Design Optimization of Active and Passive Structural Control Systems

Nikos D. Lagaros
National Technical University of Athens, Greece

Vagelis Plevris
School of Pedagogical & Technological Education, Greece

Chara Ch. Mitropoulou
National Technical University of Athens, Greece

Information Science
REFERENCE

Managing Director: Lindsay Johnston
Senior Editorial Director: Heather A. Probst
Book Production Manager: Sean Woznicki
Development Manager: Joel Gamon
Development Editor: Myla Merkel
Assistant Acquisitions Editor: Kayla Wolfe
Typesetter: Alyson Zerbe
Cover Design: Nick Newcomer

Published in the United States of America by
Information Science Reference (an imprint of IGI Global)
701 E. Chocolate Avenue
Hershey PA 17033
Tel: 717-533-8845
Fax: 717-533-8661
E-mail: cust@igi-global.com
Web site: http://www.igi-global.com

Library of Congress Cataloging-in-Publication Data

Design optimization of active and passive structural control systems / Nikos D. Lagaros, Vagelis Plevris, and Chara Ch. Mitropoulou, editors.
p. cm.
Includes bibliographical references and index.
Summary: "This book addresses the design optimization of active and passive control systems including earthquake engineering and tuned mass damper research topics and their link"-- Provided by publisher.
ISBN 978-1-4666-2029-2 (hardcover) -- ISBN 978-1-4666-2030-8 (ebook) -- ISBN 978-1-4666-2031-5 (print & perpetual access) 1. Structural control (Engineering) 2. Structural optimization. I. Lagaros, Nikos D., 1970- II. Plevris, Vagelis, 1976- III. Mitropoulou, Chara Ch., 1983-
TA654.9.D47 2013
624--dc23

2012009917

British Cataloguing in Publication Data
A Cataloguing in Publication record for this book is available from the British Library.

All work contributed to this book is new, previously-unpublished material. The views expressed in this book are those of the authors, but not necessarily of the publisher.

Preface

A typical engineering task during the development of any system is, among others, to improve its performance in terms of cost and response. Improvements can be achieved either by simply using design rules based on the experience or in an automated way by using optimization methods that lead to optimum designs.

Structural control is an expanding field in the family of control systems, also known as earthquake protective systems, including passive, active, and hybrid systems. Applications to buildings, bridges, and power plants have been made in many seismically active countries (primarily in Italy, Japan, New Zealand, and the United States). Structural control provides an alternative to conventional structural design methods. In many applications, elastic performance during large earthquake events is economically feasible, and the methodology permits performance-based design criteria, now required in many modern seismic design codes, to be satisfied more readily than with conventional methods. Applications to the retrofit of existing structures have been particularly attractive, especially to the upgrading of historical buildings. Passive control systems include tuned mass dampers, base isolation systems, mechanical energy dissipation systems, and others. Major developments in theory, design, and installation procedures of these systems have permitted applications to buildings, bridges, and power plants. After the development of passive control systems, the next step was to control the action of these devices in an optimal manner by an external energy source and the resulting system is known as an active control device system. In recent years significant progress has been made in the analytical study of active control systems for civil engineering structures. There are however limitations to the use of the passive and active control systems, and therefore, further study is required. These limitations include the uncertainty of the response, the non-optimal behavior of passive systems for both small and large earthquakes and others. The structural control fields described above define "hot" topics of Earthquake Engineering involving the use of advanced optimization tools.

The basic idea of this book is to include all the aforementioned research topics into a volume taking advantage of the connecting link between them, which is optimization. In this direction the book consists of 14 chapters in total, dealing with the topic of design optimization of active and passive structural control systems. The objective of chapters one to four is to evaluate different methodologies for the optimal placement and innovative design of passive energy dissipation systems used to reduce vibrations of civil engineering structures subject to earthquakes. Furthermore, the recent advances in damper placement methodologies based on optimization theory are reviewed. In addition the problems of the optimal location of viscoelastic dampers and determination of the optimal values of parameters of dampers are also considered.

In the fifth chapter, a combination of the analytic hierarchy process and first-order optimization method is formulated to optimize the seismic response control effect of the Runyang suspension bridge under earthquake, considering the traveling wave effect. In the next chapter the authors present a two-stage optimum design procedure for Multiple Tuned Mass Dampers (MTMD) with limitation of their strokes, for which new invention patents both in Taiwan and in USA have been granted. The objective of the seventh chapter is to demonstrate the outstanding features of the proposed Tuned Liquid Column Gas Damper and present its wide spectrum of applications of three design alternatives. The main objective of the next chapter is to find the optimal values of the parameters of the base isolation systems and the semi-active viscous dampers using genetic algorithms and fuzzy logic in order to simultaneously minimize the building's selected responses such as displacement of the top story, base shear, and others.

In the ninth chapter, an application of a neuromorphic controller is proposed for hazard mitigation of smart structures under seismic excitations. The new control system is developed through the integration of a brain emotional learning-based intelligent control algorithm with a proportional-integral-derivative compensator and a clipped algorithm. The authors of the next chapter perform analyses of the amplification and placement of active controlled devices on the efficiency of a control system, while in the eleventh chapter a multidimensional optimization problem is formulated in order to define the mass-spring combinations of the compensators. In the next chapter, a new seismic protection device is proposed, designed to dissipate the energy entering a structure subject to seismic action through the activation of hysteresis loops of the material. The thirteenth chapter provides an introduction to semi-active control of base isolated buildings using magnetorheological dampers. The last chapter of the book introduces three new multi-objective genetic algorithms for minimum distributions of both actuators and sensors within seismically excited large-scale civil structures in order to minimize the structural response.

Nikos D. Lagaros
National Technical University of Athens, Greece

Vagelis Plevris
School of Pedagogical & Technological Education, Greece

Chara Ch. Mitropoulou
National Technical University of Athens, Greece

Detailed Table of Contents

reduce interstorey drifts beyond the level that can be achieved using uniform or stiffness-proportional methods, though the influence on floor accelerations is less marked. The optimisation methods studied show broadly comparable performance, so ease of use becomes a significant factor in choosing between them. In this respect, Lavan's approach offers some advantages over the others.

The problems of the optimal location of viscoelastic (VE) dampers and determination of the optimal values of parameters of dampers are considered in this chapter. The optimal distributions of dampers in buildings are found for various objective functions. The optimization problem is solved using the sequential optimization method and the particle swarm optimization method. The properties of VE dampers are described using the rheological models with fractional derivatives. These models have an ability to correctly describe the behaviour of VE dampers using a small number of model parameters. Moreover, generalized classical rheological models of VE dampers are also taken into account. A mathematical formulation of the problem of dynamics of structures with VE dampers, modelled by the classical and fractional rheological models is presented. The results obtained from numerical calculation are also discussed in detail.

A consolidated review of the current-state-of-the-art on optimal damper positioning techniques is presented in this chapter. The inherent assumptions made in previous research are discussed and substantiated with numerical studies. Earlier studies have shown that optimal distribution of dampers is sensitive to in-structure damping. In this chapter the significance of optimal distribution of dampers coupled with the necessity for the use of a more realistic in-structure damping model is qualitatively illustrated using a comparative sensitivity study. The effect of inherent assumption of linearity of the parent frame on the 'optimality' is also investigated. It is shown that linearity assumption imposed on the parent frame in a major seismic event may not be justified; thereby raising doubts on the scope of optimality techniques proposed in literature.

Long-span suspension bridges are becoming prevalent globally with the rapid progress in design methodologies and construction technologies. Although with apparent progress, the balance between excessive displacement and inner forces, under dynamic loads, is still a main concern because of increased flexibility and low structural damping. Therefore, effective controllers should be employed to control the seismic responses to ensure their normal operation. In this chapter, the combination of the analytic hierarchy process (AHP) and first-order optimization method are formulated to optimize seismic response control effect of the Runyang suspension bridge (RSB) under earthquakes, considering traveling wave effect. The compositive optimal parameters of dampers are achieved on the basis of 3-dimensional nonlinear seismic response analyses for the RSB and parameters sensitivity analyses. Results show that the dampers with rational parameters can reduce the seismic responses of the bridge significantly, and the application of the AHP and first-order optimization method can lead to accurate optimization effects.

The design concept and procedure for tuned mass dampers (TMDs) have been extensively investigated through numerical simulation analyses and experimental tests. Sophisticated three-dimensional building models were developed to examine the optimum installation location in elevation and in plane, number and movement direction of the TMDs with the consideration of translation-torsion coupling and soil-structure interaction effects. Analytical and empirical formulas were also derived to determine the optimal parameters of TMD. It is well recognized that the performance of a TMD is sensitive to the slight deviation of frequency ratio between the TMD and the structure. Multiple tuned mass dampers (MTMDs) were proposed to reduce this detuning effect. It is also recognized that TMD's performance relies on its large stroke which may not be allowed due to the limitation of space and vibration components. The authors presented a two-stage optimum design procedure for MTMDs with limitation of their strokes. New invention patents both in Taiwan and in USA have been granted for the MTMD device.

Tuned liquid column damper (TLCD) show excellent energy and vibration absorbing capabilities appropriate for applications in wind- and earthquake engineering. The objective of this chapter is to demonstrate the outstanding features of the proposed Tuned Liquid Column Gas Damper (TLCGD) and present its wide spectrum of applications of three design alternatives. Among others it includes base isolation of structures, applications to lightly damped asymmetric buildings and other vibration prone structures like bridges (even under traffic loads) and large arch-dams as well as simple, ready to use design guidelines for optimal absorber placement and tuning. The evident features of TLCGDs are no moving mechanical parts, cheap and easy implementation into civil engineering structures, simple modification of the natural frequency, and even of the damping properties, low maintenance costs, little additional weight in those cases where a water reservoir is required, e.g., for the sake of fire fighting, and with a performance comparable to that of TMDs of the spring-mass- (or pendulum-)-dashpot type.

Compensators are widely used to influence the dynamic response of excited structures. The coupling of additional masses with defined stiffness and damping to the vibrating elements reduces or avoids unwanted oscillations. In earthquake engineering, compensators often consist of one or a small number of such additional mass-spring combinations. To come up with a good design of the compensators, a multidimensional optimization problem has to be solved. As there might be many local optima, evolutionary approaches are the appropriate choice of the optimization strategy. They start with some basic designs. Then a sequence of generations of design variants is studied. The members of each generation are derived from the parent generation by crossing and mutation. The best kids are the parents of the next generation. Optimization results show that the use of compensating systems may essentially reduce the impact of an earthquake.

In this chapter, a new seismic protection device is proposed. It is designed to dissipate the energy entering a structure subject to seismic action through the activation of hysteresis loops of the material that composes it. These devices are characterized by a high capacity to absorb the seismic energy and the ability to concentrate the damage on it and, consequently, to keep the structure and the structural parts undamaged. Moreover, after a seismic event they can be easily replaced. In particular, this chapter proposes a new shear device that shows the plasticity of some areas of the device at low load levels. In order to maximize the amount of dissipated energy, the design of the device was performed by requiring that the material be stressed in an almost uniform way. In particular, the device is designed to concentrate energy dissipation for plasticity in the aluminum core while the steel parts are responsible to make stiffer the device, limiting out-of-plane instability phenomena. The geometric configuration that maximizes the energy dissipation has been determined using a structural optimization routine of finite element software.

This chapter provides an introduction to semi active control of base isolated buildings using magnetorheological (MR) dampers. Recently developed nonlinear control algorithms are discussed. First a fuzzy logic control (FLC) is designed to decide how much voltage is required to be supplied to the MR damper for a desired structural response. The FLC is optimized using micro genetic algorithm. A novel geometric approach is developed to optimize the FLC rule base. Experiments are undertaken to access the efficacy of the optimal FLC. Secondly the chapter develops two model based control algorithms based on dynamic inversion and integrator backstepping approaches. A three storey base isolated building is used for experimental and numerical studies. A numerical comparison is shown with clipped optimal control.

This chapter introduces three new multi-objective genetic algorithms (MOGAs) for minimum distributions of both actuators and sensors within seismically excited large-scale civil structures such that the structural responses are also minimized. The first MOGA is developed through the integration of Implicit Redundant Representation (IRR), Genetic Algorithm (GA), and Non-dominated sorting GA 2 (NSGA2): NS2-IRR GA. The second one is proposed by combining the best features of both IRR GA and Strength Pareto Evolutionary Algorithm (SPEA2): SP2-IRR GA. Lastly, Gene Manipulation GA (GMGA) is developed based on novel recombination and mutation mechanism. To demonstrate the effectiveness of the proposed three algorithms, two full-scale twenty-story buildings under seismic excitations are investigated. The performances of the three new algorithms are compared with the ones of the ASCE benchmark control system while the uncontrolled structural responses are used as a baseline. It is shown that the performances of the proposed algorithms are slightly better than those of the benchmark control system. In addition, GMGA outperforms the other genetic algorithms.

Chapter 1
Optimal Placement of Controller for Seismic Structures

Gian Paolo Cimellaro
Politecnico di Torino, Italy

ABSTRACT

The objective of this chapter is to evaluate different methodologies for the optimal placement and innovative design of passive energy dissipation systems which are being used to reduce vibrations of civil engineering structures subject to earthquakes. For large civil engineering structures it is necessary to install a sufficient number of dampers to achieve a reduction of the building response and the performance of these dampers depends on their location in the structures. The selection of few locations out of a large number of locations for the placement of passive dampers is typically a nonlinear constrained optimization problem. This problem can be solved either by simple heuristic search approaches which can be easily integrated in conventional design procedures used by practicing engineers dealing with damper-added structures, and they yield a solution which may be close to the optimal solution, but computationally expensive. Three different heuristic search strategies will be used to optimize four objective functions, and results will be compared for three different building typologies.

INTRODUCTION

Earthquakes pose a major threat to society and to the economic development of a nation. An earthquake disaster is generally associated with the collapse of building structures, but most severely with a large number of casualties and enormous economic losses.

The dynamic response of civil engineering structures subjected to earthquake excitation can be reduced by using passive control systems such as energy dissipation devices (e.g. viscous dampers, etc.). The advantage of these systems with respect to active and semi-active control systems consist in the fact that they don't require any power supply, therefore are quite reliable and they require least maintenance.

DOI: 10.4018/978-1-4666-2029-2.ch001

For large civil engineering structures it is necessary to install a sufficient number of dampers to achieve a reduction of the structural response due to earthquake and the performance of these dampers depends on their location in the structures. The selection of few locations out of a large number of locations for the placement of passive dampers is typically a nonlinear constrained optimization problem. This problem can be solved either by simple heuristic search approaches or through integral optimization. The first ones are simple and they yield a solution which may be close to the optimal solution, but computationally expensive, instead the second ones are fast but solution is complex.

In this chapter heuristic search methods have been investigated in detail using four different objective functions and applied to three building typologies that have been modeled as linear behavior for simplicity, however these methods can also be applied nonlinear structures.

BACKGROUND

The seismic response of structures subjected to earthquake excitations may be effectively reduced by incorporating any of various kinds of available passive energy dissipation devices (Soong and Dargush 1997). Numerous are the studies related to optimal placement and capacity of damping coefficient for linear multistory buildings.

Tsuji and Nakamura (1996) proposed an algorithm that finds the optimal story stiffness distribution and the optimal damper distribution for a shear building model subjected to a set of spectrum-compatible earthquakes, but it requires high computational afford because it is necessary to run dynamic analysis and include artificial constraints like the upper bound of the damping coefficients. Nakamura et al. (1996) found a method for evaluating an ordered set of stiffness design variables of an elastic shear type building with an ordered set of damping coefficients via an inverse problem approach, under the assumption that the ratio between the mean maximum interstory drift due to a spectrum compatible earthquake and the target specified value remains constant. Gluck, Reinhorn et al. (1996) suggested a method for the design of supplemental dampers and stiffness based on optimal control theory using a linear quadratic regulator (LQR) that minimizes a performance cost function, but the algorithm is valid under the assumption of white noise input and it is effective only for systems where the first mode effects are predominant.

Takewaki (1997) proposed a stiffness-damping simultaneous optimization procedure where the sum of mean square responses to stationary random excitations is minimized subjected to the constraints on total stiffness and damping capacity. It is a two-step optimization method where, in the first step, the optimal design is found for a specified value of total stiffness and damping, while in the second step the procedure is repeated for a set of total stiffness and damping capacity.

All methods mentioned above, even if they lead to an optimal damper configuration, are not practical, because they are not simple enough to be used routinely by practical engineers. An ideal method should be practical and capable of controlling the number of different damper sizes to be used. The method should be also efficient, in the sense that the resulting damper configuration (i.e., size and location of added dampers) minimizes the total amount of added damping necessary to reach a given performance objective.

A practical method is the one proposed by Zhang and Soong (1992), who suggested a sequential procedure to find the optimal placement of viscoelastic dampers, based on the controllability index method presented by Cheng and Pantelides (1988). The procedure consists in adding dampers one by one to the structure in the story where the optimal location index is maximum, assuming that all the dampers have the same size. Since all dampers have the same size the method is more practical than other optimization methods, which usually lead to a different damper size at each story. The method can be referred to as a Sequential Search algorithm (SS) and it can be included in a broader category of methods called heuristic search methods. These methods are very flexible, because they provide designer and engineers a number of possible choices: if the damper size is constrained, then the number of damper can be adjusted and if the number of dampers is subjected to limitations, then the damper size can be conveniently selected. Therefore in this chapter, three simple heuristic search methods that can be easily used by practical engineers are compared using four different objective functions and applied to three different building typologies.

OBJECTIVE FUNCTIONS

Average Dissipated Energy (J1)

This objective function represents the average energy dissipated by the dampers; in this case, to determine the optimal placement of passive energy dissipation systems, it is necessary to maximize *J1*.

Consider an n story linear shear-type building structure, equipped with r passive energy dissipation systems in various story units. Masses, stiffnesses and damping coefficients for different floors of the building are contained in $(n \times n)$ matrices, respectively called **M, K, C**.

The state equation of motion is

$$\dot{\mathbf{z}}(t) = \mathbf{Az}(t) + \mathbf{Bu}(t) + \mathbf{Ew}(t) \tag{1}$$

where $\mathbf{z}(t) = [\mathbf{x}(t), \dot{\mathbf{x}}(t)]^T$ is a $2n$ state vector, $\mathbf{u}$(t) is a r vector whose each element is a function of nonlinear stiffness and damping forces from the damper installed in the ith story unit, $w(t)$ is an n vector of external excitations, **A** is a $(2n \times 2n)$ system matrix, **B** is $(2n \times r)$ damper location matrix and **E** is a $(2n \times n)$ matrix. **A, B** and **E** can be written as

$$\mathbf{A} = \begin{bmatrix} 0 & \mathbf{I} \\ -\mathbf{M}^{-1}\mathbf{K} & -\mathbf{M}^{-1}\mathbf{C} \end{bmatrix}, \mathbf{B} = \begin{bmatrix} 0 \\ \mathbf{M}^{-1}\mathbf{H} \end{bmatrix}, \mathbf{E}(t) = \begin{bmatrix} 0 \\ \mathbf{M}^{-1} \end{bmatrix} \tag{2}$$

in which **H** is a $(n \times r)$ location matrix for passive dampers. The damper force $\mathbf{u}$(t) can be written as

$$\mathbf{u}(t) = -\mathbf{Gz}(t) \tag{3}$$

where **G** is a $(r \times 2n)$ damper parameter matrix given as

$$\mathbf{G} = \begin{bmatrix} k_{d1} & 0 & . & . & . & 0 & c_{d1} & 0 & . & . & . & 0 \\ 0 & k_{d2} & 0 & . & 0 & 0 & 0 & c_{d2} & . & 0 & 0 & 0 \\ . & . & . & . & . & . & . & . & . & . & . & . \\ 0 & 0 & . & k_{dr} & . & 0 & 0 & 0 & . & c_{dr} & . & 0 \end{bmatrix} \tag{4}$$

By substituting Equation 3 in Equation 1 and neglecting *w(t)*, Equation 1 can be written as

$$\begin{aligned} \dot{\mathbf{z}}(t) &= (\mathbf{A} - \mathbf{BG})\mathbf{z}(t); \\ \mathbf{z}(t = 0) &= z_0 \end{aligned} \tag{5}$$

where z_0 expresses any initial condition. The average dissipated energy is given by

$$J_1 = \int_0^\infty \dot{\mathbf{x}}^T \mathbf{C}_d \dot{\mathbf{x}} dt \tag{6}$$

in which C_d is a (n×n) diagonal matrix that contains the damping coefficients of the dampers installed in each story units. J_1 is the objective function that represents the total energy dissipated by the dampers when the structure is subjected to a free vibration. Integrating Equation 5, it can be written as

$$\begin{aligned} \mathbf{z}(t) &= \Phi(t) z_0; \\ \Phi(t) &= e^{(\mathbf{A}-\mathbf{BG})t} \end{aligned} \tag{7}$$

and consequently the velocity vector $\dot{\mathbf{x}}(t)$ can be expressed as

$$\dot{\mathbf{x}} = \mathbf{T}\mathbf{z}(t) = \mathbf{T}\Phi z_0 \qquad (8)$$

where $\mathbf{T} = \begin{bmatrix} 0 & \mathbf{I}_n \end{bmatrix}$ is a *(n×2n)* transformation matrix. Substituting Equation 8 in Equation 6, it is possible to express objective function J_1 as

$$J_1 = \int_0 z_0{}^T \Phi^T \bar{\mathbf{C}}_d \Phi z_0 \, dt \qquad (9)$$

where

$$\bar{\mathbf{C}}_d = \mathbf{T}^T \mathbf{C}_d \mathbf{T} \qquad (10)$$

As expressed in Equation 9, the Average Dissipated Energy J_1 depends on the initial conditions z_0, therefore the maximization of J_1 assumes different values for different initial conditions. In order to eliminate this dependence, z_0 is assumed like a random variable (uniformly distributed on the surface of the $2n$-dimensional unit sphere), so the expression of J_1 becomes

$$J_1 = \mathbf{E}[J] = trace\left[\int_0^\infty \Phi^T \bar{\mathbf{C}}_d \Phi \, dt\right] \qquad (11)$$

It is possible to introduce the matrix **P**, defined as

$$\mathbf{P} = \int_0^\infty \Phi^T \bar{\mathbf{C}}_d \Phi \, dt \qquad (12)$$

that is definite because, since civil engineering structures are stable and ***u(t)*** always enhances the stability of the structure, the system matrix *(***A-BG***)* will always be stable.

The previous matrix **P**, according to Lyapunov's method, satisfies

$$\mathbf{P}(\mathbf{A} - \mathbf{B}\mathbf{G}) + (\mathbf{A} - \mathbf{B}\mathbf{G})^T \mathbf{P} = -\bar{\mathbf{C}}_d \qquad (13)$$

Consequently, the performance index J_1 in Equation 11 becomes

$$J_1 = trace[\mathbf{P}] \qquad (14)$$

The main advantage of this objective function is that it is independent of external excitations.

Weighted Sum of Damping Ratios for Dominant Modes (J2)

This objective function derives from Ashour and Hanson's studies (1987), which have studied the problem of optimal placement of dampers by modeling the building as a continuous shear beam and then using numerical procedures to maximize the damping in the fundamental mode. Their results show that the fundamental mode has a maximum damping ratio when all the dampers are placed in the first story unit. However, their discovery is useful only for shear-type buildings with identically constructed story units, so it is possible to define a generalized objective function which is the weighted sum of damping ratios for q dominant modes, valid for any kind of civil engineering structure. The damping ratio of the i^{th} mode can be obtained as

$$\zeta_i = \frac{-\mathrm{Re}(\lambda_i)}{|\lambda_i|} \qquad (15)$$

where λ_i is obtained by the complex eigenvalue analysis of the state Equation 5. In the case of systems with a small number of degrees of freedom, the eigenvalues can be calculated easily, instead for very large order systems, eigenvalue analysis is very difficult.

Hence, Milman and Chu (1994) proposed to use the Ritz reduction method to calculate damping ratio.

Generally the structures are dominated by the first q modes of vibration, consequently the objective function can be written as

$$J_2 = \sum_{j=1}^{q} \psi_i \zeta_i \tag{16}$$

where q indicates the first dominant modes, ψ_i is the scalar weighting factor for the i[th] mode. J_2 objective function represents the weight average damping ratios, which it is necessary to maximize, to determine the optimal placement of passive energy dissipation systems.

Maximum Peak Absolute Accelerations (J3)

For particular type of buildings such as health care facilities, control towers, etc., the goal of installing dampers is to reduce the absolute accelerations to reduce damage to mechanical equipments, computers etc. Therefore it may be interesting to investigate the optimal location of dampers for an objective function which represents the maximum of the peak absolute accelerations of all story units, which will be minimized. Then the objective function, representing the maximum of all peak absolute accelerations, can be defined as

$$J_3 = \max\left\{\bar{\ddot{x}}_{pi},\ \text{i=1,2,...,n}\right\} \tag{17}$$

where the maximum accelerations can be written as

$$\bar{\ddot{x}}_{pi} = \max_t \left|x_i(t)\right| \tag{18}$$

Maximum Peak Interstory Drifts (J4)

Buildings are usually planned by using the design earthquakes for a particular site. Since the objective of installing dampers on buildings is to reduce the interstory drifts, it may be interesting to investigate the optimal location of dampers for an objective function which represents the maximum of the peak drift of all story units which will be minimized. For the system in Equation 5, for a design earthquake ground acceleration $\ddot{x}_0(t)$, the equation of motion can be expressed as

$$\dot{\mathbf{z}}(t) = (\mathbf{A} - \mathbf{BG})\mathbf{z}(t) + \mathbf{E}_0\ddot{x}_0(t) \tag{19}$$

where $\mathbf{E}_0 = \left[0_{(1,n)}, -\mathbf{M}^{-1}\mathbf{m}_v\right]$

Equation 19 can be integrated for a particular ground acceleration time-history, obtaining $x_i(t)$, from which peak interstory drift can be written as

$$\bar{x}_{pi} = \max_t \left|x_i(t)\right| \tag{20}$$

Then the objective function, representing the maximum of all peak interstory drifts, can be defined as

$$J_4 = J_{4Dbe} = \max\left\{\bar{x}_{pi},\ \text{i=1,2,...,n}\right\} \tag{21}$$

INTEGER HEURISTIC PROGRAMMING

Once the objective functions are defined in previous paragraph then the optimal location of energy dissipation dampers needs be determined. Three types of heuristic search algorithms can be used in order to solve the nonlinear constrained optimization problem:

- The Sequential Search algorithm (SS)
- The Worst-Out-Best-In algorithm (WOBI)
- The Exhaustive-Single-Point-Substitution algorithm (ESPS)

The Sequential Search (SS) Algorithm

The method consists of placing r dampers in n story units. It starts by placing the first damper in a particular story unit and evaluating the corresponding objective function. This process is repeated for all story units and the story unit, which corresponds to the best objective function, is selected as the optimal location for the first damper (Table 1). After that the first damper is located in its optimal location, this procedure is repeated for all remaining dampers (Figure 1).

This method can be used for two types of damper placement strategies:

1. **Distinctive Locations:** With this strategy only one damper can be located in a story unit, while the second damper can be placed in the rest of (n-1) story units. So the required number of evaluations for the objective function is {n×r-[r×(r-1)/2]}.
2. **Repeated Locations:** With this strategy, more than one damper can be located in a story unit, while the second damper can be placed in all story units. So the required number of evaluations for the objective function is n×r.

The Worst-Out-Best-In (WOBI) Search Algorithm

This method starts with an initial configuration of *r* dampers, denoted by I_0, and the corresponding objective function is denoted by f_0. Generally, I_0 corresponds to the configuration obtained by either the sequential search method (SS) or any given pre-design method. In the WOBI search algorithms the objective function *f* is calculated

Table 1. The sequential search method

Step by Step Procedure
Step 1: For the placement of the first damper, set $k=1$.
Step 2: Select stiffness k_d and damping coefficients c_d.
Step 3: Assemble the vector *Ivec(k)* that containing optimal locations. Set it null.
Step 4: Assemble the damper matrix **G** (set **G**=0)
Step 5: For distinct locations, evaluate the objective function *f* at each of the *(n-k-1)* story units; for repeated locations, evaluate the objective function *f* at each of the *n* story units.
Step 6: The i^{th} story unit with the best value of objective function is identified as the optimal location for the first damper, so add it to the list of optimal locations.
Step 7: Set *Ivec(k)*=I.
Step 8: Set $k=k+1$.
Step 9: if $k>r$, stop; if $k<r$ go to step 4.

for each of the *r* configurations of *(r-1)* dampers, obtained by removing one damper from I_0. The configuration of *(r-1)* dampers, obtained by eliminating the worst damper, is denoted by I_1. Then, the removed damper is placed in the *(n-r)* story units and the performance index is evaluated for every configuration. The configuration corresponding to the optimal objective function is denoted by I_2. This procedure is an iterative one, and evaluations are continued till no improvement in the objective function is possible (Figure 2). In WOBI search, a total of $r+(n-r)=n$ evaluations of the objective function are required in each iteration to find the optimal locations (for the case of distinctive location strategy). The method is summarized in a step by step procedure in Table 2.

The Exhaustive-Single-Point Substitution (ESPS) Search Algorithm

The ESPS method, like the WOBI method, starts with an initial configuration of *r* dampers, denoted by I_0, and the corresponding objective function is denoted by f_0. Generally I_0 corresponds to the configuration obtained by either the sequential

Figure 1. Flow chart of the sequential search method

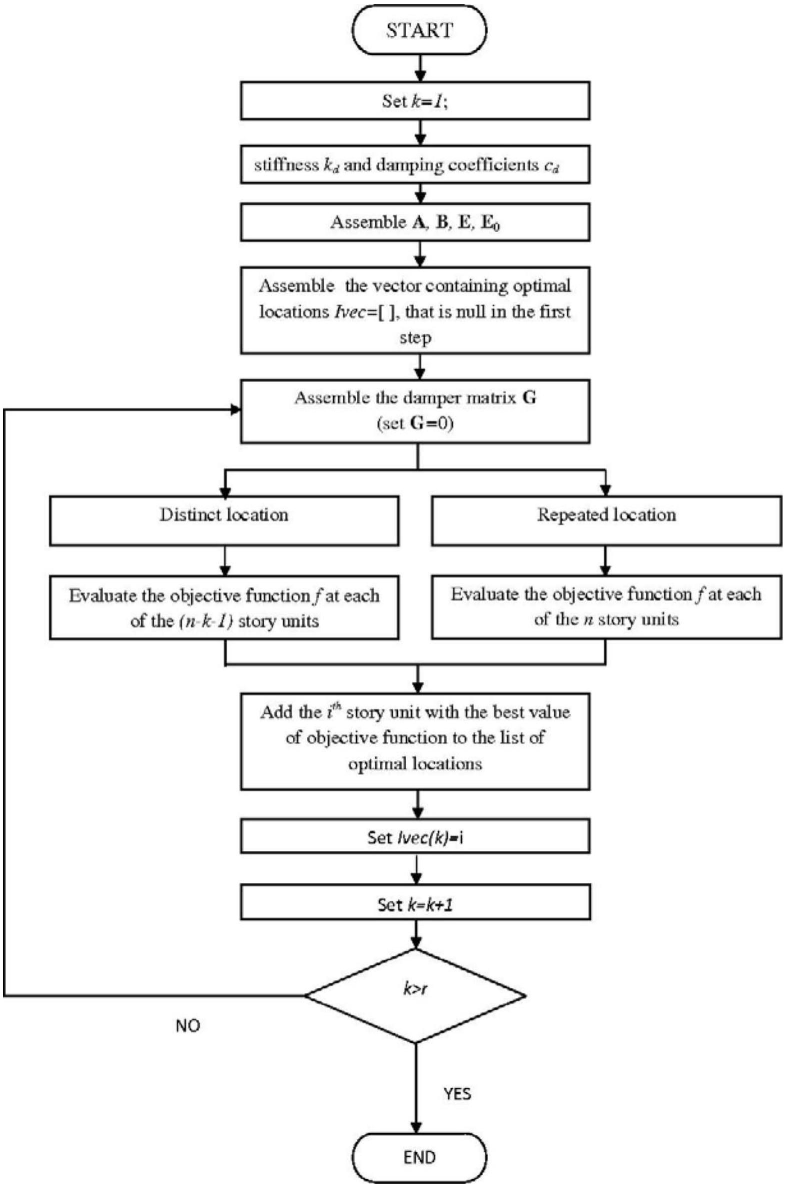

search method or any given pre-design method. Then, one damper of I_0 is removed by its initial position and it is placed at each of *(n-r)* unused locations (not included in I_0) and the objective function is evaluated. This process is repeated for each of the *r* dampers of I_0 so globally $r \times (n-r)$ combinations are considered and the corresponding objective functions are evaluated (Table 3 and Figure 3). Then, the configuration with the best objective function is denoted by I_2. It is obvious from above discussion that the ESPS search method is more general than WOBI one, because it considers all possible configurations. In ESPS search, a total of $r \times (n-r)$ evaluations of the objective function are required in each iteration to find the optimal location, while WOBI search tries only *n* configurations.

Figure 2. Flow chart of worst-out-best-in algorithm (WOBI)

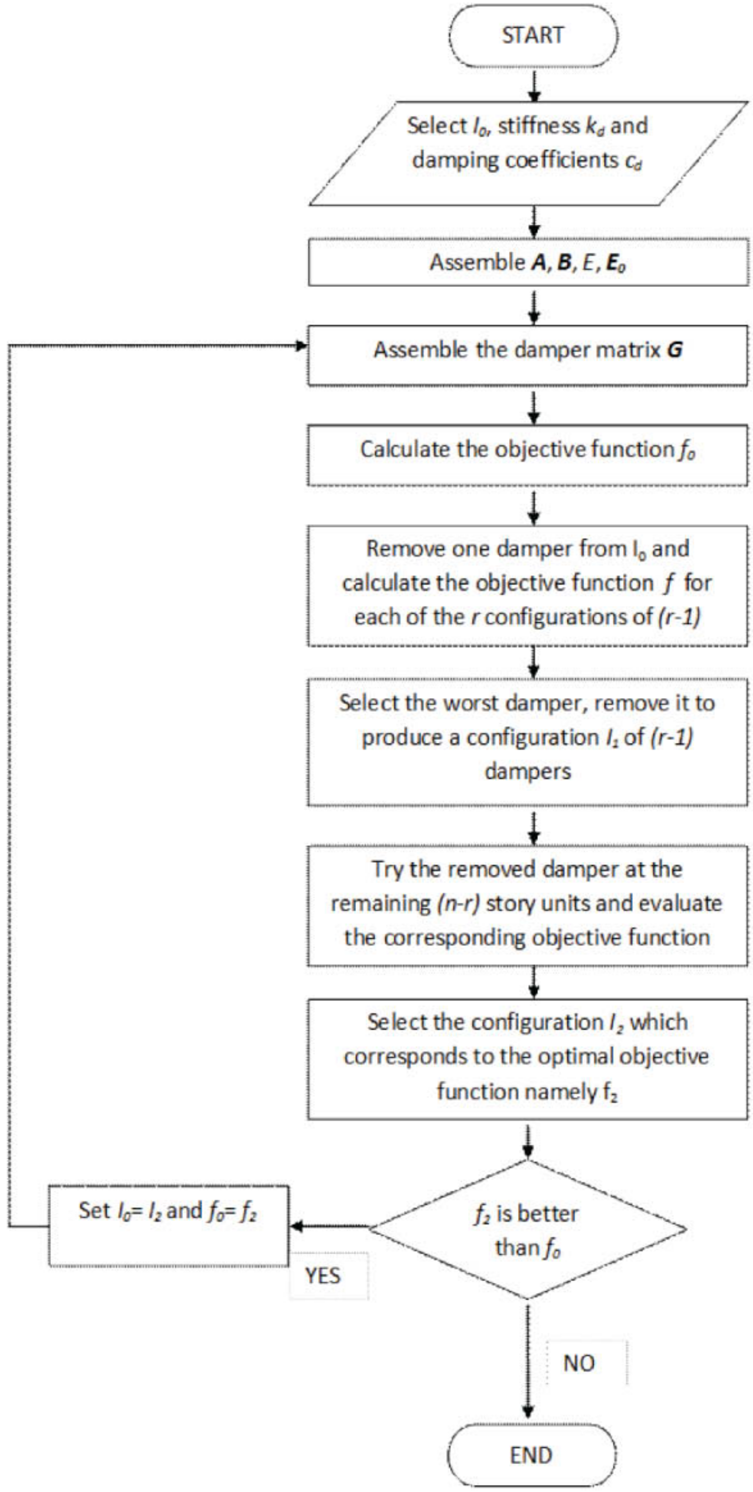

Table 2. The worst-out-best-in method

Step by Step Procedure
Step 1: Select I_0 (a r vector containing initial configuration of damper locations obtained by either the sequential search method or any given pre-design method), stiffness k_d and damping coefficients c_d.
Step 2: Assemble **A**, **B**, E, $\mathbf{E_0}$ matrices.
Step 3: Assemble the damper matrix **G.**
Step 4: Evaluate the objective function f_0, corresponding to the initial damper configuration I_0.
Step 5: Remove one damper from I_0 and calculate the objective function f for each of the r configurations of *(r-1)*.
Step 6: Select the worst damper and remove it in order to produce a configuration I_1 of *(r-1)* dampers.
Step 7: Try the removed damper at the remaining *(n-r)* story units and evaluate the corresponding objective function.
Step 8: The configuration which corresponds to the optimal objective function, namely f_2, is denoted by I_2.
Step 9: If f_2 is better than f_0, the next iteration is started by I_0=I_2 and go to step 3.

Instead, if f_0 is better than f_2, the iteration ends.

Table 3. The exhaustive-single-point substitution search method

Step by Step Procedure
Step 1: Select I_0 (a r vector containing initial configuration of damper locations obtained by either the sequential search method or any given pre-design method), stiffness k_d and damping coefficients c_d.
Step 2: Assemble **A**, **B**, E, $\mathbf{E_0}$ matrices.
Step 3: Assemble the damper matrix **G**.
Step 4: Evaluate the objective function f_0, corresponding to the initial damper configuration I_0.
Step 5: Remove one damper from I_0 and place it at each of *(n-r)* unused locations (not included in I_0).
Step 6: Evaluate the objective function f for each of the *(n-r)* r configurations.
Step 7: Label the objective function with best f as f_1 and the corresponding configuration as I_1.
Step 8: If f_1 is better than f_0, the next iteration is started by I_0=I_1 and go to step 3.

Instead, if f_0 is better than f_1, the iteration ends.

PRELIMINARY DESIGN

The preliminary design of viscous dampers of the framed structure can be done starting from the dynamic characteristics of the unbraced building and in particular from the fundamental period T_{1U}. The approximate method is based on the following steps:

1. The damping ratio ξ_1 related to the first mode T_{1u} of the unbraced structures is selected.

2. The fundamental period of the braced structure with fictitious springs is obtained using the following expression:

$$T_{1f} = \frac{T_{1u}}{\sqrt{2\xi_1 + 1}} \tag{22}$$

3. An initial stiffness value k_{o_trial} of the fictitious springs equivalent t_{oe} the viscous dampers is assumed. A new stiffness matrix is obtained considering the additional stiffness of the equivalent braces. For preliminary design it is assumed to have one damper for story;

4. 4.Modal analysis of the building is obtained using the stiffness matrix obtained from point 3 and a new value of the fundamental period $T_{1f,trial}$ is obtained;

5. The new stiffness values of the braced structures are evaluated with the following expression:

$$k_{1,trial} = \frac{k_{0,trial}}{1 - \left(\dfrac{T_{1f}^2 - T_{1f,trial}^2}{T_{1f}^2 - T_{1u}^2} \right)} \tag{23}$$

6. Repeat step 4 and 5 iteratively until the i^{th} iteration satisfies the condition $k_{i,trial} \simeq k_{i-1,trial}$ e $T_{if,trial} \simeq T_{i-1f,trial}$ .Asingle iteration is sufficient, because the stiffness variation is linearly proportional to the square of the period of the building;

Figure 3. Flow chart of exhaustive-single-point-substitution algorithm (ESPS)

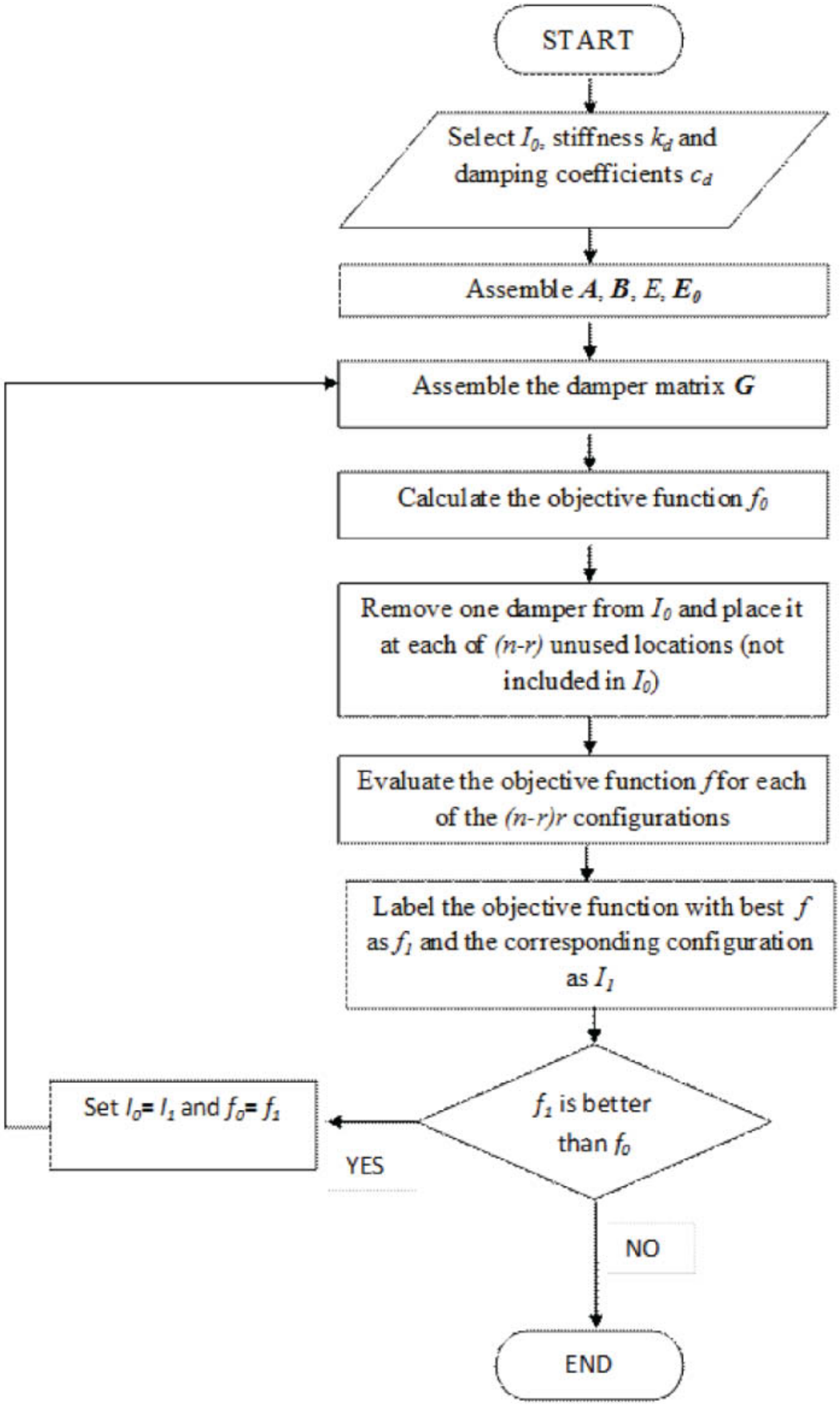

7. Once the stiffness of the fictitious springs is evaluated, the respective viscous coefficients can be obtained as:

$$c = \frac{T_{1u}}{2\pi} k_{0f} \tag{24}$$

Preliminary design is used to select the size of the damper unit which will be used during the optimization process. In the next sessions are shown the results of preliminary design obtained for three different buildings.

NUMERICAL RESULTS

The three integer heuristic approaches presented in previous paragraphs called SS, WOBI and ESPS are used to find the optimal location for dampers. The search methods described can be applied using the Distinctive Location Strategy and the Repeated Location Strategy. In the following numerical examples only the repeated location strategy is applied. The optimization process starts with a uniform distribution of the damper unit (one for each story) which is selected by the preliminary design. Then the search methods will re-allocate the dampers 'position. The heuristic search methods described in previous paragraphs for optimal location of passive energy dissipation systems will be investigated numerically for three different types of buildings: (1) a six story shear building with soft story behavior; (2) a 10 story shear building with uniform stiffness through the story height; (3) a thirty story shear building with non uniform stiffness through the story height. (Figure 4). The performance of each search method for optimizing different objective functions will be investigated based on four earthquake records that were selected from a benchmark problem (Ohtori 2004). The earthquakes selected for the analysis correspond to the earthquake of: El Centro (1940), Hachinohe (1968), Northridge (1994) and Kobe (1995). The first two are far-field earthquakes, while the other two are near field earthquakes.

Dynamic time history analyses are performed to demonstrate the validity of the proposed design methodology, using four earthquake records representative of near field and far field conditions.

Six Story Building with Soft Story Behavior

The building is modeled as a *6 DOF* shear type model with soft story behavior. This type of behavior is observed in most real buildings that usually have openings and shops at the first story. The mass is assumed uniform at all story levels and equal to $m_i = 3.2\times10^4 kg$. The lateral stiffness is

$$\begin{aligned} k_i &= 56.40\times10^3\ kN/m \quad i = 2,\ldots,6 \\ k_1 &= 39.48\times10^3\ kN/m \qquad i = 1 \end{aligned}$$

and it has been considered for determining the optimal locations of viscous dampers, by optimizing the objective functions described in previous paragraph. The natural periods of the six modes of the building are: *T=0.66, 0.22, 0.13, 0.10, 0.08 and 0.07 sec*, and it is assumed a damping ratio of *5%* on the first and the third mode. Dynamic properties of the building, including the modal damping ratio and the mass participation factor are given in Table 4.

The story height considered is $h = 3.0\ m$, the same in all levels, while the total weight of the building is *1882.88kN*. The structural response in term of interstory drifts and absolute accelerations for the uncontrolled structures (unbraced) are shown in Figure 5.

Preliminary design was performed assuming 25% damping ratio on the first mode assuming one damper placed at every story unit (uniform distribution), therefore the fictitious lateral stiffness at a given story is $k_{of} = 34000\ kN/m$, while the equivalent damping coefficient is $c_o = 3588.7\ kN{*}s/m$.

Figure 4. Response spectra of the four selected earthquakes

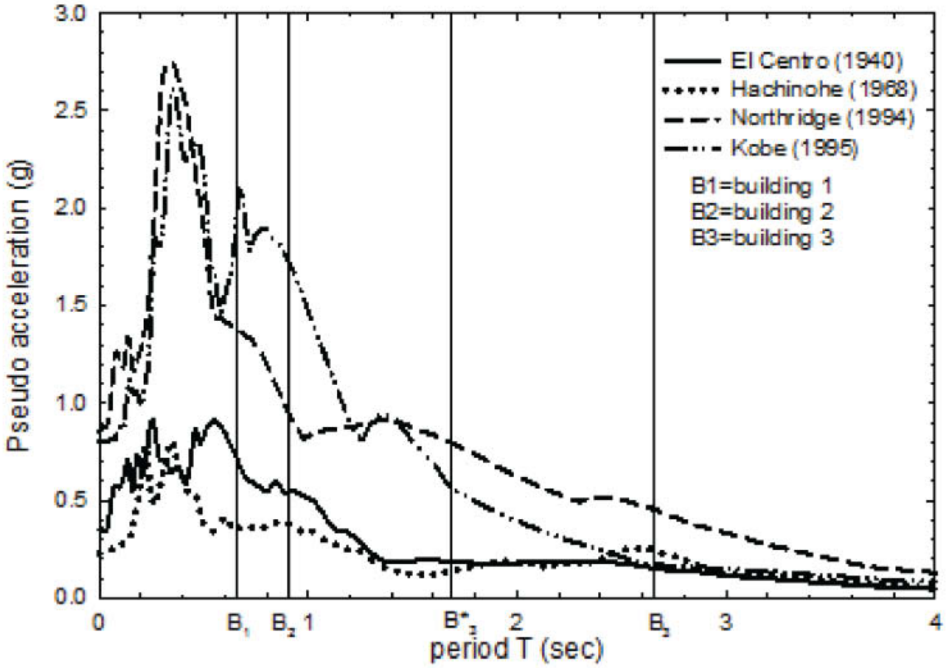

The structural responses of the uniformly braced structure for different seismic events are shown in Figure 6.

The base shear coefficient normalized with respect to the total weight of the building is shown in Figure 7, comparing the uncontrolled and the controlled structure. An average reduction of the base shear is observed for all the earthquake records of about 26%, while the higher reduction is obtained with Hachinobe earthquake (47%).

The structural response in term of drift and absolute accelerations are shown in Figure 8 when El Centro earthquake is considered using the sequential search algorithm (SS) with the maximum absolute acceleration (J3) and the interstory drift (J4) as objective functions. Both distributions obtained with the two indices have similar performances even if *J3* will perform slightly better in accelerations and *J4* slightly better in interstory drifts as expected.

When analyzing the six story building there are no differences among the three algorithms: SS, WOBI and ESPS when the maximum drift (*J4*) is considered as objective function (Figure 9). This brings to the conclusions that both for near field that far field earthquakes the damper distribution obtained using the index *J4* is very stable and it is not affected by the search algorithm adopted. Small differences can be observed instead

Table 4. Dynamic properties of the unbraced six story building

Story	ω [rad/s]	T [s]	ζ [%]	ϵ [%]
1	9.51	0.661	5.00	90.09
2	28.30	0.222	3.94	7.56
3	46.07	0.136	5.00	1.70
4	61.62	0.102	6.18	0.48
5	73.69	0.085	7.16	0.14
6	81.35	0.077	7.80	0.03

Figure 5. Unbraced structural responses for different seismic events

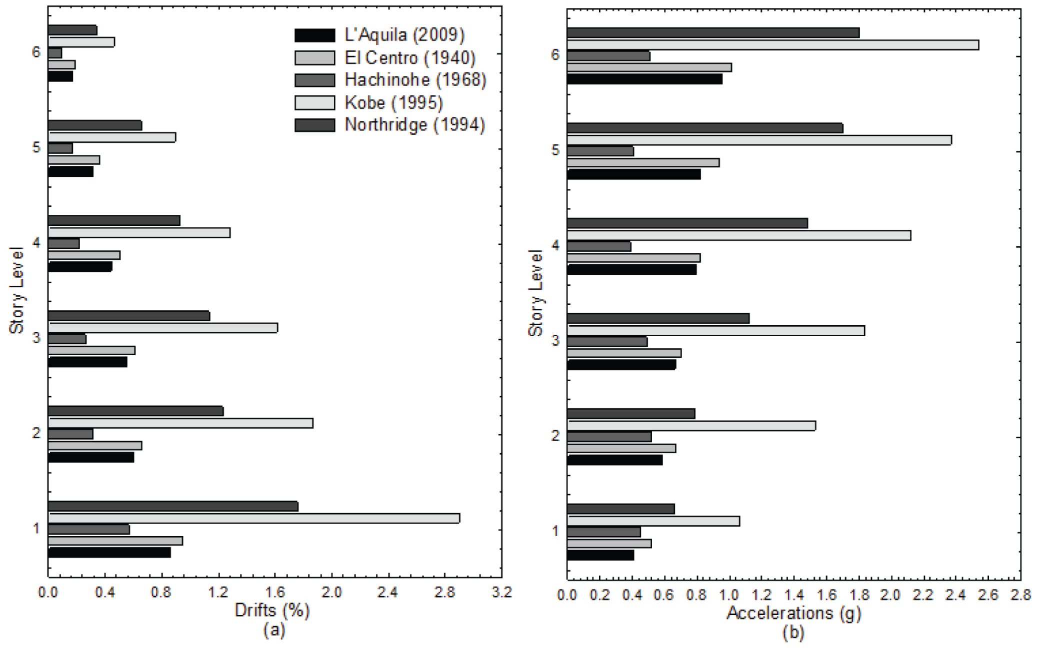

Figure 6. Structural responses of the uniformly braced structure for different seismic events

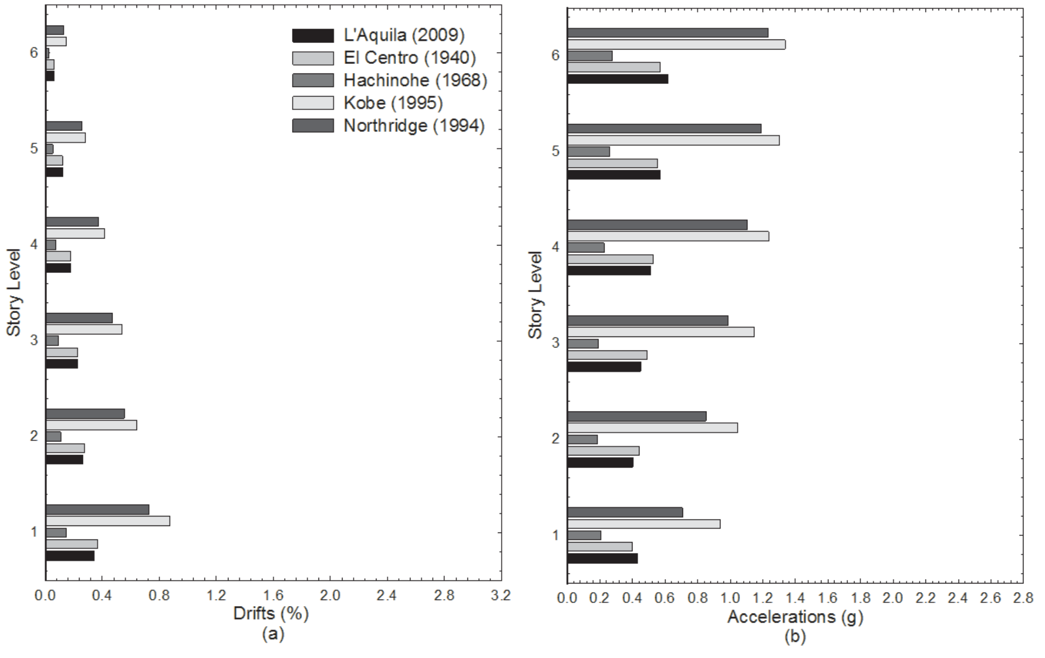

Figure 7. Base shear comparison with uniformly braced structure

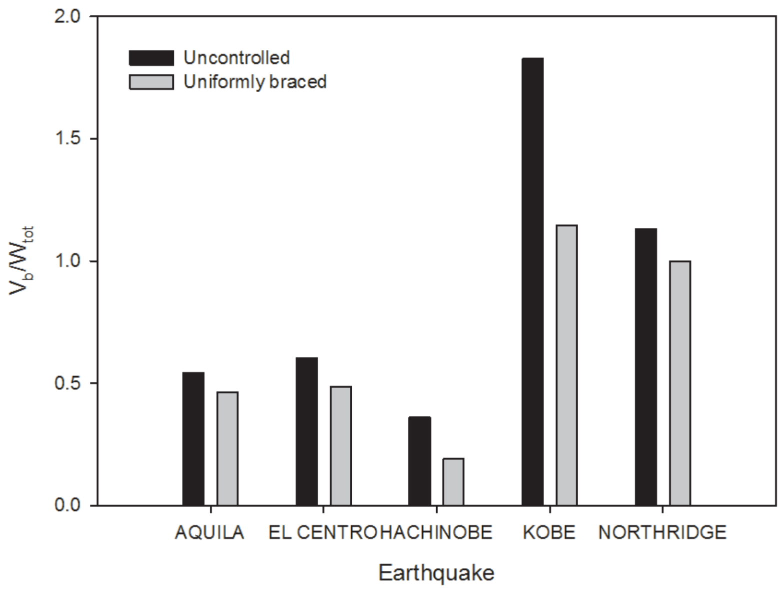

when the maximum acceleration (*J3*) is used as objective function (Figure 10).

For both indices instead different damper distributions can be obtained using different earthquake records that can be caused by the different frequency content of each earthquake (Figure 4). Hence it has been found that the optimal distributions obtained with *J3* and *J4* as objective functions strongly depend on the nature of the earthquake record at the site. Hence, the optimal damper distribution for seismic excited buildings can be obtained by minimizing *J4* using the design earthquake of the particular site.

The index that maximizes the energy dissipated by the viscous dampers (*J1*) tends to locate dampers where the velocity is higher and this usually happens in the upper floors. Therefore this performance index moves the dampers in the uppers floors. Instead the index that maximizes the damping ratio (*J2*) is not very sensitive and it does not bring to realistic distributions.

In summary, it has been observed that when the DOFs of the building are reduced such as in the 6 story building, then SS, WOBI and ESPS search methods bring to the same damper distribution for the various objective functions considered.

Ten Story Building

A ten story shear building with story mass of $m_i = 20786kg$ and lateral stiffness of

$$
\begin{aligned}
k_i &= 687.1 \times 10^5 \; kN/m \quad & i &= 1,\dots,2 \\
k_i &= 540.1 \times 10^5 \; kN/m \quad & i &= 3,\dots,4 \\
k_i &= 421.7 \times 10^5 \; kN/m \quad & i &= 5,\dots,6 \\
k_i &= 286.6 \times 10^5 \; kN/m \quad & i &= 7,\dots,8 \\
k_i &= 164.5 \times 10^5 \; kN/m \quad & i &= 9,\dots,10
\end{aligned}
$$

and it has been considered for determining the optimal locations of viscous dampers, by optimizing the objective functions described in the previous paragraph. The natural periods of the first three modes of the building are: *T=0.66, 0.22, 0.13, 0.10, 0.08* and *0.07 sec*, and it is assumed a damping ratio of 5% on the first and the third mode. Dynamic properties of the building,

Figure 8. Structural response using sequential search algorithm (SS) with J3 and J4 performance index respectively

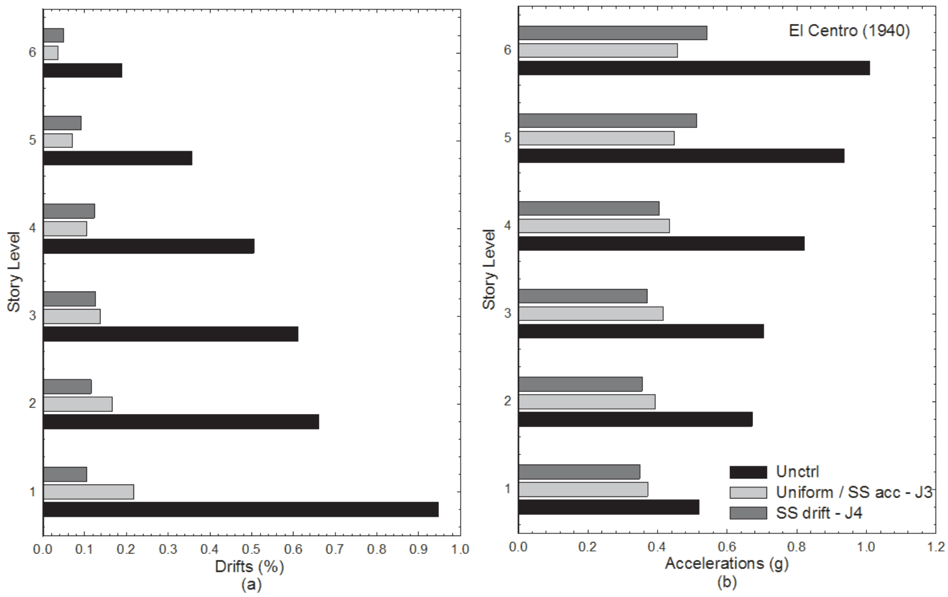

Figure 9. Damper distributions using the maximum interstory drift (J4)

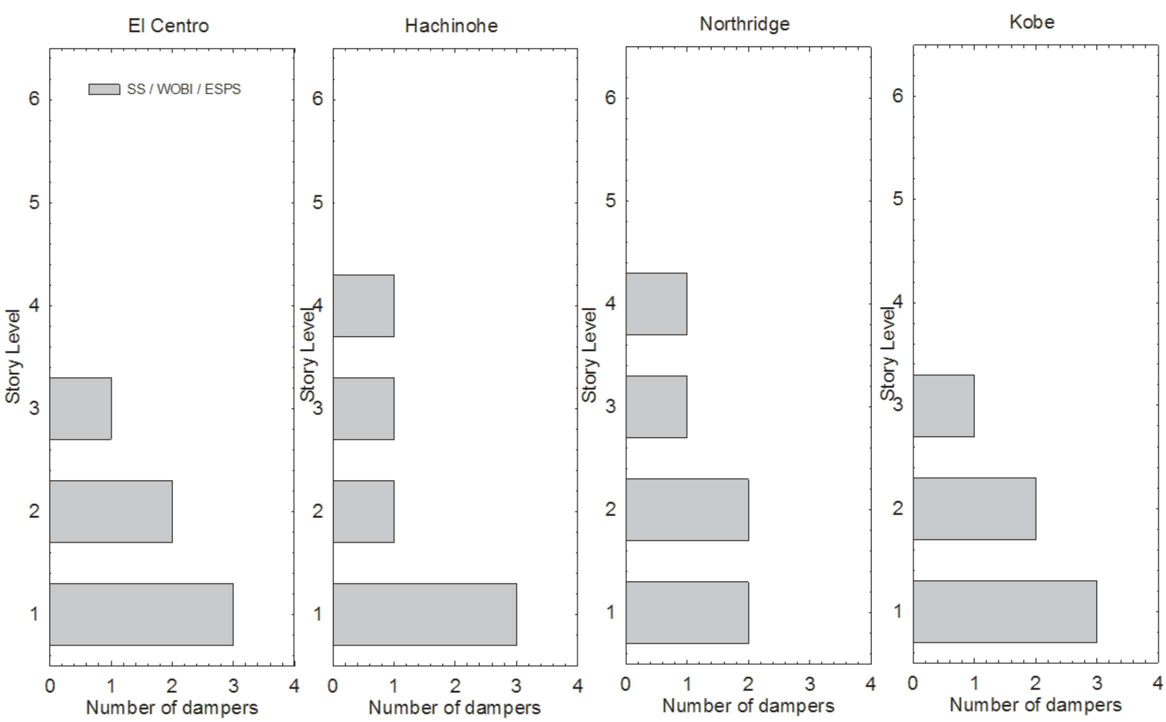

Figure 10. Damper distribution using the maximum absolute acceleration (J3) for different search algorithms

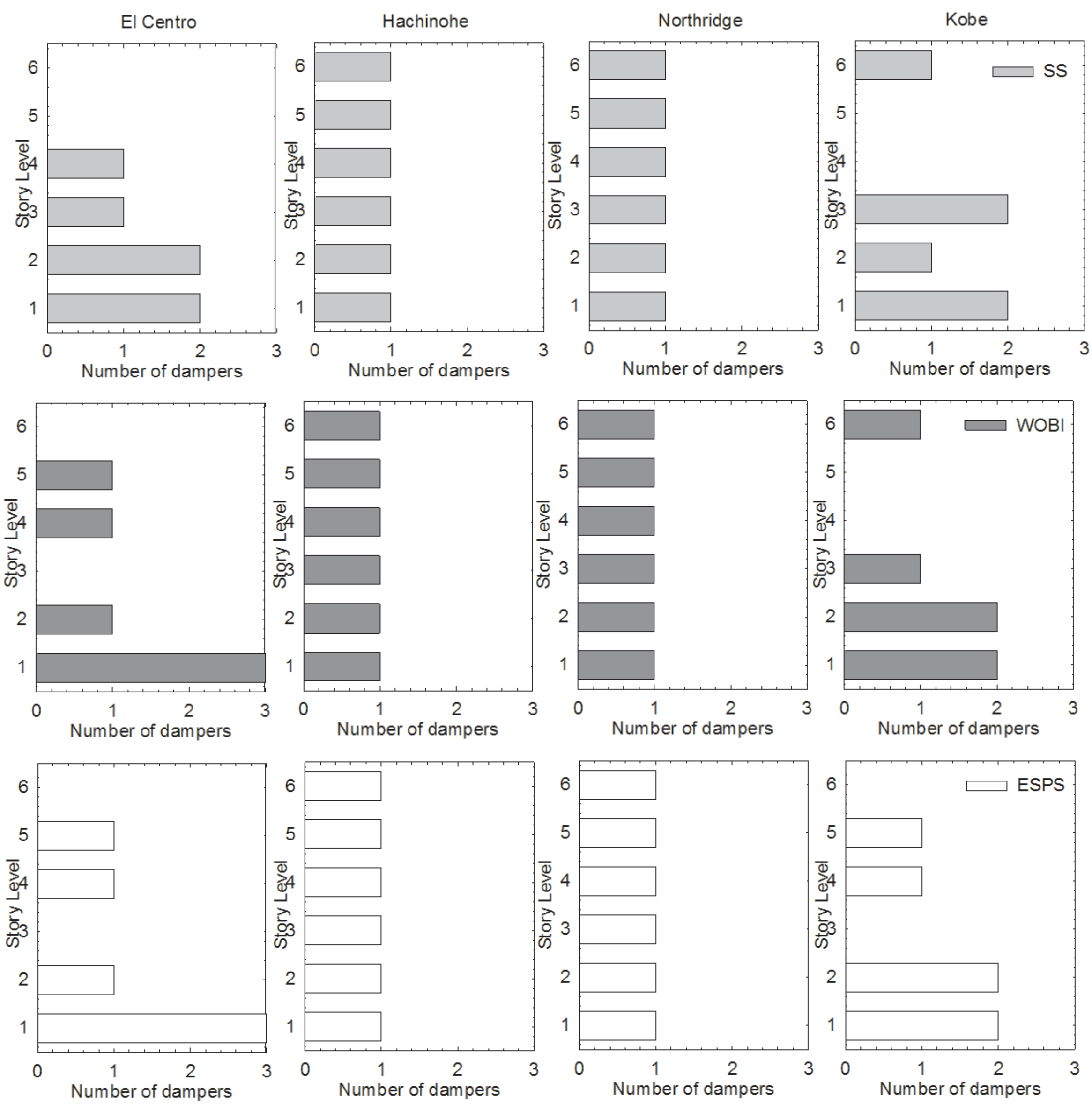

including the modal damping ratio and the mass participation factor are given in Table 5.

The interstory height is *3m*, while the total weight of the building is 2038.41 *kN*. The structural response in term of interstory drifts and absolute accelerations are shown in Figure 11 for the uncontrolled structures.

In the first step, a viscous damper was designed and used such that the fundamental mode has 25% damping ratio, when one damper is placed at every story unit (uniform distribution). The structural responses of the uniformly braced structure for different seismic events are shown in Figure 12.

The base shear coefficient normalized with respect to the total weight of the building is shown in Figure 13, comparing the uncontrolled structure with the uniformly distributed dampers and the two optimal distributions obtained using the maximum interstory drift (*J4*) and the maximum absolute acceleration (*J3*) performance indices. A reduction of the base shear is observed for all the earthquake records that is slightly improved when also the optimal damper distributions are considered.

When considering a 10 story building there is no difference among SS, WOBI and ESPS when using the maximum drift (J4) or the maximum absolute acceleration (J3) as index when El Centro earthquake is used as shown in Figure 14. In this particular case using *J3* or *J4* does not bring to substantial improvements in the performance of the building.

This conclusion can be generalized, because the distribution is independent from the earthquake record selected, as shown in Figure 15, where there is almost no difference among SS, WOBI and ESPS when using the maximum drift (J4) as index, while small differences can be found when index J3 is adopted as shown in Figure 16.

Figure 17 shows that the algorithm that maximize the energy dissipated by the viscous dampers (J1) is the ESPS, regardless the earthquake record selected, however when comparing the maximum interstory drift obtained with ESPS, the performance of the obtained damper distribution is worst (Figure 17b), therefore this bring to the conclusion that the objective function J1 might not be a good candidate to find a practical damper distribution that is able to reduce the damage in the building.

Table 5. Dynamic properties of the unbraced ten story building

Story	ω [rad/s]	T [s]	ζ [%]	ϵ [%]
1	22.64	0.277	5.00	80.29
2	56.42	0.111	4.08	11.16
3	91.72	0.069	5.00	3.99
4	127.21	0.049	6.28	1.97
5	151.45	0.041	7.22	1.05
6	182.02	0.035	8.46	0.55
7	208.21	0.030	9.54	0.27
8	244.64	0.026	11.07	0.26
9	280.94	0.022	12.61	0.23
10	323.38	0.019	14.42	0.21

Thirty Story Building

In order to show the applicability of the methodology for tall buildings, a 2D model of 30-story shear building has been considered for determining the optimal locations of viscous dampers, by optimizing the objective functions described in previous paragraph. The properties of the lateral story stiffness are summarized below

$$
\begin{array}{llll}
k_i = 150\times10^3\, kN/m & i=1,\dots,4 & k_i = 125\times10^3\, kN/m & i=5,\dots,10 \\
k_i = 100\times10^3\, kN/m & i=11,\dots,14 & k_i = 85\times10^3\, kN/m & i=15,\dots,18 \\
k_i = 72.5\times10^3\, kN/m & i=19,\dots,22 & k_i = 62\times10^3\, kN/m & i=23,\dots,26 \\
k_i = 53\times10^3\, kN/m & i=27,\dots,30 & &
\end{array}
$$

while the story mass is assumed constant and equal to $51.2\ kN{\bullet}sec^2/m$. The first natural frequency is $\omega_0=2.36\ rad/sec$ that correspond to a period of $T=2.65sec$ and it is assumed a damping ratio equal to *2%* on the first and the second mode. Dynamic properties of the building, including the modal damping ratio and the mass participation factor are given in Table 6.

The story height considered is $h = 3.0\ m$, the same in all levels, while the total weight of the building is *15063.01 kN*. The structural response in term of interstory drifts and absolute accelerations for the uncontrolled structures (unbraced) are shown in Table 7.

In the first step, a viscous damper was designed and used such that the fundamental mode has 25% damping ratio, when one damper is placed at every story unit (uniform distribution).

Figure 11. Unbraced structural responses of the 10 story building for different seismic events

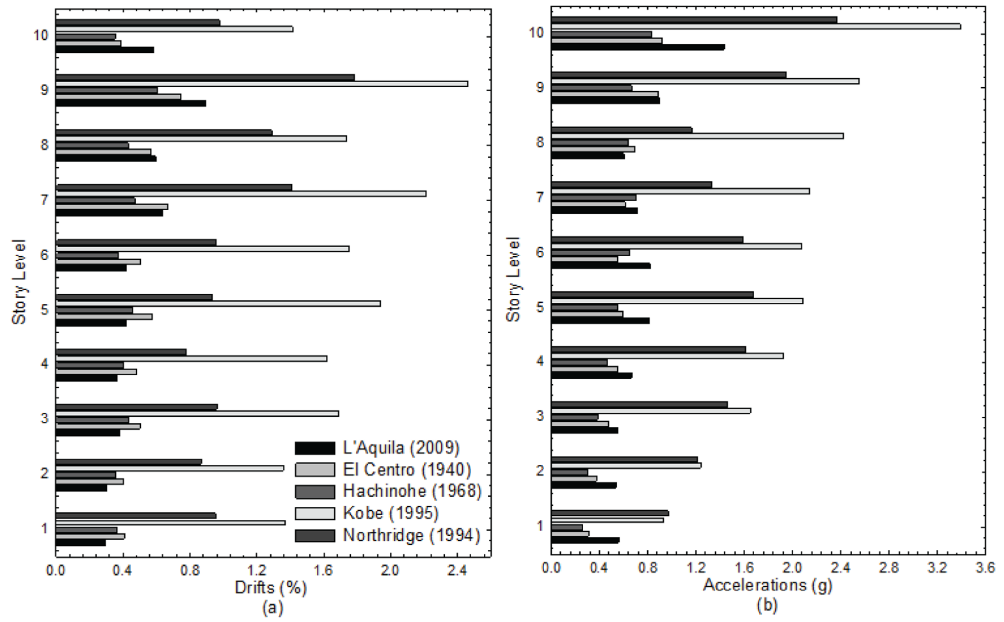

Figure 12. Uniformly braced structural responses of the 10 story building for different seismic events

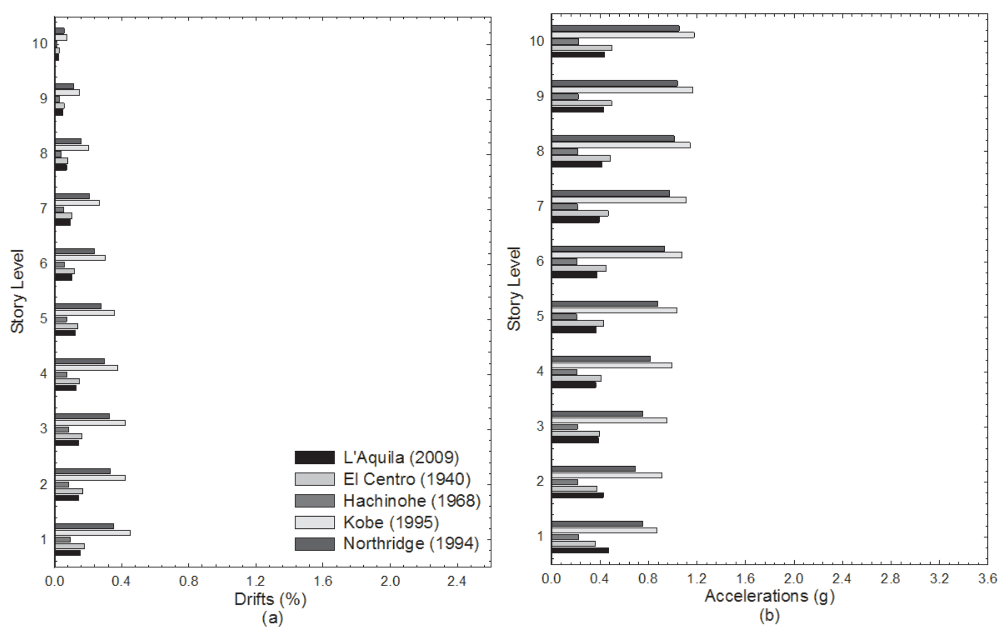

Figure 13. Base shear comparison

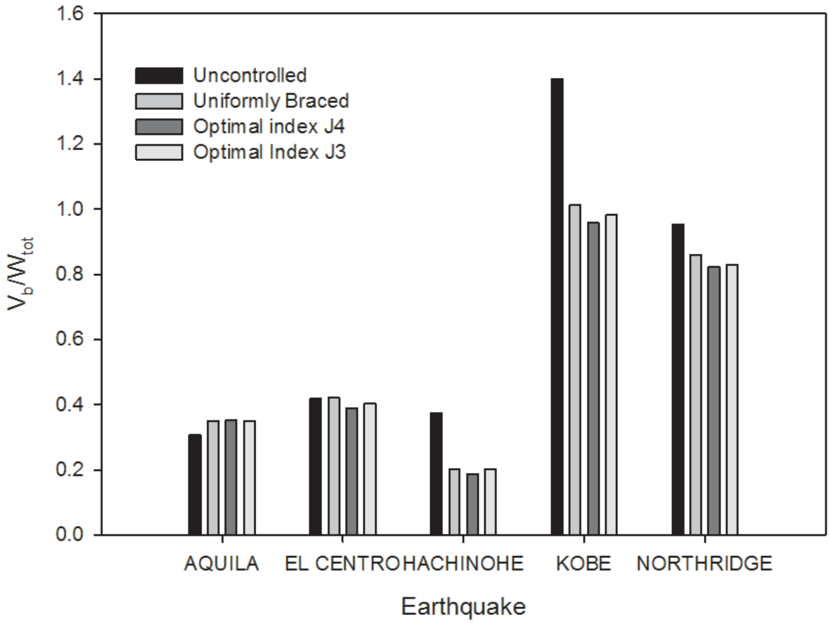

When increasing the DOFs of the building the Sequential Search (SS) using El Centro Earthquake does not converge to a reasonable solution even when the more stable performance index (*J4*) is used. Stable and practical configuration can be obtained instead using either WOBI or ESPS search algorithms (Figure 18). When considering also the damper distributions obtained with the other four earthquake records that are shown in Figure 19, it can be assumed that they all converge to similar distribution when WOBI and ESPS search algorithms are adopted except for the case of Kobe earthquake where more dampers are needed at the upper floors. This can be explained by the higher mode effects, that in tall buildings is more evident and by the frequency content of the earthquake. The damper distributions obtained with the performance index *J3* bring to more stable distributions when the WOBI and ESPS search algorithms are used, while the SS does not converge to an optimal solution (Figure 20). Repeating the procedure for all the four earthquake records bring to the same conclusion that the damper distributions obtained with *J3* index are unstable when SS algorithm is adopted, while it converges to similar distributions with WOBI and ESPS.

All distributions are however affected by the type of ground motion selected and therefore are affected by the frequency content of the earthquake ground motion (Figure 21).

CONCLUSION

Passive energy dissipation systems (e.g. viscous dampers, metallic dampers, friction dampers etc) have been used extensively for the protection of civil engineering structures against strong earthquakes, therefore in this chapter are shown and compared three practical search methods for the optimal placement and design of dampers. They are called:

- Sequential Search (SS)
- Worst-Out-Best-In (WOBI)

Figure 14. Structural response using sequential search algorithm (SS) with J3 and J4 performance index respectively

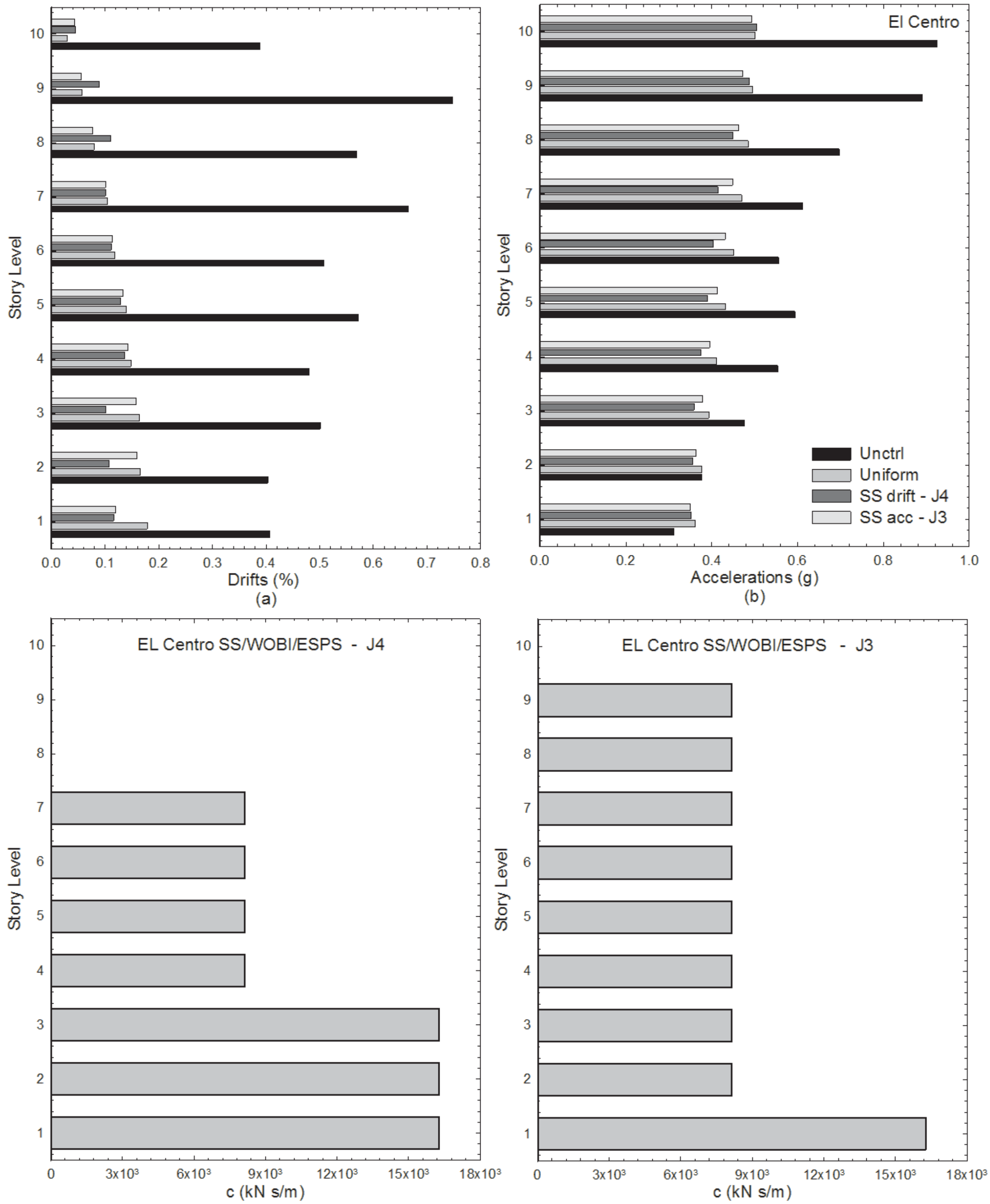

Figure 15. Damper distributions using the maximum interstory drift (J4) for different search algorithms

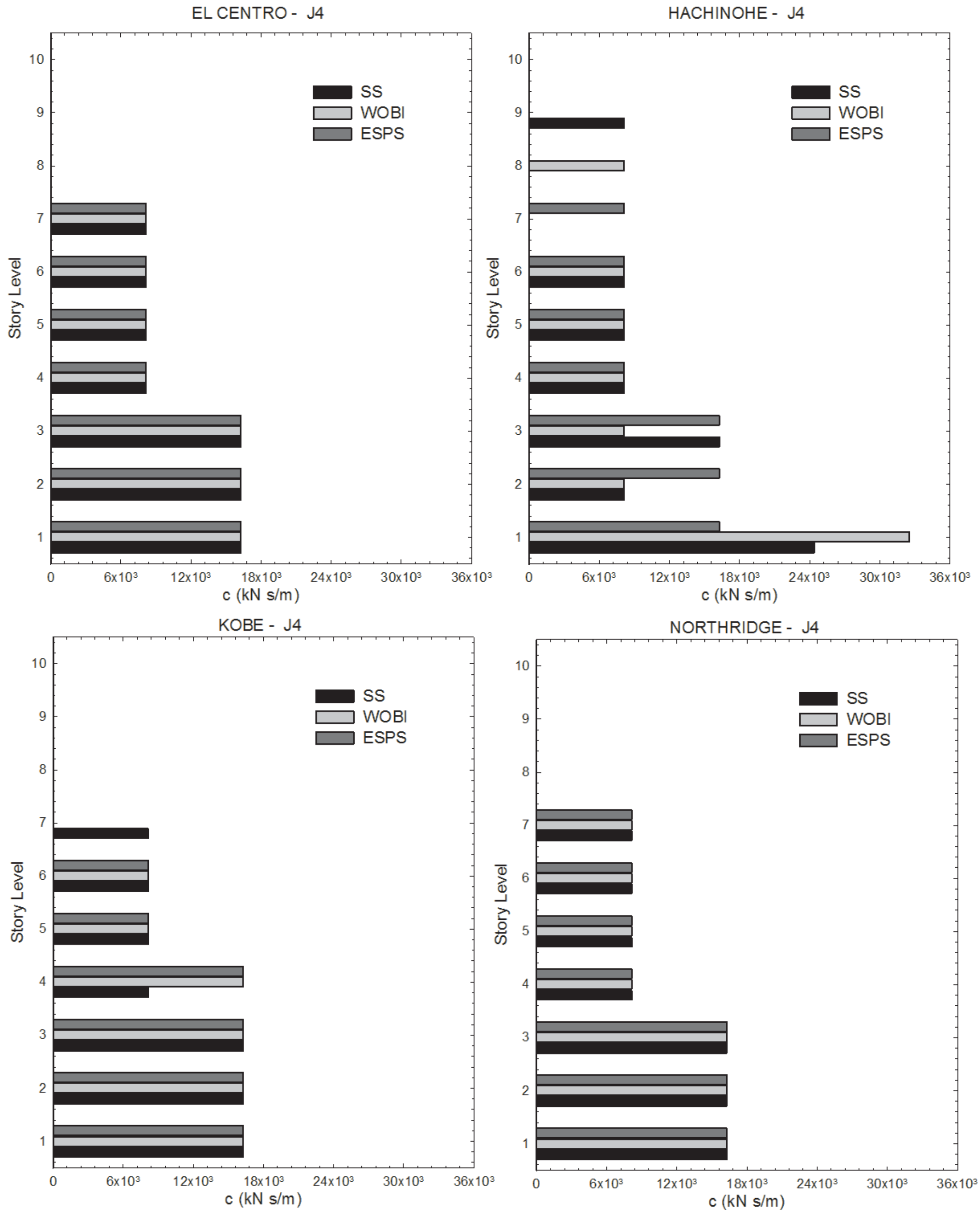

Figure 16. Damper distributions using the maximum absolute acceleration drift (J3) for different search algorithms

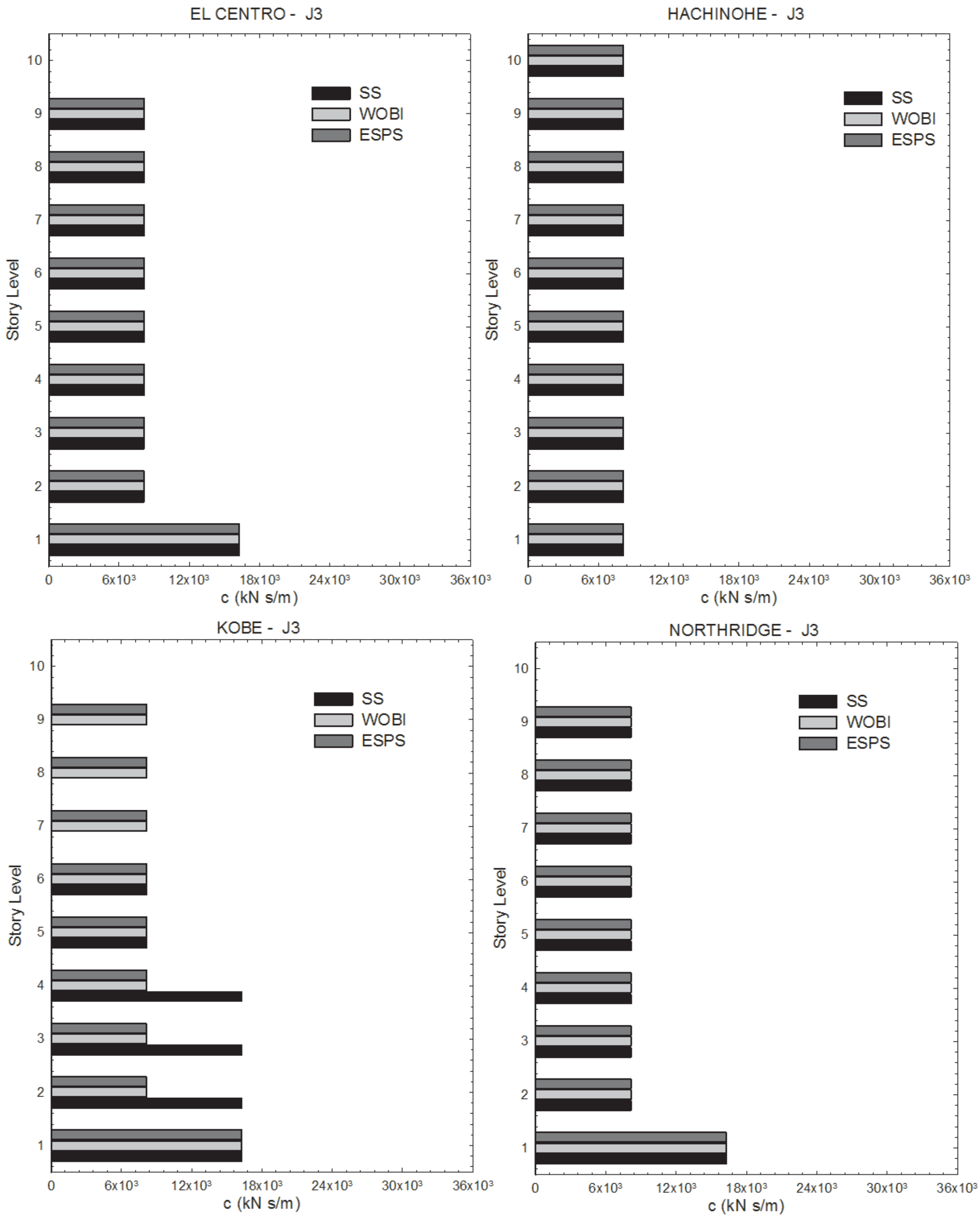

Figure 17. Objective function J1 vs. different algorithms and ground motions

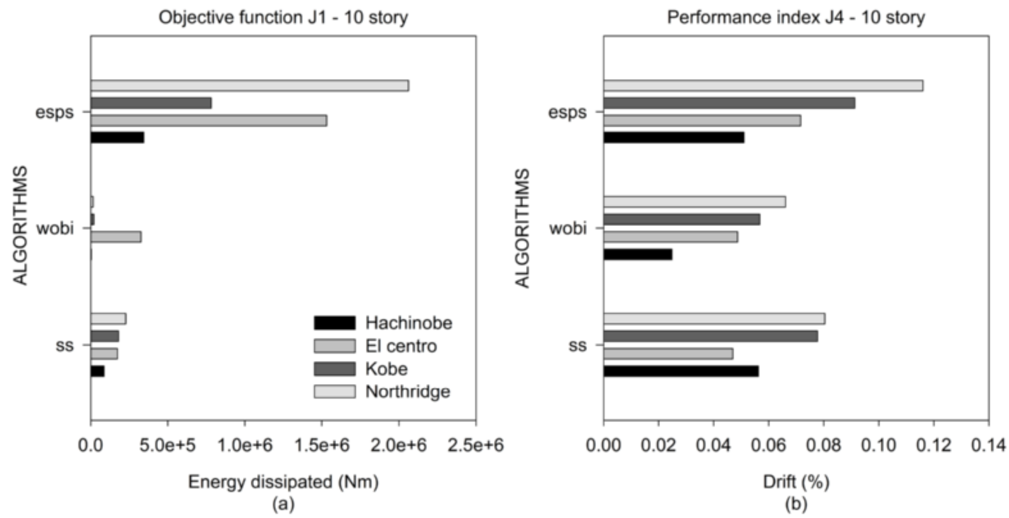

- Exhaustive Single Point Substitution (ESPS)

Two types of damper placement strategies can be adopted:

- Distinctive Location, with only one damper in any story unit
- Repeated Location, with more than one damper in any story unit

Numerical results presented in this chapter are obtained using the Repeated Location damper placement. The optimal locations of dampers have been investigated by optimizing the following types of objective functions:

1. The average dissipated energy by dampers (J1)
2. The weighted sum of damping ratios of selected modes of the building (J2)
3. The maximum story absolute acceleration (J3)
4. The maximum of peak interstory drifts of buildings subjected to a given earthquake (J4)

Four different earthquake records have been considered to investigate the dependence of the optimal locations on the stochastic nature of the earthquake excitation.

- Two are near field earthquakes: Kobe (1995) and Northridge (1994)
- Two are far-field earthquakes: El Centro (1940) and Hachinohe (1968)

The applications of the proposed methods for the optimal locations of dampers are investigated for three types of buildings:

1. A 6 story building with soft story behavior
2. A 10 story building with identically constructed story units
3. A 30 story building with stiffness variation along the story height

Table 6. Dynamic properties of the unbraced thirty story building

Story	ω [rad/s]	T [s]	ζ [%]	ϵ [%]
1	2.37	2.65	2.00	76.03
2	6.39	0.98	2.00	12.04
3	10.52	0.60	2.73	4.34
4	14.68	0.43	3.59	2.16
5	18.81	0.33	4.48	1.37
6	22.82	0.28	5.36	1.00
7	26.88	0.23	6.26	0.72
8	30.59	0.21	7.10	0.37
9	34.66	0.18	8.01	0.33
10	38.23	0.16	8.82	0.28
11	41.83	0.15	9.63	0.19
12	45.47	0.14	10.46	0.15
13	48.88	0.13	11.23	0.12
14	51.75	0.12	11.88	0.12
15	55.02	0.11	12.62	0.12
16	57.52	0.11	13.19	0.09
17	60.25	0.10	13.81	0.05
18	62.24	0.10	14.27	0.05
19	64.59	0.10	14.80	0.08
20	66.82	0.09	15.31	0.04
21	68.68	0.09	15.73	0.05
22	71.79	0.09	16.44	0.03
23	73.87	0.09	16.91	0.03
24	77.44	0.08	17.72	0.04
25	79.74	0.08	18.25	0.03
26	84.24	0.07	19.27	0.03
27	87.40	0.07	19.99	0.05
28	92.48	0.07	21.15	0.05
29	96.82	0.06	22.14	0.01
30	103.61	0.06	23.69	0.03

It has been observed that when the DOFs of the building are reduced such as in the 6 story building, then SS, WOBI and ESPS search methods bring to the same damper distribution for various objective functions considered. However when the complexity of the building increases such as in the 30 story building, then the applications of WOBI and ESPS search methods for various objective functions resulted in an improved performance over those obtained by the sequential search (SS) method.

It has been found that the optimal distribution obtained with *J4* is very stable and not affected by the selection of the search algorithm, but it strongly depends on the nature of the earthquake record at the site. Hence the best results for seismic excited building can be obtained by minimizing J4 using the design earthquake of the particular site.

Heuristic search methods using performance indices have the advantage to be practical and easy to implement and they can be applied both to linear and nonlinear structures. However there are some weaknesses in the methods:

1. A trial and error procedure must be employed.
2. A large computing cost is required, because the time history structural response need to be evaluated.
3. The optimal device distribution is affected by the specific earthquake record employed in the analysis.

Due to the great uncertainties in the nature of the earthquake excitations, using different earthquake records can yield different optimal locations. Therefore there is need for further research in developing statistical methods that can overcome the weaknesses of the above approaches.

FUTURE RESEARCH DIRECTIONS

Much of structural control research and applications in civil engineering have been concerned with structures equipped with passive, hybrid, or active control devices in order to enhance structural performance under extraordinary loads. In most cases, the structure and the control system are independently designed and optimized. On the other hand, an exciting consequence of

Table 7. Structural response of the thirty story uncontrolled structure using different seismic events

	Drift (%)					Acc(g)				
	L'Aquila	El Centro	Hachinohe	Kobe	Northridge	L'Aquila	El Centro	Hachinohe	Kobe	Northridge
1	0.25	0.49	0.66	1.00	1.12	**0.49**	0.34	0.23	0.82	0.83
2	0.24	0.49	0.66	0.98	1.14	**0.46**	0.34	0.23	0.80	0.82
3	0.23	0.49	0.65	0.96	1.15	**0.46**	0.34	0.23	0.79	0.81
4	0.23	0.49	0.64	0.92	1.16	**0.45**	0.34	0.22	0.77	0.79
5	0.26	0.58	0.75	1.07	1.39	**0.44**	0.35	0.21	0.74	0.77
6	0.25	0.56	0.74	1.02	1.38	**0.42**	0.35	0.23	0.72	0.77
7	0.25	0.54	0.73	0.98	1.36	**0.41**	0.35	0.23	0.71	0.77
8	0.24	0.51	0.71	0.93	1.33	**0.40**	0.36	0.23	0.74	0.77
9	0.23	0.50	0.69	0.89	1.30	**0.40**	0.36	0.23	0.80	0.77
10	0.22	0.49	0.66	0.85	1.26	**0.40**	0.36	0.25	0.88	0.76
11	0.27	0.59	0.79	1.00	1.51	**0.39**	0.37	0.26	0.99	0.74
12	0.26	0.56	0.76	0.95	1.45	**0.39**	0.37	0.27	1.09	0.71
13	0.26	0.54	0.73	0.89	1.42	**0.39**	0.35	0.29	1.14	0.68
14	0.25	0.51	0.72	0.83	1.40	**0.39**	0.32	0.30	1.15	0.64
15	0.30	0.56	0.84	0.93	1.63	**0.38**	0.31	0.31	1.10	0.64
16	0.30	0.60	0.83	0.88	1.59	**0.37**	0.32	0.30	1.00	0.64
17	0.31	0.63	0.82	0.84	1.55	**0.37**	0.34	0.28	0.87	0.63
18	0.31	0.65	0.80	0.85	1.51	**0.34**	0.35	0.28	0.87	0.62
19	0.38	0.78	0.90	1.12	1.71	**0.31**	0.36	0.28	0.84	0.60
20	0.38	0.77	0.86	1.21	1.65	**0.33**	0.37	0.28	0.77	0.66
21	0.38	0.75	0.82	1.24	1.57	**0.33**	0.35	0.27	0.68	0.66
22	0.36	0.71	0.77	1.22	1.47	**0.33**	0.31	0.29	0.59	0.80
23	0.39	0.77	0.83	1.50	1.60	**0.34**	0.31	0.32	0.58	1.02
24	0.34	0.69	0.75	1.55	1.45	**0.32**	0.35	0.34	0.77	1.15
25	0.35	0.60	0.67	1.55	1.28	**0.32**	0.38	0.36	0.86	1.16
26	0.40	0.50	0.58	1.47	1.11	**0.30**	0.40	0.38	0.83	1.03
27	0.47	0.47	0.57	1.55	1.21	**0.24**	0.39	0.40	0.89	0.77
28	0.42	0.38	0.44	1.27	1.03	**0.34**	0.37	0.44	1.17	0.88
29	0.32	0.28	0.30	0.90	0.76	**0.47**	0.41	0.47	1.38	1.13
30	0.17	0.15	0.15	0.47	0.40	**0.55**	0.48	0.49	1.49	1.28

Figure 18. Structural response using J4 performance index and different search algorithms

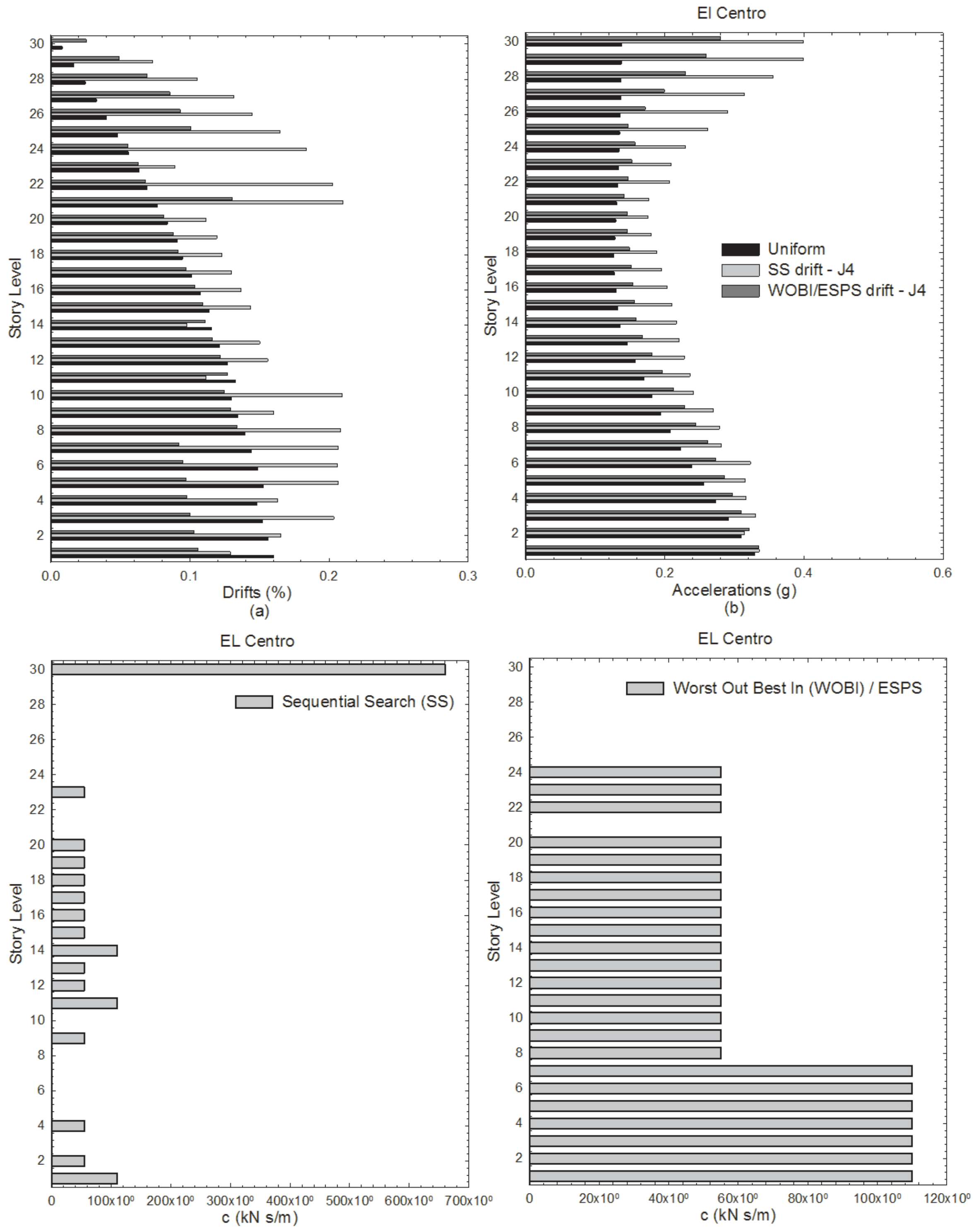

Figure 19. Damper distribution using the maximum interstory drift (J4) for different search algorithms

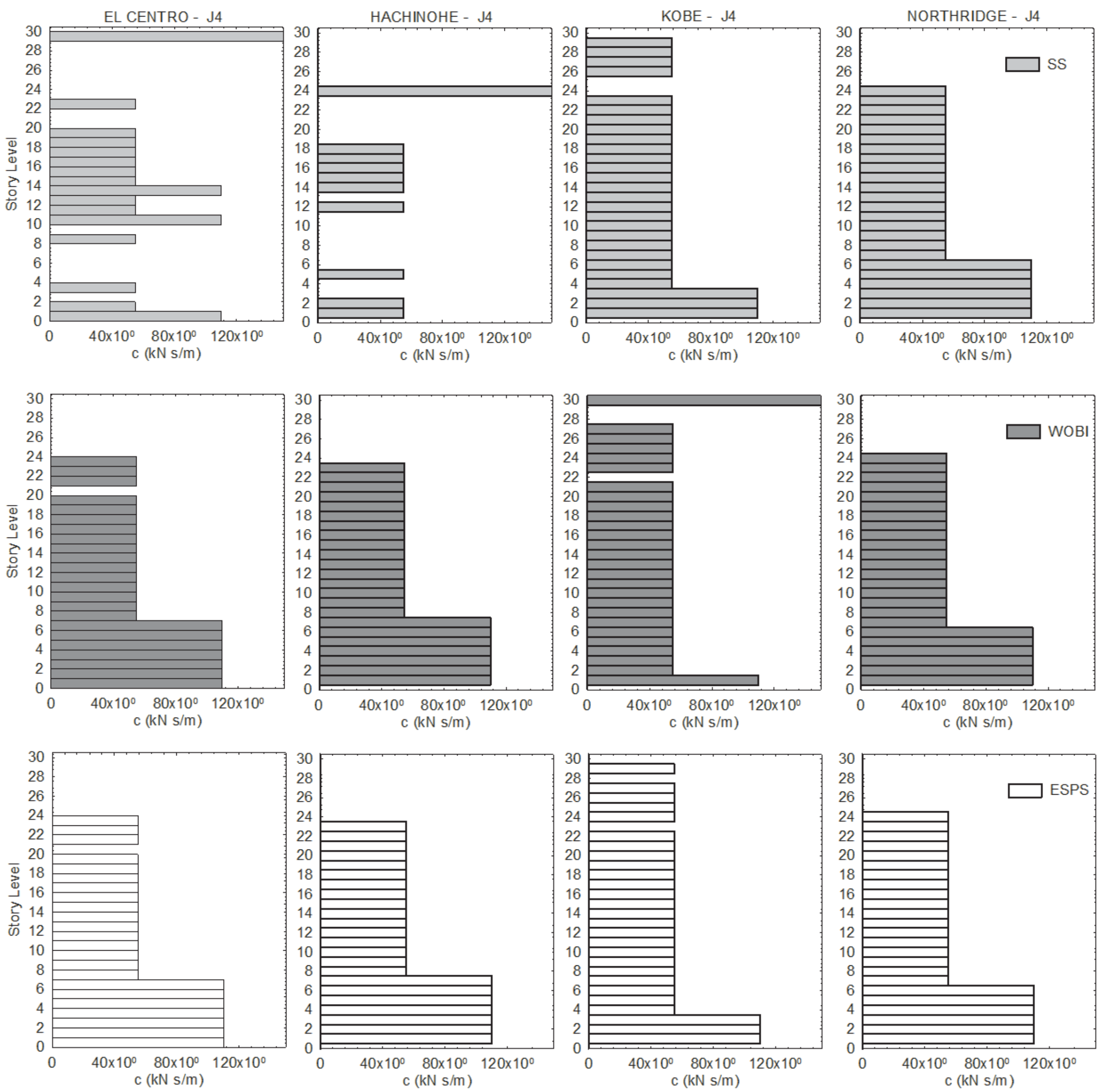

structural control research is that it also opens the door to new possibilities in structural forms and configurations, such as slender buildings or bridges with longer spans without compromising on structural performance. This can only be achieved through integrated design of structures with control elements as an integral part. In the last thirty years, much research has been done on integrated design of structural/control systems. Integrated optimal structural/control system design has been acknowledged as an advanced design methodology for space structures, but only few applications can be found in civil engineering

Figure 20. Structural response using J3 performance index and different search algorithms

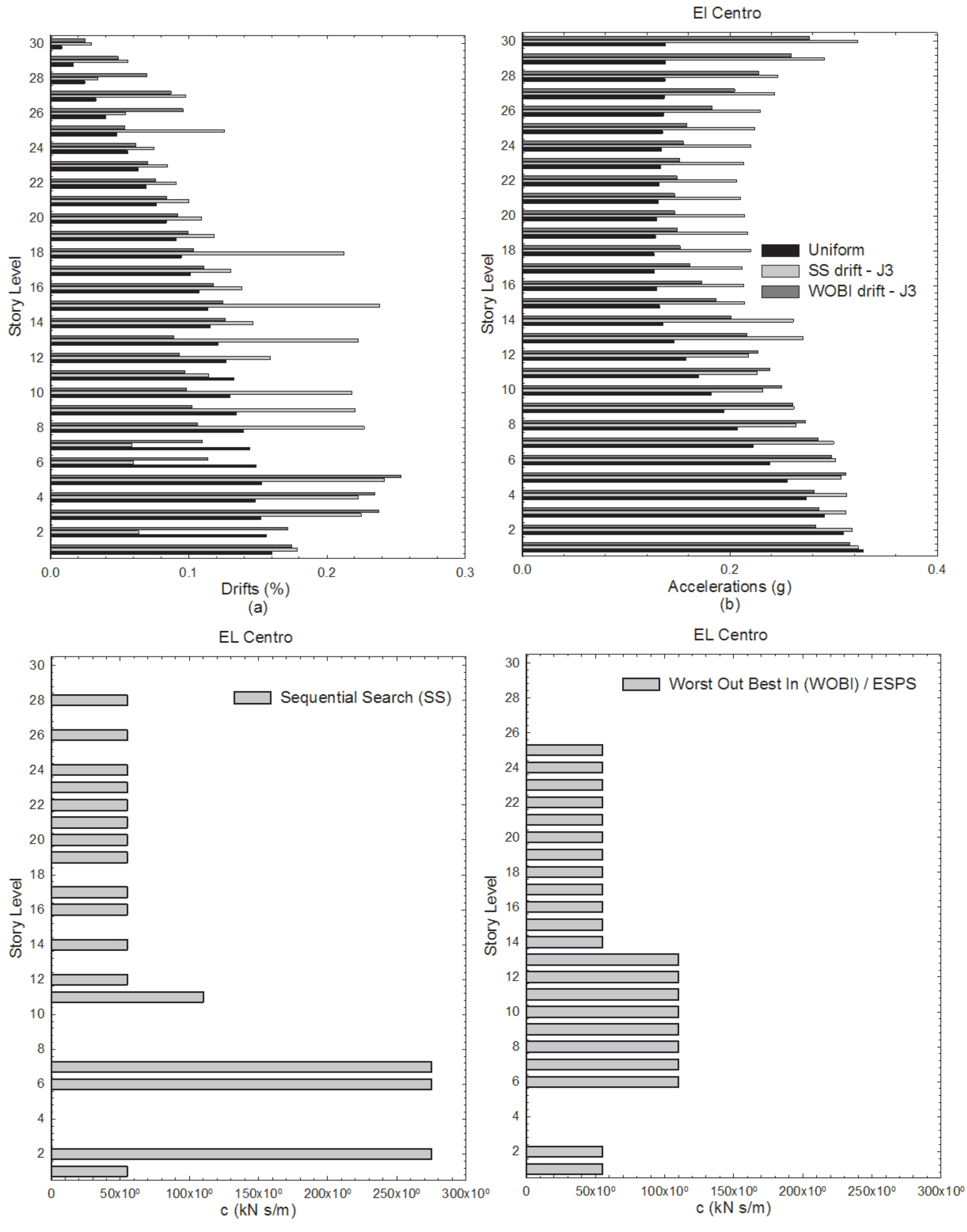

Figure 21. Damper distributions using the maximum absolute acceleration drift (J3) for different search algorithms

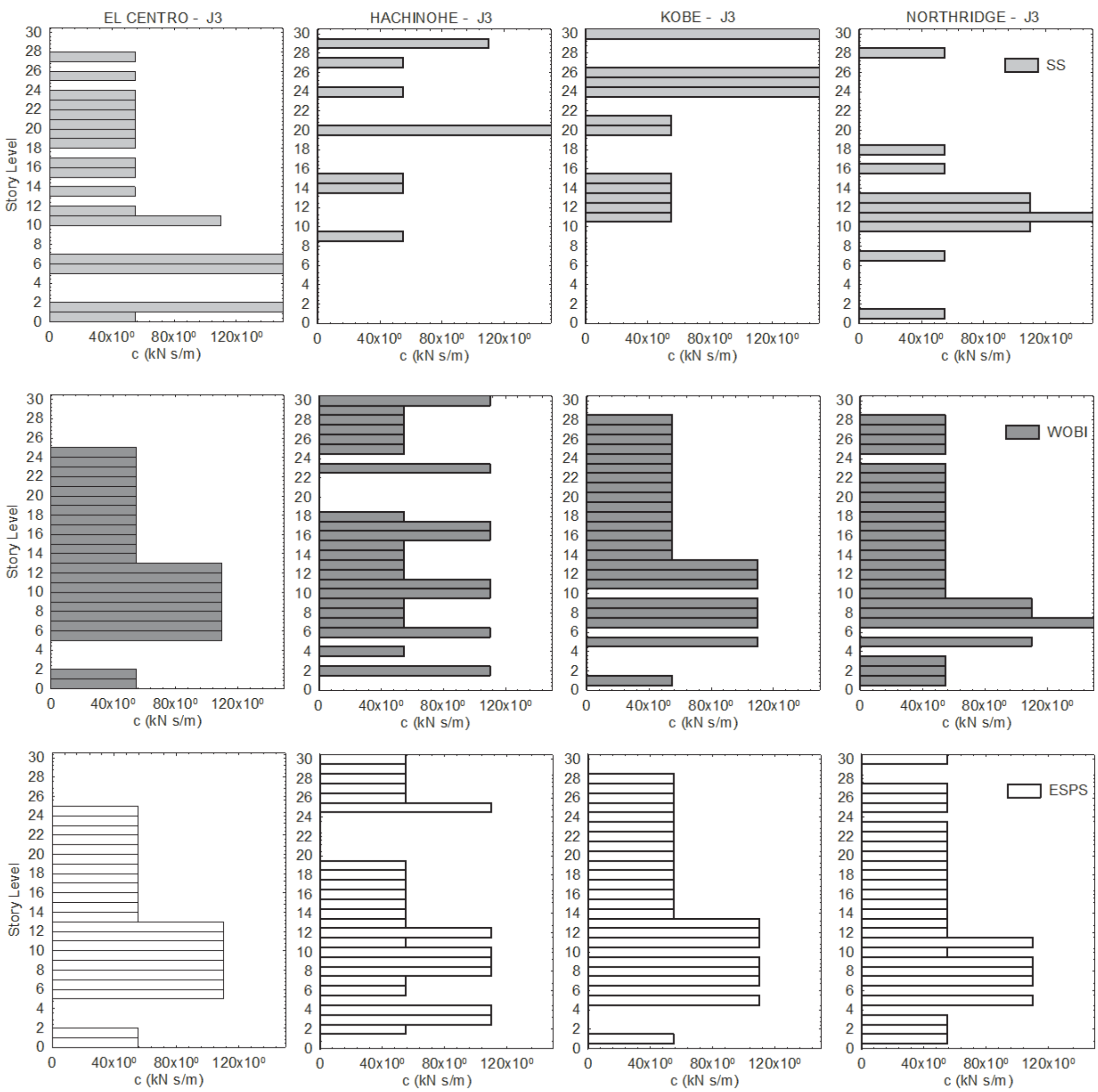

(Cimellaro et al. 2009) and this can be the future research trend in the years to come.

ACKNOWLEDGMENT

The research leading to these results has received funding from the European Community's Seventh Framework Programme - Marie Curie International Reintegration Actions - FP7/2007-2013 under the Grant Agreement n° PIRG06-GA-2009-256316 of the project ICRED - Integrated European Disaster Community Resilience. The author is grateful for the assistance in the editorial part of the M.S. students Valentina Cavallo, Caterina Chiofalo, Giuseppina Divita and Leonardo Isgro`.

REFERENCES

Ashour, S. A., & Hanson, R. D. (1987). *Elastic seismic response of buildings with supplemental damping. Report No. UMCE- 87-1*. Department of Civil Engineering, University of Michigan.

Cimellaro, G. P., Soong, T. T., & Reinhorn, A. M. (2009). Integrated design of controlled linear structural systems. *Journal of Structural Engineering*, *135*(7), 853–862. doi:10.1061/(ASCE)ST.1943-541X.0000032

Gluck, N., Reinhorn, A., & Levy, R. (1996). Design of supplemental dampers for control of structures. *Journal of Structural Engineering*, *122*(12), 1394–1399. doi:10.1061/(ASCE)0733-9445(1996)122:12(1394)

Milman, M. H., & Chu, C.-C. (1994). Optimization methods for passive damper placement and tuning. *Journal of Guidance, Control, and Dynamics*, *17*(4), 848–856. doi:10.2514/3.21275

Nakamura, T., & Tsuji, M. (1996). Inverse damping perturbation for stiffness design of shear buildings. *Journal of Structural Engineering*, *122*(6), 617–625. doi:10.1061/(ASCE)0733-9445(1996)122:6(617)

Ohtori, Y., Christenson, R. E., Spencer, B. F., & Dyke, S. J. (2004). Nonlinear benchmark control problem for seismically excited buildings. *Journal of Engineering Mechanics*, *130*(4), 366–385. doi:10.1061/(ASCE)0733-9399(2004)130:4(366)

Soong, T. T., & Dargush, G. (1997). *Passive energy dissipation systems in structural engineering*. Chichester, UK: John Wiley & Sons.

Takewaki, I. (1997). Optimal damper placement for minimum transfer function. *Earthquake Engineering & Structural Dynamics*, *26*(11), 1113–1124. doi:10.1002/(SICI)1096-9845(199711)26:11<1113::AID-EQE696>3.0.CO;2-X

Tsuji, M., & Nakamura, T. (1996). Optimal viscous dampers for stiffness design of shear buildings. *Structural Design of Tall Buildings*, *5*, 217–234. doi:10.1002/(SICI)1099-1794(199609)5:3<217::AID-TAL70>3.0.CO;2-R

Zhang, R. H., & Soong, T. T. (1992). Seismic design of viscoelastic dampers for structural applications. *Journal of Structural Engineering*, *118*(5), 1375–1392. doi:10.1061/(ASCE)0733-9445(1992)118:5(1375)

ADDITIONAL READING

Aydin, E., Boduroglu, M. H., & Guney, D. (2006). Optimal damper distribution for seismic rehabilitation of planar building structures. *Engineering Structures*, *29*(2).

Bhaskararao, A. V., & Jangid, R. S. (2006). Seismic analysis of structures connected with friction dampers. *Engineering Structures*, *28*(5), 690–703. doi:10.1016/j.engstruct.2005.09.020

Cimellaro, G. P. (2007). Simultaneous stiffness-damping optimization of structures with respect to acceleration, displacement and base shear. *Engineering Structures*, *29*(11), 2853–2870. doi:10.1016/j.engstruct.2007.01.001

Cimellaro, G. P. (2009). Optimal weakening and damping using polynomial control for seismically excited nonlinear structures. *Earthquake Engineering and Engineering Vibration*, *8*(4), 607–616. doi:10.1007/s11803-009-9124-2

Cimellaro, G. P., Lavan, O., & Reinhorn, A. M. (2009). Design of passive systems for controlled inelastic structures. *Earthquake Engineering & Structural Dynamics*, *38*(6), 783–804. doi:10.1002/eqe.867

Cimellaro, G. P., & Retamales, R. (2007). Optimal softening and damping design for buildings. *Journal of Structural Control and Health Monitoring*, *14*, 831–857. doi:10.1002/stc.181

Cimellaro, G. P., Soong, T. T., & Reinhorn, A. M. (2009). Integrated design of controlled linear structural systems. *Journal of Structural Engineering*, *135*(7), 853–862. doi:10.1061/(ASCE)ST.1943-541X.0000032

Dargush, G., & Soong, T. T. (1995). Behavior of metallic plate dampers in seismic passive energy dissipation systems. *Earthquake Spectra*, *11*(4), 545–568. doi:10.1193/1.1585827

Gluck, N., Reinhorn, A., & Levy, R. (1996). Design of supplemental dampers for control of structures. *Journal of Structural Engineering*, *122*(12), 1394–1399. doi:10.1061/(ASCE)0733-9445(1996)122:12(1394)

Hahn, G. D., & Sathiavageeswaran, K. R. (1992). Effects of added-damper distribution on the seismic response of buildings. *Computers & Structures*, *43*(5), 941–950. doi:10.1016/0045-7949(92)90308-M

Kim, H., & Adeli, H. (2005). Hybrid control of irregular steel highrise building structures under seismic excitations. *International Journal for Numerical Methods in Engineering*, *63*(12), 1757–1774. doi:10.1002/nme.1336

Kim, J., Ryu, J., & Chung, L. (2006). Seismic performance of structures connected by viscoelastic dampers. *Engineering Structures*, *28*(2), 183–195. doi:10.1016/j.engstruct.2005.05.014

Lavan, O., Cimellaro, G. P., & Reinhorn, A. M. (2008). Noniterative optimization procedure for seismic weakening and damping of inelastic structures. *Journal of Structural Engineering*, *134*(10), 1638–1648. doi:10.1061/(ASCE)0733-9445(2008)134:10(1638)

Lavan, O., & Levy, R. (2006). Optimal design of supplemental viscous dampers for linear framed structures. *Earthquake Engineering & Structural Dynamics*, *35*(3), 337–356. doi:10.1002/eqe.524

Lopez-Garcia, D. (2001). A simple method for the design of optimal damper configurations in MDOF structures. *Earthquake Spectra*, *17*(3), 387–398. doi:10.1193/1.1586180

Lopez-Garcia, D. (2002). Efficiency of a simple approach to damper allocation in MDOF structures. *Journal of Structural Control*, *9*, 19–30. doi:10.1002/stc.3

Milman, M. H., & Chu, C.-C. (1994). Optimization methods for passive damper placement and tuning. *Journal of Guidance, Control, and Dynamics*, *17*(4), 848–856. doi:10.2514/3.21275

Occhiuzzi, A. (2009). Additional viscous dampers for civil structures: Analysis of design methods based on effective evaluation of modal damping ratios. *Engineering Structures*, *31*(5), 1093–1101. doi:10.1016/j.engstruct.2009.01.006

Ribakov, Y., & Reinhorn, A. M. (2003). Design of amplified structural damping using optimal considerations. *Journal of Structural Engineering*, *129*(10), 1422–1427. doi:10.1061/(ASCE)0733-9445(2003)129:10(1422)

Roh, H. S., & Cimellaro, G. P. (2010). (in review). Fragility evaluation of structures with controlled rocking columns and viscous dampers. *Journal of Earthquake Engineering*.

Singh, M. P., & Moreschi, L. M. (2001). Optimal seismic response control with dampers. *Earthquake Engineering & Structural Dynamics*, *30*(4), 533–572. doi:10.1002/eqe.23

Soong, T. T., & Dargush, G. (1997). *Passive energy dissipation systems in structural engineering*. New York, NY: John Wiley & Sons.

Takewaki, I. (1997). Optimal damper placement for minimum transfer function. *Earthquake Engineering & Structural Dynamics*, *26*(11), 1113–1124. doi:10.1002/(SICI)1096-9845(199711)26:11<1113::AID-EQE696>3.0.CO;2-X

Trombetti, T., & Silvestri, S. (2004). Added viscous dampers in shear-type structures: The effectiveness of mass proportional damping. *Journal of Earthquake Engineering*, *8*(2), 275–313. doi:10.1080/13632460409350490

Tsuji, M., & Nakamura, T. (1996). Optimal viscous dampers for stiffness design of shear buildings. *Structural Design of Tall Buildings*, *5*, 217–234. doi:10.1002/(SICI)1099-1794(199609)5:3<217::AID-TAL70>3.0.CO;2-R

Wang, J. F., & Lin, C. C. (2005). Seismic performance of multiple tuned mass dampers for soil-irregular building interaction systems. *International Journal of Solids and Structures*, *42*(20), 5536–5554. doi:10.1016/j.ijsolstr.2005.02.042

Yaomin, F., & Kazuhiko, K. (1998). Comparative study of frames using viscoelastic and viscous dampers. *Journal of Structural Engineering*, *124*(5), 513–522. doi:10.1061/(ASCE)0733-9445(1998)124:5(513)

Yoshida, O., & Dyke, S. J. (2005). Response control of full-scale irregular buildings using magnetorheological dampers. *Journal of Structural Engineering*, *131*(5), 734–742. doi:10.1061/(ASCE)0733-9445(2005)131:5(734)

Zhang, R. H., & Soong, T. T. (1992). Seismic design of viscoelastic dampers for structural applications. *Journal of Structural Engineering*, *118*(5), 1375–1392. doi:10.1061/(ASCE)0733-9445(1992)118:5(1375)

Zhu, H. P., & Xu, Y. H. (2005). Optimum parameters of Maxwell model-defined dampers used to link adjacent structures. *Journal of Sound and Vibration*, *279*(1-2), 253–274. doi:10.1016/j.jsv.2003.10.035

APPENDIX A

In linear algebra, the trace of a (n×n) square matrix A is defined to be the sum of the diagonal elements.

$$\mathbf{A} = \begin{bmatrix} a_{11} & . & . & a_{1n} \\ a_{21} & a_{22} & . & a_{2n} \\ . & . & . & . \\ a_{n1} & . & . & a_{nn} \end{bmatrix}$$

$$trace\left(\mathbf{A}\right) = a_{11} + a_{22} + \ldots + a_{nn} = \sum_{i=1}^{n} a_{ii}$$

where a_{ii} represents the entry on the ith row and ith column of A. Equivalently, the trace of a matrix is the sum of its eigenvalues, making it an invariant with respect to a change of basis. This characterization can be used to define the trace for a linear operator in general. The trace is only defined for a square matrix (n×n). Geometrically, the trace can be interpreted as the infinitesimal change in volume, as the derivative of the determinant, which is made precise in Jacobi's formula.

Chapter 2
Optimal Placement of Viscous Dampers for Seismic Building Design

Jessica K. Whittle
University of Oxford, UK

Martin S. Williams
University of Oxford, UK

Theodore L. Karavasilis
University of Warwick, UK

Anthony Blakeborough
University of Oxford, UK

ABSTRACT

While the use of supplemental damping for improving the seismic performance of buildings has gained acceptance in recent years, there remains a lack of consensus over how dampers should be optimally arranged within a structure. The authors review recent advances in damper placement methodology based on optimisation theory, and present a detailed comparative study of five selected methods: two using simple empirical rules – uniform and stiffness-proportional damping distributions; and three more advanced, iterative methods – the simplified sequential search algorithm (SSSA), Takewaki's method based on minimising transfer function drifts, and Lavan's fully-stressed analysis/redesign approach. The comparison of the selected methods is based on the performance enhancement of a ten-story, steel moment-resisting frame. It is shown that even very crude placement techniques can achieve substantial improvements in building performance. The three advanced optimisation methods show the potential to reduce interstory drifts beyond the level that can be achieved using uniform or stiffness-proportional methods, though the influence on floor accelerations is less marked. The optimisation methods studied show broadly comparable performance, so ease of use becomes a significant factor in choosing between them. In this respect, Lavan's approach offers some advantages over the others.

DOI: 10.4018/978-1-4666-2029-2.ch002

INTRODUCTION

The addition of supplemental damping to buildings is becoming an increasingly popular seismic design strategy, and with it has come the evolution of building guidelines to include supplementally damped structures. A critical design concern is the placement of dampers, as the distribution of damping may greatly affect a building's dynamic response and the resulting damping cost (Soong and Dargush, 1997). However, despite the variety of optimal damper placement methods available, there is no clear consensus on which method is best. Building codes say little on the issue, and few thorough comparisons of damper placement techniques have been conducted for realistic building scenarios.

The purpose of this chapter is to present some of the most notable efforts in optimal damper placement, and to explore the potential of a subset of these for improving building performance. After a general review of available methods, we present a comparison of three optimal placement techniques with two simpler, standard techniques. To do this, the five damper placement techniques are applied to a supplementally damped steel moment resisting frame building. Using nonlinear time history analysis, a suite of twenty ground motions, and two seismic hazard levels (DBE and MCE), the effectiveness of the optimal damper placement schemes is gauged by the reduction in peak interstory drifts, total accelerations, residual drifts, and overall ability to meet the expected performance objective.

REVIEW OF DAMPER PLACEMENT TECHNIQUES

A large variety and quantity of damper placement methods have been proposed; these can be categorised, as shown in Figure 1.

Stochastic Methods

Heuristic approaches are particularly applicable to structural engineering problems because they allow for problem-specific a priori knowledge (Liu et al., 2005). The adaptation of the controllability index, previously used to determine optimal actuator locations for active structural control (Cheng and Pantelides, 1988), to sequentially place dampers where their effects are maximised (Zhang and Soong, 1992) was an innovative

Figure 1. Classification of optimised damper placement approaches (adapted from Liu et al., 2005)

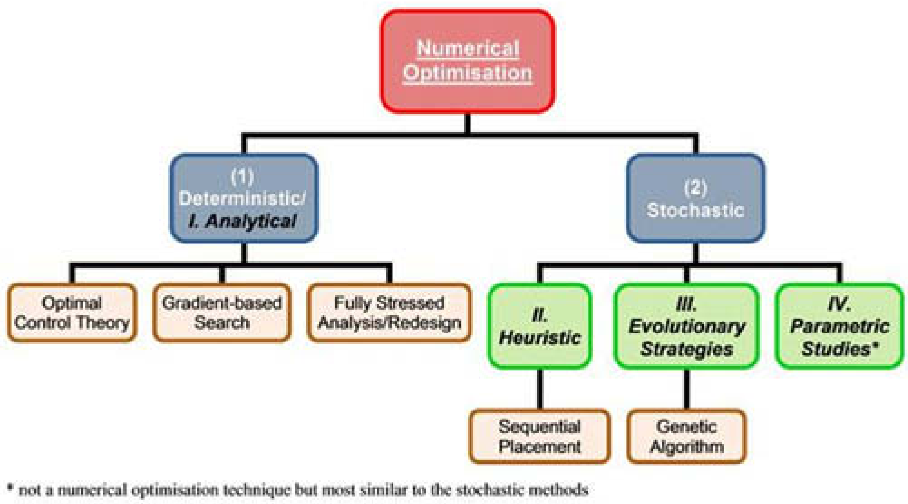

heuristic placement method. This method, the Sequential Search Algorithm (SSA), was considered an advancement in the field because of its practicality. Zhang and Soong (1992) compared SSA to Uniform damping, concluding that with SSA, 2-5 dampers were saved for a 10-story structure with viscoelastic dampers using drift as the performance criterion. Additional performance objectives, such as absolute accelerations, were not considered, and a relatively small amount of damping (10% effective damping ratio) was selected. Other researchers verified the SSA method for viscoelastic dampers and a shear-frame model (Shukla and Datta, 1999) and for torsional effects of a three-dimensional model (Wu et al., 1997).

An evolution of the SSA method was the Simplified Sequential Search Algorithm (SSSA) (Lopez-Garcia, 2001), which sought to further simplify the method for passive devices by decreasing the computational-effort of determining optimal locations and simulating stochastic ground motions. It claimed simplicity and practicality over existing methods due to its sequential procedure, use of tools familiar to designers, and inherent consideration of discrete damper sizes.

Limitations of the original SSSA study include the use of few ground motions, small unrealistic damping levels (less than 10% effective damping ratio with dampers) for comparing SSSA to other methods, and the use of example structures and damper placement distributions from previous researchers. The last limitation implies that the placement methods compared to SSSA were not followed in full and therefore, usability of the methods could not be adequately compared. The method's dependency on specific ground motions and proven effectiveness limited to linear structures were two inherent limitations of the technique. However, Lopez-Garcia and Soong (2002) confirm that the sensitivity of the SSSA damper distribution to ground motion characteristics decreases with increasing levels of damping. Minor differences were found in SSSA damper distributions for four different ground motions with 18% damping as compared to much larger discrepancies in distribution when using 6% damping for the same structure and ground motions.

An alternative stochastic approach is the use of genetic algorithms. These are evolutionary techniques specifically applied to combined global optimisation problems (Pintér 2008). The algorithm evolves based on user-provided fitness functions; new generations 'reproduce' until some termination criterion is satisfied. Examples of application to the damper placement problem include Movaffaghi and Friberg (2006), who proposed optimisation using genetic algorithms with discrete variables (using the IDESIGN software interfaced with ABAQUS). Singh and Moreschi (2002) developed a genetic algorithm method to optimally place and size viscous and viscoelastic dampers. The method was demonstrated for various linear dampers and linear, shear and torsional structures and assessed for interstory drifts, floor accelerations, and shear forces. Although the genetic algorithm is a powerful optimisation method, its main disadvantage is high computational time.

Deterministic Methods

Many analytical optimal placement methods have been proposed, including methods based on the principles of optimal control theory, gradient-based search methods, and an analysis/redesign method.

Gluck et al. (1996) adapted optimal control theory (OCT) to the damper placement problem. OCT is used to minimise the performance objective by optimising the location of linear passive devices. Since passive dampers cannot provide feedback in terms of optimal control gains, three approaches (response spectrum approach, single mode approach, and truncation approach) are proposed to remove the off-diagonal state interactions within the gain matrix and allow approximation of floor damping coefficients. Combination of these methods with OCT and passive devices achieves an equivalent effect compared to active control, but is limited to structures dominated by a single mode response. The OCT approach was demonstrated with passive linear viscous and viscoelastic devices within a braced multistory building.

A good example of a gradient-based search method is the optimum for minimum transfer functions (Takewaki, 1997). This damper placement technique takes as its objective the minimisation of the sum of the interstory drifts of the transfer function, evaluated at the structure's undamped fundamental frequency. The method has since been developed further for more complex structures, multiple performance objectives, and optimal sensitivity design to optimise total damping and distribution (Takewaki, 2009). Since the damper placement schemes are based on the dynamic behaviour of the structure alone, the Takewaki method is independent of the ground motion. The method was demonstrated for two shear buildings and assumed stationary ground motions. A possible weakness of the technique is its objective of minimising the sum of a performance indicator as opposed to the peak value, which is a more appropriate damage indicator, and the exclusion of design objectives in the method. The method's status as an early benchmark method for damper placement, its claimed independence from ground motion characteristics, and the lack of verification of the 1997 method for realistic building designs and ground motions warrant further investigation.

The fully-stressed analysis/redesign procedure is an analytical placement method that uses engineering knowledge and a simple numerical approach for damper placement (Levy and Lavan, 2006). Based on the principle of fully-stressed design of truss members, the Lavan A/R method uses a recurrence relationship to maximise ('fully-stress') the dampers influence on the performance parameter (e.g. drift or acceleration allowance) of the building and minimise the total adding damping necessary. The original procedure may be adapted to constrain the total damping (Lavan and Levy, 2009). The Lavan method has been verified by formal gradient-based optimisation and has been applied to shear-frames, industrial frames (Levy and Lavan, 2006), and 3D irregular frames (Lavan and Levy, 2006). Levy and Lavan (2006) claim the method achieves the optimal design, with a desired uniform damage distribution, an inherent consideration of performance based design objectives, and efficiency based on realistic ground motion records and structures. The Lavan method is shown to be more effective than an active control method (Gluck et al., 1996) in terms of interstory drifts for multiple structures and ground motions (Lavan and Levy, 2009).

Techniques Chosen for Further Study

To assess and illustrate the performance of a variety of placement techniques, five methods were applied to the retrofit of steel moment-resisting frames under a range of seismic hazard levels. Two are simple empirical rules, while the other three attempt some form of optimisation. In each case the key constraint is that the total added damping is fixed at the same, constant value, enabling fair comparisons of the schemes' performance.

1. **Uniform:** The total added damping C_t is uniformly distributed over the n storys, so that the damping at floor i is simply:

$$C_i = \frac{C_t}{n} \tag{1}$$

2. **Stiffness-Proportional:** The total added damping C_t is distributed over the n storys in proportion to the stiffness k_i at floor i:

$$C_i = C_t \frac{k_i}{\sum_{i=1}^{n} k_i} \tag{2}$$

3. **Simplified Sequential Search Algorithm (SSSA):** This iterative approach does not explicitly minimise an objective function, but seeks to optimise the dampers' contribution by sequentially placing them where they can be expected to generate the greatest resisting force (Lopez-Garcia, 2001). The total damping to be provided is divided between the number of equally-sized discrete devices. Device placement is governed by an optimal location index γ_i given by

$$\gamma_i = \alpha_1 \delta_i + \alpha_2 \dot{\delta}_i \tag{3}$$

where δ_i is the interstory drift at story i, $\dot{\delta}_i$ the interstory velocity and the coefficients α_1 and α_2 can be chosen according to the dissipater type. For a purely viscous damper (as in our study) $\alpha_1 = 0$ and $\alpha_2 = 1$, so that γ_i is simply equal to the interstory velocity. A time history analysis of the bare frame is performed and a device added to the story giving the highest γ_i value. The process is repeated until all the devices have been distributed. To reduce the dependence on one time history, we suggest that the process should be based on a set of spectrum-compatible accelerograms (three in our analyses), with the damper added to the floor that most frequently gives the highest γ_i value.

4. **Takewaki Method:** The aim of the Takewaki (1997) method is to minimise an objective function given by the sum of the amplitudes of the interstory drifts of the transfer function, evaluated at the undamped natural frequency of the structure, subject to a constraint on the total amount of added viscous damping. Initially the added damping is uniformly distributed and the optimum distribution is then achieved using a gradient-based search algorithm, that is, the damping distribution is altered in a way that maximises the rate of change of the objective function towards its minimum value. This is achieved by computing an optimality index for each floor j given by the differential of the objective function with respect to the damping at floor $j + 1$, normalised by the differential with respect to the damping at floor 1, i.e.:

$$\gamma_j = \frac{\left(\sum_{i=1}^{n} \left|\hat{\delta}_i\right|\right)_{,j+1}}{\left(\sum_{i=1}^{n} \left|\hat{\delta}_i\right|\right)_{,1}} \tag{4}$$

where $\hat{\delta}_i$ is the peak interstory drift of the transfer function at floor i, n is the number of floors and the subscripts such as $_{,j+1}$ indicate differentiation with respect to the damping at that level. Thus, floors with large values of γ_j are those where a change in the damping will cause the most rapid change in the objective function. The change in damping distribution is therefore weighted according to the γ_j values. An optimal solution is achieved when the damping distribution is such that all γ_j values tend to unity, implying that changing the damping at one floor is no more beneficial than doing so at any other floor.

5. **Lavan Method:** The Levy and Lavan (2006) fully stressed analysis/redesign procedure uses a single 'active' ground motion, selected based on its high displacement or energy demands. A response analysis is performed using this ground motion, and the objective function, or performance index, p_i is calculated as the value of a chosen response parameter at story i normalised by an allowable value. In this study the parameter chosen is the interstory drift δ_i:

$$p_i = \max\left(\frac{\left|\delta_i(t)\right|}{\delta_{all,i}}\right) \quad (5)$$

A 'fully-stressed' design is achieved when all p_i values tend to unity, i.e. the damping distribution is such that the drift limit is just achieved at each story. If this optimum is not achieved in iteration (k), then the damping levels are adjusted in step (k+1) according to:

$$C_i^{(k+1)} = C_t \frac{C_i^{(k)}\left(p_i^{(k)}\right)^{1/q}}{\sum_{i=1}^{n} C_i^{(k)}\left(p_i^{(k)}\right)^{1/q}} \quad (6)$$

where q is a convergence parameter with recommended values of 0.5 for linear analysis and 5 for non-linear analysis. The analysis-redistribution process is repeated until all the constraint errors (differences of p_i values from unity) have been minimised and the damping distribution does not change significantly between iterations.

ANALYSIS METHODOLOGY

To assess the different damper placement methods, they were applied to the retrofit of conventionally designed steel moment-resisting frames. Performance of the different schemes was then compared by analysing the retrofitted frames under a suite of earthquake ground motions. Both regular and irregular frames were considered; results presented here focus on the regular frame, with other results given elsewhere (Whittle et al., 2012).

Building Design

Two ten-story, steel MRF buildings, one regular and another irregular in elevation, were designed according to the Eurocodes 3 and 8. Both buildings had floor heights of 3.2 m and the same first floor plan, comprising three 8m bays in each direction, with a lateral force resisting system of MRFs in the north-south direction and braced frames in the east-west direction. While the regular building had a uniform elevation (with section sizes reducing with height), the irregular building had setbacks at the first and sixth storys. A single MRF in the north-south direction was designed, with gravity loads of 4 kN/m^2 dead load and 2 kN/m^2 live load, and an assumed 5% inherent damping. The MRFs were designed using response spectrum analysis and 0.3g PGA and Eurocode soil B site conditions. A high behaviour factor of 6.5 was selected for the regular building, and a reduced factor of 5.2 for the irregular building, to account for vertical irregularities. Basic details of the designs are shown in Figure 2, with fuller information presented in Whittle et al. (2012).

SAP2000 (CSI, 2009) was employed for modelling the frames and aiding the design process. Seismic performance levels selected include the frequently occurring earthquake (FOE), which is 40% of the design basis earthquake (DBE), the DBE (10% probability of exceedance in 50 years), and the maximum considered earthquake (MCE) (2% probability of exceedance in 50 years), which is 150% of the DBE (Somerville et al., 1997). A serviceability limit of 1% peak interstory drift under the FOE was selected. This achieves the Immediate Occupancy performance based design level for the FOE and Life Safety for the DBE (FEMA, 2000). Key building properties are presented in Table 1, where the peak drift is based on the response spectrum analysis.

Damping Design

A strategic amount of added damping in the form of linear viscous dampers was calculated to improve the performance of the buildings. The objective was to add dampers to achieve a linear elastic building performance under the DBE, causing

Figure 2. Layout and section sizes for 10-story MRFs

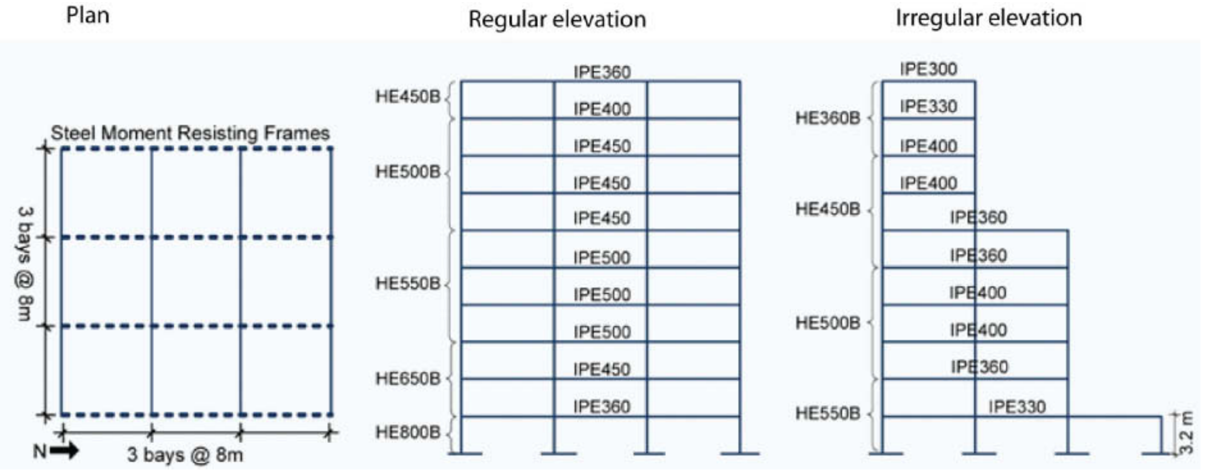

no permanent damage to structural members, and thereby increasing the building performance from a Life Safety level to an Immediate Occupancy level under the DBE.

For the regular building, this design process yielded a requirement for the dampers to provide an increase in the equivalent viscous damping ratio from 5% to 37%, necessitating a total added damping of C_t = 812 kNs/cm. Application of the five damper placement techniques then resulted in damping distributions over the structure as shown in Table 2. It can be seen that the stiffness-proportional approach is the most different from the others, and that none of the optimisation schemes results in any damping being added at the bottom story.

Table 1. Building properties, prior to damper retrofit

	Peak Interstory Drift (%)		Period (sec)		
	FOE	DBE	Mode 1	Mode 2	Mode 3
Regular	0.88	2.20	2.05	0.70	0.38
Irregular	0.99	2.47	2.31	0.93	0.47

Ground Motion Suite

A set of twenty ground motion records were selected from the Pacific Earthquake Engineering Research Center Next-Generation Attenuation Relationships strong-motion database (PEER, 2005). The primary selection criteria were the absence of near-fault characteristics and Eurocode soil B classification (Table 3). Ground motions were normalised to the same hazard level (i.e. DBE or MCE), so that performance objectives at specific hazard levels could be evaluated from the ground motions. This was performed by scaling the ground motions to the same pseudo-spectral acceleration (PSA) at the buildings' fundamental frequencies and 5% inherent damping.

RESULTS AND DISCUSSION

Performance Indicators

Peak interstory drift, absolute acceleration, and residual interstory drift were selected as the main performance indicators. Interstory drift indicates potential damage to primary structural members, while absolute floor acceleration corresponds to damage of building contents and sensitive

Table 2. Damping distributions in the regular building (kNs/cm)

Floor	Uniform	Stiffness Prop.	SSSA	Takewaki	Lavan
10	81.2	27.6	40.6	0.0	9.1
9	81.2	42.9	40.6	46.3	39.9
8	81.2	51.0	81.2	70.1	60.7
7	81.2	55.3	121.8	89.4	92.1
6	81.2	63.3	81.2	102.2	96.7
5	81.2	70.1	81.2	114.0	101.3
4	81.2	73.8	121.8	126.2	133.5
3	81.2	81.5	121.8	134.8	155.2
2	81.2	101.9	121.8	128.9	123.4
1	81.2	244.5	0.0	0.0	0.0
Total	812.0	812.0	812.0	812.0	812.0

Table 3. Ground motion suite

	Ground Motion	Station Name	Component	PGA (g)
1	Imperial Valley 1979	Cerro Prieto	H-CPE237	0.157
2	Loma Prieta 1989	Hollister - S & P	HSP000	0.371
3	Loma Prieta 1989	Woodside	WDS000	0.080
4	Manjil 1990	Abbar	ABBAR--T	0.496
5	Cape Mendocino 1992	Fortuna - Fortuna Blvd	FOR000	0.116
6	Landers 1992	Desert – Hot Springs	LD-DSP000	0.171
7	Northridge 1994	LA - W 15th St	W15090	0.104
8	Northridge 1994	Moorpark - Fire Sta	MRP180	0.292
9	Northridge 1994	N Hollywood - Cw	CWC270	0.271
10	Northridge 1994	Santa Susana Ground	5108-360	0.232
11	Northridge 1994	LA - Brentwood VA	0638-285	0.164
12	Northridge 1994	LA - Wadsworth VA	5082-235	0.303
13	Kobe 1995	Nishi-Akashi	NIS090	0.503
14	Kobe 1995	Abeno	ABN090	0.235
15	ChiChi 1999	TCU105	TCU105-E	0.112
16	ChiChi 1999	CHY029	CHY029-N	0.238
17	Hector 1999	Hector	HEC090	0.337
18	Imperial Valley 1940	USGS 117 El Centro	I-ELC180	0.313
19	New Zealand 02 1987	99999 Matahina Dam	A-MAT083	0.256
20	Nahinni Canada 1985	Site 3	S3270	0.148
21*	Victoria Mexico 1980	UNAMUCSD6604	CPE045	0.621

*Not included in the final ground motion suite; used as the active ground motion for Lavan method.

equipment. Residual interstory drift indicates the permanent damage to the structural members and feasibility of economic repair of the building after the earthquake. Residual drifts were determined by continuing analyses for at least 20 seconds beyond the end of the ground motion record, until the structure was stationary. The residual drifts were then calculated as the difference between the final displacements of adjacent floors.

Performance of Regular Building

The results of the regular building's performance are presented in Figures 3-6. Figure 3 compares the added damper placement schemes in terms of the median peak interstory drift distributions under both the DBE and the MCE. The drift design objectives of the bare frame under the DBE (2.2%) and of the frame with dampers (1.1%) are noted with solid lines. Under the DBE (Figure 3(a)), all the damper schemes achieve less than 1.10% peak interstory drift, thereby meeting the DBE design objective and reducing the bare frame drifts by more than half. Both the Takewaki and Lavan schemes result in peak interstory drifts best approaching a desirable, uniform drift distribution. The stiffness-proportional and uniform distributions produce the least uniform drift profiles, with the uniform scheme overdamping the upper floors and the stiffness-proportional approach overdamping the first floor such that floors three and four are not effectively damped. Figure 3(b) compares the distributions under the MCE. The MCE drift distributions mirror the DBE results, and display a 50% increase in the drifts of the damped frame, as to be expected for a predominantly linear building response. Under the MCE, the design objective for added dampers (1.65% interstory drift) is met by all of the damper placement schemes.

Table 4 presents the maximum interstory drifts of all floors. The uniform and stiffness-proportional damper schemes produce very similar maximum interstory drifts, while the three advanced techniques all result in lower peak drifts, with little disparity between the three schemes. Drifts in millimetres particularly highlight the small differences between the methods.

The peak interstory drifts for the regular building are analysed further in Figure 4. The standard deviations of drift under the DBE are similar amongst the damper placement methods at each floor (an average of 0.24% maximum standard deviation, with all methods within 8% of the average maximum standard deviation) and greatest for the bare frame (0.40% and 0.84% maximum standard deviations under the DBE and MCE, respectively).

A larger dispersion of drifts occurs in the damped frame under the MCE, with an average of 0.39% maximum standard deviation, with all methods within 11% of the average maximum standard deviation. The dispersion is largest in the internal floors (2-7) corresponding to the largest peak interstory drifts in the frame.

Figure 5 compares the placement techniques in terms of absolute accelerations. For the DBE (Figure 5(a)), all the damper placement schemes reduce the absolute accelerations of the bare frame at all floors except the 1st floor. The maximum peak accelerations in the damped frames occur at the first floor and are within a narrow range of 6.17 m/s^2 to 6.30 m/s^2. Similar distributions and narrow maximum peak acceleration range (9.25 m/s^2 to 9.46 m/s^2) are exhibited in the damped

Table 4. Regular building – Maximum of peak interstory drifts

	DBE Ground Motion Suite		MCE Ground Motion Suite	
	%	mm	%	mm
No Dampers	2.27	72.5	3.28	104.9
Uniform	1.08	34.7	1.64	52.6
Stiffness Proportional	1.07	34.3	1.62	52.0
SSSA	0.94	30.1	1.41	45.2
Takewaki	0.90	28.7	1.34	43.0
Lavan	0.87	27.7	1.30	41.6

Figure 3. Median of peak interstory drifts under (a) DBE, (b) MCE

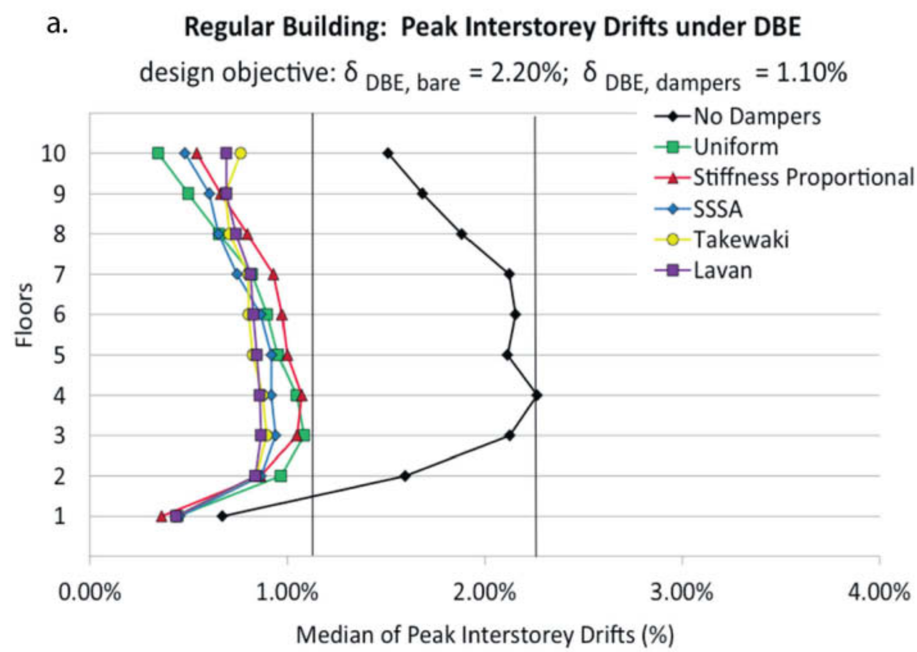

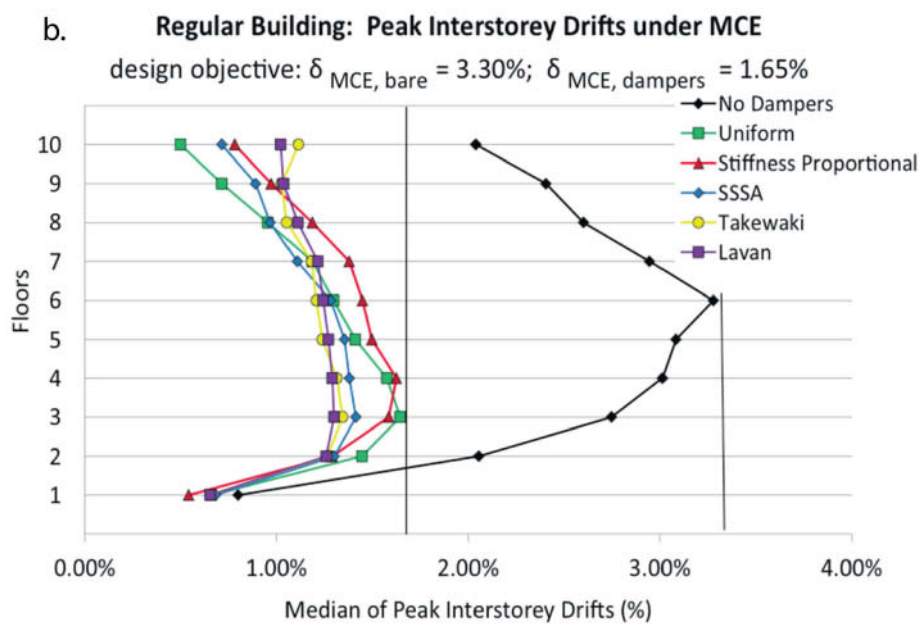

Figure 4. Mean and standard deviation of peak interstory drifts under (a) DBE, (b) MCE

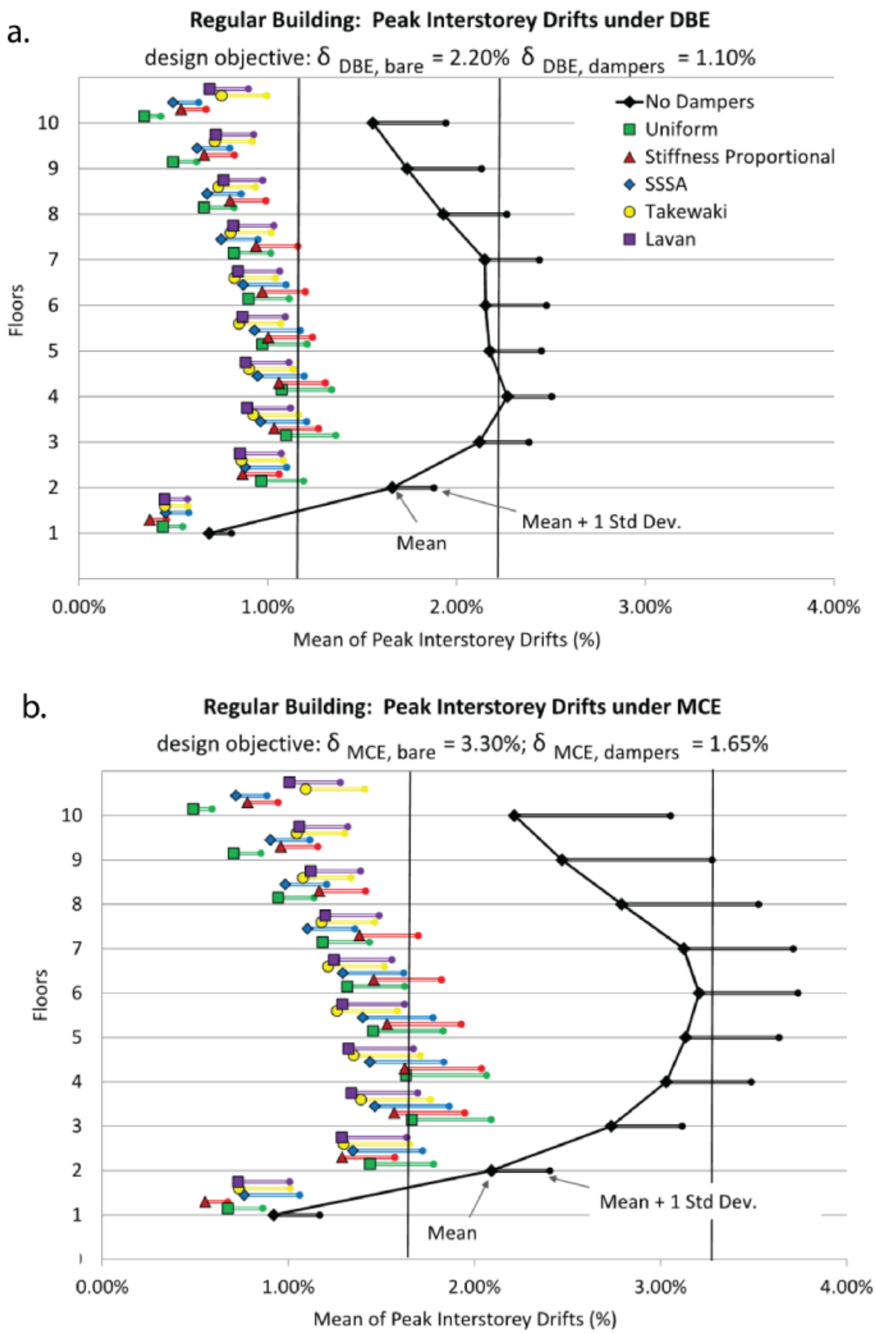

Figure 5. Median of absolute floor acceleration under (a) DBE, (b) MCE

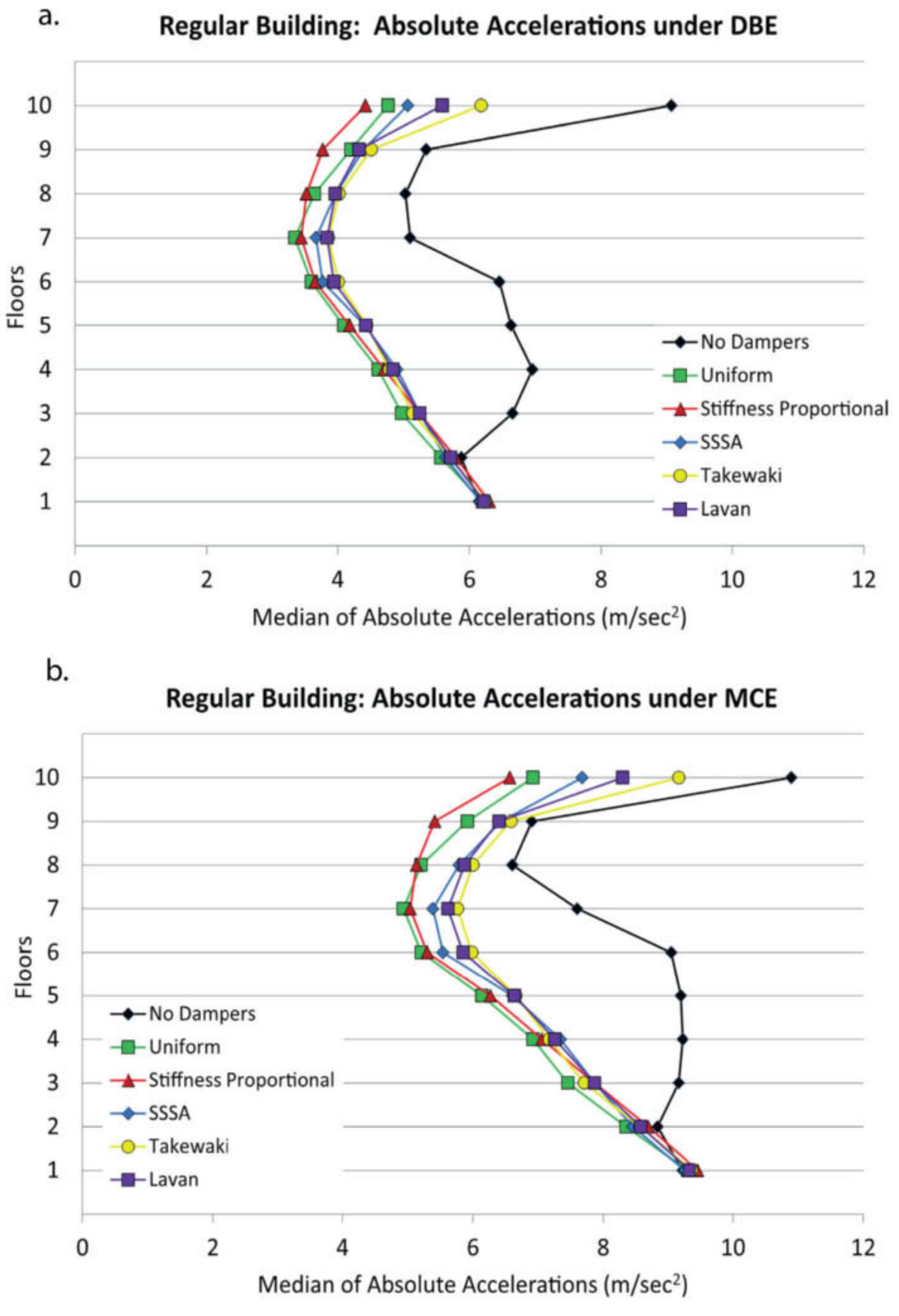

Figure 6. Median of residual interstory drifts under (a) DBE, (b) MCE

a.

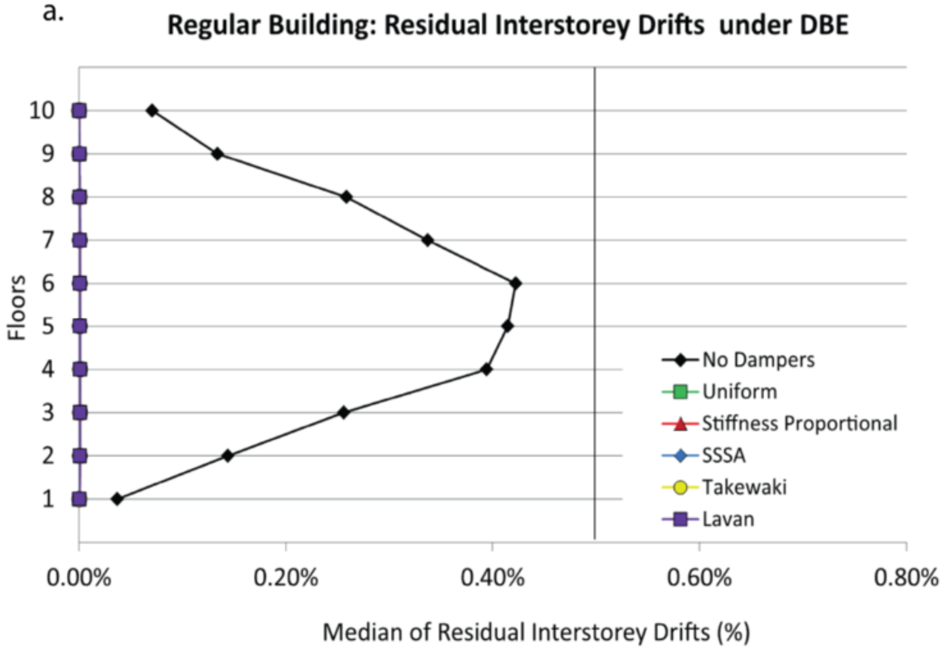

b.

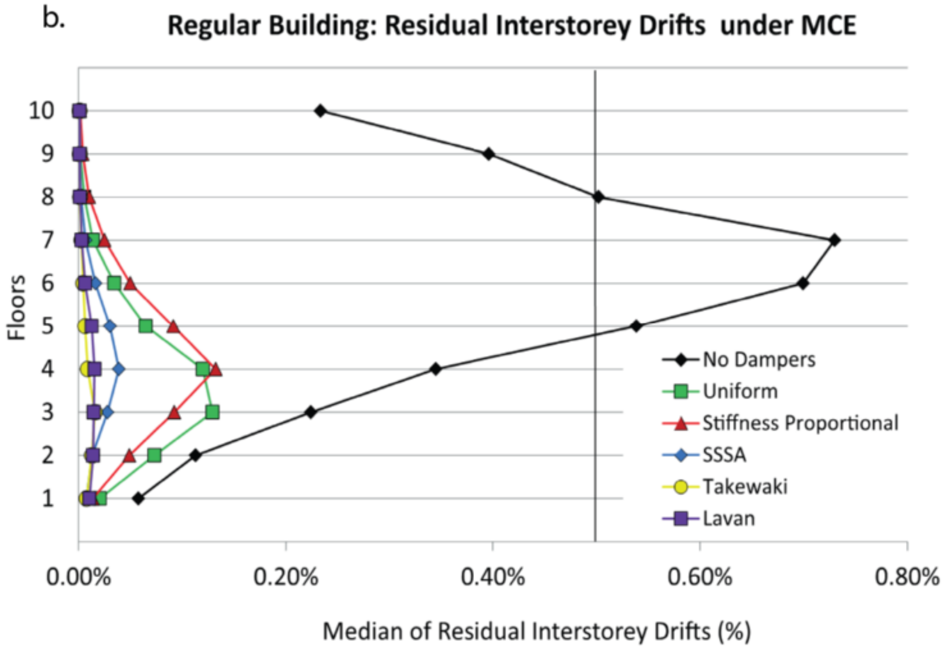

frame under the MCE (Figure 5(b)). The maximum peak accelerations of the bare frame (at the roof) are reduced by an average of 30% under the DBE and 14% under the MCE with the added dampers (peak occurring at the first floor).

In terms of overall distribution, the uniform and stiffness-proportional schemes are the most effective at reducing accelerations at floors 5-10. For example, under the MCE at the roof, the uniform scheme achieves a 10% reduction and the stiffness proportional approach a 14% reduction from the nearest of the advanced methods, SSSA. This may be attributed to the standard methods apportioning large damping at the base and roof of the building.

Figure 6 presents residual interstory drifts. The building with added dampers experiences negligible residual interstory drifts under the DBE, confirming that the addition of dampers has in all cases resulted in linear building performance. This compares favourably with the large residual drifts in the bare frame, 0.42% at floor 6 (Figure 6(a)). McCormick et al. (2008) recommend a permissible residual drift limit of less than 0.5%, based on realistic repair costs and human tolerance of drifts. The bare frame under the MCE (Figure 6(b)) achieves peak residual drifts near 0.75%; these would render the building economically unsalvageable after the earthquake. However, the addition of viscous dampers reduces the residual drifts to less than 0.15% for the standard placement methods and less than 0.05% for the advanced placement methods.

Finally, we offer some comments on the ease of implementation of the schemes, based on adherence to the damper placement methods' procedures as outlined in literature. The uniform and stiffness proportional methods are the simplest to apply while still achieving the desired drift limit. Although requiring the use of only three time histories, the SSSA method is the most time consuming because it requires three time domain analyses at each of the twenty steps used in our analysis (i.e. a total of sixty linear time history analyses). The Takewaki technique requires significant up-front effort in developing the necessary programming script; once this is achieved the method is reasonably efficient, requiring only minimal inputs and operating independently from ground motions. Selection of the correct step-size greatly influences convergence time. Of the three optimisation techniques, the Lavan technique is the easiest to implement from scratch. Although it does depend on an iterative analysis with specific ground motions, this can be conducted with the same tools used for the SSSA method and requires fewer ground motions and steps; for our structures, convergence occurred in less than 10 iterations.

While controlling the total added damping permits a fair comparison of the placement methods, the advanced placement schemes could achieve a reduced damping while still meeting the drift performance objectives. Further research is needed to conduct thorough comparisons of the existing damper placement methods that consider both the optimal placement of dampers and reduction of total damping to meet specific performance criteria. In addition, investigation of a wider range of effective damping ratios and structural properties would provide additional insight into the efficiency and robustness of the damper placement methods.

CONCLUSION

The effectiveness and usability of five damper placement methods has been evaluated by using them to achieve response reductions in ten-story, moment-resisting frames. It was shown that even the simplest methods can provide substantial improvements in building performance, as demonstrated by the median responses to a suite of 20 ground motions. In our example, all the schemes considered were able to meet the design drift limits, reduce floor accelerations and eliminate non-linearity at the DBE, resulting in zero residual drift.

While all methods investigated were effective, the three optimal placement techniques studied, the SSSA, Takewaki and Lavan methods, all offered greater reductions in interstory drifts than the uniform and stiffness-proportional schemes. It is therefore evident that there is benefit to be gained from the additional effort of implementing an iterative scheme, in terms of further response reductions for a given outlay. It is notable that this benefit of the advanced schemes is not so evident when considering peak absolute floor accelerations, which do not reveal large differences between any of the added damper schemes, apart from consistently smaller acceleration distributions in the upper floors for the standard placement methods.

Of all the advanced placement techniques tested here, the Lavan method achieves the best performance with the least complexity and time expended to achieve the damper distribution scheme. However, the differences between the advanced techniques should not be exaggerated, as all three produced similar placement schemes and extremely similar drift and acceleration results.

REFERENCES

Cheng, F. Y., & Pantelides, C. P. (1988). *Optimal placement of actuators for structural control*. Technical Report NCEER-88-0037, National Centre for Earthquake Engineering Research, State University of New York, Buffalo, N.Y.

CSI. (2009). *SAP2000, version 11*. Berkeley, CA: Computers and Structures, Inc.

FEMA. (2000). *FEMA 356: Prestandard and commentary for the seismic rehabilitation of buildings*. Washington, DC: Federal Emergency Management Agency.

Gluck, N., Reinhorn, A. M., Gluck, J., & Levy, R. (1996). Design of supplemental dampers for control of structures. *Journal of Structural Engineering*, *122*(12), 1394–1399. doi:10.1061/(ASCE)0733-9445(1996)122:12(1394)

Lavan, O., & Levy, R. (2006). Optimal peripheral drift control of 3D irregular framed structures using supplemental viscous dampers. *Journal of Earthquake Engineering*, *10*(6), 903–923. doi:10.1080/13632460609350623

Lavan, O., & Levy, R. (2009). Simple iterative use of Lyapunov's solution for the linear optimal seismic design of passive devices in framed buildings. *Journal of Earthquake Engineering*, *13*, 650–666. doi:10.1080/13632460902837736

Levy, R., & Lavan, O. (2006). Fully stressed design of passive controllers in framed structures for seismic loadings. *Structural and Multidisciplinary Optimisation*, *32*(6), 485–498. doi:10.1007/s00158-005-0558-5

Levy, R., & Lavan, O. (2009). Quantitative comparison of optimization approaches for the design of supplemental damping in earthquake engineering practice. *Journal of Structural Engineering*, *135*(3), 321–325. doi:10.1061/(ASCE)0733-9445(2009)135:3(321)

Liu, W., Tong, M., & Lee, G. (2005). Optimization methodology for damper configuration based on building performance indices. *Journal of Structural Engineering*, *131*(11), 1746–1756. doi:10.1061/(ASCE)0733-9445(2005)131:11(1746)

Lopez-Garcia, D. (2001). A simple method for the design of optimal damper configurations in MDOF structures. *Earthquake Spectra*, *17*(3), 387–398. doi:10.1193/1.1586180

Lopez-Garcia, D., & Soong, T. T. (2002). Efficiency of a simple approach to damper allocation in MDOF structures. *Journal of Structural Control*, *9*, 19–30. doi:10.1002/stc.3

McCormick, J., Aburano, H., Ikenaga, M., & Nakashima, M. (2008). Permissible residual deformation levels for building structures considering both safety and human elements. *Proceedings of the 14th World Conference on Earthquake Engineering*, Beijing, China, Paper No. 05-06-0071.

Movaffaghi, H., & Friberg, O. (2006). Optimal placement of dampers in structure using genetic algorithm. *Engineering Computations*, *23*(6), 597–606. doi:10.1108/02644400610680324

PEER. (2005). *Next generation attenuation relationships – Strong motion database*. Pacific Earthquake Engineering Research Center. Retrieved from http://peer.berkeley.edu/nga.

Pintér, J. (2008). *Global optimization*. Retrieved from http://mathworld.wolfram.com/GlobalOptimization.html

Shukla, A. K., & Datta, T. K. (1999). Optimal use of viscoelastic dampers in building frames for seismic force. *Journal of Structural Engineering*, *125*(4), 401–409. doi:10.1061/(ASCE)0733-9445(1999)125:4(401)

Singh, M. P., & Moreschi, L. M. (2002). Optimal placement of dampers for passive response control. *Earthquake Engineering & Structural Dynamics*, *31*, 955–976. doi:10.1002/eqe.132

Somerville, P., Smith, N., Punyamurthula, S., & Sun, J. (1997). *Development of ground motion histories for phase 2 of the FEMA/SAC steel project*. Report No. SAC/BD-97/04.

Soong, T. T., & Dargush, G. F. (1997). *Passive energy dissipation systems in structural engineering*. Chichester, UK: John Wiley & Sons.

Takewaki, I. (1997). Optimal damper placement for minimum transfer functions. *Earthquake Engineering & Structural Dynamics*, *26*, 1113–1124. doi:10.1002/(SICI)1096-9845(199711)26:11<1113::AID-EQE696>3.0.CO;2-X

Takewaki, I. (2009). *Building control with passive dampers: Optimal performance based design for earthquakes*. London, UK: John Wiley & Sons. doi:10.1002/9780470824931

Whittle, J. K., Williams, M. S., Karavasilis, T. L., & Blakeborough, A. (2012). A comparison of viscous damper placement methods for improving seismic building design. *Journal of Earthquake Engineering*, *16*(4), 540-560.

Wu, B., Ou, J. P., & Soong, T. T. (1997). Optimal placement of energy dissipation devices for three-dimensional structures. *Engineering Structures*, *19*(2), 113–125. doi:10.1016/S0141-0296(96)00034-X

Zhang, R., & Soong, T. T. (1992). Seismic design of viscoelastic dampers for structural applications. *Journal of Structural Engineering*, *118*(5), 1375–1392. doi:10.1061/(ASCE)0733-9445(1992)118:5(1375)

Chapter 3
Optimal Placement of Viscoelastic Dampers Represented by the Classical and Fractional Rheological Models

Roman Lewandowski
Poznan University of Technology, Poland

Zdzisław Pawlak
Poznan University of Technology, Poland

ABSTRACT

The problems of the optimal location of viscoelastic (VE) dampers and determination of the optimal values of parameters of dampers are considered in this chapter. The optimal distributions of dampers in buildings are found for various objective functions. The optimization problem is solved using the sequential optimization method and the particle swarm optimization method. The properties of VE dampers are described using the rheological models with fractional derivatives. These models have an ability to correctly describe the behaviour of VE dampers using a small number of model parameters. Moreover, generalized classical rheological models of VE dampers are also taken into account. A mathematical formulation of the problem of dynamics of structures with VE dampers, modelled by the classical and fractional rheological models is presented. The results obtained from numerical calculation are also discussed in detail.

DOI: 10.4018/978-1-4666-2029-2.ch003

INTRODUCTION

Passive damping systems consist of various mechanical devices which are mounted on structures and dissipate a portion of the energy introduced by excitation forces affecting the structures. Different kinds of mechanical devices, such as viscous dampers, viscoelastic dampers, tuned mass dampers, or base isolation systems, can be used as passive systems. In contrast with the active and semi-active systems, the passive ones require no amount of energy to operate. Online measurements of the dynamical state of the structure are not necessary. Books by Soong and Dargush (1997), by Constantinou *et al.* (1998), and Hanson and Soong (2001) contain important basic information concerning many aspects of passive control of civil structures. Moreover, fundamental information concerning passive control systems can be found in books by Mead ((1998), by Jones D.I.G. (2001), and De Silva (2007).

In civil engineering, VE dampers are successfully applied to reduce excessive vibrations of buildings caused by winds and earthquakes. It was found that incorporation of VE dampers in a structure leads to a significant reduction of unwanted vibrations; see the paper by Soong and Spencer (2002). A number of applications of VE dampers in civil engineering are listed in a book by Christopoulos and Filiatrault (2006).

The VE dampers' behaviour depends mainly on the rheological properties of the VE material and the dampers are made of. In the past, several rheological models were proposed to describe the dynamic behaviour of VE materials and dampers. Both the classical and the so-called fractional-derivative models of dampers and VE materials are available. In the classical approach, the mechanical models consisting of springs and dashpots are used to describe the rheological properties of VE dampers, see, for example the paper by Park (2001). A good description of the VE dampers requires mechanical models consisting of a set of appropriately connected springs and dashpots. In this approach, the dynamic behaviour of a single damper is described by a set of differential equations. The rheological properties of VE dampers could be also described using the fractional calculus and the fractional mechanical models. This approach has received considerable attention and has been used in modelling the rheological behaviour of VE materials and dampers (Bagley and Torvik, 1989; Rossikhin and Shitikova, 2001; Chang and Singh, 2002). The fractional models have an ability to correctly describe the behaviour of VE materials and dampers using a small number of model parameters. A single equation is enough to describe the VE damper dynamics, which is an important advantage of the discussed model. However, in this case, the VE damper equation of motion is the fractional differential equation.

An optimal distribution of the damping properties of dampers and optimal positioning of dampers are important from the designer's point of view. The optimal positioning of a single viscous damper based on the energy criterion was considered by Gurgoze and Muller (1992). Takewaki (2009) used a gradient-based approach for the optimal placement of passive, mainly viscous, dampers and modelled by the simple Maxwell model by minimizing the norm of the response transfer function calculated for the undamped fundamental frequency of structure. Singh and Moreschi (2001) used a gradient–based optimization procedure to obtain the optimal distribution of viscous dampers. Moreover, the genetic algorithm was used by Singh and Moreschi (2002) to find the optimal size and location of viscous and viscoelastic dampers. Tsuji and Nakamura (1996) described a method to find the optimal storey stiffness distribution and the optimal damper distribution for structures subjected to a set of earthquakes. A sequential search algorithm was presented by Zhang and Soong (1992) and by Garcia and Soong (2002) for the design of an optimal damper configuration. Aydin *et al.* (2007) considered the optimal distribution of viscous dampers, as used for the rehabilitation of an existing building with soft storeys. The method of simultaneous optimal distribution of stiffness and damping for the rehabilitation of existing buildings was also proposed in the paper by Cimellaro (2007). The objective function of his method combines the displacement, absolute acceleration, and base shear transfer function. Lavan and Levy (2005) proposed a method for the optimal design of viscous dampers based on a global damage index. In several papers, the active control theory is used to optimize the size and location of dampers. For example, the H_2 method and the H_∞ methods are used by Yang *et al.* (2002) while the linear quadratic regulation (LQR) method is used by Gluck et al. (1996), Agrawal and Yang (2000), and by Loh et al. (2000) to determine damper allocations. Interesting studies concerning the allocation and sizing of viscous dampers were presented by Main and Krenk (2005) and by Engelen *et al.* (2007). Recently, the issue of the optimal placement of VE dampers was considered in two papers by Fujita *et al.* (2010a, 2010b) and by Pawlak and Lewandowski (2010), who used the fractional Kelvin model of VE dampers. Moreover, the optimal connections of parallel structures by VE dampers were considered by Zhu *et al.* (2010). A study of the effect of hysteretic damper's stiffness on energy distribution among building stories was presented in two papers by Nakashima *et al.* (1996 a, b).

The aims of the chapter are to find the optimal location of VE dampers and to determine their optimal parameters. Several objective functions, which are minimized, are taken into account. One of the objective functions is the weighted sum of amplitudes of the transfer functions of interstorey drifts, evaluated at the fundamental natural frequency of the frame with such dampers. Another objective functions are taken as the extreme displacement within the structure or as the extreme bending moment in the supporting columns. The optimization constraints are formulated, based on the properties of dampers. The considered optimization problem is solved using the sequential optimization method (SOM) and the particle swarm optimization (PSO) method. Moreover, a mathematical formulation of the problem of dynamics of structures with VE dampers, modelled by classical and fractional rheological models, is presented. The fractional models of dampers have an ability to correctly describe the behaviour of VE dampers using a small number of model parameters. Advanced classical rheological models of VE dampers are also taken into account. The equations of motion of the considered frame structures, expressed in physical co-ordinates and in the state space, are derived. The optimal distributions of dampers in buildings are found for various objective functions using the above mentioned damper models.

FORMULATION OF THE OPTIMIZATION PROBLEM AND DESCRIPTION OF THE SOLUTION METHOD

In the considered optimization problem, the following objective functions to be minimized are taken into account:

1. The weighted sum of amplitudes of the transfer functions of interstorey drifts, evaluated at the fundamental natural frequency of the frame with the dampers
2. The weighted sum of amplitudes of the transfer functions of displacements evaluated at the fundamental natural frequency of the frame with dampers
3. The extreme bending moment in columns caused by a real earthquake

The above mentioned objective functions may be described as follows:

$$F = \mathbf{w}^T \mathbf{h} \tag{1}$$

where $\mathbf{w} = [w_1, w_2, ..., w_r]^T$ is the vector of weight coefficients, and *r* stands for the number of quantities taken into account in the objective function. The vector $\mathbf{h} = [h_1, h_2, ..., h_r]^T$ consists of the values of the above mentioned amplitudes of the transfer functions of interstorey drifts (case 1), displacements (case 2), or values of the bending moments in columns (case 3). The weight factor w_i could be chosen more or less arbitrarily or, which is more reasonable, it could reflect the designer's preferences.

The considered optimization problem is subjected to some constraints. Due to limitations resulting from the building's functionality and manufacturing constraints, the dampers' positions cannot be freely chosen. Therefore, it is reasonable to assume that during the building design process some, say *m*, places in the building are chosen as acceptable damper locations. Moreover, it is reasonable to assume that the properties of VE dampers cannot be freely changed and only the size of dampers is changeable. This means that all parameters in the *i-th* VE damper's model are proportional to one parameter, say, the damping factor $c_{d,i}$ which will be called the main damping factor. In the case of the fractional model, it is assumed that the parameter α, which describes the order of the fractional derivative in the model, is constant and cannot be changed during the optimization procedure. If the damper model contains more than one damping parameter, one of them may be chosen as the main damping factor. For the above-mentioned reasons, it is assumed that the sum of damping coefficients is known and constant. Moreover, the values of the main damping factor $c_{d,i}$ of every damper must be non-negative. The above constraints are written as:

$$\sum_{i=1}^{m} c_{d,i} = C_d, \qquad c_{d,i} \geq c_{\min} \tag{2}$$

where C_d is the assumed total amount of main damping factors and $i = 1, 2, .., m$. Moreover, $c_{\min} = 0$ or $c_{\min}$ is the low-value positive number if the particle swarm optimization method is used to optimize the structure with dampers modelled using the fractional Maxwell model.

The equations of motion of a structure with dampers are treated as additional implicit constraints. Moreover, it is assumed that the damper's damping factors are continuous design variables. However, in practical applications, the damper's capacity and size can be found only from a set of actually manufactured dampers. Dampers are fixed to a structure with the help of braces, which are treated as elastic elements or as rigid elements when the shear frame is used as the model of a real structure.

The considered optimization problem is formulated as follows:

For a given set of *m* possible damper locations, find the positions of dampers and the value of their main damping factors $c_{d,i}$ which minimize the objective function (1) and fulfill the explicit constraints of Equation (2) and other implicit constraints mentioned above.

The solution is obtained using the sequential optimization method and the particle swarm optimization method (see, Kennedy and Eberhart (2001), Clerc (2006), Gazi and Passino (2011)). In the first method, for each possible location of one damper the values of the objective function are calculated. The optimal, most appropriate location of the damper is the position for which the minimum value of the objective function is obtained. When the first damper location is determined, the procedure is repeated until all locations for the dampers are found. This procedure is very simple. However, there is no proof for the solution's convergence although many examples show that the method is efficient in a number of engineering applications (see, for example, the papers by Zhang and Soong (1992) and by Lewandowski (2008)). Moreover, the order of convergence of

Figure 1. The flowchart of the sequential optimization method

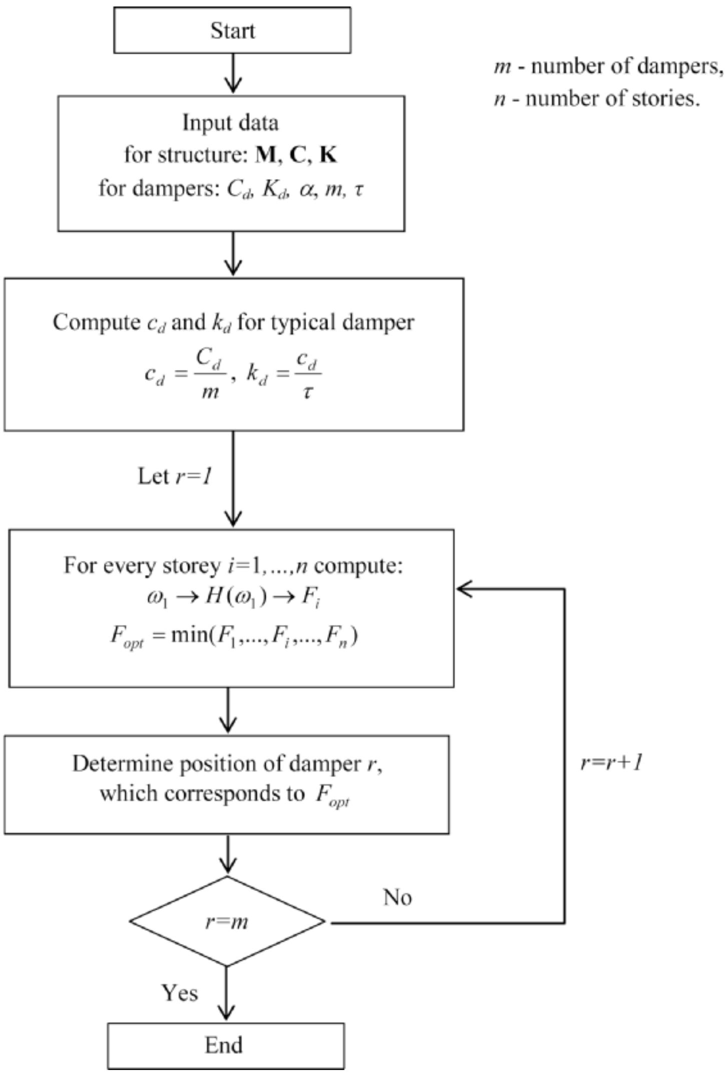

this method is also an open question. The flowchart of SOM is presented in Figure 1.

The PSO algorithm, which is based on the study of social behaviour in a self–organized population system (i.e., ant colonies, fish schools), searches a space by adjusting the trajectories of so-called particles. Every particle is characterized by the vector of particle position $\mathbf{p}_i$ and the vector of particle velocity $\mathbf{v}_i$. In this paper, the position vector $\mathbf{p}_i$ of the i-th particle contains the main damping coefficients of dampers currently mounted on the structure, i.e., $\mathbf{p}_i = [c_{d,1}^{(i)}, c_{d,2}^{(i)}, \ldots, c_{d,m}^{(i)}]^T$. The dimension of the vector $\mathbf{p}_i$ is equal to the number of acceptable damping locations. The search for an optimal solution is performed by updating the subsequent positions of particles. Moreover, every particle keeps record of its best fitness achieved so far as the vector $\mathbf{b}_i$ and the best fitness and corresponding solution achieved in the particle's neighbourhood as the vector $\mathbf{g}_i$.

A population of particles is initialized with random positions and velocities. Every time instances *k* of the PSO, the velocities of the particles are changed (accelerated) towards the $\mathbf{b}_i(k)$ and the $\mathbf{g}_i(k)$ and the particles are moved to new positions according to the following formulae:

$$\mathbf{v}_i(k+1) = w(k)\mathbf{v}_i(k) + \frac{c_1}{\Delta t}\mathbf{R}_1(k)\big(\mathbf{b}_i(k) - \mathbf{p}_i(k)\big) + \frac{c_2}{\Delta t}\mathbf{R}_2(k)\big(\mathbf{g}_i(k) - \mathbf{p}_i(k)\big),$$

$$\mathbf{p}_i(k+1) = \mathbf{p}_i(k) + \mathbf{v}_i(k+1)\Delta t \quad (3)$$

where Δt is the time step (here $\Delta t = 1$ sec), $\mathbf{p}_i(k)$ is the position of the *i*-th particle at the *k*-th iteration, $\mathbf{v}_i(k)$ is the corresponding velocity vector, $\mathbf{R}_1(k)$, $\mathbf{R}_2(k)$ are the diagonal matrices of independent random numbers, uniformly distributed in the range (0, 1); $w(k)$ is the inertia factor providing balance between exploration and exploitation, c_1 is the individuality constant, and c_2 is the sociality constant. To speed up convergence, the inertia weight was linearly reduced from $w_{\max}$ to $w_{\min}$, i.e.:

$$w(k+1) = w_{\max} - \frac{(w_{\max} - w_{\min})}{k_{\max}} k \quad (4)$$

where $k_{\max}$ denotes the maximal number of iterations.

A new velocity, which moves the particle in the direction of a potentially better solution, is calculated based on its previous value, and the particle location at which the best fitness so far has been achieved.

The initial values of the elements $v_{i,j}(0)$ of the velocity vector $\mathbf{v}_i(0)$ are calculated from the following formula:

$$v_{i,j} = r_3 \ C_d \varepsilon_0 \quad (5)$$

where r_3 is the random number taken from the range (0, 1) and ε_0 is a low-value number which assure that initial velocities are not too large (here $\varepsilon_0 = 0.05$). The initial values of elements of the vector $\mathbf{p}_i(0)$ are determined from the following relationship:

$$c_{d,i}(0) = \frac{\tilde{r}_i C_d}{\sum_{j=1}^{m} \tilde{r}_j} \quad (6)$$

where $\tilde{r}_i$ is the random number taken from the range (0, 1). The above choices assure that all of the assumed initial approximations of damper parameters, i.e., vectors $\mathbf{p}_i(0)$ and $\mathbf{v}_i(0)$ fulfil the optimization constraints (2).

The way of handling the constraints introduced in the optimization problem is an important part of the PSO algorithm. The following very simple procedure is used here to fulfil the constraints (2):

- If non-admissible values $c_{d,i}(k+1) < 0$ result from the relationship (3), then $c_{d,i}(k+1) = c_{\min}$ is artificially introduced,
- In order to fulfil the constraint (2.1), elements of the vector $\mathbf{p}_i(k+1)$ are normalized in such a way that

$$\tilde{c}_{d,i} = \frac{c_{d,i}}{\sum_{j=1}^{m} c_{d,j}} C_d \quad (7)$$

Figure 2. The flowchart of the PSO method

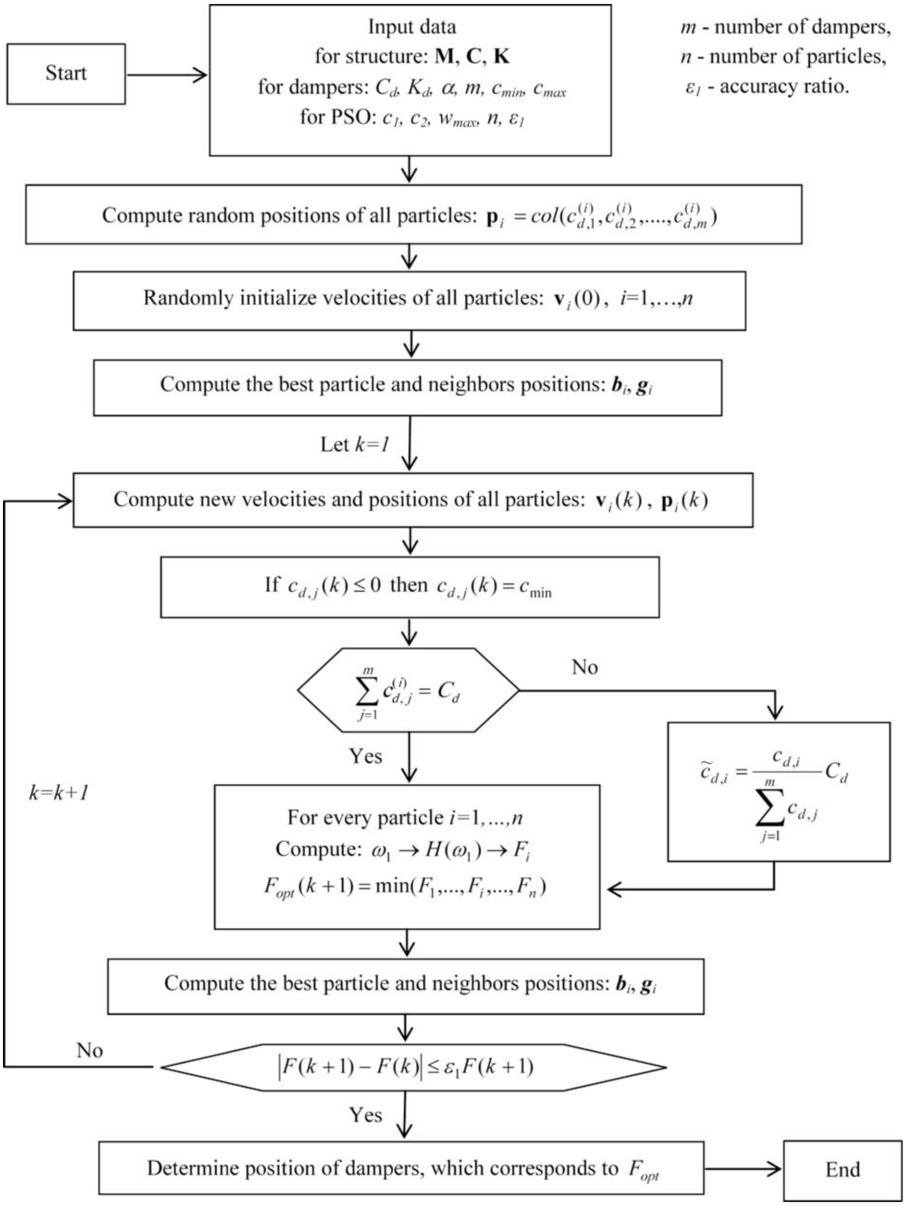

The PSO procedure is ceased if the change of the best value of objective function is sufficiently small for a given number of time steps l, i.e., when

$$\left|F(k+l) - F(k)\right| \le \varepsilon_1 F(k+l), \tag{8}$$

where ε_1 is an assumed low-value number.

The flowchart of the PSO method is presented in Figure 2.

The optimization problem presented above could also be solved using another evolution optimization method, such as genetic algorithm, evaluation strategies or ant colony method. For example, the genetic algorithm was used by Singh

Figure 3. A schematic of the generalized Kelvin model

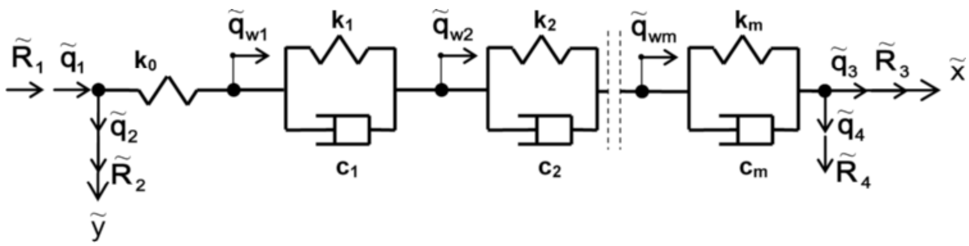

and Moreschi (2002), Alkhatib et al. (2004) and Wu et al. (1997). An interesting comparison between the properties of PSO and the genetic method is presented by Plevris and Papadrakakis (2011). Compared with other evolutionary algorithms, like genetic algorithm and ant colony optimization algorithm, PSO has some appealing features including easy implementation, few parameters tuning and fast convergence rate. Some applications of ant colony optimization method to solve structural optimization problems are presented by Viana *et al.* (2008) and by Kaveh A. and Talatahari S. (2009).

DESCRIPTION OF MODELS OF VE DAMPERS

The properties of VE dampers can be properly captured using generalized rheological models like the generalized Kelvin model and the generalized Maxwell model, shown in Figure 3 and Figure 4, respectively. The generalized Kelvin model is built from the spring and a set of the *m* Kelvin elements connected in series while the generalized Maxwell model is built from the spring and a set of the *m* Maxwell elements connected in parallel. In this paper, a serially connected spring and dashpot will be referred to as the Maxwell element while the Kelvin element is the spring and dashpot connected in parallel.

The behaviour of the generalized Kelvin model of damper can be described by means of the following equations:

$$u_0(t) = k_0[\tilde{q}_{w,1}(t) - \tilde{q}_1(t)],$$

$$u_i(t) = k_i[\tilde{q}_{w,i+1}(t) - \tilde{q}_{w,i}(t)] + c_i[\dot{\tilde{q}}_{w,i+1}(t) - \dot{\tilde{q}}_{w,i}(t)],$$

$$u_m(t) = k_m[\tilde{q}_3(t) - \tilde{q}_{w,m}(t)] + c_m[\dot{\tilde{q}}_3(t) - \dot{\tilde{q}}_{w,m}(t)] \tag{9}$$

where $u_i(t)$ is the force in the *i-th* element of the model ($i = 0,1,..,m$). Symbols k_i and c_i are the spring stiffness and the damping factor of the dashpot of the *i-th* element of the model, respectively, and $\tilde{q}_1(t)$ and $\tilde{q}_3(t)$ denote the external nodes displacements given in the local coordinate system. Moreover, the dot stands for differentiation with respect to time t and the symbol $\tilde{q}_{w,i}(t)$ denotes additional displacements, called “the internal variable” ($i = 1,..,m$).

After introducing the vector of external reactions $\tilde{\mathbf{R}}_z(t) = [\tilde{R}_1(t),\ \tilde{R}_2(t),\ \tilde{R}_3(t),\ \tilde{R}_4(t)]^T$ and utilizing the equilibrium conditions of the external nodes: $\tilde{R}_1(t) = -u_0(t)$, $\tilde{R}_2(t) = 0$, $\tilde{R}_1(t) = u_m(t)$ and $\tilde{R}_4(t) = 0$ the following matrix equation can be written:

$$\tilde{\mathbf{R}}_z(t) = \tilde{\mathbf{K}}_{zz}\tilde{\mathbf{q}}_z(t) + \tilde{\mathbf{K}}_{zw}\tilde{\mathbf{q}}_w(t) + \tilde{\mathbf{C}}_{zz}\dot{\tilde{\mathbf{q}}}_z(t) + \tilde{\mathbf{C}}_{zw}\dot{\tilde{\mathbf{q}}}_w(t) \tag{10}$$

where $\tilde{\mathbf{q}}_z(t) = [\tilde{q}_1(t),\ \tilde{q}_2(t),\ \tilde{q}_3(t),\ \tilde{q}_4(t)]^T$, $\tilde{\mathbf{q}}_w(t) = [\tilde{q}_{w,1}(t), \ldots\ldots,\ \tilde{q}_{w,m}(t)]^T$ and the symbols $\tilde{\mathbf{K}}_{zz}$, $\tilde{\mathbf{K}}_{zw}$, $\tilde{\mathbf{C}}_{zz}$ and $\tilde{\mathbf{C}}_{zw}$ denote the stiffness and

Figure 4. A schematic of the generalized Maxwell model

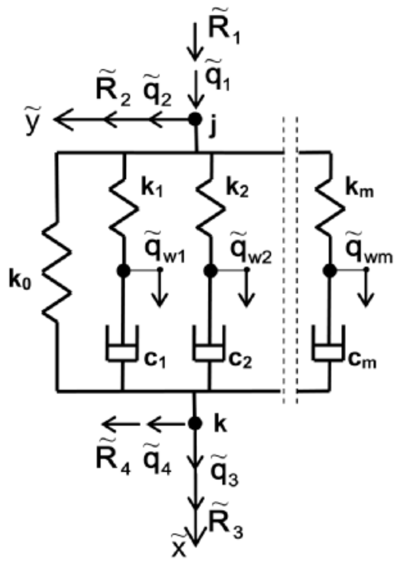

damping matrices given in the local coordinate system, respectively.

The equilibrium conditions of the internal nodes, i.e., $u_{i-1}(t) - u_1(t) = 0$ for $i = 1,..,m$ lead to the following matrix equation:

$$\tilde{\mathbf{K}}_{wz}\tilde{\mathbf{q}}_z(t) + \tilde{\mathbf{K}}_{ww}\tilde{\mathbf{q}}_w(t) + \tilde{\mathbf{C}}_{wz}\dot{\tilde{\mathbf{q}}}_z(t) + \tilde{\mathbf{C}}_{ww}\dot{\tilde{\mathbf{q}}}_w(t) = \mathbf{0} \tag{11}$$

where $\tilde{\mathbf{K}}_{wz} = \tilde{\mathbf{K}}_{zw}^T$, $\tilde{\mathbf{C}}_{wz} = \tilde{\mathbf{C}}_{zw}^T$.

The equation of the generalized Kelvin model written in the local coordinate system can be finally presented in the form:

$$\tilde{\mathbf{R}}_d(t) = \tilde{\mathbf{K}}_d\tilde{\mathbf{q}}_d(t) + \tilde{\mathbf{C}}_d\dot{\tilde{\mathbf{q}}}_d(t) \tag{12}$$

where $\tilde{\mathbf{R}}_d(t) = [\tilde{\mathbf{R}}_z(t), \ \mathbf{0}]^T$, $\tilde{\mathbf{q}}_d(t) = [\tilde{\mathbf{q}}_z(t), \ \tilde{\mathbf{q}}_w(t)]^T$,

$$\tilde{\mathbf{K}}_d = \begin{bmatrix} \tilde{\mathbf{K}}_{zz} & \tilde{\mathbf{K}}_{zw} \\ \tilde{\mathbf{K}}_{wz} & \tilde{\mathbf{K}}_{ww} \end{bmatrix}, \qquad \tilde{\mathbf{C}}_d = \begin{bmatrix} \tilde{\mathbf{C}}_{zz} & \tilde{\mathbf{C}}_{zw} \\ \tilde{\mathbf{C}}_{wz} & \tilde{\mathbf{C}}_{ww} \end{bmatrix} \tag{13}$$

A typical transformation of nodal parameters to the global coordinate system is used. The displacements of the damper's external nodes are transformed as usual but the internal variables of the damper are still defined in the local coordinate system. This means that the transformation matrix is:

$$\mathbf{T}_d = \begin{bmatrix} \tilde{\mathbf{T}}_d & \mathbf{0} \\ \mathbf{0} & \mathbf{I} \end{bmatrix} \tag{14}$$

where

$$\tilde{\mathbf{T}}_d = \begin{bmatrix} \tilde{\mathbf{T}} & \mathbf{0} \\ \mathbf{0} & \tilde{\mathbf{T}} \end{bmatrix}, \qquad \tilde{\mathbf{T}} = \begin{bmatrix} c & s \\ -s & c \end{bmatrix} \tag{15}$$

$c = \cos\beta$, $s = \sin\beta$, β is the angle between the global and the local coordinate systems and $\mathbf{I}$ is the $(m \times m)$ identity matrix.

The equation of the considered model, written in the global coordinate system, has the form:

$$\mathbf{R}_d(t) = \mathbf{K}_d\mathbf{q}_d(t) + \mathbf{C}_d\dot{\mathbf{q}}_d(t) \tag{16}$$

where

$$\mathbf{R}_d(t) = [\mathbf{R}_z(t), \ \ \mathbf{0}]^T = \mathbf{T}_d^T\tilde{\mathbf{R}}_d\mathbf{T}_d,$$
$$\mathbf{R}_z(t) = [R_1(t), \ R_2(t), \ R_3(t), \ R_4(t)]^T,$$
$$\mathbf{q}_d(t) = [\mathbf{q}_z(t), \ \ \mathbf{q}_w(t) = \tilde{\mathbf{q}}_w(t)]^T = \mathbf{T}_d^T\tilde{\mathbf{q}}_d\mathbf{T}_d,$$
$$\mathbf{q}_z(t) = [q_1(t), \ q_2(t), \ q_3(t), \ q_4(t)]^T$$

are the vector of nodal reactions and the vector of nodal parameters, respectively, written in the global coordinate system. The explicit forms of matrices $\mathbf{K}_d$ and $\mathbf{C}_d$ are given in Appendix A.

The equation of the generalized Maxwell model could be derived in a similar way. In the global coordinate system the equation mentioned above has the form of Equation (16) though with the matrices $\mathbf{K}_d$ and $\mathbf{C}_d$ as given in Appendix A.

Figure 5. A schematic of the fractional derivative Kelvin model

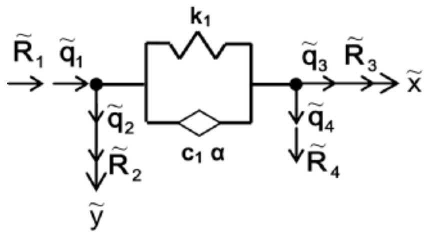

Many particular rheological models existing in the literature may be obtained by varying the number of elements in the generalized models mentioned above.

The fractional-derivative Kelvin model is shown in Figure 5. Its equation of motion can be written in the following form:

$$u(t) = k_1(\tilde{q}_3(t) - \tilde{q}_1(t)) + c_1 D_t^{\alpha}(\tilde{q}_3(t) - \tilde{q}_1(t)) \tag{17}$$

where the symbol $D_t^{\alpha}(\bullet)$ denotes the Riemann-Liouville fractional-derivative of the order α $(0 < \alpha \leq 1)$ with respect to time, *t*. Additional information concerning the Riemann-Liouville fractional-derivative is given in the book by Podlubny (1999).

The matrix equation of the fractional-derivative Kelvin model could be written, in the global coordinate system, in the form:

$$\mathbf{R}_d(t) = \mathbf{K}_d \mathbf{q}_d(t) + \mathbf{C}_d D_t^{\alpha} \mathbf{q}_d(t) \tag{18}$$

where, again, the matrices $\mathbf{K}_d$ and $\mathbf{C}_d$ are given in Appendix A.

The fractional-derivative Maxwell model of a VE damper is shown in Figure 6. Its equations of motion can be written in the following form:

$$u_s(t) = k_1(\tilde{q}_w(t) - \tilde{q}_1(t)),$$
$$u_d(t) = c_1 D_t^{\alpha}(\tilde{q}_3(t) - \tilde{q}_w(t)) \tag{19}$$

where the symbols $u_s(t)$ and $u_d(t)$ denote force in the spring and the dashpot, respectively.

Proceeding as described above, the matrix equation of the fractional-derivative Maxwell model written in the global coordinate system is obtained. The equation has the form of Equation (18) where the vector $\mathbf{q}_d(t)$ and matrices $\mathbf{K}_d$ and $\mathbf{C}_d$ are as defined in Appendix A.

EQUATIONS OF MOTION FOR A STRUCTURE WITH VE DAMPERS

Equation of Motion for a Structure with VE Dampers Modelled Using Classical Rheological Models

Plane frame structures, treated as elastic systems with VE dampers, are modelled using the finite element method. A two-node bar element with six nodal parameters is used to describe the structure. The mass and stiffness matrices together with the vector of nodal forces of the element can be found in many sources. The equation of motion of a structure with VE dampers modelled using the generalized rheological models can be written in the following form:

$$\mathbf{M}_{ss}\ddot{\mathbf{q}}_s(t) + \mathbf{C}_{ss}\dot{\mathbf{q}}_s(t) + \mathbf{C}_{sd}\dot{\mathbf{q}}_d(t) + \mathbf{K}_{ss}\mathbf{q}_s(t) + \mathbf{K}_{sd}\mathbf{q}_d(t) = \mathbf{p}_s(t) \tag{20}$$

$$\mathbf{C}_{ds}\dot{\mathbf{q}}_s(t) + \mathbf{C}_{dd}\dot{\mathbf{q}}_d(t) + \mathbf{K}_{ds}\mathbf{q}_s(t) + \mathbf{K}_{dd}\mathbf{q}_d(t) = \mathbf{0} \tag{21}$$

where the symbols $\mathbf{M}_{ss}$, $\mathbf{C}_{ss}$, $\mathbf{C}_{sd} = \mathbf{C}_{ds}^T$, $\mathbf{C}_{dd}$, $\mathbf{K}_{ss}$, $\mathbf{K}_{sd} = \mathbf{K}_{ds}^T$ and $\mathbf{K}_{dd}$ denote the global mass, damping and stiffness matrices of the system (i.e., structure with dampers), respectively. The dimension of the matrices $\mathbf{M}_{ss}$, $\mathbf{C}_{ss} = \mathbf{C}_{ss}^{(s)} + \mathbf{C}_{ss}^{(d)}$ and $\mathbf{K}_{ss} = \mathbf{K}_{ss}^{(s)} + \mathbf{K}_{ss}^{(d)}$ is $(n \times n)$. The matrices $\mathbf{M}_{ss}$, $\mathbf{C}_{ss}^{(s)}$ and $\mathbf{K}_{ss}^{(s)}$ describe the inertia, damping and elastic properties of the structure without

Figure 6. A schematic of the fractional derivative Maxwell model

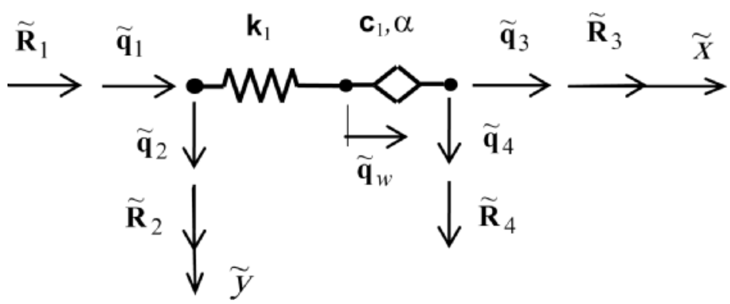

dampers, while the matrices $\mathbf{C}_{ss}^{(d)}$, $\mathbf{K}_{ss}^{(d)}$ and the ($n \times r$) matrices $\mathbf{C}_{sd} = \mathbf{C}_{ds}^T$, $\mathbf{K}_{sd} = \mathbf{K}_{ds}^T$ represent the effect of the coupling of dampers with the structure. The ($r \times r$) matrices $\mathbf{C}_{dd}$ and $\mathbf{K}_{dd}$ describe the damping and stiffness properties of dampers with braces, respectively. Moreover, $\mathbf{q}_s(t)$, $\mathbf{q}_d(t)$ and $\mathbf{p}_s(t)$ are the global vectors of nodal generalized displacements, internal variables and nodal excitation forces, respectively. The concept of proportional damping is used to model the damping properties of the structure, i.e.: $\mathbf{C}_{ss}^{(s)} = \alpha\ \mathbf{M}_{ss} + \kappa\ \mathbf{K}_{ss}^{(s)}$ where α and κ are proportionality factors.

The equation of motion, written in terms of state variables, will also be useful. After introducing the following state vector $\mathbf{x}(t) = [\mathbf{q}_s(t),\ \ \dot{\mathbf{q}}_s(t),\ \ \mathbf{q}_d(t)]^T$ the following state equation could be written

$$\mathbf{A}\dot{\mathbf{x}}(t) + \mathbf{B}\mathbf{x}(t) = \mathbf{s}(t) \tag{22}$$

where

$$\mathbf{A} = \begin{bmatrix} \mathbf{C}_{ss} & \mathbf{M}_{ss} & \mathbf{C}_{sd} \\ \mathbf{M}_{ss} & \mathbf{0} & \mathbf{0} \\ \mathbf{C}_{ds} & \mathbf{0} & \mathbf{C}_{dd} \end{bmatrix},$$

$$\mathbf{B} = \begin{bmatrix} \mathbf{K}_{ss} & \mathbf{0} & \mathbf{K}_{sd} \\ \mathbf{0} & -\mathbf{M}_{ss} & \mathbf{0} \\ \mathbf{K}_{ds} & \mathbf{0} & \mathbf{K}_{dd} \end{bmatrix},$$

$$\mathbf{s}(t) = \begin{Bmatrix} \mathbf{p}(t) \\ \mathbf{0} \\ \mathbf{0} \end{Bmatrix} \tag{23}$$

If the structure with VE dampers modelled using the simple Maxwell model is considered, then all of the relationships presented above are valid, provided that the appropriate matrices given in Appendix A are used to generate the global matrices appearing in Equations (20) and (21).

In the case of the structure with dampers modelled by the simple Kelvin model, the equation of motion (20) takes the form:

$$\begin{aligned} &\mathbf{M}_{ss}\ddot{\mathbf{q}}_s(t) + (\mathbf{C}_{ss} + \mathbf{C}_{dd})\ \dot{\mathbf{q}}_s(t) \\ &+(\mathbf{K}_{ss} + \mathbf{K}_{dd})\ \mathbf{q}_s(t) = \mathbf{p}_s(t) \end{aligned} \tag{24}$$

because internal variables do not exist.

The matrices $\mathbf{C}_{dd}$ and $\mathbf{K}_{dd}$ appearing in (24) are built from the matrices $\mathbf{C}_d$ and $\mathbf{K}_d$ given by Equation (A.12). The state equation has the form of Equation (20) where now

$$\mathbf{x}(t) = \begin{Bmatrix} \mathbf{q}_s(t) \\ \dot{\mathbf{q}}_s(t) \end{Bmatrix},$$

$$\mathbf{A} = \begin{bmatrix} \mathbf{C}_{ss} + \mathbf{C}_{dd} & \mathbf{M}_{ss} \\ \mathbf{M}_{ss} & \mathbf{0} \end{bmatrix},$$

$$\mathbf{B} = \begin{bmatrix} \mathbf{K}_{ss} + \mathbf{K}_{dd} & \mathbf{0} \\ \mathbf{0} & -\mathbf{M}_{ss} \end{bmatrix},$$

$$\mathbf{s}(t) = \begin{Bmatrix} \mathbf{p}(t) \\ \mathbf{0} \end{Bmatrix} \tag{25}$$

The solution to the homogenous state equation, i.e., when $\mathbf{s}(t) = \mathbf{0}$ in (22), is assumed to be in the form:

$$\mathbf{x}(t) = \mathbf{a} \ \exp(st) \tag{26}$$

This leads to the following linear eigenvalue problem:

$$(s\mathbf{A} + \mathbf{B})\ \mathbf{a} = \mathbf{0} \tag{27}$$

from which the $(2n + r)$ eigenvalues s_i and eigenvectors $\mathbf{a}_i$ can be determined. In the case of an undercritically damped structure, the $2n$ eigenvalues (eigenvectors) are complex and conjugate numbers (vectors) while the remaining r eigenvalues (eigenvectors) are real numbers (vectors).

The frame with VE dampers is characterized by the natural frequencies ω_i and the non-dimensional damping parameters γ_i. The above-mentioned quantities are defined as:

$$\omega_i^2 = \mu_i^2 + \eta_i^2, \qquad \gamma_i = -\mu_i / \omega_i \tag{28}$$

where $\mu_i = \mathrm{Re}(s_i)$, $\eta_i = \mathrm{Im}(s_i)$. Equation (28) refer to complex eigenvalues only.

The considered system can also be characterized by the frequency response functions. To determine these functions the steady state harmonic responses of the system are considered. If the excitation forces vary harmonically in time, i.e., when

$$\mathbf{p}(t) = \mathbf{P}\exp(\mathrm{i}\lambda t) \tag{29}$$

then the steady state response of the structure and the vector of internal variables can be expressed as

$$\mathbf{q}_s(t) = \mathbf{Q}_s \exp(\mathrm{i}\lambda t),$$
$$\mathbf{q}_d(t) = \mathbf{Q}_d \exp(\mathrm{i}\lambda t) \tag{30}$$

After substituting relationships (29) and (30) into Equations (20) and (21), the following relationships are obtained:

$$\mathbf{D}_{ss}(\lambda)\mathbf{Q}_s(\lambda) + \mathbf{D}_{sd}(\lambda)\mathbf{Q}_d(\lambda) = \mathbf{P},$$

$$\mathbf{D}_{ds}(\lambda)\mathbf{Q}_s(\lambda) + \mathbf{D}_{dd}(\lambda)\mathbf{Q}_d(\lambda) = \mathbf{0} \tag{31}$$

where

$$\mathbf{D}_{ss}(\lambda) = -\lambda^2\mathbf{M}_{ss} + \mathrm{i}\lambda\ \mathbf{C}_{ss} + \mathbf{K}_{ss},$$
$$\mathbf{D}_{sd}(\lambda) = \mathrm{i}\lambda\ \mathbf{C}_{sd} + \mathbf{K}_{sd},$$
$$\mathbf{D}_{ds}(\lambda) = \mathrm{i}\lambda\ \mathbf{C}_{ds} + \mathbf{K}_{ds},$$
$$\mathbf{D}_{dd}(\lambda) = \mathrm{i}\lambda\ \mathbf{C}_{dd} + \mathbf{K}_{dd} \tag{32}$$

Finally, it is possible to write the relationships

$$\mathbf{Q}_s(\lambda) = \mathbf{H}_{ss}(\lambda)\mathbf{P},$$
$$\mathbf{Q}_d(\lambda) = \mathbf{H}_{ds}(\lambda)\mathbf{P} \tag{33}$$

where the frequency response functions $\mathbf{H}_{ss}(\lambda)$ and $\mathbf{H}_{rd}(\lambda)$ could be written in the following form:

$$\mathbf{H} \equiv \mathbf{H}_{ss}(\lambda) = \left[\mathbf{D}_{ss}(\lambda) - \mathbf{D}_{sd}(\lambda)\mathbf{D}_{dd}^{-1}\mathbf{D}_{ds}(\lambda)\right]^{-1},$$

$$\mathbf{H}_{ds}(\lambda) = -\mathbf{D}_{dd}^{-1}(\lambda)\mathbf{D}_{ds}(\lambda)\mathbf{H}_{ss}(\lambda)$$
$$= -\mathbf{D}_{dd}^{-1}(\lambda)\mathbf{D}_{ds}(\lambda)\left[\mathbf{D}_{ss}(\lambda) - \mathbf{D}_{sd}(\lambda)\mathbf{D}_{dd}^{-1}\mathbf{D}_{ds}(\lambda)\right]^{-1} \tag{34}$$

When the structure is subjected to base acceleration $\ddot{u}_g(t)$, the excitation vector is written as $\mathbf{p}(t) = -\mathbf{M}\ \mathbf{r}\ \ddot{u}_g(t)$, where $\mathbf{r}$ is the influence vector with values 0 or 1. For harmonic external forces, we have $\ddot{u}_g(t) = \ddot{U}_g \exp(i\lambda t)$, where $\ddot{U}_g$ is the amplitude of base acceleration. The displacement response of the structure is given by relationship (30), and $\mathbf{Q}_s(\lambda)$ is determined from:

$$\mathbf{Q}_s(\lambda) = \tilde{\mathbf{H}}(\lambda)\ddot{U}_g \tag{35}$$

where the vector $\tilde{\mathbf{H}}(\lambda) = -\mathbf{H}(\lambda)\mathbf{M}\mathbf{r}$ will be called the vector of frequency transfer functions of displacements caused by kinematic excitation.

Equation of Motion for a Structure with VE Dampers Modelled Using Fractional Rheological Models

If the dampers are modelled using the fractional derivative Maxwell model, then the equation of motion of structures with dampers could be written in the form (see also the paper by Lewandowski and Pawlak 2010):

$$\begin{aligned}&\mathbf{M}_{ss} D_t^2 \mathbf{q}_s(t) + \mathbf{C}_{ss} D_t^1 \mathbf{q}_s(t)\\ &+\mathbf{C}_{ss}^d D_t^\alpha \mathbf{q}_s(t) + (\mathbf{K}_{ss} + \mathbf{K}_{ss}^d)\ \mathbf{q}_s(t)\\ &+\ \mathbf{C}_{sd}^d D_t^\alpha \mathbf{q}_d(t) - \mathbf{K}_{sd}^d \mathbf{q}_d(t) = \mathbf{p}(t)\end{aligned} \tag{36}$$

$$\begin{aligned}&\mathbf{C}_{ds}^d D_t^\alpha \mathbf{q}_s(t) + \mathbf{C}_{dd}^d D_t^\alpha \mathbf{q}_d(t)\\ &-\mathbf{K}_{ds}^d \mathbf{q}_s(t) + \mathbf{K}_{dd}^d \mathbf{q}_d(t) = \mathbf{0}\end{aligned} \tag{37}$$

where the symbols $D_t^2 \mathbf{q}_s(t) = \ddot{\mathbf{q}}_s(t)$ and $D_t^1 \mathbf{q}_s(t) = \dot{\mathbf{q}}_s(t)$ are used in order to be consistent with the notation. Here, it is assumed that for all dampers the values of the parameter α are identical.

The equations of motion in the state space can also be derived for a structure with dampers modelled by the fractional derivative Maxwell model. In this case, the vector of state variables and the vectors of state variables' derivatives are defined as:

$$\begin{aligned}&\mathbf{z}(t) = [\mathbf{q}_d(t),\quad \mathbf{q}_s(t),\quad D_t^1\mathbf{q}_s(t)]^T,\\ &D_t^1\mathbf{z}(t) = [D_t^1\mathbf{q}_d(t),\quad D_t^1\mathbf{q}_s(t),\quad D_t^2\mathbf{q}_s(t)]^T,\\ &D_t^\alpha\mathbf{z}(t) = [D_t^\alpha\mathbf{q}_d(t),\quad D_t^\alpha\mathbf{q}_s(t),\quad D_t^{\alpha+1}\mathbf{q}_s(t)]^T\end{aligned} \tag{38}$$

The equation of motion written in state space takes the form:

$$\mathbf{A}\ D_t^1\mathbf{z}(t) + \mathbf{A}_1 D_t^\alpha \mathbf{z}(t) + \mathbf{B}\mathbf{z}(t) = \tilde{\mathbf{p}}(t) \tag{39}$$

where

$$\mathbf{A} = \begin{bmatrix} \mathbf{0} & \mathbf{0} & \mathbf{0}\\ \mathbf{0} & \mathbf{C}_{ss} & \mathbf{M}_{ss}\\ \mathbf{0} & \mathbf{M}_{ss} & \mathbf{0}\end{bmatrix},\ \mathbf{A}_1 = \begin{bmatrix} \mathbf{C}_{dd}^d & \mathbf{C}_{ds}^d & \mathbf{0}\\ \mathbf{C}_{sd}^d & \mathbf{C}_{ss}^d & \mathbf{0}\\ \mathbf{0} & \mathbf{0} & \mathbf{0}\end{bmatrix},$$
$$\mathbf{B} = \begin{bmatrix} \mathbf{K}_{dd}^d & -\mathbf{K}_{ds}^d & \mathbf{0}\\ -\mathbf{K}_{sd}^d & \mathbf{K}_{sd} + \mathbf{K}_{ss}^d & \mathbf{0}\\ \mathbf{0} & \mathbf{0} & -\mathbf{M}_{sd}\end{bmatrix},\ \tilde{\mathbf{p}}(t) = \begin{Bmatrix} \mathbf{0}\\ \mathbf{p}(t)\\ \mathbf{0}\end{Bmatrix} \tag{40}$$

In the case of a structure with dampers modelled using the fractional-derivative Kelvin model the equation of motion can be written in the form (see also the paper by Lewandowski and Pawlak 2010):

$$\begin{aligned}&\mathbf{M}_{ss} D_t^2 \mathbf{q}_s(t) + \mathbf{C}_{ss} D_t^1 \mathbf{q}_s(t) + \mathbf{C}_{dd} D_t^\alpha\ \ \mathbf{q}_s(t)\\ &+(\mathbf{K}_{ss} + \mathbf{K}_{dd})\ \mathbf{q}_s(t) = \mathbf{p}_s(t)\end{aligned} \tag{41}$$

Thus, the state equation is:

$$\mathbf{A}\ D_t^1\mathbf{z}(t) + \mathbf{A}_1 D_t^\alpha \mathbf{z}(t) + \mathbf{B}\mathbf{z}(t) = \mathbf{s}(t) \tag{42}$$

where $\mathbf{z}(t) = [\mathbf{q}_s(t),\ D_t^1\mathbf{q}_s(t)]^T$,
$\mathbf{s}(t) = [\mathbf{p}_s(t),\ \mathbf{0}]^T$,

$$\mathbf{A} = \begin{bmatrix} \mathbf{C}_{ss} & \mathbf{M}_{ss} \\ \mathbf{M}_{ss} & \mathbf{0} \end{bmatrix},\quad \mathbf{A}_1 = \begin{bmatrix} \mathbf{C}_{dd} & \mathbf{0} \\ \mathbf{0} & \mathbf{0} \end{bmatrix},$$

$$\mathbf{B} = \begin{bmatrix} \mathbf{K}_{ss} + \mathbf{K}_{dd} & \mathbf{0} \\ \mathbf{0} & -\mathbf{M}_{ss} \end{bmatrix} \tag{43}$$

The eigenvalue problem, which can be solved to determine the eigenvalue s and the eigenvector **a**, is nonlinear and has the following form:

$$(s\mathbf{A} + s^{\alpha}\mathbf{A}_1 + \mathbf{B})\ \mathbf{a} = \mathbf{0} \tag{44}$$

The above nonlinear eigenvalue problem can be solved using the continuation method described by Lewandowski and Pawlak (2010). Moreover, relationships (28) can be used to determine the natural frequencies and non-dimensional damping ratios.

For the fractional derivative Kelvin model of dampers, the frequency response functions are defined as:

$$\mathbf{H}(\lambda) = \left[-\lambda^2\mathbf{M}_{ss} + \mathrm{i}\lambda\mathbf{C}_{ss} + (\mathrm{i}\lambda)^{\alpha}\mathbf{C}_{dd} + \mathbf{K}_{ss} + \mathbf{K}_{dd}\right]^{-1} \tag{45}$$

The shear frame model is also used as a structure model in this chapter. The detailed derivation of the equation of motion is given by Lewandowski and Pawlak (2010). The final form of the equation of motion, the eigenvalue problem and the matrix of transfer functions can be written in the form of relationships (41), (42), (44) and (45), respectively.

In the case of a structure with the fractional derivative Maxwell dampers, after substituting relationships (29) and (30) into Equations (36) and (37), the following relationships are obtained:

$$\mathbf{D}_{ss}(\lambda)\mathbf{Q}_s(\lambda) + \mathbf{D}_{sd}(\lambda)\mathbf{Q}_d(\lambda) = \mathbf{P},$$

$$\mathbf{D}_{ds}(\lambda)\mathbf{Q}_s(\lambda) + \mathbf{D}_{dd}(\lambda)\mathbf{Q}_d(\lambda) = \mathbf{0} \tag{46}$$

where

$$\begin{aligned}
\mathbf{D}_{ss}(\lambda) &= -\lambda^2\mathbf{M}_{ss} + \mathrm{i}\lambda\mathbf{C}_{ss} + (\mathrm{i}\lambda)^{\alpha}\mathbf{C}^d_{ss} + \mathbf{K}_{ss} + \mathbf{K}^d_{ss},\\
\mathbf{D}_{sd}(\lambda) &= (\mathrm{i}\lambda)^{\alpha}\mathbf{C}^d_{sd} - \mathbf{K}^d_{sd},\\
\mathbf{D}_{ds}(\lambda) &= (\mathrm{i}\lambda)^{\alpha}\mathbf{C}^d_{ds} - \mathbf{K}^d_{ds},\\
\mathbf{D}_{dd}(\lambda) &= (\mathrm{i}\lambda)^{\alpha}\mathbf{C}^d_{dd} + \mathbf{K}^d_{dd}
\end{aligned} \tag{47}$$

Finally, it is possible to write the relationships

$$\mathbf{Q}_s(\lambda) = \mathbf{H}_{ss}(\lambda)\mathbf{P},\ \mathbf{Q}_d(\lambda) = \mathbf{H}_{ds}(\lambda)\mathbf{P} \tag{48}$$

where the frequency response functions $\mathbf{H}_{ss}(\lambda)$ and $\mathbf{H}_{rd}(\lambda)$ could be written in the following form:

$$\mathbf{H} \equiv \mathbf{H}_{ss}(\lambda) = \left[\mathbf{D}_{ss}(\lambda) - \mathbf{D}_{sd}(\lambda)\mathbf{D}^{-1}_{dd}\mathbf{D}_{ds}(\lambda)\right]^{-1},$$

$$\begin{aligned}
\mathbf{H}_{ds}(\lambda) &= -\mathbf{D}^{-1}_{dd}(\lambda)\mathbf{D}_{ds}(\lambda)\mathbf{H}_{ss}(\lambda) = \\
&-\mathbf{D}^{-1}_{dd}(\lambda)\mathbf{D}_{ds}(\lambda)\left[\mathbf{D}_{ss}(\lambda) - \mathbf{D}_{sd}(\lambda)\mathbf{D}^{-1}_{dd}\mathbf{D}_{ds}(\lambda)\right]^{-1}
\end{aligned} \tag{49}$$

The vector $\mathbf{H}_d(\lambda)$ of the frequency transfer functions of interstorey drifts can be calculated from the following formula:

$$\mathbf{H}_d(\lambda) = \mathbf{T}\ \mathbf{H}(\lambda) \tag{50}$$

where $\mathbf{T}$ is the transformation matrix. In the case of a share frame, the transformation matrix is:

$$\mathbf{T} = \begin{bmatrix} 1 & 0 & 0...0 & 0 & 0 \\ -1 & 1 & 0...0 & 0 & 0 \\ \cdots & \cdots & \cdots & \cdots & \cdots \\ 0 & 0 & 0...0 & -1 & 1 \end{bmatrix} \tag{51}$$

When the structure is subjected to base acceleration $\ddot{u}_g(t)$, the excitation vector is written as $\mathbf{p}(t) = -\mathbf{M}\ \mathbf{r}\ \ddot{u}_g(t)$, where $\mathbf{r}$ is the influence vector with values 0 or 1. For harmonic external forces, we have $\ddot{u}_g(t) = \ddot{U}_g \exp(i\lambda t)$, where $\ddot{U}_g$ is the amplitude of base acceleration. The displacement response of the structure is given by relationship (30), and $\mathbf{Q}_s(\lambda)$ is determined from:

$$\mathbf{Q}_s(\lambda) = \tilde{\mathbf{H}}(\lambda)\ddot{U}_g \tag{52}$$

where the vector $\tilde{\mathbf{H}}(\lambda) = -\mathbf{H}(\lambda)\mathbf{M}\mathbf{r}$ will be called the vector of frequency transfer functions of displacements caused by kinematic excitation.

NUMERICAL EXAMPLES

Four examples are presented in this section to illustrate several aspects of the considered optimization problem. Among others, one aim of all the examples is to illustrate the possibility of reduction of vibrations of frame structures with the help of VE dampers. In the chapter a few structures are analyzed in order to enlarge the diversity of the considered problems.

Optimal Placement of Dampers for Frame Structures: Classical Rheological Models of Dampers

The first example shows the influence of dampers on dynamic characteristics of structure. The main objective of the second example is to show that dynamic characteristics of a structure with dampers, modelled using two different rheological models of dampers is practically identical if both models have approximately equal possibilities to dissipate energy. A frame very similar to the one analyzed in Example 1 is considered in Example 3. However, the structure is now analyzed in a time domain and the optimal location of dampers is found for structures loaded by forces excited by one specific earthquake (El Centro). Moreover, the objective function is different. Now the maximal peak values of the bending moment in columns is the objective function. The aim of this example and Example 1 is to show how different can be the optimal solution for various objective functions.

Example 1: An Eight-Storey Frame

An eight-storey RC frame with three bays is selected for which the optimized position of VE dampers and the optimal parameters of dampers are determined. The frame is designed according to the requirements of EC8 Part 1 for Class B (stiff soils). The height of the columns is 3.0 m, the span of the beams is 5.0 m and Young's modulus for concrete is 31.0 GPa. The dimensions of the cross-section of structural elements are presented in Table 1 while the unit masses of the frame elements are given in Table 2. The frame is treated as a planar structure. The axial deformations and internal damping of the structure are neglected. However, the internal damping of structure can be taken into account assuming that the damping matrix is in the form $\mathbf{C} = a_0\mathbf{M} + a_1\mathbf{K}$, where a_0 and a_1 are some constant (see Chopra (2000) for details). In this example, internal damping of structure is neglected because our aim is to show the influence of dampers on dynamic characteristics of structure only. Of course, in real structures more or less internal damping always exists and it enlarges the modal damping ratios of structures.

It is assumed that the dampers could be placed on all the floors of the structure, in the middle bay. The dampers are modelled using the generalized models with seven parameters. In this example we introduce the comparative damper for which the storage and loss modulus are calculated from the formulae:

Table 1. Dimensions of the eight-storey frame elements

Storey	Lateral column [cm]	Central column [cm]	Beams [cm]
7, 8	35×35	40×40	30×40
5, 6	40×40	45×45	30×45
3, 4	45×45	53×53	30×50
1, 2	50×50	60×60	30×50

Table 2. Unit mass of the eight-storey frame elements

Storey	Unit lateral column mass [kg/m]	Unit central column mass [kg/m]	Unit beam mass [kg/m]
7, 8	306.2	400.0	15000.0
5, 6	400.0	506.2	15000.0
3, 4	506.2	702.2	15000.0
1, 2	625.0	900.0	15000.0

Table 3. Parameters of generalized Kelvin and Maxwell models

Stiffness [MN/m]			Damping factor [MN sec/m]		
	Kelvin model	Maxwell model		Kelvin model	Maxwell model
k_0	57.650	0.1065		–	–
k_1	18.350	33.385	c_1	2.729	1.478
k_2	6.160	3.310	c_2	6.190	1.732
k_3	0.5545	1.443	c_3	8.675	8.305

$$K'(\lambda) = k + c\lambda^{\alpha}\cos(\alpha\pi / 2),$$
$$K''(\lambda) = c\lambda^{\alpha}\sin(\alpha\pi / 2) \tag{53}$$

The expressions (53) are analytical formulae for the fractional-derivative Kelvin model of dampers. The chosen parameters of the fractional-derivative Kelvin model are $\alpha = 0.63$, $k = 0.4\times10^{6}\,\mathrm{N/m}$, and $c = 3.6\times10^{6}\,\mathrm{Nsec}^{\alpha}/\mathrm{m}$. The value of the parameter α is similar to the one used by Chang and Singh (2009) and by Singh and Chang (2009) except that the original values of *k* and *c* are divided by 2.0.

In the paper by Chang and Singh (2009), the parameters of generalized models are obtained by minimizing the mean square norm of the differences between the targeted modules and analytical modules of the considered model. The parameters of the generalized Kelvin model (which are used in this example) and the generalized Maxwell model (which will be used in Example 2), both with seven parameters, are given in Table 3.

The energy dissipated by the damper is calculated by assuming that a damper executes harmonically varying vibrations. This energy can be calculated using the following formula:

$$E_d = \int_0^T u(t)\dot{x}(t)dt \tag{54}$$

where *T* is the period of excitation and *x(t)* is the relative displacement of damper, i.e., the difference between displacements of the right and the left end of damper, respectively.

The amplitude of displacements is equal to 0.01 m in all of the considered cases. A comparison of dissipated energy calculated for the considered models of a VE damper is shown in Figure 7. From this calculation, it may be concluded that the dissipation energies of the fractional-derivative Kelvin model and both generalized models are approximately equal in the range 0 – 15.0 rad/sec of excitation frequency. This range of frequency covers the range of the first three natural frequencies of vibration of the con-

Figure 7. Comparison of dissipated energy

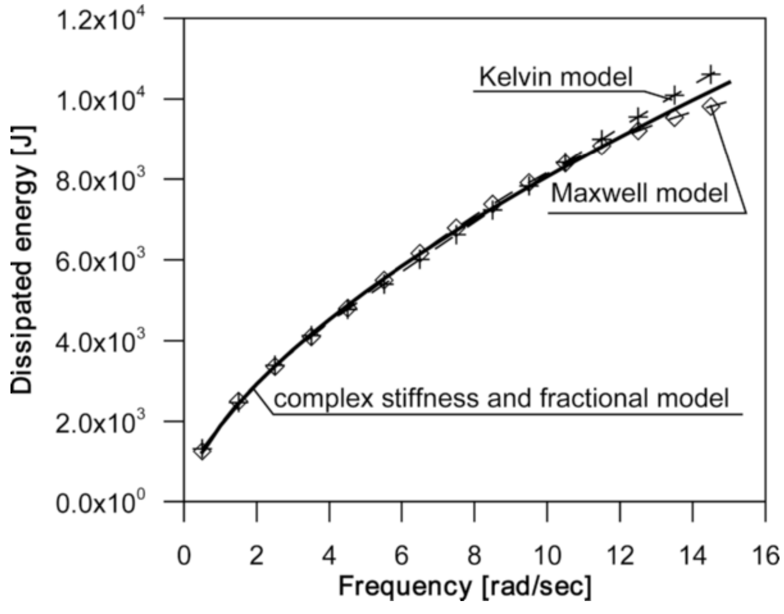

sidered structure. Chevron braces are used to connect the dampers with the structure. The braces are made of wide flange beams HEB 200 stainless steel profiles of which the parameters are: $EA = 1.60105 \times 10^9$ N and $EJ = 1.1685 \times 10^7$ Nm^2, where *E, A*, and *J* is the Young's modulus, the area of the cross section, and the moment of inertia of the cross section, respectively.

Here, the objective function is the maximum value of the modulus of the transfer function of horizontal displacement for the top floor, evaluated at the fundamental natural frequency of the frame with dampers. This function is the appropriate element of vector $\tilde{\mathbf{H}}(\lambda) = -\mathbf{H}(\lambda)\mathbf{Mr}$ defined above. The values of weight coefficients are equal to zero except for one of them, which is equal to 1. The modulus of transfer function of different kinds was widely used in the objective function considered by Takewaki (2009). It is assumed that the value of the main damping factor is $c_{d,3} = 8.675$ MNs/m and that the total capacity of the dampers is $C_d = 69.4$ MNs/m. This means that the eight dampers must be optimally located within the structure. Moreover, $c_{\min} = 0.0$. The sequential optimization method is used to determine the optimal position of the dampers. As a result of the optimization procedure, an almost uniform distribution of the dampers is obtained, i.e., there are no dampers on the first and eighth storeys, there are two dampers each on the third and fifth storeys and only one damper is located on each of the other storeys. The sequence of successive optimal position of dampers was obtained as follows: the first damper on the fifth storey, the second damper on the third storey, the third damper on the sixth storey, the fourth damper on the third storey, the fifth damper on the fourth storey, the seventh damper on the seventh storey, the sixth damper on the second storey and the eighth damper on the fifth storey. The effect of introduction of VE dampers is shown in Figure 8, where the top floor displacement of frame versus a number of dampers is presented. A significant reduction of displacement is visible. Introduction of the first few dampers is the most effective. At the end of the optimization process

Figure 8. Top floor displacement versus number of added dampers

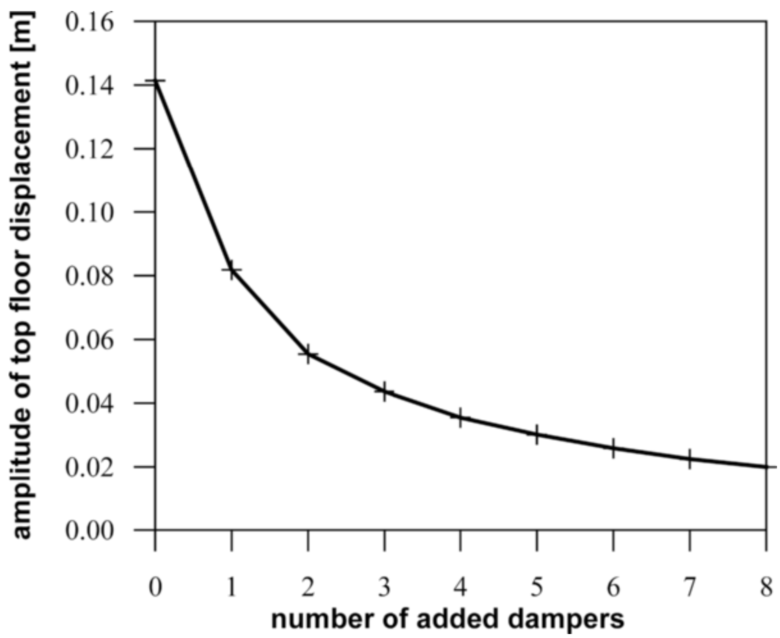

the modulus of the considered transfer function is calculated for a range of excitation frequencies which contains the first few natural frequencies of the structure. The results clearly show that the maximal value of this function is still at the fundamental natural frequency of the structure.

Example 2: A Four-Storey Shear Frame

As the second example, the four-storey shear frame analyzed by Singh and Chang (2009) is considered. The following data are used: the storey stiffness $k_1 = 18.0\ \mathrm{MN/m}$, $k_2 = k_3 = 12.0\ \mathrm{MN/m}$, $k_4 = 10.0\ \mathrm{MN/m}$, the floor masses $m_1 = m_2 = 40.0\ \mathrm{Mg}$, $m_3 = m_4 = 36.0\ \mathrm{Mg}$. The first two non-dimensional damping ratios of frame without dampers, used to calculate the damping matrix of the frame, are $\gamma_1 = \gamma_2 = 0.02$. The generalized Kelvin and Maxwell models are used as the VE damper models. The parameters of both models are twice as high as the ones shown in Table 3. One damper is located on the first storey of the frame. The energy dissipated in both damper models is almost identical to that shown in Figure 7. The horizontal stiffness of the brace is $k_b = 184.3\ \mathrm{MN/m}$. The structure is loaded by harmonically varied displacements of supports, i.e., $u_g(t) = U_g \sin \lambda t$ for $0 \le t \le 4.72\ \mathrm{sec}$ and $u_g(t) = 0$ for $t > 4.72\ \mathrm{sec}$, where $U_g = 0.01\ \mathrm{m}$ and $\lambda = 6.663\ \mathrm{rad/sec}$. The equations of motion are solved with the help of average acceleration ver-

Table 4. Logarithmic decrements of damping of frame with VE dampers

	Generalized Kelvin model	Generalized Maxwell model
Logarithmic decrement of damping	0.178	0.171
Peak value of displacement [cm]	10.21	10.25
Peak value of acceleration [m/s^2]	4.62	4.63

sion of the Newmark method. The chosen parameters of the Newmark method are: $\gamma = 0.5$ and $\beta = 0.25$ (see book by Chopra (2000)).

It is the main objective of this example to show that some dynamic characteristics of a structure with dampers, modelled using the above mentioned models is practically identical if both models possess approximately equal possibilities to dissipate energy. This conclusion is supported by the results presented in Table 4. This table contains logarithmic decrements of damping and the peak values of displacements and accelerations of the fourth-floor, calculated from the obtained solutions to the equations of motion for both damper models.

Example 3: An Eight-Storey Frame

A frame very similar to the one presented in Example 1 is considered. Here, the frame with granulated masses is taken into account, with masses concentrated at the floor levels. The value of every mass is 225.0 Mg. The first two non-dimensional damping ratios of frame without dampers, used to calculate the damping matrix of the frame, are $\gamma_1 = \gamma_2 = 0.02$. The generalized Kelvin model is used as the model of VE damper. The model parameters are sixteen times as great as the ones shown in Table 3. It is assumed that ten dampers are located on the frame. The chevron braces used are as the ones described in Example 1.

The structure is loaded with forces caused by the horizontal North South component of the El Centro earthquake (Peknold Version). The commercial program Autodesk® Robot™ Structural Analysis (2010) is used to solve the equations of motion with the help of the average acceleration version of the Newmark method.

The sequential optimization method is used to solve the optimization problem. The maximal peak value of the bending moments in columns is chosen as the objective function.

As the result of the optimization procedure, the following distributions of dampers are obtained: there are six dampers on the first storey, four dampers on the second storey, one damper on the sixth storey, and two dampers on the seventh storey. The sequence of the successive optimal positions of dampers was obtained as follows: the first damper on the sixth storey, the second damper on the seventh storey, the third damper on the first storey, the fourth damper on the second storey, and the remaining five dampers are located on the first storey.

In Figure 9, the peak values of the bending moments for columns on all storeys are presented. The results of calculation for three cases are presented: i) the dampers in the optimal positions, ii) all dampers are on the first storey, and iii) the dampers are uniformly distributed on the frame. In the last case, there are eight dampers within the structure but the parameters of a single damper are 1.25 times as great as in the other cases. Results for all of the considered cases are shown by the bar with forward slashes, the bar with diagonal crosses, and the bar with backward slashes, respectively. It is easy to notice that the peak values of the bending moments for all storeys are greater in the case 2. Comparing the results for cases 1 and 3, it can be seen that the peak values of the bending moment for the first storey are smaller in the case 1, but on the higher storeys, these peak values of the bending moments are smaller in the case 3.

Because the algorithm of sequential optimization method is very simple in Example 1 and 3 all steps of this algorithm were done using Excel or manually except the calculation of the values of objective function.

A similar comparison between the peak values of the horizontal displacements of floors is presented, in the same manner, in Figure 10. The peak values of horizontal displacement obtained for the frame with the optimal distribution of dampers are greater than those for the frame with uniformly distributed dampers and smaller than

Figure 9. Peak values of bending moments for different configurations of dampers

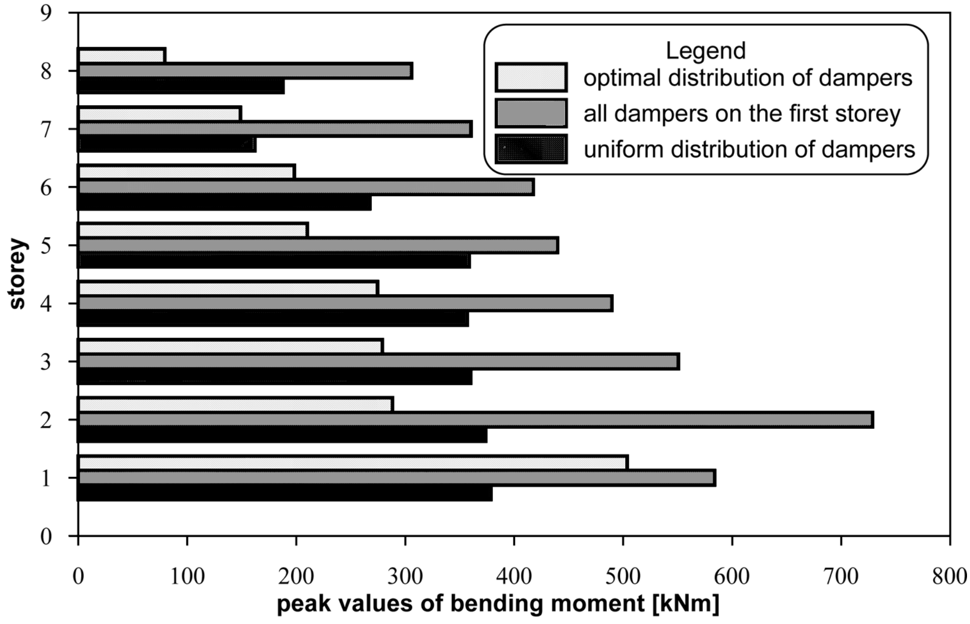

Figure 10. Peak values of horizontal displacements of storeys for different configurations of dampers

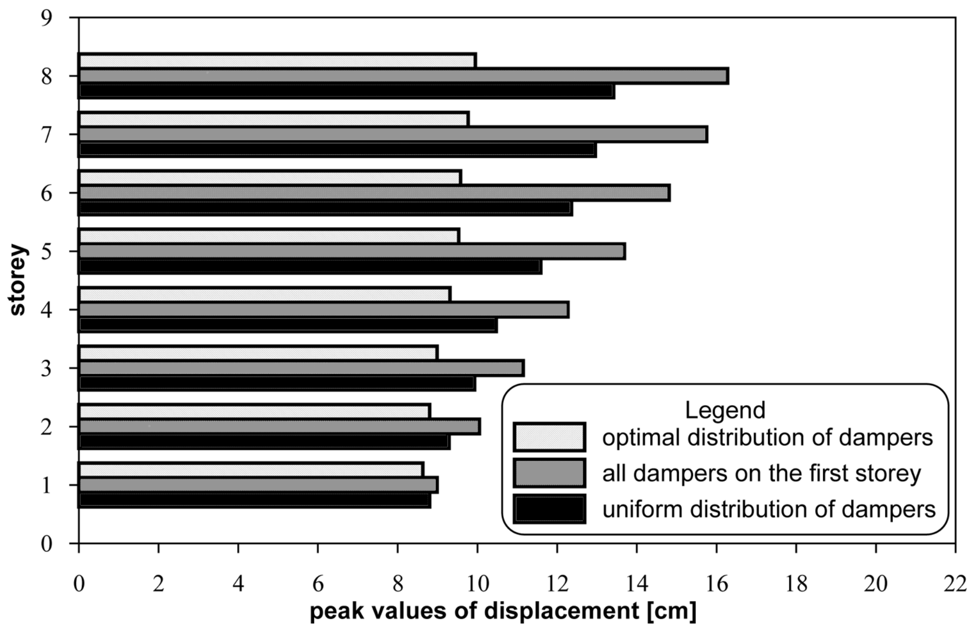

Figure 11. Peak values of horizontal acceleration of storeys for different configuration of dampers

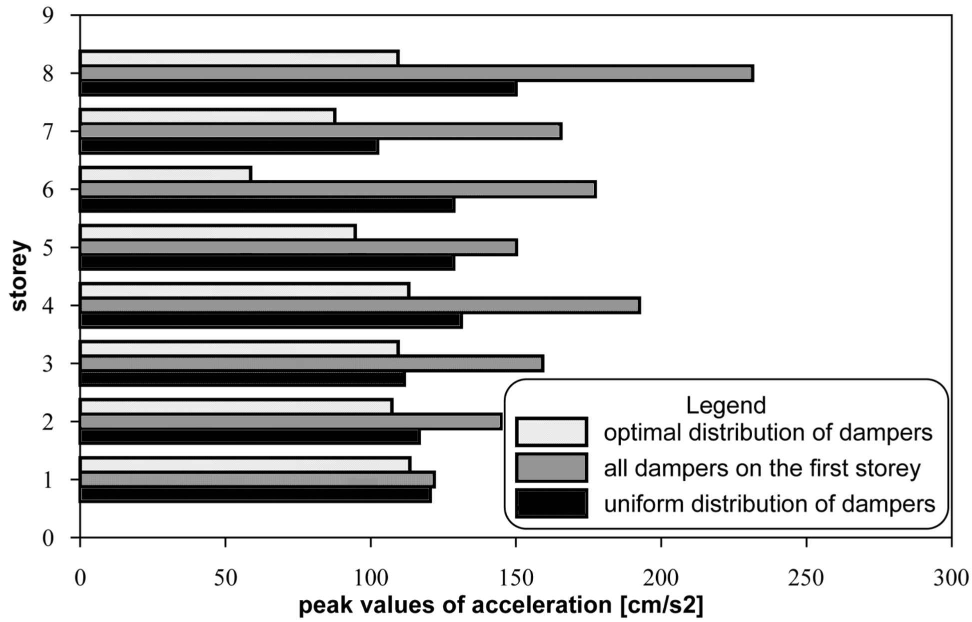

for the frame with dampers concentrated on the first storey. Identical conclusions can be drawn from the peak values of acceleration shown in Figure 11.

Optimal Placement of Dampers for Frame Structures: Fractional Rheological Models of Dampers

The aim of the fourth example is to illustrate the optimal position of dampers on structure when dampers are modelled using the fractional Kelvin model and the fractional Maxwell model. Moreover, it is shown that results obtained using the sequential optimization method (which is a heuristic method) and using the PSO method are very similar. It justifies that it is possible to find, using the sequential optimization method, a solution which is near the global optimum of the optimization problem at hand.

Example 4: A Ten-Storey Shear Frame

In the next numerical example, a ten-storey building structure, modelled as a shear plane frame with VE dampers mounted on it is considered. The bending rigidity of columns varies in sequence, for every two storeys:

$$k_1 = k_2 = 68710 \ \ \mathrm{kN/m}$$
$$k_3 = k_4 = 54010 \ \ \mathrm{kN/m}$$
$$k_5 = k_6 = 42170 \ \ \mathrm{kN/m}$$
$$k_7 = k_8 = 28660 \ \ \mathrm{kN/m}$$

Table 5. Natural frequencies ω_i for the frame structure

Mode Number	Natural Frequency [rad/sec]	Mode Number	Natural Frequency [rad/sec]
1	22.690	6	182.399
2	56.534	7	208.638
3	91.909	8	245.147
4	127.472	9	281.524
5	151.769	10	324.052

Table 6. Non-dimensional damping ratios γ_i

Mode Number	Frame without dampers	Uniform distribution of dampers		Optimal distribution of dampers	
		Kelvin model	Maxwell model	Kelvin model	Maxwell model
1	0.0008	0.0038	0.0036	0.0043	0.0049
2	0.0022	0.0099	0.0087	0.0085	0.0139
3	0.0035	0.0137	0.0113	0.0107	0.0148
4	0.0047	0.0162	0.0129	0.0118	0.0094
5	0.0061	0.0231	0.0177	0.0181	0.0251
6	0.0066	0.0195	0.0143	0.0200	0.0150
7	0.0073	0.0219	0.0157	0.0261	0.0218
8	0.0085	0.0208	0.0151	0.0237	0.0230
9	0.0097	0.0209	0.0154	0.0228	0.0111
10	0.0112	0.0212	0.0160	0.0214	0.0112

$k_9 = k_{10} = 16450 \ \mathrm{kN/m}$, but the mass value is the same for every floor: $m_s = 2.07 \ \mathrm{Mg}$. The structure's damping factors are: $c_1 = c_2 = 4.76 \ \mathrm{kNsec/m}$

$c_3 = c_4 = 3.73 \ \mathrm{kNsec/m}$

$c_5 = c_6 = 2.91 \ \mathrm{kNsec/m}$

$c_7 = c_8 = 1.98 \ \mathrm{kNsec/m}$

$c_9 = c_{10} = 1.44 \ \mathrm{kNsec/m}$.

The data is taken from Zhang and Soong (1992). Two rheological models describing the dynamic behaviour of dampers were applied in the calculations; the Kelvin fractional model and the Maxwell fractional model.

Firstly, the calculations were carried out for a frame without dampers, only the damping properties of the structure were taken into account. The solution to Equation (44), where $\mathbf{A}_1 = \mathbf{0}$ and $\mathbf{K}_{dd} = 0$, leads to the eigenvalues s_i which enables determination of the dynamic properties of the structure described by Equation (28). The results, the natural frequencies of the structure and the values of non-dimensional damping ratios are presented in Table 5 and in the second column of Table 6, respectively.

Next, the authors investigated a structure with one damper mounted on every storey (see Figure 12a). The assumed values of the sum of the damping coefficients and the sum of the stiffness parameters are: $C_d = 500 \ \mathrm{kNsec}^\alpha/\mathrm{m}$, and $K_d = 25000 \ \mathrm{kNm}^2$, respectively. If dampers are uniformly distributed within a structure, then the data for every single damper are: $k_d = 2500 \ \mathrm{kNm}^2, c_d = 50 \ \mathrm{kNsec}^\alpha/\mathrm{m}$, $\tau_d = c_d / k_d = 0.02$. The values of fractional parameters for all dampers are identical, i.e., $\alpha = 0.6$. The above values of damper parameters are used for both of the considered fractional models. Using the suggested procedure, the dynamic properties of the considered system were computed (see Table 6). These results show that a frame with uniformly distributed dampers is less damped by the fractional Maxwell damper than by the fractional Kelvin damper if both dampers have identical values of parameters. The optimization procedures provide lower values of damping ratios in the case of the Kelvin model of damper for the first, second, third and fifth modes of vibration in comparison with the Maxwell model. But the results of optimization correspond to the different dampers distribution at frame structure (see Table 6 and Figure 12).

Figure 12. A 10-storey frame with different distributions of dampers: a) structure with uniformly distributed dampers, b) structure with optimally located dampers modelled using fractional Kelvin model, c) structure with optimally located dampers modelled using fractional Maxwell model

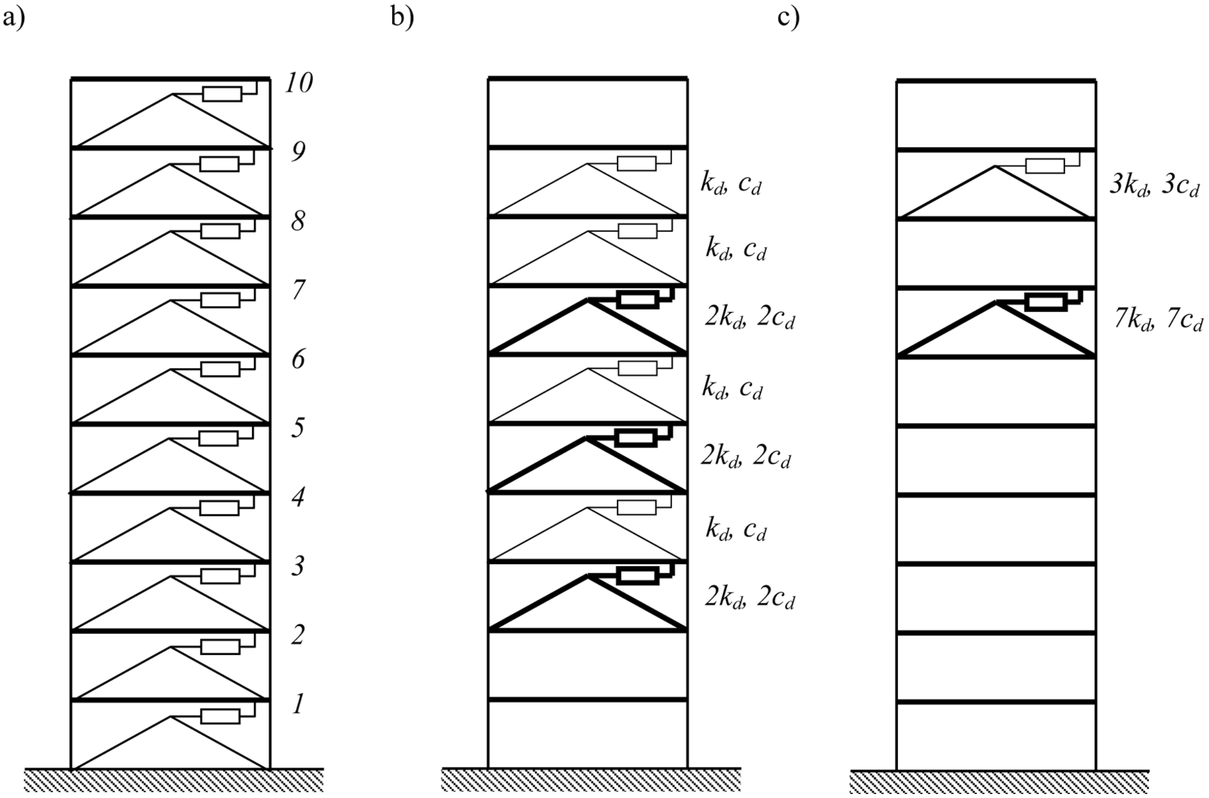

In this example the objective function is the weighted sum of amplitudes of the transfer functions of interstorey drifts calculated at the fundamental natural frequency of the structure with dampers. All weight factors are equal to 1.0, i.e., $\mathbf{w} = [1.0,\ 1.0,...,1.0]^T$.

A first solution to the optimization problem is obtained using the sequential optimization method. For every possible location of one damper, the values of fundamental frequency and non-dimensional damping ratios are calculated (see Figure 13 and 14). Next, the objective function is evaluated for the frame, taking into account every possible position of the damper. The results are presented in Figure 15.

The correct fixed location of the first damper is at the seventh storey, for which the minimum value of the objective function is obtained. When the first damper's location is determined, the procedure is repeated until all locations for the dampers are found. The optimal locations of ten successive dampers are found to be: no dampers on the first, second and tenth storeys, one damper on the fourth, sixth, eighth, and ninth storeys, and two dampers on the third, fifth, and seventh storeys for the fractional Kelvin model (see also Figure 12b). In the case of the fractional Maxwell model, the optimal locations of dampers are: seven dampers on the seventh storey and three dampers on the ninth storey (see also Figure 12c). The dynamic properties of structures with optimally distributed dampers are shown in Tables 5 and 6. It can be noticed that the non-dimensional damping ratio of the first mode of vibration is

Figure 13. Non-dimensional damping factors versus first damper's position

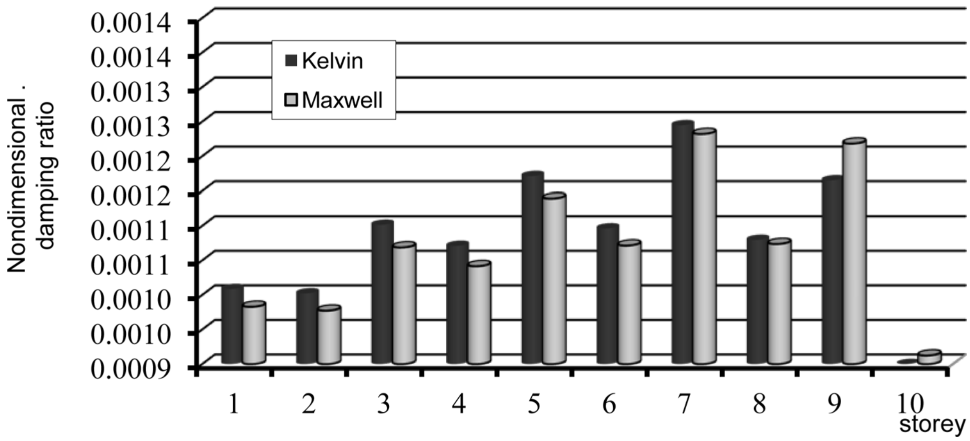

Figure 14. The first natural frequency versus first damper's position

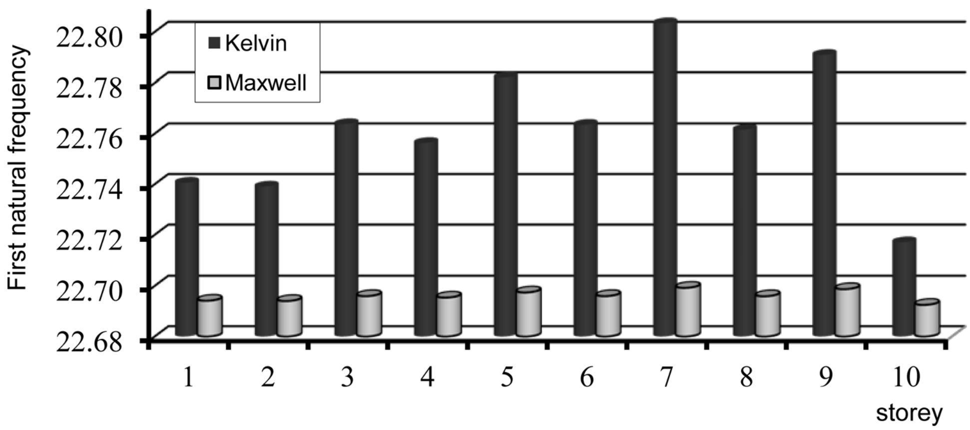

Figure 15. Objective function versus first damper's position

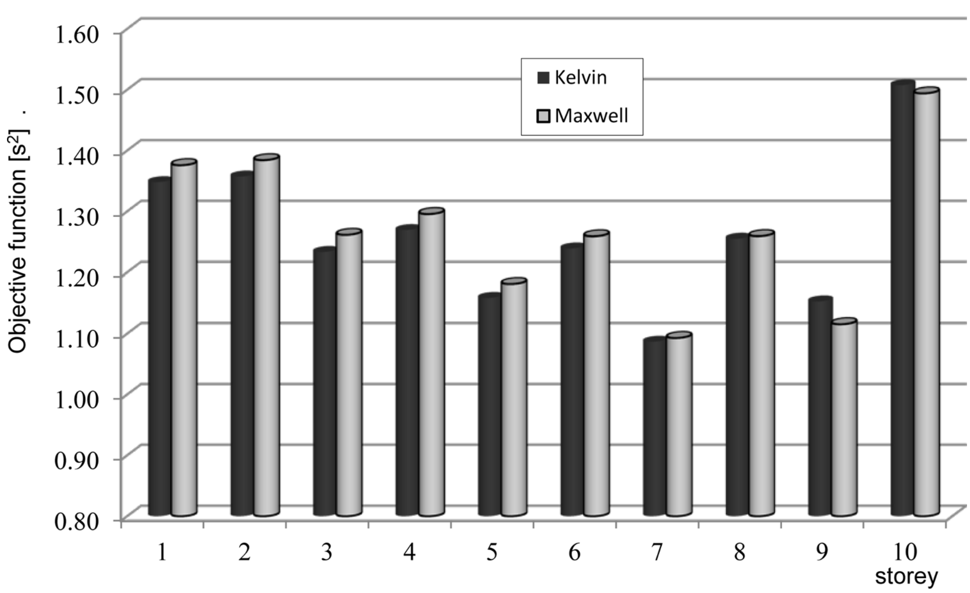

Figure 16. Convergence of objective function at PSO iteration

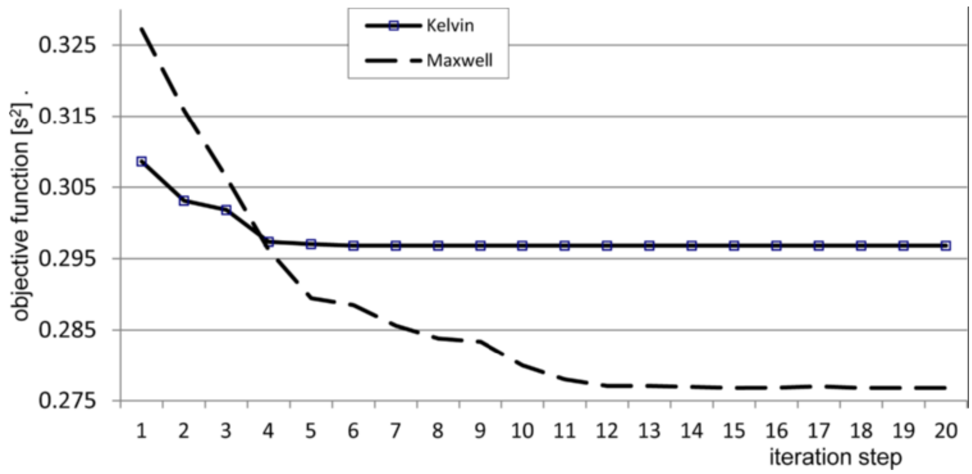

greater, by about 13% and 36%, for the Kelvin and the Maxwell models, respectively, compared with the same ratio for the structure with uniformly distributed dampers.

In the second approach, the PSO method is applied. In Equation (3), the values of the coefficients $c_1 = c_2 = 2$ and the declining value of the inertia factor are defined; starting with $w = 0.9$, it decreased by 0.005 at every step of iteration. A population of ten particles was initialized with random positions. The position coordinates for every particle describe the current distribution of damping properties on the frame. On every storey, the value of the damping coefficient must be non-negative and smaller than the assumed constant value $C_d = 500\ \mathrm{kNsec}^{\alpha}/\mathrm{m}$ (i.e., $c_{\min} \le c_{d,i} \le C_d$). The stiffness parameters of the dampers are calculated from the ratio $c_{d,i} / k_{d,i}$, which is equal to 0.02 and constant for every damper.

Variations of the best value of the objective function during the iteration process are presented in Figure 16. The solution to the optimization problem, i.e., the optimal distribution of VE dampers obtained by both optimization methods, is shown in Table 7.

The objective function, the weighted sum of amplitudes of the transfer functions of interstorey drifts is $F_0 = 1.7053\ \mathrm{sec}^2$, $F_{U,K} = 0.3286\ \mathrm{sec}^2$, $F_{U,M} = 0.3739\ \mathrm{sec}^2$ for the frame without dampers and for uniformly distributed Kelvin and Maxwell dampers, respectively. The optimal solution obtained by the sequential and the PSO methods for the frame with the Kelvin fractional dampers $F_{S,K} = 0.2972\ \mathrm{sec}^2$ differ from the results obtained when the Maxwell fractional dampers are applied:

$$F_{S,M} = 0.2759\ \mathrm{sec}^2$$

It can be concluded that the results obtained by both methods yield similar dampers' distributions within the frame. Differences between the optimal values of damping coefficients, obtained as the result of optimization procedures, are partially affected by an incremental way of distribution of the damping coefficients in the sequential optimization method. Moreover, in the PSO method the values of the damping $c_{d,i}$ parameters must be positive for every damper. During the iteration process, negative or zero values of parameters $c_{d,i}$ were substituted by $c_{\min}$ and normal-

Table 7. Optimal distribution of VE dampers

Storey	Damping coefficient $c_{d,i}$			
	Fractional Kelvin model		Fractional Maxwell model	
	Sequential method	PSO method	Sequential method	PSO method
1	0	0	0	0.78
2	0	0	0	0.78
3	100.0	87.57	0	0.78
4	50.0	47.68	0	0.78
5	100.0	106.18	0	0.78
6	50.0	56.68	0	0.78
7	100.0	120.77	350.0	347.23
8	50.0	26.68	0	0.78
9	50.0	54.45	150.0	146.48
10	0	0	0	0.78
Total	500.0	500.01	500.0	499.95

ized using Equation (7), therefore, the values given in Table 7 differ from $c_{\min} = 1$. It justifies, for example, that it is possible to find, using the sequential optimization method, a solution which is near the global optimum of the considered optimization problem.

The Maple program was used to obtain all of the results presented in this example.

CONCLUDING REMARKS AND FUTURE RESEARCH WORKS

The problems of the optimal location of VE dampers on the planar frame structures and determination of the optimal values of parameters of dampers are considered in this chapter. VE dampers are modelled using several rheological models, i.e., the generalized Kelvin and Maxwell models, both with seven parameters, and the three-parameter Kelvin and Maxwell models with fractional derivatives. The mathematical formulation for structures with VE dampers, modelled by the classical and fractional rheological models, is presented. The resulting matrix equation of motion is the fractional differential equation for the models with fractional derivative or the classical differential equation when the dampers are modelled using the classical rheological models. The dynamics properties of structures are determined as the solution to the appropriately defined linear or non-linear eigenvalue problems and as the solution to the appropriately defined set of algebraic equations.

The optimal damper distributions in buildings are found for various objective functions. The weighted sum of amplitudes of the transfer functions of interstorey drifts and the weighted sum of amplitudes of the transfer functions of displacements evaluated at the fundamental natural frequency of the frame with the dampers are most frequently used as the objective function. The optimization problem is solved using the sequential optimization method and the particle swarm optimization method. Several numerical solutions to the considered optimization problem are presented and discussed in detail.

Based on the results presented above, the following main conclusions can be formulated:

- The problem of optimal distribution of VE dampers modelled using the rheological models with fractional derivative or using the generalized classical rheological models is solved for the first time.
- The results presented prove the effectiveness and applicability of the proposed approach.
- The optimal distribution of dampers within a structure strongly depends on the adopted objective function and the structure characteristics.
- The results of optimization of problems in which VE dampers are modelled using the generalized Kelvin model and the generalized Maxwell model are almost identical

providing the dissipation energy of each model is approximately equal.

- The frequency response functions change very fast in the vicinity of their maximal value and it is necessary to take into account small changes of the natural frequencies of vibration when calculating the maximal values of the frequency response functions.

The advantage of the optimization methods used in the chapter is that they are non-gradient methods and only calculation of the values of the objective function is required. An advantage of the PSO method is its ability to solve optimization problems when the objective function has many local minima. However, usually many iteration and many evaluations of the values of the objective function are necessary. The advantage of sequential optimization method is its simplicity and clear physical justification of optimal position of dampers. The lack of a formal proof of convergence of the solution to the global minima is the main drawback of this method. However, numerical results reported in the chapter and previously by Lewandowski (2008) suggest that, for the considered particular optimization problems, the method gives us an optimal or nearly optimal solution, acceptable from the practical point of view.

The considered optimization methods for optimal location of dampers could also be used, without significant changes, to find optimal positions of dampers on 3D structures. Of course, 3D frames have usually many more degrees of freedom than planar ones, which means that the computational effort needed to find an optimal solution could be substantially greater. Moreover, additional details, such as specification of acceptable locations of dampers on the structure, must be specified in order to reduce the number of variables in the optimization problem.

In this chapter structures are treated as linear elastic systems. In reality, elastoplastic deformations of structures will occur when structures are subjected to very strong earthquakes. In such a case, analyses of structures in the frequency domain are not possible or they are very tedious and only analyses in a time domain could be done. This fact makes it impossible to use or significantly complicates the optimization methods presented above and could drastically increase computational efforts necessary to obtain the optimal solution. In particular, objective functions which are written in terms of transfer functions cannot be used. Moreover, for example, specification of a set of accelerograms compatible with the design spectra is necessary.

In conclusion, reformulation of optimization procedure for optimal location of dampers on elastoplastic structures which will be effective and efficient is desirable and could be the direction of future works. Other direction of future research works could be a more thorough examination of optimization results obtained for structures with dampers modelled using generalized rheological models and ones with fractional derivatives. The influence of uncertainty of structures and dampers parameters on optimal positions and optimal parameters of dampers has not been analyzed yet and seems to be an important problem from a practical point of view.

ACKNOWLEDGMENT

The authors wish to acknowledge the financial support received from the Poznan University of Technology (Grant No. DS 11 - 068/11) in connection with this work. The authors are also thankful to anonymous referees for their careful reading of the chapter and their several suggestions, which have helped improve the chapter.

REFERENCES

Agrawal, A. K., & Yang, J. N. (2000). Design passive energy dissipation systems based on LQR methods. *Journal of Intelligent Material Systems and Structures*, *10*, 933–944. doi:10.1106/FB58-N1DG-ECJT-B8H4

Alkhatib, R., Jazar, G. N., & Golnaraghi, M. F. (2004). Optimal design of passive linear suspension using genetic algorithm. *Journal of Sound and Vibration*, *275*, 665–691. doi:10.1016/j.jsv.2003.07.007

Autodesk, Inc. (2010). *Autodesk® Robot™ structural analysis*. San Rafael, CA: Author.

Aydin, E., Boduroglu, M. H., & Guney, D. (2007). Optimal damper distribution for seismic rehabilitation of planar building structures. *Engineering Structures*, *29*, 176–185. doi:10.1016/j.engstruct.2006.04.016

Bagley, R. L., & Torvik, P. J. (1989). Fractional calculus – A different approach to the analysis of viscoelastically damped structures. *AIAA Journal*, *27*, 1412–1417. doi:10.2514/3.10279

Chang, T., & Singh, M. P. (2002). Seismic analysis of structures with a fractional derivative model of viscoelastic dampers. *Earthquake Engineering and Engineering Vibration*, *1*, 251–260. doi:10.1007/s11803-002-0070-5

Chang, T. S., & Singh, M. P. (2009). Mechanical model parameters for viscoelastic dampers. *Journal of Engineering Mechanics*, *135*, 581–584. doi:10.1061/(ASCE)0733-9399(2009)135:6(581)

Chopra, A. K. (2000). *Dynamics of structures, Theory and applications to earthquake engineering*. Upper Saddle River, NJ: Prentice Hall.

Christopoulos, C., & Filiatrault, A. (2006). *Principles of passive supplemental damping and seismic isolation*. Pavia, Italy: IUSS Press.

Cimellaro, G. P. (2007). Simultaneous stiffness-damping optimization of structures with respect to acceleration, displacement and base shear. *Engineering Structures*, *29*, 2853–2870. doi:10.1016/j.engstruct.2007.01.001

Clerc, M. (2006). *Particle swarm optimization*. Wiley-ISTE. doi:10.1002/9780470612163

Constantinou, M. C., Soong, T. T., & Dargush, G. F. (1998). *Passive energy dissipation systems for structural design and retrofit. Monograph No.1*. Buffalo, NY: Multidisciplinary Center for Earthquake Engineering Research.

De Silva, C. W. (2007). *Vibration damping, control, and design*. Boca Raton, FL: CRC Press/Taylor & Francis Group.

Engelen, K., Ramon, H., Saeys, A., Franssens, W., & Anthonis, J. (2007). Positioning and tuning of viscous damper on flexible structure. *Journal of Sound and Vibration*, *304*, 845–862. doi:10.1016/j.jsv.2007.03.020

Fujita, K., Moustafa, A., & Takewaki, I. (2010a). Optimal placement of viscoelastic dampers and supporting members under variable critical excitations. *Earthquakes and Structures*, *1*, 43–67.

Fujita, K., Yamamoto, K., & Takewaki, I. (2010b). An evolutionary algorithm for optimal damper placement to minimize interstorey-drift transfer function in shear building. *Earthquakes and Structures*, *1*, 289–306.

Garcia, L., & Soong, T. T. (2002). Efficiency of a simple approach to damper allocation in MDOF structures. *Journal of Structural Control*, *9*, 19–30. doi:10.1002/stc.3

Gazi, V., & Passino, K. M. (2011). *Swarm stability and optimization*. Springer Verlag. doi:10.1007/978-3-642-18041-5

Gluck, N., Reinhorn, A. M., Gluck, J., & Levy, R. (1996). Design of supplemental dampers for control of structure. *Journal of Structural Engineering*, *122*, 1394–1399. doi:10.1061/(ASCE)0733-9445(1996)122:12(1394)

Gurgoze, M., & Muller, P. C. (1992). Optimal positioning of dampers in multi-body systems. *Journal of Sound and Vibration*, *158*, 517–530. doi:10.1016/0022-460X(92)90422-T

Hanson, R. D., & Soong, T. T. (2001). *Seismic design with supplemental energy dissipation devices. EERI Monograph No. 8*. Oakland, CA: Earthquake Engineering Research Institute.

Jones, D. I. G. (2001). *Handbook of viscoelastic vibration damping*. Chichester, UK: Wiley.

Kaveh, A., & Talatahari, S. (2009). Particle swarm optimizer, ant colony strategy and harmony search scheme hybridized for optimization of truss structures. *Computers & Structures*, *87*, 267–283. doi:10.1016/j.compstruc.2009.01.003

Kennedy, J., & Eberhart, R. (2001). *Swarm intelligence*. San Francisco, CA: Morgan Kaufmann Publishers.

Lavan, O., & Levy, R. (2005). Optimal design of supplemental viscous dampers for irregular shear frames in the presence of the yielding. *Earthquake Engineering & Structural Dynamics*, *34*, 889–907. doi:10.1002/eqe.458

Lewandowski, R. (2008). Optimization of the location and damping constants of viscous dampers. In B. H. V. Topping & M. Papadrakakis (Eds.), *Proceedings of the Ninth International Conference on Computational Structures Technology, Civil-Comp Press, Stirlingshire, Scotland*, Athens, Greece, 2-5 September, 2008, Paper 193, (pp. 1-16).

Lewandowski, R., & Pawlak, Z. (2010). Dynamic analysis of frames with viscoelastic dampers modelled by rheological models with fractional derivatives. *Journal of Sound and Vibration*, *330*, 923–936. doi:10.1016/j.jsv.2010.09.017

Loh, C. H., Lin, P. Y., & Chung, N. H. (2000). Design of dampers for structures based on optimal control theory. *Earthquake Engineering & Structural Dynamics*, *29*, 1307–1323. doi:10.1002/1096-9845(200009)29:9<1307::AID-EQE972>3.0.CO;2-D

Main, J. A., & Krenk, S. (2005). Efficiency and tuning of viscous dampers on discrete systems. *Journal of Sound and Vibration*, *286*, 97–112. doi:10.1016/j.jsv.2004.09.022

Maplesoft Inc. (n.d.). *Maple 13.02*. Waterloo, Canada: Author.

Mead, D. J. (1999). *Passive vibration control*. Chichester, UK: Wiley.

Nakashima, M., & Mitani, T. (1996b). Distribution of energy input and dissipation along stories in steel building structures with hysteretic dampers. *Proceedings of the 11th World Conference on Earthquake Engineering 1996*, Paper No. 260.

Nakashima, M., Saburi, K., & Tsuji, B. (1996a). Energy input and dissipation behaviour of structures with hysteretic dampers. *Earthquake Engineering & Structural Dynamics*, *25*, 483–496. doi:10.1002/(SICI)1096-9845(199605)25:5<483::AID-EQE564>3.0.CO;2-K

Park, S. W. (2001). Analytical modelling of viscoelastic dampers for structural and vibration control. *International Journal of Solids and Structures*, *38*, 8065–8092. doi:10.1016/S0020-7683(01)00026-9

Pawlak, Z., & Lewandowski, R. (2010). Optimization of viscoelastic dampers as described by the fractional rheological model. In B. H. V. Topping et al., (Eds.), *Proceedings of The Tenth International Conference on Computational Structural Technology*, (pp. 1-15). Stirlingshire, UK: Civil-Comp Press.

Plevris, V., & Papadrakakis, M. (2011). A hybrid particle swarm—gradient algorithm for global structural optimization. *Computer-Aided Civil and Infrastructure Engineering*, *26*, 48–68.

Podlubny, I. (1999). *Fractional differential equations*. Academic Press.

Rossikhin, Y. A., & Shitikova, M. V. (2001). A new method for solving dynamic problems of fractional derivative viscoelasticity. *International Journal of Engineering Science*, *39*(2), 149–176. doi:10.1016/S0020-7225(00)00025-2

Singh, M. P., & Chang, T. S. (2009). Seismic analysis of structures with viscoelastic dampers. *Journal of Engineering Mechanics*, *135*, 571–580. doi:10.1061/(ASCE)0733-9399(2009)135:6(571)

Singh, M. P., & Moreschi, L. M. (2001). Optimal seismic response control with dampers. *Earthquake Engineering & Structural Dynamics*, *30*, 553–572. doi:10.1002/eqe.23

Singh, M. P., & Moreschi, L. M. (2002). Optimal placement of dampers for passive response control. *Earthquake Engineering & Structural Dynamics*, *31*, 955–976. doi:10.1002/eqe.132

Soong, T. T., & Dargush, G. F. (1997). *Passive energy dissipation systems in structural engineering*. London, UK: Wiley.

Soong, T. T., & Spencer, B. F. (2002). Supplemental energy dissipation: State-of-the-art and state-of-the-practice. *Engineering Structures*, *24*, 243–259. doi:10.1016/S0141-0296(01)00092-X

Takewaki, L. (2009). *Building control with passive dampers. Optimal performance-based design for earthquakes*. Singapore: Wiley. doi:10.1002/9780470824931

Tsuji, M., & Nakamura, T. (1996). Optimum viscous dampers for stiffness design of shear buildings. *Structural Design of Tall Buildings*, *5*, 217–234. doi:10.1002/(SICI)1099-1794(199609)5:3<217::AID-TAL70>3.0.CO;2-R

Viana, F. A. C., Kotinda, G. I., Rade, D. A., & Steffen, V. (2008). Tuning dynamic vibration absorbers by using ant colony optimization. *Computers & Structures*, *86*, 1539–1549. doi:10.1016/j.compstruc.2007.05.009

Wu, B., Ou, J. P., & Soong, T. T. (1997). Optimal placement of energy dissipation devices for three-dimensional structures. *Engineering Structures*, *19*, 113–125. doi:10.1016/S0141-0296(96)00034-X

Yang, J. N., Kim, J. H., & Agrawal, A. K. (2002). Optimal design of passive energy dissipation systems based on $H\infty$ and H_2 performances. *Earthquake Engineering & Structural Dynamics*, *31*, 921–936. doi:10.1002/eqe.130

Zhang, R. H., & Soong, T. T. (1992). Seismic design of viscoelastic dampers for structural applications. *Journal of Structural Engineering*, *118*, 1375–1392. doi:10.1061/(ASCE)0733-9445(1992)118:5(1375)

Zhu, H. P., Ge, D. D., & Huang, X. (2010). Optimum connecting dampers to reduce the seismic responses of parallel structures. *Journal of Sound and Vibration*, *330*. doi:doi:10.1016/j.jsv.2010.11.016

KEY TERMS AND DEFINITIONS

Active Systems: Active Vibration Control involves the use of actuators (e.g., motors for vibration) along with sensors and controllers (analog or digital) to produce an actuation with the right timing to counteract the resonant oscillation. Due to remarkable advances in sensor, actuator and, more importantly, computer technologies in recent years active systems have become cost effective solutions to most sound and vibration control problems.

Fractional Derivative: A generalization of the well known derivative in the case when the derivative order is a real number. A few definitions of the fractional derivative are known and the most popular ones are those proposed by Riemann and Liouville, Caputo and by Grunwald and Letnikov.

Models with Fractional Derivative: Models which contain spring-pot elements. Differential equations with fractional derivatives describe the behaviour of such models.

Particle Swarm Optimization (PSO): The optimization method based on the study of social behaviour in a self–organized population system (i.e., ant colonies, fish schools). It is a non-gradient, heuristic method which requires calculation of the objective function only. This method is able to find a global solution to non-convex optimization problem and problems which have many local minima.

Passive Systems: The most commonly applied vibration control techniques are based on the use of passive technologies. The majority of these applications are based on passive damping using viscoelastic materials. The traditional passive damping methods include the use of broadband dissipative solutions such as viscoelastic, viscous, and friction dampers, as well as narrowband reactive solutions such as tuned mass dampers. Although most passive damping treatments are inexpensive to fabricate, their successful application requires a thorough understanding of the vibration problem in hand and the properties of the damping materials. Viscous dampers (dashpots), tuned-mass dampers, dynamic absorbers, shunted piezoceramic dampers, and magnetic dampers are other mechanisms of passive vibration control. Passive vibration control has its limitations such as: lack of versatility, large size and weight when used for low-frequency vibration control, and detuning of tuned treatments.

Rheological Models: One-dimensional constitutive models for viscoelasticity based on spring, dashpot, and spring-pot elements. The elements may be connected in series or in parallel. In models where the elements are connected in series the strain is additive while the stress is equal in each element. In parallel connections, the stress is additive while the strain is equal in each element.

Semi-Active (Adaptive-Passive) Systems: Refer to an adjustable passive vibration control scheme, that is, the passive treatment can adjust itself in response to changes in the structure. For example, the stiffness, damping coefficient or other variables of the passive control scheme can change automatically so that optimal vibration mitigation is induced. These variable components, also known as "tunable parameters" of the control system, are re-tailored via a properly developed semi-active control algorithm. Being more versatile than passive control techniques and more affordable (in terms of cost and energy consumption) than active control schemes, has made semi-active control methods very popular.

Spring-Pot Element (also known as the Scott–Blair's Element): An element which combines elastic and viscous properties of spring and dashpot elements. The spring-pot element satisfies the constitutive equation: $u(t) = c\ D_t^{\alpha} x(t)$, where $u(t)$ is the force in element, c and α are models parameters and $D_t^{\alpha} x(t)$ is the fractional derivative of the order α with respect to time t. The spring-pot element is often schematically shown as rhombus in rheological model diagrams. The spring-pot element can be understood as an interpolation between the spring element and the dashpot element: spring-pot is a spring when $\alpha = 0$ and a dashpot when $\alpha = 1$.

Transfer Function (also known as the System Function or Network Function): A mathematical representation, in terms of spatial or temporal frequency, of the relationship between the input and output of a linear time-invariant system.

Viscoelastic (VE) Dampers: A wide class of energy dissipation devices whose force-displacement relationship has viscoelastic mechanical properties. In recent decades, VE dampers have been widely used to reduce vibration in civil engineering structures caused by various excitations, including traffic load, wind load and seismic load. A VE damper is usually connected to a structure through braces and is activated by the relative motion of the structure to which it is connected. The VE dampers could be divided broadly into fluid and solid VE dampers. Silicone oil is used to build the fluid dampers while the solid dampers are made of copolymers or glassy substances.

APPENDIX A

Finite Element Matrices of Different VE Damper Models

The explicit form of the matrices used to describe the generalized Kelvin model is given by:

$$\mathbf{K}_d = \mathbf{T}_d^T \tilde{\mathbf{K}}_d \mathbf{T}_d = \begin{bmatrix} \mathbf{K}_{zz} & \mathbf{K}_{zw} \\ \mathbf{K}_{wz} & \mathbf{K}_{ww} \end{bmatrix}, \qquad \mathbf{C}_d = \mathbf{T}_d^T \tilde{\mathbf{C}}_d \mathbf{T}_d = \begin{bmatrix} \mathbf{C}_{zz} & \mathbf{C}_{zw} \\ \mathbf{C}_{wz} & \mathbf{C}_{ww} \end{bmatrix} \tag{A.1}$$

$$\mathbf{K}_{zz} = \begin{bmatrix} c^2k_0 & csk_0 & 0 & 0 \\ csk_0 & s^2k_0 & 0 & 0 \\ 0 & 0 & c^2k_m & csk_m \\ 0 & 0 & csk_m & s^2k_m \end{bmatrix}, \qquad \mathbf{C}_{zz} = \begin{bmatrix} 0 & 0 & 0 & 0 \\ 0 & 0 & 0 & 0 \\ 0 & 0 & c^2c_m & \mathrm{csc}_m \\ 0 & 0 & \mathrm{csc}_m & \mathrm{csc}_m \end{bmatrix} \tag{A.2}$$

$$\mathbf{K}_{zw} = \mathbf{K}_{wz}^T = \begin{bmatrix} -ck_0 & 0.....\ 0....... & 0 \\ -sk_0 & 0.....\ 0....... & 0 \\ 0 & 0.....0..... & -ck_m \\ 0 & 0.....0...... & -sk_m \end{bmatrix}, \qquad \mathbf{C}_{zw} = \mathbf{C}_{wz}^T = \begin{bmatrix} 0 & 0.....\ 0....... & 0 \\ 0 & 0.....\ 0....... & 0 \\ 0 & 0.....0..... & -cc_m \\ 0 & 0.....0..... & -sc_m \end{bmatrix} \tag{A.3}$$

$$\mathbf{K}_{ww} = \tilde{\mathbf{K}}_{ww} = diag\left(k_1, \quad k_2, ..., k_m,\right), \qquad \mathbf{C}_{ww} = \tilde{\mathbf{C}}_{ww} = diag\left(c_1, \quad c_2, ..., c_m,\right) \tag{A.4}$$

where $c = \cos\beta$, $s = \sin\beta$, β is the angle between the global and the local coordinate systems

The explicit form of the matrices used to describe the generalized Maxwell model is given by:

$$\mathbf{K}_d = \mathbf{T}_d^T \tilde{\mathbf{K}}_d \mathbf{T}_d = \begin{bmatrix} \mathbf{K}_{zz} & \mathbf{K}_{zw} \\ \mathbf{K}_{wz} & \mathbf{K}_{ww} \end{bmatrix}, \qquad \mathbf{C}_d = \mathbf{T}_d^T \tilde{\mathbf{C}}_d \mathbf{T}_d = \begin{bmatrix} \mathbf{C}_{zz} & \mathbf{C}_{zw} \\ \mathbf{C}_{wz} & \mathbf{C}_{ww} \end{bmatrix} \tag{A.5}$$

$$\mathbf{K}_{zz} = \begin{bmatrix} c^2\left(k_0 + \sum_{i=1}^{m} k_i\right) & cs\left(k_0 + \sum_{i=1}^{m} k_i\right) & -c^2k_0 & -csk_0 \\ cs\left(k_0 + \sum_{i=1}^{m} k_i\right) & s^2\left(k_0 + \sum_{i=1}^{m} k_i\right) & -csk_0 & -s^2k_0 \\ -c^2k_0 & -csk_0 & c^2k_0 & csk_0 \\ -csk_0 & -s^2k_0 & csk_0 & s^2k_0 \end{bmatrix} \tag{A.6}$$

$$\mathbf{C}_{zz} = \begin{bmatrix} 0 & 0 & 0 & 0 \\ 0 & 0 & 0 & 0 \\ 0 & 0 & c^2 \sum_{i=1}^{m} c_i & cs \sum_{i=1}^{m} c_i \\ 0 & 0 & cs \sum_{i=1}^{m} c_i & s^2 \sum_{i=1}^{m} c_i \end{bmatrix} \tag{A.7}$$

$$\mathbf{K}_{zw} = \mathbf{K}_{zw}^{T} = \begin{bmatrix} -ck_1 & -ck_2 \ldots\ldots & -ck_i \ldots\ldots\ldots & -ck_m \\ -sk_1 & -sk_2 \ldots\ldots & -sk_i \ldots\ldots\ldots & -sk_m \\ 0 & 0 \ldots\ldots\ldots & 0 \;\; \ldots\ldots\ldots & 0 \\ 0 & 0 \ldots\ldots\ldots & 0 \;\; \ldots\ldots\ldots & 0 \end{bmatrix} \tag{A.8}$$

$$\mathbf{C}_{zw} = \mathbf{C}_{zw}^{T} = \begin{bmatrix} 0 & 0 \ldots\ldots\ldots & 0 \;\; \ldots\ldots\ldots & 0 \\ 0 & 0 \ldots\ldots\ldots & 0 \;\; \ldots\ldots\ldots & 0 \\ -cc_1 & -cc_2 \ldots\ldots & -cc_i \ldots\ldots\ldots & -cc_m \\ -sc_1 & -sc_2 \ldots\ldots & -sc_i \ldots\ldots\ldots & -sc_m \end{bmatrix} \tag{A.9}$$

$$\mathbf{K}_{ww} = \tilde{\mathbf{K}}_{ww} = diag\left(k_1, \quad k_2, \ldots\ldots\ldots\ldots, k_m,\right), \qquad \mathbf{C}_{ww} = \tilde{\mathbf{C}}_{ww} = diag\left(c_1, \quad c_2, \ldots\ldots\ldots\ldots, c_m,\right) \tag{A.10}$$

The explicit form of the vectors and matrices used to describe the simple Kelvin model and the fractional-derivative Kelvin model of a VE damper is:

$$\mathbf{q}_d(t) = \mathbf{q}_z(t) = [q_1(t), \; q_2(t), \; q_3(t), \; q_4(t)]^T \tag{A.11}$$

$$\mathbf{K}_d = \mathbf{K}_{zz} = k_1 \begin{bmatrix} c^2 & cs & -c^2 & -cs \\ cs & s^2 & -cs & -s^2 \\ -c^2 & -cs & c^2 & cs \\ -cs & -s^2 & cs & s^2 \end{bmatrix}, \qquad \mathbf{C}_d = \mathbf{C}_{zz} = c_1 \begin{bmatrix} c^2 & cs & -c^2 & -cs \\ cs & s^2 & -cs & -s^2 \\ -c^2 & -cs & c^2 & cs \\ -cs & -s^2 & cs & s^2 \end{bmatrix} \tag{A.12}$$

The explicit form of the matrices used to describe the simple Maxwell model and the fractional Maxwell model of a VE damper is:

$$\mathbf{q}_d(t) = [\mathbf{q}_z(t), \quad \mathbf{q}_w(t)]^T \tag{A.13}$$

$$\mathbf{q}_z(t) = [q_1(t), \; q_2(t), \; q_3(t), \; q_4(t)]^T, \qquad \mathbf{q}_w(t) = [q_{w,1}(t)]^T \tag{A.14}$$

$$\mathbf{K}_{d} = \begin{bmatrix} \mathbf{K}_{zz} & \mathbf{K}_{zw} \\ \mathbf{K}_{wz} & \mathbf{K}_{ww} \end{bmatrix}, \qquad \mathbf{C}_{d} = \begin{bmatrix} \mathbf{C}_{zz} & \mathbf{C}_{zw} \\ \mathbf{C}_{wz} & \mathbf{C}_{ww} \end{bmatrix} \tag{A.15}$$

$$\mathbf{K}_{zz} = k_1 \begin{bmatrix} c^2 & cs & 0 & 0 \\ cs & s^2 & 0 & 0 \\ 0 & 0 & 0 & 0 \\ 0 & 0 & 0 & 0 \end{bmatrix}, \qquad \mathbf{K}_{zw} = \mathbf{K}_{zw}^{T} = k_1 \begin{bmatrix} -c \\ -s \\ 0 \\ 0 \end{bmatrix}, \qquad \mathbf{K}_{ww} = \begin{bmatrix} k_1 \end{bmatrix} \tag{A.16}$$

$$\mathbf{C}_{zz} = c_1 \begin{bmatrix} 0 & 0 & 0 & 0 \\ 0 & 0 & 0 & 0 \\ 0 & 0 & c^2 & cs \\ 0 & 0 & cs & s^2 \end{bmatrix}, \qquad \mathbf{C}_{zw} = \mathbf{C}_{zw}^{T} = c_1 \begin{bmatrix} 0 \\ 0 \\ -c \\ -s \end{bmatrix}, \qquad \mathbf{C}_{ww} = \begin{bmatrix} c_1 \end{bmatrix} \tag{A.17}$$

Chapter 4
Optimal Passive Damper Positioning Techniques:
State-of-the-Art

Arun M. Puthanpurayil
University of Canterbury, New Zealand

Rajesh P Dhakal
University of Canterbury, New Zealand

Athol J. Carr
University of Canterbury, New Zealand

ABSTRACT

A consolidated review of the current-state-of-the-art on optimal damper positioning techniques is presented in this chapter. The inherent assumptions made in previous research are discussed and substantiated with numerical studies. Earlier studies have shown that optimal distribution of dampers is sensitive to in-structure damping. In this chapter the significance of optimal distribution of dampers coupled with the necessity for the use of a more realistic in-structure damping model is qualitatively illustrated using a comparative sensitivity study. The effect of inherent assumption of linearity of the parent frame on the 'optimality' is also investigated. It is shown that linearity assumption imposed on the parent frame in a major seismic event may not be justified; thereby raising doubts on the scope of optimality techniques proposed in literature.

INTRODUCTION

The effectiveness of control strategies in achieving the objectives of performance based design is well accepted in structural engineering community. The theory of structural control as a field in itself was mainly enriched by mechanical and aerospace engineering and its adoption in structural engineering is rather more recent. The introduction of control techniques in structural engineering was mainly necessitated due to the growing demand for minimizing damage during a seismic event.

DOI: 10.4018/978-1-4666-2029-2.ch004

The adoption of control strategies to structures presented the structural engineering community with new challenges due to the inherent uncertainties associated with the system as well as with the excitation sources. The uncertainties associated with the excitation sources result in the inherent record to record randomness at a location. As no two earthquake-induced ground motions are similar, it is uncertain if a system proven to work for a structure in one ground motion will work equally efficiently in another ground motion. The inherent system uncertainties differ with respect to the type of control strategy adopted. Before delving into the details, we briefly describe the classification and types of structural control used in practice. Structural control is mainly divided into four types (Wada et al. 2004):

- **Seismic Isolation:** The art of insertion of mechanical devices between the sub-structure and super-structure which decouples the system from the damaging components of the earthquake ground motion.
- **Passive Control:** Mechanical devices distributed through the structure to provide "added damping" to the system to reduce the response to controllable limits.
- **Active Control:** Includes computer controlled actuators which provide seismic resistance by imposing forces on the structure to counter-balance the ground motion induced forces.
- **Semi-Active Control / Hybrid Control:** A combination of active and passive control which includes a combination of dampers and isolators.

The main focus of this chapter is on the passive control techniques. In line with this focus, the issues discussed herein would be limited to those associated with passive control. In deciding a passive control strategy, say for a building, two questions need to be answered: (1) What type of device is the most efficient? and (2) How should they be positioned in different floors and distributed across the height of the building? In the process, two system uncertainties associated with passive control have to be dealt with (Takewaki 2009):

- Local amplification of responses in the elements where a control device is attached
- The interaction between the structure and dampers distributed throughout the structure.

The first uncertainty needs to be addressed mainly in the structural design process, whereas the second needs to be addressed in the optimal positioning strategies (Takewaki 2009). Focusing on the second system uncertainty, the main purpose of this chapter is to present a consolidated review of the existing state-of-the-art on optimal positioning of dampers. Some inherent assumptions made in deciding the optimal positioning techniques in previous studies are critically scrutinized based on simplified numerical studies to assess their validity in the real world scenario. The authors have selected the most representative works known to them, and it is acknowledged that some important and stimulating works may have been unknown to the authors and unintentionally omitted.

Following the background presented in this section, the next section (i.e. *Significance of Optimal Distribution*) establishes significance of optimal distribution of dampers in controlling structural response. In this section, the need for optimal distribution of the dampers is emphasized with the help of numerical simulations. *Previous Studies* summarizes the current state-of-the-art. A consolidated review on the past researches in optimal damper positioning techniques is presented in this section. *Effect of In-Structure Damping Models on Optimal Distribution of Dampers* investigates and discusses the effect of in-structure damping models on optimal distribution of dampers. In this section, issues associated with the use of classical viscous damping model are discussed and a short insight into other damping models is also presented. In order to investigate the effect of the different damping models, a comparative numerical study is also performed. *Discussions on Realism of Linearity Assumption* investigates the validity of the linearity assumption (which is inherent in most of the previous studies on optimal positioning of dampers) in a realistic situation. Finally, the chapter ends with conclusions in the final section.

SIGNIFICANCE OF OPTIMAL DISTRIBUTION

In practice, there is often a belief that an increase in damping would always result in a better performance, which may not always be true. In order to justify this argument we present two studies; the first is based on the reduction of elastic response spectra of a record from the Chi-Chi earthquake by increasing the equivalent viscous damping which conceptually illustrates the significance of optimal positioning; and the second study is carried out on a twenty storey reinforced concrete frame emphasizing the relevance of optimal positioning in more realistic terms.

Figure 1 depicts the response acceleration reduction obtained as a result of an increase in the equivalent viscous damping. The solid curve represents the conventional elastic response spectra obtained with 5% equivalent viscous damping. The dotted curves represent the reduced equivalent elastic spectral ordinates obtained with higher values of equivalent viscous damping.

It could be observed that though there is a reduction in the peak acceleration response, a uniform reduction in response is not guaranteed; an increase in response is observed in some period ranges, which could be different for different earthquakes. This is a clear indication that an increase in added damping may not always result in a response reduction.

In order to further emphasize this fact in quantitative terms, an analytical investigation is carried out on a twenty storey reinforced concrete

Figure 1. Elastic response spectra of a Chi-Chi earthquake ground motion with varying levels of damping

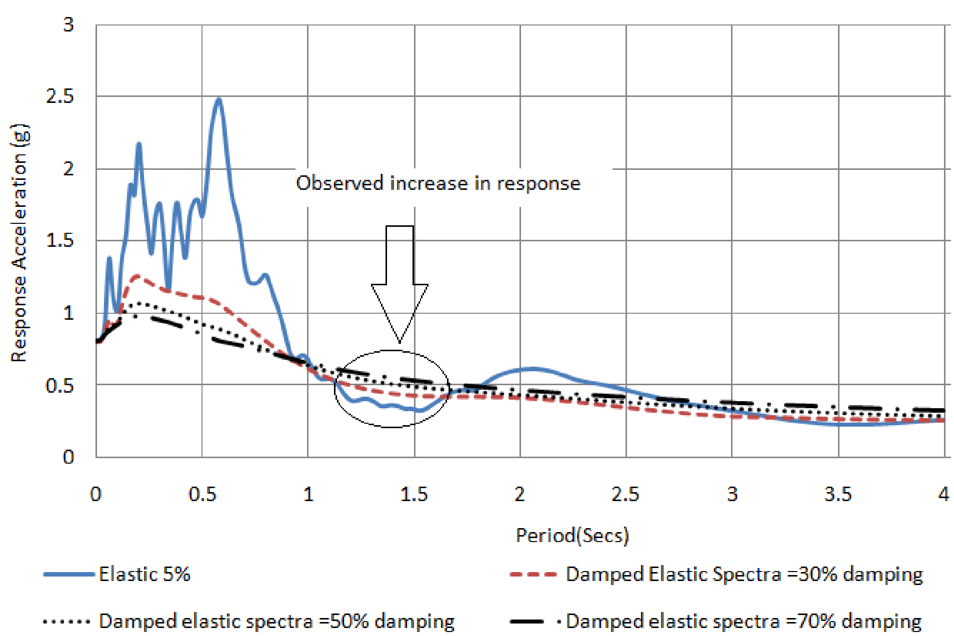

frame subjected to the ground motion recorded at Sakaria station in the 1999 Kocaeli earthquake. The two dimensional concrete frame model used for the study consists of three bays and the base is assumed to be fixed, neglecting the effect of soil-structure interaction. The fundamental period of the un-damped frame is 1.31 seconds. This period falls in the range where additional damping was found to increase the response in Figure 1. The frame is fitted uniformly with viscous dampers with a capacity of 9000 kN (Taylor 1999). A uniform distribution of the dampers is adopted as shown in Figure 2.

Assuming that the parent (i.e. uncontrolled) frame remains elastic during the seismic event, a linear time history analysis using the Newmark Beta scheme is performed using SAP 2000. Both acceleration and displacement time histories at the top floor are recorded and the results are presented in Figures 3 and 4. Figure 3 compares the displacement time history at the roof for both the controlled and the un-controlled frames. Similarly, Figure 4 compares the acceleration time history at the roof for both the controlled and un-controlled frames.

Figure 2. Controlled 20-storey frame with a uniformly distributed damper arrangement

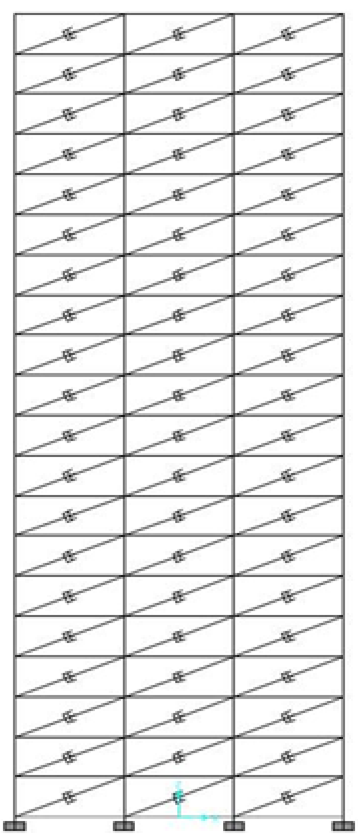

Figure 3 clearly illustrates the displacement response reduction achieved by the controlled frame. For this specific case, a reduction of approximately 80% is achieved in the peak displacement. On the contrary, Figure 4 depicts the fact that at certain specific times, there is an increase in the acceleration response of the controlled frame as compared to the un-controlled frame. For example, the acceleration response between 2 and 3 seconds is considerably higher for the controlled frame than for the uncontrolled frame. This reinforces the significance of optimal positioning by highlighting the fact that "a uniform increase in damping" might not always be beneficial from a response reduction point of view.

PREVIOUS STUDIES

This section presents a consolidated review on the state-of-the-art for optimal passive damper placement. Wherever possible and relevant, comprehensive outlines of the contents of respective works are presented. At the end of this section, some limitations inherent in the current optimal damper placement methods are pointed.

The majority of earlier research on structural control science has primarily focused on the design and installation techniques (i.e., the first system uncertainty discussed in Section 1). Extensive studies have been carried out on these aspects of structural control and considerable progress has been made. In comparison, studies associated with optimal positioning (i.e., the second system uncertainty) are very limited. Classically, optimal

Figure 3. Roof displacement time histories for the controlled and un-controlled frames

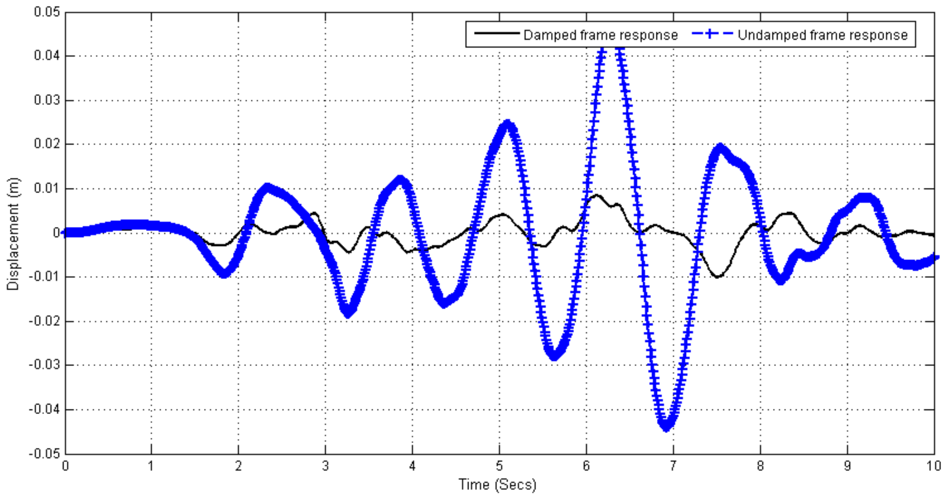

Figure 4. Roof acceleration time histories for the controlled and un-controlled frames

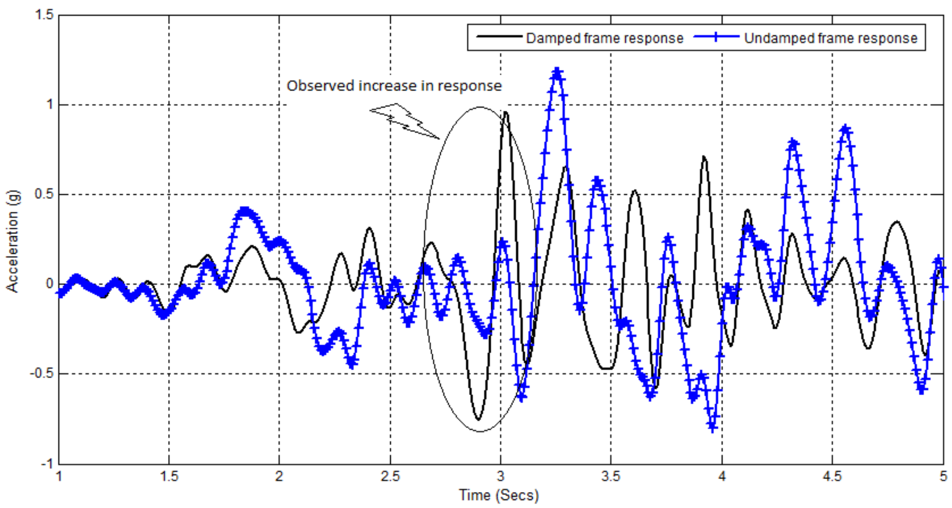

positioning techniques principally aim at developing strategies for the placement of the control devices with optimal capacity for the reduction of the target indices; the primarily chosen target indices would be drift and acceleration.

One of the early major works in this direction was the study carried out by Desilva (1981) in which he derived a gradient algorithm for controlling the vibration of a flexible system by optimally inserting control devices. His work included a complete mathematical formulation for slender beams in vibration due to flexure. Thereafter, Constantinou and Tadjabakhsh (1983) obtained an optimum damping coefficient for a damper located in the first story of a shear building subjected to stationary white noise ground accelerations. In this work, analytical expressions were formulated for calculating the maximum displacements of each floor. Parametric studies were conducted to determine the effect of structural damping and the inherent structural flexibility on the control parameters.

Cheng and Pantelides (1988) pioneered an approach in which the locations of active controllers were optimized in terms of a controllability index. This controllability index as defined by them is a measure associated with the structure's response to a specific earthquake. The basic idea underlying the controllability index method is that a controller is optimally placed when it is located at a position where the displacement or relative displacement response of the uncontrolled system is the maximum. Though it was done in the context of active control, the philosophy was very much applicable for addressing the positioning issues in passive control.

Zhang and Soong (1992) pioneered an extension to the above described controllability index method to address the issue of locating passive dampers. They developed a sequential procedure for the optimal placement of the damper devices. This procedure is called the Sequential Search Algorithm (SSA), and it determines the optimal location index by evaluating the random seismic response of a structure using the transfer matrix method. The mean square values of the inter-story drifts are used as optimal location indices. The procedure starts with determining the best location for the first damper. It was shown that the best position for the first damper is the location where the inter-story drift of the uncontrolled frame is the maximum (Cheng and Pantelides 1988). After determining this location, the damper is added and the procedure is repeated incorporating the added stiffness and damping and the optimal location for the second damper is determined. This procedure is repeated till all dampers are placed. In this method, the earthquake excitation is modeled as a stationary stochastic process.

Hahn and Sathiavageeswaran (1992) proved through a series of sensitivity analyses that in order to get an optimum response for a shear building with uniform stiffness during an earthquake, the dampers should be placed in the lower half of the building. This study mainly focused on assessing the effect of distribution of visco-elastic dampers. They also proved that tall buildings are more sensitive to changes in the distribution of dampers as compared to short buildings. Gurgoze and Muller (1992) came up with a numerical method for optimally placing the dampers and to determine their capacities based on an energy criterion. One common observation that could be made in these works is that all of them considered shear buildings with either uniform story stiffness or with specified story stiffness. In other words, in the optimality problem considered, stiffness of the parent frame was never considered as a design variable.

Tsuji and Nakamura (1996) made a significant advancement by pioneering an algorithm to derive an optimum set of stiffness of a shear building frame along with the optimum set of viscous damping devices, imposing necessary behavioral constraints. The constraints imposed were on maximum inter-story drifts due to a set of spectrum compatible ground motions, on upper bounds of the damping coefficient of each damper and on the sum of the damping coefficients of all dampers. Optimum problem addressed in this study was to find a minimum cost design. The method proposed by Tsuji and Nakamura was more efficient in the sense that it produces an ordered set of optimum design of shear buildings with viscous dampers by minimizing the sum of the story stiffness subjected to the current constraints, and each design in the ordered set could be considered to be a 'candidate design' corresponding to various upper bound levels of damper damping coefficients. On the other hand, the method developed by Zhang and Soong (1992) was more intuitive as their ultimate solution only approximately optimizes the objective function. Connor and Klink (1996) and Connor *et al.* (1997) introduced the concept of a quasi-optimal distribution in which the damper devices are proportional to the stiffness distribution.

Takewaki (1997a, 1997b, 1998) opened a new approach of smart passive damper placement techniques with a series of algorithms based on the concepts of inverse problem and optimal criteria based design approaches. The problem pioneered by Takewaki was to find the optimal damper placement to minimize the sum of the amplitudes of the transfer functions evaluated at the undamped fundamental natural frequency of the structural system. A constraint was imposed on the sum of the damping coefficients of the added dampers. This was a single criterion approach because only the damping coefficients of the added dampers were considered as a design variable, whereas the story stiffness was pre-specified.

Subsequently, Takewaki (1999) came up with an approach of stiffness-damping simultaneous optimization for displacement-acceleration simultaneous control. The structural system considered was a shear building model and both stiffness and damping coefficients of the added dampers were considered as design variables. This is a two-step design method. In the first step, a design is obtained by satisfying the optimality conditions for a specified set of total story stiffness capacity and total damper capacity. In the second step, a series of optimal designs is obtained sequentially for various stiffness and damping capacity levels. Deformation is reduced in both the steps while acceleration is reduced only in the second step. This is a very significant work as it considers acceleration also as a quantity that needs to be controlled. To the authors' knowledge most of the earlier works were mainly concentrated on drift reduction as the primary objective, whereas this was the first work which explicitly aimed to minimize both displacement and acceleration responses through minimization of the weighted sum of mean-square inter-story drifts and a mean square top floor absolute acceleration. Takewaki also showed that increases in total stiffness capacity and total damper capacity are effective in reducing the inter-story drift, but increase of only the total damper capacity reduces the floor acceleration.

Takewaki and Yoshitomi (1998), Takewaki and Uetani (1999) and Takewaki (2000) described a systematic procedure for determining the optimal positioning of dampers in planar moment resisting frames by minimizing the dynamic compliance subjected to a constraint on the sum of the damping coefficients of the dampers. Dynamic compliance is defined as the sum of the transfer function amplitudes of inter-story drifts evaluated at the undamped fundamental natural frequency. The systematic procedure developed is called the steepest direction search algorithm. This again is a significant advancement because most of the earlier researchers were only considering shear building models. Takewaki consolidated all his work on optimal damper positioning in the form of a textbook (Takewaki 2009). In addition to the works mentioned above, the book illustrates the procedures by which the steepest direction search algorithm could be extended to three dimensional systems. This book also describes the procedures by which the effect of soil structure interaction could be incorporated in optimal positioning of dampers and gives an overview of the design of shear buildings with uncertainties using the principle of critical excitation. Some additional useful references on this are Takewaki and Nakamura (1995, 1997), and Takewaki (2000a, 2000b).

Gluck et al (1996) pioneered and adapted the optimal control theory using a quadratic regulator to design and place control devices based on their deformations and velocities. They considered linear passive viscous and visco-elastic devices, represented them by a fully effective Kelvin model using a full state static feedback. This work holds a significant place in the literature, as it adapted the well established active control theories for passive devices. Wu et al. (1997) applied the sequential search algorithm (SSA) developed by Zhang and Soong (1992) to 3-D torsionally-coupled structures and carried out an investigation into the effect of ground motion characteristics on optimal distribution.

Shukla and Datta (1999) reconfirmed the efficiency of the SSA method through a parametric study using visco-elastic dampers. Frequency domain approach was employed for determining the responses to both broad and narrow band ground motions. The study shows that the optimal placement of dampers is sensitive to the nature of excitation force. This is an important observation because it implies that what is optimal in one specific ground motion need not be optimal in a different ground motion. This opens up a whole lot of concern on the use of the term 'optimality' because of the high inherent uncertainty in the ground motions. One approach to address this uncertainty is to use the principle of critical excitation (Takewaki 2007). As it falls beyond the scope of the present chapter we will not further discuss on this aspect; interested readers should refer to other relevant works such as Takewaki (2000a-d, 2001a-g, 2004a-b, 2005, 2007), Ahmadi (1979), Drenick (1970, 1973, 1977a-b), Drenick and Park (1975), Iyengar (1970, 1972, 1989), Iyengar and Manohar (1985, 1987); to name a few.

Moreschi (2000) and Singh and Moreschi (2001, 2002) introduced a gradient based approach and also employed genetic algorithm approaches as an alternative to address the problem of optimal placement of dampers. The performance index to be minimized was defined as a function of the system response obtained by considering a stochastic description of the input motion defined by Kanai-Tajimi spectral density function. The application of genetic algorithm is especially suitable where the performance index is not a continuous function of the design variables. The basic assumption in the study was that the parent frame remains linear. State space approach was used for the analysis. Numerical results were reported for both shear and torsional building models.

Garcia (2001), and Garcia and Soong (2002) developed the simplified sequential search algorithm method (SSSA) which is basically a simplified form of the SSA method originally developed by Soong. In order to show the efficiency of the proposed method a comparison of the proposed SSSA with other methods was presented. The other methods used for comparison were the optimal design using optimal control theory (Gluck et al 1996) and the optimal design using the minimum transfer functions (Takewaki 1997). It was shown that the optimal distribution of dampers obtained is sensitive to ground accelerations. In this study too, the parent frame was assumed to remain linear. Palazzo et al (2004) presented a new approach to optimally locate dampers by assessing the power balance of structures subjected to seismic actions described by a response spectrum. Modal state space approach was used for response evaluation and optimization.

Trombetti and Silvestri (2004, 2006, 2007) developed an efficient mass proportional damping (MPD) system and showed its utility. In this scheme, the dampers are placed in such a way that they are connected to a fixed point and are sized to be proportional to each storey mass. The scheme is based on the mass proportional damping component of the Rayleigh viscous damping matrices. Shear building model was used for the study, and it is assumed that the first mode of vibration controls the dynamic response. In an earlier work (Trombetti et al. 2003), they had proved that within the class of Rayleigh damping, the first modal damping ratio of the mass proportional damping system is always higher than the first modal damping ratio of stiffness proportional damping system and other Rayleigh damping systems. They compared their scheme with the algorithm proposed by Takewaki (1997) to show its efficiency. Later, Takewaki (2009) agreed that the MPD scheme is efficient, but expressed his concern regarding its practical application. From an implementation perspective, we also wish to emphasis here that the MPD scheme would be impracticable unless there is a fixed point associated with every degree of freedom to which the dampers could be attached.

Martinez-Rodrigo and Romero (2003) described a simple numerical methodology that leads to an optimum retrofitting option with nonlinear fluid viscous dampers. Subsequently, Lavan and Levy (2005) presented a methodology for the optimal design of supplemental viscous dampers for regular and irregular building models by minimizing the added damping subjected to a constraint on energy based global damage index for an ensemble of realistic ground motions. A gradient based optimization scheme was used in this study, which tried to address the effect of strength irregularity caused by different story stiffness. This work was definitely an improvement as compared to most of the studies documented earlier because it considered nonlinearity in the parent frame. Lavan and Levy (2004, 2006a) also presented a methodology for the optimal design of supplemental viscous dampers in which the parent frame remains elastic. The problem of minimizing the added damping was achieved by solving an equivalent optimization problem subjected to a constraint on the maximum inter-story drift for a frame excited by an ensemble of ground motion records. The other significant contribution of these two works is that they achieved the optimum design for an ensemble of realistic ground motions rather than for a stationary or non-stationary stochastic excitation as used in majority of the other methods recorded in this section. Again, Lavan and Levy (2006b) extended this methodology into the optimal design of viscous dampers for 3D irregular framed structures. In this study too, an ensemble of realistic ground motions was used and the parent frame is assumed to be linear. The added damping was minimized and subjected to a constraint on inter-story drifts on floor edges. A gradient based optimization algorithm was used and a variational approach was adopted for the derivation of the gradient of the constraint.

In the last decade, there have been several studies on optimal damper positioning. Aydin et al (2007) presented an alternative to Takewaki's method by considering the transfer function amplitude of base shear evaluated at the fundamental frequency as the objective function. Planar building frames with a soft storey were investigated in this study. The efficiency of the proposed method was illustrated by a comparison with Takewaki's method. Ajeet and Shirkhande (2007) showed that the efficiency of optimally placed dampers is maximised in symmetric buildings and its efficiency reduces as plan irregularity increases. Cimellaro (2007) addressed the issue of simultaneous optimal distribution of stiffness and damping for retrofitting structures by optimizing a generalized objective function that combines absolute acceleration, displacement and base shear transfer function. This method basically modified the method proposed by Takewaki (1997). In order to highlight the efficiency of the proposed method a comparison with the methods of Takewaki (1997) and Aydin et al (2007) was carried out. Lavan et al (2008) developed a non-iterative optimization procedure for seismic weakening and damping of inelastic structures. The procedure determines the optimal location and amount of weakened structural components and added damping devices in inelastic structures. The methodology proposed assumes proportional changes in strength and stiffness which is a limitation. Cimellaro et al. (2009) extended the above proposed methodology into a more generic design strategy in which uncoupled changes of strength and stiffness are allowed for the control of buildings experiencing inelastic deformations during seismic response.

More recently, Lavan and Dargush (2009) examined a multi-objective seismic design optimization in which the maximum interstorey drift and maximum acceleration were considered as the primary control parameters. The multi-objective problem was formulated in Pareto optimal sense (Pareto 1927) and a genetic algorithm based approach was adopted to identify the Pareto front. The end result of this multi-objective optimization is a family of Pareto front solutions providing the decision makers with an opportunity to understand the tradeoff between the drift and acceleration.

Both linear and nonlinear parent structural frames were considered in the study. The nonlinear parent frame was idealized as a yielding shear frame which also takes into account the new retrofitting techniques based on weakening and damping described in Lavan et al (2008). The other most important contribution of this work was the consideration of 'cost of the damper' as an external constraint. Paola and Navarra (2009) discussed the stochastic responses of MDOF structures with nonlinear viscous dampers to a seismic excitation.

Although not described here in detail, some other related studies include: Takewaki et al (2010), Viola and Guidi (2009), Cimellaro and Retamales (2007), Wongprasert and Symans (2004), Xu et al (2003, 2004), Tan et al (2005) and Xi Lin (1999) and interested readers should refer to these.

All the above mentioned studies investigated different optimal positioning techniques; but some of the assumptions adopted remain common to all. Reviewing these assumptions we identify the following limitations:

- **Inherent assumption of Rayleigh's viscous damping model for representing in-structure damping of parent frame.** Almost all studies recorded above assume the Rayleigh viscous model for representing in-structure damping. Reviewing the available literature on damping we have strong concerns regarding the use of this model for representing in-structure damping of the parent frame (Adhikari 2000, Adhikari and Woodhouse 2003, Woodhouse 1998, Brenal 1994, Leger and Duassault 1992, Hall 2006, Charney 2008, Zareian and Medina 2010). In the next section, we further substantiate our concern through a numerical sensitivity study.
- **Inherent assumption of linear elastic behavior of the parent frame.** Except for Lavan and Levy (2005), Lavan et al (2008), Cimellaro et al (2008), and Lavan and Dargush (2009), majority of all other studies discussed above assumed the parent frame to remain elastic during a seismic action. Even in the aforementioned studies, although yielding in the parent frame was considered, the model was not adequately set up to reflect reality. Most of them adopted a yielding shear story frame idealization, but if a frame is designed to a seismic code based on capacity design principles, yielding tends to happen in the beams to avoid the formation of a soft storey failure mechanism which might result in a global collapse. As the shear story frame models do not consider columns or beams separately, they fail to capture the realistic yielding behavior. Hence, considering the majority of the documented past research, we can say that linearity of the parent frame is an inherent assumption in the existing optimal positioning techniques. In Section 5, we discuss in detail the consequences of this assumption on the optimality criteria and substantiate it with a numerical sensitivity study.

EFFECT OF IN-STRUCTURE DAMPING MODELS ON OPTIMAL DISTRIBUTION OF DAMPERS

Takewaki (2009) has shown that the optimal distribution of added dampers is sensitive to the in-structure damping inherent in the structure. The sensitivity study emphasized the fact that the distribution of the capacity of the added dampers changes with the extent of in-structure damping. This means if the in-structure damping model fails to capture the realistic damping in the system, then what seems optimal in analysis might not be optimal in reality. This signifies the necessity of the use of a more realistic model of in-structure damping imperative.

This section mainly reviews the interaction of the in-structure damping models with the optimal distribution of dampers and attempts to qualitatively evaluate the influence of the various models on optimality in terms of response. Though no specific conclusions are drawn, our main intention here is to highlight the issues associated with certain prevalent assumptions regarding the in-structure damping and its effect on the optimal distribution of dampers.

Discussions on the Realism of Classical Viscous Damping

The sensitivity studies by Takewaki (2009) implicitly pose a big question as to what is the correct model of in-structure damping that represents the true nature of the system. Common practice is to use the classical viscous damping model originated by Rayleigh, through his famous 'Rayleigh dissipation function', in which only the instantaneous velocities are considered as the relevant state variables and on employing Taylor's expansion results in a model which captures the damping through the formation of a 'dissipation matrix' (Adhikari 2000). In strict mathematical sense, Rayleigh's matrix is actually representative of a system which is mainly driven by fluid damping due to its inherent dependence on the instantaneous velocity. This model is commonly used to model damping in MDOF systems and its popularity is mainly due to the fact that it uses the already computed mass *(M)* and stiffness *(K)* matrices $\left(C = \alpha M + \beta K\right)$ and demands only the calculation of the constants α and β (Carr 2007). The main advantage of this model is that the orthogonality of the modes is preserved; thereby facilitating the classical modal analysis to be performed more or less similar to the un-damped vibration.

In the case of a controlled frame, due to the addition of dampers, damping becomes non-classical and the orthogonality of the modes no longer exists. So using the classical in-structure damping model (Rayleigh model) does not add any benefit. Moreover, from a realistic perspective there are a lot of issues associated with this model, some of which are discussed briefly hereafter. One of the main issues is the proportionality phenomenon exhibited by the Rayleigh model. In reality, the test results indicate complex nature of the eigen modes, which implies non-orthogonality of the mode shapes and indicates the presence of non-classical damping (Adhikari 2000). The other main issue with this model is the strong dependence on the frequency of the structure as the constants $\left(\alpha \text{ and } \beta\right)$ are evaluated as a function of the frequency. There have been a large number of studies investigating the frequency dependence of the analytical model used in practice, and interestingly the majority of these studies emphasize that material level damping is a strong function of x^n and a frail function of *w*, where *x* refers to the displacement and *w* refers to the angular frequency (Adhikari 2000, Bandstra 1983, Baburaj and Matsukai 1994). The facts highlighted above raise a huge concern regarding the optimality criterion achieved in terms of response reduction when the classical Rayleigh model is used for the in-structure damping. So here we give a brief overview of other models of damping reported in literature and perform a numerical sensitivity study to see the effect of different models on the response of optimally controlled frame.

Brief Overview of the Models of Damping

A full detail review on all models of damping is beyond the scope of this chapter and interested readers should refer to Banks and Inman (1991), Woodhouse (1998), Adhikari (2000), Muravski (2004), Puthanpurayil et al (2011), Smyrou et al (2011). In this section, we restrict our discussion to non-viscous damping models and frequency-independent damping models.

Models in which the damping force is a function of past history of motion via convolution integrals over a suitable Kernel function constitutes non-viscous damping. They are called non-viscous because the force depends on state variables other than just the instantaneous velocity (Adhikari et al 2003). The most generic form of linear non-viscous damping given in the form of modified dissipation function is as follows (Woodhouse 1998, Adhikari 2000):

$$F == \frac{1}{2}\dot{q}\,'\int_0^t g\left(t-\tau\right)\dot{q}(\tau)d\tau \qquad (1)$$

where $g(t)$ represents the Kernel function and $\dot{q}(\tau)$ represents system velocity. This could also be looked as a time hysteresis model applied to discrete systems. The generality of this model is evident from the aspect that the Kernel function $g(t)$ could adopt any causal model where the energy functional is non-negative (Adhikari et al 2003). Incorporating this model, the equation of motion of the system can be expressed as

$$M\ddot{u} + \int_0^t g\left(t-\tau\right)\dot{u}\left(\tau\right)d\tau + Ku = f(t) \qquad (2)$$

where M is the mass, K the stiffness, $f(t)$ the applied force, $\ddot{u}$ the acceleration, $\dot{u}$ the velocity and u the displacement of the system.

The other most popular model is the frequency independent damping model. The concept of frequency independent damping arose when in 1927 Kimball and Lovell claimed that hysteretic damping is universal in nature. Since then there has been several studies which further strengthened their claim. One of the most popular models in this category is the linear Coulomb friction force model given as (Reid 1956, Muravski 2004)

$$F = k\left[x + \eta \mid x \mid \frac{\dot{x}}{\mid \dot{x} \mid}\right] \qquad (3)$$

This model could be in general a better representation of the boundary/structural damping occurring at structural joints. As material damping is negligible in comparison to the boundary damping, it could well be assumed that the use of this model in dynamic analysis would give a better representation of the overall damping phenomenon.

It should also be noted that, in this section, we are discussing damping models suited only for linear dynamic analysis. Detail literature on damping models suited for nonlinear dynamic analysis is available and interested readers should refer to Brenal (1994), Leger and Dussault (1992), Carr (1997, 2005), Hall (2006), Charney (2008), and Zareian and Medina (2010). These studies mainly propose modeling approaches to overcome the limitations of Rayleigh damping based on initial stiffness.

Numerical Study

A numerical study is carried out for illustrating the effect of in-structure damping models on the optimal distribution of dampers. Models used for the study are the classical Rayleigh model and the non-viscous model given by Equation (1) as it represents the most general damping model within the scope of a linear analysis (Woodhouse 1998).

Description of the Frame

The optimal distribution of dampers derived by Takewaki (1997) in a six storey shear building model is used for the study. The shear building model is shown in Figure 5. All masses are assumed to be lumped at storey levels with m_1=m_2…..=m_6= 0.8x10^5 kg. A uniform storey stiffness is assumed with k_1=k_2=………=k_6=4.0x10^7 N/m. The optimal damper locations are indicated in Figure 5.

The value of the optimal damper coefficients as calculated by Takewaki is as follows: c_1= 4.8x10^6 N-s/m and c_2= 4.2x10^6 N-s/m. One fact to be noted is that Takewaki neglected the contribution of the in-structure damping while calculating these coefficients. From our sensitivity analysis point of view, this is ideal because the damper coefficient values obtained do not have any contribution from in-structure damping; thereby providing us with a flexibility of incorporating different in-structure damping models with apparently no significant error. The undamped frequencies of the uncontrolled frame are recorded in Table 1.

Description of the Ground Motions

In order to assess the sensitivity of the optimally controlled frame to different in-structure damping models, the controlled frame is subjected to two different earthquake ground motions: the Chi-Chi and the Sakaria. The Fourier amplitude spectra of both ground motions are presented in Figure 6 and Figure 7.

Figure 6 shows that the Chi-Chi record has a narrow band spectrum with a predominant frequency content of 1.7Hz. On the other hand, the Sakaria record has a broad band spectrum with Fourier peaks occurring between 0.5 and 10 Hz as is evident in Figure 7.

The choice of the ground motion records is made with a focus to excite as many modes as possible. For example, reviewing the modal frequencies given in Table 1 it becomes evident that in the case of the Chi-Chi record the predominant excitation is expected to happen in the first 2 modes, whereas the Sakaria record is expected to excite several higher order modes to varying degrees. Since our intention is only to highlight the possible uncertainties arising due to the interaction between the inherent in-structure damping of the system and the 'added damping' supplied by the mechanical dampers, the choice of these two ground motions may be deemed to be appropriate.

Figure 5. Uncontrolled shear frame building (left) and optimally controlled shear frame building (right)

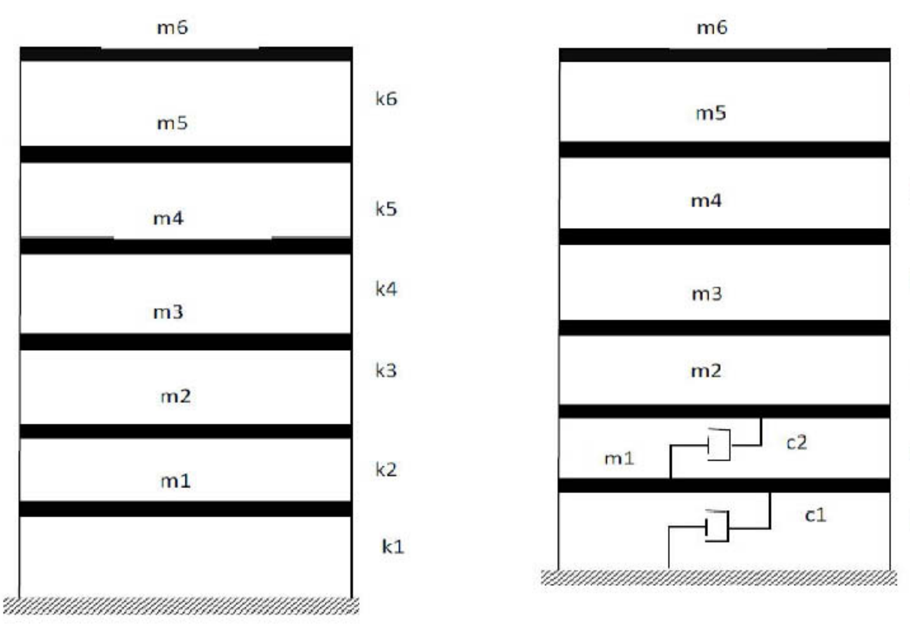

Table 1. Modal frequencies

Modes	Frequency (Hz)
1	0.85793
2	2.5239
3	4.0433
4	5.3276
5	6.3023
6	6.9108

Analysis of the Controlled Frame

Direct time integration is performed using the Newmark total equilibrium method (Carr 2007). MATLAB codes were developed for the time domain analysis incorporating both classical Rayleigh viscous and non-viscous damping models. In the case of non-viscous damping, a single exponential model called Biot's relaxation function is used as the Kernel function. Biot's relaxation function is of the form

$$g(t) = \mu e^{-\mu t} \tag{4}$$

where μ is a dissipation constant. A very low value of μ indicates strong non-viscous characteristics and a high value of μ indicates close to viscous characteristics (Adhikari 2000). Now the interesting question is which of these μ values would reflect reality? At this point of time unfortunately this question remains unanswered and demands further research. In this sensitivity study we use μ =1.0, 5.0 and 50.0, based on past research evidence (Adhikari, 2000).

Results and Discussions

Figures 8 and 9 represent the time histories of the displacement and acceleration responses of the roof due to the Chi-Chi ground motion with the classical viscous damping model and non-viscous damping models with different values of μ. The duration of the Chi-Chi ground motion used is 40 seconds and the response is evaluated till 60 seconds. The comparisons plotted in the figures can be used to investigate the effect of different non-viscous damping models in comparison with the classical viscous damping model. One qualitative observation that could be made from both

Figure 6. Fourier amplitude spectra of the Chi-Chi and the Sakaria

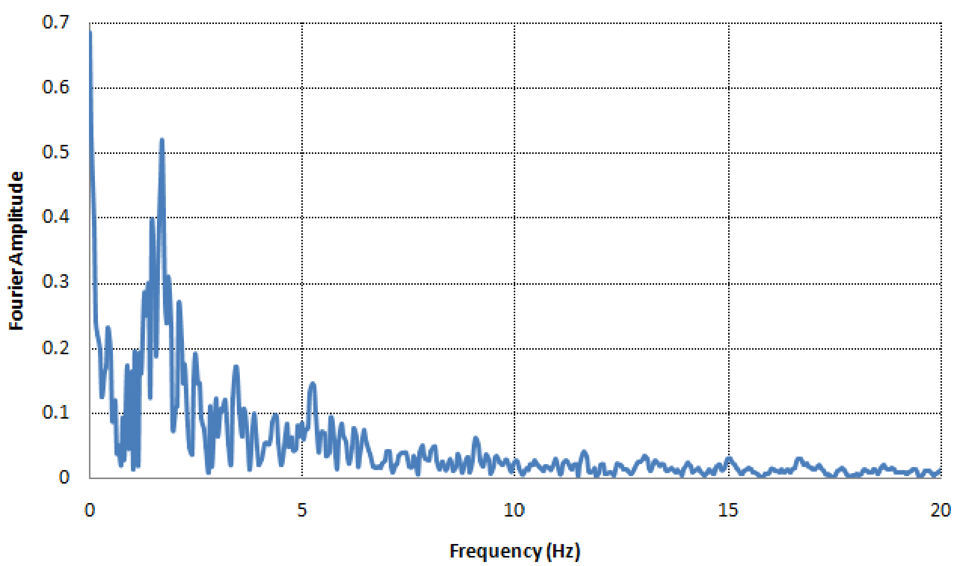

Figure 7. Fourier amplitude spectra of the Chi-Chi ground motion records

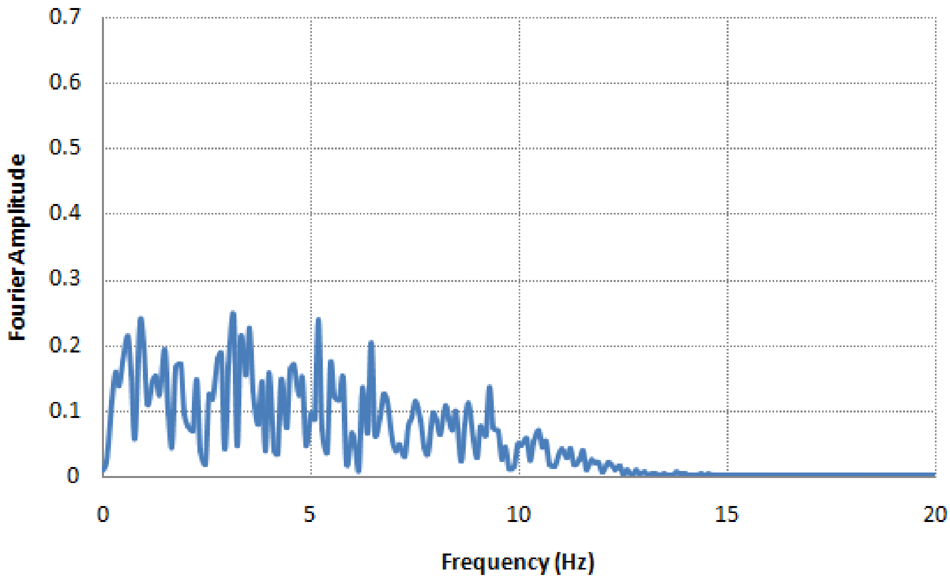

the plots is that a lower value of μ has a lesser decay rate for the vibration response.

Qualitatively observing the plots recorded in Figures 8 and 9 shows that there is a clear distinction between the responses obtained using non-viscous models with μ=50.0, μ =5.0 and μ =1.0. In order to get a better insight, zoomed in plots are shown in Figures 10 through 13. Figure 10 represents the zoomed in plots for roof displacement and Figure 11 represents roof acceleration due to the Chi-Chi ground motion. Similarly, Figures 12 and 13 represent the roof displacement and roof acceleration responses due to the Sakaria ground motion.

In all the plots it can be seen that there is a difference in the response amplitudes between the viscous and non-viscous models. μ=1.0 represents highly non-viscous nature and μ =50.0 indicates close to viscous nature. In almost all cases the response due to classical viscous damping model is closer to or follows the response with μ =50.0, justifying the statement made in section 4.3.3, 'a higher value of μ indicates close to viscous characteristics'. It is evident from these plots, that a smaller value of μ shows lesser decay and hence higher amplitude of response. The peak displacement amplitude in the μ =1.0 case is approximately two times that of the peak displacement amplitude associated with the classical viscous damping model.

Unfortunately, in reality, very little is known about structural damping. Free vibration testing of real buildings indicates that the damping in the first mode, though not purely viscous, is very close to viscous and we could say that $\left(\mu = 50.0\right)$ represents a realistic behavior, at least in the first mode. Our intention in plotting the highly non-viscous $\left(\mu = 1.0\right)$ and close to viscous $\left(\mu = 50.0\right)$ is to highlight this inherent variability existing in the modeling. There are other models such as the frequency independent damping model (described in section 4.2) which would again give an entirely different set of responses. All these observations raises a question on the optimality, because what is optimal in one analysis using a specific damping model might not be optimal in terms of response if we use a different damping model. It has also been shown by earlier studies (Val &Se-

Figure 8. Roof displacement histories due to the Chi-Chi ground motion

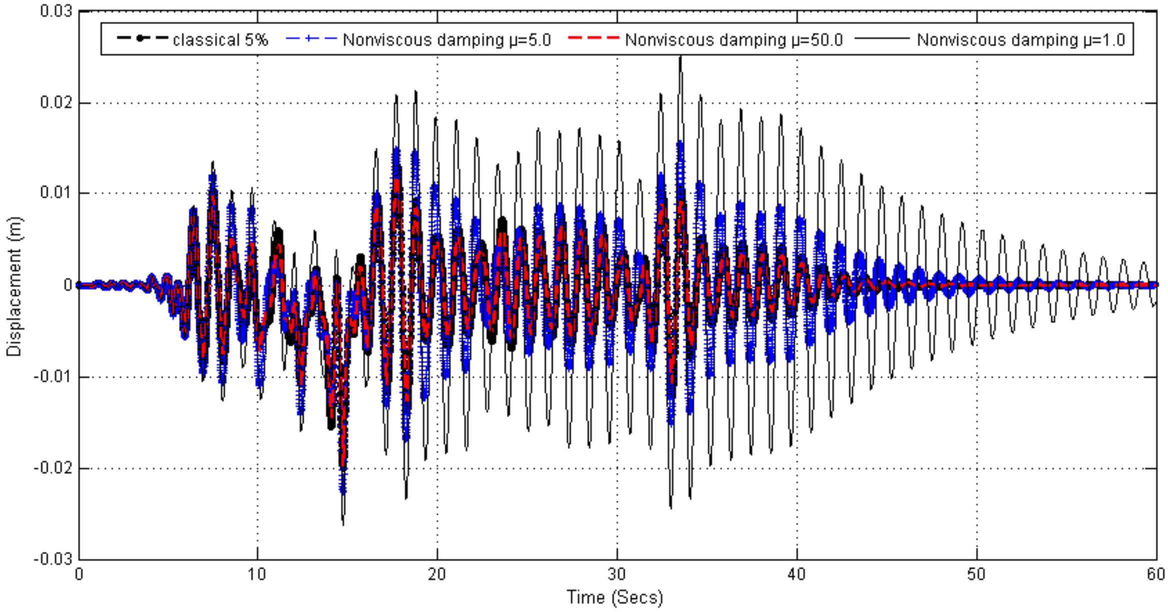

Figure 9. Roof acceleration histories due to the Chi-Chi ground motion

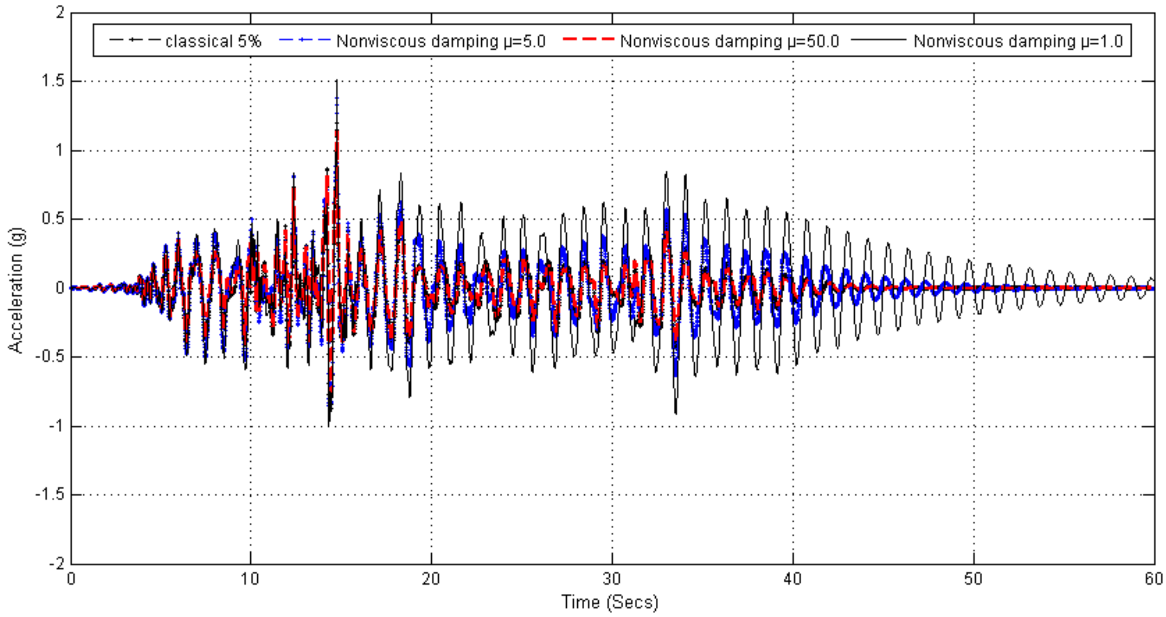

Figure 10. Roof displacement histories and roof acceleration histories

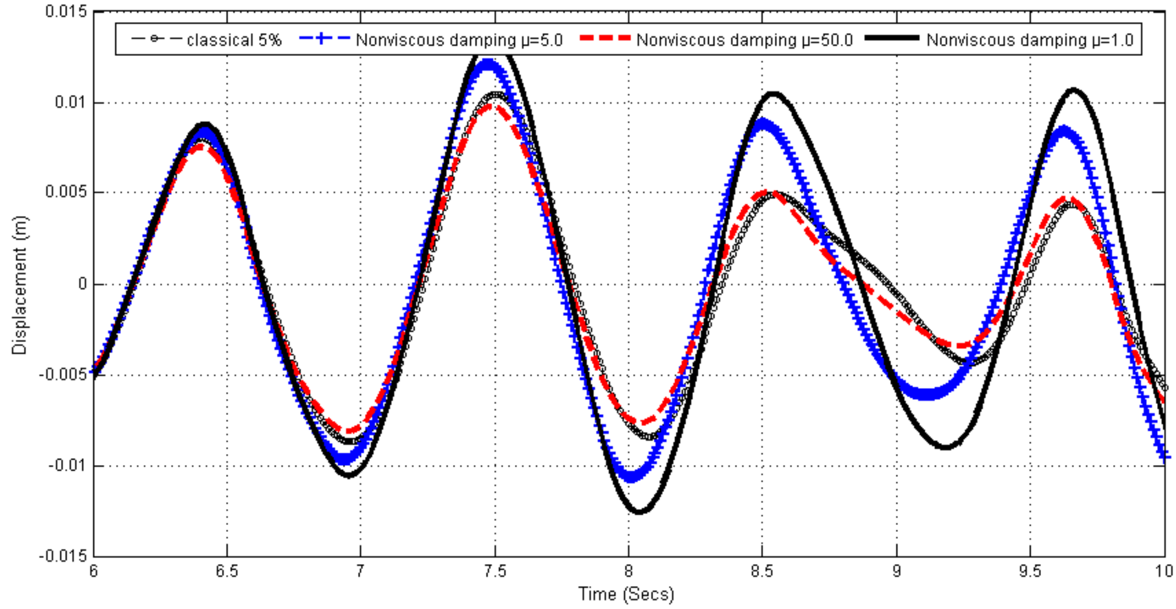

Figure 11. Roof displacement histories due to the Chi-Chi record

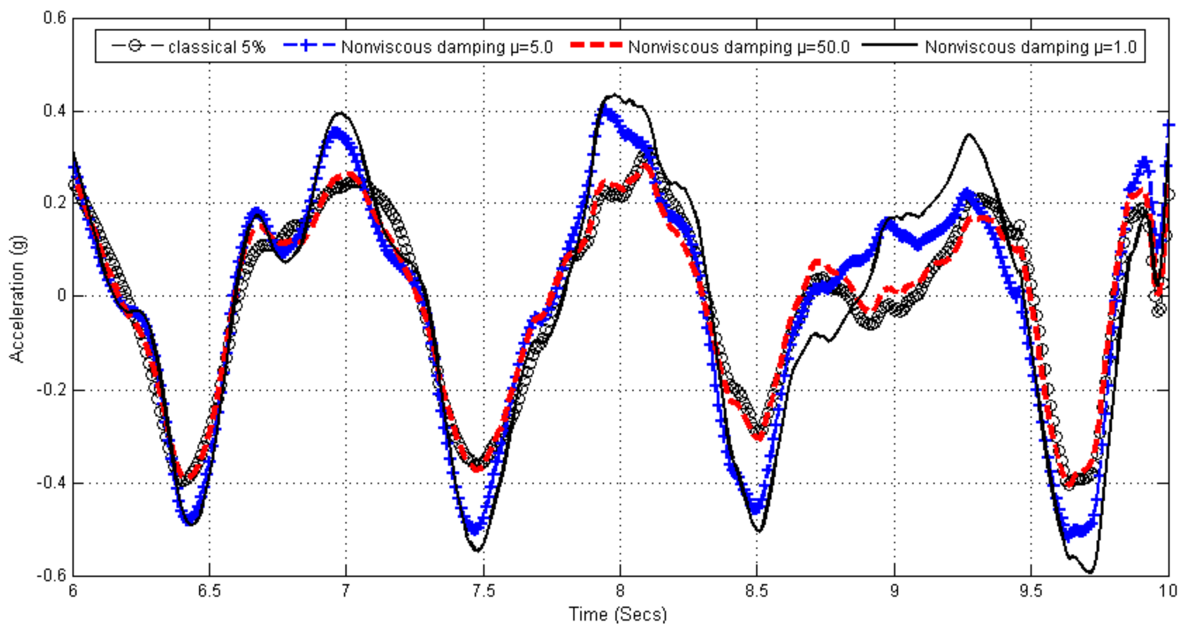

Figure 12. Roof displacement histories and roof acceleration histories

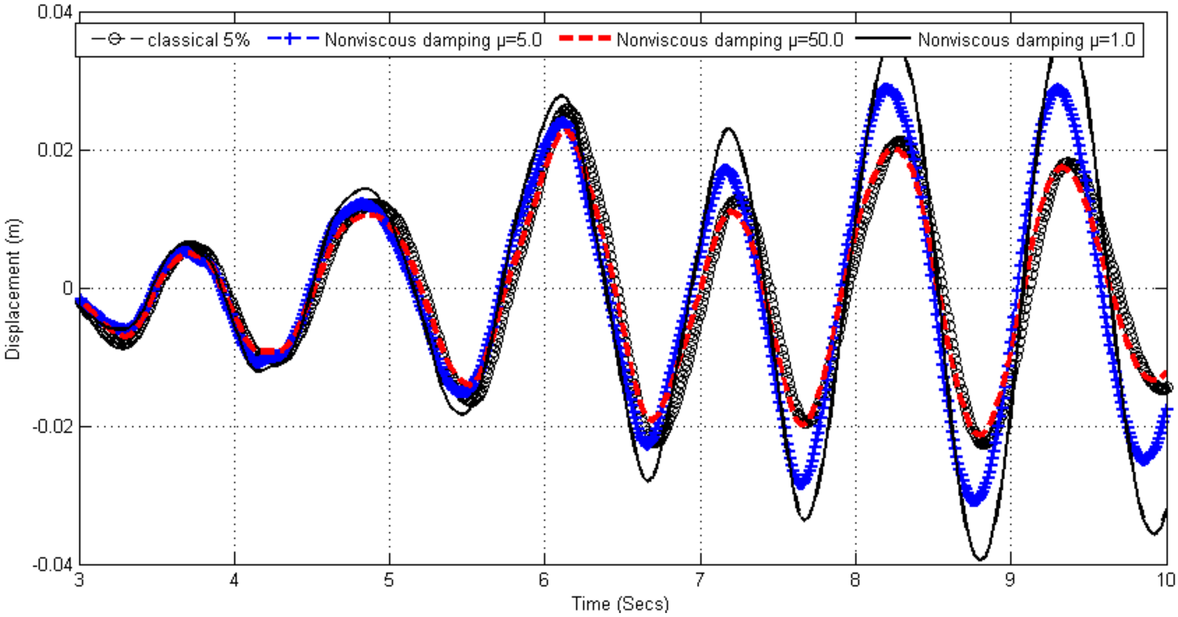

Figure 13. Roof displacement histories due to the Sakaria record

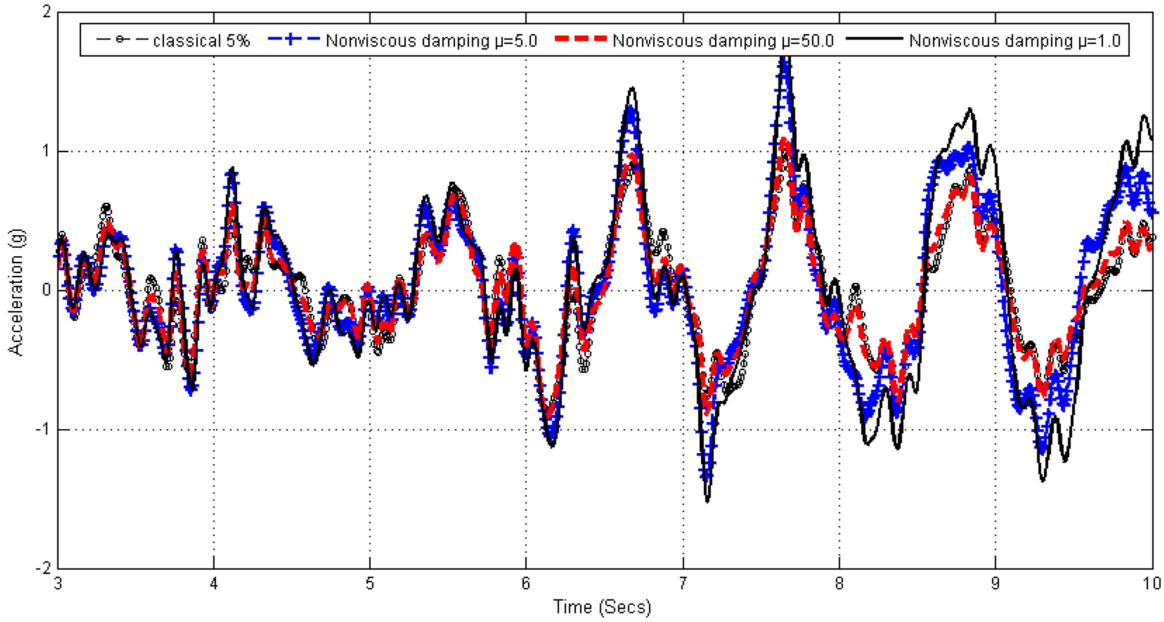

gal, 2005), that there would be instances when the classical viscous damping assumption would underestimate the peak deflection and fail to capture the occurrence of nonlinearity in the parent frame. So this aspect poses a risk of the parent frame becoming nonlinear and the damping model used in the analysis might fail to capture that effect, meaning that the resulting optimal distribution might no longer be optimal.

In this section we have only qualitatively emphasized the significance of the contribution of the in-structure damping in the overall structural response. From the studies carried out in this section we can state that in-structure damping models affect the optimal distribution of dampers; but at this point of time we are unable to define the extent of its effect. Further research is needed in this area.

DISCUSSIONS ON REALISM OF LINEARITY ASSUMPTION

In this section we intend to review the implications of the linearity assumption from a real world implementation point of view. Most of the research summarized in Section 3 investigated novel techniques for arriving at an optimal distribution of dampers and presented very useful methods; but one common fact that could be observed in majority of these methods is that most of the techniques require the parent frame to be linearly elastic during the seismic excitation. Also majority of the techniques are formulated in the frequency or state space domain where eigenvalues and eigenvectors determine the dynamic performance. This implies that in order for the above recorded techniques to be valid in a major seismic event, the frame has to remain linearly elastic. The other concern is that if in case the parent frame becomes inelastic, there would be stability issues (Cimellaro et al. 2009). This would make most of the optimal positioning techniques presented in literature invalid. The remaining part of this section focuses mainly on the realism of the linearity assumption rather than delving into the details of stability issues associated with development of the nonlinearity. Readers interested in the techniques of circumventing of the stability issues associated with inelasticity in the parent frame should refer to Lavan et al. (2008), and Cimellaro et al. (2009).

At first the effect of adding dampers into a parent structure is illustrated schematically. Figures 14a and 14b illustrate the effect of adding dampers into a building frame and the effect is expressed in terms of reduction in seismic input energy dissipated by the frame. E1 represents the total input energy and E2 represents the energy dissipated by the parent frame fitted with dampers. Evidently it could be seen that once a damper is added into the frame there is a reduction in the seismic energy that needs to be dissipated by the parent frame (E2<E1 in Figure 14b). But a closer look at Figure 14b epitomizes the fact that there is still a specific amount of energy that needs to be dissipated by the parent frame. This specific amount of dissipated energy would determine whether the parent frame remains elastic or not. So as demanded by the algorithms used in the literature, if the parent frame needs to remain in the elastic state (with no ductility mobilized) the input energy should be reduced to that level so as to cause only elastic stresses in the parent frame. In other words, this means that dampers would need to dissipate all the excess energy that might cause inelastic excursions in the parent frame.

Now what could this requirement mean in realistic terms? To answer this question, we use the results obtained from the Chi-Chi earthquake ground motion. The study mainly attempts to qualitatively illustrate the amount of damping required for a reduction of the input energy to a desired level so that the frame remains elastic. In order to satisfy this objective, the amount of damping required to reduce the original elastic spectra to an equivalent spectra is calculated, such that the newly derived equivalent elastic spectra has force amplitudes similar to a spectra of the

Figure 14. Effectiveness of passive dampers (a) uncontrolled frame, (b) controlled frame. Adapted from Takewaki 2009.

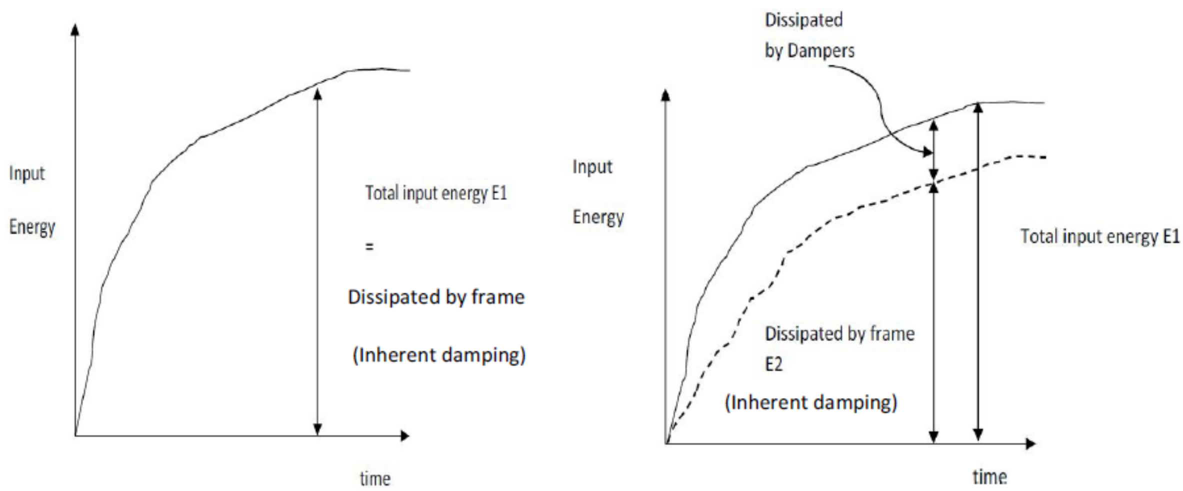

same earthquake with a ductility of 4.0. So in simple terms, we are attempting to match the acceleration amplitude of the elastic spectra (5% damping) to the spectra corresponding to a ductility of 4 by increasing the effective damping. Plots in Figure 15 depict the above stated objective.

Figure 15 illustrates the elastic response spectra and spectra with ductility equal to 4.0 with the standard 5% damping. Now the aim is to make the elastic amplitudes coincide with the amplitudes of spectra with ductility 4.0 by adding extra damping. In order to achieve this objective, the damping ratio is increased and is found that at a damping ratio of 30%, the amplitudes of elastic spectra are still slightly higher than the peak amplitudes of the spectra with ductility 4.

So in effect this study signifies that in order for the parent frame to remain elastic, for this particular case, from the very beginning there needs to be a system of dampers capable of imparting more than 25% damping in addition to the in-structure damping. The whole optimization algorithms reduce to a series of iterations on this damping level and in effect in strict mathematical sense the iterations would need to increase the overall damping, as a decrease might cause the algorithms to be invalid (i.e., the frame might become inelastic and the basic assumption in the algorithm development is violated). This is an interesting aspect because since the analysis itself is in the frequency/state space domain which is an inherent elastic method, the response evaluations could be deceptive in the sense that it might not capture the inelastic excursions which might occur in reality, should the overall damping not be sufficiently high.

CONCLUSION

A consolidated state of the art review on the optimal positioning techniques for passive dampers has been presented. The significance of the optimal distribution of dampers coupled with the necessity for the use of a more realistic in-structure damping model is illustrated with the help of a comparative sensitivity study. It is observed that different damping models give different responses highlighting the need for a realistic representation of the in-structure damping to achieve optimality in terms of response reduction. Realism of the basic inherent assumption of linearity of the

Figure 15. Response spectra of Chi-Chi ground motion for elastic and ductility=4.0

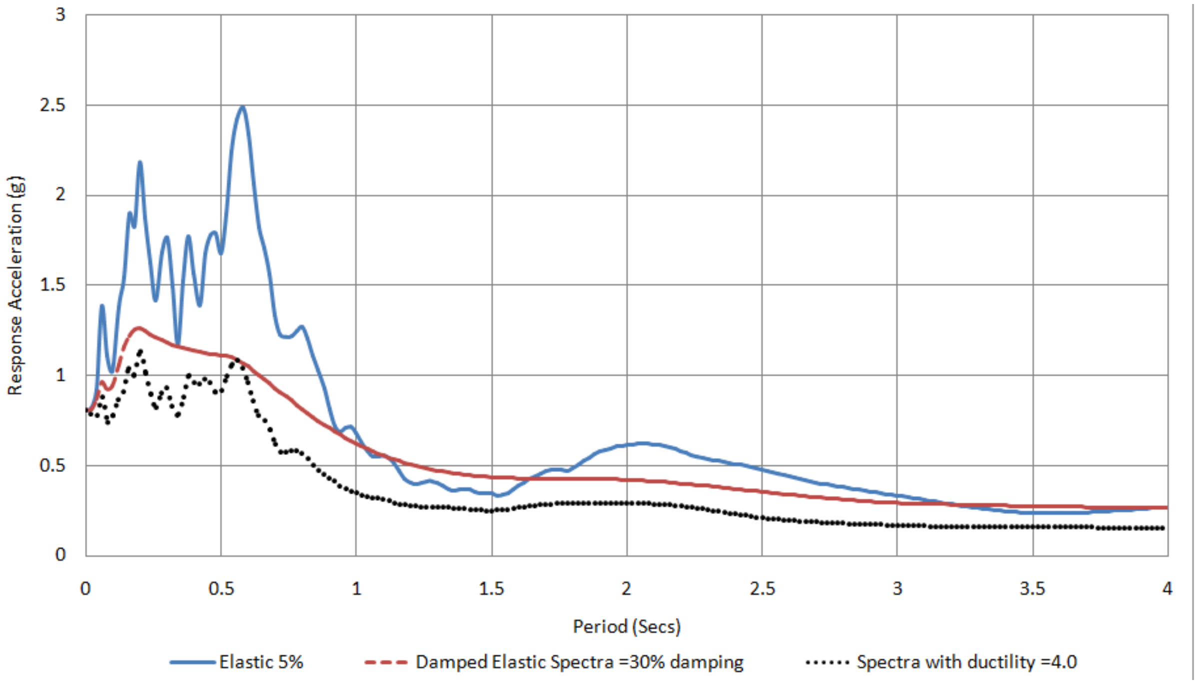

parent frame is explored. From a simple study it is shown that in a major seismic event it might not be possible to have the frame remain elastic. Certain areas which require further research have also been highlighted.

REFERENCES

Adhikari, S. (2000). *Damping models for structural vibration.* PhD Dissertation, University of Cambridge.

Adhikari, S., & Woodhouse, J. (2003). Quantification of non-viscous damping in discrete linear systems. *Journal of Sound and Vibration*, *260*, 499–518. doi:10.1016/S0022-460X(02)00952-5

Ahmadi, G. (1979). On the application of the critical excitation method to aseismic design. *Journal of Structural Mechanics*, *7*, 55–63. doi:10.1080/03601217908905312

Ajeet, S. K., & Shirkhande, M. (2007). Optimal placement of supplemental dampers in seismic design of structures. *Japanese Society of Engineering Education*, *9*(3), 125–135.

Aydin, E., Boduroglub, M. H., & Guney, D. (2007). Optimal dampers placements for seismic rehabilitation of planar building structures. *Engineering Structures*, *29*, 176–185. doi:10.1016/j.engstruct.2006.04.016

Baburaj, V., & Matsukai, Y. (1994). A study on the material damping of thin angle-ply laminated plates. *Journal of Sound and Vibration*, *172*(3), 415–419. doi:10.1006/jsvi.1994.1184

Bandstra, J. P. (1983). Comparison of equivalent viscous damping in discrete and continuous vibrating system. *Transaction of ASME, Journal of Vibration, Acoustics. Stress and Reliabilityin Design*, *105*, 382–392. doi:10.1115/1.3269117

Banks, H. T., & Inman, D. J. (1991). On damping mechanisms in beams. *Transactions of ASME. Journal of Applied Mechanics*, *58*, 716–723. doi:10.1115/1.2897253

Bernal, D. (1994). Viscous Damping in inelastic structural response. *Journal of Structural Engineering*, *120*(4), 1240–1254. doi:10.1061/(ASCE)0733-9445(1994)120:4(1240)

Carr, A. J. (1997). Damping models for inelastic structures. *Proceedings of Asia Pacific Vibration Conference '97*, Kyongju, Korea, Nov. 9–13, Vol. 1 (pp. 287–293).

Carr, A. J. (2005). Damping models for time-history structural analyses. *Proceedings of Asia Pacific Vibration Conference '05*, Langkawi, Malaysia, Nov 27 (pp. 42–48).

Carr, A. J. (2007). *Ruaumoko manual - Theory* (pp. 3–14). University of Canterbury Press.

Charney, F. A. (2008). Unintended consequences of modelling damping in structures. *Journal of Structural Engineering*, *134*(4), 581–592. doi:10.1061/(ASCE)0733-9445(2008)134:4(581)

Cheng, F. Y., & Pantelides, C. P. (1988). *Optimal placement of actuators for structural control*. Technical Report NCEER-88-0037, State University of New York, Buffalo, New York.

Cimellaro, G. P. (2007). Simultaneous stiffness-damping optimization of structures with respect to acceleration, displacement and base shear. *Engineering Structures*, *29*, 2853–2870. doi:10.1016/j.engstruct.2007.01.001

Cimellaro, G. P., Lavan, O., & Reinhorn, A. M. (2009). Design of passive systems for control of inelastic structures. *Earthquake Engineering & Structural Dynamics*, *38*, 783–804. doi:10.1002/eqe.867

Cimellaro, G. P., & Retamales, R. (2007). Optimal softening and damping design for buildings. *Structural Control and Health Monitoring*, *14*(6), 831–857. doi:10.1002/stc.181

Connor, J. J., & Klink, B. S. A. (1996). *Introduction to motion-based design*. WIT Press.

Connor, J. J., Wada, A., Iwata, M., & Huang, Y. H. (1997). Damage-controlled structures, I: Preliminary design methodology for seismically active regions. *Journal of Structural Engineering*, *123*(4), 423–431. doi:10.1061/(ASCE)0733-9445(1997)123:4(423)

Constantinou, M. C., & Tadjabakhsh, I. G. (1983). Optimum design of a first story damping system. *Computers & Structures*, *17*(2), 305–310. doi:10.1016/0045-7949(83)90019-6

De Silva, C. W. (1981). An algorithm for the optimal design of vibration controllers for flexible systems. *Journal of Sound and Vibration*, *75*(4), 495–502. doi:10.1016/0022-460X(81)90437-5

Drenick, R. F. (1970). Model-free design of aseismic structures. *Journal of the Engineering Mechanics Division*, *96*(4), 483–493.

Drenick, R. F. (1973). Aseismic design by way of critical excitation. *Journal of the Engineering Mechanics Division*, *99*(4), 649–667.

Drenick, R. F. (1977a). On a class of non-robust problems in stochastic dynamics. In Clarkson, B. L. (Ed.), *Stochastic problems in dynamics* (pp. 237–255). London, UK: Pitman.

Drenick, R. F. (1977b). The critical excitation of nonlinear systems. *Journal of the Engineering Mechanics Division*, *44*(2), 333–336.

Drenick, R. F., & Park, C. B. (1975). Comments on worst inputs and a bound on the highest peak statistics of a class of non-linear systems. *Journal of Sound and Vibration*, *41*, 129–131. doi:10.1016/S0022-460X(75)80203-3

Garcia, D. L. (2001). A simple method for the design of optimal damper configuration in MDOF structures. *Earthquake Spectra*, *17*(3), 38–398. doi:10.1193/1.1586180

Garcia, D. L., & Soong, T. T. (2002). Efficiency of a simple approach to damper allocation in MDOF structures. *Journal of Structural Control*, *9*(1), 19–30. doi:10.1002/stc.3

Gluck, N., Reinhorn, A. M., Gluck, J., & Levy, R. (1996). Design of supplemental dampers for control of structures. *Journal of Structural Engineering*, *122*(12), 1394–1399. doi:10.1061/(ASCE)0733-9445(1996)122:12(1394)

Gurgoze, M., & Muller, P. C. (1992). Optimal positioning of dampers in multi-body systems. *Journal of Sound and Vibration*, *158*(3), 517–530. doi:10.1016/0022-460X(92)90422-T

Hahn, G. D., & Sathiavageeswaran, K. R. (1992). Effects of added-damper distribution on the seismic response of buildings. *Computers & Structures*, *43*(5), 941–950. doi:10.1016/0045-7949(92)90308-M

Hall, J. F. (2006). Problems encountered from the use (or misuse) of Rayleigh damping. *Earthquake and Structural Dynamics*, *35*, 522–545.

Iyengar, R. N. (1970). *Matched inputs*. Report No. 47, Series J, Center for Applied Stochastics, Purdue University, W. Lafayette, IN.

Iyengar, R. N. (1972). Worst inputs and a bound on the highest peak statistics of a class of non-linear systems. *Journal of Sound and Vibration*, *25*, 29–37. doi:10.1016/0022-460X(72)90593-7

Iyengar, R. N. (1989). Critical seismic excitation for structures. *Proceedings of the 5th ICOSSAR*, San Francisco. New York, NY: ASCE Publications.

Iyengar, R. N., & Manohar, C. S. (1985). System dependent critical stochastic seismic excitations. *M15/6, Proceedings of the 8th International Conference on SMiRT*, Brussels, Belgium.

Iyengar, R. N., & Manohar, C. S. (1987). Nonstationary random critical seismic excitations. *Journal of Engineering Mechanics*, *113*(4), 529–541. doi:10.1061/(ASCE)0733-9399(1987)113:4(529)

Lavan, O., Cimellaro, G. P., & Reinhorn, A. M. (2008). Noniterative optimization procedure for seismic weakening and damping of inelastic structures. *Journal of Structural Engineering*, *134*(10), 1638–1648. doi:10.1061/(ASCE)0733-9445(2008)134:10(1638)

Lavan, O., & Dargush, G. F. (2009). Multi-objective Evolutionary seismic design with passive energy dissipation systems. *Journal of Earthquake Engineering*, *13*, 758–790. doi:10.1080/13632460802598545

Lavan, O., & Levy, R. (2004). Optimal design of supplemental viscous dampers for linear framed structures. *Proceedings of 13th World Conference on Earthquake Engineering,* Paper no: 42.

Lavan, O., & Levy, R. (2005). Optimal design of supplemental viscous dampers for irregular shear frames in the presence of yielding. *Earthquake Engineering & Structural Dynamics*, *34*(8), 889–907. doi:10.1002/eqe.458

Lavan, O., & Levy, R. (2006a). Optimal design of supplemental viscous dampers for linear framed structures. *Earthquake Engineering & Structural Dynamics*, *35*(3), 337–356. doi:10.1002/eqe.524

Lavan, O., & Levy, R. (2006b). Optimal peripheral drift control of 3D irregular framed structures using supplemental viscous dampers. *Journal of Earthquake Engineering*, *10*(6), 903–923. doi:10.1080/13632460609350623

Leger, P., & Dussault, S. (1992). Seismic energy dissipation in MDOF structures. *Journal of Structural Engineering*, *118*(5), 1251–1269. doi:10.1061/(ASCE)0733-9445(1992)118:5(1251)

Martinez-Rodrigo, M., & Romero, M. L. (2003). An optimum retrofit strategy for moment resisting frames with nonlinear viscous dampers for seismic applications. *Engineering Structures*, *25*(2), 913–925. doi:10.1016/S0141-0296(03)00025-7

Moreschi, L. M. (2000). *Seismic design of energy dissipation systems for optimal performance.* PhD. Dissertation, Virginia Polytechnic Institute and State University.

Muravski, G. B. (2004). On frequency independent damping. *Journal of Sound and Vibration*, *274*, 653–668. doi:10.1016/j.jsv.2003.05.012

Palazzo, B., Petti, L., & De Iuliis, M. (2004). A modal approach to optimally place dampers in framed structures. *Proceedings of 13th World Conference on Earthquake Engineering,* Paper no: 769.

Palazzo, B., Petti, L., & De Iuliis, M. (2004). A modal approach to optimally place dampers in framed structures. *Proceedings of 13th World Conference on Earthquake Engineering,* Paper no: 769.

Paola, M. D., & Navarra, G. (2009). Stochastic seismic analysis of MDOF structures with nonlinear viscous dampers. *Structural Control and Health Monitoring*, *16*(3), 303–318. doi:10.1002/stc.254

Pareto, V. (1927). *Manuel d'e'conomie politique*. Paris, France: Giard.

Puthanpurayil, A. M., Dhakal, R. J., & Carr, A. J. (2011). Modelling of in-structure damping damping: A review of the state of the art. *Proceedings of 9th Pacific Conference on Earthquake Engineering,* Paper no: 091.

Reid, T. J. (1956). Free vibration and hysteretic damping. *Journal of Royal Aeronautical Society*, *60*, 283.

Shukla, A. K., & Datta, T. K. (1999). Optimal use of viscoelastic dampers in building frames for seismic force. *Journal of Structural Engineering*, *125*(4), 401–409. doi:10.1061/(ASCE)0733-9445(1999)125:4(401)

Singh, M. P., & Moreschi, L. M. (2001). Optimal seismic response control with dampers. *Earthquake and Structural Dynamics*, *30*(4), 553–572. doi:10.1002/eqe.23

Singh, M. P., & Moreschi, L. M. (2002). Optimal placement of dampers for passive response control. *Earthquake and Structural Dynamics*, *31*(4), 955–976. doi:10.1002/eqe.132

Smyrou, E., Priestley, M. J., & Carr, A. J. (2011). Modelling of elastic damping in nonlinear time-history analyses of cantilever RC walls. *Bulletin of Earthquake Engineering*, *9*(5). doi:10.1007/s10518-011-9286-y

Takewaki, I. (1997a). Optimal damper placements for minimum transfer functions. *Earthquake Engineering & Structural Dynamics*, *26*(11), 1113–1124. doi:10.1002/(SICI)1096-9845(199711)26:11<1113::AID-EQE696>3.0.CO;2-X

Takewaki, I. (1997b). Efficient redesign of damped structural systems for target transfer functions. *Computer Methods in Applied Mechanics and Engineering*, *147*(3-4), 275–286. doi:10.1016/S0045-7825(97)00022-4

Takewaki, I. (1998). Optimal damper positioning in beams for minimum dynamic compliance. *Computer Methods in Applied Mechanics and Engineering*, *156*(1-4), 363–373. doi:10.1016/S0045-7825(97)00221-1

Takewaki, I. (1999). Displacement-acceleration control via stiffness-damping collaboration. *Earthquake Engineering & Structural Dynamics*, *28*, 1567–1585. doi:10.1002/(SICI)1096-9845(199912)28:12<1567::AID-EQE882>3.0.CO;2-1

Takewaki, I. (2000). Optimal damper placement for planar building frames using transfer functions. *Structural and Multidisciplinary Optimization*, *20*(4), 280–287. doi:10.1007/s001580050158

Takewaki, I. (2000a). Optimal damper placement for critical excitation. *Probabilistic Engineering Mechanics*, *15*(4), 317–325. doi:10.1016/S0266-8920(99)00033-8

Takewaki, I. (2000b). *Effective damper placement for critical excitation* (pp. 558–561). Confronting Urban Earthquakes, Report of Fundamental Research on the Mitigation of Urban Disasters Caused by Near-Field Earthquakes.

Takewaki, I. (2000c). A new probabilistic critical excitation method. *Journal of Structural and Construction Engineering*, *533*, 69–74.

Takewaki, I. (2000d). A nonstationary random critical excitation method for MDOF linear structural models. *Journal of Structural and Construction Engineering*, *536*, 71–77.

Takewaki, I. (2001a). Anewmethod for nonstationary random critical excitation. *Earthquake Engineering & Structural Dynamics*, *30*(4), 519–535. doi:10.1002/eqe.21

Takewaki, I. (2001b). Nonstationary random critical excitation for nonproportionally damped structural systems. *Computer Methods in Applied Mechanics and Engineering*, *190*(31), 3927–3943. doi:10.1016/S0045-7825(00)00354-6

Takewaki, I. (2001c). Nonstationary random critical excitation for acceleration response. *Journal of Engineering Mechanics*, *127*(6), 544–556. doi:10.1061/(ASCE)0733-9399(2001)127:6(544)

Takewaki, I. (2001d). Critical excitation for elastic–plastic structures via statistical equivalent linearization. *Probabilistic Engineering Mechanics*, *17*(1), 73–84. doi:10.1016/S0266-8920(01)00030-3

Takewaki, I. (2001e). Critical excitation for MDOF elastic–plastic structures via statistical equivalent linearization. *Journal of Structural Engineering*, *47B*, 187–194.

Takewaki, I. (2001f). Probabilistic critical excitation for MDOF elastic–plastic structures on compliant ground. *Earthquake Engineering & Structural Dynamics*, *30*(9), 1345–1360. doi:10.1002/eqe.66

Takewaki, I. (2001g). Maximum global performance design for variable critical excitations. *Journal of Structural and Construction Engineering*, *539*, 63–69.

Takewaki, I. (2004a). Critical envelope functions for non-stationary random earthquake input. *Computers & Structures*, *82*(20–21), 1671–1683. doi:10.1016/j.compstruc.2004.04.004

Takewaki, I. (2004b). Bound of earthquake input energy. *Journal of Structural Engineering*, *130*(9), 1289–1297. doi:10.1061/(ASCE)0733-9445(2004)130:9(1289)

Takewaki, I. (2005). Bound of earthquake input energy to soil–structure interaction systems. *Soil Dynamics and Earthquake Engineering*, *25*(7–10), 741–752. doi:10.1016/j.soildyn.2004.11.017

Takewaki, I. (2007). *Critical excitation methods in earthquake engineering*. Netherlands: Elsevier.

Takewaki, I. (2009). *Building control with passive dampers: Optimal performance based design of earthquakes*. John Wiley and Sons. doi:10.1002/9780470824931

Takewaki, I., Fujita, K., Yamamoto, K., & Takabatake, H. (2010). Smart passive damper control for greater building earthquake resilience in sustainable cities. *Sustainable Cities and Society*, *1*(1). doi:doi:10.1016/j.scs.2010.08.002

Takewaki, I., & Nakamura, T. (1995). Hybrid inverse mode problems for FEM-shear models. *Journal of Engineering Mechanics*, *121*(8), 873–880. doi:10.1061/(ASCE)0733-9399(1995)121:8(873)

Takewaki, I., & Nakamura, T. (1997). Hybrid inverse mode problems for a structure-foundation system. *Journal of Engineering Mechanics*, *123*(4), 312–321. doi:10.1061/(ASCE)0733-9399(1997)123:4(312)

Takewaki, I., & Uetani, K. (1999). *Optimal damper placement in shear-flexural building models. Proceedings of second world conference on structural control* (*Vol. 2*, pp. 1273–1282). Chichester, UK: John Wiley & Sons Ltd.

Takewaki, I., & Yoshitomi, S. (1998). Effects of support stiffnesses on optimal damper placement for a planar building frame. *Journal of the Structural Design of Tall Buildings*, *7*(4), 323–336. doi:10.1002/(SICI)1099-1794(199812)7:4<323::AID-TAL115>3.0.CO;2-L

Tan, P., Dyke, S. J., Richardson, A., & Abdullah, M. (2005). Integrated device placement and control design in civil structures using genetic algorithms. *Journal of Structural Engineering*, *131*(10), 1489–1496. doi:10.1061/(ASCE)0733-9445(2005)131:10(1489)

Taylor, D. P. (1999). *Buildings: Design for damping*. New York, NY: Taylor Devices Inc.

Trombetti, T., & Silvestri, S. (2004). Added viscous dampers in shear type structures: The effectiveness of mass proportional damping. *Journal of Earthquake Engineering*, *8*(2), 275–313. doi:10.1080/13632460409350490

Trombetti, T., & Silvestri, S. (2006). On the modal damping ratios of shear-type structures equipped with Rayleigh damping systems. *Journal of Sound and Vibration*, *292*(1-2), 21–58. doi:10.1016/j.jsv.2005.07.023

Trombetti, T., & Silvestri, S. (2007). Novel schemes for inserting seismic dampers in shear type systems based upon the mass proportional component of Rayleigh damping matrix. *Journal of Sound and Vibration*, *302*(3), 486–526. doi:10.1016/j.jsv.2006.11.030

Trombetti, T., Silvestri, S., & Ceccoli, C. (2003). *On the first modal damping ratio of MPD and SPD systems. Technical Report, Department DISTART*. Italy: University of Bologna.

Tsuji, M., & Nakamura, T. (1996). Optimum viscous dampers for stiffness design of shear buildings. *Journal of the Structural Design of Tall Buildings*, *5*, 217–234. doi:10.1002/(SICI)1099-1794(199609)5:3<217::AID-TAL70>3.0.CO;2-R

Val, V. D., & Segal, F. (2005). Effect of damping model on pre-yielding earthquake response of structures. *Engineering Structures*, *27*, 1968–1980. doi:10.1016/j.engstruct.2005.06.018

Viola, E., & Guidi, F. (2009). Influence of the supporting braces on the dynamic control of buildings with added viscous dampers. *Structural Control and Health Monitoring*, *16*(3), 267–286. doi:10.1002/stc.234

Wada, A., Huang, Y., & Bertero, V. V. (2004). Innovative strategies in earthquake engineering. In Bozorgnia, Y., & Bertero, V. V. (Eds.), *Earthquake engineering: From engineering seismology to performance-based engineering* (pp. 10-1–10-33). London, UK: CRC Press.

Wongprasert, N., & Symans, M. D. (2004). Application of a genetic algorithm for optimal damper distribution within the nonlinear seismic benchmark building. *Journal of Engineering Mechanics*, *130*(4), 401–406. doi:10.1061/(ASCE)0733-9399(2004)130:4(401)

Woodhouse, J. (1998). Linear damping models for structural vibration. *Journal of Sound and Vibration*, *215*(3), 547–569. doi:10.1006/jsvi.1998.1709

Wu, B., Ou, J. P., & Soong, T. T. (1997). Optimal placement of energy dissipation devices for three-dimensional structures. *Engineering Structures*, *19*, 113–125. doi:10.1016/S0141-0296(96)00034-X

Xi, L. (1999). *Analysis and design of building structures with supplemental lead dampers under earthquake and wind loads.* PhD. Dissertation, University of Canterbury, Christchurch.

Xu, Z. D., Shen, Y. P., & Zhao, H. T. (2003). A synthetic optimization analysis method on structures with viscoelastic dampers. *Soil Dynamics and Earthquake Engineering*, *23*, 683–689. doi:10.1016/j.soildyn.2003.07.003

Xu, Z. D., Zhao, H. T., & Li, A. Q. (2004). Optimal analysis and experimental study on structures with viscoelastic dampers. *Journal of Sound and Vibration*, *273*(3), 607–618. doi:10.1016/S0022-460X(03)00522-4

Zareian, F., & Medina, R. A. (2010). A practical methof for proper modelling of structural damping in inelastic plane structural systems. *Computers & Structures*, *88*, 45–53. doi:10.1016/j.compstruc.2009.08.001

Zhang, R. H., & Soong, T. T. (1992). Seismic design of visco-elastic dampers for structural applications. *Journal of Structural Engineering*, *118*(5), 1375–1392. doi:10.1061/(ASCE)0733-9445(1992)118:5(1375)

KEY TERMS AND DEFINITIONS

Classical Viscous Damping: The model of damping based on Rayleigh's dissipation function where the damping force depends on instantaneous velocities.

Damper: A mechanical device added into the parent structure to control the responses to permissible limits.

Nonviscous Damping: The model of damping in which the damping force depends on the past history of velocities.

Optimal Positioning: Procedure for placement of control devices in the parent frame to get an optimal response.

Chapter 5

Damper Optimization for Long-Span Suspension Bridges:
Formulations and Applications

Hao Wang
Southeast University, China

Aiqun Li
Southeast University, China

Zhouhong Zong
Southeast University, China

Teng Tong
Southeast University, China

Rui Zhou
Southeast University, China

ABSTRACT

Long-span suspension bridges are becoming prevalent globally with the rapid progress in design methodologies and construction technologies. Although with apparent progress, the balance between excessive displacement and inner forces, under dynamic loads, is still a main concern because of increased flexibility and low structural damping. Therefore, effective controllers should be employed to control the seismic responses to ensure their normal operation. In this chapter, the combination of the analytic hierarchy process (AHP) and first-order optimization method are formulated to optimize seismic response control effect of the Runyang suspension bridge (RSB) under earthquakes, considering traveling wave effect. The compositive optimal parameters of dampers are achieved on the basis of 3-dimensional non-linear seismic response analyses for the RSB and parameters sensitivity analyses. Results show that the dampers with rational parameters can reduce the seismic responses of the bridge significantly, and the application of the AHP and first-order optimization method can lead to accurate optimization effects.

DOI: 10.4018/978-1-4666-2029-2.ch005

INTRODUCTION

Long-span suspension bridges are always attractive because of their magnificence, symbolization and convenience. Currently this bridge type is becoming prevalent globally with the rapid progress of design methodologies and construction technologies. Take China for instance, numerous suspension bridges have been constructed, such as the Humen Bridge (main span: 888 m), the Xiling Bridge (main span: 900 m), the Jiangyin Bridge (main span: 1385 m) and the Runyang Bridge (main span: 1490 m). Nevertheless, some issues existing in long-span suspension bridges still challenge engineers, as dynamic behavior subjected to earthquakes. How to ensure an adequate level of safety against earthquakes for both new and existing long-span suspension bridges is important (Fan, 1997).

Rigid connections between the main girder and towers would transmit to foundations inertial forces generated by the superstructure, magnifying shear forces and overturning moments at the bottom of towers. In order to reduce seismic forces of towers, the seismic isolation system forming the floating system is generally adopted to supplant rigid connections. It is notable that for such case the seismic displacement at the end of the main girder may potentially exceed the threshold (Park et al., 2005; He et al., 2001). Dampers intended to control the seismic displacement of long-span bridges are therefore installed between towers and the main girder and has been proved to be an effective approach (He, Agrawal, & Mahmoud, 2001; Erkus, Abe, & Fujino, 2002; Murphy & Collins, 2004). The application of the seismic isolation system with dampers is by far the most practical solution to control the seismic responses of structures and a number of studies have been conducted on damper optimization for seismic response control of buildings (Furuya, Hamazaki, & Fujita, 1998; Shukla & Datta, 1999; Chen & Wu, 2001; Aydin, Boduroglu, & Guney, 2007) and bridges (Kawashima & Unjoh, 1994; Symans & Kelly, 1999; Abe & Fujino, 1998).

In this chapter, principle introductions are conducted in terms of seismic response control, the analytic hierarchy process (AHP) and first-order optimization method. Through the parameters sensitivity analyses of 3-dimensional model for the Runyang Suspension Bridge (RSB), damper optimization for seismic control of the RSB under certain seismic input are realized, on the basis of the combination of the AHP and first-order optimization method.

FOUNDATIONS OF OPTIMIZATION THEORY

Optimization theory is widely used in civil engineering to combat various issues such as sensor placement for structural health monitoring (Heo, Wang, & Satpathi, 1997; Meo & Zumpano, 2005), finite element model updating (Wang, Li, & Miao, 2005), cable force optimization of the cable-stayed bridges (Zhang & Xiao, 2005), bridge design (Ming, Hu, & Huang, 2007), acoustic design (Duhring, Jensen, & Sigmund, 2008), structural damage identification (Andrzej, Przemyslaw, & Jan, 2008), et cetera. Generally, the constrained optimization problem can be expressed as:

$$\text{Minimize } J = J\left(x\right) \tag{1}$$

subjected to:

$$\underline{x}_i \le x_i \le \overline{x}_i \quad (i=1,2,3,\ldots,N)$$

$$g_j(x) \le \overline{g}_j \quad (j=1,2,3,\ldots,m_1)$$

$$\underline{h}_k \le h_k(x) \quad (k=1,2,3,\ldots, m_2)$$

$$\underline{w}_l \le w_l(x) \le \overline{w}_l \quad (l=1,2,3,\ldots, m_3)$$

where x_i is the design variable; g_j, h_k, and w_l represent the state variables; N is the number of design variables and m_1+m_2+m_3 is the number of state variables. The bar above/below variables represents the lower/upper bound.

Analytical Hierarchy Process (AHP)

The AHP is a decision-aiding method proposed by Saaty (1980). It aims at quantifying relative priorities for a given set of alternatives on a ratio scale, based on the judgment of the decision-maker, and stresses the importance of the intuitive judgments of a decision-maker as well as the consistency of the comparison of alternatives in the decision-making process. The AHP method has been widely used in evaluation system of many fields (Skibniewski & Chao, 1992; Mikhailov, 2004; Zhang et al., 2005) and improved or combined with other analysis methods in evaluation (Klocke et al., 1997; Bao et al., 2004).

Procedures of the AHP solution are generally as follows (Skibniewski, 1988): (1) A complex problem is structured by decomposing it into a hierarchy with enough levels to include all attribute elements to reflect the goals and concerns of decision-makers; (2) Elements are compared in a systematic manner using the same scale to measure their relative importance, and the overall priorities among the elements within the hierarchy are established; (3) The relative standing of each alternative with respect to each criterion element in the hierarchy is determined using the same scale; (4) The overall score for each alternative can then be aggregated, and the sensitivity analysis can be performed to see the effect of change in the initial priority setting, while the consistency of comparison can be measured using Saaty's consistency ration.

First-Order Optimization Method

The first-order optimization method (Wang, Li, & Mao, 2005; Jaishi & Ren, 2005), the zero order optimization method and the differential equation method can all solve constrained optimization problems. In this chapter, the first-order optimization method and the penalty concept are utilized. With regard to this optimization method, Equation (1) for the constrained case is transformed into an unconstrained one through penalty functions, expressed as:

$$Q(x,q) = \frac{J}{J_0} + \sum_{i=1}^{N} P_x(x_i) + q\left[\sum_{j=1}^{m_1} P_g(g_j) + \sum_{k=1}^{m_2} P_h(h_k) + \sum_{l=1}^{m_3} P_w(w_l)\right] \tag{2}$$

where $Q(x,q)$ is the unconstrained objective function; q is the bound control parameter; J_0 is the reference objective function value that is selected from the current group of design sets; P_x, P_g, P_h and P_w represent penalties of the constrained design and state variables respectively. The optimization iteration formula is:

$$x^{(j+1)} = x^{(j)} + s_j d^{(j)} \tag{3}$$

where s_j is the line search parameter and $d^{(j)}$ is the search direction vector which leads to the minimum value of $Q(x,q)$. Various slopes and direction searches are performed for the iteration until convergence is obtained.

$$\left|J^{(j)} - J^{(j-1)}\right| \le \tau \text{ and } \left|J^{(j)} - J^{(b)}\right| \le \tau \tag{4}$$

where $J^{(j)}$, $J^{(j-1)}$ and $J^{(b)}$ refer to the current, previous and best objective function values, respectively (Jaishi & Ren, 2005). τ is the objective function tolerance.

The zero-order optimization method is similar to the first-order optimization method with the main difference being in the disposition of variables. Derivatives of the variables are used in the first-order optimization method whereas variables themselves are used in the zero-order optimization method.

RESEARCH BACKGROUND

Description and FEM Model of RSB Bridge

The RSB is a single-span hinged and simply supported steel box girder bridge with a main span of 1490 m, shown in Figure 1. It is the longest suspension bridge in China and ranks the third in the globe. In addition, the central buckle is for the first time used in suspension bridges in China. The control of seismic responses involved in this striking bridge under earthquakes is undoubtedly crucial.

A 3-dimensional model for the bridge is established on finite element program ANSYS, with reference to design drawings of the RSB, to study the structural seismic response. In the FE model, the beam element with six degrees of freedom for each node is employed to simulate the girder, the central buckle and the towers. The massless rigid element placed perpendicular to the spine which is intended for modelling the main girder is to simulate the connections between the suspenders and the girder. The 3-dimensional linear elastic truss element is to simulate main cables and the suspenders whose nonlinear stiffness characteristic due to gravity effect is approximately simulated by linearizing the cable stiffness by the Ernst equation of equivalent modulus of elasticity (Ernst, 1965). In addition, the pavement and the railings on the steel box girder were simulated by mass elements without stiffness.

The main girder and the relevant tower cross-beams are coupled in three DOFs including vertical displacement, lateral displacement and rotation in longitudinal direction. The central buckle, applied in China for the first time, is precisely simulated, and the main girder and cables at the central buckle are also coupled with references to the practical design. The main cables are fixed at both the top of towers and anchorages and towers are fixed at their foundations (Wang, Li, & Mao, 2005). The spatial FE model of RSB is shown in Figure 2.

Foundations for Dynamic Behavior in Bridges

The dynamic force equilibrium equation for bridges can be written as:

$$M\ddot{u}(t) + C\dot{u}(t) + Ku(t) = F(t) = \sum_{j=1}^{J} f_j g(t)_j \tag{5}$$

All possible types of time-dependent loading, including wind, wave and seismic, can be represented by a sum of "J" space vectors f_j, which are nit a function of time and J time functions $g(t)_j$, where J cannot be greater than the number of displacements N. To combat the above equation, the following three methods are generally employed.

1. **Static or Quasistatic Analysis Tools:** In many cases of seismic analysis it is most convenient to apply the seismic actions in the form of an equivalent static force to the bridge model, particular when seismic distributions or likely deformation modes can be estimated. The equivalent earthquake force is:

   $$F = W_s a_s \tag{6}$$

   where W_s is the total seismic weight, a_s is the absolute acceleration coefficient. The equivalent force is lumped at the centroid of seismic mass, or distributed proportional to the expected fundamental mode force.
2. **Response Spectrum Analysis:** Analysis models used for modal spectral analysis are linear elastic models based on effective stiffness prosperities and on assumed equivalent viscous damping ratios. Many modal analysis programs provide an effective mass or mass participation factor for

Figure 1. Configuration of RSB: (a) two photos of RSB, (b) elevation and plan (unit: m), (c) cross section of the steel box girder (unit: min)

(a)

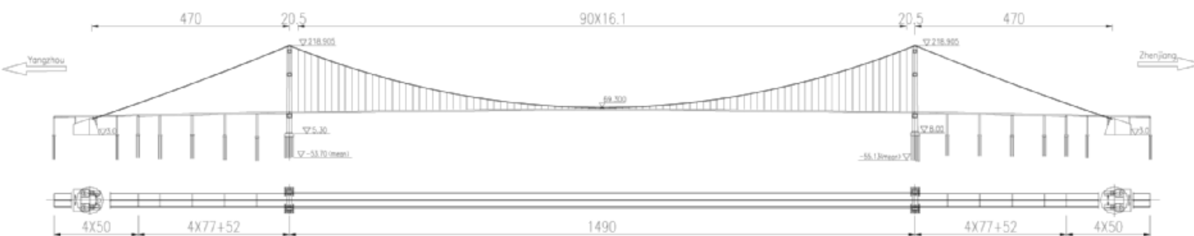

(b)

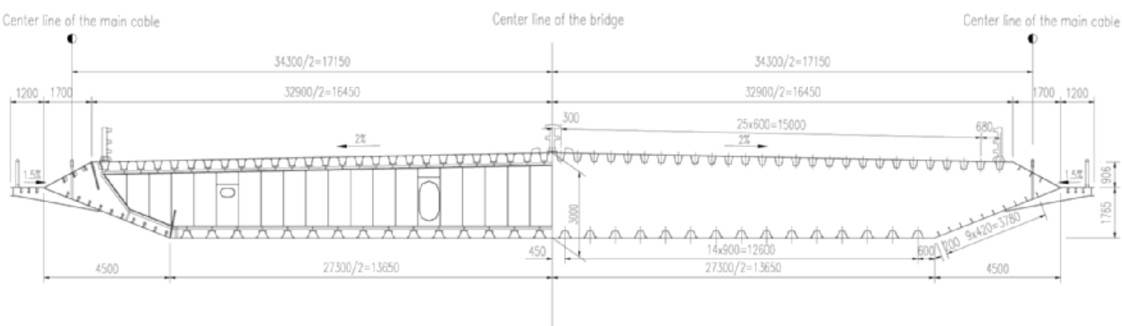

(c)

Figure 2. Spatial FE model of RSB

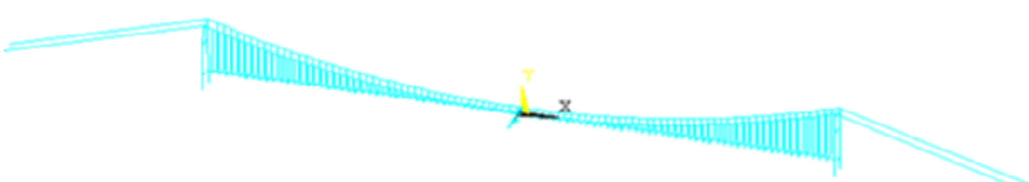

each mode. The sum of the effective must equal the total mass of the bridge. Effective mass participation of 80 to 90% of the total mass in any given response direction can be considered sufficient.

3. **Time-History Analysis:** For the earthquake time-history analysis of bridge models, three analysis tools are available. Among them, the approach (a) is adopted universally.
   a. Step-by-step integration in the time domain
   b. Superstition of normalized modal time histories in the time domain
   c. Evaluation of frequency-dependent response contributions with transformation to and superposition in the time domain.

Numerical integration schemes for the time domain can have problems with accuracy or period distortion as well as numerical stability when the integration step Δt is not small enough. As a general rule, numerical stability in conditionally stable explicit time integration schemes can be achieved when the time step Δt is selected such that:

$$\Delta t = \frac{T_n}{\pi} \tag{7}$$

where T_n represents the period of the highest significant mode of vibration.

Damper Simulation

Numerous dampers have been developed to release seismic forces such as soft steel damper, friction damper, magneto-rheological (MR) damper, viscous fluid damper, etc. In this study, the relative mature viscous fluid damper is applied. The force of damper varying with the relative velocity can be formed as:

$$F = CV^{\alpha} \tag{8}$$

where F is the force of damper, C is the damping coefficient, V is the relevant velocity and α is the exponent generally varying from 0.2 to 1.0. The linear relationship between F and V occurs when α equals 1.0, and is named the linear damper. Because of the 90^0 phase between the damp and elastic force, the linear damper would give no contributions to internal structural forces.

The dampers can only be simulated by software with nonlinearity damp element. The COMBIN14 element whose nodes have three DOFs in the ANSYS software is employed, accounting for the compression and tension in the axis direction and no bending and torsion, as shown in Figure 3.

Seismic Input

Two levels of seismic waves (10% and 2% probability in 50 years respectively) are provided by Jiangsu Provincial Institute of Earthquake Engineering. These waves, located at different points along the RSB, include data in all the three directions (longitudinal, vertical and lateral directions). In this chapter, the group of five seismic waves with the 2% probability of exceedance is employed as the seismic acceleration input, and the wave leading to the most adverse situation is selected for the further analysis.

Analysis results have shown that the lateral seismic motion has little influence on the girder displacement of long-span cable-supported bridges in along-bridge direction, and the opposite is obtained as to the vertical seismic motion. Hence longitudinal + vertical seismic input is taken into account, the seismic waves corresponding to the most adverse case is shown in Figure 4.

The travelling wave effect is obvious for the RSB case because of its long span (Abdel-Ghaffar & Rubin, 1982; 1983a; 1983b; Abdel-Ghaffar, 2000) and thus should be considered when performing time domain analysis. The design seismic

Figure 3. Combin14 element in ANSYS

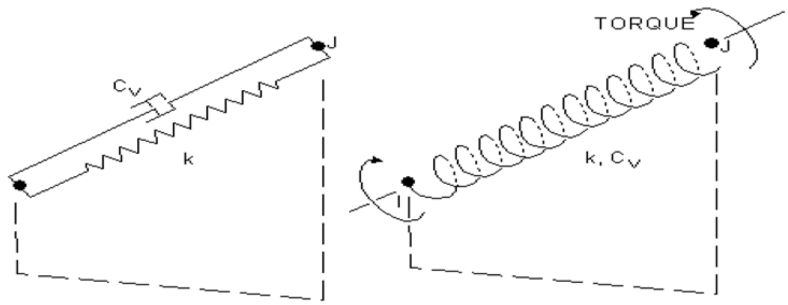

parameter analysis on the ground soil of the RSB is also conducted by Jiangsu Provincial Institute of Earthquake Engineering, and the seismic wave velocities of ground are obtained. According to the ground soil analysis results and the pile length of the RSB, the shear wave velocity and the longitudinal wave velocity are set to 263 m/s and 1332 m/s, respectively.

OPTIMIZATION FOR DAMPERS

Time history analysis shows that the maximum longitudinal displacement at the end of the girder is 0.42 m and the maximum overturning moment at the base of the tower is 1.89×10^7 kN·m. Although seismic forces of such bridges with floating system are not the dominant loads governing the design,

Figure 4. Seismic input used in the analysis

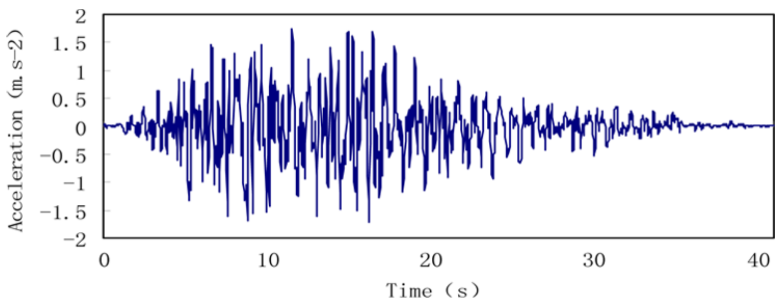

(a) Longitudinal seismic acceleration

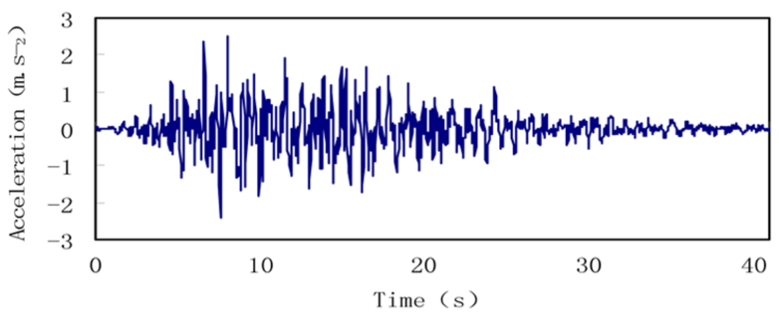

(b) Vertical seismic acceleration

the isolation system with dampers is usually applied to restrain the large girder displacement. The following is about how to achieve the most satisfied seismic control effect by optimizing the damping coefficient C and damper placement in the two towers.

Parameter Sensitivity Analysis of Dampers

Parameter sensitivity analysis of dampers is adequate because it can reveal the correlation between dampers and structural responses, therefore is conducive to the damper optimization. Various damping coefficients C are employed to conduct the parameter sensitivity study of dampers. The value of C ranges from 1×10^3 to 20×10^3 kN·s/m, and α is 1.0, according to the linear damper.

The relationships between damping coefficient C and the girder displacement, tower moment, damper force and displacement are shown in Figure 5. Obviously, the girder displacement, tower moment and damper displacement decrease with the rise of C, while the damper force varies inversely. Dampers can therefore reduce structural response significantly if C is selected appropriately.

Optimization Model Based on AHP

When carrying out an optimization based on the AHP, a correct optimization model including the selection of evaluation parameters and the determination of their weighting factors is significant for the accuracy of the analysis results since it is a decision-aiding method. To simplify calculations, only one kind of seismic input (longitudinal + vertical input) which could lead to the most adverse internal responses is employed.

Six evaluation parameters are usually considered when performing a assessment of seismic control effect for long-span suspension bridges (Wang, Li, & Guo, 2006), and they are: D_1 (displacement at the end of the girder), M_1 (moment at the base of the tower), D_2 (the along-span displacement at the top of the tower), M_2 (the moment at mid-span of the crossbeam below), D_3 (the displacement of the damper), and F_3 (the force of the damper). These evaluation parameters are also adopted for damper optimization of the RSB.

Furthermore, it is notable that traveling wave effect is considered when conducting the seismic analysis of the RSB. However, traveling wave effect is merely a simple form of multi-support seismic excitation where incoherence effect and site-response effect should also be considered. In addition, traveling wave effect is significantly dependent on the apparent wave velocity, the seismic input direction and some other factors which are uncertain. Therefore it is recommendable to conduct analysis of uniform seismic input, traveling wave effect and multi-support seismic excitation, and a comprehensive investigation is adopted for optimization (Figure 6). However, in this chapter only optimization under traveling wave effect is conducted for simplification, as shown in shadow part of Figure 6.

It is notable that other factors can be added for assessment if necessary, such as lateral seismic input, multiple-point seismic input, shear force at the base of the tower, displacement response at the middle of the deck and displacement response at the top of the tower, etc.

Determining Assessment Functions Based on First-Order Optimization Method

The optimization model and procedure has been established, with reference to the idea of the AHP. The next step is to ascertain the optimization criteria (Optimization J_1-J_4 in Figure 6) for dampers. However this is a complicated case for that six evaluation parameters and their weighting factors are not an easy task to be determined. In this case, four assessment functions for seismic control are formulated as the object functions during the optimization, which are as follows:

Figure 5. The influence of damping coefficient C on: (a) girder displacement, (b) tower moment, (c) damper force, (d) damper displacement

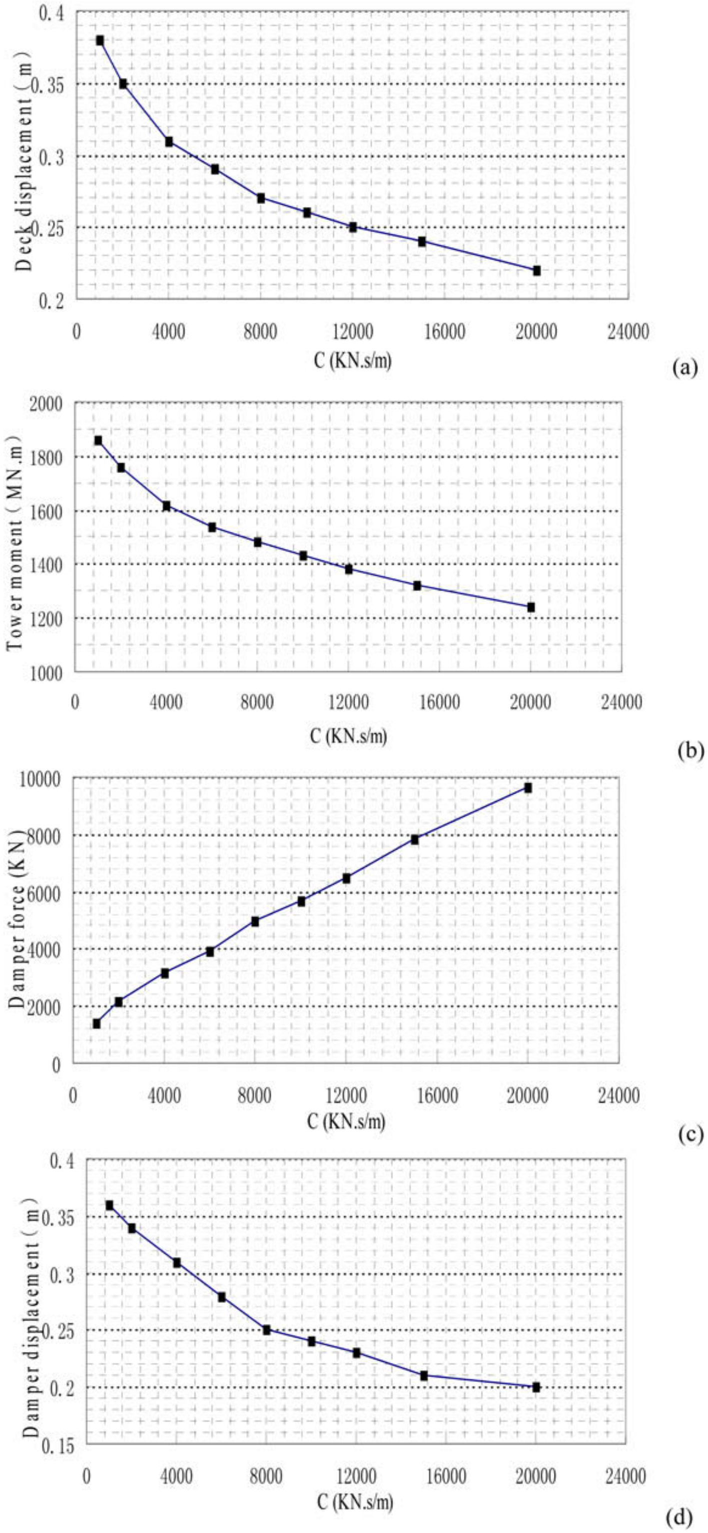

Figure 6. Assessment model for compositive optimal control

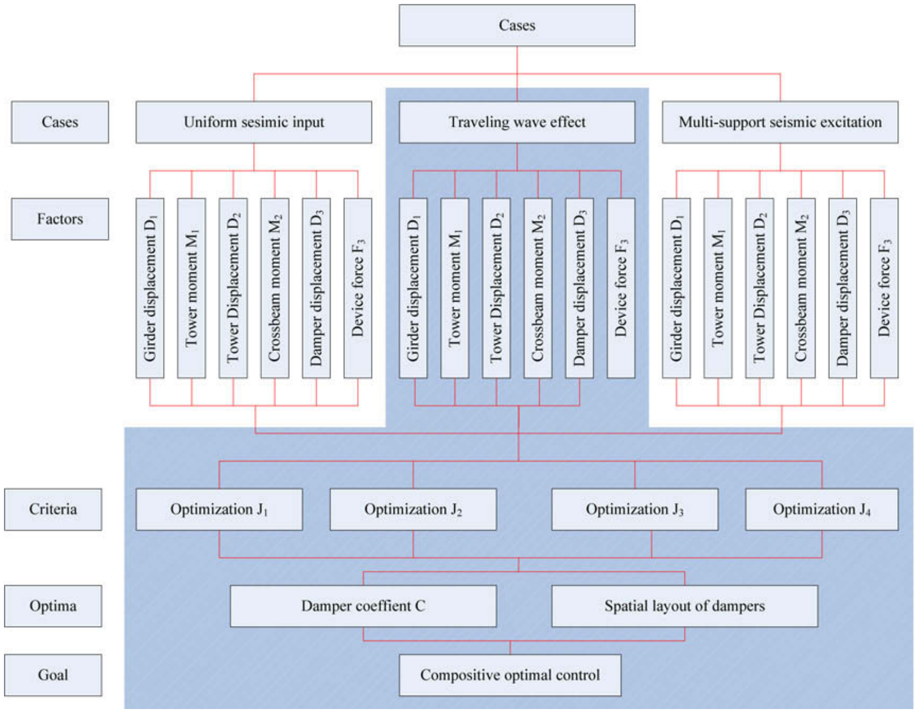

$$J = J_1 = \left| D_1 \right| \tag{9}$$

$$J = J_2 = \left| M_1 \cdot D_1 \right| \tag{10}$$

$$J = J_3 = \left| M_1 \cdot D_1 \right| \cdot \left| M_2 \cdot D_2 \right|^{1/2} \tag{11}$$

$$J = J_4 = \left| M_1 \cdot D_1 \right| \cdot \left| F_3 \cdot D_3 \right|^{1/2} \tag{12}$$

J_1 is the most simplest and convenient and merely one dominating factor D_1 is considered whereas it may be inadequate to deal with a complex structure as the RSB. Another relative important factor M_1 is therefore added into J_2. Furthermore, two more factors of M_2 and D_2 are considered in J_3, and F_3 and D_3 in J_4.

It is notable that J_3 and would be suitable when the calculation is near the optimization and the opposite is suitable for J_4. When responses of two towers are different during the optimization, the one with larger responses is selected for calculation. The lower and upper bounds of the design parameters are set as follows:

10000 kN·s/m≤C_1≤20000 kN·s/m

10000 kN·s/m≤C_2≤20000 kN·s/m

C_1+C_2=30000 kN·s/m

$$\left| D_1 \right| \le 0.3m$$

where C_1 and C_2 represent damper coefficients at the south and north towers respectively. C_1 and C_2 are set to an integer multiplied by 1000 to decrease iterations. The range of C_1 and C_2 is set from 10000 kN·s/m to 20000 kN·s/m for that initial analysis shows that the control effect is not perfect when the C_1 is greatly different from C_2. Consider the response control effect turns unobvious when the damp coefficient C is greater than 15000 kN·s/m (Figure 5), the total damper of the two towers of the RSB is set as 30000 kN·s/m.

Results of Damper Optimization

Table 1 shows the optimization analysis results under 5 cases. Note that case 1 is without dampers, and Cases 2, 3, 4 and 5 correspond to Equations (9), (10), (11) and (12), respectively.

When compared with results of Case 1, Table 1 shows that values of M_1 and D_3 reduce significantly and values of M_2 turn larger, indicating effects in seismic control induced by the application of dampers.

When only the girder displacement D_1 is regarded, the optimization is achieved in Cases 2 and 3 whose dampers are not evenly distributed between the left and right towers. This phenomenon is mainly derived from the traveling wave effect in this chapter. However, consider the complication and uncertainty of traveling wave effect, equal distribution of dampers on the two towers is the most general choice. In addition, values of M_2, D_2, F_3 and D_3 are larger in cases 2 and 3 when compared to those of cases 4 and 5, indicating the other advantages of adopting equal distribution approach. Therefore the spatially equal distribution of dampers in the two towers is recommended.

CONCLUSION

In this chapter, the damper optimization of the RSB is conducted under seismic input considering the traveling wave effect, based on the combination of the AHP and first-order optimization method. The following conclusions could be drawn:

- Dampers with appropriate parameters can reduce the seismic displacement of super-long-span suspension bridges significantly. The parameter sensitive analysis involved in influence of damping coefficient C on the structural responses will necessarily facilitate the damper optimization.
- When creating evaluation model based on AHP method, a correct evaluation model, adequate evaluation parameters and the determination of their weighting factors are significant for the accuracy and credibility of the analysis results. In this chapter, the model is established on the author's experience. More research is required to refine the model for better damper optimization.
- Four assessment functions are proposed as the optimization criteria, by first-order optimization method to deal with quantitive assessment. Different functions can lead to different optimization results and their optimization results are compared with each other to indentify the most effective one.
- Although spatially unequal damper distribution on the two towers can lead to the

Table 1. Comparison of optimization result

Case	C_1 (kN·s/m)	C_2 (kN·s/m)	M_1×10^6 (kN· M)	D_1 (m)	M_2×10^3 (kN· M)	D_2 (m)	F_3 (kN)	D_3 (m)
1			1.890	0.423	81.52	0.372		
2	18000	12000	1.429	0.235	103.8	0.263	9160	0.216
3	18000	12000	1.429	0.235	103.8	0.263	9160	0.216
4	15000	15000	1.382	0.243	95.3	0.238	7850	0.207
5	15000	15000	1.382	0.243	95.3	0.238	7850	0.207

minimum displacement of the main girder, the spatially equal damper distribution is recommended for the uncertainty of the traveling wave effect. The value of damping coefficient C is set as 15000 kN·s/m when control efficiency are considered.

- Analysis results show that the combination of the AHP and first-order optimization method is effective and reliable methods in damper optimization for seismic control of long-span suspension bridges. However, more researches are required for the accurate optimization of seismic control effect of long-span suspension bridges.

REFERENCES

Abdel-Ghaffar, A. M. (2000). Vibration studies and tests of a suspension bridge. *Computers & Structures*, *76*(6), 787–797.

Abdel-Ghaffar, A. M., & Rubin, L. I. (1982). Suspension bridge response to multiple-support excitations. *Journal of Engineering Mechanics*, *108*(2), 419–435.

Abdel-Ghaffar, A. M., & Rubin, L. I. (1983a). Vertical seismic behavior of suspension bridges. *Earthquake Engineering & Structural Dynamics*, *11*(1), 1–19. doi:10.1002/eqe.4290110103

Abdel-Ghaffar, A. M., & Rubin, L. I. (1983b). Lateral earthquake response of suspension bridges. *Journal of Engineering Mechanics*, *109*(3), 664–675.

Abe, M., & Fujino, Y. (1998). Optimal design of passive energy dissipation devices for seismic protection of bridges. [in Japanese]. *J Struct Mech Earthquake Eng*, *605*(45), 41–52.

Agrawal, A. K., & Yang, J. N. (2000). Optimal placement of passive dampers on seismic and wind-excited buildings using combinatorial optimization. *International Mater System Structure*, *10*(12), 997–1014.

Andrzej, S., Przemyslaw, K., & Jan, H. S. (2008). Damage identification in skeletal structures using the virtual distortion method in frequency domain. *Mechanical Systems and Signal Processing*, *22*(8), 1826–1839. doi:10.1016/j.ymssp.2008.03.009

Aydin, E., Boduroglu, M. H., & Guney, D. (2007). Optimal damper distribution for seismic rehabilitation of planar building structures. *Structure Engineering*, *29*(2), 176–185. doi:10.1016/j.engstruct.2006.04.016

Bao, Y. D., Wu, Y. P., He, Y., et al. (2004). An improved AHP method in performance assessment. *WCICA 2004-Fifth World Congress on Intelligent Control and Automation, Conference Proceedings,* Vol. 1, (pp. 177-180).

Chen, G., & Wu, J. (2001). Optimal placement of multiple tune mass dampers for seismic structures. *Structure Engineering*, *127*(9), 1054–1062. doi:10.1061/(ASCE)0733-9445(2001)127:9(1054)

Dühring, M. B., Jensen, J. S., & Sigmund, O. (2008). Acoustic design by topology optimization. *Sound and Vibration*, *317*(3), 557–575. doi:10.1016/j.jsv.2008.03.042

Erkus, B., Abe, M., & Fujino, Y. (2002). Investigation of semi-active control for seismic protection of elevated highway bridges. *Structure Engineering*, *24*(3), 281–293. doi:10.1016/S0141-0296(01)00095-5

Ernst, J. H. (1965). Der E-Modul von Seilen unter Berucksichtigung des Durchhanges. *Der Bauingenieur*, *40*(2), 52–55.

Fan, L. C. (1997). *Seismic analysis of bridge*. Shanghai, China: Tongji University Press.

Furuya, O., Hamazaki, H., & Fujita, S. (1998). Study on proper distribution of storey-installation type damper for vibration control of slender structures using genetic algorithm. *Joint Pressure Vessels and Piping Conference, 364*, 297-304.

He, W. L., Agrawal, A. K., & Mahmoud, K. (2001). Control of seismically excited cable-stayed bridge using resetting semiactive stiffness dampers. *Bridge Engineering*, *6*(6), 376–384. doi:10.1061/(ASCE)1084-0702(2001)6:6(376)

Heo, G., Wang, M. L., & Satpathi, D. (1997). Optimal transducer placement for health monitoring of long span bridge. *Structure Engineering*, *16*(7-8), 495–502.

Jaishi, B., & Ren, W. X. (2005). Structural finite element model updating using ambient vibration test results. *Structure Engineering*, *131*(4), 617–628. doi:10.1061/(ASCE)0733-9445(2005)131:4(617)

Kawashima, K., & Unjoh, S. (1994). Seismic response control of bridges by variable dampers. *Journal of Structural Engineering*, *120*(9), 2583–2601. doi:10.1061/(ASCE)0733-9445(1994)120:9(2583)

Klocke, F., Weck, M., & Schell, H. (1997). Evaluating alternative production cycles using the extended fuzzy AHP method. *European Journal of Operational Research*, *100*(2), 351–366. doi:10.1016/S0377-2217(96)00295-0

Meo, M., & Zumpano, G. (2005). On the optimal sensor placement techniques for a bridge structure. *Structure Engineering*, *27*(10), 1488–1497. doi:10.1016/j.engstruct.2005.03.015

Mikhailov, L. (2004). Group prioritization in the AHP by fuzzy preference programming method. *Computers & Operations Research*, *31*(2), 293–301. doi:10.1016/S0305-0548(03)00012-1

Ming, T. Z., Hu, G. W., & Huang, W. (2007). Multiple-objective optimum design of pavement system for long-span steel bridges. *China Civil Engineering*, *40*(2), 70–73.

Murphy, T. P., & Collins, K. R. (2004). Retrofitting suspension bridges using distributed dampers. *Structure Engineering*, *130*(10), 1466–1474. doi:10.1061/(ASCE)0733-9445(2004)130:10(1466)

Park, K. S., Koh, H. M., Ok, S. Y., & Seo, C. W. (2005). Supervisory control of earthquake-excited cable-stayed bridges. *Engineering Structures*, *27*, 1086–1100. doi:10.1016/j.engstruct.2005.02.007

Saaty, T. L. (1980). *The analytic hierarchy process*. New York, NY: McGraw-Hill.

Shukla, A. K., & Datta, T. K. (1999). Optimal use of viscoelastic dampers in building frames for seismic force. *Structure Engineering*, *125*(4), 401–409. doi:10.1061/(ASCE)0733-9445(1999)125:4(401)

Skibniewski, M., & Chao, L. C. (1992). Evaluation of advanced construction technology with AHP method. *Journal of Construction Engineering and Management*, *118*(3), 577–593. doi:10.1061/(ASCE)0733-9364(1992)118:3(577)

Skibniewski, M. J. (1988). Framework for decision-making on implementing robotics in construction. *Journal of Computing in Civil Engineering*, *2*(2), 188–200. doi:10.1061/(ASCE)0887-3801(1988)2:2(188)

Symans, M. D., & Kelly, S. W. (1999). Fuzzy logic control of bridge structures using intelligent semi-active seismic isolation systems. *Earthquake Engineering & Structural Dynamics*, *28*(1), 37–60. doi:10.1002/(SICI)1096-9845(199901)28:1<37::AID-EQE803>3.0.CO;2-Z

Wang, H., Li, A. Q., & Guo, T. (2006). Compositive optimal control of the seismic response for super-long-span suspension bridges. *Hunan University*, *33*(3), 6–10.

Wang, H., Li, A. Q., & Miao, C. Q. (2005). FE model updating and validating of Runyang Suspension Bridge based on SHMS. *Southeast University*, *21*(4), 474–479.

Wang, H., Li, A. Q., & Miao, C. Q. (2005). FE model and model updating of Runyang Suspension Bridge. *The 2nd International Conference on Structural Health Monitoring of Intelligent Infrastructure,* (pp. 1235-1241).

Ye, A. J., Hu, S. D., & Fan, L. C. (2004). Seismic displacement control for super-long-span cable-stayed bridges. *China Civil Engineering Journal*, *37*(12), 38–43.

Zhang, J. M., & Xiao, R. C. (2005). Study on the prearranged angle of girders in construction state for a thousand-meter scale cable-stayed bridge. *Computational Mechanics*, *22*(5), 618–622.

Zhang, Q., Zhu, S. T., & Zhou, Z. W. (2005). Study of advanced evaluation system based on a fuzzy AHP method for nuclear reactors. *Nuclear Power Engineering*, *26*(1), 91–95.

Chapter 6
Optimal Design and Practical Considerations of Tuned Mass Dampers for Structural Control

Chi-Chang Lin
National Chung Hsing University, Taiwan, R.O.C.

Jer-Fu Wang
National Museum of Natural Science, Taiwan, R.O.C.

ABSTRACT

The design concept and procedure for tuned mass dampers (TMDs) have been extensively investigated through numerical simulation analyses and experimental tests. Sophisticated three-dimensional building models were developed to examine the optimum installation location in elevation and in plane, number and movement direction of the TMDs with the consideration of translation-torsion coupling and soil-structure interaction effects. Analytical and empirical formulas were also derived to determine the optimal parameters of TMD. It is well recognized that the performance of a TMD is sensitive to the slight deviation of frequency ratio between the TMD and the structure. Multiple tuned mass dampers (MTMDs) were proposed to reduce this detuning effect. It is also recognized that TMD's performance relies on its large stroke which may not be allowed due to the limitation of space and vibration components. The authors presented a two-stage optimum design procedure for MTMDs with limitation of their strokes. New invention patents both in Taiwan and in USA have been granted for the MTMD device.

INTRODUCTION

Vibration control of structures using supplemental devices against natural and man-made excitations has been a topic of interest in civil engineering in recent decades. Among those devices, tuned mass damper (TMD) is one kind of passive-type devices and it can be incorporated into an existing structure with less interference compared with others. Since 1971, TMDs have been successfully installed in high-rise buildings, observatory towers, long-span bridge towers and decks, and pedestrian bridges.

DOI: 10.4018/978-1-4666-2029-2.ch006

All of these applications show that TMDs can reduce structural vibrations effectively. However, a TMD could face some drawbacks in seismic applications: large stroke and detuning problem, due to large earthquake forces. To solve the detuning problem, a new device, called multiple tuned mass dampers (MTMD), with less sensitivity to frequency change was first proposed by Xu and Igusa in 1992. Followed by numerous studies (i.e., Yamaguchi & Harnpornchai, 1993; Abe & Fujino, 1994, 1995; Kareem & Kline, 1995; Jangid, 1995; Li, 2000, 2002, 2003, Lin et al., 1999; Lin et al., 2005; Wang & Lin, 2005; Hoang & Warnitchai, 2005; Zuo & Nayfeh, 2005; Li & Ni, 2007), various design theories and control efficiency of an MTMD were well established. Still, the large stroke problem was not taken into account. In 2010, a research paper by the authors using a brand-new MTMD design theory with the consideration of stroke limitation was published. A shaking table test was also conducted to verify the control effectiveness of a fabricated MTMD device for a large-scale building. The objective of this chapter is to provide a quick review on the development of TMD and MTMD and to introduce the new findings by Lin *et al*. (2010).

BACKGROUND

A TMD is a single-degree-of-freedom (SDOF) dynamic system. The design of TMD is to determine its mass, damping coefficient, and stiffness coefficient based on the characteristics of primary structure to which it is installed and/or the external excitation. The time-domain equations of motion of a linear structure-TMD system involves second-order differential. In the early stage, the application of TMD mainly focused on the vibration problem of mechanical systems. Although the concept of TMD dated back to 1909 (Frahm, 1911), Den Hartog (1956) could be the first one who provided a detail description and design formulas for TMD.

Den Hartog's Design Formulas for Undamped Structures

In Den Hartog's study, an undamped SDOF dynamic system subjected to sinusoidal loading was considered. For a given mass ratio of TMD to the primary structure, μ, he suggested that the optimal frequency ratio of the TMD to the primary, $(r_f)_{opt}$ and the optimal damping ratio of TMD, $(\xi_s)_{opt}$, can be calculated by the following equations

$$(r_f)_{opt} = \frac{1}{1+\mu} \text{ and } (\xi_s)_{opt} = \sqrt{\frac{3\mu}{8(1+\mu)}} \tag{1}$$

From Equation (1), the physical parameters (e.g., mass, damping coefficient, and stiffness coefficient) of a TMD can be obtained if the mass and natural frequency of the primary structure are given. Although the design problem is significantly simplified, it appears that the damping ratio of the primary structure is unrelated to the design of a TMD. As a result, the applicability of the equation to damped structures is not clear. The equation also implies that the larger the TMD mass, the smaller the value of $(r_f)_{opt}$. It is a reasonable situation because a larger TMD mass means larger system mass which will have a smaller resonant frequency to which a TMD is tuned.

Optimally Designed Formulas for Damped Structures

After Den Hartog's work, numerous studies have investigated the TMD design for damped structural systems. Lin *et al*. (1994) developed theories for optimal design of TMD's parameters and investigated its vibration control effectiveness for building structures. In their study, a linear multistory planar building model with viscous damping was applied. The earthquake excitation was considered as a random process of white noise or filtered white noise. Because of structural damping, analytical solutions for the optimal frequency ratio, $(r_f)_{opt}$, and optimal damping ratio, $(\xi_s)_{opt}$ of TMD with a given mass ratio, μ, are inaccessible. Instead, by conventional curve fitting, the optimal design parameters of TMD were obtained as

$$\begin{aligned}&(r_f)_{opt} = (\frac{a}{1+\mu})^b;\\&a = 1.0 - \frac{\xi_p}{4},\ \ b = 1.35e^{3.2\xi_p}\ \text{ and}\\&(\xi_s)_{opt} = 0.46\mu^{0.48}\end{aligned} \tag{2}$$

where ξ_p is the structural damping ratio. Comparing with Equation (1), it is seen that the influence of structural damping on $(r_f)_{opt}$ is included in Equation (2).

Philosophy and Advantages of TMD

The vibration control effectiveness of TMD is achieved by changing the dynamic characteristics, specifically the damping properties, of the structure by tuning its vibration frequency to that of the structure. Figure 1(a) gives plots of typical transfer functions of a building with fundamental frequency $\omega_p = 1.5$ Hz and damping ratio $\xi_p = 2$ %, without and with TMD $\left(\mu = 2.85\%\right)$. Here, two different TMD design parameter sets were utilized: (a) optimal TMD: $r_f = 0.953$, $\xi_s = 8.3\%$ obtained from Equation (2); (b) Den Hartog's TMD: $r_f = 0.972$, $\xi_s = 10.2\%$ obtained from Equation (1). It is seen that the amplitude of transfer function is significantly reduced near the resonant frequency (1.5Hz) when the structure is equipped with TMD. The frequency bandwidth where TMD is effective is called the operating range. Notice that insignificant amplifications are observed outside the operating range. Figure 1(a) also shows that the optimal TMD can suppress the transfer function amplitude more than the Den Hartog's TMD near the resonant frequency of the structure.

This simple case shows a TMD, merely requiring a small room compared to the primary structures, is able to reduce structural resonant response by means of increasing additional damping. This is economically advantageous for gigantic structures with enough stiffness but limited inherent damping, such as a high-rise building or a long-

Figure 1. Transfer functions of (a) structure without and with TMD based on two different design equations ("optimal TMD": based on Eq. (2); "Den Hartog's TMD": based on Eq. (1)); (b) TMD's stroke

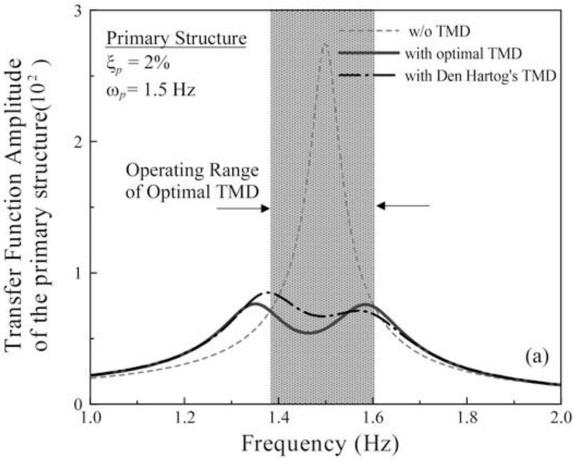

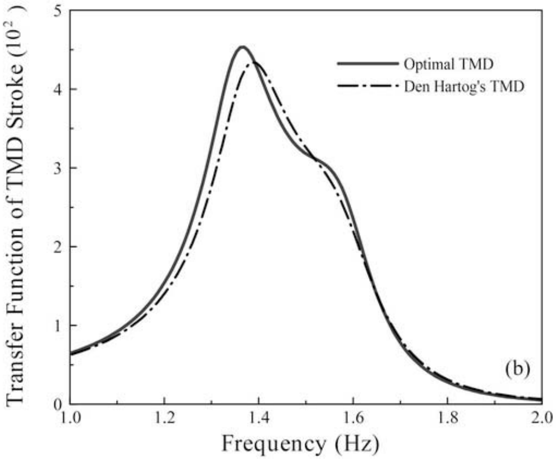

span bridge made of steel under the threat of wind resonance. An article written by Morgenstern (1995) describing the history of the tuned mass damper in Citicorp Center, New York, points out how these advantages are important to an existing structure when most of its structural elements are not accessible and immediate retrofit is demanded.

Practical Issues of Single TMD

Figure 1(a) implies that minimizing the area of transfer function can statistically reduce the seismic response of a structure under unpredictable ground excitations, which usually have wide-banded frequencies. Therefore, in conventional design of TMD, structural response-based parameters are usually defined as the objective function in optimization process. When TMD absorbs some of the vibration energy, the structural vibration is reduced. Inevitably, significant TMD stroke (displacement relative to the installed place) is the consequence, as shown in Figure 1(b). Figure 1(b) also implies that the more the structural response reduction, the larger the TMD stroke. In practice, TMD stroke demand for seismic application is larger than that of the wind application since an earthquake can induce more energy to structures. This may not be allowed due to the limitation of installation space and TMD's components. In addition, the difference in control performance of two TMD designs shown in Figure 1(a) results mainly from the difference in TMD design frequency($r_f = 0.953$ or 0.972), even though there is only 2% difference. Results of previous studies have also shown that any slight change in TMD design frequency can significantly deteriorate the control effectiveness. This "detuning effect" is another issue in real world application since the natural frequency of a structure is usually evaluated by employing system identification techniques from field measurements contaminated by machine and environment noises, which always induce errors to the outcome.

OPTIMAL DESIGN OF MULTIPLE TUNED MASS DAMPERS

To solve the detuning effect of single TMD, a multiple-TMD (MTMD) comprising of multiple units of SDOF substructures arranged in parallel was first proposed by Xu and Igusa (1992). Since then, numerous studies on the design approach and control efficiency have been carried out theoretically. Most of the previous studies did not consider the stroke problem of the control device. Lin *et al*. (2010) by expanding the efforts of Wang *et al*. (2009) for single TMD were among the first to study the stroke parameter in MTMD design.

Building-MTMD System Model

The equations of motion of a general n-DOF building equipped with an MTMD of p units at the ith floor, as shown in Figure 2, can be expressed as

$$\mathbf{M}\ddot{\mathbf{x}}(t) + \mathbf{C}\dot{\mathbf{x}}(t) + \mathbf{K}\mathbf{x}(t) = \mathbf{M}_f \mathbf{r}\ddot{x}_g(t) \tag{3}$$

in which

$$\mathbf{M} = \begin{bmatrix} \mathbf{M}_p & \mathbf{0} \\ \mathbf{M}_{sp} & \mathbf{M}_s \end{bmatrix}$$

$$\mathbf{C} = \begin{bmatrix} \mathbf{C}_p & \mathbf{C}_{ps} \\ \mathbf{0}^{\mathrm{T}} & \mathbf{C}_s \end{bmatrix}$$

$$\mathbf{K} = \begin{bmatrix} \mathbf{K}_p & \mathbf{K}_{ps} \\ \mathbf{0}^{\mathrm{T}} & \mathbf{K}_s \end{bmatrix}$$

$$\mathbf{M}_f = \begin{bmatrix} \mathbf{M}_p & \mathbf{0} \\ \mathbf{0}^{\mathrm{T}} & \mathbf{M}_s \end{bmatrix}$$

are $(n+p)\times(n+p)$ mass, damping and stiffness matrices of the entire system. $\mathbf{M}_p$, $\mathbf{C}_p$, and $\mathbf{K}_p$

Figure 2. A multi-story building equipped with multiple tuned mass dampers (Lin et al., 2010)

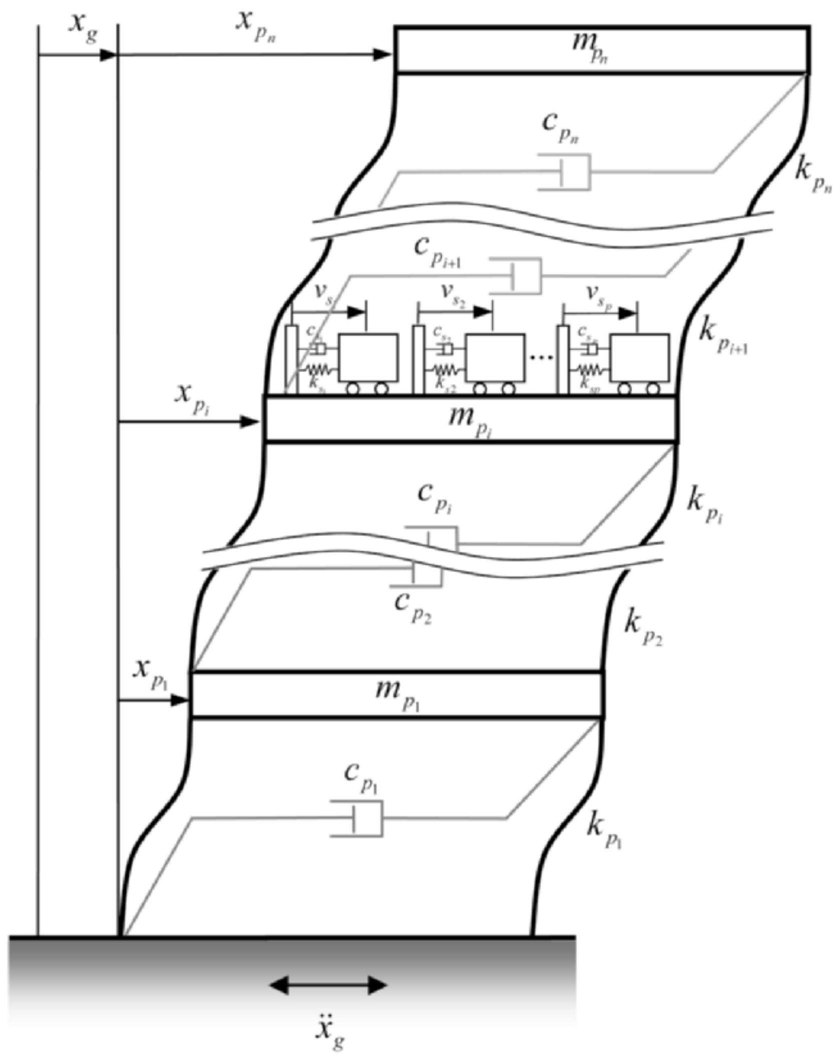

are $n \times$ n mass, damping and stiffness matrices of the primary building, respectively. $\mathbf{M}_s = diag.[m_{s_k}]$, $\mathbf{C}_s = diag.[c_{s_k}]$, $\mathbf{K}_s = diag.[k_{s_k}]$, $\mathbf{M}_{sp} = \mathbf{M}_s\mathbf{u}$, $\mathbf{C}_{ps} = -(\mathbf{C}_s\mathbf{u})^{\mathrm{T}}$, $\mathbf{K}_{ps} = -(\mathbf{K}_s\mathbf{u})^{\mathrm{T}}$ where $\mathbf{M}_s$, $\mathbf{C}_s$, and $\mathbf{K}_s$ are $p \times$ p diagonal matrices; m_{s_k}, c_{s_k}, and k_{s_k} are mass, damping coefficient and stiffness coefficient of the kth unit of MTMD $(k = 1,\ 2, \ldots, p)$; $\mathbf{u} = [\mathbf{0} \quad \mathbf{0} \quad \ldots \quad \mathbf{1}^{(i)} \quad \ldots \quad \mathbf{0}]_{p \times n}$ where 0 and 1 are $p \times 1$ vectors with each element equal to 0 and 1, respectively. The superscript (i) indicates the position of vector 1 in matrix $\mathbf{u}$. $\mathbf{x}(t) = [\mathbf{x}_p^{\mathrm{T}}(t) \quad \mathbf{v}_s^{\mathrm{T}}(t)]^{\mathrm{T}}$ is the displacement vector. $\mathbf{x}_p(t)$ and $\mathbf{v}_s(t)$ denote the vector of displacement of building relative to the ground and the vector of MTMD's displacement relative to the ith floor (called stroke), respectively. $\mathbf{r}$ is $(n+p) \times 1$ influence vector with each element equal to -1. $\ddot{x}_g(t)$ represents the ground acceleration.

Let Φ be the $n \times$ n mode shape matrix of the building and $\eta(t)$ be the $n \times 1$ modal displacement vector. By substituting $\mathbf{x}_p(t) = \Phi\eta(t)$ into Equation (3) and premultiplying two sides of the building part by Φ^{T} to transform the system coordinates from physical domain to modal domain, the equations of motion become

$$\begin{bmatrix} \mathbf{M}_p^* & \mathbf{0} \\ \mathbf{M}_{sp}^* & \mathbf{M}_s^* \end{bmatrix} \begin{Bmatrix} \ddot{\eta}(t) \\ \ddot{\mathbf{v}}_s(t) \end{Bmatrix} + \begin{bmatrix} \mathbf{C}_p^* & \mathbf{C}_{ps}^* \\ \mathbf{0}^{\mathrm{T}} & \mathbf{C}_s^* \end{bmatrix} \begin{Bmatrix} \dot{\eta}(t) \\ \dot{\mathbf{v}}_s(t) \end{Bmatrix} + \begin{bmatrix} \mathbf{K}_p^* & \mathbf{K}_{ps}^* \\ \mathbf{0}^{\mathrm{T}} & \mathbf{K}_s^* \end{bmatrix} \begin{Bmatrix} \eta(t) \\ \mathbf{v}_s(t) \end{Bmatrix} = \begin{bmatrix} \Gamma_p \\ \Gamma_s \end{bmatrix} \ddot{x}_g(t) \tag{4}$$

where the modal parameters of the primary building and the MTMD are involved.

Conventional MTMD Parameter Design

The *j*th modal displacement of the building and the stroke of the *k*th MTMD unit can be represented in frequency domain as

$$\eta_j(\omega) = H_{\eta_j \ddot{X}_g}(\omega)\ddot{X}_g(\omega) \tag{5a}$$

$$v_{s_k}(\omega) = H_{v_{s_k} \ddot{X}_g}(\omega)\ddot{X}_g(\omega) \tag{5b}$$

Statistically, the MTMD control effectiveness can be evaluated by the performance index, R_j, defined as

$$R_j = \frac{E[\eta_j^2]_{\text{with MTMD}}}{E[\eta_j^2]_{\text{w/o MTMD}}} \tag{6}$$

that is, the ratio of mean square response of displacement or acceleration of the *j*th structural mode with MTMD to that without MTMD. R_j is a function of *j*th modal damping ratio of the primary building, ξ_j, *j*th mode shape at *i*th floor of the building, φ_{ij}, ratio of the *k*th MTMD unit mass to the *j*th modal mass of the building, $\mu_{s_k,j}$, damping ratio of the *k*th MTMD unit, ξ_{s_k}, and frequency ratio of the *k*th MTMD unit to the *j*th modal frequency of the building, $r_{f_k} = \left(\omega_{s_k} / \omega_j\right)$ where k =1, 2, …, p. With the prior knowledge of structural parameters, ω_j, ξ_j, and φ_{ij}.

Considering the most economical MTMD layout, identical stiffness coefficient, k_{s_0}, and damping coefficient, c_{s_0}, are given. It can be expressed as:

$$k_{s_0} = \frac{m_{st}}{\sum_{k=1}^{p} \frac{1}{\omega_j^2 r_{f_k}^2}} \tag{7a}$$

$$c_{s_0} = \frac{\xi_{s_k}}{r_{f_k}\omega_j} k_{s_0} \tag{7b}$$

$$m_{s_k} = \frac{k_{s_0}}{r_{f_k}^2 \omega_j^2} \tag{7c}$$

where $m_{st} = \sum_{k=1}^{p} m_{s_k}$ is the total mass of MTMD units. Based on Equations (7a), (7b), and (7c), the damping ratio of each MTMD unit, $\xi_{s_1}, \xi_{s_2}, \ldots,$ and ξ_{s_p} can be expressed as $\xi_{s_k} = \xi_{s_0} r_{f_k}$ where ξ_{s_0} is a constant. Moreover, with the given MTMD mass ratio, $\mu_{st,j} = \varphi_{ij} m_{st} / m_j^*$, the modal mass ratio of the *k*th MTMD unit can be calculated by

$$\mu_{s_k,j} = \mu_{st,j} \frac{1/r_{f_k}^2}{\sum_{l=1}^{p} 1/r_{f_l}^2} \tag{8}$$

Without any restriction on the frequency distribution of MTMD units, the optimization of

MTMD with identical stiffness and damping coefficient involves (p + 1) independent parameters, $r_{f_1}, r_{f_2}, \ldots, r_{f_p}$ and ξ_{s_0}. Theoretically, with given ω_j, ξ_j, and φ_{ij}, the optimal MTMD parameters, $(r_{f_1})_{\mathrm{opt}}$, $(r_{f_2})_{\mathrm{opt}}, \ldots,$ $(r_{f_p})_{\mathrm{opt}}$, and $(\xi_{s_0})_{\mathrm{opt}}$ can be obtained by solving the following system of equations which are established by differentiating R_j with respect to the (p + 1) parameters and equating to zero, respectively, to minimize R_j.

$$\frac{\partial R_j}{\partial r_{f_1}} = 0, \quad \frac{\partial R_j}{\partial r_{f_2}} = 0, \quad \ldots, \quad \frac{\partial R_j}{\partial r_{f_p}} = 0, \quad \frac{\partial R_j}{\partial \xi_{s_0}} = 0 \tag{9}$$

Then, the optimum stiffness coefficient, $(k_{s_0})_{\mathrm{opt}}$, optimum damping coefficient, $(c_{s_0})_{\mathrm{opt}}$, and optimum mass for kth MTMD unit, $(m_{s_k})_{\mathrm{opt}}$ can be obtained. The optimization process can also be performed by numerical seaching techniques which can be found in mathematical software packages, such as MATLAB.

A New Optimization Criterion: Considering Stroke Limitation

To consider the stroke of each MTMD unit in design stage, the kth stroke ratio, $R_{v_{s_k}}$, which is used to measure the reduction of stroke, is defined as

$$R_{v_{s_k}} = \frac{E[v_{s_k}^2]_{\text{with MTMD}}}{E[v_{s_k}^2]_{\text{with MTMD}^0}} \tag{10}$$

where $E[v_{s_k}^2]_{\text{with MTMD}^0}$ represents the mean square stroke of the kth MTMD unit based on the optimum parameters obtained by the first-stage optimization procedure. Because there are k units of MTMDs, it can be a complicated problem if all units' strokes are considered. An alternative strategy is to select only one of them as a representative.

From Equation (7c), it can be seen that the first MTMD unit (m_{s_1}, called Unit1) has the heaviest weight among the MTMD units if r_{f_1} is the smallest frequency ratio and r_{f_p} is the largest one. Since each MTMD unit has the same stiffness and damping coefficients, Unit 1 would probably experience the largest stroke. Consequently, the stroke of Unit1 is selected to be reduced.

Now, a modified performance index, R_j^{α} with the consideration of stroke, is defined as

$$R_j^{\alpha} = (1-\alpha)R_j + \alpha R_{v_{s_1}} \tag{11}$$

where α is the stroke weighting factor ranging from 0 to 1.0. $R_{v_{s_1}}$ means the stroke ratio of Unit1. When $\alpha = 0$, R_j^{α} reduces to the conventional performance index with unlimited movement of MTMD, while $\alpha = 1.0$ indicates that the MTMD are locked. To associate the parameters of Unit1 with the rest of MTMD units, the frequency differences between Unit1 and the other MTMD units ($r_{f_2} - r_{f_1}, r_{f_3} - r_{f_1}, \ldots, r_{f_p} - r_{f_1}$) from the first-stage design are assumed unchanged in the second-stage. With the new performance index R_j^{α} which includes the first-stage optimization result, the second-stage optimization can be proceeded in the same manner as Equation (9) as

$$\frac{\partial R_j^{\alpha}}{\partial r_{f_1}} = 0, \quad \frac{\partial R_j^{\alpha}}{\partial \xi_{s_0}} = 0 \tag{12}$$

By solving Equation (12), the optimum damping ratio, $(\xi_{s_1})^{\alpha}_{\mathrm{opt}}$, $(\xi_{s_2})^{\alpha}_{\mathrm{opt}}, \ldots, (\xi_{s_p})^{\alpha}_{\mathrm{opt}}$, and optimum frequency ratio, $(r_{f_1})^{\alpha}_{\mathrm{opt}}$, $(r_{f_2})^{\alpha}_{\mathrm{opt}}, \ldots,$ $(r_{f_p})^{\alpha}_{\mathrm{opt}}$ can be obtained with a prior selection of MTMD mass ratio and the weighting factor, α.

The new optimization criterion is demonstrated by an example of a three-story shear building with 2% damping ratio in each mode. With total MTMD mass ratio, $\mu = 2\%$, the optimum parameters of MTMD with five units (p=5) versus α are presented in Figure 3(a). Comparing with conventional design parameters (when α= 0, e.g., $(\xi_s)^{\alpha}_{\text{opt}}$=3.03%, $(r_{f_1})^{\alpha}_{\text{opt}}$ ~ $(r_{f_5})^{\alpha}_{\text{opt}}$: 0.860, 0.922, 0.977, 1.032, and 1.093), it is seen that the frequency ratio parameters are almost unchanged for most ranges of α, whereas the larger α, the greater optimal damping ratio is required. This result reflects that accurate frequency parameters are more important to MTMD's control effectiveness than the damping ratio parameter. Therefore, the increase of MTMD's damping can reduce the MTMD's stroke and avoid detuning. However, when α = 1, each MTMD unit becomes very stiff and highly-damped. It is true because the structural response is not considered and the suppression of MTMD stroke is the only concern under this condition.

Figure 3(b) presents the first modal displacement ratio of the structure, R_1, and the stroke ratio of the first MTMD unit, $R_{v_{s_1}}$, versus α. It is shown that the suppression of the MTMD stroke by increasing α decreases the control effectiveness of structural response. However, it is seen that when 0 < α < 0.15, the MTMD stroke is significantly reduced with little loss of control efficiency of structural responses. Hence, there exists an appropriate α which corresponds to an MTMD with acceptable structural control performance and smaller stroke. Figure 4 illustrates the transfer functions of roof displacement and MTMD's stroke with respect to base acceleration for different α. When α increases, the strokes of MTMD decrease and structural response increases, which agree with the results in Figure 3(b).

AN EXPERIMENTAL STUDY

To verify the control effectiveness of MTMD, Lin *et al*. (2010) conducted shaking-table tests of a large-scale building-MTMD system at the National Center for Research on Earthquake Engineering (NCREE) in Taipei, Taiwan. In their

Figure 3. (a) Optimal damping ratio (ξ_{s_0}) and optimal frequency ratios of the five MTMD units versus stroke weighting factor (α); (b) First modal displacement ratio of the structure (R_1) and stroke ratio of Unit1 TMD ($R_{v_{s_1}}$) versus stroke weighting factor (α)

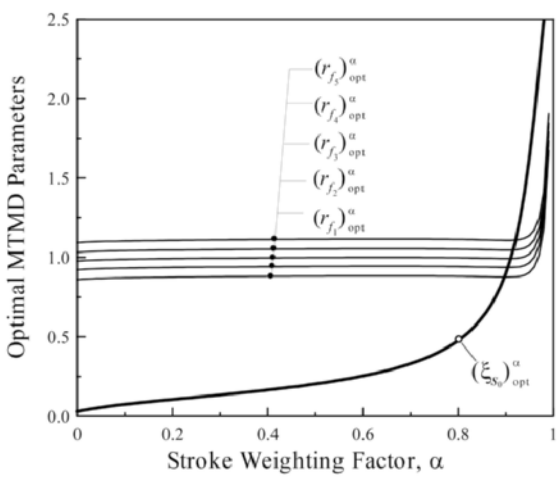

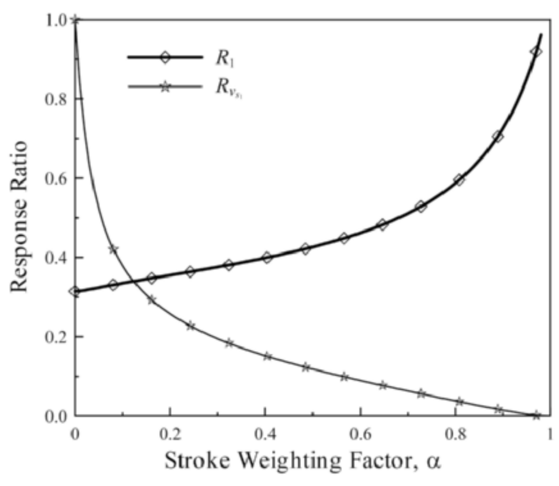

Figure 4. (a) Transfer function of roof displacement of a 3-story building-MTMD system with different α; (b) Transfer function of MTMD stroke with different α

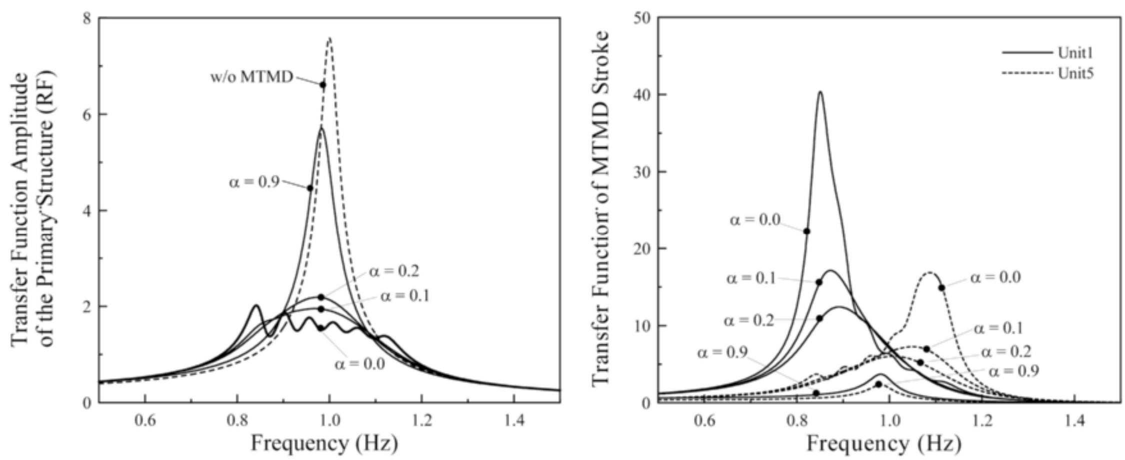

study, a real MTMD device was designed and fabricated. Then, experiments were performed on a 5m ×5m three-dimensional shake table. This section describes the details and the results of the study. It also provides a useful reference when a real-life case is implemented.

Test Program and Sensors Setup

The experimental structure used in the experimental study was a large-scale three-story steel frame as shown in Figure 5. This structure is regarded as a benchmark building designed for the demonstration of research on structural control and health monitoring in Taiwan. It was a uniform building with total of 18 tons in weight and 9 m in height. The dimension of the rectangular floor is 3 m × 2 m. Four columns of H-shape (H150×150×7×10) section with the same section orientation are used for support. The weak axis of the column section is also the test direction.

The test program includes three major steps: (1) Bare building test: to identify the dynamic parameters of the building at the time and to establish the uncontrolled response for future comparisons; (2) MTMD design and fabrication: to create the control device based on the identified building parameters; (3) Building-MTMD system test: to evaluate the control effectiveness of MTMD.

Two acceleration sensors and two displacement sensors along the excitation direction at each floor were deployed.

Figure 5. Configuration of 3-story building and MTMD device

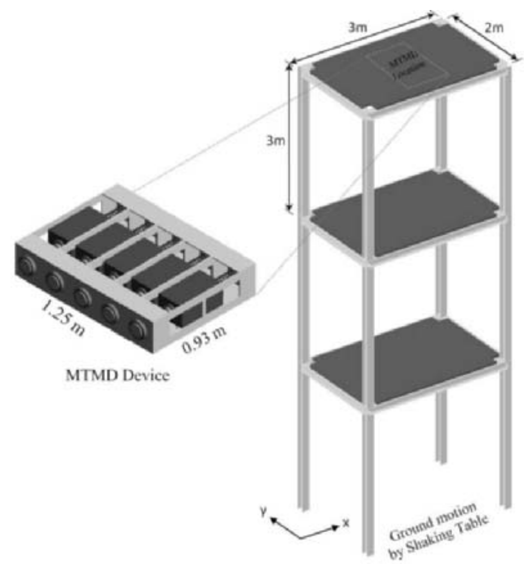

Parameter Identification of the Bare Building

After the setup of the bare building, a shaking table test was conducted first. The excitation used for the test was the ground acceleration recorded during the 1999 Chi-Chi earthquake on the campus of National Chung Hsing University (NCHU) in Taiwan along the E-W direction. The original PGA (360 gal) was scaled down to 30 gal to ensure that the building remained linear and the strokes of MTMD units were within the allowable range.

After collecting and processing the acceleration measurements, the SRIM (System Realization using Information Matrix) system identification technique (Juang, 1997; Lin *et al.*, 2005) was employed using the second floor (2F), third floor (3F), and roof (RF) accelerations as output and the base acceleration as input. The identified modal frequencies, damping ratios, and mode shapes are presented in Table 1. It can be seen that the first modal damping of the steel building is normal (around 2%) but the second and third modal damping ratios are extremely low (0.21 and 0.17%, respectively).

Design and Fabrication of MTMD

The given mass of the MTMD was 360 kg $\left(\mu = 2\%\right)$ consisting of five units. Due to the light damping in higher modes of the building, the MTMD units were divided into two groups: four units were tuned to the first structural mode and one unit to the second structural mode. The distribution of the 2% MTMD mass ratio was 1.69% to the first group and 0.31% to the second group, which was obtained by minimizing the mean square roof acceleration under the condition of two single TMDs controlling two structural modes. With the given masses, the optimal parameters of the first-mode MTMD and second-mode TMD with $\alpha = 0$ are first obtained based on the design theory stated earlier. The optimal parameters are presented in Table 2.

The mass block of each MTMD unit was a steel cuboid with four bearing wheels and was placed in a metal box of 93 cm in length. Inside the box, there were two parallel guiding rails. Two compression coil springs were used to generate the resilient force of each MTMD unit. Based on the optimum masses and designed stiffness coefficient in Table 2, mass blocks and springs were made. The simulation 3D view of the finished MTMD device is shown in Figure 5. The installed location of this MTMD was on the roof at which the maximum of the first mode shape located (Ueng *et al.*, 2008).

According to the design parameters in Table 2, each MTMD unit of the first-mode MTMD is supposed to give a supplemental damping device with optimal c_{s_0}. However, measurements of the free vibration of the SDOF mass-spring system of the fabricated MTMD unit showed that due to contact friction, an equivalent damping coefficient of 71.0 N·s / m, exceeding the demand optimum damping coefficient, 27.8 N·s/m, in the case of $\alpha = 0$, was observed. Consequently, no additional supplementary damping was installed. The

Table 1. Identified modal parameters of the 3-story experimental building

Modal frequency (Hz)	Modal damping ratio (%)	Mode shape
$\begin{Bmatrix} 1.08 \\ 3.24 \\ 5.02 \end{Bmatrix}$	$\begin{Bmatrix} 1.95 \\ 0.21 \\ 0.17 \end{Bmatrix}$	$\begin{array}{cc} \begin{bmatrix} 0.4933 & 0.3576 & 0.1362 \\ 0.9791 & 0.1695 & -0.1586 \\ 1.2383 & -0.3088 & 0.0783 \end{bmatrix} & \begin{matrix} 2F \\ 3F \\ RF \end{matrix} \end{array}$

Table 2. Design parameters of the fabricated MTMD

<table>
<tr><th rowspan="2">Parameters</th><th colspan="4">1st-Mode MTMD</th><th>2nd-Mode TMD</th></tr>
<tr><th>Unit 1</th><th>Unit 2</th><th>Unit 3</th><th>Unit 4</th><th>Unit 5</th></tr>
<tr><td rowspan="2">Designed mass, kg
(μ_s)</td><td>93.2</td><td>79.9</td><td>70.0</td><td>61.0</td><td>56.0</td></tr>
<tr><td colspan="4">(1.69%)</td><td>(0.31%)</td></tr>
<tr><td>Optimal frequency ratio</td><td>0.87</td><td>0.94</td><td>1.01</td><td>1.08</td><td>0.99</td></tr>
<tr><td>Designed k_{s_0} , N / m</td><td colspan="4">3,361</td><td>22,746</td></tr>
<tr><td rowspan="2">Optimal c_{s_0} , N·s / m
(ξ_s)</td><td colspan="4">27.8</td><td>68.2</td></tr>
<tr><td>(2.5%)</td><td>(2.7%)</td><td>(2.9%)</td><td>(3.1%)</td><td>(3.0%)</td></tr>
<tr><td rowspan="2">Designed c_{s_0} , N·s / m
(ξ_s)</td><td colspan="4">71.0</td><td>71.0</td></tr>
<tr><td>(6.5%)</td><td>(7.0%)</td><td>(7.4%)</td><td>(7.9%)</td><td>(3.1%)</td></tr>
<tr><td>Designed α</td><td colspan="4">0.1</td><td>0.0</td></tr>
<tr><td rowspan="2">Designed R_j
$(R_{v_{s_i}})$</td><td colspan="4">0.36</td><td>0.60</td></tr>
<tr><td>(0.38)</td><td>(0.40)</td><td>(0.38)</td><td>(0.34)</td><td>(0.97)</td></tr>
</table>

inherent damping of the first-mode MTMD was equivalent to the case of $\alpha = 0.1$. For the second-mode TMD, the inherent damping ratio, 3.1%, was very close to the optimal damping ratio, 3.0%. Since the stiffness of the second-mode TMD was large enough, there was no stroke problem and stroke-reduction design was not required. Hence, no supplementary damping was installed as well.

Building-MTMD System Tests

In this experimental study, three different acceleration time histories, i.e., an artificial white noise, the 1940 El Centro earthquake, and the 1999 Chi-Chi earthquake at NCHU, were used as input excitations of the shaking table. The PGA of the three inputs was scaled to 30 gal so that the PGA effect between these input forces could be eliminated.

After the tests, the system matrices of the experimental building were identified by employing SRIM technique based on the recorded acceleration measurements. With the identified controlled and uncontrolled systems, transfer functions of roof displacement and roof acceleration of the building can be obtained as shown in Figure 6. It shows that the displacement of the uncontrolled building is dominated by the first mode, whereas the acceleration is dominated by the second mode. With the MTMD installed, both displacement and acceleration resonance peaks of the first and second modes were significantly reduced. Comparing with Figure 4(a), the unclear local five peaks near the first mode of the controlled system also revealed that $\alpha > 0$ for the first-mode MTMD. On the other hand, $\alpha = 0$ for the second-mode TMD resulted in two clear local peaks near the second mode.

Figure 7 presents the recorded time-history accelerations and displacements at roof with and without the MTMD device under the three input excitations along with the peak values and reduc-

Figure 6. Transfer functions of displacement and acceleration at roof of the experimental building near the first and second modal frequencies (1.08Hz and 3.42Hz) with and without MTMD

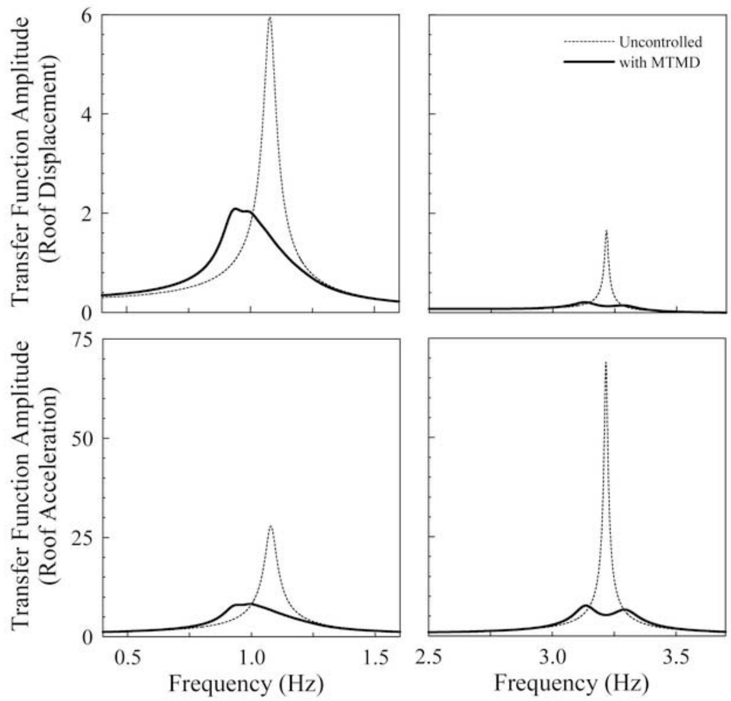

tion percentages in root-mean-square (r.m.s.) response. It is seen that different MTMD control effectiveness is observed even though all input excitations have the same PGA. This is because the frequency content of each input excitation varies from that of one another, whereas MTMD is only effective for the structural response of the frequencies in the MTMD operating range. In the cases of El Centro earthquake and Chi-Chi earthquake, the reductions in peak acceleration were 34.8% and 33.1%, respectively. In contrast, the MTMD seemed ineffective for the white-noise case. However, it is seen that the amplification of acceleration from base (30gal) to roof (38gal, 44.5gal) is small, which means there is no need to control this white noise induced vibration. These results showed that the vibration control effectiveness of MTMD was highly frequency-dependent. It is always useful once the excitation frequencies are within its operating range and the structural response is significant.

ISSUES ON BUILDING MODEL

Since MTMD/TMD is highly frequency-dependent, the accuracy of the building model used for MTMD/TMD design will be a concern in practical application. Most of the previous studies regarded building as a fix-based symmetrical structure. In real-life situations, a building usually has flexible foundation and contains some degrees of asymmetry. Therefore, more or less, the soil-structure interaction (SSI) effect and torsion-translation coupling (TC) effect may affect the dynamic parameters of the building used for MTMD/TMD design. A building model with TC and SSI effects suggested by Wu *et al.* (2001) is shown in Figure8.

Figure 7. Time-history measurements of absolute acceleration and relative displacement at roof of the experimental building with and without the TYPE-II (two-mode) MTMD subjected to earthquakes

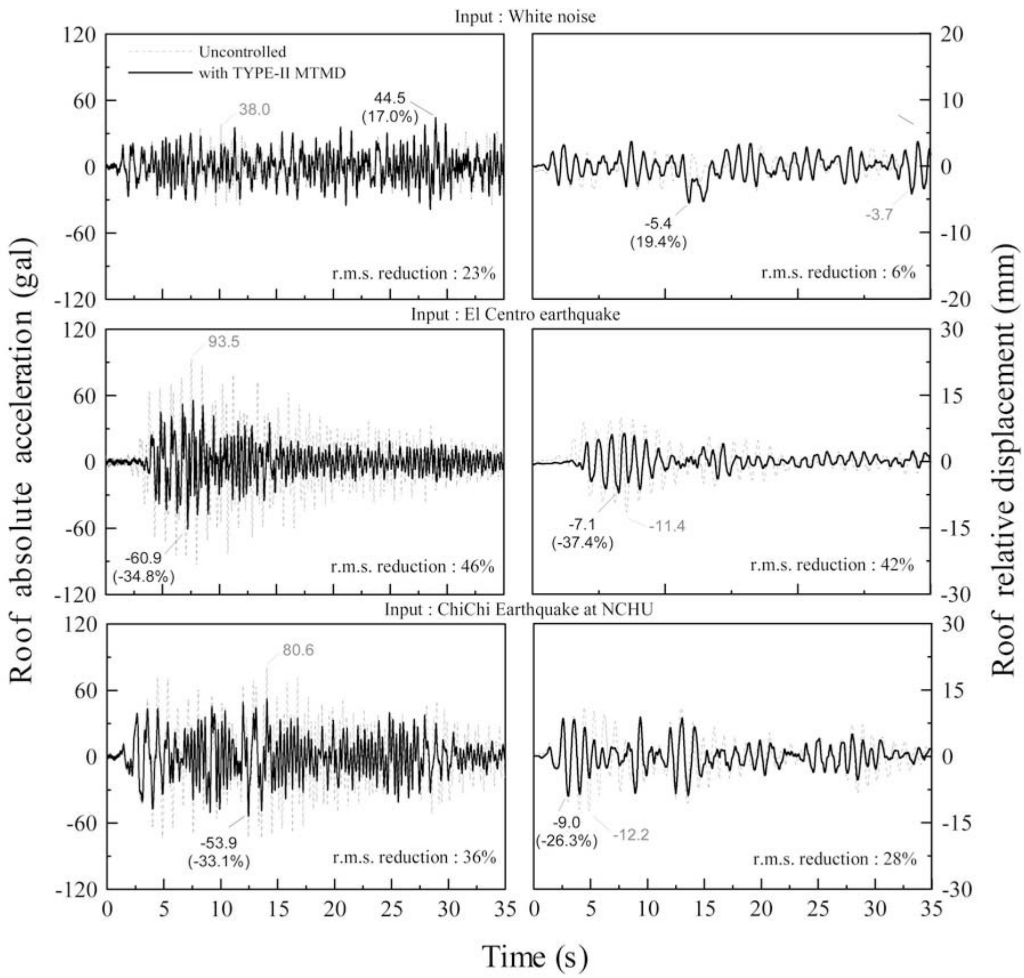

Torsion-Coupling (TC) Effect

The building model in Figure 8(a) was a single floor building with mass lumped at the center of mass (CM). The center of rigidity (CR) contributed by the lateral resisting elements (e.g., columns) was not located on the vertical line passing through the C.M. Under the x-direction ground motion, $\ddot{x}_g$, the floor encounters not only the translation but also torsion due to the inconsistency between the C.R. and the C.M. This is called torsion-coupling effect, which occurs when the lateral resisting elements are asymmetrically arranged. In addition, because the soil is flexible, the base experiences not only the free-field ground motion in x-direction, but also the foundation motion, including x-directional translation, $\ddot{x}_b$, θ- directional torsion, $\ddot{\theta}_b$, and x-directional rocking (with respect to y-axis), φ_b. The lateral displacement of the floor at the C.M. relative to the base is contributed by the shear deformation of the building, x_p, and rocking of the entire building, $h\varphi_b$.

Figure 8. (a) An irregular building-soil interaction model before and after deformation (Wu et al., 2001), (b) Top-view of floor equipped with MTMD (c) Top-view of foundation with ground reaction forces

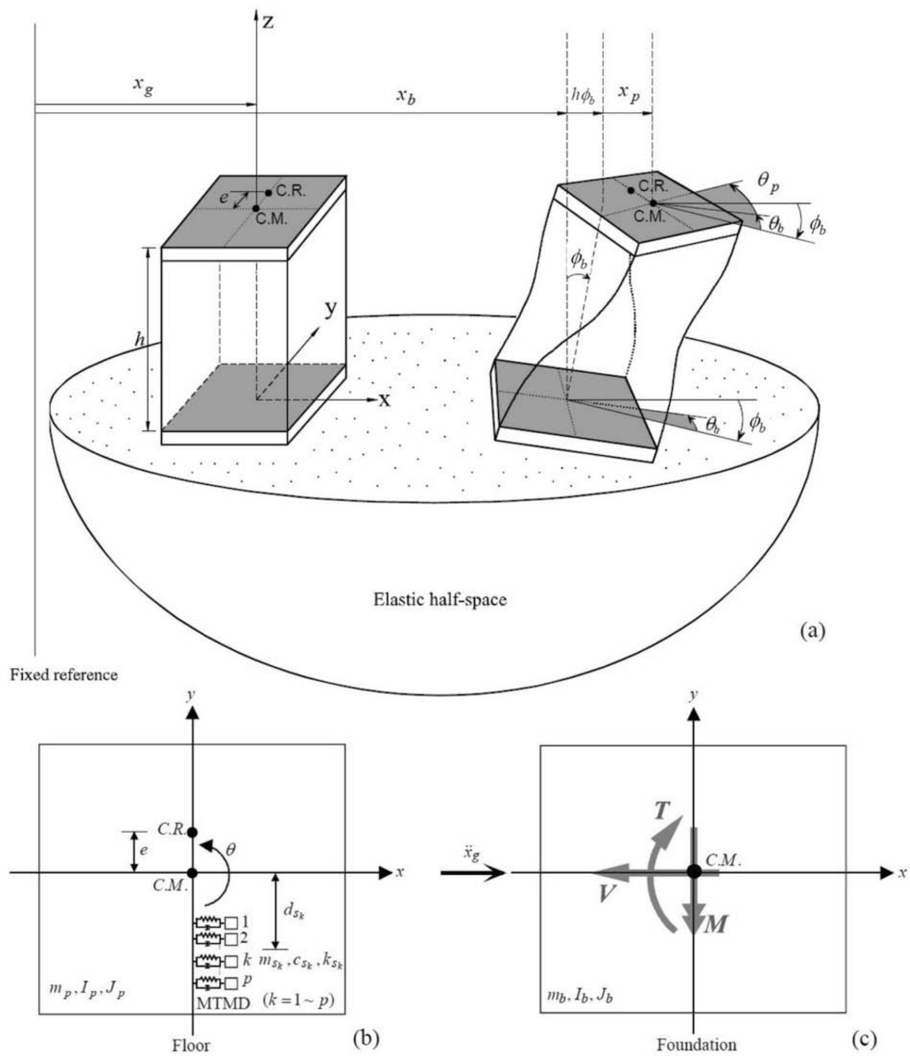

The mass and stiffness matrices of the fixed-base building can be given by

$$\mathbf{M}_p = \begin{bmatrix} m_p & 0 \\ 0 & J_p \end{bmatrix} \text{ and } \mathbf{K}_p = \begin{bmatrix} k_x & -ek_\theta \\ -ek_\theta & k_\theta{}^2 + e^2 k_x^2 \end{bmatrix} \tag{12}$$

where m_p and J_p are the mass and polar moment of inertia of the floor, respectively. k_x and k_θ are the uncoupled lateral stiffness and torsional stiffness, respectively; e is the one-way eccentricity of the C.R. from the C.M. The displacement vector is represented by $\mathbf{U}_p = \{x_p \quad \theta_p\}^T$, which can also be expressed by the product of mode shape matrix and modal displacement vector as

$$\mathbf{U}_p = \Phi\eta \tag{13}$$

where

$$\Phi = \begin{bmatrix} \varphi_{11} & \varphi_{12} \\ \varphi_{21} & \varphi_{22} \end{bmatrix}, \ \eta = \begin{Bmatrix} \eta_1 \\ \eta_2 \end{Bmatrix} \tag{14}$$

According to the study by Ueng *et al.* (2008), the building floor is equipped with an MTMD system with *p* units along the y-axis, as shown in Figure 8(b), and considering flexible foundation, the equations of motion of the building-MTMD system can be given in modal domain by

$$\begin{bmatrix} \mathbf{M}_p^* & \mathbf{0} \\ \mathbf{M}_{sp}^* & \mathbf{M}_s \end{bmatrix} \begin{Bmatrix} \ddot{\eta}(t) \\ \ddot{\mathbf{v}}_s(t) \end{Bmatrix} + \begin{bmatrix} \mathbf{C}_p^* & \mathbf{C}_{ps}^* \\ \mathbf{0}^{\mathrm{T}} & \mathbf{C}_s \end{bmatrix} \begin{Bmatrix} \dot{\eta}(t) \\ \dot{\mathbf{v}}_s(t) \end{Bmatrix} + \begin{bmatrix} \mathbf{K}_p^* & \mathbf{K}_{ps}^* \\ \mathbf{0}^{\mathrm{T}} & \mathbf{K}_s \end{bmatrix} \begin{Bmatrix} \eta(t) \\ \mathbf{v}_s(t) \end{Bmatrix} = \begin{bmatrix} \Gamma_p \\ \Gamma_s \end{bmatrix} \ddot{\mathbf{X}}_b(t) \tag{15}$$

where

$$\mathbf{M}_p^* = \begin{bmatrix} 1 & 0 \\ 0 & 1 \end{bmatrix}, \ \mathbf{C}_p^* = \begin{bmatrix} 2\xi_1\omega_1 & 0 \\ 0 & 2\xi_2\omega_2 \end{bmatrix}, \ \mathbf{K}_p^* = \begin{bmatrix} \omega_1^2 & 0 \\ 0 & \omega_2^2 \end{bmatrix}$$

$$\mathbf{M}_s = \mathbf{I}, \ \mathbf{C}_s = diag.(2\xi_{s_k}\omega_{s_k}), \ \mathbf{K}_s = diag.(\omega_{s_k}^2)$$

$$(\mathbf{M}_{sp}^*)^{\mathrm{T}} = \begin{bmatrix} \varphi_{11} + \varphi_{21}d_{s_1} & \varphi_{11} + \varphi_{21}d_{s_2} & \cdots & \varphi_{11} + \varphi_{21}d_{s_p} \\ \varphi_{12} + \varphi_{22}d_{s_1} & \varphi_{12} + \varphi_{22}d_{s_2} & \cdots & \varphi_{12} + \varphi_{22}d_{s_p} \end{bmatrix}$$

$$\mathbf{C}_{ps}^* = \begin{bmatrix} -2\xi_{s_1}\omega_{s_1}\rho_{s_1}(\varphi_{11} + \varphi_{21}d_{s_1}) & -2\xi_{s_2}\omega_{s_2}\rho_{s_2}(\varphi_{11} + \varphi_{21}d_{s_2}) & \cdots & -2\xi_{s_p}\omega_{s_p}\rho_{s_p}(\varphi_{11} + \varphi_{21}d_{s_p}) \\ -2\xi_{s_1}\omega_{s_1}\rho_{s_1}(\varphi_{12} + \varphi_{22}d_{s_1}) & -2\xi_{s_2}\omega_{s_2}\rho_{s_2}(\varphi_{12} + \varphi_{22}d_{s_2}) & \cdots & -2\xi_{s_p}\omega_{s_p}\rho_{s_p}(\varphi_{12} + \varphi_{22}d_{s_p}) \end{bmatrix}$$

$$\mathbf{K}_{ps}^* = \begin{bmatrix} -\omega_{s_1}^2\rho_{s_1}(\varphi_{11} + \varphi_{21}d_{s_1}) & -\omega_{s_2}^2\rho_{s_2}(\varphi_{11} + \varphi_{21}d_{s_2}) & \cdots & -\omega_{s_p}^2\rho_{s_p}(\varphi_{11} + \varphi_{21}d_{s_p}) \\ -\omega_{s_1}^2\rho_{s_1}(\varphi_{12} + \varphi_{22}d_{s_1}) & -\omega_{s_2}^2\rho_{s_2}(\varphi_{12} + \varphi_{22}d_{s_2}) & \cdots & -\omega_{s_p}^2\rho_{s_p}(\varphi_{12} + \varphi_{22}d_{s_p}) \end{bmatrix}$$

$$\Gamma_b = -\begin{bmatrix} \varphi_{11} & \varphi_{11} & \varphi_{21} \\ \varphi_{12} & \varphi_{12} & \varphi_{22} \end{bmatrix}$$

$$\Gamma_s = -\begin{bmatrix} 1 & 1 & d_{s_1} \\ 1 & 1 & d_{s_2} \\ \vdots & \vdots & \vdots \\ 1 & 1 & d_{s_p} \end{bmatrix}$$

$$\ddot{\mathbf{X}}_b^T = \begin{Bmatrix} \ddot{x}_b \\ \ddot{\varphi}_b \\ \ddot{\theta}_b \end{Bmatrix}$$

where ξ_j and ω_j $(j = 1 \sim 2)$ are the *j*th modal damping ratio and modal frequency of the primary building; ρ_{s_k}, ξ_{s_k}, and ω_{s_k} are the mass ratio, damping ratio and natural frequency of the *k*th MTMD unit; d_{s_k} is the distance between the *k*th MTMD unit and the C.M. of the floor.

It is seen that Equation (15) is similar to Equation (4) except multiple input excitations, $\ddot{\mathbf{X}}_b$, rather than single input excitation, $\ddot{x}_g$. Taking Fourier transform on Equation (15), the modal displacement of the *j*th mode of the building can be expressed in terms of transfer functions as

$$\eta_j(\omega) = H_{\eta_j\ddot{x}_b}(\omega)\ddot{X}_b(\omega) + H_{\eta_j\ddot{\varphi}_b}(\omega)\ddot{\Phi}_b(\omega) + H_{\eta_j\ddot{\theta}_b}(\omega)\ddot{\Theta}_b(\omega) \tag{16}$$

where $\ddot{X}_b(\omega)$, $\ddot{\Phi}_b(\omega)$, and $\ddot{\Theta}_b(\omega)$ are the Fourier transform of $\ddot{x}_b(t)$, $\ddot{\varphi}_b(t)$, and $\ddot{\theta}_b(t)$, respectively. Equation (16) takes the similar form to Equation (5a) except that three transfer functions are involved. Since $\ddot{X}_b(\omega)$, $\ddot{\Phi}_b(\omega)$, and $\ddot{\Theta}_b(\omega)$ are independent and the ratio between them is uncertain, it is not proper to use $\eta_j(\omega)$ to measure the performance of MTMD. In turn, the reduction of area of transfer function can be a useful option because earthquake usually has wide-band frequency content. Therefore, the performance index can be defined as

$$R_j = \frac{\int_0^\infty \left| H_{\eta_j \ddot{x}_i}(\omega) \right|^2_{\mathrm{MTMD}} d\omega}{\int_0^\infty \left| H_{\eta_j \ddot{x}_i}(\omega) \right|^2_{\mathrm{NOMTMD}} d\omega} \tag{17}$$

where $\ddot{x}_i = \ddot{x}_b$, $\ddot{\varphi}_b$, or $\ddot{\theta}_b$. In Equation (17), the selection of $H_{\eta_j \ddot{x}_i}(\omega)$ is dependent upon the MTMD control goal. Moreover, R_j is recognized as a function of structural parameters: ξ_1, ξ_2, and $\mathbf{\Phi}$, which should be known *in priori*, and the MTMD parameters: ρ_{s_k}, ξ_{s_k}, r_{f_k} (the frequency ratio of the *k*th unit to the controlled mode of the structure) and d_{s_k}. The MTMD mass ratio is assigned based on both considerations of construction cost and structural capacity before the MTMD design. Considering the same stiffness and damping coefficients condition, which the physical parameters of the MTMD unit can be obtained by Equation (7), the MTMD parameters to be optimized become

$$\begin{cases} (r_{f_1})_{\mathrm{opt}}, \ (r_{f_2})_{\mathrm{opt}}, \ \ldots, \ (r_{f_p})_{\mathrm{opt}} \\ (\xi_{s_0})_{\mathrm{opt}} \\ d_{s_0} \end{cases} \tag{18}$$

where d_{s_0} is the distance from center of MTMD to the C.M of the building floor. Comparing with Equation (9), it is found that with the TC effect of the building, multiple structural modes should be taken into account. Besides, the installed location of the MTMD is also an essential issue.

According to the study by Wang and Lin (2005), two parameters govern the TC effect of a building, i.e., eccentricity, e, and uncoupled torsion/translation stiffness ratio, k_θ / k_x. In addition, the optimal locations for MTMD controlling the first mode and the second mode can be obtained by

$$\begin{cases} (d_{s_0})_{\mathrm{opt}} = -\dfrac{\varphi_{12}}{\varphi_{22}} & \text{for 1st mode} \\ (d_{s_0})_{\mathrm{opt}} = -\dfrac{\varphi_{11}}{\varphi_{21}} & \text{for 2nd mode} \end{cases} \tag{19}$$

Figure 9 are plots of the optimal MTMD location, $(d_{s_0})_{\mathrm{opt}}$, for a square floor TC building under two eccentricity cases, $e / r = 0$ and $e / r = 0.3$ (*r* = radius of gyration of the floor plan) and three different uncoupled torsion/translation stiffness ratios, $k_\theta / k_x = 4$ (white arrow), $k_\theta / k_x = 1$ (gray arrow), and $k_\theta / k_x = 0.25$ (black arrow). It is seen that when $k_\theta / k_x = 4$, which means that the torsional stiffness is large, only one MTMD for the first structural mode is needed. The optimal location is basically near the C.M. of the floor when $e / r < 0.3$. It is reasonable because the first mode is dominated by floor translation. When $k_\theta / k_x = 0.25$, which means the building motion is dominated by floor torsion, only one MTMD for the first mode is needed. The corresponding optimal location, $(d_{s_0})_{\mathrm{opt}} = 1.45r$, is near the positive edge of the floor. In this situation, the MTMD is used to control the torsional motion, so MTMD far away from the C.M. can generate larger torque to the floor. When $k_\theta / k_x = 1$, both the first and the second structural modes are important. Two MTMDs respectively located at opposite sides of the floor are required. The optimal locations of both MTMDs are between the C.M. and the floor side.

Figure 9. Optimal location of MTMD for three different uncoupled torsion/translation stiffness ratios: $k_\theta / k_x = 4$, $k_\theta / k_x = 1$, $k_\theta / k_x = 0.25$

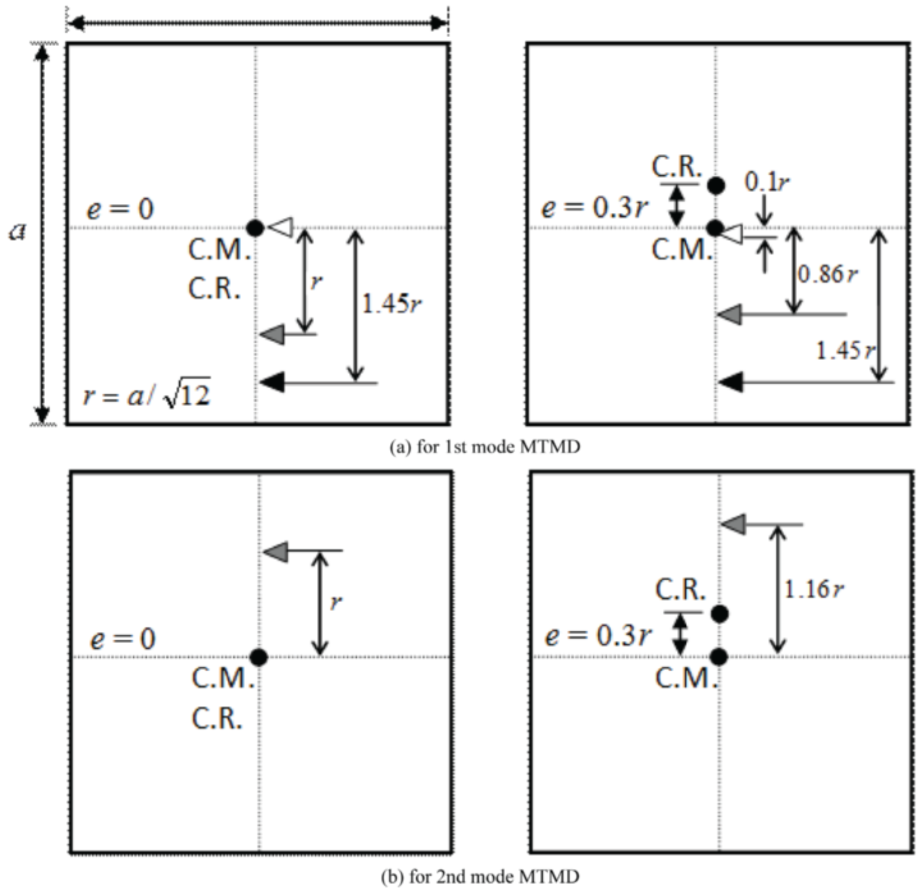

Soil-Structure Interaction (SSI) Effect

As mentioned previously, the building model in Figure 8 has flexible foundation and the base excitations are different from those of fixed-base model. This is called the soil-structure interaction (SSI) effect. It is well recognized that two parameters govern the SSI effect:

$$\sigma = \frac{V_s}{h\omega_x} \text{ and } \lambda_h = \frac{h}{r} \tag{20}$$

where V_s = the shear wave velocity of the soil, h = the height of the building, $\omega_x = \sqrt{k_x / m_p}$. Parameter σ is the relative stiffness of soil to structure, whereas λ_h is the height-to-base ratio of structure. Small σ and large λ_h represent significant SSI effect.

The SSI effect on the MTMD control effectiveness has been evaluated by Lin *et al*. (2005) with the employment of a methodology developed by Wu *et al*. (2001). With and without TMD/MTMD, the mean-square-response ratio of floor translation with respect to free-field ground acceleration, $R_{x_p \ddot{x}_g}$, versus σ ranging from 0.5 to 5.0 for $\lambda_h = 3$ and $\lambda_h = 5$ are shown in Figure 10. The design parameters of TMD and MTMD(7) are presented in Table 3, where '(7)' means the number of MTMD units (p=7) installed.

The dash line and dot line in Figure 10 show that a very small σ can significantly deteriorate the control effectiveness of TMD and MTMD. This is because the soft soil decreases the frequencies and increases the damping of the SSI system causes the detuning effect. So is a large λ_h. In most cases, MTMD(7) has better control effectiveness than TMD except when σ is smaller than about 0.75 and $\lambda_h = 5$. This phenomenon indicates that the sensitivity of MTMD to the variations in system parameters is higher than that of TMD. In order to reduce the detuning problem, enlarging frequency spacing between MTMD units with 100% and the corresponding mean-square response ratio, $R_{x_p\ddot{x}_g}$, is shown in Figure 10 (labeled as MTMD(7)*). It is seen that although MTMD(7)* is less effective than MTMD(7) for large σ, but control effectiveness for small σ is significantly improved. Figure10 also shows that Case 2 MTMD controlling both two structural modes has better performance than Case 1 MTMD in most situations.

The MTMD effectiveness in terms of dynamic responses is demonstrated using the 1995 Kobe earthquake as ground excitation. This ground acceleration with peak value of 0.821g was recorded in the KJM000 component of the Japanese KJMA station during the earthquake. To con-

Figure 10. Mean-square-response ratio of floor displacement with respect to free-field ground acceleration versus σ with and without TMD/MTMD in the cases of $\lambda_h = 3$ and $\lambda_h = 5$

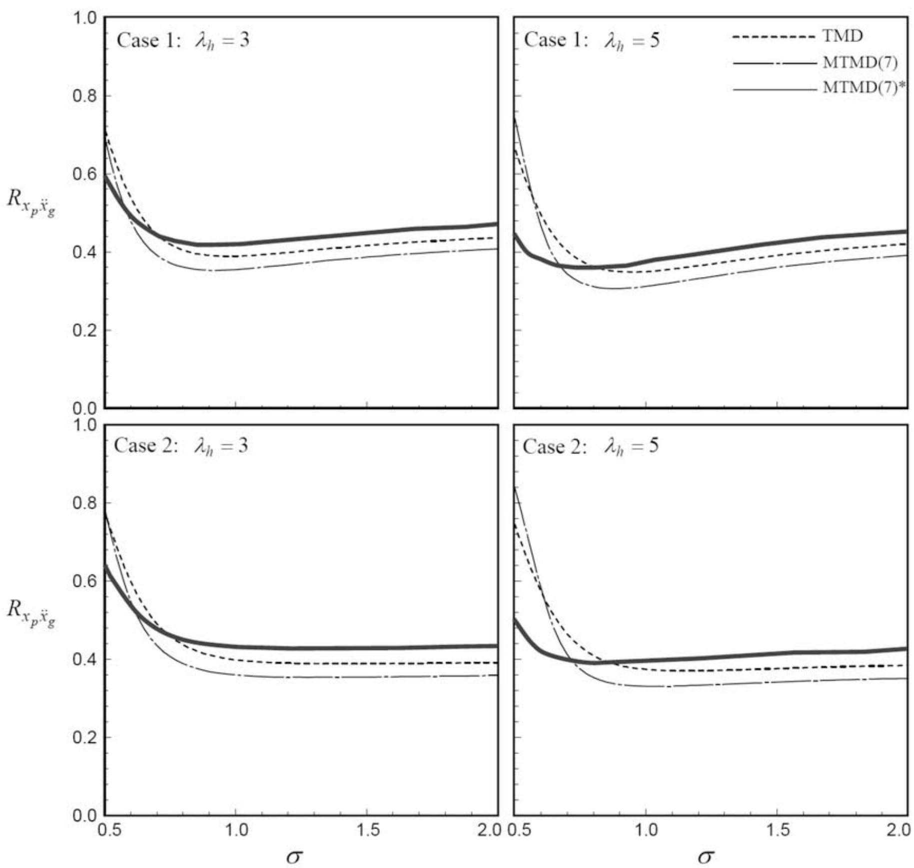

Table 3. Optimal TMD/MTMD(7) parameters for Case 1 and Case 2 irregular building-MTMD systems (structural damping ratio = 2%)

Case	Building Parameters	Controlled mode (Mass ratio)	Number of MTMD units, p	Location ratio, d_{s_k}/r	Damping ratio, ξ_{s_0}	Frequency ratio, r_{f_k}
1	$\lambda_e = 0.3$ $\lambda_\omega = 1.0$	first mode (2%)	1	0.86	9.2%	0.948
			7	0.71, 0.76, 0.81, 0.86, 0.91, 0.96, 1.01	2.5%	0.826, 0.864, 0.901, 0.939, 0.982, 1.032, 1.098
2	$\lambda_e = 0.3$ $\lambda_\omega = 1.0$	first mode (1.59%)	1	0.86	8.2%	0.958
			7	0.71, 0.76, 0.81, 0.86, 0.91, 0.96, 1.01	2.2%	0.846, 0.881, 0.915, 0.950, 0.988, 1.033, 1.091
		second mode (0.41%)	1	-1.16	4.9%	1.324
			7	-1.206, -1.191, -1.176, -1.161, -1.146, -1.131, -1.116	1.2%	1.230, 1.266, 1.297, 1.328, 1.359, 1.393, 1.435

sider SSI parameters, $h\omega_x \approx 60\pi$ and $\lambda_h = 2T_u$ where $T_u (= 2\pi / \omega_x)$ is the fundamental period in second suggested by Sikaroudi and Chandler (1992) were used. In addition, the value $\sigma = 1.5$ corresponding to soft soil ($V_s \cong 280$ m/s) was used to represent the site conditions of the Kobe earthquake. The value $\sigma = \infty$ representing the fixed-base condition was also investigated for comparison. Figure 11 presents the peak floor translational acceleration of the irregular building versus T_u under the Kobe earthquake. Comparing the curves with and without the SSI effect, it is found that the building response would generally be overestimated if the SSI effect is ignored. These figures also show that the TMD and MTMD control effectiveness is strongly dependent upon the frequency content of the earthquake. Moreover, the SSI effect decreases the TMD and MTMD effectiveness since the detuning effect occurs. If the SSI effect is not considered, the vibration control effectiveness will be overestimated. The time history accelerations illustrated in Figure 12 are the dynamic responses of floor translation for the building of $T_u = 0.4$ sec in Case 1 (or Case 2) without and with MTMD(7) considering SSI effect. It is clearly shown that not only the peak amplitude but the entire trace of the acceleration responses are significantly reduced due to the installation of MTMD, in particular for the Case 2 MTMD system in controlling two structural modes.

FUTURE RESEARCH DIRECTIONS

Since a TMD/MTMD is a frequency-sensitive device, the accuracy of dynamic properties of primary structures is a key issue in designing this type of device. Although this could be achieved by employing system identification techniques directly based on the vibration measurements of the structures, using a more precise mathematical model to simulate the controlled system is still worthy for the prediction of the TMD/MTMD vibration control effectiveness. The authors suggest that a more accurate system model, such as an SSI model of multi-story, nonlinear TC building under bi-directional ground motions or vertical ground motion and so on, be developed in the future. Another direction is to develop a different TMD/MTMD mechanism to solve the stroke problem, which may completely change the original behavior of a TMD/MTMD system.

Figure 11. Response spectra of floor translation of building-MTMD systems with and without considering SSI effect under the 1995 Kobe earthquake

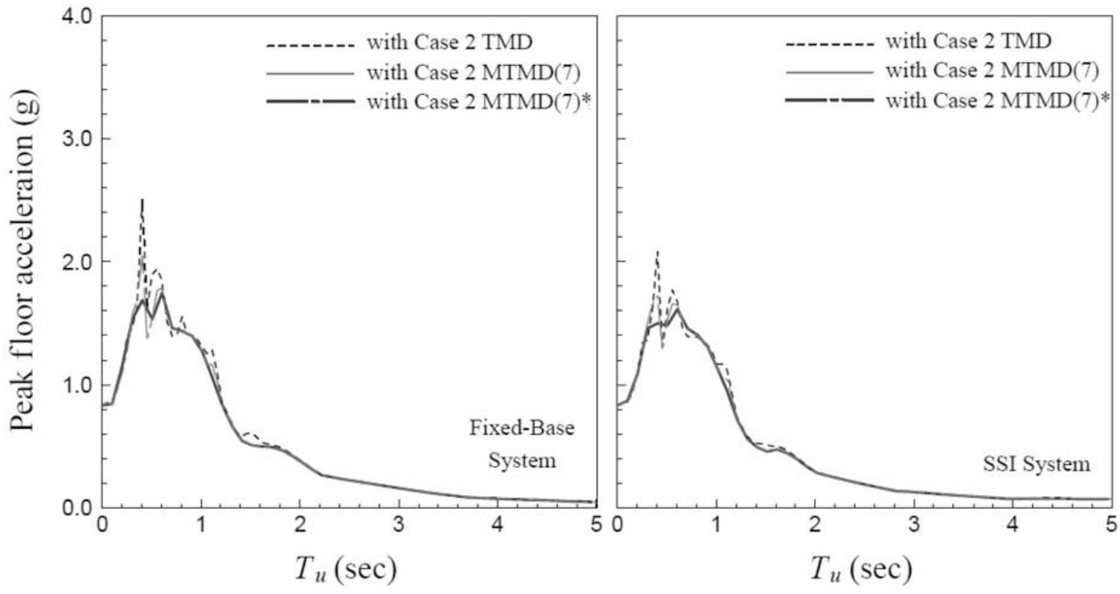

Figure 12. Time history absolute acceleration of floor translation of a TC building without and with MTMDs (case 1 and case 2) considering SSI effect under the 1995 Kobe earthquake

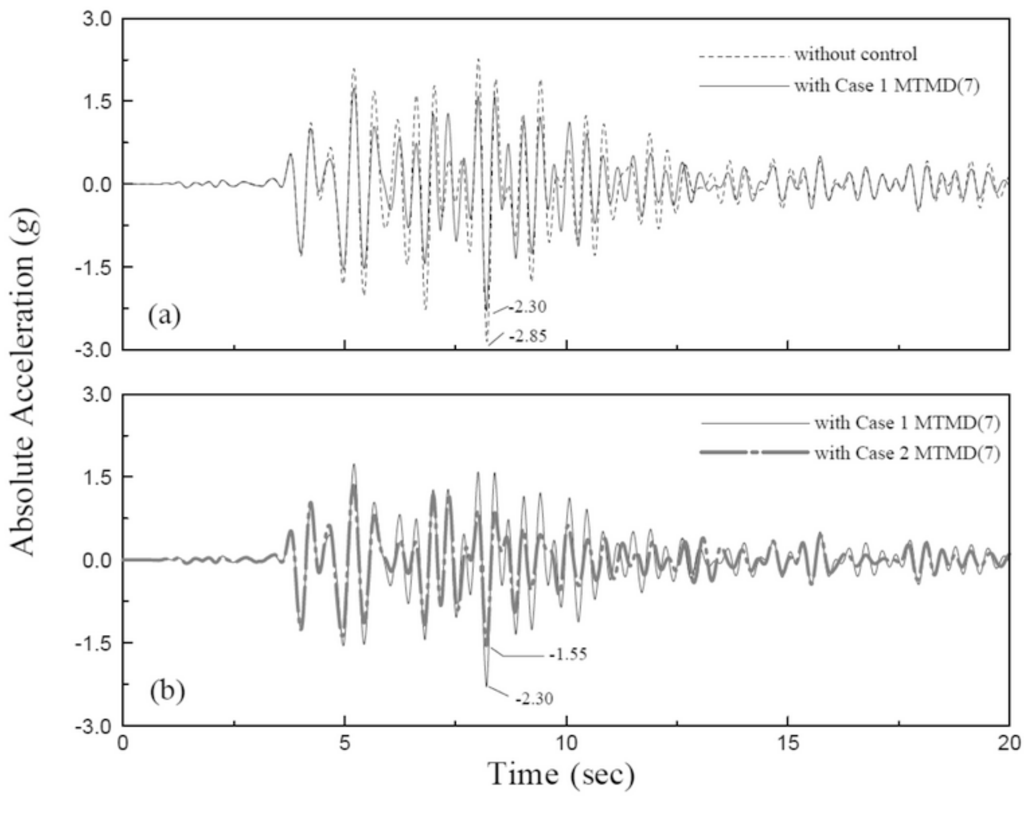

CONCLUSION

TMD has at least one hundred years of history, while its enhanced version, MTMD, has been proposed for nearly twenty years. The large stroke and detuning effect are two major problems for TMD in seismic applications. MTMD is one of the solutions to reduce the detuning problem. For the stroke problem, this chapter provides a new methodology for MTMD system designers to deal with it in design stage. The methodology is primarily to include the stroke related factors into the performance index of MTMD in the optimization procedure. The outcome is a more damped MTMD than that by the conventional design method which the MTMD units usually have small damping demand. It also implies that the new methodology is more favorable for real implementation because the limitation of little contact friction between MTMD and controlled structure is eliminated. Instead, the unavoidable friction could turn into the required damping of MTMD unit and lead to reducing the construction cost of MTMD.

REFERENCES

Abe, M., & Fujino, Y. (1994). Dynamic characterization of multiple tuned mass dampers and some design formulas. *Earthquake Engineering & Structural Dynamics*, *23*, 813–835. doi:10.1002/eqe.4290230802

Abe, M., & Igusa, T. (1995). Tuned mass dampers for structures with closely spaced natural frequencies. *Earthquake Engineering & Structural Dynamics*, *24*, 247–261. doi:10.1002/eqe.4290240209

Chang, M. L., Lin, C. C., Ueng, J. M., Hsieh, K. H., & Wang, J. F. (2010). Experimental study on adjustable tuned mass damper to reduce floor vibration due to machinery. *Structural Control and Health Monitoring*, *17*(5), 532–548.

Den Hartog, J. P. (1956). *Mechanical vibrations* (4th ed.). New York, NY: McGraw-Hill.

Frahm, H. (1911). *Device for damping vibrations of bodies*. U.S. Patent 989-958.

Hoang, N., & Warnitchai, P. (2005). Design of multiple tuned mass dampers by using a numerical optimizer. *Earthquake Engineering & Structural Dynamics*, *34*, 125–144. doi:10.1002/eqe.413

Jangid, R. S. (1995). Dynamic characteristics of structures with multiple tuned mass dampers. *Structural Engineering & Mechanics*, *3*, 497–509.

Juang, J. N. (1997). System realization using information matrix. *Journal of Guidance, Control, and Dynamics*, *21*(3), 492–500. doi:10.2514/2.4068

Kareem, A., & Kline, S. (1995). Performance of multiple mass dampers under random loading. *Journal of Structural Engineering*, *121*, 348–361. doi:10.1061/(ASCE)0733-9445(1995)121:2(348)

Li, C. (2000). Performance of multiple tuned mass dampers for attenuating undesirable oscillations of structures under the ground acceleration. *Earthquake Engineering & Structural Dynamics*, *29*, 1405–1421. doi:10.1002/1096-9845(200009)29:9<1405::AID-EQE976>3.0.CO;2-4

Li, C. (2002). Optimum multiple tuned mass dampers for structures under the ground acceleration based on DDMF and ADMF. *Earthquake Engineering & Structural Dynamics*, *31*, 897–919. doi:10.1002/eqe.128

Li, C., & Liu, Y. (2003). Optimum multiple tuned mass dampers for structures under the ground acceleration based on the uniform distribution of system parameters. *Earthquake Engineering & Structural Dynamics*, *32*, 671–690. doi:10.1002/eqe.239

Li, H., & Ni, X. (2007). Optimization of non-uniformly distributed multiple tuned mass damper. *Journal of Sound and Vibration*, *308*, 80–97. doi:10.1016/j.jsv.2007.07.014

Lin, C. C., Hu, C. M., Wang, J. F., & Hu, R. Y. (1994). Vibration control effectiveness of passive tuned mass dampers. *Journal of the Chinese Institute of Engineers*, *17*, 367–376. doi:10.1080/02533839.1994.9677600

Lin, C. C., Ueng, J. M., & Huang, T. C. (1999). Seismic response reduction of irregular buildings using passive tuned mass dampers. *Engineering Structures*, *22*(5), 513–524. doi:10.1016/S0141-0296(98)00054-6

Lin, C. C., Wang, C. E., Wu, H. W., & Wang, J. F. (2005). On-line building damage assessment based on earthquake records. *Smart Materials and Structures*, *14*, S137–S153. doi:10.1088/0964-1726/14/3/017

Lin, C. C., Wang, J. F., & Chen, B. L. (2005). Train-induced vibration control of high-speed railway bridges equipped with multiple tuned mass dampers. *Journal of Bridge Engineering*, *10*(4), 398–414. doi:10.1061/(ASCE)1084-0702(2005)10:4(398)

Lin, C. C., Wang, J. F., Lien, C. H., Chiang, H. W., & Lin, C. S. (2010). Optimum design and experimental study of multiple tuned mass dampers with limited stroke. *Earthquake Engineering & Structural Dynamics*, *39*, 1631–1651. doi:10.1002/eqe.1008

Lin, C. C., Wang, J. F., & Ueng, J. M. (2001). Vibration control identification of seismically excited m.d.o.f structure-PTMD systems. *Journal of Sound and Vibration*, *240*(1), 87–115. doi:10.1006/jsvi.2000.3188

Morgenstern, J. (199, May 295). City perils: The fifty-nine-story crisis. *The New Yorker*, 45-53. Retrieved from http://www.duke.edu/~hpgavin/ce131/citicorp1.htm

Sikaroudi, H., & Chandler, A. M. (1992). Structure-foundation interaction in the earthquake response of torsionally asymmetric buildings. *Soil Dynamics and Earthquake Engineering*, *11*(1), 1–16. doi:10.1016/0267-7261(92)90022-6

Ueng, J. M., Lin, C. C., & Wang, J. F. (2008). Practical design issues of tuned mass dampers for torsionally-coupled buildings under earthquake loadings. *Structural Design of Tall and Special Buildings*, *17*(3), 133–165. doi:10.1002/tal.336

Wang, J. F., & Lin, C. C. (2005). Seismic performance of multiple tuned mass dampers for soil-irregular building interaction systems. *International Journal of Solids and Structures*, *42*(20), 5536–5554. doi:10.1016/j.ijsolstr.2005.02.042

Wang, J. F., Lin, C. C., & Chen, B. L. (2003). Vibration suppression for high speed railway bridges using tuned mass dampers. *International Journal of Solids and Structures*, *40*(2), 465–491. doi:10.1016/S0020-7683(02)00589-9

Wang, J. F., Lin, C. C., & Lian, C. H. (2009). Two-stage optimum design of tuned mass dampers with consideration of stroke. *Structural Control and Health Monitoring*, *16*, 55–72. doi:10.1002/stc.312

Wu, W.-H., Wang, J. F., & Lin, C. C. (2001). Systematic assessment of irregular building-soil interaction using efficient modal analysis. *Earthquake Engineering & Structural Dynamics*, *30*, 573–594. doi:10.1002/eqe.25

Xu, K., & Igusa, T. (1992). Dynamic characteristics of multiple substructures with closely spaced frequencies. *Earthquake Engineering & Structural Dynamics*, *21*(12), 1059–1070. doi:10.1002/eqe.4290211203

Yamaguchi, H., & Harnpornchai, N. (1993). Fundamental characteristics of multiple tuned mass dampers for suppressing harmonically forced oscillations. *Earthquake Engineering & Structural Dynamics*, *22*, 51–62. doi:10.1002/eqe.4290220105

Zuo, L., & Nayfeh, S. A. (2005). Optimization of the individual stiffness and damping parameters in multiple-tuned-mass-damper system. *Journal of Vibration and Acoustics*, *127*(1), 77–83. doi:10.1115/1.1855929

ADDITIONAL READING

Chen, G., & Wu, J. (2001). Optimal placement of multiple tuned mass dampers for seismic structures. *Journal of Structural Engineering*, *127*(9), 1054–1062. doi:10.1061/(ASCE)0733-9445(2001)127:9(1054)

Chen, G., & Wu, J. (2003). Experimental study on multiple tuned mass dampers to reduce seismic responses of a three-storey building structure. *Earthquake Engineering & Structural Dynamics*, *32*, 793–810. doi:10.1002/eqe.249

Du, D., Gu, X., Chu, D., & Hua, H. (2007). Performance and parametric study of infinite-multiple TMDs for structures under ground acceleration by H∞ optimization. *Journal of Sound and Vibration*, *305*, 843–853. doi:10.1016/j.jsv.2007.05.003

Hoang, N., Fujino, Y., & Warnitchai, P. (2008). Optimal tuned mass damper for seismic applications and practical design formulas. *Engineering Structures*, *30*, 707–715. doi:10.1016/j.engstruct.2007.05.007

Hwang, J. S., Kim, H., & Kim, J. (2006). Estimation of the modal mass of a structure with a tuned-mass damper using H-infinity optimal model reduction. *Engineering Structures*, *28*, 34–42. doi:10.1016/j.engstruct.2005.06.022

Korenev, B. G., & Reznikov, L. M. (1993). *Dynamic vibration absorbers: Theory and technical applications* (1st ed.). England: John Wiley & Sons Ltd.

Krenk, S. (2005). Frequency analysis of the tunes mass damper. *Journal of Applied Mechanics*, *72*, 936–942. doi:10.1115/1.2062867

Lee, C. L., Chen, Y. T., Chung, L. L., & Wang, Y. P. (2006). Optimal design theories and applications of tuned mass dampers. *Engineering Structures*, *28*, 43–53. doi:10.1016/j.engstruct.2005.06.023

Li, C. (2006). Performance of dual-layer multiple tuned mass dampers for structures under ground excitations. *International Journal of Structural Stability and Dynamics*, *6*(4), 541–557. doi:10.1142/S0219455406002106

Li, C., & Zhang, J. (2005). Evaluation of arbitrary integer based multiple tuned mass dampers for structures. *International Journal of Structural Stability and Dynamics*, *5*(3), 475–488. doi:10.1142/S0219455405001659

Li, C., & Zhu, B. (2006). Estimating double tuned mass dampers for structures under ground acceleration using a novel optimum criterion. *Journal of Sound and Vibration*, *298*, 280–297. doi:10.1016/j.jsv.2006.05.018

Park, J., & Reed, D. (2001). Analysis of uniformly and linearly distributed mass dampers under harmonic and earthquake excitation. *Engineering Structures*, *23*, 802–814. doi:10.1016/S0141-0296(00)00095-X

Pinkaew, T., Lukkunaprasit, P., & Chatupote, P. (2003). Seismic effectiveness of tuned mass dampers for damage reduction of structures. *Engineering Structures*, *25*, 39–46. doi:10.1016/S0141-0296(02)00115-3

Rasouli, S. K., & Yahyai, M. (2002). Control of response of structures with passive and active tuned mass dampers. *Structural Design of Tall Buildings*, *11*, 1–14. doi:10.1002/tal.181

Singh, M. P., Singh, S., & Moreschi, L. M. (2002). Tuned mass dampers for response control of torsional buildings. *Earthquake Engineering & Structural Dynamics*, *31*, 749–769. doi:10.1002/eqe.119

Soong, T. T., & Dargush, G. F. (1997). *Passive energy dissipation systems in structural engineering* (1st ed.). England: John Wiley & Sons Ltd.

Takewaki, I. (2009). *Building control with passive dampers: optimal performance-based design for earthquakes*, 1st ed. Singapore: John Wiley & Sons (Asia) Pte. Ltd.

Verdirame, J. M., Nayfeh, S. A., & Zuo, L. (2002). Design of multi-degree-of-freedom tuned-mass dampers. *Proceedings of the Society for Photo-Instrumentation Engineers*, *4697*, 98–108.

Wang, A.-P., & Fung, R.-F. (2001). Dynamic analysis of a tall building with a tune-mass-damper device subjected to earthquake excitations. *Journal of Sound and Vibration*, *244*(1), 123–136. doi:10.1006/jsvi.2000.3480

Wang, A.-P., & Lin, Y. H. (2007). Vibration control of a tall building subjected to earthquake excitation. *Journal of Sound and Vibration*, *299*, 757–773. doi:10.1016/j.jsv.2006.07.016

Wong, K. K. F. (2008). Seismic energy dissipation of inelastic structures with tuned mass dampers. *Journal of Engineering Mechanics*, *134*(2), 163–172. doi:10.1061/(ASCE)0733-9399(2008)134:2(163)

Wong, K. K. F., & Chee, Y. L. (2004). Energy dissipation of tuned mass dampers during earthquake excitations. *Structural Design of Tall and Special Buildings*, *13*, 105–121. doi:10.1002/tal.244

Wong, W. O., & Cheung, Y. L. (2008). Optimal design of a damped dynamic vibration absorber for vibration control of structure excited by ground motion. *Engineering Structures*, *30*, 282–286. doi:10.1016/j.engstruct.2007.03.007

Zuo, L., & Nayfeh, S. A. (2004). Minimax optimization of multi-degree-of-freedom tuned-mass dampers. *Journal of Sound and Vibration*, *272*, 893–908. doi:10.1016/S0022-460X(03)00500-5

Zuo, L., & Nayfeh, S. A. (2006). The two-degree-of-freedom tuned-mass damper for suppression of single-mode vibration under random and harmonic excitation. *Journal of Vibration and Acoustics*, *128*, 56–65. doi:10.1115/1.2128639

KEY TERMS AND DEFINITIONS

Den Hartog: A researcher who first proposes a complete design theory for TMD and is one of the most referred authors in TMD literatures.

Detuning Effect: An effect that induces reduction of control effectiveness of a TMD/MTMD due to mistuning in frequency.

Multiple Tuned Mass Dampers (MTMD): A passive vibration control device which is composed by multiple TMDs arranged in parallel.

Operating Range: Frequency range in which a TMD/MTMD is effective.

Passive Control System: A system of structural control whose characteristic is determined once by an appropriate design method before the device is in place.

Soil-Structure Interaction (SSI) Effect: An effect that describes the interaction between soil and structure motions due to a flexible foundation.

Stroke: Displacement of TMD/MTMD unit relative to the installed place.

Torsionally Coupled (TC) Effect: An effect that describes the coupling of translation and torsion of a building due to the inconsistency of the center of rigidity and the center of mass.

Tuned Mass Damper (TMD): A passive vibration control device which is a single-degree-of-freedom system consisting of mass, damping, and stiffness components.

Chapter 7
Tuned Liquid Column Gas Damper in Structural Control:
The Salient Features of a General Purpose Damping Device and its Application in Buildings, Bridges, and Dams

Markus Hochrainer
University of Applied Sciences, Wiener Neustad,t Austria

Franz Ziegler
Vienna University of Technology, Austria

ABSTRACT

Tuned liquid column damper (TLCD) show excellent energy and vibration absorbing capabilities appropriate for applications in wind- and earthquake engineering. The objective of this chapter is to demonstrate the outstanding features of the proposed Tuned Liquid Column Gas Damper (TLCGD) and present its wide spectrum of applications of three design alternatives. Among others it includes base isolation of structures, applications to lightly damped asymmetric buildings and other vibration prone structures like bridges (even under traffic loads) and large arch-dams as well as simple, ready to use design guidelines for optimal absorber placement and tuning. The evident features of TLCGDs are no moving mechanical parts, cheap and easy implementation into civil engineering structures, simple modification of the natural frequency and even of the damping properties, low maintenance costs, little additional weight in those cases where a water reservoir is required, e.g., for the sake of fire fighting, and a performance comparable to that of TMDs of the spring-mass- (or pendulum-)-dashpot type.

DOI: 10.4018/978-1-4666-2029-2.ch007

INTRODUCTION

The basic idea of most vibration reducing devices is the absorption of vibrational energy, thereby reducing the ductility demand of the main structure and thus preventing it from serious structural damage. A well accepted damping principle is the transfer of energy from critical building vibration modes to dynamic damping devices which are designed to absorb and dissipate energy to protect a structure from excessive dynamic loads. This method of energy dissipation incorporates dynamic absorber like tuned mass damper (TMD), tuned liquid damper (TLD also called sloshing motion damper) or tuned liquid column damper (TLCD). A different concept is to prevent the accumulation of seismic energy by uncoupling the structure-base and the surrounding soil by base isolation elements. This type of earthquake protection is very effective because it reduces the energy dissipation demand of the higher structural vibration modes. If base isolation is combined with other earthquake defending measures a high level of protection can be achieved.

Besides base isolation, probably the most commonly used passive device is the tuned mass damper, which consists of a mass attached to the vibrating structure through a spring and a dashpot. TMD have been applied successfully in symmetric high raised buildings where the motion of a single mass can be used to absorb two bending and a torsional motion. However, it is difficult to guarantee a smooth, frictionless motion for huge masses, and in order to avoid the application of hydrodynamic bearings or friction compensating actuators the mass is often suspended vertically on cables, thereby forming a pendulum type mass damper which is used in high raise buildings, e.g. the Taipei 101 tower. Pendulum type absorbers represent the ideal alternative to TMD of spring-mass-dashpot type when considering symmetric high raised buildings.

For other applications TLD are optimal, e.g. to suppress wind induced vibrations of smokestacks or wind turbines, but they suffer from difficult tuning, variable damping and a comparatively low active mass. Tuned liquid column damper (TLCD) overcome these drawbacks by a controlled and guided liquid motion in a rigid piping system. Originally developed to reduce the rolling motion of ships, they were first proposed for civil engineering structures about 20 years ago. The working principle is to transfer structural vibration energy into a liquid movement and dissipate it by viscous and turbulent damping. Since the restoring forces are due to gravity, the extremely low natural frequencies in real size applications are in the range of about 0.1 - 0.5Hz. Although this excellent low frequency characteristic might be feasible for very large structures, the invention of the modified tuned liquid column gas damper (TLCGD) expands the possible field of applications to structures with critical natural frequencies, say up to 5Hz, see Hochrainer (2001). The classic TLCD is closely related to the TMD of pendulum type: both are only applicable for structures with extremely low natural frequencies (high raised buildings) and the restoring forces are due to gravity only. The main advantages of TLCGD include comparably low installation costs, easy application to new buildings or in retrofitting existing structures, a simple tuning mechanism which allows for adaptation to modified (degraded) building dynamics, no moving mechanical parts, virtually no maintenance requirements and little additional weight in those cases where a water reservoir is required, e.g. for the sake of firefighting.

TLCD have shown to be effective in reducing structural vibrations in recent years and the research work of the last decade has culminated in simple guidelines for optimal placement and tuning of the TLCD. So far, all research results indicate that the TLCD is competitive when compared to TMD (spring-mass-dashpot type) and it could replace the TMD in many structural application. Due to their salient features, TLCD have caused an increased research interest, resulting in both, analytical and experimental analyses.

Real size applications have been reported in a 26 storey, 106 m high hotel in Japan, Teramura et al. (1996), and the tallest building in Vancouver, Canada, the 48 storey One Wall Center, RWDI consultant engineers (2011). The focus of the present work is to introduce the TLCGD as flexible, extremely simple and efficient vibration reducing device with possible applications as dynamic absorber in base excited asymmetric high raised buildings, additional damping device for a novel base isolation system, temporary mobile unit applied to the cantilever method of bridge construction, a permanent vibration reducing device for earthquake, wind or traffic induced coupled bending torsional bridge vibrations as well as earthquake protection for large dams. For bridges with dominating vertical flexural vibrations the novel space saving pipe-in-pipe design of vertical TLCGD (VTLCGD) renders additional efficient damping.

TLCGD DYNAMICS

In this section a universal description of the TLCGD dynamics is given based on the nonstationary Bernoulli's equation applied in a moving frame. Since the TLCGD is considered independently, its application to civil engineering structures is based on substructure synthesis. Consequently the TLCGD equations of motion and the interaction forces have to be determined before coupling absorber and host structure. Many different TLCGD geometries have been proposed, all of them result from a derivation of the original U-shaped device. It consists of one horizontal and two symmetric vertical pipe sections of length B and H with piecewise constant cross sectional areas, A_H and A_B. The V-shaped TLCGD is obtained by inclining the vertical sections by an opening angle β, see Figure 1a.

The most comprehensive description for combined multi-axial translations and rotations can be obtained applying the non-stationary Bernoulli equation generalized for moving reference

Figure 1. a) TLCGD of general shape with a relative streamline from 1-2 at a time instant t, symmetric arrangement with rigid pipe b) Analogy between TMD and TLCGD, the liquid mass m_f is split into an active mass m^* and a dead weight load $\bar{m} = m_f - m^*$

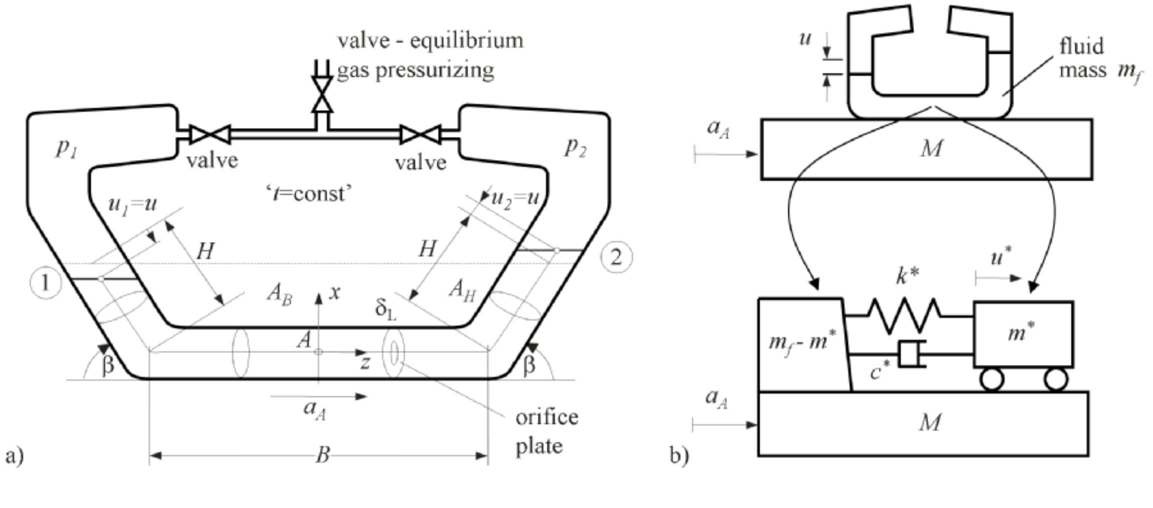

frames, Ziegler (1998), p.497. Assuming that the liquid motion is characterized by the ideal fluid flow along a representative streamline, the standard form of the non-stationary Bernoulli equation has to be extended to account for the relative fluid motion with respect to a moving reference system A, see e.g. Hochrainer (2005). For the symmetric arrangement the liquid stroke is $u = u_1 = u_2$ and the equation of motion is given by

$$L_{eff}\ddot{u} + 2gu\sin\beta = -\frac{1}{\rho}\left(p_2 - p_1\right) - \int_1^2 \mathbf{a}_A \cdot \mathbf{e}'_t \, ds',$$
$$L_{eff} = 2H + B\frac{A_H}{A_B} \tag{1}$$

where g and $\rho = 1000\, kg/m^3$ denote the constant of gravity, and the density, e.g. of water, respectively. The scalar integral expression $\int_1^2 \mathbf{a}_A \cdot \mathbf{e}'_t \, ds'$ accounts for the moving reference frame, with $\mathbf{e}'_t$ and $\mathbf{a}_A$ denoting the relative streamline's tangential direction and the absolute acceleration of the moving reference point A. If the pipe endings are kept open (classical TLCD) the pressure difference $p_2 - p_1$ vanishes approximately, if the pipes are sealed (the novel proposal of the TLCGD) the liquid stroke u will compress and expand the enclosed gas mass thereby building up a gas-spring. Under the assumption that the TLCGD operating range is limited to low frequencies, the inertia of the gas is small, and a quasi-static approach applies to approximate the pressure difference $p_2 - p_1$. With the weakly nonlinear polytropic material law for ideal gases the pressure difference can be sufficiently well approximated in the range $\left|u\right| / H_a \leq 0.3$ by just considering the linearized portion in the series

$$p_2 - p_1 = 2n\, p_0 \frac{u}{H_a} + O\left(\frac{u}{H_a}\right)^3,$$
$$H_a = \frac{V_0}{A_H} \tag{2}$$

where V_0, p_0, n denote the gas volume and the equilibrium gas pressure as well as the polytropic index, respectively. The invention of the gas spring also protects the TLCGD from excessive vibrations because extreme stroke amplitudes cause a nonlinear stiffening effect, thereby limiting the maximum liquid displacement. For extremely slow vibrations the gas spring will operate under isothermal conditions (n=1), at high frequencies an adiabatic change will occur and the polytropic index becomes n=1.4. For all other operating conditions n is in the range of $1 \leq n \leq 1.4$. To prevent the rigid piping from buckling due to low pressure during the gas expansion phase, the equilibrium gas pressure should be chosen above the atmospheric pressure. Since all discussed advantageous effects of the gas spring have been proved experimentally under laboratory conditions by Khalid (2010) it is one of the most promising developments of recent research activities.

To include energy losses by the experimentally observed turbulent fluid flow an averaged nonlinear pressure loss $\delta_L \left|\dot{u}\right| \dot{u}$ is added to the equation of motion. The head loss factor δ_L accounts for the losses in the elbows and the hydraulic roughness of the pipe walls. If necessary, damping can be reduced by a smooth and continuous change in the cross sectional area from A_B to A_H, however at the price of an additional nonlinearity, or increased by the insertion of additional hydraulic orifices into the liquid path. In the design stage and for the sake of tuning this nonlinear damping term is equivalently linearized by substituting viscous damping where the linear viscous damping coefficient $\zeta_A = 4U_{\max}\delta_L / 3\pi$

depends on the amplitude $U_{\max}$ of a time harmonic vibration of the liquid column. This relation is used for any forced vibration. Numerical simulations of a main structure with a TLCGD attached under earthquake load, see e.g. Hochrainer (2001), have shown that the turbulent damping performs even better when compared to the linearized one. For small amplitude excitation the TLCGD is lightly damped and thus promptly starts to oscillate with comparatively large fluid strokes, thereby absorbing energy and keeping the structural vibrations small. When coming to peak vibrations with maximum energy dissipation the turbulent damping prevents the TLCGD from excessive liquid strokes.

If the cross sectional dimensions are small when compared to the liquid column length it is straightforward to define a representative streamline to evaluate Eq.(1), thereby averaging the liquid flow over the cross sectional area, absolute acceleration a_A of the frame is in the horizontal direction of the trace of the TLCGD-midplane,

$$\ddot{u} + 2\zeta_A\omega_A\dot{u} + \omega_A^2 u = -\kappa a_A,\ f_A = \frac{\omega_A}{2\pi} = \sqrt{\frac{g/\pi^2}{4L_0}},$$
$$L_0 = L_{eff}/2\left(\sin\beta + h_0/H_a\right),\ h_0 = np_0/\rho g,$$
$$\kappa = \frac{B + 2H\cos\beta}{L_{eff}} \tag{3}$$

L_{eff} is the equivalent length of the fluid column with constant cross sectional area A_H rendering the same natural circular frequency ω_A. κ is a geometry dependent coupling factor determining the TLCGD excitation. The n-multiplied static pressure head, h_0, when related to the virtual height H_a of the gas volume serves as the most convenient frequency tuning parameter for the TLCGD allowing for its application in an extended range of frequencies when compared to the classical TLCD. Without the passive gas spring TLCD are restricted to frequencies, say below 0.5 Hz in practical applications. Only by the invention of the passive gas spring this serious limitation is bypassed and TLCGD frequencies say up to 5Hz are possible in practical implementations. For proper application of the piston theory, the frequency is actually limited by the (relative) maximum fluid speed, $\dot{u} = \omega_A u$, which must stay below the critical speed of $\dot{u}_{\max} < 12\,\mathrm{m}/\mathrm{s}$ to keep the fluid-gas interface intact, Ziegler (2008). Hence, for a given fluid stroke, the practicable frequency-range in Eq.(3) is limited.

For a subsequent substructure synthesis the horizontal structure-TLCGD interaction force F_A is obtained applying the conservation of momentum of the fluid mass m_f with respect to its center of mass in horizontal direction of the trace,

$$F_A = m_f\left(a_A + \bar{\kappa}\ddot{u}\right),\ m_f = \rho A_H L_1,\ L_1 = 2H + \frac{A_B}{A_H}B,$$
$$\bar{\kappa} = \kappa\frac{L_{eff}}{L_1} \tag{4}$$

where a_A denotes the absolute horizontal acceleration of the TLCGD housing, and $\bar{\kappa}$ is a geometry dependent force factor. Furthermore, there exist undesired moments resulting from the displacement of the fluid center of mass with respect to the reference point A, and a contribution from gravity forces acting at the displaced center of mass. However, it is common practice to neglect the influence of the undesired moments that party also exist for TMD of the spring-mass-dashpot type.

Any vertical floor acceleration, commonly assumed proportional to the horizontal component, $\lambda_x a_g$, $0 < \lambda_x \leq 1.2$, depending on the site condition, adds parametric forcing to Eq.(3). Detailed analytical and experimental investigations, Reiterer et al. (2004), have proven that parametric resonance does not occur if sufficient damping is provided. The cut-off value of the equivalent linearized damping turns out to be dependent on both, the maximum stroke of the fluid motion and the amplitude of the time harmonic vertical vibration of the most critical double frequency parametric resonance,

$$\zeta_A = \frac{4\max|u|}{3\pi}\delta_L > \zeta_{A,0} = \frac{\max|\lambda_x a_g|/g}{4\left(1 + h_0/H_a \sin\beta\right)} \tag{5}$$

The gas spring effect of the TLCGD, h_0/H_a, lowers the required damping even further and any effects of the vertical excitation become negligible if the inequality (5) holds.

TLCGD-TMD ANALOGY

By inspection of the absorber control force and the equations of motion it is possible to establish a convenient analogy that proves the equivalence of TLCGD and TMD with respect to vibration reduction, Hochrainer (2001). Considering only horizontal frame acceleration a_A, the TLCGD equation of motion is given by Eq.(3), with the corresponding interaction force F_A of Eq.(4). Setting virtually $\kappa = \bar{\kappa} = 1$, these expressions turn out to be identical to those of a TMD of the spring-mass-dashpot type. Since the TLCGD must have inclined pipe sections, this condition is not possible from a physical point of view. However, when considering the liquid displacement scaled by $u^* = u/\kappa$ the plane TLCGD motion can be described by

$$\ddot{u}^* + 2\zeta_A\omega_A\dot{u}^* + \omega_A^2 u^* = -a_A \tag{6}$$

with the corresponding horizontal interaction force changed to

$$F_A = \bar{m}\,a_A + m^*\left(a_A + \ddot{u}^*\right),\ m^* = \kappa\bar{\kappa}\,m_f,\quad \bar{m} = m_f - m^* \tag{7}$$

Eq. (6) corresponds to that of an equivalent TMD whose displacement is characterized by u^* and the reaction force F_A splits into two parts: The first term corresponds to the reaction force of a dead weight load of mass $\bar{m}$ attached to the supporting host structure. The second term, $m^*(a_A + \ddot{u}^*)$, represents the reaction force of a corresponding TMD of mass m^* and displacement u^*. Consequently, there is a simple TMD-TLCGD analogy, see Figure 1b: The total liquid mass m_f is split into the equivalent TMD mass, the “active mass” m^*, and the dead weight mass $\bar{m}$.

From the analogy it follows that the geometry factor $\kappa\bar{\kappa}$ should be as large as possible to assure that most liquid mass is used for vibration absorption. Although not obvious from the analogy, the liquid part acting as dead weight load is mainly moving vertically, thereby providing the gravitational restoring force. Demanding $\kappa\bar{\kappa} = 1$ would lead to a degenerated TLCGD with no inclined pipe sections. However, the ratio B/H should be maximized combined with an opening angle $\beta \geq 30°$ to minimize the dead fluid mass. Having selected a suitable TLCGD geometry and the fluid mass, the analogy can be used to obtain optimal frequency and damping parameter from the large number of design and optimization criteria that have been originally developed for TMD.

If the TLCGD is attached to a generalized SDOF main structure with mass M and natural frequency Ω, the mass of the host structure is increased by the dead fluid mass $\bar{m}$. Given the mass ratio $\mu = m_f/M$, the properties of the equivalent TMD-main system, become slightly altered,

$$M^* = M\left(1+\mu\left(1-\kappa\bar{\kappa}\right)\right),\ \Omega^* = \frac{\Omega}{\sqrt{1+\mu\left(1-\kappa\bar{\kappa}\right)}},$$
$$\mu^* = \frac{m_f \kappa\bar{\kappa}}{M^*} = \mu\frac{\kappa\bar{\kappa}}{1+\mu\left(1-\kappa\bar{\kappa}\right)} < \mu \tag{8}$$

All properties of the equivalent TMD system are denoted by a star *. Optimal tuning for a two DOF system is classically done by applying the Den Hartog criterion (Hartog 1956),

$$\delta^* = \frac{\omega^*_{A,opt}}{\Omega^*} = \frac{1}{1+\mu^*},\ \zeta^*_{opt} = \sqrt{\frac{3\mu^*}{8\left(1+\mu^*\right)}} \tag{9}$$

that minimizes the dynamic magnification factor of absolute floor acceleration in case of time harmonic base excitation. The same parameters apply for minimizing the displacement magnification factor under the condition of time harmonic forcing, Warburton (1981). Since the TLCGD is fully described by the equivalent TMD system their natural frequencies and damping ratios are identical, $\omega_{A,opt} = \omega^*_{A,opt}$, $\zeta_{opt} = \zeta^*_{opt}$ and can be calculated evaluating Eq.(9), with Eq.(8) substituted,

$$\delta_{opt} = \frac{\omega_{A,opt}}{\Omega} = \frac{\sqrt{1+\mu\left(1-\kappa\bar{\kappa}\right)}}{1+\mu},\ \zeta_{opt} = \sqrt{\frac{3\kappa\bar{\kappa}\mu}{8\left(1+\mu\right)}} \tag{10}$$

APPLICATION TO MULTIPLE STOREY ASYMMETRIC BUILDINGS

The damping of excessive vibrations of asymmetric plan multiple purpose buildings is a common task in civil engineering. Even discomfort of people living in lightly damped tall buildings is observed under wind excitation. Since the direct application of viscous or frictional damping devices to increase the structural damping suffers from small storey drifts, TLCGD should be preferred. Assuming that each floor can be represented by a rigid diaphragm with three degrees of freedom (e.g. by applying static condensation of a finite element discretization), its motion is given by the horizontal displacements of its center of mass *w* and *v* together with a rotation θ about the vertical axis. For the subsequent section the choice of the coordinate system is in accordance with literature: the vertical axis is denoted *x*, the horizontal axes are *y* and *z*, respectively. Recent research on the application of TLCGD on multiple purpose buildings has revealed that it is favorable to distinguish between moderate and strong asymmetry. In terms of modal floor displacements strong asymmetry is observed if the modal center of velocity lies within the floor plan but distinct from the center of mass, $C_M = \left[y_{C_M}, z_{C_M}, 0\right]$. In this case the rotation of the floor dominates and, e.g., is excited by the horizontal ground acceleration of an earthquake. In a perfect symmetric structure modal center of stiffness, $C_K = \left[y_{C_K}, z_{C_K}, 0\right]$, and center of mass coincide and the rotational mode is seismically not forced. If the modal center of velocity lies outside the geometrically regular floor plan, translation dominates and the building is considered moderately asymmetric. Given the modal floor displacement with respect to the center of mass by the (modal) displacement vector, mode number *j* understood, $\boldsymbol{\phi} = \left[\phi_y, \phi_z, \phi_{u_T}\right]$ the coordinates of the modal center of velocity $C_V = \left[y_{C_V}, z_{C_V}, 0\right]$ for small rotations become, see Figure 2a,

$$y_{C_V} = y_{C_M} - \frac{\phi_z r_S}{\phi_{u_T}},\ z_{C_V} = z_{C_M} + \frac{\phi_y r_S}{\phi_{u_T}},\ \phi_{u_T} \neq 0 \tag{11}$$

$u_T = r_S\theta$, where r_S denotes the radius of inertia with respect to the mass of the properly selected floor (the top floor is always eligible). For moderate asymmetry the plane TLCGD is preferred, for strong asymmetry the redesigned torsional TLCGD, TTLCGD, is recommended. Since the multiple purpose building considered is asymmetric, its center of mass and the center of stiffness do not coincide. An arbitrary distribution of floor mass and stiffness furthermore causes the mass and stiffness centers not to be aligned vertically along the *x*-axis.

In the following section moderate asymmetry is assumed, thus the popular plane U- or V-shaped TLCGD is perfectly suited as the proper absorber. If the position of the TLCGD is given with respect to its reference point $A = \left[y_A, z_A, 0\right]$ and its angular orientation by the angle γ with respect to the *y*-axis, rotation of the floor about the vertical *x*-axis is denoted θ, see Figure 2b, proper generalization of Eq. (1) renders

$$\ddot{u} + 2\zeta_A\omega_A\dot{u} + \omega_A^2\left(1 - \kappa_1\frac{\dot{\theta}^2}{\omega_A^2}\right)u = -\kappa\mathbf{a}_A\cdot\mathbf{e}'_A, \;\; \kappa_1 = \kappa\cos\beta \tag{12}$$

Figure 2. a) Top floor of a moderately asymmetric building: Position of the velocity-center C_V is outside of the floor plan. Rotation exaggerated. b) TLCGD in horizontal general motion. Unit vector $\mathbf{e}'_A$ in direction of its trace. Instant position of the fluid mass center C_f marked. c) Torsional TLCGD (TTLCGD) in plan view. The pipe encloses the modal center of velocity C_V. (Adapted from Fu et al. (2010)).

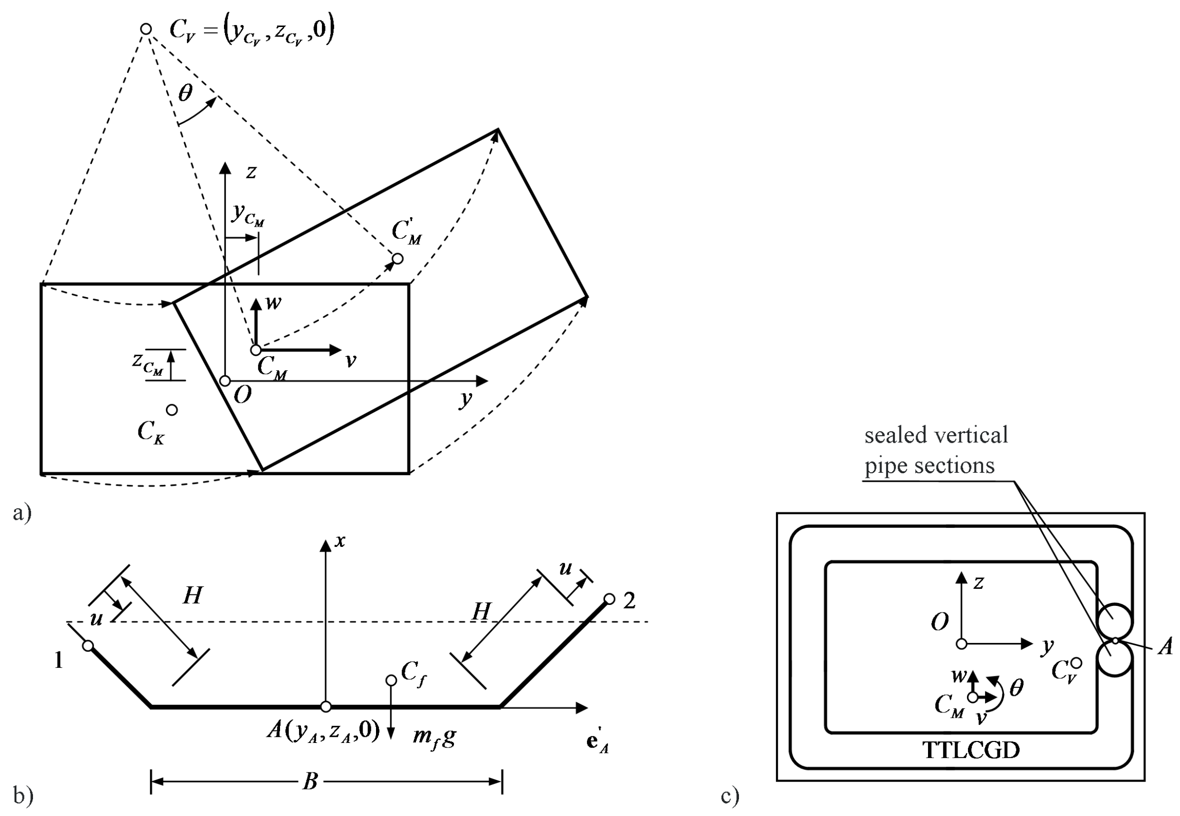

The excitation of the TLGGD is due to projection of the floor absolute acceleration $\mathbf{a}_A$ in the trace of the TLCGD-mid-plane, unit vector $\mathbf{e}'_A$, as in Eq.(1).

Given the relative floor acceleration of the floor's center of mass C_M with respect to ground, $\mathbf{a}_{C_M} = \left[\ddot{v}_M,\ \ddot{w}_M,\ \ddot{u}_T\right]$, and a single point uniaxial obliquely incident seismic ground excitation $\ddot{v}_g = a_g \cos\alpha$, $\ddot{w}_g = a_g \sin\alpha$, further assuming that the TLCGD is installed with its trace in a general direction γ with respect to the y-axis, evaluation of Eq.(12) yields, for details see Fu et al. (2010) or Fu (2008),

$$\begin{aligned}\ddot{u} + 2\zeta_A\omega_A\dot{u} + \omega_A^2 u = -\kappa\{ & a_g\cos(\alpha-\gamma) \\ & +[\ddot{v}_M - (z_A - z_{C_M})\frac{\ddot{u}_T}{r_S}]\cos\gamma \\ & +[\ddot{w}_M + (y_A - y_{C_M})\frac{\ddot{u}_T}{r_S}]\sin\gamma\}\end{aligned} \tag{13}$$

For sake of substructure synthesis the generalized interaction forces are calculated applying the conservation of momentum and angular momentum of the fluid mass m_f, with respect to its center of mass, C_f. Neglecting all undesired nonlinear parts and assuming small floor rotations $\theta \ll 1$ the linearized interaction forces become

$$\begin{aligned}F_{Ay} &= m_f\left[a_g\cos\alpha + \ddot{v}_M - \left(z_A - z_{C_M}\right)\ddot{u}_T/r_S\right] \\ &\quad + \bar{\kappa} m_f \ddot{u}\cos\gamma \\ F_{Az} &= m_f\left[a_g\sin\alpha + \ddot{w}_M + \left(y_A - y_{C_M}\right)\ddot{u}_T/r_S\right] \\ &\quad + \bar{\kappa} m_f \ddot{u}\sin\gamma\end{aligned} \tag{14}$$

$\bar{\kappa}$ is defined in Eq.(4). The resulting moment about the vertical axis becomes, transformation from point C_f to the center of floor mass C_M is understood,

$$\begin{aligned}M_{C_M x} &= m_f\bar{\kappa}_T H^2\ddot{u}_T/r_S - F_{Ay}\left(z_A - z_{C_M}\right) \\ &\quad + F_{Az}\left(y_A - y_{C_M}\right)\end{aligned} \tag{15}$$

In case of strong asymmetry the application of a more efficient torsional TLCGD (TTLCGD) is recommended. A schematic view of the TTLCGD is given in Figure 2c. Its horizontal ring shaped pipe system forms an almost closed loop enclosing the modal center of velocity, ending with two, sealed vertical pipe sections close to each other at the optimally selected reference point A.

Based on the properly adapted generalized Bernoulli equation, Eq.(1), the linearized equation of motion of the relative fluid flow in the TTLCGD results,

$$\begin{aligned}&\ddot{u} + 2\zeta_A\omega_A\dot{u} + \omega_A^2 u = -\kappa_{T0}\ddot{u}_{TT}, \\ &\kappa_{T0} = \frac{2A_p}{r_f L_{eff}},\ \ddot{u}_{TT} = r_f\ddot{\theta},\ I_{fx} = m_f r_f^2\end{aligned} \tag{16}$$

where A_p denotes the area enclosed by the TTLCGD-loop projected onto the floor plane. The control and interaction moment with respect to the floor's center of mass C_M becomes, see Fu et al. (2010),

$$\begin{aligned}&M_{C_M x} = m_f r_f\left(\ddot{u}_{TT} + \frac{\bar{\kappa}_{T3} y_A}{r_f}a_{Az} - \frac{\bar{\kappa}_{T3} z_A}{r_f}a_{Ay}\right) + m_f r_f\bar{\kappa}_{T0}\ddot{u}, \\ &F_{C_M y} = m_f\left(a_g\cos\alpha + \ddot{v}_M - \bar{\kappa}_{T3}\ddot{u}_{TT}\frac{z_A}{r_f}\right), \\ &F_{C_M z} = m_f\left(a_g\sin\alpha + \ddot{w}_M + \bar{\kappa}_{T3}\ddot{u}_{TT}\frac{y_A}{r_f}\right), \\ &\bar{\kappa}_{T0} = \kappa_{T0}\frac{L_{eff}}{L_1},\ \bar{\kappa}_{T3} = 2H/L_1\end{aligned} \tag{17}$$

It can be concluded that the TTLCGD should be installed on the floor with largest modal rotation to get the most effective energy absorption: from inspection of the excitation term on the right hand side of Eq.(16) large angular floor accelerations maximise the forced liquid motion and consequently the energy absorption and thus the effective damping. Similarly, for plane TLCGD, a large component of the floor acceleration $\mathbf{a}_A$ parallel to the horizontal pipe section will induce strong TLCGD liquid movements and consequently the desired high energy absorption. It has been shown that the TLCGD should be installed at the maximum normal distance from the floor's center of velocity allowed by the floor's plan.

MODAL TRANSFORMATION OF BUILDING VIBRATIONS

Considering a discretized asymmetric building properly condensed to account for rigid floor motions, the undamped dynamic equations, in matrix form become

$$\mathbf{M}\ddot{\mathbf{x}} + \mathbf{K}\mathbf{x} = -\mathbf{M}\mathbf{E}_N\ddot{\mathbf{x}}_g + \mathbf{F} + \mathbf{F}_A,$$
$$\mathbf{E}_N = \begin{bmatrix} 1 & 0 & 0 & 1 & 0 & 0 & 1 & \cdots \\ 0 & 1 & 0 & 0 & 1 & 0 & 0 & \cdots \\ 0 & 0 & 0 & 0 & 0 & 0 & 0 & \cdots \end{bmatrix}^T \tag{18}$$

where $\mathbf{x} = \left[y_1,\ z_1,\ u_{T1}, y_2,\ z_2,\ u_{T2},\dots, u_{TN}\right]^T$ denotes the vector of floor displacements, with $u_{Ti} = \theta_i r_{Si}$. r_{Si} is the radius of inertia with respect to the floors center of mass, storey number *i*, **M** and **K** are the mass and stiffness matrix, respectively, $\mathbf{F} = \left[F_{y1}, F_{z1}, M_{1x}/r_{S1}, F_{y2},\dots, M_{Nx}/r_{SN}\right]^T$ and $\mathbf{F}_A$ are the wind (inwind or lateral) and TLCGD-structure interaction (control) force, respectively, and $\ddot{\mathbf{x}}_g = \left[\ddot{v}_g, \ddot{w}_g, 0\right]^T$ is the vector of horizontal ground acceleration. $\mathbf{E}_N$ is the influence matrix of the ground excitation for the N-storey asymmetric structure. Modal expansion of Eq.(18) using the mass normalized (ortho-normalized) modal transformation matrix $\left[\boldsymbol{\phi}_1, \boldsymbol{\phi}_2, \dots, \boldsymbol{\phi}_N\right]$ renders the modal equations of motion with light modal structural damping $2\zeta_{Sj}\omega_{Sj}$ added, thus decoupled on their left hand side,

$$\ddot{q}_j + 2\zeta_{Sj}\omega_{Sj}\dot{q}_j + \omega_{Sj}^2 q_j = -\boldsymbol{\phi}_j^T\mathbf{M}\mathbf{E}_N\ddot{\mathbf{x}}_g + \boldsymbol{\phi}_j^T\mathbf{F} + \boldsymbol{\phi}_j^T\mathbf{F}_A \tag{19}$$

However, the right hand side decouples only approximately with respect to in- wind or lateral wind forces and with respect to the control forces of the absorbers as well. The floor displacements (and rotations) in Cartesian coordinates can subsequently be determined by modal superposition, $\mathbf{x} = \sum_{j=1}^{N} \boldsymbol{\phi}_j q_j$.

OPTIMIZATION BY MODAL TUNING BY MEANS OF THE TLCGD-TMD ANALOGY

During the design stage, optimization in a first step is proposed applying the TLCGD-TMD analogy.

Assuming that the geometrical constraints are known from the building construction and dimension the maximum physical size of the absorber can be determined in terms of pipe section lengths and cross sectional areas. For given design earthquakes the TLCGD is optimized in an iterative process using the TLCGD-TMD analogy. This renders the maximum absolute liquid displacement $|U_{\max}|$ needed to determine the virtual height $H_a \geq 3|U_{\max}|$. However, even if this inequality cannot be met for excessive liquid strokes, the TLCGD will not be damaged since the nonlinear air spring effect renders increased restoring forces and the smooth liquid flow breaks down temporarily when the water column enters the slightly inclined horizontal pipe sections of the air spring.

If modal vibrations are approximately isolated for the displacements of a selected mode *j* at floor number i, $v_{i,j} = \phi_{j,(3i-2)} q_j$, $w_{i,j} = \phi_{j,(3i-1)} q_j$, $u_{Ti,j} = \phi_{j,3i} q_j$ and inserted into the control forces, Eq.(14), and into the absorber equation, Eq.(13), the structure-TLCGD interaction is determined with respect to the selected modal generalized coordinate q_j. Considering base excitation only, the dynamic structural behavior can be approximated by the isolated two degree of freedom system in combination with Eq.(19), Fu et al. (2010)

$$\begin{bmatrix} 1+\mu_j & \bar{\kappa}_j V_{\gamma i,j} \dfrac{m_{fj}}{m_j} \\ \kappa_j V_{\gamma i,j} & 1 \end{bmatrix} \begin{bmatrix} \ddot{q}_j \\ \ddot{u}_j \end{bmatrix} + \begin{bmatrix} 2\zeta_{Sj}\omega_{Sj} & 0 \\ 0 & 2\zeta_{Aj}\omega_{Aj} \end{bmatrix} \begin{bmatrix} \dot{q}_j \\ \dot{u}_j \end{bmatrix} + \begin{bmatrix} \omega_{Sj}^2 & 0 \\ 0 & \omega_{Aj}^2 \end{bmatrix} \begin{bmatrix} q_j \\ u_j \end{bmatrix} = - \begin{bmatrix} \dfrac{L_{jy}\cos\alpha + L_{jz}\sin\alpha}{m_j} \\ \kappa_j \cos\left(\alpha - \gamma_j\right) \end{bmatrix} a_g, \tag{20}$$

$$V_{\gamma i,j} = v_{Ai,j}\cos\gamma_j + w_{Ai,j}\sin\gamma_j$$

$$v_{Ai,j} = \phi_{j,(3i-2)} - \phi_{j,3i}\left(z_{Ai,j} - z_{C_M i}\right)\Big/ r_{Si}$$

$$w_{Ai,j} = \phi_{j,(3i-1)} + \phi_{j,3i}\left(y_{Ai,j} - y_{C_M i}\right)\Big/ r_{Si}$$

$$\mu_j = V_{i,j}^2 m_{fj} \Big/ m_j$$

$$V_{i,j}^2 = v_{Ai,j}^2 + w_{Ai,j}^2 + \bar{\kappa}_3 \left(\frac{H\phi_{j,3i}}{r_{Si}}\right)^2$$

$$L_{jy} = \sum_{n=1}^{N} m_{Sn}\phi_{j,(3n-2)} + m_{fj} v_{Ai,j}$$

$$L_{jz} = \sum_{n=1}^{N} m_{Sn}\phi_{j,(3n-1)} + m_{fj} w_{Ai,j} \tag{21}$$

where μ_j, ζ_{Sj}, ζ_{Aj}, ω_{Sj} and ω_{Aj} are the generalized mass ratio, the light modal structural damping, the TLCGD damping, the circular natural frequency of the original structure and the circular natural frequency of the TLCGD, respectively. m_{Si}, m_j and L_j denote the mass of floor *i*, the modal mass and the modified participation factor, respectively. $v_{Ai,j}$ and $w_{Ai,j}$ denote the modal displacements of the reference point *A* in *y*- and *z*-direction, respectively. Again the dead fluid mass $\bar{m} = m_f\left(1-\kappa\bar{\kappa}\right)$ reduces the frequency of the main structure. The dead weight of the rigid TLCGD pipe is neglected at this stage of the tuning process. It is accounted for during the fine tuning in state space. According to the TLCGD-TMD analogy the equivalent TMD system is obtained setting $\kappa = \bar{\kappa} = 1$. If the properties of the equivalent TMD system are again denoted by a star *, Eqs.(20) and (21) render

$$\begin{bmatrix} 1+\mu_j^* & V_{\gamma i,j} \dfrac{m_{Aj}^*}{m_j^*} \\ V_{\gamma i,j} & 1 \end{bmatrix} \begin{bmatrix} \ddot{q}_j \\ \ddot{u}_j^* \end{bmatrix} + \begin{bmatrix} 2\zeta_{Sj}^*\omega_{Sj}^* & 0 \\ 0 & 2\zeta_{Aj}^*\omega_{Aj}^* \end{bmatrix} \begin{bmatrix} \dot{q}_j \\ \dot{u}_j^* \end{bmatrix} + \begin{bmatrix} \omega_{Sj}^{*2} & 0 \\ 0 & \omega_{Aj}^{*2} \end{bmatrix} \begin{bmatrix} q_j \\ u_j^* \end{bmatrix} = - \begin{bmatrix} \dfrac{L_{jy}^*\cos\alpha + L_{jz}^*\sin\alpha}{m_j^*} \\ \cos\left(\alpha - \gamma_j\right) \end{bmatrix} a_g \tag{22}$$

$$\mu_j^* = V_{i,j}^{*2} m_{Aj} \Big/ m_j^*$$

$$V_{i,j}^{*2} = v_{Ai,j}^2 + w_{Ai,j}^2$$

$$L_{jy}^* = \sum_{n=1}^{N} m_{Sn}^*\phi_{j,(3n-2)} + m_{Aj}^* v_{Ai,j}$$

$$L_{jz}^* = \sum_{n=1}^{N} m_{Sn}^*\phi_{j,(3n-1)} + m_{Aj}^* w_{Ai,j} \tag{23}$$

Considering equal seismic excitation and comparing the dynamic equations, Eqs.(20) and

(22), there is again a complete TLCGD-TMD-analogy if $u^* = u/\kappa$. The equivalent mass ratio and the TLCGD frequency ratio can be identified as

$$\mu_j^* = \mu_j \frac{\kappa\bar{\kappa}\left(V_{i,j}^*/V_{i,j}\right)^2}{1+\mu_j\left[1-\kappa\bar{\kappa}\left(V_{i,j}^*/V_{i,j}\right)^2\right]} < \mu_j,$$
$$\delta_{jopt} = \frac{\omega_{Aj,opt}}{\omega_{Sj}} \frac{\delta_{jopt}^*}{\sqrt{1+\mu_j\left(1-\kappa\bar{\kappa}\left(V_{i,j}^*/V_{i,j}\right)^2\right)}} \tag{24}$$

Together with $\zeta_{Aj}^* = \zeta_{Aj}$, $\omega_{Aj}^* = \omega_{Aj}$ the optimal tuning values are again given by (9),

$$\delta_{jopt} = \frac{\sqrt{1+\mu_j\left(1-\kappa\bar{\kappa}\left(V_{i,j}^*/V_{i,j}\right)^2\right)}}{1+\mu_j},$$
$$\zeta_{jopt} = \sqrt{\frac{3\mu_j\kappa\bar{\kappa}\left(V_{i,j}^*/V_{i,j}\right)^2}{8\left(1+\mu_j\right)}} \tag{25}$$

The optimal tuning values are recommended initial values for a subsequent fine-tuning in state space which also takes the influence of the neighbouring modes into account. From the definition of the generalized equivalent mass ratio μ_j^*, the damping coefficient ζ_{Sj}^* and the angular frequency ω_{Sj}^* of the equivalent TMD system it is apparent that the TLCGD geometry (factor $\bar{\kappa}\kappa$), the TLCGD position and direction (factor $V_{\gamma i,j}^2/V_{i,j}^2$) as well as the earthquake angle of incidence α influence more or less the optimal tuning values.

OPTIMIZATION AND FINE-TUNING OF TLCGD IN STATE SPACE

After a preliminary modal TLCGD design, fine-tuning in state space is recommended as it allows optimizing any dynamic system independent of the number of degrees of freedom. Therefore it is possible to split the TLCGD into smaller units in case of a too large cross-sectional area to keep the flow one-dimensional, to account for the influence of neighboring vibration modes during the optimization and to select the performance criteria as a linear combination of the system states. Combining the structure's equation of motion (18), however modally expanded (possibly using some appropriate modal truncation) with the dynamic absorber Eq. (13) via the modally expanded linearized interaction forces (17) for all installed TLCGD renders a coupled system in state space formulation. With the state hyper vector $\mathbf{z} = \left[\mathbf{q}^T \quad \mathbf{u}^T \quad \dot{\mathbf{q}}^T \quad \dot{\mathbf{u}}^T\right]^T$ with generalized modal coordinates collected in $\mathbf{q}$ and the liquid strokes, collected in $\mathbf{u}$, the entire system dynamics can be given by the lightly coupled system of first order differential equations,

$$\dot{\mathbf{z}} = \mathbf{A}_r\mathbf{z} + \mathbf{E}_g\ddot{\mathbf{x}}_g \tag{26}$$

where $\mathbf{A}_r$ denotes the system matrix containing all system information, e.g. natural frequencies and light damping of the host structure, mass and stiffness distribution but also the TLCGD design parameter (of all smaller units) to be optimized during fine-tuning. $\mathbf{E}_g$ is the base excitation influence matrix and $\ddot{\mathbf{x}}_g$ the oblique uniaxial ground excitation. Assuming $\ddot{\mathbf{x}}_g$ to be time harmonic with amplitude a_0 and forcing frequency ω,

$$\ddot{\mathbf{x}}_g = a_0 \mathbf{e}_S e^{i\omega t}, \ \mathbf{e}_S = \begin{bmatrix} \cos\alpha \\ \sin\alpha \\ 0 \end{bmatrix} \tag{27}$$

the complex steady state solution depends on the angle of incidence α of the earthquake and on the excitation frequency, $\mathbf{z}(\omega,\alpha) = (i\omega\mathbf{I} - \mathbf{A}_r)^{-1} \mathbf{E}_g \mathbf{e}_S a_0$. The optimal tuning parameter are found by minimizing the response for given α over the entire forcing frequency range. Introducing the positive definite weighing matrix $\mathbf{S}$ a suitable quadratic performance index, expressed by the system state vector $\mathbf{z}_S = \begin{bmatrix} \mathbf{q}^T & \dot{\mathbf{q}}^T \end{bmatrix}^T$ can be given by

$$\begin{aligned} J &= \int_{-\infty}^{\infty} \mathbf{z}_S^T(\omega) \mathbf{S} \mathbf{z}_S(\omega) d\omega \\ &= 2\pi \left[\mathbf{E}_g \mathbf{e}_S a_0\right]^T \mathbf{P}\, \mathbf{E}_g \mathbf{e}_S a_0 \rightarrow \min \end{aligned} \tag{28}$$

The positive definite weighing matrix is chosen to optimize the structural response with respect to certain system states, e.g. floor displacements. The covariance matrix $\mathbf{P}$ is defined as the solution of the Ljapunov matrix equation, see e.g. Müller et al. (1976),

$$\mathbf{A}_r^T \mathbf{P} + \mathbf{P} \mathbf{A}_r = -\mathbf{S} \tag{29}$$

Although derived for harmonic excitation the state space optimization can also be interpreted in terms of stochastic quantities. Assuming the ground excitation to be a stationary random white noise process, the structural vibration response can be characterized by a random process with zero mean, and a covariance matrix given by $\mathbf{P}$, see again Müller et al. (1976). The covariance matrix is an important response measure, since the standard deviation of the states is given by diagonal elements. This property of the covariance matrix can be applied directly for a stochastic optimization by minimizing a properly weighed sum of its diagonal elements. The minimization of the scalar function J is generally performed numerically as unconstrained quadratic optimization with initial tuning parameters obtained by Den Hartog's formula. The parameter optimization of Eq.(28) may also include structural uncertainty by generalizing the performance criterion. If e.g. the extreme variations in the mass and stiffness distribution (due to structural deterioration) are considered in addition to the ideal structure by adding the associated performance indices $J_{A_{r\min}}$ and $J_{A_{r\max}}$

$$J = J_{A_r} + J_{A_{r\min}} + J_{A_{r\max}} \tag{30}$$

where J_{A_r} refers to the performance index of the ideal main system. The minimum of Eq.(30) renders a robust optimization accounting for all uncertainties considered in the extended performance criterion, Hochrainer et al. (2006). All structural modifications and uncertainties are hidden in the performance indices $J_{A_{r\min}}$ and $J_{A_{r\max}}$ as they include the influence of the corresponding system matrices $A_{r\min}$ and $A_{r\max}$. If required the summation in Eq.(30) can be extended to additional performance indices and even weighing factors to account for further structural uncertainties in the optimization process.

APPLICATION TO ASYMMETRIC THIRTY STOREY BUILDING

To demonstrate the effectiveness of the proposed damping system, a thirty-storey moderately asymmetric building with rectangular cross section is analysed under seismic excitation. The building data were obtained by Huo et al. (2001), the dynamic analysis and optimization is described in detail in Fu et al. (2010). The building mass is homogenously distributed over the storeys with a floor mass of $m = 384 \times 10^3$ kg and a moment of inertia of $I_x = 5.96 \times 10^6 \mathrm{kg} \cdot \mathrm{m}^2$. The anisotropic shear stiffness in y and z direction are $k_y = 8.64 \times 10^5 \mathrm{kN/m}$ and $k_z = 7.80 \times 10^5 \mathrm{kN/m}$, and the torsional stiffness is $k_t = 1.38 \times 10^8 \mathrm{kNm/rad}$. The center of stiffness is eccentrically located at $C_K = (e_y, e_z, 0)$ with $e_y = 4\mathrm{m}$, $e_z = 3\mathrm{m}$. With three dynamic degrees of freedom for each floor assigned the model is described by 90 DOF. A model reduction is performed by applying a modal truncation to include the first twelve modes, with an assigned constant modal damping coefficient of 1% and the natural (undamped) frequencies are 0.348, 0.384, 1.042, 1.151, 1.343, 1.734, 1.915, 2.421, 2.673, 3.102, 3.425 and 3.774Hz, respectively. The modal analysis of the structure revealed that three relevant centers of velocity are outside the floor plan, therefore three plane TLCGD are installed in the building. The maximum modal displacements for these modes occur in the 30th floor (top floor) and the 10th floor, respectively, indicating the best positions for the TLCGD. The alignments of the absorber is parallel to the building floor plan with maximum distance from the floor's modal center of velocity, see Figure 3a. With a selected fluid mass of $m_{f1} = 270 \times 10^3 \mathrm{kg}$ $m_{f2} = 250 \times 10^3 \mathrm{kg}$ and $m_{f3} = 50 \times 10^3 \mathrm{kg}$, $\beta = \pi/4$ and $\kappa = \bar{\kappa} = 0.85$, the absorber in a first step were tuned using Den Hartog's formula, Eq.(25). For the selected structural modes the effective modal damping coefficients are increased from 1% to 7.08%, 6.47% and 3.77% respectively. The optimal absorber frequencies, damping ratios and appropriate gas pressure heads (with gas volume and effective fluid column length kept properly assigned as in the first Den Hartog tuning) are given by $f_{A1} = 0.33\mathrm{Hz}$, $f_{A2} = 0.37\mathrm{Hz}$, $f_{A3} = 1.03\mathrm{Hz}$, $\zeta_{A1} = 12.09\%$, $\zeta_{A2} = 10.93\%$, $\zeta_{A3} = 4.62\%$, $h_{0A1} = 35.47\mathrm{m}$, $h_{0A2} = 39.14\mathrm{m}$ $h_{0A3} = 30.00\mathrm{m}$. With an effective length of $L_{eff1} = 20.8\mathrm{m}$, $L_{eff2} = 20.0\mathrm{m}$ and $L_{eff3} = 5\mathrm{m}$, respectively, the constant cross -sectional area of $A_1 = 12.98\mathrm{m}^2$, $A_2 = 12.50\mathrm{m}^2$, $A_3 = 10.00\mathrm{m}^2$ are too large for practical applications. Therefore TLCGD1 and TLCGD2 are split into 6, and TLCGD3 is split into 4 smaller units keeping the effective fluid column lengths unchanged, thus rendering altogether 16 TLCGD. The final optimization is done by numerical fine-tuning in the frequency domain in state space, Eq.(28), the weighed sum of the generalized coordinates is given in Figure 3b in the relevant frequency window. The function *fminsearch* of the Matlab optimization toolbox renders the optimal parameters quite fast when starting the search with the Den Hartog parameters.

APPLICATION TO BASE ISOLATION SYSTEM

Base isolation has become an increasingly applied technique in structural design to protect civil engineering structures with natural frequencies, say above about 1Hz against earthquakes. Base isolation techniques are used to decouple the structure from ground motions using a mechanical low pass filter. The decoupling is achieved by inserting a layer of low horizontal and high vertical stiffness between structure and foundation. Isolated this way, a structure has a mode of vibration, commonly referred to as base isolation mode, with a natural frequency much lower than the fixed base structure and certainly lower than the predominant frequencies of the expected ground motion. The most common laminated isolation elements consist of alternating layers of steel and rubber which need additional damping usually provided by lead core plugs, hydraulic or mechanical dampers. This type of isolation system has a limited lifetime since the lead core or rubber may melt due to overheating during the earthquake or the aftershocks. Therefore a

Figure 3. a) Modal displacements of first three modes of vibration with modal centers of velocity b) Weighed sum of amplitude response functions (generalized coordinates) of the thirty storey, moderately asymmetric building with linearized TLCGD attached, $\alpha = 0$*. (Adapted from Fu et al. (2010)).*

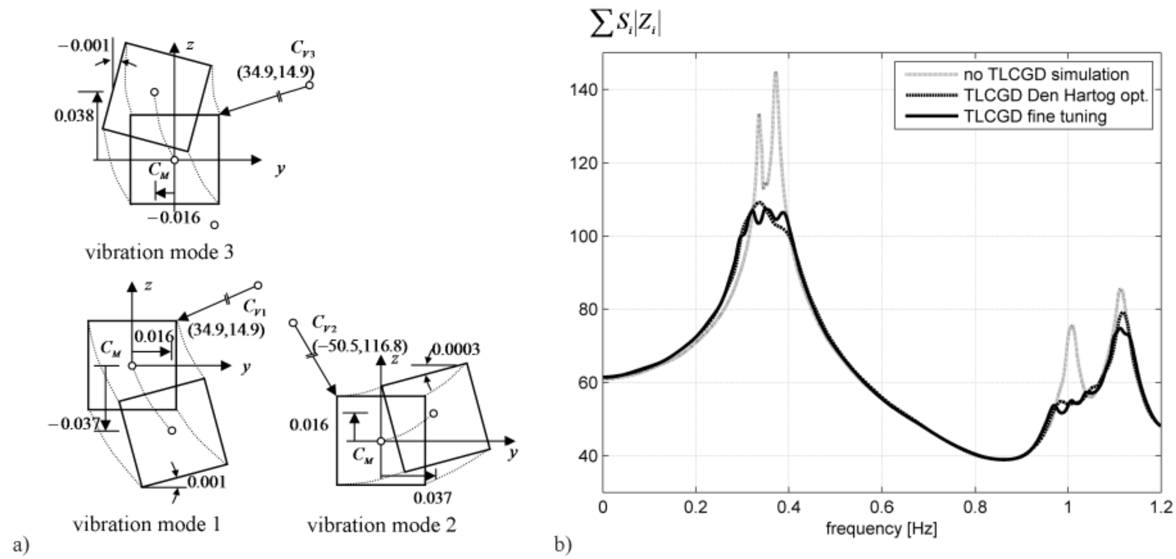

new type of base isolation element provides high vertical and low lateral stiffness and virtually no damping. Bachman (2010) developed a base isolation system separated into two parts: the classical reinforced rubber element together with separately arranged sliding elements operating in dry friction. In order to resist (minor) wind gusts and small seismic disturbances (e.g. also of traffic origin) without base isolation motion, these elements must supply sufficient static friction. During an earthquake or strong wind incident the entire vibration energy is permanently dissipated by the sliding elements in dry friction which are thus suffering from wear. Khalid et al. (2010) avoided such abrasive processes and adapted the concept of a functionally separated modular base isolation system by providing the required energy dissipation for excessive horizontal vibrations of the isolation modes by TLCGD installed in the basement. Experimental verification is given in Khalid et al. (2009) and the new isolation system is partly presented in Ziegler et al. (2011). It consists of three main elements, developed in full detail in Kahlid (2010): the novel pendulum spring base isolation element, an innovative sliding element to resist minor dynamic loads and a TLCGD to dissipate vibrational energy during the strong motion phase of an earthquake.

The novel pendulum-spring base isolation element consists of a pivoted upright-pendulum encapsulated by a coil steel spring acting in shear, see Figure 4a for the element designed for a typical residential house (more building details are presented in the following numerical study). The maximum vertical stiffness is about 13-times the horizontal stiffness allowing for a base isolated natural frequency of about 0.5 Hz, thereby forming a suitable low pass filter. Only some fraction of the vertical dead weight load of the building is supported by the steel springs, the remaining part is carried by the (stainless) steel columns of length l with spherical ends pivoted between spherical bearing cups. A horizontal displacement of the pendulum $\delta_h = l \sin \varphi$ with a tilt angle limited to about $|\varphi| \leq 15°$, causes a

Figure 4. a) Pendulum-spring base isolation: pivoted upright-pendulum encapsulated by a steel coil spring acting in shear. b) Scaled sketch of novel sliding element without continuous energy dissipation. Three levers in contact with the upper sliding plate by roller bearings. Note the bolt connection to the lower sliding plate moving axially in a slit of the lever. c) Plan view of base isolated building with alternative arrangements of three TLCGD. Eight novel sliding elements are indicated by circle. (Adapted from Khalid (2010)).

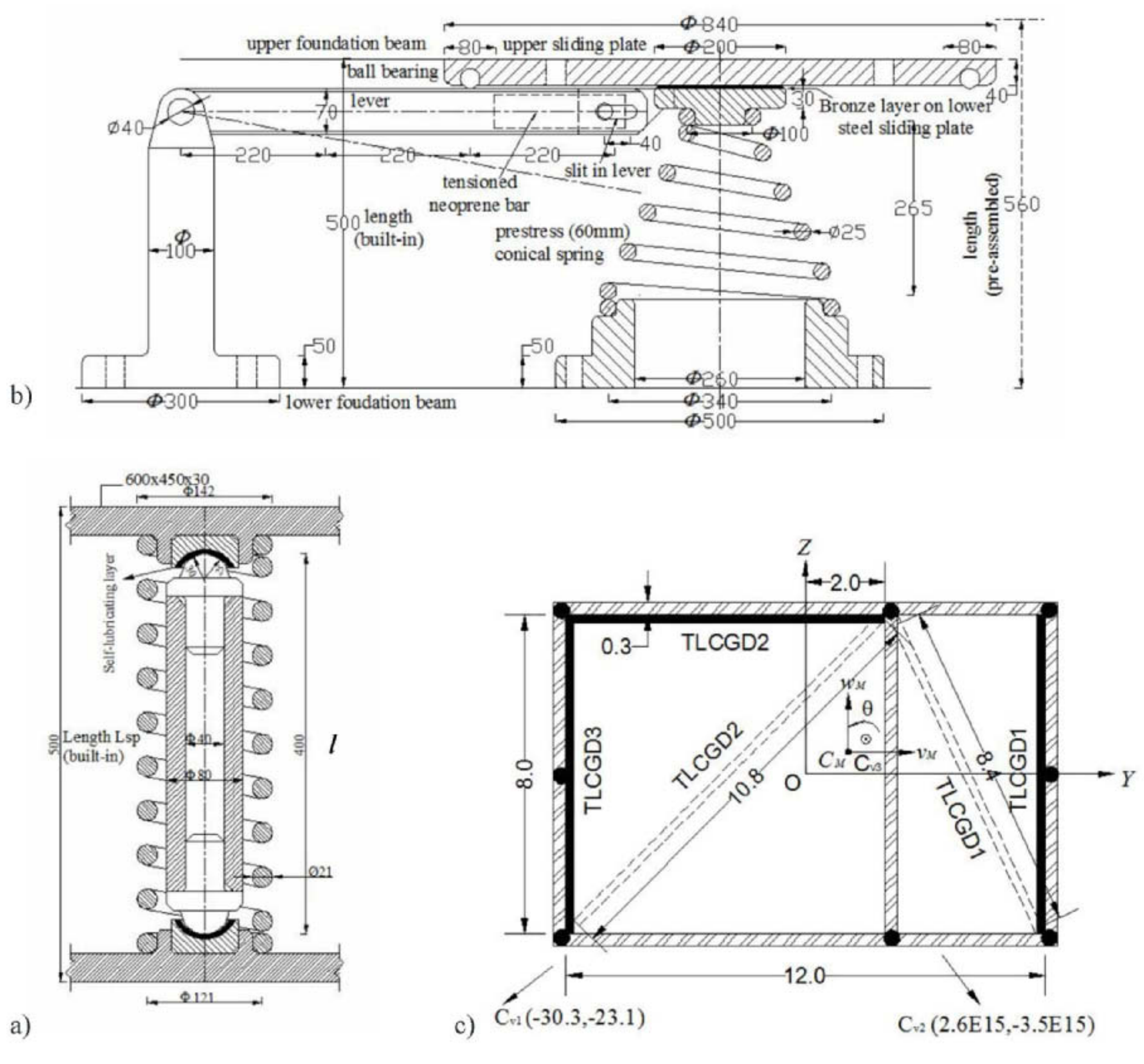

small vertical deflection $\delta_v = l(1-\cos\varphi)$ of the bearing and thus of the building. The base isolation element can be arranged in compact units; e.g. a four spring pendulum unit with a mass of about 50 kg, which can be manipulated and exchanged easily.

To avoid abrasive dry friction, a novel sliding element has been developed by Khalid (2010) that consists of a bronze-steel interface of two contacting circular plates to provide the static friction. The adjustable pressure of the contacting plates is provided by an axially pre-stressed conical steel spring. Above the static friction limit the relative horizontal motion will cause a small vertical deflection of the basement, thereby separating the friction elements via a magnifying lever mechanism and thus avoiding continuous contact and the abrasive sliding in dry friction. Figure 4b shows the design applied in the base isolation.

The effectiveness of TLCGD in providing efficient damping of the three base isolated rigid body modes is demonstrated by the numerical analysis of a simple single-storey asymmetric building, see again Khalid (2010). It has a rectangular plan rigid base of $A = a \cdot b = 12 \cdot 8\text{m}^2$ and a total mass of $m = 244 \times 10^3 kg$. Due to asymmetric walls and distributed load the center of mass is defined by $C_M = \left[y_{C_M}, z_{C_M}, 0\right]$, $y_{C_M} = 1.07\text{m}$, $z_{C_M} = 0.56\text{m}$ with respect to the origin $O(y,z)$, see Figure 4c. To decouple foundation and basement 60 spring pendulum units (240 spring pendulum elements) are distributed over the floor plan as well as eight novel sliding elements. The horizontal stiffness of the spring pendulum units was determined by demanding that the natural frequencies of the first three modes of vibration (base isolation modes) of the isolated building are around 0.5 Hz. A modal analysis of the system modeled as three DOF rigid body renders a set of three ortho-normalised modal vectors with natural frequencies of $f_1 = 0.49\text{Hz}$, $f_2 = 0.50\text{Hz}$, and $f_3 = 0.82\text{Hz}$. Assuming small modal displacements, the modal centers of velocity, determined from Eq. (11), are given by, Khalid (2010),

$$C_{V1} = \begin{bmatrix}-30.3\\-23.1\end{bmatrix} m,\quad C_{V2} = 10^{15}\begin{bmatrix}2.6\\-3.5\end{bmatrix} m,\quad C_{V3} = \begin{bmatrix}1.5\\0.9\end{bmatrix} m \tag{31}$$

The first rigid body mode is dominated by a translation, the second is a pure translational mode, both refer to moderate asymmetry of the building. The center of modal velocity of the third mode, lies within the floor plan, but distinct from C_M and is dominated by a rotational seismically forced motion thus referring to strong asymmetry of the building for this mode. The placement of the absorber would be optimal with a maximum normal distance from the modes of vibration, see dashed TLCGD in Figure 4c. However, to avoid a diagonal installation in the building, the less effective three TLCGD might be aligned parallel to the outer perimeter.

For efficient design the geometric dimensions of the TLCGD are selected to utilize the maximum available lengths in the plan of the base isolated building. The vertical liquid column length H is selected to fulfill the limiting conditions of a maximum stroke of $|u_{\max}| = 2H/3$ and $|u_{\max}| = H_a/3$ for the design earthquake load given by the El Centro 1940 seismogram scaled to 0.32 g. It is checked that the maximum liquid speed remains well below the limit of $|\dot{u}_{\max}| \le 12\text{m/s}$, Ziegler (2008), for three TLCGD with a fluid mass of $m_{f1} = 5000\text{kg}$, $m_{f2} = 4200\text{kg}$ and $m_{f3} = 1000\text{kg}$, Khalid (2010). The extremely low structural damping of such a base isolated building is less than 1%, even with linearized frictional damping of the novel sliding elements during their short time contact of the sliding plates taken into account. The main parameter of the three TLCGD (diagonally orientated TLCGD1 and TLCGD2, z-parallel TLCGD3) obtained by Den Hartog's optimal tuning formulas and their transformations result for the effective lengths of the fluid columns $L_{eff1} = 11.7\mathrm{m}$, $L_{eff2} = 14.3\mathrm{m}$, $L_{eff3} = 9.0\mathrm{m}$, and the modal mass ratios $\mu_1 = 2.25\%$, $\mu_2 = 1.72\%$, $\mu_3 = 0.6\%$: optimal absorber frequencies $f_{A1} = 0.486\mathrm{Hz}$, $f_{A2} = 0.493\mathrm{Hz}$, $f_{A3} = 0.814\mathrm{Hz}$, and optimal linear damping coefficients $\zeta_{A1} = 6.51\%$, $\zeta_{A2} = 6.02\%$, $\zeta_{A3} = 3.97\%$. Because of the extremely low frequencies of the base isolated building, the gas compression might be close to isothermal conditions. A subsequent state space optimization quickly renders the optimal natural frequencies slightly lowered and the optimal linearized damping coefficients reduced. The increase in effective damping of the base isolated building with TLCGD installed is illustrated in Figure 5. The weighed sum of the building response, again modal generalized coordinates are used in $\sum S_i \left|z_{Si}\right|$, is reduced tremendously at the resonant peaks for a critical angle of earthquake incidence, $\alpha = 125°$.

APPLICATION TO LONG SPAN BRIDGES AND FOR THE CANTILEVER METHOD OF BRIDGE CONSTRUCTION

Long span bridges with low structural damping generally perform coupled, oblique bending and torsional vibrations. Depending on the source of excitation, e.g. traffic flow, trains moving sinusoidally on the rails, critical gusty winds or even pedestrians, and seismic forcing, the bridge vibrations can increase up to critical levels. Especially

Figure 5. Weighed sum of amplitude response function (expressed in generalized modal coordinates) for the base isolated building with and without TLCGD installed

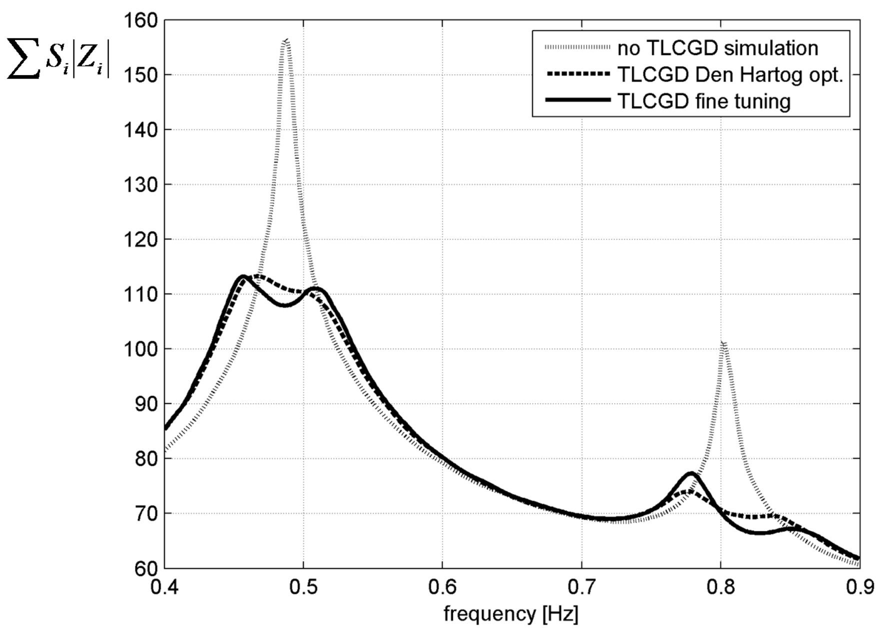

strong wind excitation, a well known problem, e.g. limiting the cantilever method of bridge construction, can be reduced substantially by the application of TLCGD. If lateral horizontal and torsional vibrations dominate, the U- or V-shaped plane TLCGD is perfectly suited to increase the effective damping of the bridge. Tall supporting columns of bridges in seismic zones should be effectively damped by TLCGD mounted on top, analogous to tall buildings as discussed above.

The analytical investigation is based on a modal approximation of the bridge dynamics, selecting a rigid plane cross section with a TLCGD attached. Modal tuning is performed with respect to the dominating horizontal or alternatively rotational motion. Classical Den Hartog tuning is performed before fine tuning the multiple degree of freedom main structure with several TLCGD attached in state space.

Again the TLCGD dynamic equations have to be adapted to the possible lateral deflection of a bridge cross-section, which comprises of the two translational displacements *w* and *v* and the rotation ϑ about the (horizontal) bridge axis (*x*-axis), see Figure 6a. Eq.(1) with absolute accelerations prescribed renders for sufficiently small rotational angles, $|\vartheta| \ll 1$, a linearized equation of motion for the TLCGD stroke *u*, see e.g. Reiterer et al. (2006)

$$\ddot{u} + 2\zeta_A\omega_A\dot{u} + \omega_A^2\left(1 - \kappa_1\frac{\ddot{w}}{H\omega_A^2} + \left(\kappa_1\frac{d_A}{H} - \kappa_2\right)\frac{\dot{\vartheta}^2}{\omega_A^2}\right)u = \kappa\left(\ddot{v} - g\vartheta\right) - \left(\kappa d_A + \kappa_1\frac{B}{2}\right)\ddot{\vartheta}$$

$$\kappa = \frac{B + 2H\cos\beta}{L_{eff}},\quad \kappa_1 = \frac{2H\sin\beta}{L_{eff}},\quad \kappa_2 = \frac{B\cos\beta + 2H}{L_{eff}} \tag{32}$$

with the geometry dependent factors κ_1 and κ_2. The interaction forces are obtained by the basic law of conservation of momentum and generalized conservation of the moment of momentum of the fluid body with respect to the moving reference point A. Introducing the geometry dependent

Figure 6. a) Free body diagram of symmetrically designed TLCGD with moving reference frame (y', z') b) symmetric cross section of the bridge with absorber forces applied, note the distinct centers of mass and stiffness. (Adapted from Reiterer et al. (2006)).

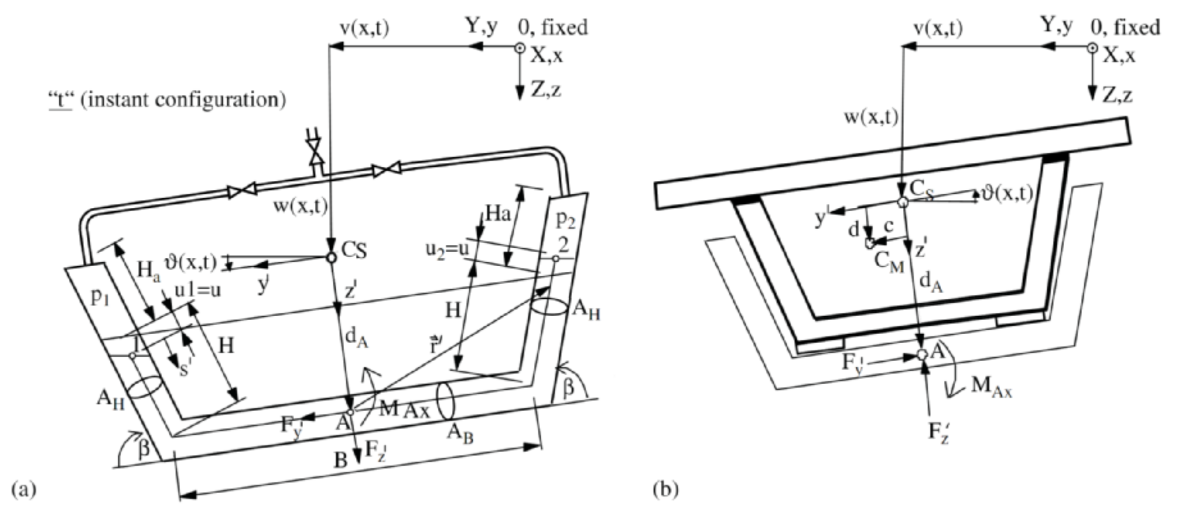

coefficients $\bar{\kappa}_1$, $\bar{\kappa}_2$ and $\bar{\kappa}_3$ renders the interaction forces in the relative coordinates, Reiterer et al. (2006),

$$F_{y'} = m_f \left(a_{y'} - \bar{\kappa}\left(\ddot{u} - u\dot{\vartheta}^2\right) + \frac{\bar{\kappa}_1}{2H}\left(\left(H^2 + u^2\right)\ddot{\vartheta} + 4u\dot{u}\dot{\vartheta}\right)\right)$$

$$F_{z'} = \\ m_f \left(a_{z'} - \bar{\kappa}\left(u\ddot{\vartheta} + 2\dot{u}\dot{\vartheta}\right) + \frac{\bar{\kappa}_1}{2H}\left(\left(H^2 + u^2\right)\dot{\vartheta}^2 - 2\left(\dot{u}^2 + u\ddot{u}\right)\right)\right)$$

$$M_{Ax} = \\ m_f \left(\bar{\kappa}_3 H^2 \ddot{\vartheta} + \frac{\bar{\kappa}_1 B}{2}\ddot{u} - \bar{\kappa} u a_{z'} + \frac{\bar{\kappa}_1}{2H}\left(H^2 + u^2\right)a_{y'} + \bar{\kappa}_2\left(u^2\ddot{\vartheta} + 2u\dot{u}\dot{\vartheta}\right)\right) \\ + M_{AG}$$

$$M_{AG} = m_f g\left(\bar{\kappa} u + \frac{\bar{\kappa}_1}{2H}\left(H^2 + u^2\right)\vartheta\right)$$

$$\bar{\kappa} = \frac{B + 2H\cos\beta}{L_1},\ \bar{\kappa}_1 = \frac{2H\sin\beta}{L_1},\ \bar{\kappa}_2 = \frac{B\cos\beta + 2H}{L_1}$$

$$\bar{\kappa}_3 = \frac{2H}{3L_1}\left(1 + \frac{3B^2}{4H^2} + \frac{3B\cos\beta}{2H} + \frac{A_B}{A_H}\frac{B^3}{8H^3}\right) \tag{33}$$

From Eq.(32) a parametric excitation by vertical flexural accelerations $\ddot{w}$ as well as by angular velocities $\dot{\vartheta}^2$ is apparent. Reiterer (2004) has shown theoretically and by experiments that the parametric excitation of the bridge remains ineffective if the linearized damping coefficient is sufficiently large and thus can be omitted.

To obtain a dynamic model of the bridge, two straightforward approaches are possible. Most accurate and flexible is a numeric approach using the finite element method with subsequent modal analysis. Having calculated the mode shape vector and the natural frequency a modal truncation becomes necessary to reduce the dynamic degrees of freedom substantially. The resulting low order bridge model is coupled with the TLCGD and analyzed as MDOF system. Alternatively, a more analytic approach is to describe the long span bridge of length *l* as a vibrating beam with coupled oblique bending torsional vibrations. The dynamic equation can be solved for a selected isolated mode using the single term Ritz approximations of the deformations,

$$v(x,t) = Y(t)\chi(x),\ \ w(x,t) = Y(t)\phi(x)$$

$$u_T(x,t) = \vartheta(x,t)e = Y(t)\psi(x) \tag{34}$$

Together with the Ritz-Galerkin approximation the coupled dynamic bending torsional differential beam equations can be solved. The linearized equation of motion of a mode number *j* is obtained as a function of the generalized coordinate $Y(t) = q_j\left(t\right)$, light modal structural damping has been added, see Reiterer et al. (2006)

$$\ddot{Y} + 2\zeta\,\Omega\,\dot{Y} + \Omega^2 Y = \\ \frac{1}{M}\left[-F_{y'}\left(\chi + \phi\psi\frac{Y}{e} - \frac{d_A}{e}\psi\right) - F_{z'}\left(\phi - \chi\psi\frac{Y}{e}\right) - \psi\frac{M_{Ax}}{e}\right]_{x=\xi} \\ + \frac{F(t)}{M} \tag{35}$$

where $M = I_e / e^2$ is the effective modal mass and $\Omega = \omega_{Sj}$ the natural circular frequency of the mode considered. $e^2 = c^2 + d^2 + I_0 / A$ denotes the radius of gyration with respect to the center of stiffness, see Figure 6b, and ξ the position of the TLCGD on the span. The effective external load *F(t)* is obtained from the projection of the distributed bridge load p_y, p_z and when including a distributed moment m_x / e onto the Ritz approximations of the modal shape

$$F(t) = \int_0^l \chi(x) p_y(x,t) + \phi(x) p_z(x,t) + \psi(x) m_x(x,t)/e \, dx \tag{36}$$

The linearized interaction forces determined by Eq.(34) together with Eq.(33) render

$$F_{y'} \approx m_f \left[\left(\chi - \frac{d_A}{e} \psi \right) \ddot{Y} - \bar{\kappa} \ddot{u} \right]_{x=\xi}$$

$$F_{z'} = m_f \phi \ddot{Y} \Big|_{x=\xi}$$

$$M_{Ax} \approx m_f \left(\bar{\kappa}_3 \frac{H^2}{e} \psi \ddot{Y} + \frac{\bar{\kappa}_1 B}{2} \ddot{u} + g \bar{\kappa} u \right) \tag{37}$$

Neglecting the TLCGD parametric excitation, $-\kappa_1 \ddot{w} u/H + \left(\kappa_1 d_A/H - \kappa_2\right) \dot{\vartheta}^2 u$, in Eq.(32) renders, together with the bridge dynamics (represented by a generalized SDOF system), a linear coupled matrix equation of motion of the two DOF isolated system

$$\mathbf{M}_S \begin{bmatrix} \ddot{Y} \\ \ddot{u} \end{bmatrix} + \mathbf{C}_S \begin{bmatrix} \dot{Y} \\ \dot{u} \end{bmatrix} + \mathbf{K}_S \begin{bmatrix} Y \\ u \end{bmatrix} = \begin{bmatrix} 1/M \\ 0 \end{bmatrix} F(t)$$

$$\mathbf{M}_S = \begin{bmatrix} 1 + \mu a_{11} & \mu a_{21} \\ a_{12} & 1 \end{bmatrix}_{x=\xi}$$

$$\mathbf{C}_S = \begin{bmatrix} 2\zeta\Omega & 0 \\ 0 & 2\zeta_A \omega_A \end{bmatrix}$$

$$\mathbf{K}_S = \begin{bmatrix} \Omega^2 & \mu \psi \bar{\kappa} g/e \\ \psi \kappa g/e & \omega_A^2 \end{bmatrix}_{x=\xi} \tag{38}$$

with constant coefficients, position ξ, see Eqs. (32) and (33) for the geometry factors,

$$a_{11} = \chi^2 + \phi^2 + \left(\frac{\psi d_A}{e} \right)^2 \left(1 + \bar{\kappa}_3 \frac{H^2}{d_A^2} \right) - \frac{2 d_A}{e} \psi \chi$$

$$a_{12} = -\chi \kappa + \frac{B}{2e} \psi \kappa_1 + \frac{d_A}{e} \psi \kappa$$

$$a_{21} = -\chi \bar{\kappa} + \frac{B}{2e} \psi \bar{\kappa}_1 + \frac{d_A}{e} \psi \bar{\kappa} \tag{39}$$

If the bridge is modeled as an MDOF system using a finite series Ritz approximation, and multiple TLCGD are installed, Eq.(37) still holds in a hypermatrix notation, Reiterer et al. (2006).

In case of a low order bridge model, the equations of motion of a TMD and a TLCGD can be compared to get the optimal tuning values. For dominating lateral vibrations the vertical and torsional mode shapes ϕ and ψ are set to zero in Eq.(38), and the mass ratio μ^* of the equivalent TMD results

$$\mu^* = \left. \frac{\mu \chi^2 \kappa \bar{\kappa}}{1 + \mu \chi^2 (1 - \kappa \bar{\kappa})} \right|_{x=\xi}, \quad \mu = \frac{m_f}{M} \tag{40}$$

According to the optimal Den Hartog tuning, see Eq. (9), the optimal frequency tuning becomes

$$\delta_{opt} = \frac{\omega_{A,opt}}{\Omega} = \left. \frac{\delta^*_{opt}}{\sqrt{1 + \mu \chi^2 (1 - \kappa \bar{\kappa})}} \right|_{x=\xi}, \quad \zeta_{A,opt} = \zeta^*_{A,opt} \tag{41}$$

The active TLCGD absorber mass is defined by $m^* = m_f \kappa \bar{\kappa} \chi^2 \big|_{x=\xi}$ and thus determines the optimal absorber placement at the position of maximum horizontal modal displacement χ. The possible parametric excitation from vertical bending remains ineffective for sufficiently large damping, because the cut-off value $\zeta_{A,0}^{(w)}$ for time harmonic vertical excitation can be given by, Reiterer (2004),

$$\zeta_{A,opt} = \frac{4U_0\delta_L}{3\pi} > \zeta_{A,0}^{(w)} = \kappa_1 \frac{\max\left|w\left(x=\xi\right)\right|}{H} \tag{42}$$

If the bridge vibration is dominated by torsional vibrations, oblique bending is assumed zero, $\phi \approx 0$, $\chi \approx 0$ and the equivalent mass ratio changes accordingly to

$$\mu^* = \left.\frac{\mu\left(\bar{\kappa}_1 B + 2\bar{\kappa} d_A\right)\left(\kappa_1 B + 2\kappa d_A\right)\psi^2}{4e^2\left[1+\mu\psi^2\left(\bar{\kappa}_3\frac{H^2}{e^2}+\frac{d_A^2}{e^2}-\frac{1}{4e^2}\left(\bar{\kappa}_1 B + 2\bar{\kappa} d_A\right)\left(\kappa_1 B + 2\kappa d_A\right)\right)\right]}\right|_{x=\xi}$$

$$\mu = \frac{m_f e^2}{I_e} \tag{43}$$

with the optimal tuning parameter determined by

$$\delta_{opt} = \frac{\omega_{A,opt}}{\Omega} = \left.\frac{\delta_{opt}^*}{\sqrt{1+\mu\psi^2\left(\bar{\kappa}_3\frac{H^2}{e^2}+\frac{d_A^2}{e^2}-\frac{1}{4e^2}\left(\bar{\kappa}_1 B + 2\bar{\kappa} d_A\right)\left(\kappa_1 B + 2\kappa d_A\right)\right)}}\right|_{x=\xi}$$

$$\zeta_{A,opt} = \zeta_{A,opt}^* \tag{44}$$

Again parametric excitation remains ineffective for pure torsional motion, w=0 in Eq. (32), if the equivalent viscous damping is above the critical cut-off damping $\zeta_{A,0}^{(\vartheta)}$ for time harmonic torsional vibrations,

$$\zeta_{A,opt} = \frac{4U_0\delta_L}{3\pi} > \zeta_{A,0}^{(\vartheta)} = \frac{1}{8}\left|\kappa_1\frac{d_A}{H} - \kappa_2\right| \operatorname{maxangle}\left|\vartheta_0^2(x=\xi)\right| \tag{45}$$

Due to the different type of excitation, the critical damping differs from Eq.(42).

To demonstrate the increase of effective bridge damping by TLCGD, a scaled model of a cable-stayed bridge (see Figure 7a) is tested dynamically under laboratory conditions. This model refers to the cantilever method of bridge construction. Harmonic horizontal forcing at the position of the cantilever carriage was used to excite the dynamic laboratory model, and vibration measurements rendered the dynamic magnification factor given in Figure 7b). The substantial reduction of displacements proves that the TLCGD

Figure 7. a) Scaled model of the bridge with TLCGD and harmonic excitation at the position of the cantilever carriage, b) Dynamic magnification factor of predominant horizontal motion (Adapted from Ziegler, 2008)

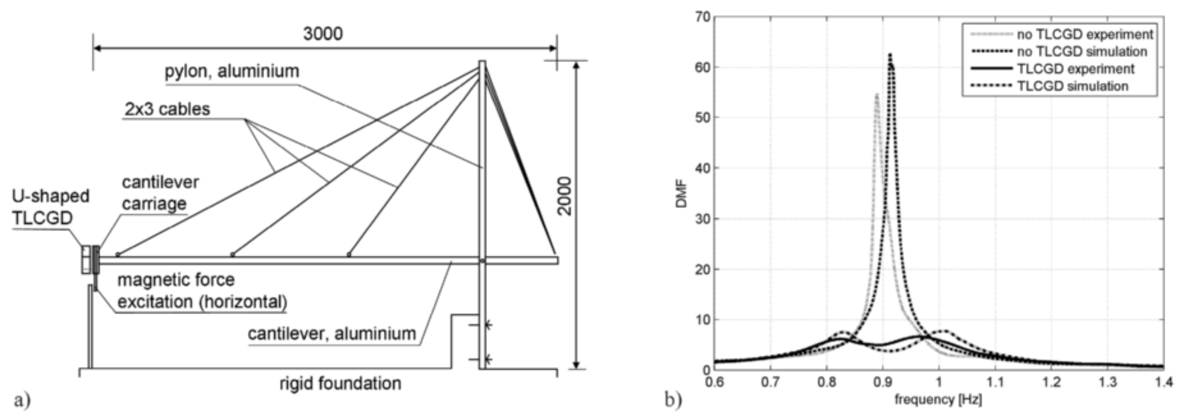

is perfectly suited to reduce bridge vibrations. If e.g. the cantilever method of bridge construction is limited by (wind excited) dominantly horizontal vibrations a single TLCGD carried along with the progress of the construction work, can reduce the vibrations significantly allowing for considerably longer cantilever arm length. In such an application vibration measurements identify the permanently changing bridge dynamics the TLCGD has to be tuned to the fundamental bridge frequency. The static pressure head in the gas vessel serves as convenient frequency tuning parameter for the TLCGD without changing the geometry or the effective liquid column length.

THE VERTICALLY ACTING TUNED LIQUID COLUMN GAS DAMPER

The classical U- or V-shaped TLCGD is perfectly suited to mitigate lateral or torsional vibrations. For dominating vertical vibrations, e.g. in case of flexural bridge vibrations, the absorber setup is modified in the following way: the length B of the horizontal pipe section is reduced until the pipe sections are close to each other and one of the closed pipe sections is charged with static over-pressure resulting in a static liquid surface displacement. The remaining small asymmetry of the liquid filled vertical pipe sections is eliminated by the novel symmetric vertical pipe-in-pipe TLCGD (VTLCGD), see Figure 8a). The geometric analogy between the VTLCGD and the TMD still exists allowing a classical modal Den Hartog tuning in a first design step, before splitting the absorber into smaller units in parallel action or considering neighboring modes of vibration during subsequent fine tuning in state space. Again, the experimentally observed averaged turbulent damping of the relative fluid flow and the weakly nonlinear gas-spring render the

Figure 8. a) Novel symmetric design of VTLCGD for vertical vibration damping, shown with a curved bottom. $B/H \ll 1$. Static over-pressure head H_0 indicated in the "equilibrium2" position. b) Dynamic magnification factor of the vertical deflection at mid-span of a standard 50m-span, SS-steel bridge in the critical frequency window around the first mode. Single force excitation, (Adapted from Ziegler (2008)).

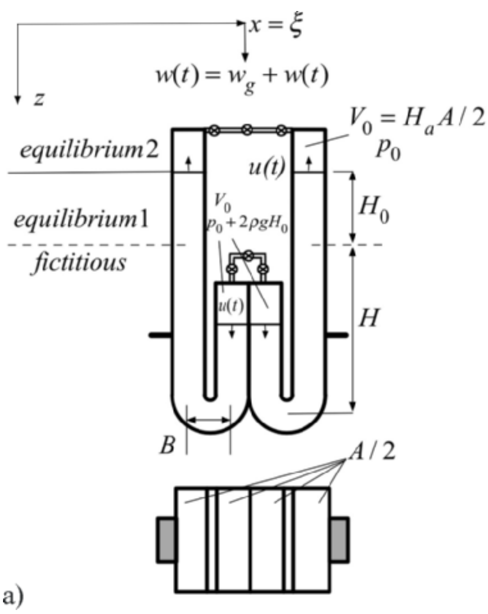

a)

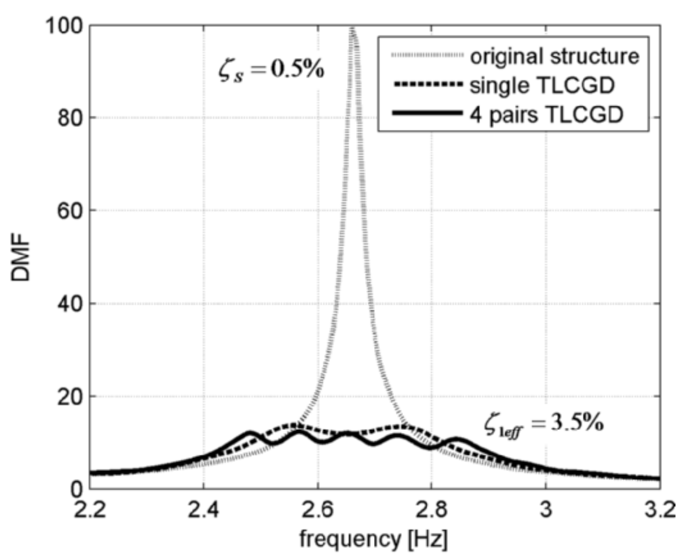

b)

VTLCGD insensitive to overloads and to the parametric forcing caused by the vertical motion.

Considering a force and base excited SDOF host structure with mass, damping and natural frequency denoted M_S, ζ_S and Ω_S, respectively, with a VTLCGD attached renders, with proper linearization, a linear coupled matrix equation of motion of the two DOF isolated system, see Ziegler (2008),

$$\begin{bmatrix} 1+\mu & -\mu\kappa_0 \\ -\kappa_0 & 1 \end{bmatrix}\begin{bmatrix} \ddot{w} \\ \ddot{u} \end{bmatrix} + \begin{bmatrix} 2\zeta_S\Omega_S & 0 \\ 0 & 2\zeta_A\omega_A \end{bmatrix}\begin{bmatrix} \dot{w} \\ \dot{u} \end{bmatrix} + \begin{bmatrix} \Omega_S^2 & 0 \\ 0 & \omega_A^2 \end{bmatrix}\begin{bmatrix} w \\ u \end{bmatrix} = -\begin{bmatrix} 1+\mu \\ -\kappa_0 \end{bmatrix}\lambda_z a_g + \begin{bmatrix} \dfrac{F(t)}{M_S} \\ 0 \end{bmatrix} \tag{46}$$

$$\mu = \frac{m_F}{M_S},\ \kappa_0 = \frac{2H_0}{L},\ f_A = \frac{\omega_A}{2\pi} = \sqrt{\frac{g/\pi^2}{4L_0}},$$
$$L_0 = \frac{L/2}{1+\left(h_0 + nH_0\right)/H_a},\ h_0 = \frac{np_0}{\rho g} \tag{47}$$

Assuming constant cross sectional areas of the piping system, the linearized VTLCGD-structure interaction force F_z, the liquid column length L as well as the active fluid mass m_A^* can be given by

$$F_z = m_f\left(\ddot{w}_g + \ddot{w} \quad \kappa_0\,\ddot{u}\right)$$

$$L_{eff} = L = 2H + B$$

$$m_A^* = \kappa_0^2 m_f \tag{48}$$

Like all TLCGD, the vertical absorber is susceptible to parametric excitation, but with sufficient absorber damping understood, the most critical double frequency parametric resonance becomes negligible with the cut-off value in this case given by (the vertical ground acceleration is assumed proportional to the horizontal component, $\lambda_z a_g$, $0 < \lambda_z \leq 1.2$

$$\zeta_A > \zeta_{A,0}^{(w)} = \max\left|\lambda_z a_g + \ddot{w}\right| / \left(L/2\right) << 1 \tag{49}$$

Comparing Eq.(46) with that of a TMD attached to a properly altered main SDOF-system Den Hartog tuning is possible with the equivalent mass ratio defined by

$$\mu^* = \frac{m_A^*}{M_S^*} = \mu\frac{\kappa_0^2}{1+\mu\left(1 \quad \kappa_0^2\right)} \tag{50}$$

where all the relevant parameter are denoted by a star *. The formula remains applicable for modal tuning if the normal mode is normalized to one at the position of the VTLCGD. The optimal tuning values are simply given by the transformation, Eq. (9), together with $\zeta_{Aj}^* = \zeta_{Aj}$, $\omega_{Aj}^* = \omega_{Aj}$ they become

$$\delta_{opt} = \frac{\omega_{A,opt}}{\Omega_S} = \frac{\delta_{opt}^*}{\sqrt{1+\mu\ \left(1-\kappa_0^2\right)}} = \frac{\sqrt{1+\mu\ \left(1-\kappa_0^2\right)}}{1+\mu},$$
$$\zeta_{jopt} = \sqrt{\frac{3\mu\ \kappa_0^2}{8\left(1+\mu\ \right)}} \tag{51}$$

Equation (46) takes on a hyper matrix form for a multiple-degree-of-freedom main system (preferably described in modal coordinates) with several VTLCGDs attached at properly selected positions, and possibly converted into smaller units in parallel action at one and the same location. In such a case, fine-tuning in state space is recommended.

The increase in effective structural damping is demonstrated convincingly by numerical simulations of a simply supported standard steel bridge of span 50 meter, time-harmonically forced at mid-span.

The modally tuned VTLCGD with $m_f = 2000kg$ is designed to suppress the fundamental bridge mode with a modal mass of $m_S = ml / 2 = 35720kg$ within the critical frequency window. With the pressure in equilibrium state 1 prescribed, $p_0 = 1.2 \times 10^5 \,\mathrm{Pa}$, the surplus pressure head $H_0 = 0.70\mathrm{m}$ chosen in the equilibrium state 2, $\kappa_0 = 2H_0 / L = 0.40$ inserted in Eq. (50) to obtain the equivalent mass ratio $\mu^* = 0.9\%$, the optimal Den Hartog parameters of a single VTLCGD become $f_{A1\,opt} = 2.64\,\mathrm{Hz}$ and $\zeta_{A1\,opt} = 5.6\,\%$.

Assuming n=1.4 yields the height of the gas volume H_a=0.380m, Eq. (47), and with the cross-sectional area of A=0.571m^2 the design of the single VTLCGD is completed. The linearly estimated maximum fluid stroke of $\max|u| = 0.05\mathrm{m}$ is compatible within the design dimensions, and the parametric forcing proven to be fully negligible, $\zeta_{A1\,opt} = 5.6\% > \zeta_{A,0}^{(w)} = 0.08\%$. Converting the single VTLCGD into four pairs of smaller VTLCGD units with fine tuning in state space renders slightly modified absorber frequencies and heights of gas volumes as well as much lower optimal damping ratios,

$f_{A1,8,opt} = 2.80$ Hz, $H_{A1,8} = 0.32m$, $\zeta_{A1,8,opt} = 1.85\%$, $f_{A2,7,opt} = 2.51$ Hz, $H_{A2,7} = 0.40m$, $\zeta_{A2,7,opt} = 1.73\%$, $f_{A3,6,opt} = 2.61$ Hz, $H_{A3,6} = 0.37m$, $\zeta_{A3,6,opt} = 1.70\%$ and $f_{A4,5,opt} = 2.70$ Hz, $H_{A4,5} = 0.34m$, $\zeta_{A4,5,opt} = 1.73\%$.

Consequently almost doubling maximum liquid strokes the parametric excitation remains insignificant, while the control becomes more robust, Figure 8b. With a simulated maximum relative fluid speed of 1.7 m/s < 12 m/s, the liquid surface is expected to stay intact, and no problems with respect to the piston theory are expected.

APPLICATION OF TLCGD IN LARGE DAMS

Another promising field of application of TLCGD is the passive control of seismically activated arch dams. The structural damping can be increased significantly which is of particular importance for the retrofit of existing structures which do not meet the criteria of modern seismic civil engineering codes. Assuming a low water level, neither the hydrostatic pressure nor the hydrodynamic forces are considered, and radiation damping into the water is absent. Such a structure is conveniently analyzed by commercially available finite element programs, which will also perform a modal analysis of the arch dam, thereby accounting for the proper foundation in the surrounding bed-rock. The structure of the modal model is identical to the MDOF system, Eq.(18), and for well separated natural frequencies in a critical resonance range, the dam-dynamics can be represented by a single mode of vibration, see Eq.(19). The low frequency modes show maximum modal displacements at the dam crest, but it is necessary to distinguish between symmetric and anti-symmetric modes. The first show maximum displacements close to the center of the dam, the latter, depending on the dam geometry, rather at the ends of the middle third. For effective damping by the action of TLCGD, the modal structural damping is as low as about 1% (for the free-standing dam a result of material damping and radiation damping into the bed-rock). Due to the enormous modal masses of a dam the necessary liquid column cross-sectional areas are much too large for a single TLCGD.

Therefore the TLCGD is split into several smaller units acting in parallel keeping the length of the fluid column constant. The recommended subsequent fine tuning in state space renders the optimal frequencies slightly modified and more robust when compared to traditional Den Hartog tuning. Since the modal equations of motion are identical to those given for the asymmetric building, however without rotation of the frame, the reduction of the dynamic magnification factor only depends on the mass ratio. A possible installation in the selected vertical section of a double curved dam is sketched in Figure 9. By changing the gas pressure, thus adapting the static pressure head, it is even possible to adjust the TLCGD to modified dynamic parameter e.g. to adapt it to the natural frequency changing with the water level in the reservoir. However, the optimal position might become sub-optimal with changing modal shapes.

CONCLUSION

Tuned liquid column gas dampers show excellent vibration and energy absorbing capabilities appropriate for many applications in earthquake engineering. It has been shown that the vibration reduction is equal to well established dynamic absorber e.g. the TMD of spring-mass-dashpot type, if the vibration is dominantly horizontal, which occurs e.g., either if the main system is a moderately asymmetric space frame or if the main system is a bridge with critical lateral flexural-torsional natural modes, as made evident in this paper. However, its salient features make the TLCD superior to commonly applied alternative systems: they neither have moving parts nor elements which suffer from friction, wear and tear. One of the most important developments was the recently established TLCGD-TMD analogy facilitating a simple design and tuning process for almost all civil engineering structures.

Figure 9. a) Vertical section of a double curved dam with symmetric TLCGD b) detailed schematic view of TLCGD smoothly integrated below the dam crest. Closed pressurized pipe sections have equal volume.

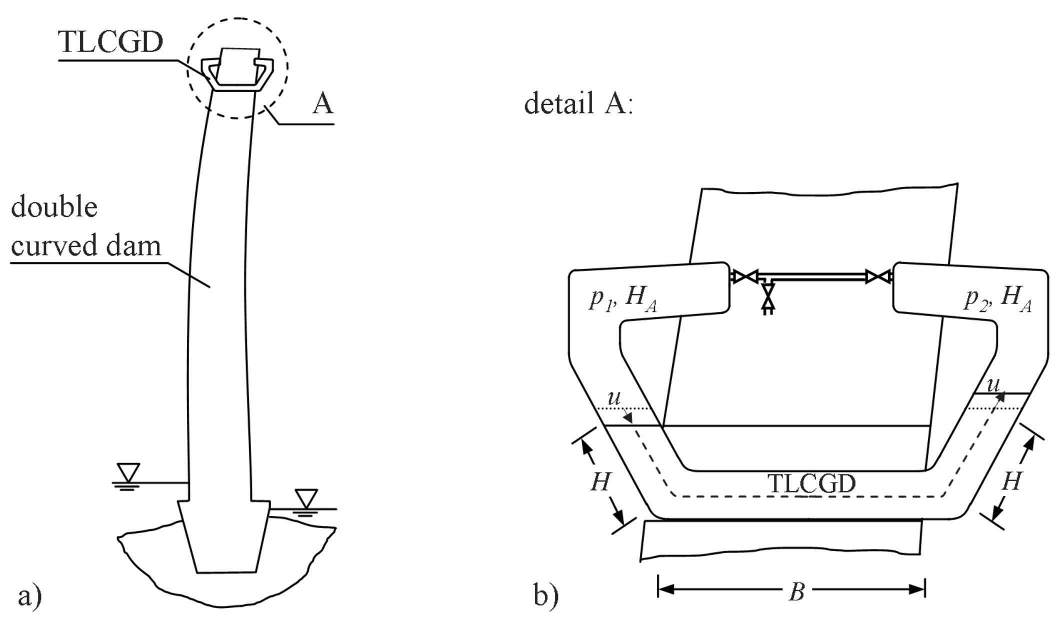

For practical purposes the liquid column length has to be in the range of several meters to thirty meters and more for large structures, causing the classical TLCD's natural frequency to be far below 1Hz. The invention of the gas spring effect by properly sealing and pressurizing the rigid pipe not only has extended the practical frequency range say up to 5Hz, but also renders an easily accessible tuning parameter, namely the static equilibrium gas pressure in the symmetrically arranged gas containers above the inclined pipe sections. Furthermore, additional desired properties were obtained, particularly the passive protection against overload and excessive liquid column strokes and the reduced sensitivity against parametric excitation. The simple tuning mechanism allows for very promising applications of TLCGD in case of continuous adjustment of the frequency e.g. in the course of the cantilever method of bridge construction. Den Hartog's optimal tuning is recommended for preliminary modal design, before splitting the TLCGD into smaller units in parallel action to achieve an additional gain in structural damping and a more robust control of the response in the neighborhood of resonance frequencies by fine tuning in state space. As a general rule the TLCGD should be installed at the position of largest modal displacements. For the low vibration modes of a building the top floor is appropriate, for higher modes an intermediate floor might be equally adequate. For strongly asymmetric buildings a redesigned torsional TLCGD (TTLCGD) is recommended. Applying the device to increase the effective damping of a lightly damped base isolation mode, the base slab is proposed for TLCGD placement because it is easy to meet the requirements for the additional mass load as well as the space specifications for the TLCGD piping system. Besides the classical V-or U-shaped TLCGD a novel design of a VTLCGD is analyzed that mitigates dominating vertical vibrations, e.g., of bridges and large floor-plates. For a practical design of the symmetric VTLCGD unit and to safely avoid unsymmetric flows and sloshing, two separate TLCGDs are to be combined, Ziegler et al. (2013).

The advances made in the last decade have led to an increased insight and the understanding of TLCGD has grown in C.E. practice a great deal. As a result simple guidelines for optimal placement and tuning are readily available for buildings, bridges and recently even for large arch-dams. So far, all research results indicate that the TLCGD is more competitive when compared to TMD so that it should replace the TMD (possibly except the pendulum-dashpot type) in almost any structural application.

REFERENCES

Bachmann, H. (2010). Seismic upgrading of a fire-brigade building by base isolation in Basel, Switzerland. *Structural Engineering International*, *20*(7), 268–274. doi:10.2749/101686610792016880

Den Hartog, J. P. (1956). *Mechanical vibrations* (4th ed.). New York, NY: McGraw-Hill.

Fu, C. (2008). *Effective damping of vibrations of plan-asymmetric buildings.* Doctoral dissertation, Vienna University of Technology, Austria. Retrieved from http://www.ub.tuwien.ac.at/diss/AC05037516.pdf

Fu, C., & Ziegler, F. (2010). Vibration prone multi-purpose buildings and towers effectively damped by tuned liquid column-gas dampers. *Asian Journal of Civil Engineering*, *10*(1), 21–56.

Hochrainer, M. J. (2001). *Control of vibrations of civil engineering structures with special emphasis on tall buildings*. Doctoral dissertation, Vienna University of Technology, Austria. Retrieved from http://www.ub.tuwien.ac.at/diss/AC03322409.pdf

Hochrainer, M. J. (2005). Tuned liquid column damper for structural control. *Acta Mechanica*, *175*(1-4), 57–76. doi:10.1007/s00707-004-0193-z

Hochrainer, M. J., & Ziegler, F. (2006). Control of tall building vibrations by sealed tuned liquid column dampers. *Structural Control and Health Monitoring*, *13*(6), 980–1002. doi:10.1002/stc.90

Huo, L. S., Li, H. N., & Sun, L. (2001). Parameter study of TLCD control system excited by multidimensional ground motions. *Earthquake Engineering and Engineering Vibration*, *4*(21), 147–153.

Khalid, B. (2010). *Control of seismically forced vibrations of asymmetric buildings by means of a novel base isolation system.* Doctorial dissertation, Vienna University of Technology, Austria. Retrieved from http://www.ub.tuwien.ac.at/diss/AC07809200.pdf

Khalid, B., & Ziegler, F. (2009). Experimental verification of control of asymmetric building vibrations by tuned liquid column gas dampers. *Proceedings of the 3rd International Conf. Experiments / Process / System Modeling / Simulation and Optimisation*, Athens, 8-11 July, 2009. Retrieved from http://epsmso.gr/2009/default.htm, CD-ROM paper: epsmso09_142.pdf

Khalid, B., & Ziegler, F. (2010). A novel base isolation system for asymmetric buildings effectively damped by tuned liquid column-gas dampers. *Proceedings of the 14th European Conference on Earthquake Engineering* (14.ECEE), Ohrid, 30. 08.- 03. 09. 2010. Abstract ID 1048. Retrieved from http://www.14ecee.mk/

Müller, P. C., & Schiehlen, W. O. (1976). *Lineare Schwingungen*. Wiesbaden, Germany: Akademische Verlagsgesellschaft.

Reiterer, M. (2004). *Damping of vibrational civil engineering structures with emphasis on bridges*. Doctoral dissertation, Vienna University of Technology, Austria. Retrieved from http://www.ub.tuwien.ac.at/diss/AC04250350.pdf

Reiterer, M., & Ziegler, F. (2004). Bi-axial seismic activation of civil engineering structures equipped with tuned liquid column dampers. *Journal of Seismology and Earthquake Engineering*, *6*(3), 45–60.

Reiterer, M., & Ziegler, F. (2006). Control of pedestrian-induced vibrations of long-span bridges. *Structural Control and Health Monitoring*, *13*, 1003–1027. doi:10.1002/stc.91

RWDI Consultant Engineers, (2011). *Projects from RWDI.* Retrieved March 28, 2011, from http://www.rwdi.com/project/one_wall_centre

Teramura, A., & Yoshida, O. (1996). Development of vibration control system using u-shaped water tank. In *Proceedings of the 11th World Conference on Earthquake Engineering* (Sociedad Mexicana de Ingenieria Sismica, A.C.), paper no. 1343, Elsevier Science Ltd.

Warburton, G. B. (1982). Optimum absorber parameters for various combinations of response and excitation parameters. *Earthquake Engineering & Structural Dynamics*, *10*, 381–401. doi:10.1002/eqe.4290100304

Ziegler, F. (1998). Mechanics of solids and fluids, 2nd ed. New York, NY: Springer.

Ziegler, F. (2008). Special design of tuned liquid column-gas dampers for the control of spatial structural vibrations. *Acta Mechanica*, *201*, 249–267. doi:10.1007/s00707-008-0062-2

Ziegler, F., & Khalid, B. (2011). A novel base isolation system for asymmetric buildings in seismic active zones: damping supplied by tuned liquid column-gas dampers. In Belyaev, A. K., Irschik, H., & Krommer, M. (Eds.), *Advanced dynamics and model based control of structures and machines* (pp. 225–234). Wien, Austria: Springer-Verlag. doi:10.1007/978-3-7091-0797-3_26

Ziegler F. & Kazemi A.A. (2013), Bridge vibrations effectively damped by means of tuned liquid column gas dampers. *Asian Journal of Civil Engineering* (BHRC), *14*(1), 1-16

ADDITIONAL READING

Chang, C. C., & Hsu, C. T. (1998). Control performance of liquid column vibration absorbers. *Engineering Structures*, *20*, 580–586. doi:10.1016/S0141-0296(97)00062-X

Gao, H., Kwok, K. S. C., & Samali, B. (1999). Characteristics of multiple tuned liquid column dampers in suppressing structural vibration. *Engineering Structures*, *21*, 316–331. doi:10.1016/S0141-0296(97)00183-1

Haroun, M. A., Pires, J. A., & Won, A. Y. J. (1996). Suppression of environmentally-induced vibrations in tall buildings by hybrid liquid column dampers. *Structural Design of Tall Buildings*, *5*, 45–54. doi:10.1002/(SICI)1099-1794(199603)5:1<45::AID-TAL58>3.0.CO;2-F

Hitchcock, P. A., Kwock, K. C. S., & Watkins, R. D. (1997). Characteristics of liquid column vibration absorbers (LCVA). *Engineering Structures*, *19*, 126–144. doi:10.1016/S0141-0296(96)00042-9

Idelchick, I. E. (2005). *Handbook of hydraulic resistance*. Jaico Publishing House.

Kagawa, K., Yoshimura, Y., Fujita, K., Yamasaki, Y., & Ayabe, S. (1994). Semi-active and passive vibration control of structure by fluid system. *Active and Passive Control of Mechanical Vibration*, *289*, 41–48, New York, NY: ASME..

Sakai, F., Takaeda, S., & Tamaki, T. (1989). Tuned liquid column dampers – New type device for suppression of building vibrations. *Proceedings of the International Conference on High-rise Buildings*, Nanjing, (pp. 926-931).

Shum, K. M., & Xu, Y. L. (2002). Multiple-tuned liquid column dampers for torsional vibration control of structures: Experimental investigation. *Earthquake Engineering & Structural Dynamics*, *31*, 977–991. doi:10.1002/eqe.133

Soong, T. T., & Dargush, G. F. (1997). *Passive energy dissipation systems in structural engineering*. Chichester, UK: John Wiley & Sons.

Souza, S. L. T., Caldas, I. L., Vianab, R. L., Balthazar, J. M., & Brasil, R. M. L. R. F. (2006). Dynamics of vibrating systems with tuned liquid column dampers and limited power supply. *Journal of Sound and Vibration*, *289*, 987–998. doi:10.1016/j.jsv.2005.03.001

Spencer, B. F., & Sain, M. K. (1997). Controlling buildings: A new frontier in feedback. *IEEE-Control Systems Magazine on Emerging Technology*, *17*, 19–35. doi:10.1109/37.642972

Wu, J. C., Wang, Y. P., Lee, C. L., Liao, P. H., & Chen, Y. H. (2008). Wind-induced interaction of a non-uniform tuned liquid column damper and a structure in pitching motion. *Engineering Structures*, *30*, 3555–3565. doi:10.1016/j.engstruct.2008.05.029

Yalla, S. K., Kareem, A., & Kantor, J. C. (2001). Semi-active tuned liquid column dampers for vibration control of structures. *Engineering Structures*, *23*, 1469–1479. doi:10.1016/S0141-0296(01)00047-5

KEY TERMS AND DEFINITIONS

Den Hartog Optimization: Analytical optimization in frequency domain recommended for optimizing a modally isolated 2DOF generalized system (structure with a TLCGD attached). It serves as initial value for a subsequent optimization in state space.

Gas Spring: Invention to increase the restoring forces of TLCGD by the compressibility of the gas.

Passive Damping with Dynamic Absorber: Vibration reduction based on an energy transfer from a main system to a passive absorber with sufficient energy dissipation.

Pendulum Dashpot Absorber: Pendulum type dynamic absorber with restoring forces due to gravity, energy dissipation is provided by a dashpot.

Pipe in Pipe TLCGD: Novel vertical TLCGD to efficiently reduce dominantly vertical vibrations.

Spring Mass Dashpot Absorber (SMDA): Dynamic absorber whose restoring forces are provided by an elastic spring, the dashpot provides sufficient energy dissipation.

State Space Optimization: Accounting for neighboring modes of vibrations and rendering the TLCGD design parameter slightly modified and more robust. Although derived for harmonic excitation it can also be interpreted in terms of stochastic quantities. Using generalized coordinates the dynamic system is only weakly coupled and the optimization converges well to the desired TLCGD parameter.

TLCGD: Dynamic absorber using a liquid, preferably water, instead of a rigid mass. The liquid is guided in a rigid piping system and excited by floor displacements.

TMD-TLCGD Analogy: Equivalence in both damping properties and optimization procedure of TMD and TLCGD.

U- and V-shaped TLCGD: Plane TLCGD ideal to suppress horizontal and coupled bending torsional vibrations of civil engineering structures.

Chapter 8
Multi-Objective Optimization Design of Control Devices to Suppress Tall Buildings Vibrations against Earthquake Excitations Using Fuzzy Logic and Genetic Algorithms

Saeid Pourzeynali
University of Guilan, Iran

Shide Salimi
University of Mohaghegh-Ardebili, Iran

ABSTRACT

The main objective of this chapter is to find the optimal values of the parameters of the base isolation systems and that of the semi-active viscous dampers using genetic algorithms (GAs) and fuzzy logic in order to simultaneously minimize the buildings' selected responses such as displacement of the top story, base shear, and so on. In this study, performance of base isolation systems, and semi-active viscous dampers are studied separately as different vibration control strategies. In order to simultaneously minimize the objective functions, a fast and elitist non-dominated sorting genetic algorithm (NSGA-II) approach is used to find a set of Pareto-optimal solution. To study the performance of semi-active viscous dampers, the torsional effects exist in the building due to irregularities, and unsymmetrical placement of the dampers is taken into account through 3D modeling of the building.

DOI: 10.4018/978-1-4666-2029-2.ch008

INTRODUCTION

One of the most important tasks in structural engineering is to reasonably minimize the undesired vibrations of the structures due to the environmental dynamic loads such as earthquake excitations. Various strategies and theories have been investigated and developed to approach this goal over the years. Use of the control systems is one of these methods to enhance the structural performance against vibration excitations. The main purpose of these methods is to reduce the structural responses such as displacement, velocity and acceleration. Control systems are divided to four groups of passive, semi active, active and hybrid systems based on the performance and rate of the energy consumption and the kind of their installation to the main structure.

The passive systems dissipate the vibration excitations without using any external power source for operation and utilize the motion of the structure to develop the control force. Since the properties of these types of control systems cannot be modified after installation, these systems are regarded as passive. These systems add no energy to the structure, and therefore are not able to make the structure unstable. These systems are undoubtedly simple, inexpensive, and reliable to suppress the undesired vibrations of the structures. Another advantage of these systems is low cost of repairing and maintenance. Passive tuned mass dampers (TMDs) and base isolations are two kinds of these systems (Pinkaew &Fujino 2001; Yang & Agrawal 2002; Cao et al. 1998; Soong & Constantinou 1994; Soong & Dargush 1997). Although TMD control systems may be considered a hybrid of a tuned dynamic absorber, including a mass block and spring, combined with a viscous damper, however, in engineering is known as a passive control system (Pinkaew & Fujino 2001; Soong & Dargush 1997).

An active control system may be defined as a system which typically requires a large power source for operation of electrohydraulic or electromechanical actuators which supply control forces to the structure. Control forces are developed based on feedback from sensors that measure the excitation and/or the response of the structure (Symans & Constantinou 1999). Active tuned mass damper (ATMD) or hybrid mass damper is a kind of these control systems, which is considered when the required response reduction exceeds the capacity of the TMD. ATMD systems are more costly, complex, needs careful maintenance, as well needs huge source of energy difficult to provide in severe earthquakes. Moreover, the control forces which these systems apply to the structure may cause unforeseen behavior of the structure. These disadvantages made them to be less reliable than TMDs and are being used only for certain cases (Chey et al., 2009).

The limitation of passive and active control systems result in developing semi active control systems. Semi-active control systems maintain the reliability of passive control systems while taking advantage of the adjustable parameter characteristics of an active control system (Symans & Constantinou 1999). The semi-active tuned mass damper (STMD) with variable damping is a kind of these systems. Various studies confirm the efficiency of STMDs and show that the application of TMDs is much better when they behave as STMDs, especially in wind and earthquake excitations. In these systems, the stiffness or the damping ratio of the control device changes proportional to the relative displacement or relative velocity, by receiving information from sensors in every second (Mulligan, 2007). Therefore, they do not require large power supply, and they do not add additional energy to the main structure and guarantee stability of the system. In order to regulate the stiffness or the damping ratio of the STMDs, fuzzy systems can be utilized.

Hybrid control systems are the combination of some passive systems with active or semi active systems, resulting to better performance of the control device in reducing the structural responses. One of the most popular systems of them is smart isolator. Another example of hybrid control system is a combination of passive isolation bearings with some passive energy dissipating devices. Additional damping in these systems enhances control performance of them particularly in near field earthquakes.

The main objective of this chapter is to find the optimal values of the base isolation system as a kind of passive control device, and that of the STMD system as a kind of semi-active control device using genetic algorithms (GAs) and fuzzy logic to simultaneously minimize the buildings' selected responses. A comprehensive literature review of these systems is provided in the main relevant sections of each system.

AIMS AND SCOPE OF THE CHAPTER

In the present chapter, STMD system with variable viscous damper as a kind of semi-active control device; and base-isolation, and TMD systems as two kinds of passive control devices are studied. In this regard, a realistic ten story building modeled as a 2-D frame is selected to represent the results of use of the base-isolation systems; and a realistic twelve story building modeled as a 3-D frame is selected to simulate the response of the building with STMD/TMD systems against earthquake excitations. The parameters of these devices have been optimally designed by multi-objective genetic algorithms and fuzzy logic utilizing the well known MATLAB software. The results of use of base isolation systems, and those of the STMD/TMD control devices are provided in next sections. In order to study the performance of the base isolation systems, 18 worldwide strong ground motion accelerogrames, and to show the effectiveness of STMD/TMD control devices, 7 earthquake accelerogrames are selected, for which the detail descriptions will be provided in the future sections of the chapter. In both control systems, genetic algorithm (GA) is used to find the optimal values of the design parameters, moreover in semi-active control device the damping ratio is regulated by a fuzzy logic controller.

The main objective of this chapter is multi-objective optimization design of control devices to reduce the structural vibrations excited by the earthquake. In past decades, the use of evolutionary algorithms is considered by many researchers in different optimization fields (Schaffer 1985; Fonseca & Fleming 1993; Srinivas & Deb 1994; Zitzler & Thiele 1998; Knowles & Corne 1999). Genetic algorithms (GAs) are effective search methods in very large and wide space that eventually lead to the orientation towards finding an optimal answer. They can be used for solving a variety of optimization problems that are not well suited for standard optimization algorithms including problems in which the objective function is discontinuous, non-differentiable, stochastic or highly nonlinear (Pourzeynali & Mousanejad, 2010; Pourzeynali & Zarif 2008).

ASSUMPTIONS

The following simplified assumptions are made in the analyses (Matsagar & Jangid, 2003; Matsagar & Jangid, 2004):

- The main building is assumed to remain within the elastic limit during the earthquake excitation. As the control systems reduce the building response to a relatively low value, therefore this assumption would be reasonable.
- To study the effect of base-isolation systems, the building is modeled as a shear type frame having one lateral degree of freedom at each story level (lumped mass and rigid floor assumption), while in STMD/TMD systems, the building is modeled as a 3D frame having 3 degrees of freedom, two translational and one torsional, in each story level.

- The columns are inextensible and weightless providing the lateral stiffness.
- The system is subjected to horizontal components of the earthquake ground motion (single-support excitation assumption).
- No soil-structure interaction is considered in the analyses.

EARTHQUAKE GROUND MOTION TIME HISTORIES

In order to perform time history dynamic analyses, the earthquake inputs must be specified in terms of free field strong ground motion accelerogrames. For this purpose, in present study to show the performance of the base isolation systems, 18 worldwide strong ground motion accelerogrames are selected in which after performing any necessary corrections, filtering, and scaling are used in the analyses. The most important earthquake accelerogrames used for this purpose are given in reference (Pourzeynali & Zarif, 2008). A part of these accelerogrames may incorporate the near fault effect in the analyses. As well, to study the effect of STMD/TMD systems, 7 earthquake accelerogrames are selected for which detail descriptions are provided in Table 1.

GENETIC ALGORITHMS AND MULTI-OBJECTIVE OPTIMIZATION

The main purpose of this chapter is multi-objective optimization design of control devices to reduce the structural vibrations excited by the earthquake. Most of the engineering optimization problems are often very complex and difficult to solve without considering many simplifications. In recent years, the use of evolutionary algorithms is considered by many researchers in different optimization fields. Genetic algorithms (GAs) are effective search methods in very large and wide space that eventually lead to the orientation towards finding an optimal answer. They can be used for solving a variety of optimization problems that are not well suited for standard optimization algorithms including problems in which the objective function is discontinuous, non-differentiable, stochastic or highly nonlinear (Pourzeynali & Mousanejad, 2010). Genetic algorithms are very different with the traditional optimization methods; one of these differences is that GA works with a population or set of points in a certain moment, while traditional optimization methods use a special point. This means that the GA will be processed a large number of schemes at a time. Unlike conventional optimization methods that use derivative of function, genetic algorithms just use objective function

Table 1. Earthquake accelerogrames considered to show the performance of STMD/TMD devices

Earthquake	Earthquake specifications				
	Date	Station	Magnitude (Ms)	PGA (g)	Duration (sec)
Kocaeli	1999	Ambarli	7.8	0.2228	150.405
Chi-Chi	1999	CHY022	7.62	0.64	121
Duze	1999	Sakarya	7.3	0.0215	60
Kobe	1995	Kakogawa	7.2	0.2668	40.96
Cape Mendocino	1992	Eureka - Myrtle & West	7.1	0.1668	44
Northridge	1994	90088 Anaheim - W Ball Rd	6.7	0.0658	34.99
Coalinga	1983	36229 Parkfield - Cholame 12W	6.5	0.0445	40

value. In these algorithms, the design space should be converted to the genetic space; therefore genetic algorithms wok with series of coded variables. The advantage of working with coded variables is that the codes have basically capability to convert continuous space to discrete space. Another interesting point is that the principles of GA are based on the random processing, so the random operators investigate the search space comparative. The main steps of operation of genetic algorithms are: initializations, selection of chromosomes for reproduction, cross over between chromosomes and producing the next generation, mutation for search other parts of the problem (to prevent of early convergence), insertion of children in the new population. In recent years, the application of genetic algorithm is increasing with specify more and more capability, flexibility and speed of this algorithm.

The main purpose in single-objective optimization problems is to find the values of design parameters at which the value of one objective function is optimum. While, in multi-objective optimization (which is also called the vector optimization), the problem is to find the optimum value of more than one objective function, which are usually in conflict with each other in engineering optimization problems, such that improvement of one leads to the worsening of the others. Therefore, multi objective optimization offers the optimal set of solutions, rather than an optimal response. In this set we cannot find any answer which dominants the others. The optimal solutions are called Pareto points or Pareto Front (Atashkari et al., 2005).

Routine methods in solving multi-objective optimization problems are conversion of the multiple objective functions into one objective function. For this purpose, different methods are presented in scientific reports, from which the most widely used methods are: Weighted sum approach, ε-perturbation, Min-Max and non-sorting genetic algorithm. Genetic algorithms act well to solve the multi-objective optimization problems. In recent years, Srinivas and Deb (1994) found a new algorithm based on genetic algorithms for solving multi objective optimization problems. This method that is called non-sorting genetic algorithm or NSGA is more powerful than the previous algorithms in multi-objective optimization. Because of the difficulties exist in this method in solving optimization problems, the modified algorithm called NSGA-II was introduced by Deb a few years later, which acts better and faster to find the non-sorting solutions (Deb et al., 2002). In multi-objective optimization, it is tried to find a design vector $\boldsymbol{X}^* = \left[x_1^*, x_2^*, \ldots, x_n^*\right]^T$ which can optimize k objective functions, f_i, under m inequality constraints and p equality constraints, consequently. The multi objective optimization can be briefly expressed as:

$$
\begin{array}{lll}
\mathit{find} & \mathbf{X}^* & \\
\mathit{optimize} & \mathbf{F}(\mathbf{X}) & \\
\mathit{subject\ to} & \begin{cases} g_i(\mathbf{X}) \le 0 \\ h_j(\mathbf{X}) = 0 \end{cases} & \begin{array}{l} (i = 1,2,\ldots,m) \\ (j = 1,2,\ldots,p) \end{array}
\end{array}
\tag{1}
$$

where $\mathbf{X}^* \in \Re^n$ is the design variables vector; $\mathbf{F}(\mathbf{X}) = \left[f_1(\mathbf{X}), f_2(\mathbf{X}), \ldots, f_k(\mathbf{X})\right]^T$ is the vector of objective functions so that $\mathbf{F}(\mathbf{X}) \in \Re^k$; and $g_i(\mathbf{X})$ and $h_j(\mathbf{X})$ are inequality and equality constraints, respectively.

In optimization studies that include multi-objective optimization problems, the main objective is to find the global Pareto optimal solutions, representing the best possible objective values. However, in practice, users may not always be interested in finding the global best solutions, particularly if these solutions are very sensitive to variable perturbations. In such cases, practitioners are interested in finding robust solutions that are less sensitive to small changes in variables (Deb & Gupta 2004; Branke 1998).

BASE ISOLATION SYSTEMS

In August 1909 J. A. Calantarients, a medical doctor from northern English city of Scarborough, wrote a letter to the Director of the Seismological Service of Chile in Santiago to introduce him a new method of building construction which now is known as base isolation. The doctor proposed that in seismically active countries, the buildings can be built on "free joint" and a layer of fine sand, mica, or talc that would allow the building to slide in an earthquake. Dr. Calantarients had mentioned in his letter that he had made experiment with balls many years before it was done in Japan (Naeim & Kelly, 1999).

John Milne, an Englishman who was living in Tokyo in the years 1876-1895, built an example of isolated building at the University of Tokyo. This building was built on balls in Cast-iron plates with Saucer-like edges on the heads of piles. In 1885 he explained his experiment in a report to the British Association for the Advancement of Science. Likely, he was the reference of the Japan work, which Dr. Calantarients had mentioned in his letter (Naeim & Kelly, 1999).

Application of the seismic base isolation system has become a practical reality within the last 30 years with development of multilayer elastomeric bearings. Their development was an extension of the use of elastomeric bridge bearings and bearings for the vibration isolation of buildings (Naeim & Kelly, 1999).

The first use of a rubber isolation system to protect a structure from earthquakes was in 1969 from an elementary school in Skopje, Yugoslavia. The first base-isolated building built in the United States was the Foothill Communities Law and Justice Center (FCLJC), a legal services center for the County of San Bernardino, located in the city of Rancho Cucamonga. The construction of this building began in early 1984 and was completed in mid-1985. In Japan the first large modern base-isolated building was built in 1986, and increased to a level of around 10 isolated buildings per year in 1990 and 1991(Naeim & Kelly, 1999).

There are many types of isolation systems used today to protect the buildings from earthquakes. Most of these systems incorporate either elastomeric bearings, with natural rubber or neoprene, or sliding bearings, with the Teflon or Stainless steel sliding surface. However, many new and different isolation systems are proposed each year, and the number of these systems continues to increase year by year. This chapter discusses only the elastomeric base isolators.

Base isolation technology is now well accepted worldwide, and many example buildings are constructed in United States, Japan, New Zealand, Italy, and China.

Seismic isolation systems represent another form of passive control systems. In these systems, a flexible isolation system is introduced between the foundation and superstructure so as to increase the natural period of the system. Since the period of the base-isolated structures is long, in comparison with the fixed-base structures, therefore if the earthquake motion at the site has a long period, this can cause resonance phenomenon in the structure. In this situation, the isolation system may have a reverse effect and increase the response of the structure instead of reducing it. Examples of this phenomenon have been reported at Mexico City and Budapest. On the other hand, near fault effects cause large velocity pulses close to the fault rupture. Effects are greatest within 1 km of the rupture but extent out to 10 km. The UBC provisions require that near fault effects should be included by increasing the seismic loads by some factors. In time history dynamic analysis this can be incorporated by including time histories reflecting near fault effects. The near fault record produces a much greater response than the far fault record. The isolation system is being used in near fault locations, but the cost is usually higher and the evaluation more complex (Kelly, 2001).

The present investigation is a research study, and its main objective is to simultaneously minimize the seismic isolated building top story displacement and that of the base isolation system using a multi-objective optimization solution. Therefore, the far and near fault effects are implicitly considered in the earthquake acceleration time history records selected for dynamic analysis of the building. So, explicitly not much attention is given to this behavior of the base isolated building, which is needed in real design practice. Generally, many different systems of isolators are proposed and patented each year. In this investigation, elastomeric-base isolation systems are studied for which some brief descriptions are provided in the following (Pourzeynali & Zarif, 2008).

Laminated Rubber Bearings

The laminated rubber bearing (LRB) systems (or low-damping bearings) are composed of the rubber plates and steel shims built in a single unit. The internal steel plates reduce the lateral bulging of the bearings and increase the vertical stiffness (Naeim & Kelly, 1999). Low-damping bearings with low horizontal stiffness shift the fundamental time period of the structure to avoid resonance with the excitations. The damping constant of the system varies considerably with the strain of the bearings. Based on test results of Tarics (1984) the damping ratio depends on the strain level of the bearing. LRB isolators have been extensively tested at the University of California and found suitable for many applications (Kelly 1986). The main feature of the LRB systems is the parallel action of linear spring and damping (Matsagar & Jangid, 2003). The restoring force developed in the bearing, F_b, is given by (Matsagar & Jangid, 2003):

$$F_b = c_b \dot{v}_b + k_b v_b \tag{2}$$

where c_b and k_b are damping and stiffness of LRB systems, respectively; v_b *and* $\dot{v}_b$ are the relative displacement and velocity of the base slab with respect to the ground. The stiffness and damping of LRB systems are selected to provide the specific values of the two parameters namely the isolation time-period (T_b) and damping ratio $\left(\xi_b\right)$ defined as (Matsagar & Jangid, 2003):

$$T_b = 2\pi\sqrt{\frac{m_s}{k_b}} \tag{3}$$

$$\xi_b = \frac{c_b}{2m_s\omega_b} \tag{4}$$

where m_s is the total mass of the building and base slab, defined in Equation (9); and $\omega_b = 2\pi / T_b$ is the isolator frequency.

Lead-Rubber Bearings

The lead-rubber bearings were invented in New Zealand in 1975 and have been used extensively in New Zealand, Japan, and the United States (Naeim & Kelly, 1999). These systems are generally referred as N-Z systems. N-Z bearings are similar to the LRB systems, but in order to provide an additional means of energy dissipation and initial rigidity against minor earthquakes and winds, a central lead-core system is used (Skinner et al., 1975; Robinson, 1982). This system essentially behaves as hysteretic damping device (Kelly et al. 1972, 1977, and 1986; Skinner et al. 1975; Datta 1996). The force–deformation behavior of the N-Z bearings is generally represented by non-linear characteristics (see Figure 1). In the present study, the bilinear hysteretic model of these isolators is used (Matsagar & Jangid, 2004). The bilinear hysteretic loop, as shown in Figure 1, is characterized by three parameters namely: (1) yield strength F_y, (2) elastic and plastic stiffness values k_{b1} and k_{b2}, respectively, and (3) yield displacement v_y (Matsagar & Jangid, 2004). The restoring force developed in

Figure 1. Bilinear hysteretic model of the lead rubber bearings used in this study

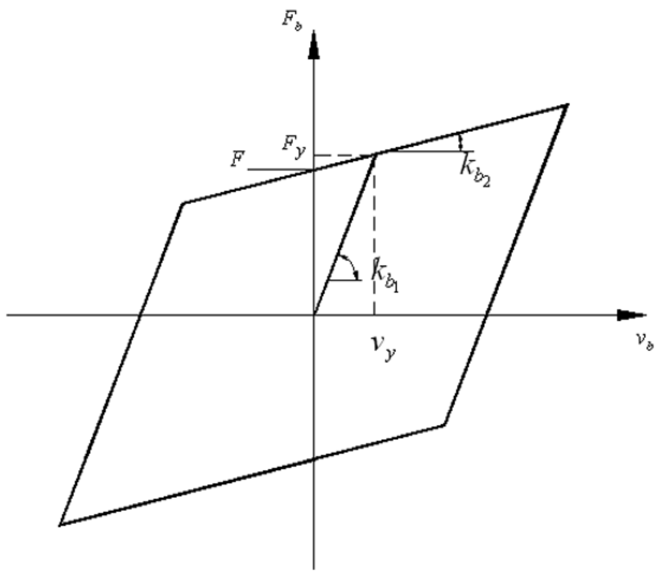

these isolation bearings can also be represented by Equation (1) by replacing the k_b by appropriate k_{b1} and k_{b2} in elastic and plastic phases, respectively. In this study, the values of v_y and $\gamma = k_{b2}/k_{b1}$ are taken about 2.50 cm and 0.142, respectively (Matsagar & Jangid, 2004; Rodellar & Manosa, 2003).

High-Damping Natural Rubber Systems (HDNR)

High damping rubber bearings are another category of elastomeric bearings. These bearings are made from a blend of filled natural rubber. The bearings are designed with flange type end plates to permit bolted structure and foundation connections. The natural rubber compound with enough inherent damping is developed in 1982 by the Malaysian Rubber Producers' Research Association (MRPRA) of the United Kingdom (Derham et al. 1985). The damping in this type of bearings is neither viscous nor hysteretic, but somewhat in between (Kelly & Naeim 1999).

Structural Model of the Base-Isolated Building

As shown in Figure 2, to study the performance of base isolation systems, the mathematical model of an N-story base-isolated building structure is idealized as a 2-D frame.

For this 2-D idealized frame, the governing equations of motion are obtained by considering the equilibrium of forces at the location of each degree of freedom, in which for a fixed base building (without any isolation system) can be written as (Naeim & Kelly, 1999):

$$M\{\ddot{X}\} + C\{\dot{X}\} + K\{X\} = -M\{R\}\ddot{x}_g \tag{5}$$

where M, C and K are the $n \times n$ mass, damping and stiffness matrices of the main structure, respectively; $\{X\}$ is the $n \times 1$ displacement vector of the building with respect to the ground; $\{R\}$ is the $n \times 1$ influence vector with unit elements in the direction of the earthquake motion; $\ddot{x}_g$ is the longitudinal acceleration of earthquake, acting on base of the main structure; and dot

Figure 2. Mathematical model of N-story base-isolated building structure (Pourzeynali & Zarif, 2008).

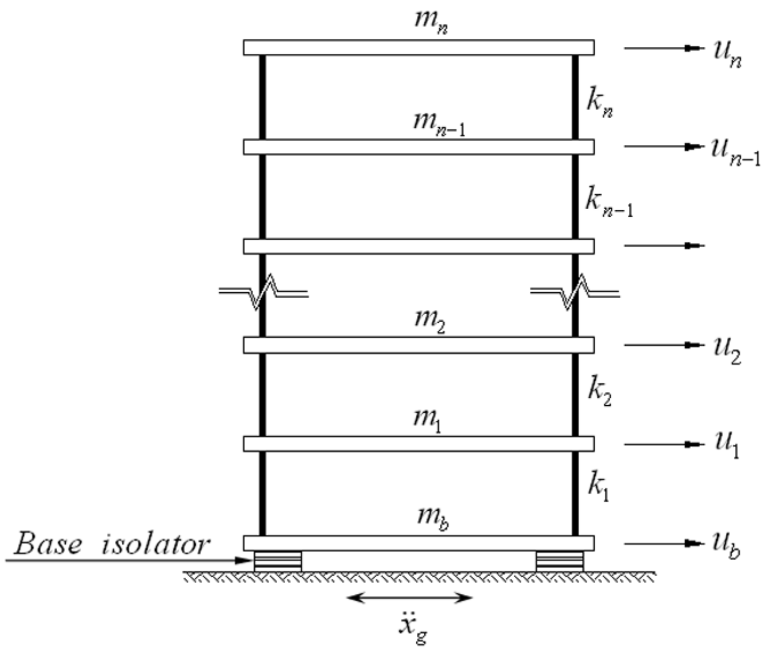

denotes to the time derivative. While for a seismically isolated structure with the base mass m_b the governing equation of motion of the building alone can be written as (Naeim & Kelly, 1999):

$$M\{\ddot{V}\} + C\{\dot{V}\} + K\{V\} = -M\{R\}\left(\ddot{x}_g + \ddot{v}_b\right) \tag{6}$$

where $\{V\}$ is the displacement vector of the building stories relative to the base slab; and v_b is the relative displacement of the base slab with respect to the ground. As well, the overall equation of motion of the combined building and base slab can be written as follow (Naeim & Kelly, 1999)

$$\begin{aligned} &\{R\}^T M\{\ddot{V}\} + (\sum_{i=1}^{n} m_i + m_b)\ddot{v}_b + \\ &c_b\dot{v}_b + k_b v_b = -(\sum_{i=1}^{n} m_i + m_b)\ddot{x}_g \end{aligned} \tag{7}$$

where n is the number of stories of the building; k_b and c_b are the stiffness and damping of the base isolator system; m_i is the mass of the building ith story; and m_b is the mass of the base slab.

This procedure of modeling the base isolated building is valid for linear behavior of the isolator systems given in detail by Kelly (1996).

By combining Equations (6) and (7) the general equation of motion of the combined seismically isolated building structure and the base slab, in the matrix format, can be expressed as the following (Naeim & Kelly, 1999):

$$M^*\{\ddot{V}^*\} + C^*\{\dot{V}^*\} + K^*\{V^*\} = -M^*\{R^*\}\ddot{x}_g \tag{8}$$

in which

$$M^* = \begin{bmatrix} m_s & \{R^T\}M \\ M\{R\} & M \end{bmatrix},\ C^* = \begin{bmatrix} c_b & \{0\}^T \\ \{0\} & C \end{bmatrix},\ K^* = \begin{bmatrix} k_b & \{0\}^T \\ \{0\} & K \end{bmatrix}$$
$$R^* = \begin{bmatrix} 1 \\ \{0\} \end{bmatrix},\ V^* = \begin{bmatrix} v_b \\ \{V\} \end{bmatrix} m_s = m_b + \sum_{i=1}^{n} m_i \tag{9}$$

where $\{0\}$ is a zero vector.

In order to solve the Equation (5), it is written in state space as given in the following:

$$\{\dot{Z}\} = A_1 \{Z\} + B_1 \{P\} \tag{10}$$

where $\{Z\}$ is the state vector; and A_1, B_1 and $\{P\}$ are, respectively, the state matrix, input matrix, and input vector given in the following:

$$\{\mathbf{Z}\} = \begin{Bmatrix} \{X\} \\ \{\dot{X}\} \end{Bmatrix} \tag{11a}$$

$$A_1 = \begin{bmatrix} 0 & I \\ -M^{-1}K & -M^{-1}C \end{bmatrix}$$
$$B_1 = \begin{bmatrix} 0 \\ I \end{bmatrix} \quad and \quad \{P\} = -\{R\}\ \ddot{x}_g(t) \tag{11b}$$

where I is an identity matrix.

The same procedure is performed for solving the Equation (8). Damping matrix of the building is also calculated using the well known Rayleigh method.

Numerical Analysis

It is well known that the base isolation systems are more effective for low buildings with low dominant vibrational periods, but in this study, their effect is studied on medium-height buildings. For this purpose, a 2-D realistic ten-story steel building frame, located in Mashhad, Iran, is selected. For this 2-D idealized frame, the mass and stiffness matrices are calculated using matrix analysis procedure. Damping matrix of the building is also calculated using the well known Rayleigh method, and for calculating the proportionality coefficients, modal damping ratios of the first two modes are assumed to be about 2% of the critical value (Pourzeynali & Zarif, 2008).

Furthermore, it should be noted that all ten vibrational modes of the building are considered in the analysis, from which the first 5 modal frequencies are given as: 1.46, 3.86, 6.27, 8.69, and 10.84 Hz.

The base isolated building is analyzed under action of the accelerogrames mentioned earlier, and the results are compared with those of fixed base building. In this step, the structural parameters of the base isolation system are taken from the references (Matsagar & Jangid, 2003; Matsagar & Jangid, 2004) as the initial values, given in the following (Pourzeynali & Zarif, 2008):

$$m_0 = m_b / m_1 = 1.0 \quad , \quad k_0 = k_b / k_1 = 0.10 \quad ,$$
$$\xi_b = c_b / (2 * m_s * \omega_b) = 0.10 \;, \quad \omega_b = \sqrt{k_b / m_s}$$

where ξ_b, is the damping ratio of base isolation system; m_1 and k_1 are the mass and stiffness of the building first story; m_0 and k_0 are the mass and stiffness ratios of the base isolation system to that of the building first story; ω_b is the natural circular frequency of the base isolation system; and m_s is given in Equation (9).

By considering the above values, equations of motion of the building are solved and the results are compared for both fixed base, and base isolated building supported on isolators with linear behavior in Tables 2 and 3, respectively (Pourzeynali & Zarif, 2008). It should be mentioned that, for brevity, only the results of the four most important earthquakes (e. g., Kobe, El Centro, Loma Prieta, and Northridge Earthquakes), as well as the ensemble average values of the responses for 18 reference earthquakes are shown in the tables.

As it is seen from the tables, displacements of the isolated building significantly are reduced. In this case, in average 43.74% reduction is obtained on building top story horizontal displacement

Table 2. Stories displacements (m) in the fixed-base building (Pourzeynali & Zarif, 2008)

Earthquake	Stories of the building									
	1st	**2nd**	**3rd**	**4th**	**5th**	**6th**	**7th**	**8th**	**9th**	**10th**
Kobe	0.049	0.094	0.141	0.186	0.227	0.269	0.307	0.339	0.365	0.378
El Centro	0.020	0.038	0.057	0.073	0.088	0.104	0.120	0.134	0.145	0.151
Loma prieta	0.035	0.067	0.098	0.171	0.153	0.179	0.202	0.222	0.237	0.245
Northridge	0.025	0.049	0.075	0.101	0.126	0.152	0.178	0.201	0.220	0.230
Ensemble average responses (m)	**0.0302**	**0.0578**	**0.0856**	**0.1304**	**0.1340**	**0.1573**	**0.1791**	**0.1996**	**0.2004**	**0.2245**

Table 3. Horizontal displacements (m) of the isolated building supported on elastomeric bearings with linear behavior (Pourzeynali & Zarif, 2008)

Earthquake	Stories of the building										
	Base	**1st**	**2nd**	**3rd**	**4th**	**5th**	**6th**	**7th**	**8th**	**9th**	**10th**
Kobe	0.173	0.034	0.064	0.093	0.120	0.144	0.168	0.189	0.208	0.223	0.230
El Centro	0.094	0.018	0.033	0.048	0.060	0.072	0.084	0.094	0.103	0.111	0.114
Loma Prieta	0.139	0.026	0.049	0.071	0.090	0.108	0.126	0.141	0.154	0.165	0.170
Northridge	0.132	0.024	0.042	0.058	0.070	0.082	0.098	0.113	0.127	0.139	0.145
Ensemble average responses (m)	0.099	0.019	0.036	0.052	0.066	0.078	0.092	0.104	0.114	0.122	0.126
Ensemble average reduction ratios (%)	------	**36.94**	**38.45**	**39.88**	**49.6**	**41.35**	**41.61**	**42.08**	**42.95**	**39.06**	**43.74**

response. The problem associated with this type of vibrational response protection system is that still the base displacement in comparison with that of the building stories is relatively high (Pourzeynali & Zarif, 2008).

Now, using a genetic algorithm (GA) optimizer, parameters of the isolators including their stiffness, damping, and the base mass are calculated to simultaneously minimize both the building top story and base isolators displacements using a multi-objective optimization procedure given in the following section. For this purpose, the variation domains (domain constraints) of the design parameters are assumed as (Pourzeynali & Zarif, 2008):

$$D_{m_0} = [0.10\ ,\ 1.50]\ ,\ D_{\xi_b} = [0.02\ ,\ 0.30]\ ,$$
$$D_{k_0} = [0.02\ ,\ 0.20]$$

in which D_{m0}, $D_{\xi b}$ and D_{k0} are, respectively, the domains of mass, damping, and stiffness ratios of the base isolators.

Multi-Objective Optimization by Considering Linear Behavior of the Bearings

In this section, in order to simultaneously minimize both the building top story displacement and that of the base isolation system, a multi-objective GA optimizer is used. For this purpose, first using a single objective GA optimizer, each of the objective functions separately is minimized. Then, using a fast and elitist non-dominated sorting genetic algorithm (NSGA-II) approach is used to find Pareto-optimal solutions in Pareto space (Pourzeynali & Zarif, 2008).

As the GA is a stochastic search methodology, it is difficult to formally specify convergence criteria. In practice, the common rule is to terminate the GA after a predefined number of generations and then test the quality of solutions. If the solutions are not acceptable, then the GA may be restarted by more generation numbers or by taking fresh initial values. For single objective GA optimizer the following parameters are chosen (Gen & Cheng, 1997):

- Number of chromosomes = 25
- Number of generations = 300
- Probability of crossover, $P_c = 0.25$
- Probability of mutation, $P_m = 0.01$

The GA iterations terminated after 300 generations and the best results for the parameters of base isolators are obtained as (Pourzeynali & Zarif, 2008):

$$m_0 = 1.20 \quad , \quad k_0 = 0.05 \quad , \quad \xi_b = 0.25$$

The results of the isolated building responses for four selected earthquakes, as well the ensemble average values of its stories responses for the 18 reference earthquakes, all optimized by GA, are shown in Table 4. In last row of the table the ensemble average reduction ratios on building stories displacements are also shown. It is seen from the table that NSGA-II is significantly effective in minimizing the objective functions and calculating the design parameters. It can be seen that in average a reduction of 64.47% is obtained on building top story horizontal displacement response (Pourzeynali & Zarif, 2008).

Multi-Objective Optimization by Considering Non-Linear Behavior of the Bearings

Herein, the material non-linearity of the isolator bearings has been taken into account by assuming that the lead rubber bearings have been used. For simplification, the non-linear hysteretic curve of the bearings, as shown in Figure 1, is divided into two linear parts (bilinear models).

Main parameters of the bilinear isolators are: the base mass shown by m_b (similar linear case); isolator stiffness in elastic phase shown by k_{b1}, and its stiffness in plastic phase k_{b2}; its time period in elastic phase and after yielding shown by

Table 4. Controlled responses (Optimized by GA) of the isolated building supported on linear isolators (Pourzeynali & Zarif, 2008)

Earthquake	Stories of the building										
	Base	1st	2nd	3rd	4th	5th	6th	7th	8th	9th	10th
Kobe	0.303	0.051	0.075	0.088	0.094	0.099	0.104	0.110	0.113	0.116	0.118
El Centro	0.168	0.025	0.044	0.056	0.063	0.068	0.073	0.082	0.090	0.095	0.097
Loma Prieta	0.207	0.032	0.053	0.065	0.070	0.074	0.084	0.094	0.100	0.104	0.107
Northridge	0.475	0.064	0.098	0.117	0.131	0.144	0.154	0.167	0.174	0.178	0.183
Ensemble average responses (m) (Optimized by GA)	0.115	0.025	0.022	0032	0.081	0.050	0.058	0.066	0.072	0.077	0.080
Ensemble average Reduction Ratios (%)	-------	**53.10**	**61.80**	**62.36**	**59.20**	**62.80**	**63.00**	**63.34**	**63.95**	**61.50**	**64.47**

T_{b1} *and* T_{b2}, respectively, which can be calculated by Equation (12); and the yield displacement, v_y, which can be calculated for different isolators by experiments. Also, the ratio of k_{b2}/k_{b1}, defined as γ, can be obtained from experiments.

In this study, the values of v_y and γ are assumed to be about 2.5 cm and 0.142, respectively, given in references (Matsagar & Jangid, 2004; Rodellar & Manosa, 2003). Finally, damping ratio of elastic phase ξ_{b1} and that of the plastic phase ξ_{b2} are defined by Equation (13).

$$T_{b_1} = 2\pi\sqrt{(m_s/k_{b_1})} \quad , \; T_{b_2} = 2\pi\sqrt{(m_s/k_{b_2})} \tag{12}$$

$$\xi_{b_1} = c_b\, T_{b_1} \,/\, (4\,\pi\, m_s) \quad , \; \xi_{b_2} = c_b\, T_{b_2} \,/\, (4\,\pi\, m_s) \tag{13}$$

Here also the same parameters of the linear isolators have been chosen for GA optimizer:

- Number of initial populations = 25
- Number of generations = 300
- P_c=0.25
- P_m=0.01

In order to apply the multi-objective genetic algorithm optimizer, first using a single objective GA, each of the objective functions is optimized and the results are shown in Figure 3 for displacement of the building top story and that of the base isolators. Then, using these results the Pareto-optimal front diagram is obtained (Figure 4), from which the following optimal values are evaluated for bilinear isolators (Pourzeynali & Zarif, 2008):

$$k_0 = k_{b1} / k_1 = 0.40, \; m_0 = m_b / m_1 = 0.35,$$
$$\xi_{b_1} = 0.19, \quad \xi_{b_2} = 0.50$$

Table 5 shows the controlled responses of the building stories for four selected earthquakes; ensemble average responses for 18 reference earthquakes; as well as, ensemble average reduction ratios for the same reference earthquakes calculated for all stories of the building. It is seen

Figure 3. Performance of the genetic algorithm with single objective function: (a) Maximum displacement of bilinear base isolator; (b) Maximum displacement of the isolated building top story

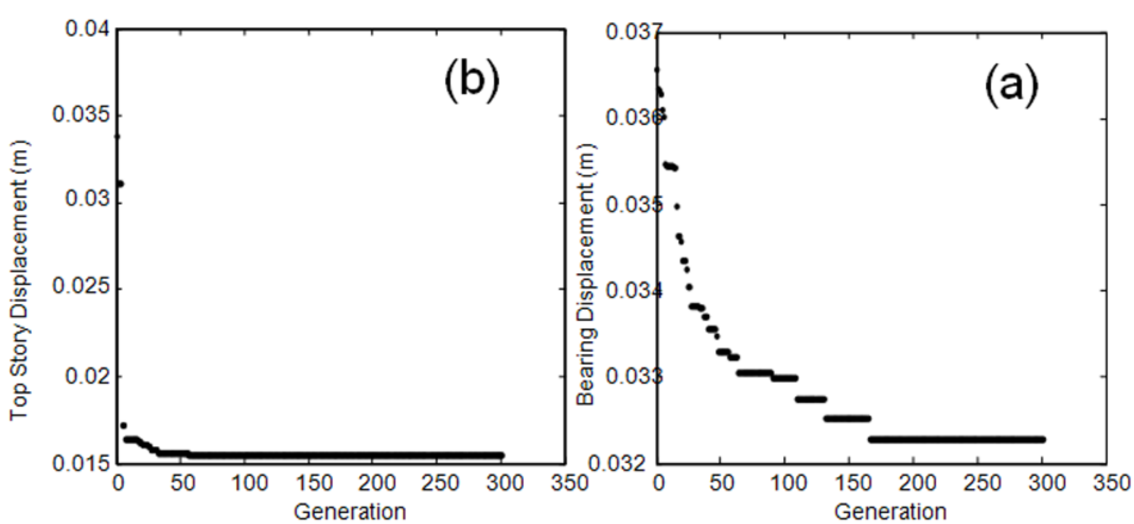

Figure 4. Optimal points of Pareto front and design range for bilinear isolators (× Feasible range), (● Pareto front)

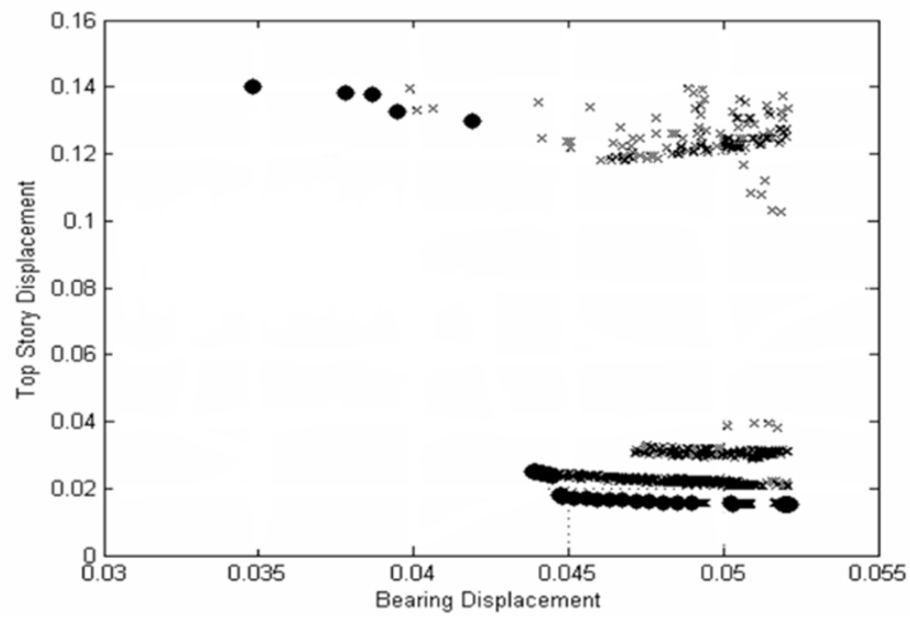

from the table that bilinear base isolators provide more reduction on building responses in comparison with the linear ones. In average 71.68% reduction is obtained on building top story horizontal displacement response (Pourzeynali & Zarif, 2008).

The results obtained from linear and bilinear modeling of the base isolators show that bilinear model needs more stiffness for base isolators in comparison with the linear model, while for this case the mass of the base slab is less. The damping ratio in elastic phase of the bilinear model is also slightly less than that of the linear one.

Table 5. Horizontal displacements (m) of the isolated building by considering non-linearity of the bearings and optimized by GA

Earthquakes	Stories of the building										
	Base	**1st**	**2nd**	**3rd**	**4th**	**5th**	**6th**	**7th**	**8th**	**9th**	**10th**
Kobe	0.151	0.010	0.015	0.022	0.028	0.033	0.038	0.043	0.047	0.052	0.056
El Centro	0.289	0.025	0.040	0.054	0.061	0.064	0.067	0.070	0.071	0.073	0.074
Loma prieta	0.201	0.041	0.063	0.072	0.079	0.084	0.087	0.089	0.091	0.093	0.096
Northridge	0.271	0.024	0.038	0.051	0.058	0.062	0.065	0.067	0.068	0.068	0.068
Ensemble average responses (m) (Optimized by GA)	0.218	0.018	0.029	0.037	0.044	0.049	0.052	0.056	0.059	0.062	0.064
Ensemble average reduction ratios (%)	-------	**34.71**	**49.50**	**56.45**	**66.44**	**63.84**	**67.05**	**68.71**	**70.46**	**69.34**	**71.68**

SEMI-ACTIVE TUNED MASS DAMPER SYSTEM

The modern concept of tuned mass dampers (TMDs) for reduction of structural vibrations, indeed, is the development of the undamped dynamic vibration absorber studied as early as 1909 by Frahm (Frahm 1909; Den Hartog 1956). Frahm's dynamic absorber was consisting of a small mass m and a spring with spring stiffness k attached to the main mass M with spring stiffness K. Under a simple harmonic load, it can be shown that the main mass M can be kept completely stationary if the natural frequency $\left(\sqrt{\frac{k}{m}}\right)$ of the attached absorber is chosen to be (or tuned to) the excitation frequency (Soong & Dargush, 1997; Grover 1996).

Den Hartog (Ormondroyd and Den Hartog, 1928) first studied the theory of undamped and damped dynamic vibration absorbers without considering damping in the main system, and developed the basic principles and the procedure for proper selection of absorber parameters. Bishop and Welbourn (1952) continued the above procedure by considering the damping in the main system. Then in 1967, Falcon et al. performed an optimization procedure to obtain minimum peak response and maximum effective damping in the main system (Soong & Dargush, 1997).

A translatory–rotary absorber system has been numerically studied by Jennige and Frohrib (1977) to control both bending and torsional modes in a building structure. Then Ioi and Ikeda (1978) developed empirical formulas for correction factors of these optimum absorber parameters by considering light damping in the main system. Warburton and Ayorinde (1980) performed another study to introduce further optimum values of the maximum dynamic amplification factor, tuning frequency ratio, and absorber damping ratio for specified values of the mass ratio and the main system damping ratio (Soong and Dargush, 1997).

Most of the above studies have related to the use of dynamic vibration absorbers in mechanical systems. While application of these systems in civil engineering structures, frequently known as tuned mass damper (TMD) systems, is expected to be different. In last decades, many research studies have been performed to show the effectiveness of the TMD system and the other control devices, derived from TMD, such as: semi-active tuned mass dampers (STMDs) and active tuned mass dampers (ATMDs) in civil engineering community in reducing the structural responses, some of which are reviewed in the following.

The tuned mass damper (TMD) system is a typical form of control devices including a mass, spring, and a viscous fluid damper, which can be attached to the main structure at one of its degrees of freedom. This system is one of the well-accepted devices to control flexible structures, particularly, tall buildings. In this passive control system, if its damping ratio or stiffness of the spring changes with time, then it is called a semi-active tuned mass damper (STMD).

Wirsching and Campbell (1974) evaluated the optimal values of the TMD parameters for one-story, and ten story building structures. It has been shown that the optimum values of TMD stiffness becomes less sensitive to structural damping and mass ratio when the number of stories increases; and the optimum TMD damping is insensitive to structural damping even for one–story buildings (Soong and Dargush, 1997).

Huffmann et al. (1987) investigated the effectiveness of two separate TMDs, installed in the center of a bridge deck, to reduce flexural and torsional vibrations. Each TMD was tuned to the corresponding eigenfrequency. Nobuto et al. (1988) performed a study to suppress the coupled flutter of long-span bridges using a 2-TMD model. They showed that the TMD frequency should be tuned to the frequency of the torsional mode of the bridge.

Warburton (1982) proposed optimal design of the TMD under different types of loads. Sadek et al. (1997) provided a single-degree-of-freedom model of the one which Villaverde et al. offered. Rana and Soong (1998) studied about TMD systems with steady-state harmonic excitation and used time-history analysis to find optimum parameters of TMD. Pourzeynali & Datta (2002) studied control of flutter of suspension bridge deck using TMD system. Cao and Li (2004) studied the application of active TMD system to control flexible structures, particularly, tall buildings. Pourzeynali and Esteki (2009) performed a comprehensive research study on optimization of the TMD parameters to suppress the vertical vibration of suspension bridges subjected to earthquake excitations.

The TMDs are undoubtedly reliable, simple and they do not require external power source, so their construction cost is low (Pinkaew & Fujino, 2001); but, inasmuch as the parameters of TMD system are constant, if there is any changes in loading conditions, then this system may not be able to control the vibrations properly. Therefore, the need to a system which is capable to be changed with different conditions is fully felt.

The semi-active tuned mass dampers (STMDs) can compensate the limitation of the passive and active systems. Various studies confirm the efficiency of STMDs and show that the application of TMDs is much better when they behave as STMDs, especially in wind and earthquake excitations. Therefore, modeling procedure of the STMD system automatically includes modeling of the TMD system which uses the passive fluid viscous damper. The theory of TMD system has been used for the first time by Frahm (1909) to reduce the movement of a structure subjected to monotonic harmonic forces reviewed above. Hrovat et al. (1983) used STMDs for the control of tall buildings against wind pressure. Kelly and Hasegawa (1992) have proposed STMD with controllable dynamic characteristics. Abe and Igusa (1996) developed analytical theory for optimum control algorithms for semi-active absorbers. Hidaka et al. (1999) investigated the operation of various dynamic absorbers which use ER liquid. Agrawal and Yang (2000) proposed particular tools namely semi-active algorithms to protect unstable structures which are subjected to near field earthquakes. Pinkaew and Fujino (2001) studied controlling effects of STMDs with different dampers for single-degree-of-freedom systems which are subjected to harmonic excitations. Lin et al. (2005) suggested a new semi-active control system that used variable damping and MR damping. Mulligan et al. (2006; & 2007) studied spectral analysis and the probabilistic design of STMDs. In these systems, the stiffness or the damping ratio of the control device changes proportional to the relative displacement or relative velocity, by receiving information from sensors in every second (Mulligan, 2007). Therefore, they do not require large power supply and they do not add additional energy to the main structure and guarantee stability of the system. In order to regulate the stiffness or the damping ratio of the STMD, fuzzy systems can be used. Pourzeynali and Datta (2005) studied application of STMD system to control the suspension bridge flutter using fuzzy logic.

In the present study, the STMD system is considered with variable damping produced by a semi-active fluid viscous damper. Fluid viscous damper, which is used in TMD system, is a device to absorb part of the input energy in buildings and reduce possible structural damage during the earthquake excitations. A passive fluid viscous damper is similar to the shock absorber in automobiles. The configuration of this damper includes a hydraulic cylinder filled with a damping fluid like silicone or oil and a piston head with a small orifice. As the damper strokes, the damping fluid flows through the orifice at high speed from one side to the other, and produces a damping pressure which creates a damping force. A semi-active fluid damper can be achieved by adding an external bypass loop which contains a controllable valve to a passive fluid damper. The behavior of the semi-active fluid damper is essentially similar to passive fluid damper, except that the semi-active fluid damper has an external valve which connects two sides of the cylinder and modulates the output force. In this kind of damper, adjustable damping property makes them capable to generate wide range of damping force. Since a small power or source just used for closing or opening external valve, it can produce very large damping force without need of large input energy and can therefore operate on batteries (Pourzeynali & Mousanejad 2010).

Structural Modeling of the Building

For a structure with a TMD and n degrees of freedom is subjected to earthquakes, the equations of motion can be given as (Cao & Li, 2004)

$$\begin{aligned} M\{\ddot{X}\} + C\{\dot{X}\} + K\{X\} = \\ -M\{R\}\ddot{x}_g + \{l\}(c_d\dot{x}_{rd} + k_d x_{rd}) \end{aligned} \tag{14}$$

$$m_d\ddot{x}_{rd} + c_d\dot{x}_{rd} + k_d x_{rd} = -m_d\{l\}^T\{\ddot{X}\} - m_d\ddot{x}_g \tag{15}$$

where x_{rd} is relative displacement of the TMD with respect to the top floor. m_d, k_d and c_d are the mass, stiffness and damping of TMD, respectively; and $\{l\}$ is the $n \times 1$ location vector of the control device.

The response of the building is depended on its mode shapes and natural frequencies and can be simulated by dominant modes. According to the reference (Zuo & Nayfeh, 2003) the first mode shape is dominant in earthquake excitation if modal frequencies are well-separated. But in this study, three first frequencies of the example building are very close, thus, three first modes of the main structure are considered for accurate modeling of the building; therefore, the displacement vector can be expressed as

$$\{X(t)\} = \sum_{i=1}^{3}\{\varphi\}_i y_i(t) \tag{16}$$

where $\{\varphi\}_i$ is the i^{th} column of the modal matrix, Φ, and $y_i(t)$ is the i^{th} generalized modal coordinate of the structure. Therefore, the equation of the motion for the three first modes can be written as follows:

$$\begin{aligned} \widehat{M}\{\ddot{y}(t)\} + \widehat{C}\{\dot{y}(t)\} + \widehat{K}\{y(t)\} = \\ -\{L\}\ddot{x}_g + [\varphi]_3^T\{l\}(c_d\dot{x}_{rd} + k_d x_{rd}) \end{aligned} \tag{17}$$

and

$$\begin{aligned} \widehat{M} = [\varphi]_3^T M[\varphi]_3, \ \widehat{C} = [\varphi]_3^T C[\varphi]_3, \\ \widehat{K} = [\varphi]_3^T K[\varphi]_3, \ \{L\} = [\varphi]_3^T M\{R\} \end{aligned} \tag{18}$$

where $[\varphi]_3$ is a matrix obtained from combination of three first mode shapes of the building. In order to optimally design of the TMD parameters, the mass of TMD is assumed as a part of total mass of the building $(m^t_{Building})$ which can be expressed as

$$m_d = m_0' \times m^t_{Building} \tag{19}$$

It should be noted that to design a proper TMD that be to absorb the entrance energy, its frequency should be tuned close to the considered frequencies of the building. In this study three first building frequencies are very close to each other, and therefore, the frequency of TMD, ω_d, can be designed based on the ratio (β) of the first mode frequency of the building,

$$\omega_d = (\beta \times \omega_1) \tag{20}$$

The damping coefficient of the TMD can be expressed as

$$c_d = 2 \times \xi_{tmd} \times \sqrt{(m_d \times k_d)} \tag{21}$$

Then m_0', β and ξ_{tmd} are considered as the design variables in the multi-objective optimization procedure.

The equation of motion of the building with a semi active tuned mass damper (STMD) control device is the same as the structure with TMD, but in this case the damping ratio of STMD is a time varying, and can be expressed as $\xi_{stmd}(t)$ which can be regulated by a fuzzy logic system, briefly described in the following.

Fuzzy Logic Controller

In this study, damping ratio of the STMD is regulated by a fuzzy logic controller. For the first time, Fuzzy set theory was proposed by Lotfi Zadeh in 1965 (Zadeh, 1965). Fuzzy set theory allows objects to have a degree of membership within a set, while traditional mathematics requires objects to have either 0 or 100 per cent membership within a set. As a result, fuzzy controller, which is based on the fuzzy set theory, is a reliable method to deal with the imprecision and uncertainty that is often present in real-world applications. Nowadays, fuzzy systems are used in a wide range of science and technology such as control, signal processing and etc. Important information of practical systems originates from two sources: the first one is experiences of human beings that define their knowledge about the systems with natural language; and the another source is measurement and mathematical models derived from physical rules. Fuzzy systems are knowledge-based or rule-based systems. The main part of a fuzzy system is a knowledge database which is composed of IF-THEN rules based on classical control theories. A fuzzy system consists of four parts, the fuzzifier, the fuzzy rule base, the inference engine, and the defuzzifier. The fuzzy rule base in this study is based on a Mamdani linguistic fuzzy model which can be written as:

$$R^i : IF\ x_1\ \ is\ \ A_{1i}\ \ AND\ \ x_2\ is\ \ A_{2i}\ \ THEN\ \ y\ \ is\ \ B \tag{22}$$

where x_1 and x_2 are input linguistic variables, y is the output linguistic variable; and A_{1i}, A_{2i}, and B are the values for each input linguistic variables and output linguistic variable, respectively. In this study, x_1 and x_2 are the displacement and velocity of the top floor, respectively; and y is the damping ratio of the STMD system. The design of a fuzzy system involves decisions about a number of important design parameters that should be determined before the actual system starts. These parameters are the fuzzy sets in the rules, the rules themselves, scaling factor in input and output, inference methods, and defuzzification procedures (Pourzeynali et al., 2007). Because of a crisp number for real application, defuzzifier maps the system output from the fuzzy domain into the crisp domain. The center of area (COA) and the mean of maximum (MOM) are the two most commonly used methods in generating the crisp system output (Shin & Xu, 2009). In this study, the center of area method is selected to produce the crisp system output in discrete universe of discourse (Shin & Xu, 2009):

$$x^* = \frac{\sum_{i=1}^{q} x_i . \mu_A\left(x\right)}{\sum_{i=1}^{q} \mu_A\left(x_i\right)} \tag{23}$$

where q is the number of the discreet elements in the universe of discourse; x_i is the value of discrete element; and $\mu_A\left(x_i\right)$ offers the corresponding membership function value at the point x_i. To achieve a fuzzy system with minimum design variables, the ideas proposed by Park et al. (1995) is used. In this method, the membership functions are considered as triangular membership functions and since often dynamic systems such as vibratory buildings behavior are symmetric, the number of membership functions should be odd which are symmetric with respect to the vertical axis. Therefore, for input and output variables, five triangular membership functions are considered. In order to design these membership functions it is assumed that all universes of discourses are normalized to lie between -1 and 1, and the first and last membership functions have their apexes at -1 and 1, respectively. Also, the apex of each triangle is in one point with the tip base of two lateral triangles, and as respects, the universe of discourse is laid between -1 and 1, so the position of the apexes of each triangular membership function $\left(C_i\right)$ can be found with the parameter P_s and the number of membership functions as bellow

$$C_i = \left(\frac{i}{n_1}\right)^{Ps},\ n_1 = \frac{N-1}{2},\ i = -n_1, ..., 0, 1, ..., n_1 \tag{24}$$

where N is the number of membership functions. It can be concluded that if P_s is less than one the centers are spaced out and if P_s is more than one, the centers are closed together in the center. Figure 5 depicts five membership functions with three different P_s values.

Another design challenge of fuzzy systems is to find the rule bases of the system. There are different strategies to get the rule bases, which most of them are often based on the experiences and knowledge of human beings, but, in intelligent design methods such as design with genetic algorithms, some characteristic parameters are considered to design rule bases. In this research, according to the reference (Park et al., 1995), two characteristic parameters are used which one is spacing parameter P_i for the inputs and the output, and the other one is the angle θ for inputs. The spacing parameter P_i determines the layout of different values of the inputs towards the origin (zero point). Therefore, the space parameter, P_i, grids the rule base space, so that these lines divide this region into different regions with the number of output linguistic variables. If the values of the

Figure 5. Designed membership functions with different P_s

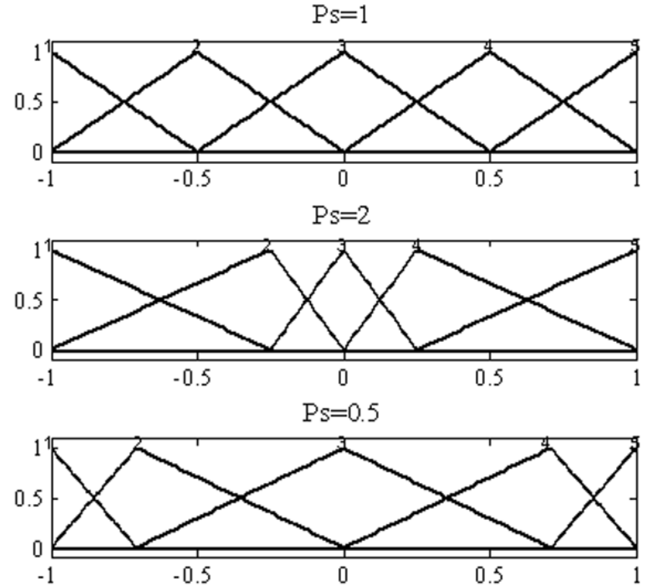

inputs are considered as: big negative (BN), small negative (SN), zero (Z), small positive (SP), and big positive (BP), and if the space between *SP* and *Z* is *a*, and that of the *SP* and *BP* is *b*, then the parameter P_i is defined as (Figure 6):

$$P_i = \frac{b}{a} \tag{25}$$

According to the symmetry between the inputs variables, the space between *SN* and *Z*, and the space between *SN* and *BN* are also *a* and *b*, respectively. Referring to Equation (25), if P_i is more than one, then the *SP* value is close to zero, and if P_i is less than one, then the *SP* value is far from the zero, and if P_i is equal to one, then the inputs values are placed with the same intervals respect to each other and to zero. These concepts are shown in Figure 7.

The angle θ is measured with respect to the horizon for the grid lines which divide the rule base space into different regions with the number of output linguistic variables. For example, in Figure 7, the angle θ is 45 degrees for all cases. In this method, it will be assumed that if the inputs are zero, then the output is, also, zero and if the inputs have their maximum value, then the output is, also, maximum. By considering above assumptions, output linguistic variables place in various regions according to Figure 7. As a result, for each combination of input linguistic variables, proper output is equal to the amount which is located in the desired area. As an example, according to Figure 7, if the first input is *SP* and the second input is *BN*, then the output is zero. Table 6 shows the obtained fuzzy rule base from Figure 7a. As mentioned, the output of the fuzzy system is $\xi_{stmd}(t)$. It has five triangular membership functions which lie between 0 and 0.5. Therefore, the damping value can guarantee the stability of the structure, and STMD system always acts as an under damped system. The design variables are P_s, P_i, θ, m_0, β and $\xi_{stmd}(t)$ that should be designed by multi-objective optimization method.

Numerical Study

In order to evaluate the performance of the proposed control devices (STMD/TMD), a reality 12-story steel building is considered and modeled as a 3-D frame, and analyzed under application of 7 earthquake accelerogrames presented in Table 1.

Three non-commensurable objective functions namely, maximum displacement, maximum velocity, and maximum acceleration of each floor are considered as the objective functions to be minimized simultaneously by multi-objective optimization process. These objective functions are expressed in the following:

$$J_1 = \max_i \left[\max_t \left(\left| D_i^c(t) \right| \Big/ \left| D_i^{uc}(t) \right| \right) \right] \tag{26}$$

Figure 6. Definition of the parameter P_i

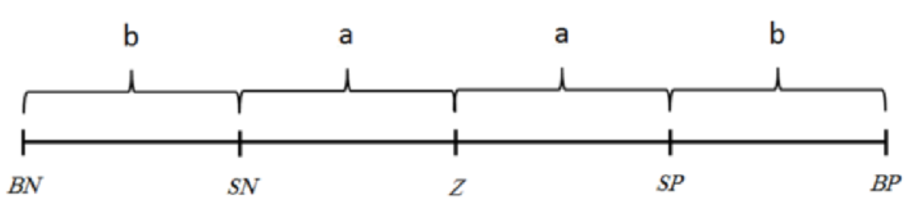

Figure 7. Rule base construction with a) $P_i = 1$, b) $P_i > 1$, c) $P_i < 1$

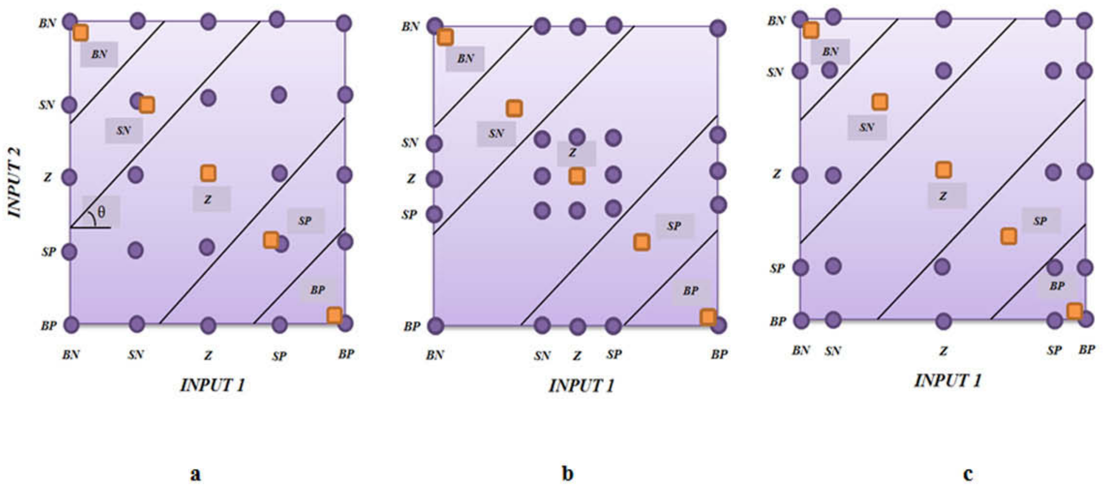

$$J_2 = \max_i \left[\max_t \left(\left| V_i^c(t) \right| \Big/ \left| V_i^{uc}(t) \right| \right) \right] \tag{27}$$

$$J_3 = \max_i \left[\max_t \left(\left| A_i^c(t) \right| \Big/ \left| A_i^{uc}(t) \right| \right) \right] \tag{28}$$

where $i = 1, \ldots, 12$ indicates the number of floors of the building; and $D_i^c(t)$, $D_i^{uc}(t)$, $V_i^c(t)$, $V_i^{uc}(t)$, $A_i^c(t)$ and $A_i^{uc}(t)$ are the displacement, velocity and acceleration of each floor of the building in controlled and uncontrolled case, respectively.

Table 6. Fuzzy rule-bases

Input	*BN*	*SN*	*Z*	*SP*	*BP*
BN	*BN*	*BN*	*Z*	*Z*	*Z*
SN	*BN*	*SN*	*Z*	*Z*	*Z*
Z	*SN*	*Z*	*Z*	*Z*	*SP*
SP	*Z*	*Z*	*Z*	*SP*	*BP*
BP	*Z*	*Z*	*SP*	*BP*	*BP*

It should be noted that it is impossible to illustrate the trade-off points when we consider more than two objective functions are being considered. To solve this difficulty, several multidimensional visualization methods are proposed. One of these methods which leads to comprehensive analysis of the Pareto front is called Level Diagrams method (Blasco et al., 2008) which is used here in to visualize the Pareto fronts of the multi-objective optimization.

In this method, each point of Pareto front must be normalized to bring them between 0 and 1 based on its minimum and maximum values (Blasco et al., 2008) as

$$J_i^M = \max J_i \ , \ J_i^m = \min J_i \ , \ i = 1, 2, 3$$
$$\bar{J}_i = \frac{J_i - J_i^m}{J_i^M - J_i^m} \tag{29}$$

The distance of each Pareto front point from origin can be used for comparison. Here, the Euclidean norm of all objective functions $\left(\left\| \bar{J} \right\|_2 = \sqrt{\sum_{i=1}^{3} \bar{J}_i^2} \right)$ is used for this purpose. To represent the Pareto front, Y axis is specified for the Euclidean norm of all objective functions and X axis is specified for each objective function; therefore, each objective function has its own graphical representation whilst Y axis of each graph would be the same. The Pareto fronts for Kobe earthquake are shown in Figures 8, 9, and 10 for STMD system.

It is obvious from Figure 8 that the point with the lowest value of J_1 has high value of objective function J_2 (Figure 9), this issue is true about the point with the lowest value of J_2 in comparison with its value for J_1, so there is a conflict between J_1 and J_2. Likewise, there is conflict between J_1 and J_3, also J_2 and J_3; as a result, three objective functions are in conflict with each other. This subject shows the Pareto concept. Therefore, selected point with the lowest value of $\|J\|_2$ is a good compromise point, because it has intermediate value of three objective functions. The maximum values of the displacement, velocity, and acceleration of each floor of the building under Kobe earthquake with lowest $\|J\|_2$ for the TMD and STMD systems are shown in Figures 11, 12, and 13.

The results of the maximum displacement, velocity, and acceleration of each floor of the building for the lowest J_1, J_2 and J_3 are the same as the results of the other point (min $\|J\|_2$). It can be concluded form Figures 11-13 that the STMD device has better performance and is more reliable in comparison with the TMD device. Moreover, Figures 14, 15, and 16 compare the uncontrolled time history responses of top floor of the building under Kobe earthquake with those controlled by STMD system for the design point with lowest value of the $\|J\|_2$. It can be seen from the figures that STMD system significantly reduces the vibrational responses of the building.

The values of the design parameters of the TMD and STMD devices and the corresponding values of the objective functions for optimum point with the lowest value of $\|J\|_2$ for Kobe

Figure 8. 2-norm level diagrams of Pareto front of the STMD for Kobe earthquake (J_1)

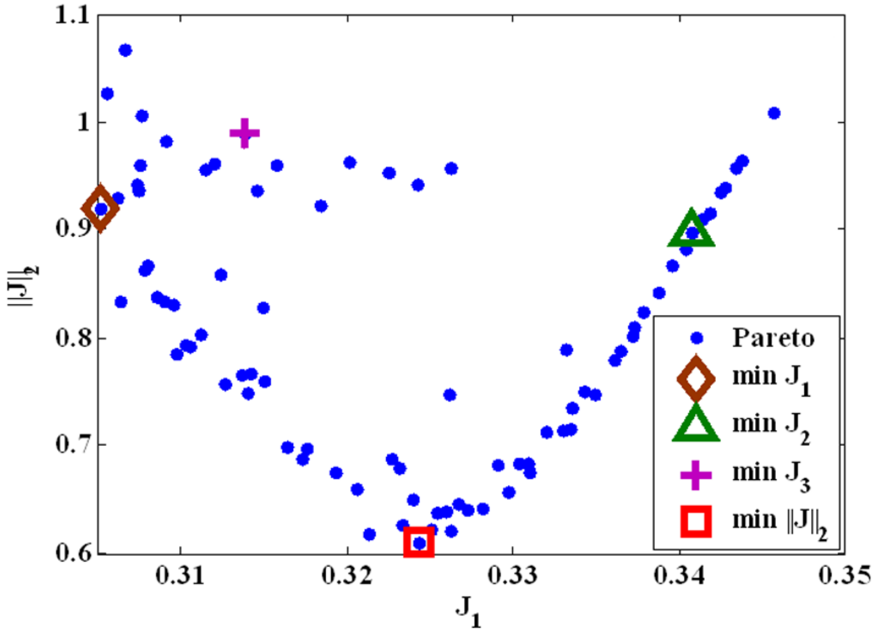

Figure 9. 2-norm level diagrams of Pareto front of the STMD for Kobe earthquake (J_2)

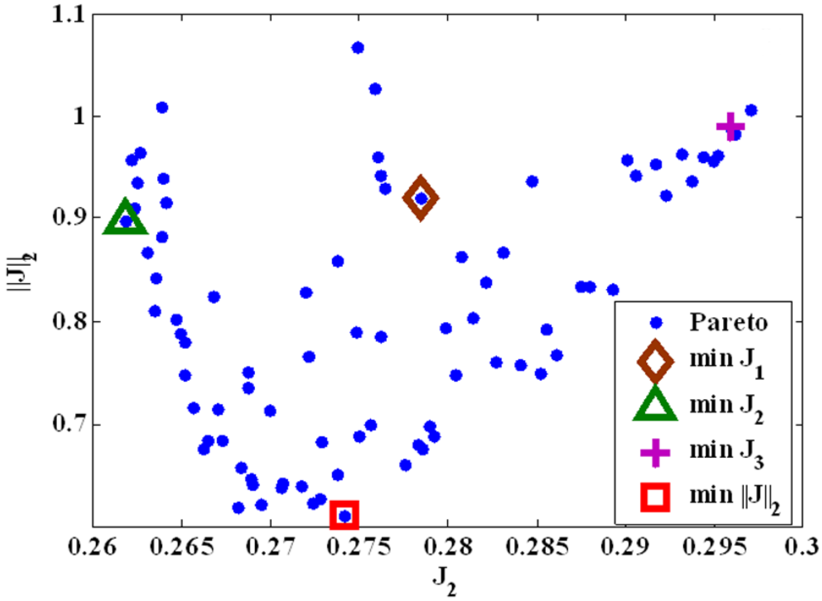

Figure 10. 2-norm level diagrams of Pareto front of the STMD for Kobe earthquake (J_3)

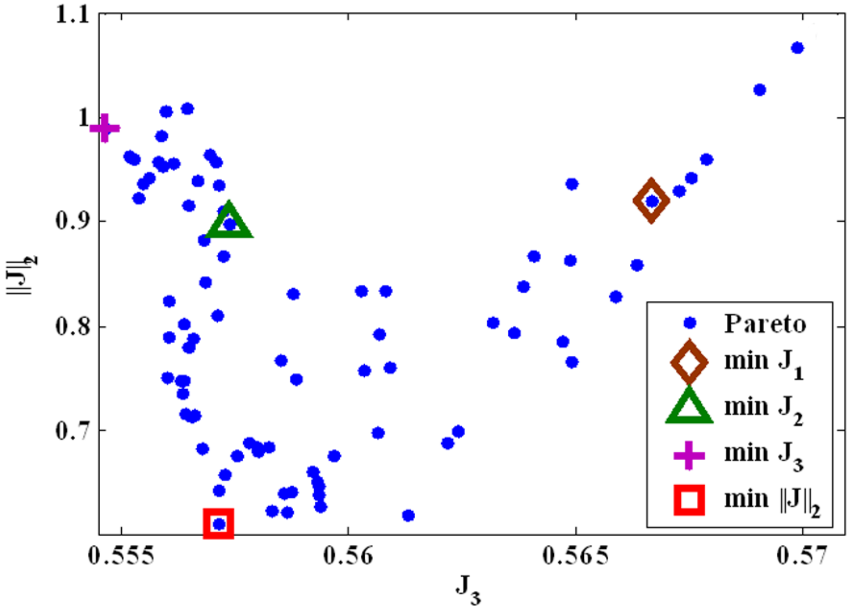

Figure 11. The responses of the building under Kobe earthquake with the optimum point with lowest $||J||_2$ *maximum displacement of each floor*

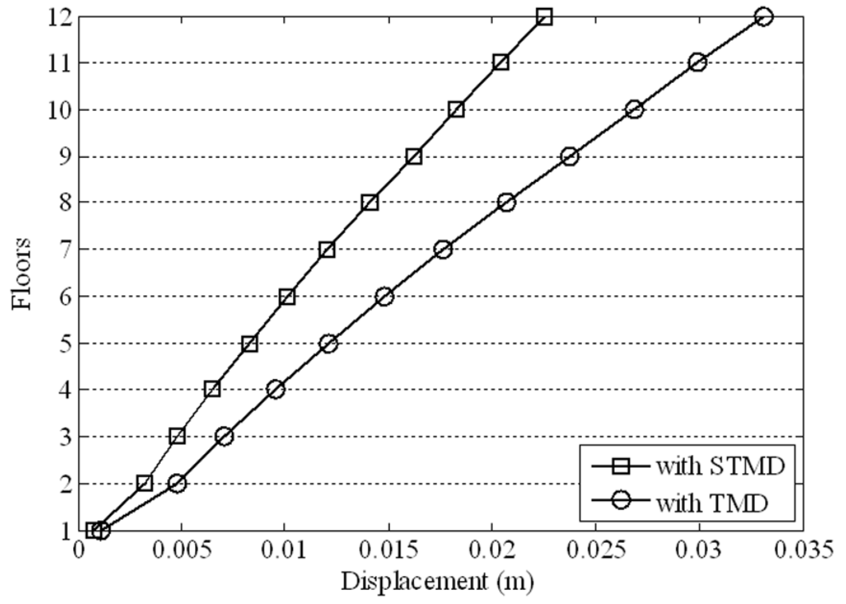

Figure 12. The responses of the building under Kobe earthquake with the optimum point with lowest $||J||_2$ *maximum velocity*

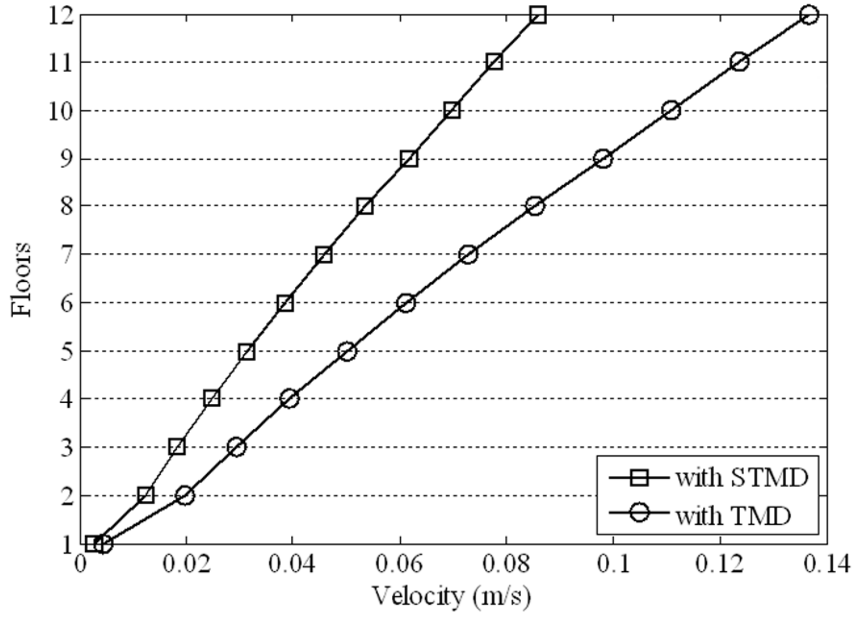

Figure 13. The responses of the building under Kobe earthquake with the optimum point with lowest $||J||_2$ *maximum acceleration*

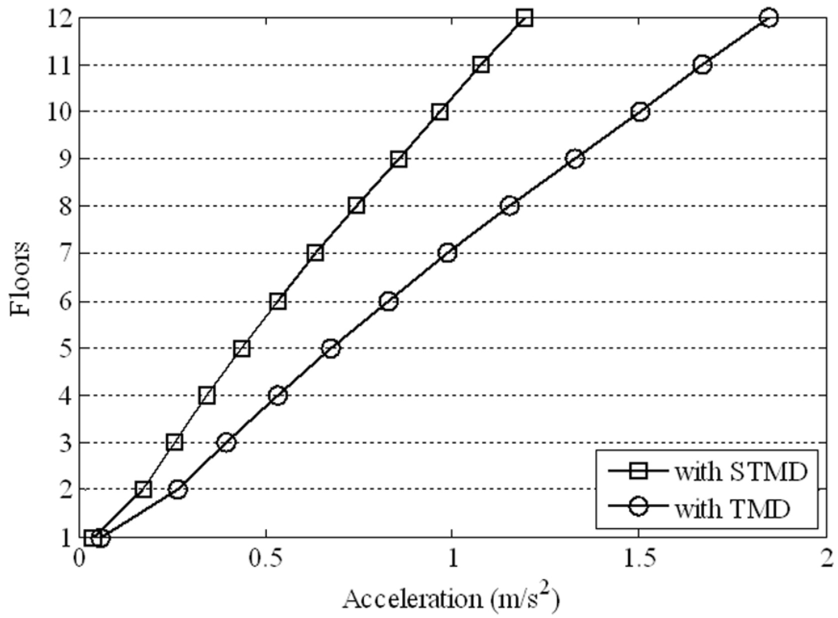

Figure 14. The time history responses of the building under Kobe earthquake with the optimum point with lowest $||J||_2$ *for STMD system compared with those of the uncontrolled ones (displacement)*

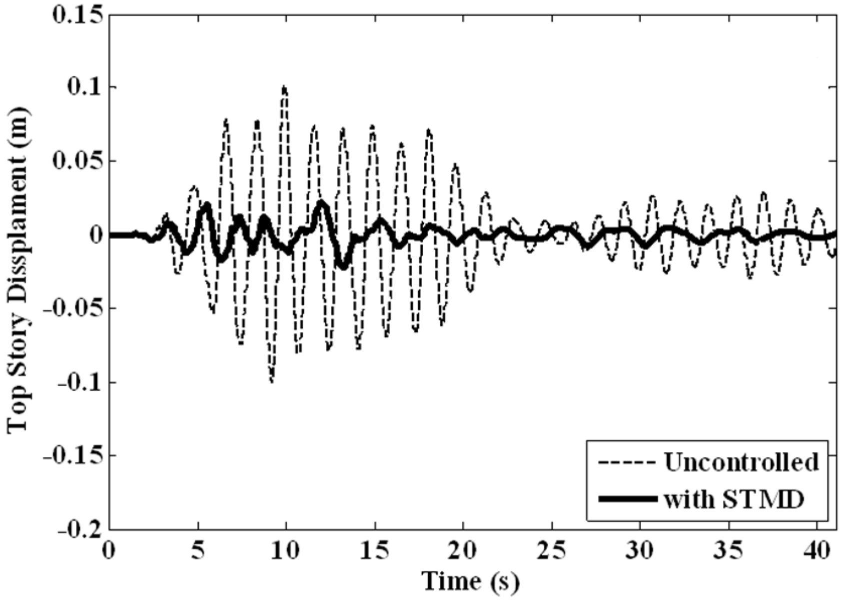

Figure 15. The time history responses of the building under Kobe earthquake with the optimum point with lowest $||J||_2$ for STMD system compared with those of the uncontrolled ones (velocity)

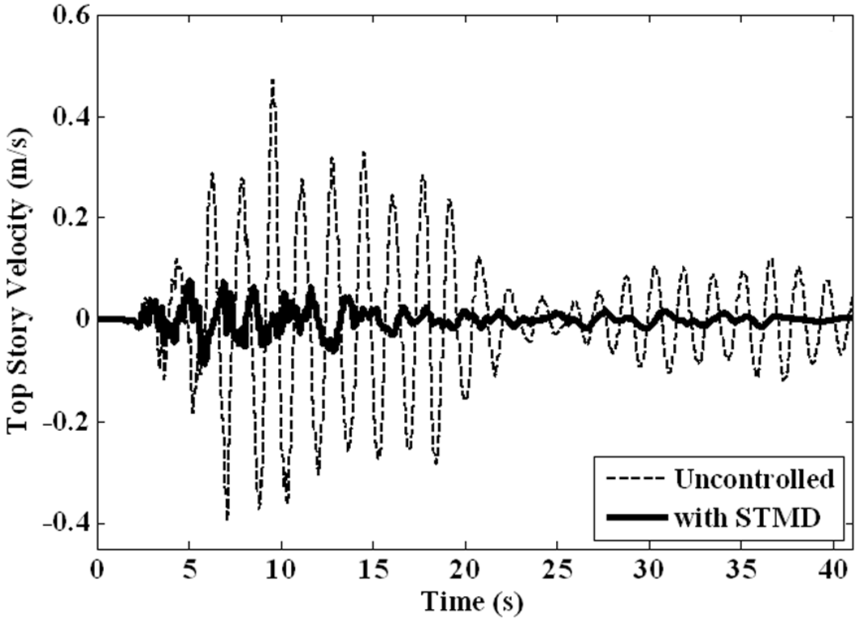

Figure 16. The time history responses of the building under Kobe earthquake with the optimum point with lowest $||J||_2$ for STMD system compared with those of the uncontrolled ones (acceleration of top floor)

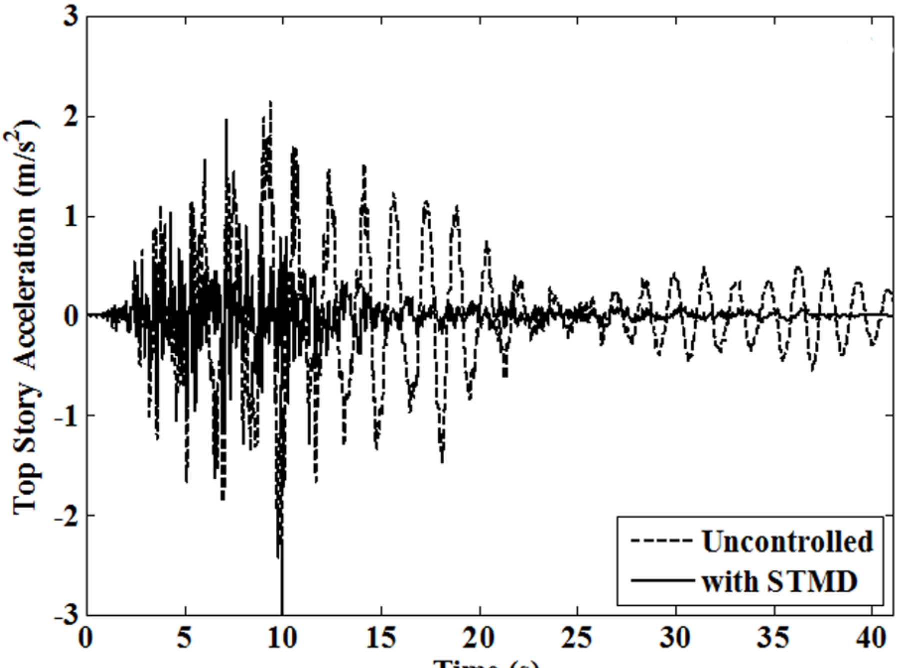

earthquake are given in Table 7 and Table 8, respectively. The time history diagram of the fuzzy tuned damping ratio of the selected optimum STMD device is shown in Figure 17. Referring to Table 8, it can be concluded that the results of the STMD system are approximately 36 percent less than those of the TMD system.

Table 9 compares the responses of the example building equipped with STMD and TMD control systems. It can be seen from the table that the average values of displacement, velocity and acceleration of the building with STMD has been decreased approximately about 61%, 73%, and 60%, respectively. It also shows the comparison of the performance of the TMD and STMD in reduction of the building responses for seven different earthquake excitations. The percentages of reduction in Table 9 are defined as $(1 - x^c / x^{uc})$ where x^c is the controlled response, and x^{uc} is the uncontrolled one.

CONCLUSION

In this chapter, multi-objective optimization of the dynamic response of base-isolated building structures, as well buildings equipped with STMD and TMD control systems are studied. The isolated building is modeled as a 2-D, planar-shear frame having one lateral degree of freedom at each story level; while the building equipped with STMD/TMD is modeled as a 3-D frame having 3 degrees of freedom, two translational and one torsional, in each story level.

In isolated building, elastomeric bearing supports are considered as one additional degree of freedom with three unknown parameters: base mass, stiffness, and damping ratio. In order to calculate the building response, the governing equations of motion of the system are solved in state-space. The building's top story horizontal displacement and that of the base isolation system are considered as the objective functions to be simultaneously minimized. The base isolators' mass, stiffness, and damping ratio are evaluated using GAs which take into account the linear and nonlinear behaviors of the isolator bearings. For this purpose, a fast and elitist NSGA-II approach is used to find a set of Pareto-optimal solutions. For a numerical example, a realistic ten-story building, located in Mashhad, Iran, was chosen and studied under action of 18 worldwide earthquake accelerogrames. From the results of the numerical studies, it is found that:

Table 7. The optimum values of design parameters evaluated for STMD/TMD devices

	P_{s1}	P_{s2}	P_{i1}	P_{i2}	$\theta(rad)$	m_0	ω_d	ξ_{tmd}	max of ξ_{STMD}
TMD						0.009	4.12	0.12	
STMD	1.82	1.79	0.59	0.82	1.52	0.009	4.01		0.33

Table 8. The values of objective functions for optimum point with lowest $||J||_2$ for STMD /TMD systems

	J_1	J_2	J_3	$\|\|J\|\|_2$
TMD	0.32	0.28	0.61	0.61
STMD	0.21	0.18	0.37	0.41

Figure 17. Time history diagram of the fuzzy tuned damping ratio

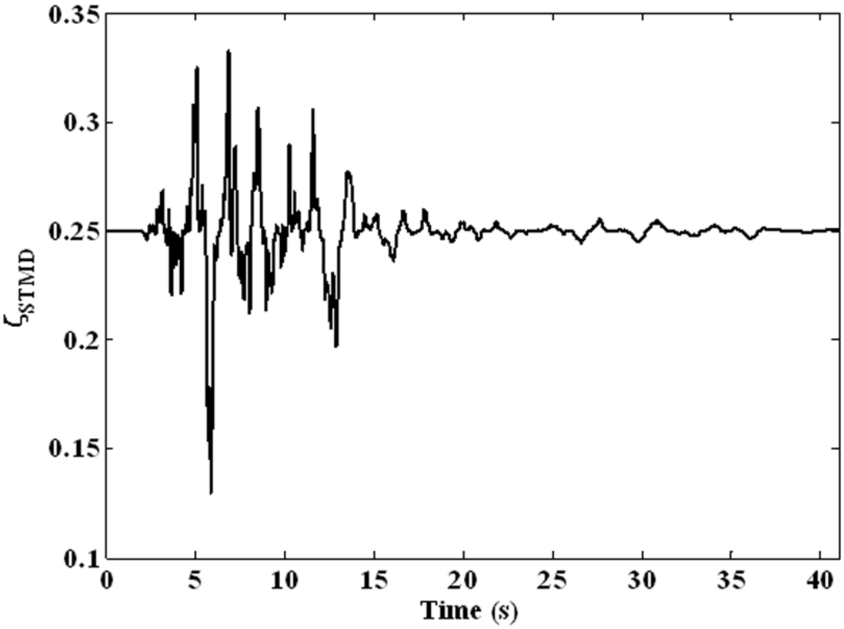

Table 9. Ratio of maximum displacement, velocity and acceleration of the STMD to the TMD and the percentage of reduction of them in seven earthquake excitations

STMD/TMD	Max controlled Displacement (m)	Percentage of reduction		Max controlled Velocity (m/s)	Percentage of reduction		max controlled Acceleration (m/s²)	Percentage of reduction	
		STMD	TMD		STMD	TMD		STMD	TMD
Kocaeli	0.08/0.12	67%	48%	0.21/0.32	80%	70%	1.17/1.82	77%	64%
Chi-Chi	0.05/0.06	51%	38%	0.15/0.21	65%	51%	1.36/1.72	40%	24%
Duze	0.06/0.1	58%	31%	0.15/0.22	72%	58%	1.28/1.88	55%	34%
Kobe	0.02/0.03	78%	75%	0.09/0.12	81%	58%	1.19/1.62	50%	33%
Cape Men-docino	0.06/0.1	56%	29%	0.22/0.31	62%	46%	1.05/1.63	57%	34%
Northridge	0.05/0.06	53%	32%	0.12/0.17	70%	57%	1.16/1.69	51%	29%
Coalinga	0.06/0.09	61%	42%	0.19/0.26	71%	60%	1.28/2.32	64%	34%
Average	**0.03/0.08**	**61%**	**42%**	**0.11/0.26**	**73%**	**61%**	**1.31/1.86**	**60%**	**40%**

- Multi-objective optimization using the NSGA-II approach is a powerful method to design the parameters of the base isolators to make the isolation system more effective.
- By calculating the parameters of the linear base-isolation system using GAs, a reduction of 64.5% is obtained for the ensemble average value (calculated for 18 worldwide earthquakes) of the building's top story horizontal displacement response.
- By considering the nonlinearity of the lead-rubber bearings and optimizing their parameters using GAs, further reduction can be obtained for the building's top story horizontal displacement. However, due to the lead-rubber bearings' plastic deformation, the horizontal displacement of the base system increases.

In buildings equipped with STMD/TMD systems also the multi-objective optimization method using GAs has been used for optimally design of the STMD and TMD control systems; and damping ratio of the STMD system is regulated by a fuzzy logic controller. The multi-objective optimization of these systems led to the discovering of some important trade-offs among the objective functions. Based on the multi-objective GAs of this work, the point which has the lowest value of the Euclidean norm of all objective functions is used to compare the application of two devices. An example 12-story building is analysed under seven different earthquake accelerogrames to investigate the effects of STMD/TMD systems, and the values of the controlled and uncontrolled responses are compared. From results of the numerical studies it is found that:

- The STMD system is more reliable than the TMD and its performance is better than TMD device. The optimum values of the mass ratio are obtained about 0.9% for both TMD and STMD, and the damping ratio is obtained to be about 12% for TMD; and as the damping ratio of STMD is variable with time, therefore its maximum value is obtained to be about 33%.
- The confliction exists between the objective functions lets the designer to choose the proper point for designing with establishment compromise between the objective functions.
- The results obtained from simulation show reduction about 60-73% for maximum value of displacement, velocity and acceleration of the example building controlled by STMD, and about 40-61% for that of the TMD. Therefore, the results represent superiority of STMD in comparison with TMD.

REFERENCES

Abe, M., & Igusa, T. (1996). Semiactive dynamic vibration absorbers for controlling transient response. *Journal of Sound and Vibration*, *198*, 547–569. doi:10.1006/jsvi.1996.0588

Agrawal, A. K., & Yang, J. N. (2000). Semiactive control strategies for building subject to near-field earthquakes. *Proceedings of SPIE 3988, Vol. 359. Smart Structures and Materials 2000: Smart Systems for Bridges, Structures, and Highways* (pp. 359-370). Newport Beach, CA, USA.

Atashkari, K., Nariman-zadeh, N., Jamali, A., & Pilechi, A. (2005). Thermodynamic Pareto optimization of turbojet using multi-objective genetic algorithm. *International Journal of Thermal Sciences*, *44*(11), 1061–1071. doi:10.1016/j.ijthermalsci.2005.03.016

Bishop, R. E. D., & Webourn, D. B. (1952). The problem of the dynamic vibration absorber. *Engineering*, *174*, 769.

Blasco, X., Herrero, J. M., Sanchis, J., & Martinez, M. (2008). A new graphical visualization of n-dimensional Pareto front for decision-making in multiobjective optimization. *Information Sciences*, *178*(20). doi:10.1016/j.ins.2008.06.010

Branke, J. (1998). Creating robust solutions by means of an evolutionary algorithm. *Proceedings of the International Conference on Parallel Problem Solving from Nature*, (pp. 119–128).

Cao, H., & Li, Q. S. (2004). New control strategies for active tuned mass damper systems. *Computers & Structures*, *82*, 2341–2350. doi:10.1016/j.compstruc.2004.05.010

Cao, H., Reinborn, A. M., & Soong, T. T. (1998). Design of an active mass damper for a tall TV tower in Nanjing, China. *Engineering Structures*, *20*(3), 134–143. doi:10.1016/S0141-0296(97)00072-2

Chey, M. H., Chase, J. G., Mander, J. B., & Carr, A. J. (2009). *Energy-dissipative semi-active tuned mass damper building systems for structural damage reduction*. Paper presented at the International Symposium.

Datta, T. K. (1996). *Control of dynamic response of structures*. Indo-US Symposium on Emerging Trends in Vibration and Noise Engineering, 18-20 March.

Deb, K., Agrawal, S., Pratap, A., & Meyarivan, T. (2002). A fast and elitist multi-objective genetic algorithm: NSGA-II. *IEEE Transactions on Evolutionary Computation*, *6*(2), 182–197. doi:10.1109/4235.996017

Deb, K., & Gupta, H. (2004). *Introducing robustness in multi-objective optimization*. Technical Report (KanGAL Report No. 2004016), Department of Mechanical Engineering, Indian Institute of Technology, Kanpur, India.

Derham, C. J., Kelly, J. M., & Thomas, A. G. (1985). Nonlinear natural rubber bearings for seismic isolation. *Nuclear Engineering and Design*, *84*(3), 417–428. doi:10.1016/0029-5493(85)90258-4

Falcon, K. C., Stone, B. J., Simcock, W. D., & Andrew, C. (1967). Optimization of vibration absorbers: A graphical method for use on idealized systems with restricted damping. *Journal of Mechanical Engineering Science*, *9*, 374–381. doi:10.1243/JMES_JOUR_1967_009_058_02

Fonseca, C. M., & Fleming, P. J. (1993). Genetic algorithms for multi-objective optimization: formulation, discussion and generalization. In S. Forrest (Ed.), *Proceedings of the Fifth International Conference on Genetic Algorithms*, Morgan Kaufmann, San Mateo, CA, (pp. 416–423).

Frahm, H. (1911). *Devices for damping vibrations of bodies*. U.S. Patent, 989, 958.

Gen, M., & Cheng, R. (1997). *Genetic algorithms and engineering design*. John Wiley & Sons Inc.

Grover, G. K. (1996). *Mechanical vibrations* (6th ed.). Roorkee, India: University of Roorkee.

Hidaka, S., Ahn, Y. K., & Morishita, S. (1999). Adaptive vibration control by a variable-damping dynamic absorber using ER fluid. *Journal of Vibration and Acoustics*, *121*, 373–378. doi:10.1115/1.2893990

Hrovat, D., Barak, P., & Rabins, M. (1983). Semi-active versus passive or active tuned mass damper for structural control. *Journal of the Engineering Mechanics Division*, *109*, 691–705. doi:10.1061/(ASCE)0733-9399(1983)109:3(691)

Huffmann, G., Freeman, R. A., & Brown, C. W. (1987). Dao Khanong cable stayed bridge: Tuned mass dampers in deck and pylon. *Proceedings of International Conference on Cable Stayed Bridges*, Bangkok, (pp. 1485-93).

Ioi, T., & Ikeda, K. (1978). On the dynamic vibration damped absorber of the vibration system. *Bulletin of Japanese Society of Mechanical Engineering*, *21*(151), 64–71. doi:10.1299/jsme1958.21.64

Jennige, R. L., & Frohrib, D. A. (1977). Alternative tuned absorbers for steady state vibration control of tall structures. *Journal of Mechanical Design*, *77*(84), 1–7.

Kelly, J. M. (1986). Aseismic base isolation: A review and bibliography. *Soil Dynamics and Earthquake Engineering*, *5*, 202–216. doi:10.1016/0267-7261(86)90006-0

Kelly, J. M. (1996). *Earthquake-resistant design with rubber* (2nd ed.). London, UK: Springer-Verlag.

Kelly, J. M., & Hasegawa, K. (1992). *Application of a mass damping system to bridge structures*. Report No. UCB/EERC 92/12. Berkeley, CA: Earthquake Engineering Research Center.

Kelly, J. M., Skinner, R. I., & Heine, A. J. (1972). Mechanisms of energy absorption in special devices for use in earthquake resistant structures. *Bulletin of the New Zealand National Society for Earthquake Engineering*, *5*, 78–89.

Kelly, J. M., & Tsztoo, D. F. (1977). Energy absorbing devices in structures under earthquake loading. *6th World Conference on Earthquake Engineering*, New Delhi, Vol. 2, (pp. 139-1374).

Kelly, T. E. (2001). *Base isolation of structures: Design guidelines*. Holmes Consulting Group Ltd.

Knowles, J., & Corne, D. (1999). The Pareto archived evolution strategy: A new baseline algorithm for multi-objective optimization. *Proceedings of the 1999 Congress on Evolutionary Computation, IEEE Service Center,* Piscataway, NJ, (pp. 98–105).

Lin, P. Y., Chung, L. L., & Loh, C. H. (2005). Semiactive control of building structures with semiactive tuned mass damper. *Computer-Aided Civil and Infrastructure Engineering*, *20*, 35–51. doi:10.1111/j.1467-8667.2005.00375.x

Matsagar, V. A., & Jangid, R. S. (2003). Seismic response of base-isolated structures during impact with adjacent structures. *Engineering Structures*, *25*, 1311–1323. doi:10.1016/S0141-0296(03)00081-6

Matsagar, V. A., & Jangid, R. S. (2004). Influence of isolator characteristics on the response of base-isolated structures. *Engineering Structures*, *26*, 1735–1749. doi:10.1016/j.engstruct.2004.06.011

Mulligan, K. (2007). *Experimental and analytical studies of semi-active and passive structural control of buildings*. PhD Thesis, University of Canterbury, Christchurch, New Zealand.

Mulligan, K., Chase, J. G., Mander, J. B., Fougere, M., Deam, B. L., Danton, G., & Elliot, R. B. (2006). Hybrid experimental analysis of semi-active rocking wall systems. *Proceedings of the New Zealand Society of Earthquake Engineering Conference (NZSEE)*, Napier, New Zealand.

Mulligan, K., Miguelgorry, M., Novello, V., Chase, J. G., Mander, J. B., & Rodgers, G. … Horn, B. (2007). *Semi-active tuned mass damper systems.* 19th Australasian Conference on Mechanics of Structures and Materials (ACMSM), Christchurch, New Zealand.

Naeim, F., & Kelly, J. M. (1999). *Design of seismic isolated structures, Earthquake resistant design.* Nabuto, J., Fujino, Y., & Ito, M. (1988). A study of the effectiveness of TMD to suppress a coupled flutter of bridge deck. *Journal of JSCE, October*, 413-16.

Ormondroyd, J., & Den Hartog, J. P. (1928). The theory of the dynamic vibration absorber. *Transactions of the American Society of Mechanical Engineers*, *50*, 9–22.

Park, Y. J., Cho, H. S., & Cha, D. H. (1995). Genetic algorithm-based optimization of fuzzy logic controller using characteristic parameters. *Proceedings of the IEEE International Conference on Evolutionary Computation* (pp. 831-836).

Pinkaew, T., & Fujino, Y. (2001). Effectiveness of semi-active tuned mass dampers under harmonic excitation. *Engineering Structures*, *23*(7), 850–856. doi:10.1016/S0141-0296(00)00091-2

Pourzeynali, S., & Datta, T. K. (2002). Control of flutter of suspension bridge deck using TMD. *International Journal of Wind and Structure*, *5*(5), 407–422.

Pourzeynali, S., & Datta, T. K. (2005). Semi active fuzzy control of suspension bridge flutter. *Journal of Structural Engineering*, *131*(6), 900–912. doi:10.1061/(ASCE)0733-9445(2005)131:6(900)

Pourzeynali, S., & Esteki, S. (2009). Optimization of the TMD parameters to suppress the vertical vibrations of suspension bridges subjected to earthquake excitations. *Iranian International Journal of Engineering*. *IJE Transaction B (Application)*, *22*(1), 23–34.

Pourzeynali, S., Lavasani, H. H., & Modarayi, A. H. (2007). Active control of high rise building structures using fuzzy logic and genetic algorithms. *Engineering Structures*, *29*, 346–357. doi:10.1016/j.engstruct.2006.04.015

Pourzeynali, S., & Mousanejad, T. (2010). Optimization of semi-active control of seismically excited buildings using genetic algorithms. *Scientia Iranica, Transaction A*. *Civil Engineering (New York, N.Y.)*, *17*(1), 26–38.

Pourzeynali, S., & Zarif, M. (2008). Multi-objective optimization of seismically isolated high-rise building structures using genetic algorithms. *Journal of Sound and Vibration*, *311*, 1141–1160. doi:10.1016/j.jsv.2007.10.008

Rana, R., & Soong, T. T. (1998). Parametric study and simplified design of tuned mass dampers. *Engineering Structures*, *202*(3), 193–204. doi:10.1016/S0141-0296(97)00078-3

Robinson, W. H. (1982). Lead rubber hysteretic bearing suitable for protecting structures during earthquakes. *Earthquake Engineering & Structural Dynamics*, *10*, 593–604. doi:10.1002/eqe.4290100408

Rodellar, J., & Manosa, V. (2003). A robust tendon control scheme for a class of cable-stayed structures. *Proceedings of the 3rd Conference on Structural Control,* Vol. 3. (pp. 184-190). Como, Italy.

Sadek, F., Mohraz, B., Taylor, A. W., & Chung, R. M. (1997). A method of estimating the parameters of tuned mass dampers for seismic applications. *Earthquake Engineering & Structural Dynamics*, *26*, 617–635. doi:10.1002/(SICI)1096-9845(199706)26:6<617::AID-EQE664>3.0.CO;2-Z

Schaffer, J. D. (1985). Multiple objective optimization with vector evaluated genetic algorithms. In J. J. Grefenstette (Ed.), *Proceedings of the First International Conference on Genetic Algorithms and their Applications,* (pp. 93–100). London, UK: Lawrence Erlbaum.

Shin, Y. C., & Xu, C. (2009). *Intelligent systems modeling, optimization, and control*. New York, NY: Taylor & Francis Group.

Skinner, R. I., Kelly, J. M., & Heine, A. J. (1975). Hysteretic damper for earthquake resistant structures. *Earthquake Engineering & Structural Dynamics*, *3*(3), 287–296. doi:10.1002/eqe.4290030307

Soong, T. T., & Constantinou, M. C. (1994). *Passive and active structural vibration control in civil engineering*. New York, NY: Springer.

Soong, T. T., & Dargush, G. F. (1997). *Passive energy dissipation systems in structural engineering*. Chichester, UK: John Wiley & Sons Ltd.

Srinivas, N., & Deb, K. (1994). Multi-objective optimization using non-dominated sorting in genetic algorithm. *Evolutionary Computation*, *2*(3), 221–248. doi:10.1162/evco.1994.2.3.221

Symans, M. D., & Constantinou, M. C. (1999). Semi-active control systems for seismic protection of structures: A state-of-the-art review. *Engineering Structures*, *21*, 469–487. doi:10.1016/S0141-0296(97)00225-3

Tarics, A. G. (1984). *The implementation of base isolation for the Foothill Communities Law and Justice Center*. Report to NSF and County of San Bernardino, San Francisco.

Warburton, G. B. (1982). Optimum absorbers parameters for various combinations of response and excitation parameters. *Earthquake Engineering & Structural Dynamics*, *10*, 381–401. doi:10.1002/eqe.4290100304

Wirsching, P. H., & Campbell, G. W. (1974). Minimal structural response under random excitation using the vibration absorbers. *Earthquake Engineering & Structural Dynamics*, *2*, 303–312. doi:10.1002/eqe.4290020402

Yang, J. N., & Agrawal, A. K. (2002). Semi-active hybrid control systems for nonlinear buildings against near-field earthquakes. *Engineering Structures*, *24*, 271–280. doi:10.1016/S0141-0296(01)00094-3

Zadeh, L. A. (1965). Fuzzy sets. *Information and Control*, *8*, 338–353. doi:10.1016/S0019-9958(65)90241-X

Zitzler, E., & Thiele, L. (1998). *An evolutionary algorithm for multi-objective optimization: The strength Pareto approach.* Technical Report 43, Computer Engineering and Federal Institute of Technology, Zurich.

Zuo, L., & Nayfeh, S. (2003). The multi-degree-of-freedom tuned-mass damper for suppression of single-mode vibration under random and harmonic excitation. *ASME*. *Proceedings on Mechanical Vibration & Noise*, *5*, 2051–2061.

ADDITIONAL READING

Aldemir, U. (2003). Optimal control of structures with semiactive-tuned mass dampers. *Journal of Sound and Vibration*, *266*(4), 847–874. doi:10.1016/S0022-460X(03)00191-3

Alhan, C., & Gavin, H. (2004). A parametric study of linear and nonlinear passively damped seismic isolation system for buildings. *Engineering Structures*, *24*, 485–497. doi:10.1016/j.engstruct.2003.11.004

Branke, J., Deb, K., Miettinen, K., & Stowinski, R. (2008). *Multiobjective optimization interactive and evolutionary approaches*. Springer.

Branke, J., & Schmidt, C. (2005). Faster convergence by means of fitness estimation. *Soft Computing- A Fusion of Foundations*. *Methodologies and Applications*, *9*(1), 13–20.

Bryson, A. E., & Ho, Y. C. (1975). *Applied optimal control*. New York, NY: John Wiley and Sons, Inc.

Charng, P. H. (1998). *Base isolation for multistory building structures*. PhD Thesis, University of Canterbury, Christchurch.

Cordon, S., Herrera, F., Haffmann, F., & Magdalena, L. (2001). *Genetic fuzzy systems: Evolutionary tuning and learning of fuzzy knowledge bases* (*Vol. 19*). World Scientific Advances in Fuzzy Systems-Applications and Theory.

Deb, K. (2001). *Multi-objective optimization using evolutionary algorithms*. John Wiley & Sons Ltd.

Deb, K., & Gupta, H. (2004). *Introducing robustness in multi-objective optimization. Technical report (KanGAL report No. 2004016)*. Kanpur, India: Department of Mechanical Engineering, Indian Institute of Technology.

Fonesca, C. M., & Fleming, P. J. (1993). Genetic algorithms for multi-objective optimization: Formulation, discussion and generalization. In S. Forrest (Ed.), *Proceedings of the Fifth International Conference on Genetic Algorithms* (pp. 416-423). San Mateo, CA: Morgan Kaufmann.

Fukushima, I., Kobori, T., Sakamoto, M., Koshika, N., Nishimura, I., & Sasaki, K. (1996, September). *Vibration control of a tall building using active–passive composite tuned mass damper*. Paper presented at the Third International Conference on Motion and Vibration Control, 1-6, Chiba, Japan.

Hadi, M. N. S., & Arfiadi, Y. (1998). Optimum design of absorber for MDOF structures. *Journal of Structural Engineering*, *124*(11), 1272–1280. doi:10.1061/(ASCE)0733-9445(1998)124:11(1272)

Hoang, N., Fujino, Y., & Warnitchai, P. (2008). Optimal tuned mass damper for seismic applications and practical design formulas. *Engineering Structures*, *30*(3), 707–715. doi:10.1016/j.engstruct.2007.05.007

Hwang, J. S., & Chiou, J. M. (1996). An equivalent linear model of lead-rubber seismic isolation bearings. *Engineering Structures*, *18*(7), 528–536. doi:10.1016/0141-0296(95)00132-8

Jangid, R. S., & Datta, T. K. (1995). Seismic behavior of base isolated building: A state-of-the-art-review. *Structures and Buildings*, *110*(2), 186–203. doi:10.1680/istbu.1995.27599

Jangid, R. S., & Kelly, J. M. (2000). Torsional displacements in base-isolated buildings. *Earthquake Spectra*, *16*, 443–454. doi:10.1193/1.1586120

Ji, H. R., Moon, Y. J., Kim, C. H., & Lee, I. W. (2005, December). Structural vibration control using semiactive tuned mass damper. *The Eighteenth KKCNN Symposium on Civil Engineering-KAIST6* (pp. 18-20). Taiwan.

Kamrani-Moghaddam, B., Rahimian, M., & Ghorbani-Tanha, A. K. (2006, October). *Performance of tuned mass dampers for response reduction of structures under near-field and far-field seismic excitations.* Paper presented at the 4th International Conference on Earthquake Engineering, No. 112, Taipei, Taiwan.

Kelly, J. M. (1990). Base isolation: Linear theory and design. *Earthquake Spectra*, *6*, 223–244. doi:10.1193/1.1585566

Kim, Y. J., & Ghaboussi, J. (1999). A new method of reduced order feedback control using genetic algorithms. *Earthquake Engineering & Structural Dynamics*, *28*, 193–212. doi:10.1002/(SICI)1096-9845(199902)28:2<193::AID-EQE811>3.0.CO;2-X

Knowles, J., & Corne, D. (1999). The Pareto archived evolution strategy: A new base line algorithm for multi-objective optimization. In *Proceedings of the 1999 Congress on Evolutionary Computation* (pp. 98-105). Piscataway, NJ: IEEE Service Center.

Komodromos, P. (2000). *Seismic isolation for earthquake resistant structures*. Southampton, UK: WIT Press.

Komodromos, P., Polycarpou, P., Papaloizou, L., & Phocas, M. C. (2007). Response of seismically isolated buildings considering poundings. *Earthquake Engineering & Structural Dynamics*, *36*, 1605–1622. doi:10.1002/eqe.692

Koo, J. H., Ahmadian, M., Setareh, M., & Murray, T. (2003). In search of suitable control methods for semi-active tuned vibration absorbers. *Journal of Vibration and Control*, *10*, 163–174. doi:10.1177/1077546304032020

Lee, C. L., Chen, Y. T., Chung, L. L., & Wang, Y. P. (2006). Optimal design theories and applications of tuned mass dampers. *Engineering Structures*, *28*(1), 43–53. doi:10.1016/j.engstruct.2005.06.023

Liedes, T. (2009). *Improving the performance of the semi-active tuned mass damper. University of Oulu*. Finland: Oulu University Press.

Meirovitch, L. (1990). *Dynamics and control of structures*. New York, NY: John Wiley and Sons, Inc.

Murudi, M. M., & Mane, S. M. (2004, August). *Seismic effectiveness of tuned mass damper (TMD) for different ground motion parameters.* Paper presented at the 13th World Conference on Earthquake Engineering, No. 2325, Vancouver, B.C., Canada.

Rudinger, F. (2006). Tuned mass damper with fractional derivative damping. *Engineering Structures*, *28*, 1774–1779. doi:10.1016/j.engstruct.2006.01.006

Sadek, F., Mohraz, B., Taylor, A. W., & Chung, R. M. (1997). A method of estimating the parameters of tuned mass dampers for seismic applications. *Earthquake Engineering & Structural Dynamics*, *26*, 617–635. doi:10.1002/(SICI)1096-9845(199706)26:6<617::AID-EQE664>3.0.CO;2-Z

Schaffer, J. D. (1985). Multiple objective optimization with vector evaluated genetic algorithms. In J. J. Grefenstette (Ed.), *Proc. of First International Conference on Genetic Algorithms and their Applications* (pp. 93-100). London, UK: Lawrence Erlbaum.

Soong, T. T., & Constantinou, M. C. (1994). *Passive and active structure vibration control in civil engineering*. New York, NY: Springer.

Soong, T. T., & Spencer, B. F. Jr. (2002). Supplemental energy dissipation: State-of-the-art and state-of-the practice. *Engineering Structures*, *24*, 243–259. doi:10.1016/S0141-0296(01)00092-X

Tanaka, N., & Kikushima, Y. (1992). Impact vibration control using a semiactive damper. *Journal of Sound and Vibration*, *158*, 277–292. doi:10.1016/0022-460X(92)90051-X

Wang, L. X. (1997). *A course in fuzzy systems and control*. Prentice-Hall International, Inc.

Wu, Y. M., & Samali, B. (2002). Shake table testing of a base isolated model. *Engineering Structures*, *24*, 1203–1215. doi:10.1016/S0141-0296(02)00054-8

Zitzler, E., & Thiele, L. (1998). *An evolutionary algorithm for multi-objective optimization: The strength Pareto approach.* Computer Engineering and Communication Networks Lab., Swiss Federal Institute of Technology, TIK-Report, No. 43, Zurich, Switzerland.\

KEY TERMS AND DEFINITIONS

Base Isolation Systems: In these systems, a flexible isolation system is introduced between the foundation and superstructure so as to increase the natural period of the system, and thereby to reduce the structural responses.

Earthquake Excitation: Earthquake excitation is light or intense vibration and movement of the ground because of releasing of the energy of quick rupture in the earth's crust fault which is happened quickly.

Fuzzy Logic: This logic uses fuzzy systems instead of crisp ones; therefore, it leads to obtaining precise results. This method is very effective in regulating the uncertain and imprecision data.

Genetic Algorithms: They are effective search methods in wide space that eventually lead to the orientation towards finding an optimal answer.

Multi-Objective Optimization: In this method, the main purpose is to find the optimum values of more than one objective function, which are usually in conflict with each other in engineering optimization problems, so that the improvement of one of them leads to worsening the others.

Semi Active Tuned Mass Damper (STMD): In passive TMD system, if its damping ratio or stiffness of the spring changes with time, then it is called a semi-active tuned mass damper (STMD). Variation of the damping ratio or stiffness of the system can be regulated by different methods such as fuzzy logic.

Tuned Mass Damper (TMD): A mechanical system including a mass block, spring, and a viscous damper able to absorb the entrance energy from the environmental hazards such as winds and earthquake excitations.

Chapter 9
Neuromorphic Smart Controller for Seismically Excited Structures

Yeesock Kim
Worcester Polytechnic Institute, USA

Changwon Kim
Texas A&M University, USA

Reza Langari
Texas A&M University, USA

ABSTRACT

In this chapter, an application of a neuromorphic controller is proposed for hazard mitigation of smart structures under seismic excitations. The new control system is developed through the integration of a brain emotional learning-based intelligent control (BELBIC) algorithm with a proportional-integral-derivative (PID) compensator and a clipped algorithm. The BELBIC control is based on the neurologically inspired computational model of the amygdala and the orbitofrontal cortex. A building structure employing a magnetorheological (MR) damper under seismic excitations is investigated to demonstrate the effectiveness of the proposed hybrid clipped BELBIC-PID control algorithm. The performance of the proposed hybrid neuromorphic controller is compared with the one of a variety of conventional controllers such as a passive, PID, linear quadratic Gaussian (LQG), and emotional control systems. It is shown that the proposed hybrid neuromorphic controller is effective in improving the dynamic responses of structure-MR damper systems under seismic excitations, compared to the benchmark controllers.

DOI: 10.4018/978-1-4666-2029-2.ch009

INTRODUCTION

The application of control technology to large structures has attracted a great attention from civil engineering because behavior of structural systems can be modified during destructive environmental forces such as earthquakes without significantly increasing the mass of structure (Yao 1972; Soong 1990; Kobori et al. 1991; Soong and Reinhorn 1993; Housner et al. 1994; Housner et al 1997; Adeli & Saleh 1999; Spencer and Nagarajaiah 2003; Agrawal et al. 1998; Kim et al. 2009; Kim et al. 2010), including passive, active, and semiactive (also called smart) systems (Nagarajaiah & Spencer 2003; Kim et al. 2010). Particularly, the smart control scheme has been used most frequently to structural control system design because it possesses the advantages of both passive and active control systems (Spencer et al. 1997). In order to improve the performance of the smart control system, the control algorithm for smart control devices has to be selected carefully (Jansen & Dyke 2000). The control algorithms that have been used for the application of smart control technology could be divided into two categories: model-based and model-free control algorithms. The typical model-based control algorithms for implementation of smart control systems in the field of structural engineering might include: linear quadratic regulator, linear quadratic Gaussian, H_∞, etc. (Chang et al. 2008; Lynch et al. 2008; Wang and Dyke 2008; Ping and Agrawal 2009; Nagarajaiah and Narasimhan 2006; Nagarajaiah et al. 2009) The model-free control system design frameworks such as fuzzy logic theory and artificial neural network have been also extensively applied to smart civil structures (Lin et al. 2007; Shook et al. 2008; Kim et al. 2009; Kim et al. 2010; Karamodin and Kazemi 2010). The reason is that the model-free control system design framework does not require for modeling nonlinear dynamic system of structures equipped with complex nonlinear smart control devices. Another new model-free smart control system design framework is the brain emotional learning-based bio-inspired control algorithm (Kim et al. 2010).

The brain limbic system, which is responsible for emotional reaction of humans (among other bio-organisms), is an available candidate as a structural control algorithm (Kim et al. 2010). Unlike rational thought that is considered to be objective, emotions have been considered a negative trait because emotional thought is considered to be involuntary and there exists little conscious control over such thought. However, scientists have recently learned about the positive aspects of human emotions. Moreover, for a number of years, the emotional signal processing in the brain limbic system has been the subject of research in cognitive science (Picard 1997; Jamali et al. 2009; Kim and Langari 2009). Rational thought can be often controlled via the involuntary emotions (Martinez-Miranda & Aldea 2005). Of special interest is that the impact of the emotional system on the cognitive system is far stronger than the impact of the cognitive system on the emotional system. For instance, one single occurrence of an emotionally significant situation is remembered far more vividly and for a longer period than a task which is repeated frequently (Meystel & Albus 2002). In other words, the emotional processing and learning are able to develop an effect that sustained cognitive inputs are not able to achieve.

To date, great attention has been paid to the application of artificial neural networks (ANNs) to bio-inspired control system design. ANNs model the synaptic connections and the Hebbian learning phenomena at the level of individual neurons that train the input-output relations of complex information. These linkages are being used for decision-making when no conventional or mathematical input-output relations are available, i.e., ANNs are trained via adjusting the weights of the various signal paths based on the error between the desired state and the current state. ANNs that are represented in networks of a number of neurons inside the human brain may be used for modeling the emotional learning and process. However, as a macro-level mechanism, the emotional learning process is at a much higher level than the ANNs that consist of a very large number of neurons. In other words, it is not necessary to apply an ANN with high-cost computational loads to system level designs. It can be inferred from this perspective that an emotion-based learning algorithm can be easily implemented without high-computational loads, compared to the ANNs. However, relatively little research has been carried out on an emotion-based control mechanism due to the fact that: (1) the properties and mechanisms of emotions in the human brain are not clearly understood and (2) a mathematical model of the emotional learning and process mechanisms in the human brain is only beginning to be developed (Balkenius & Moren 2001; Moren 2002).

Moren and Balkenius (2000) proposed a mathematical model of emotional learning process that occurs in human brain describing the physical phenomenon of the emotional processing. Since then, investigators have applied the brain emotional learning (BEL) algorithm to feedback control problems: Lucas et al. (2004) introduced the BEL algorithm for control system design; Chandra and Langari (2006) investigated the stability issues of the BEL algorithm; Mehrabian et al. (2006) used the BEL algorithm for a flight control system design by eliminating tracking errors without prior knowledge of the plant dynamics; Mehrabian and Lucas (2006) also applied the BEL algorithm to various benchmark nonlinear dynamic systems; Shahmirzadi et al. (2006) proved that the brain limbic system can be applied to a 14-DOF model of a tractor-semitrailer; Sheikholeslami et al. (2006) achieved the adaptive set point control and disturbance rejection of an HVAC system using the BEL control algorithm; based on the BEL algorithm, Rouhani et al. (2006) solved the output temperature tracking problem of the electrically heated micro-heat exchanger; Rouhani et al. (2007) also showed the excellent performance of the BEL controller for the rotor speed and position of a switched reluctance motor; the control performance of the BEL controller is also experimentally verified by Jamali et al. (2009) using a digital pendulum system; Kim and Langari (2009, 2011) proposed the BEL controller based mobile robot target tracking method; more recently, Kim and Langari (2010a, 2010b) developed autonomous vehicle functions such as lane change maneuver and adaptive cruise control by BEL control strategy. They also compared the control results with conventional control methods, i.e. Fuzzy, PID, and human driver model and showed the robustness and performance of the proposed controller. In the previous researches of the authors (Kim and Langari 2009, Kim et al. 2010, Kim and Langari 2010, and Kim and Langari 2011), the authors compared the control performances of the neuromorphic controller with those of conventional control methods such as passive, PID, PD, LQG, and fuzzy logic control method. From the comparisons it is observed that the main advantages of the neuromorphic smart control are the robustness to the parameter uncertainties, error elimination, and fast response.

In this article, a new control algorithm for seismic response control of building structure-magnetorheological (MR) systems is proposed. The control algorithm is developed through the integration of the BELBIC algorithm with a proportional-integral-derivative (PID) and a semiactive inversion algorithm. This chapter is organized as follows: Section 2 presents the proposed neuromophic control algorithm. Smart structures, i.e., building-magnetorheological damper systems, are described, including simulation results, in Section 3. Concluding remarks are discussed in Section 4.

BIO-INSPIRED SMART CONTROLLER

Neuromorphic Smart Control Formulation

The brain limbic system is an organ that is related to the emotional processing mechanism inside the mammalian brain. The limbic system is closely related to the functions of memory, emotional processing, and emotional learning (Picard 1997). The anatomical structure of the human limbic system is shown in Figure 1.

The main components of brain limbic system are amygdala, orbitofrontal cortex, sensory cortex, and thalamus. This part of brain is involved in the emotional processing and learning (Bechara et al. 2000; Rolls 2000). In what follows, the primary components of the brain limbic system are briefly described and then a mathematical model of brain limbic system is introduced. Finally, the mathematical model is integrated with a PID and a semiactive inversion algorithm to develop a hybrid neuromorphic smart controller for vibration mitigation of seismically excited structures equipped with magnetorheological dampers.

Brain Emotional Learning (BEL) Model

A mathematical relationship between the components of brain limbic system was proposed by Moren and Balkenius (2000) from the descriptive physical model of the limbic system that provides a qualitative sense of the overall functioning of the system. Figure 2 shows the structure of the Moren-Balkenius' computational BEL model. As depicted in the figure, the BEL model has four components of the so-called limbic system of the brain: amygdala, orbitofrontal cortex, sensory cortex and thalamus. Of them, amygdala and orbitofrontal cortex perform an important function in emotional processing (Moren and Balkenius 2000).

The basic idea behind the BEL-based control strategy is to generate reaction (or control output) that maximizes the emotional reward (or mini-

Figure 1. A schematic of brain limbic system

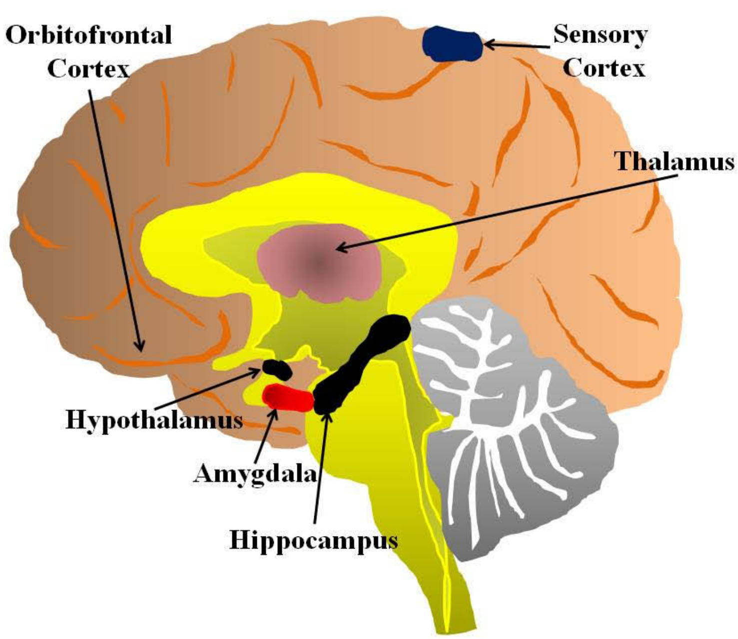

Figure 2. Schematic of the brain emotional learning model

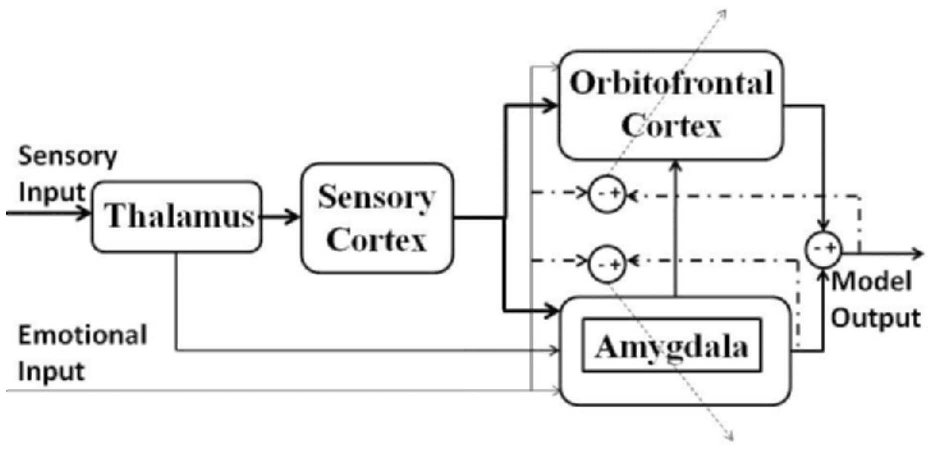

mizes the emotional punishment) under various sets of sensory inputs that the dynamic system is receiving. The sensory inputs are described as the stimulus that the dynamic system is currently experiencing. Also, the emotional signals reflect the degree of satisfaction with the linkage between the stimulus and reaction of the dynamic system at the time. In the following section, the functions of the BEL model components are briefly described.

- **Thalamus:** Initiates the emotional learning process upon the sensory inputs. Thalamus functions as a communicator between the cortical and the other parts of the loop. By passing the maximum signal over the sensory signals through the amygdale, it shows that the task of the thalamus is to provide a non-optimal but fast response from a dynamic system's perspective. The speed and fault tolerance properties of the model is improved by this shortcut route because it bypasses the sensory cortex processing and enables the model to generate a non-optimum action, called satisfactory decision, even when the sensory cortex gets damaged.
- **Sensory Cortex:** As seen in Figure 2, sensory cortex receives sensed input signals through the thalamus. There are two functions of sensory cortex; first it manipulates the sensed input to produce the sensory input that has meaning for control purpose; and the sensory cortex in real biological systems is to appropriately distribute the incoming sensory input signals to the amygdala and the orbitofrontal cortex. For instance, the sensory cortex can be represented in terms of a computational delay.
- **Amygdala:** The lobe where the stimuli from the sensory lobes are mapped to emotional responses. The amygdala receives three kinds of input signals
    - Lower level information from thalamus, e.g., visual information
    - Middle level information from all the sensory cortices, e.g., highly analyzed visual information
    - Higher level information from different parts of the prefrontal cortex. In fact, these signals are mixed to deliver complete information and context. For any sensory input signal SI_i, the output signal from the amygdala is

$$A_i = G_{A_i} \cdot SI_i \qquad (1)$$

where the subscript *i* represents the i^{th} sensing stream and G_{A_i} are the learning gains for the amygdala nodes. The sensory input is the motivation that makes the control system operates. The gain is updated according to the learning rule

$$\Delta G_{A_i} = a \cdot SI_i \cdot \max\left(0, ES - \sum_i A_i\right) \qquad (2)$$

where a is a learning rate of the amygdala node selectable between 0 (no learning) and 1 (instant adaptation) and ES is the emotional signal. Note, ES (also called the reward signal) is an internally generated signal unlike the sensory input which is an external signal that is measured by sensors. Indeed, the main learning process in the system happens in the adaptive gains of the amygdala and orbitofrontal cortex that is explained in following section.

- **Orbitofrontal Cortex (OFC):** Tracks the mismatch between the system's predictions and the actual received reinforcement, and learns to inhibit the system output in proportion to the mismatch. The OFC reduces the strength of amygdala which is no longer appropriate as the goal or the context has been changed. The OFC regulates the mapping of the stimuli to the emotional reaction occurring through the amygdala. For any sensory input signal SI_i, the output signal of a corresponding orbitofrontal cortex node OFC_i is

$$OFC_i = G_{OFC_i} \cdot SI_i, \qquad (3)$$

where G_{OFC_i} are the nodal gains for the orbitofrontal cortex nodes. The gain is updated according to the learning rule

$$\Delta G_{OFC_i} = b \cdot SI_i \cdot \left(MO - ES\right), \qquad (4)$$

where b is the learning rate for the orbitofrontal cortex nodes, ES is the emotional signal. The ES is to correlate the sensory input with the control output. In other words, the emotional signal is generated considering proper linkage between sensory input and control action. These concepts are implemented by Equations (2) and (4). The overall model output, MO is determined by the following equation

$$MO = \sum_i A_i - \sum_i OFC_i. \qquad (5)$$

From the above model output equation, it is realized that the overall model output is the subtraction of excitatory signals from the amygdala and the inhibitory signals from orbitofrontal cortex. Note, the learning trend in the amygdala is never unlearn a connection by taking maximum value between 0 and the difference between ES and amygdala gains; once learned, it is permanent, giving the system the ability to retain emotional connections for as long as necessary. However, the orbitofrontal cortex can both learn and unlearn (forget). Basically, this is inspired by biology: based on both good and bad experiences, the amygdala constantly learns the associations between the sensory input signals and the reward signal and tends to behave based on the learned associations. On the other hand, the orbitofrontal cortex inhibitory signals act to prevent any inappropriate actions to be issued by the amygdala.

Neuromorphic Control Algorithm

As previously stated, the neuromorphic controller is introduced and proved the applicability in control engineering by Lucas et al. (2004). Neuromorphic control strategy is designed by mimicking the minimum characteristics of brain emotional processing. The *MO* is actually the control output generated by the neuromorphic controller. In the control application of the neuromorphic control algorithm, the designer should determine a proper structure for the *SI* and the *ES* purposefully. In this article, the sensory input and emotional signal are defined as follows

$$SI = w_1 y_d + w_2 u, \tag{6}$$

$$ES = w_3 y_d + w_4 \int u \, dt, \tag{7}$$

where $w_1, w_2, w_3,$ and w_4 are the weight factors defining the relative importance that has to be given to either signal; y_d is the drift response of large smart civil structure; and u is the output of the neuromorphic controller. By Equations (6) and (7), the motivation of the suggested controller and the emotional evaluation for the relationship between motivation (i.e., dynamic responses of structures) and the control action (i.e., MR damper force) are defined. The weight factors are determined via trial-and-errors.

To improve the performance of the proposed neuromorphic control algorithm in Equations (6) and (7) for vibration control of large smart civil structures, a conventional controller proportional-integral-derivative (PID) is integrated with the BEL control algorithm through constructing the part of the ES using the PID, as described in later section. By defining new ES function, the appropriate degree between sensory input and controller output are evaluated in different way.

Smart Neuromorphic Control Algorithm

In control applications, the *ES* and *SI* should be appropriately defined such that the control system has the best performance. In this section, the previous form of *ES* function is redesigned using the proportional-integral-derivative (PID) controller (Mehrabian et al. 2006), i.e., the neuromorphic control algorithm is used for tuning the PID controller to improve the control performance of seismically excited civil structures as shown in Figure 3. The modified functions of the sensory input and emotional signal are given by

$$SI = w_1 y_d + w_2 u, \tag{8}$$

$$ES = K_P y_d + K_I \int y_d \, dt + K_D \frac{d}{dt} y_d + w_4 \int u \, dt, \tag{9}$$

where K_P, K_I, and K_D are the weight factors of the PID controller whose parameters are also determined via trial-and-errors. Although the parameters of the PID controller can be optimized via an optimization procedure (e.g., genetic algorithms), it is beyond the scope of the present research. However, in near future, the authors tend to optimize parameters used for the proposed control algorithms. Note that the performance of the PID controller might be sensitive to the selection of the associated weight factors: the PID controller should be re-designed for different structures via trial and errors.

The neuromorphic-PID control algorithm should be modified to operate the MR dampers for smart structure applications. It is because that the neuromorphic-PID control algorithm generates control force signals while current or voltage signals are required to operate of the MR dampers. Thus, a conversion component that converts the control force signals into current or voltage

Figure 3. PID-BELBIC control algorithm

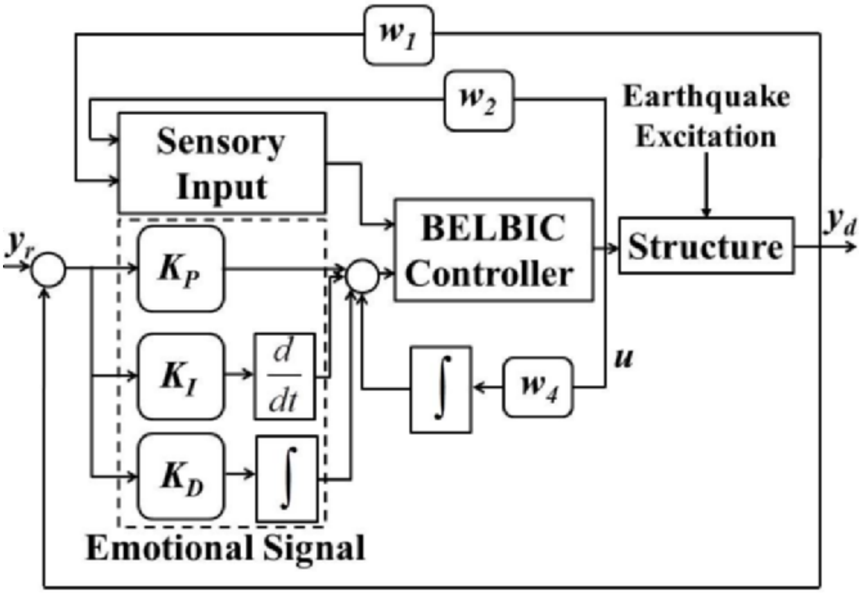

is integrated with the neuromorphic-PID control algorithm. The converting algorithm can be either an inverse MR damper model or a clipped algorithm (Kim et al. 2009). In this article, to accomplish this, a clipped algorithm is utilized. A clipped algorithm for a MR damper application is (Yoshida and Dyke 2004)

$$v = V_a \mathrm{H}\left(\left\{f_{\text{Neuromorphic-PID}} - f_{\text{m}}\right\} f_{\text{m}}\right), \tag{10}$$

where

$$V_a = \begin{cases} \mu_c \cdot f_{\text{Neuromorphic PID}} & \text{for } f_{\text{Neuromorphic PID}} \le f_{\max,} \\ V_{\max} & \text{for } f_{\text{Neuromorphic PID}} > f_{\max,} \end{cases} \tag{11}$$

where v is the voltage level, H is a Heaviside step function, f_{m} is a measured MR damper force which is calculated from Equations (14) to (20), and $f_{\text{Neuromorphic-PID}}$ is a control force signal generated by the neuromorphic-PID controller; μ_c is a value relating the MR damper force to the voltage; and $V_{\max}$ is the maximum voltage to be applied to the MR damper. A schematic diagram of the proposed hybrid neuromorphic-PID-Inv control algorithm is shown in Figure 4. The structural responses (e.g., interstory drift) and the BELBIC control force signals are used to generate predefined sensory input (*SI*) and emotional signal (*ES*) functions. In addition, the *SI* function is constructed as a linear combination of the structural responses and BELBIC control signals using the weighting factors in Equation (15). The *ES* function signal is developed through the integration of the weighted integral BELBIC control forces with the PID control signals as shown in Equation (16). Based on the *SI* and *ES* functions, the BELBIC controller is operated as previously stated: in brief, unlike classical learning or adaptive controllers, the BELBIC controller is directly inspired by biology, wherein the amygdala constantly learns the associations between the *SI* and the *ES* and functions based on these learned associations. On the other hand, the orbitofrontal

Figure 4. A schematic of hybrid clipped BEL-PID control algorithm

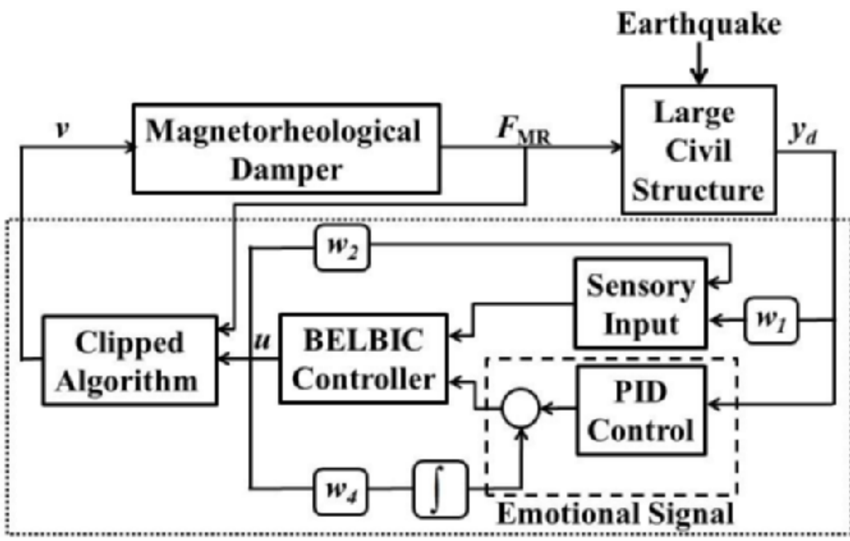

inhibitory signals act to prevent inappropriate actions issued by the amygdala (and hence, by the total model.) This is essentially the gist of the model described in the article. After the BEL controller produces appropriate control forces, the control forces are converted into current/voltage signals using a semiactive converter (i.e., clipped algorithm). Finally, the converted electrical signal is used as an input signal of the MR damper system that absorbs seismic energy of structural systems.

Case Study

Numerical Model

Building-MR Damper Model

To demonstrate the effectiveness of the proposed approach, a magnetorheological (MR) damper equipped three-story building structure is investigated. A typical example of a building structure employing an MR damper is depicted in Figure 5.

Figure 6 shows how an MR damper is implemented into a building model. The associated equation of motion is given by

$$\mathbf{M}\ddot{\mathbf{x}} + \mathbf{C}\dot{\mathbf{x}} + \mathbf{K}\mathbf{x} = \text{“}\mathbf{f}_{\text{MR}}\left(t, x_1, \dot{x}_1, v_1\right) - \mathbf{M}\text{›}\ \ddot{w}_g, \tag{12}$$

where **M**, **C**, and **K** are the mass, the damping, and the stiffness matrices, respectively; $\mathbf{f}_{\text{MR}}$ is the MR damping force; $\ddot{w}_g$ denotes the ground acceleration; the vector **x** is the displacement relative to the ground, $\dot{\mathbf{x}}$ is the velocity, $\ddot{\mathbf{x}}$ is the acceleration, x_1 and $\dot{x}_1$ are the displacement and the velocity at the 1st floor level relative to the ground, respectively, v_1 is the voltage level to be applied, and “ and › are location vectors of control forces and disturbance signal, respectively. The second order differential equation can be converted into state space

$$\begin{aligned} \dot{\mathbf{z}} &= \mathbf{A}^*\mathbf{z} + \mathbf{B}^*\mathbf{f}_{\text{MR}}\left(t, z_1, z_4, v_1\right) - \mathbf{E}^*\ddot{\mathbf{w}}_g \\ \mathbf{y} &= \mathbf{C}^*\mathbf{z} + \mathbf{D}^*\mathbf{f}_{\text{MR}}\left(t, z_1, z_4, v_1\right) + \mathbf{n}, \end{aligned} \tag{13}$$

Figure 5. A schematic of a building-MR damper system

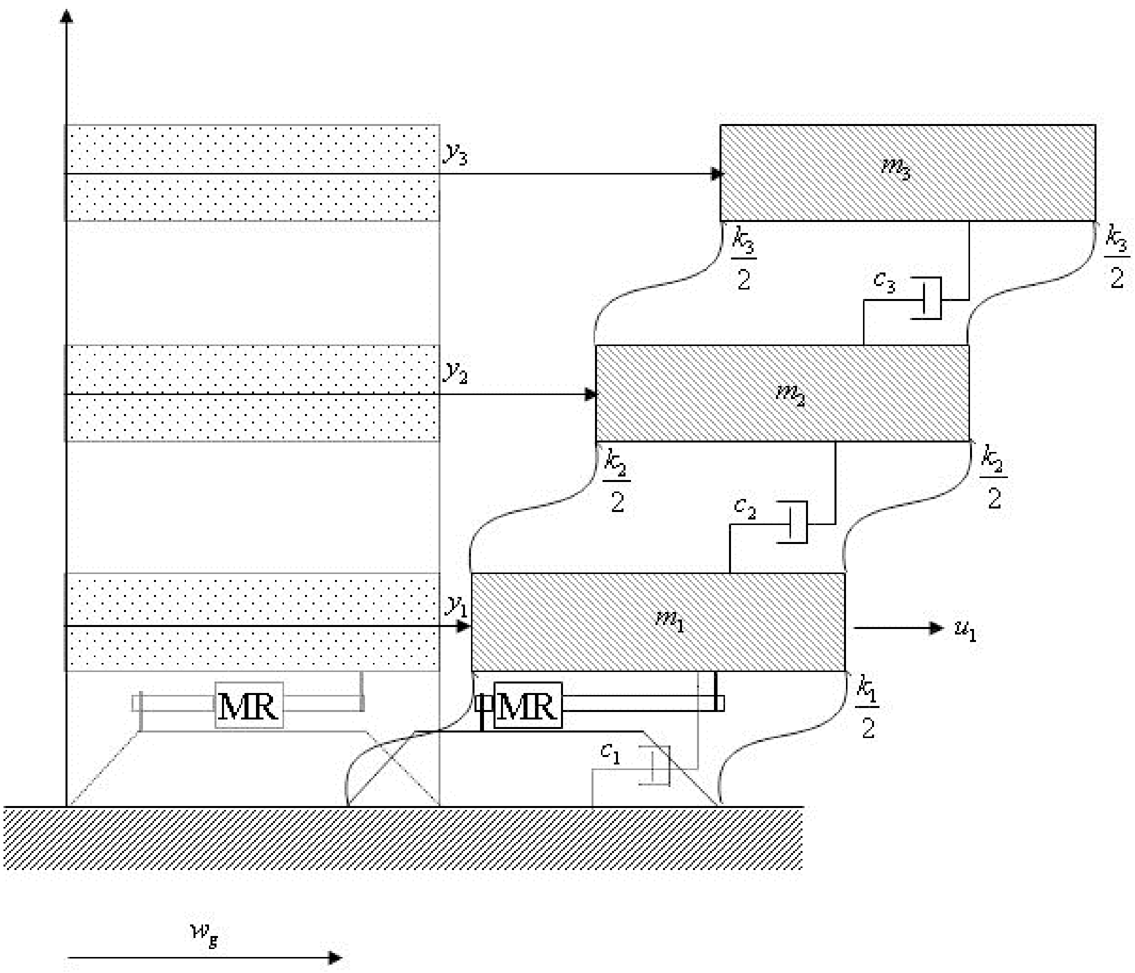

Figure 6. Integrated building structure-MR damper system

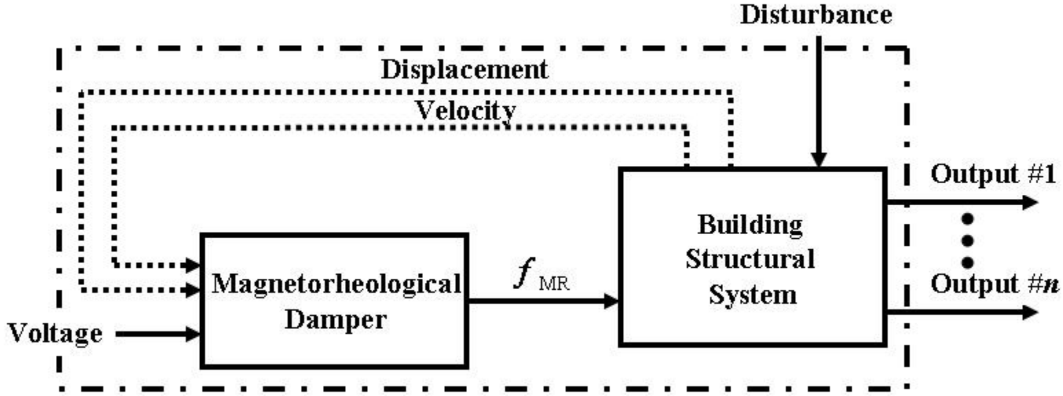

where **z** and **y** are the states and output vectors; **A**, **B**, **C**, **D**, **E** are the state, the input, the output, the feedforward, the disturbance location matrices, respectively; **n** is the noise vector, and z_1 and z_4 are the displacement and the velocity at the 1st floor level of the three-story building structure, respectively. Note that in the earthquake engineering applications, the earthquake disturbance excites all the floor levels within the building structure as the inertia forces, i.e., $\ddot{\mathbf{w}}_g$ is a vector with a dimension of 3 × 1 instead of a scalar value. Using this building-MR damper system, the performance of the proposed hybrid clipped BEL-PID control algorithm is investigated.

MR Damper

In recent years, smart control systems have been proposed for large civil structures because the smart control strategies combine the best features of both active and passive control systems. In particular, one of the controllable-fluid dampers, MR damper as shown in Kim et al. (2009) has attracted considerable attention in recent years due to its appealing characteristics: reliable operation; fast response time; low power requirements; broad temperature range; adjustable operating points; and low manufacturing cost. To make the fullest use of the advantages of the MR damper, Spencer et al. (1997) proposed a modified version of the Bouc-Wen model, as shown in Figure 7. The MR damper force $f_{\mathrm{MR}}(t)$ predicted by the modified Bouc-Wen model is governed by the following differential equations:

$$f_{\mathrm{MR}} = d_1\dot{y} + s_1(x - x_0), \tag{14}$$

$$\dot{z}_{\mathrm{BW}} = -\gamma\left|\dot{x} - \dot{y}\right| z_{\mathrm{BW}}\left|z_{\mathrm{BW}}\right|^{n-1} - \beta(\dot{x} - \dot{y})\left|z_{\mathrm{BW}}\right|^{n} + A(\dot{x} - \dot{y}), \tag{15}$$

Figure 7. Schematic of the mathematical model for the MR damper

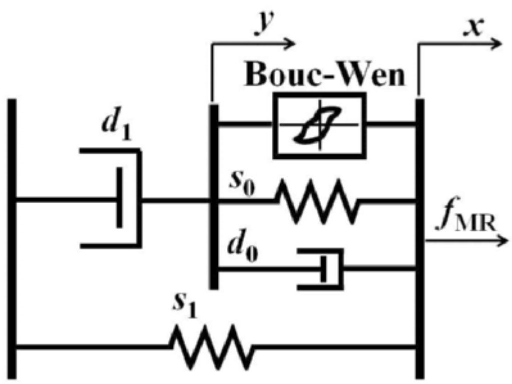

$$\dot{y} = \frac{1}{(d_0 + d_1)}\left\{\alpha z_{\mathrm{BW}} + d_0\dot{x} + s_0(x - y)\right\}, \tag{16}$$

$$\alpha = \alpha_{\mathrm{a}} + \alpha_{\mathrm{b}}u, \tag{17}$$

$$d_1 = d_{1\mathrm{a}} + d_{1\mathrm{b}}u, \tag{18}$$

$$d_0 = d_{0\mathrm{a}} + d_{0\mathrm{b}}u, \tag{19}$$

$$\dot{u} = -\eta(u - v), \tag{20}$$

where z_{BW} and α, called evolutionary variables, describe the hysteretic behavior of the MR damper; d_0 is the viscous damping parameter at high velocities; d_1 is the viscous damping parameter for the force roll-off at low velocities; α_a, α_b, d_{0a}, d_{0b}, d_{1a}, and d_{1b} are parameters that account for the dependence of the MR damper force on the voltage applied to the current driver; s_0 controls the stiffness at large velocities; s_1 represents the accumulator stiffness; x_0 is the initial displacement of the spring stiffness s_1; γ, β, n and A are adjustable shape parameters of the hysteresis loops, i.e., the linearity in the unloading and the transition between pre-yielding and post-yielding regions; v and u are input and output voltages of a first-order filter, respectively; and η is the time constant of the first-order filter. Note that nonlinear phenomena occur when the highly nonlinear MR dampers are applied to structural systems for effective energy dissipation. Such an integrated structure-MR damper system behaves nonlinearly although the structure itself is usually assumed to remain linear. Therefore, the development of an effective control algorithm for the nonlinear behavior of the structure-MR damper system would play a key role in semiactive control system design: a solution can be found in a model-free brain limbic system-based control algorithm.

Simulation

In this chapter, the performances of four controllers (i.e., passive, PID, LQG, and neuromorphic controls) are compared to demonstrate the effectiveness of the proposed hybrid neuromorphic controller for hazard mitigation of civil structures while the uncontrolled structure is used as a baseline. Properties of the three-story building employing an MR damper are adopted from a benchmark model (Dyke et al. 1996). The mass of each floor $m_1 = m_2 = m_3 = 98.3$ kg, the stiffness of each story k_1 = 516,000 N/m, k_2 = 684,000 N/m, and k_3 = 684,000 N/m; and the damping of each floor c_1 = 125 Ns/m, c_2 = 50 Ns/m, and c_3 = 50 Ns/m. The parameters of the comparative controllers are: (1) the learning rates for the amygdala and orbitofrontal cortex of the BELBIC algorithm are adopted as a = 1 and b = 1 (2) w_1 = 2, w_2 = 1, w_3 = 2, and w_4 = 1 (3) the PID control gains are K_P = 120, K_I =100, and K_D = 10, respectively (4) the parameters of the LQG control system are adopted from Dyke et al. (1996). The input signal to be fed through the each controller is the 1st floor drift response. Selected time history and interstory responses are provided.

Figure 8, Figure 9, and Figure 10 show the time history responses at the top floor of the smart structures subjected to the 1940 El-Centro earthquake with the intensity of 0.5, 1.0, and 1.5, respectively. As seen, the proposed neuromorphic control algorithm produces the best control performance over the passive, PID, and LQG control systems as far as the displacement responses of each floor are investigated. Also, all of the control algorithms have better performance than the passive control system. To further investigate of the control performances, the maximum interstory responses of the smart structure employing different control strategies are shown in Figure 11, Figure 12, and Figure 13. From the figure, it is apparent that the proposed neuromorphic control algorithm has the best performance over other control systems for most of cases. However, it is shown that the performances of the LQG and the neuromorphic control systems are similar for the case of 50% intensity of earthquake disturbance case. It is demonstrated from the simulation results that the proposed neuromorphic control algorithm is very effective in reducing vibration of the seismically excited building structure employing an MR damper.

FUTURE RESEARCH DIRECTIONS

It is recommended that the applications of the proposed neuromorphic controllers to a variety of uncertain cases be studied to demonstrate the robustness of the proposed approach. Additionally, the stability analysis of the neuromorphic control will be conducted for analytical demonstration of the given novel control strategy.

Figure 8. Displacement time history response of smart building under the 1940 El-Centro earthquake (50% intensity)

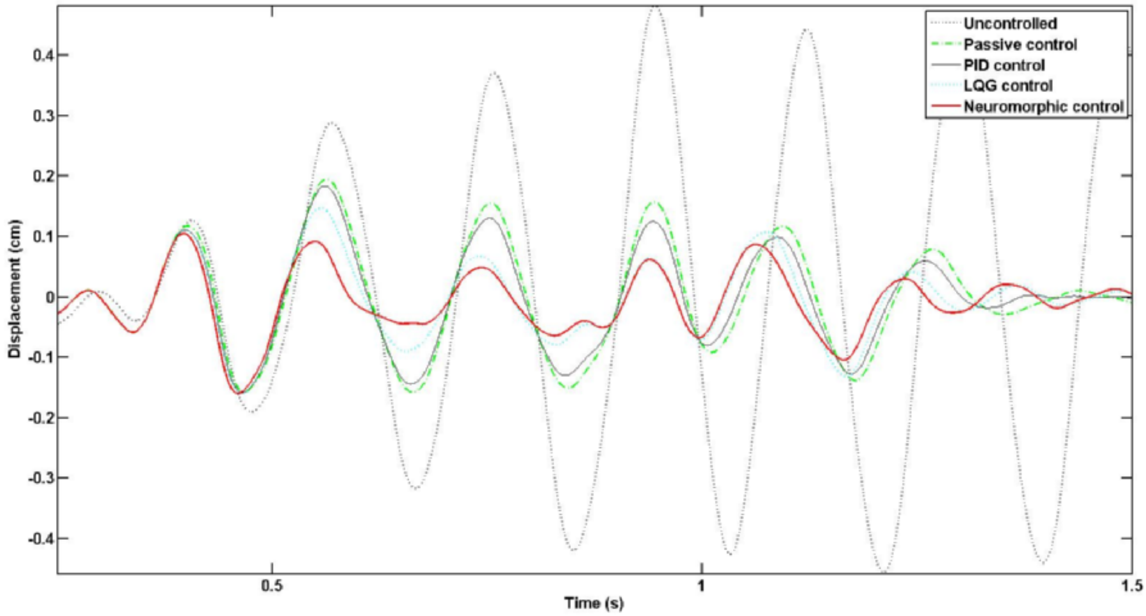

Figure 9. Displacement time history response of smart building under the 1940 El-Centro earthquake (100% intensity)

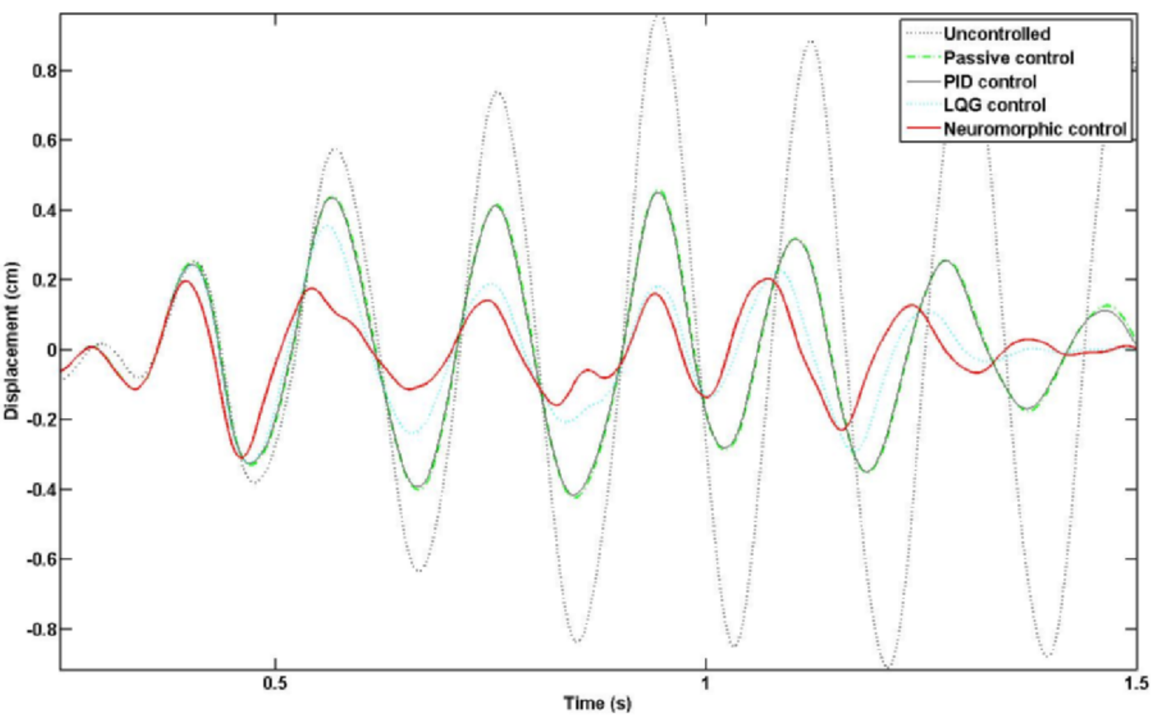

Figure 10. Displacement time history response of smart building under the 1940 El-Centro earthquake (150% intensity)

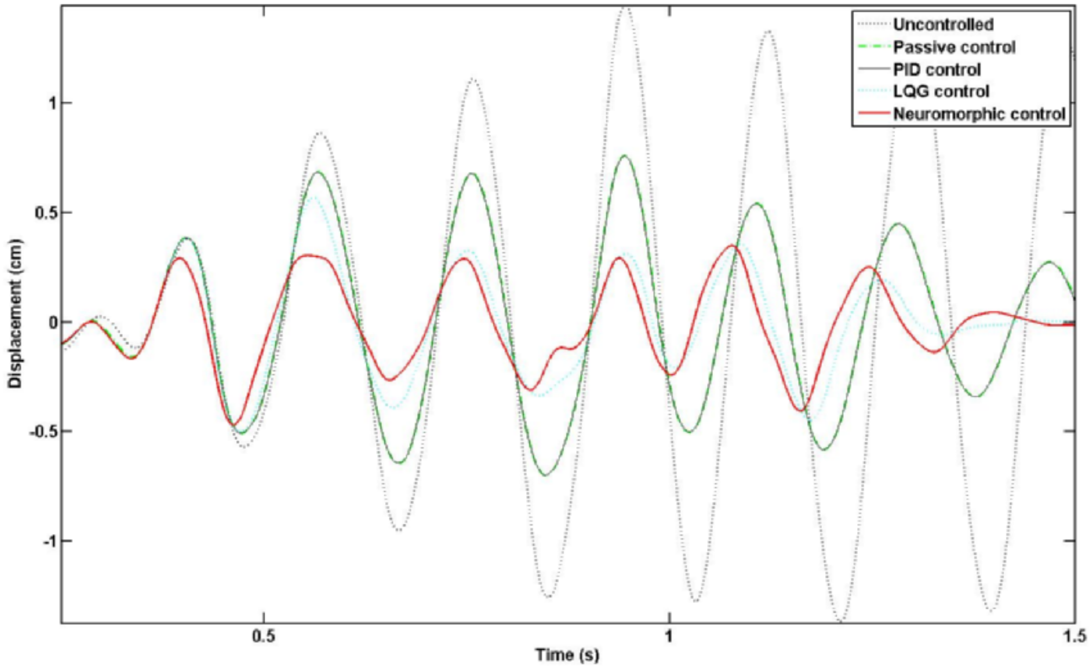

Figure 11. Maximum interstory responses of smart building under the 1940 El-Centro earthquake (50% intensity)

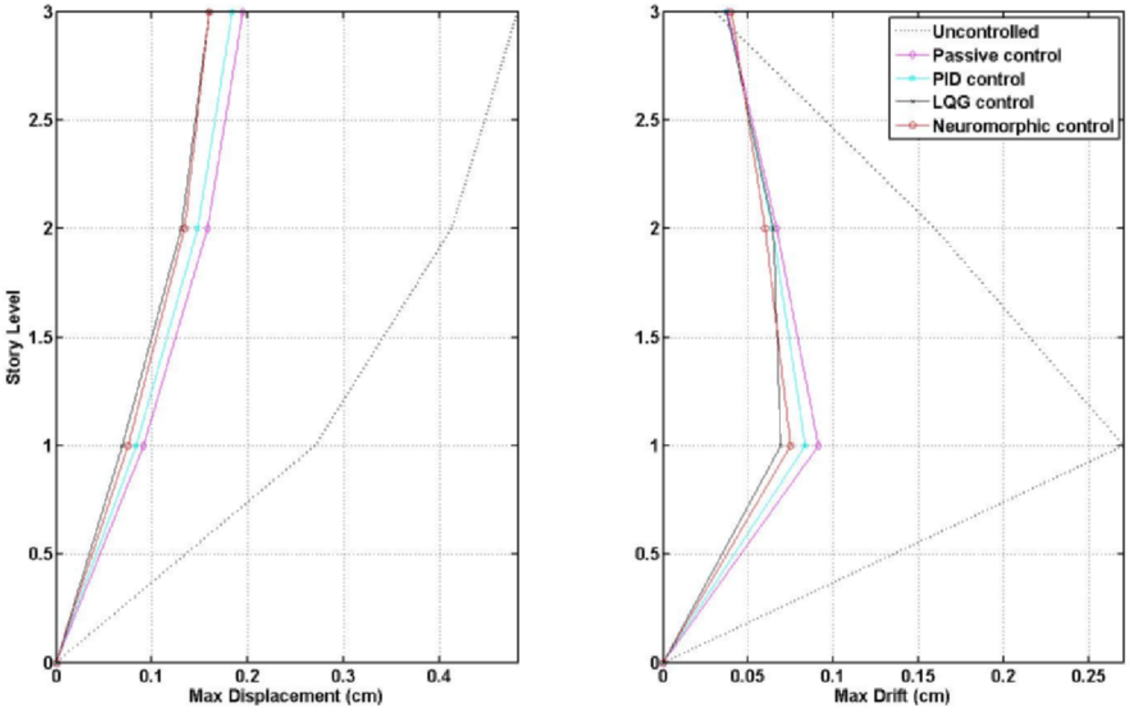

Figure 12. Maximum interstory responses of smart building under the 1940 El-Centro earthquake (100% intensity)

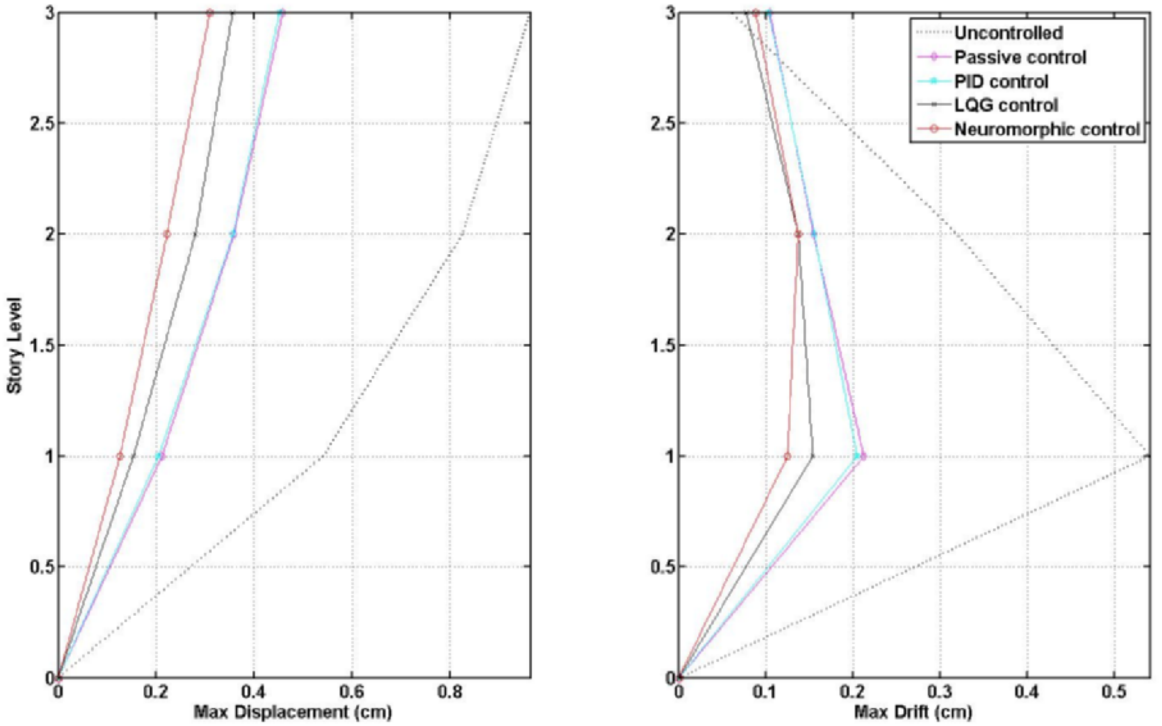

Figure 13. Maximum interstory responses of smart building under the 1940 El-Centro earthquake (150% intensity)

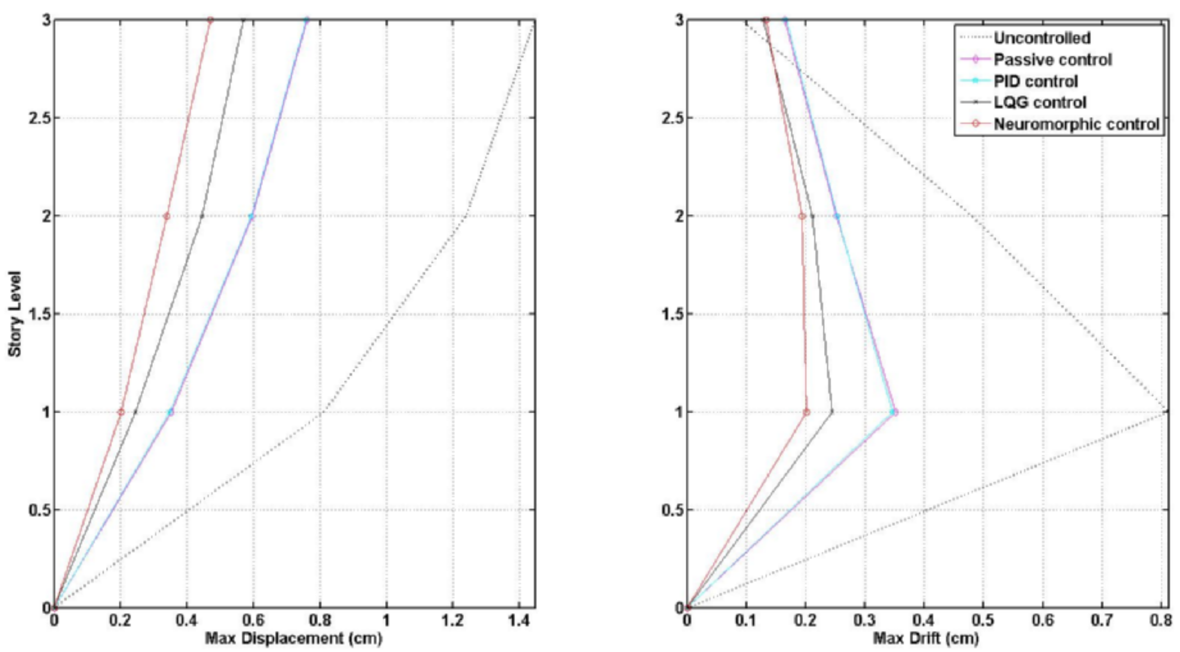

CONCLUSION

In this chapter, a novel neuromorphic smart controller is proposed for hazard mitigation of smart building structures. The controller is developed through the integration of brain emotional learning based intelligent control with the proportional-integral-derivative and a clipped algorithm. To show the performance of the proposed neuromorphic controller, a seismically excited three-story building employing an MR damper is investigated. It is demonstrated from the simulations that the proposed neuromorphic controller is effective in reducing responses of seismically excited building structure.

REFERENCES

Adeli, H., & Saleh, A. (1999). *Control, optimization, and smart structures: High-performance bridges and buildings of the future*. New York, NY: John Wiley & Sons, Inc.

Agrawal, A. K., Yang, J. N., & Wu, J. C. (1998). Application of optimal polynomial controller to a benchmark problem. *Earthquake Engineering & Structural Dynamics*, *27*, 1291–1302. doi:10.1002/(SICI)1096-9845(1998110)27:11<1291::AID-EQE784>3.0.CO;2-M

Balkenius, C., & Moren, J. (2001). Emotional learning: A computational model of the amygdala *Cybernetics and Systems*. *International Journal (Toronto, Ont.)*, *32*, 611–636.

Bechara, A., Damasio, H., & Damasio, A. R. (2000). Emotion, decision making and the orbitofrontal cortex. *Cerebral Cortex*, *10*, 295–307. doi:10.1093/cercor/10.3.295

Chandra, M., & Langari, R. (2006). Analytical study of a control algorithm based on emotional processing. *Proceedings of the the American Control Conference,* (pp. 3433-3438). Minneapolis, MN: IEEE.

Chang, C. M., Park, K. S., Mullenix, A., & Spencer, B. F. Jr. (2008). Semiactive control strategy for a phase II smart base isolated benchmark building. *Structural Control and Health Monitoring*, *15*, 673–696. doi:10.1002/stc.269

Dyke, S. J., Spencer, B. F. Jr, Sain, M. K., & Carlson, J. D. (1996). Modeling and control of magnetorheological dampers for seismic response reduction. *Smart Materials and Structures*, *5*, 565–575. doi:10.1088/0964-1726/5/5/006

Housner, G. W., Bergman, L. A., Caughey, T. K., Chassiakos, A. G., Claus, R. O., & Masri, S. F. (1997). Structural control: Past, present, and future. *Journal of Engineering Mechanics*, *123*(9), 897–971. doi:10.1061/(ASCE)0733-9399(1997)123:9(897)

Housner, G. W., Masri, S. F., & Chassiakos, A. G. (1994). *Proceedings of the 1st World Conference on Structural Control.*

Hurlebaus, S., & Gaul, L. (2006). Smart structure dynamics. *Mechanical Systems and Signal Processing*, *20*, 255–281. doi:10.1016/j.ymssp.2005.08.025

Jamali, M. R., Dehyadegari, M., Arami, A., Lucas, C., & Navabi, Z. (2009). Real-time embedded emotional controller. *Neural Computing & Applications*, *19*(1). doi:doi:10.1007/s00521-008-0227-x

Jansen, L. M., & Dyke, S. J. (2000). Semi-active control strategies for the MR damper: A comparative study ASCE. *Journal of Engineering Mechanics*, *126*, 795–803. doi:10.1061/(ASCE)0733-9399(2000)126:8(795)

Karamodin, A., & Kazemi, H. (2010). Semi-active control of structures using neuro-predictive algorithm for MR dampers. *Structural Control and Health Monitoring*, *17*, 237–253.

Kim, C., & Langari, R. (2009). Target tracking control of a mobile robot using a brain limbic system based control strategy. *Proceedings IEEE International Conference on Intelligent Robots and Systems,* (pp. 5095-5064). St. Louis, MO: IEEE.

Kim, C., & Langari, R. (2010a). Brain limbic system based intelligent controller application to lane change maneuver. *Vehicle System Dynamics*, *49*(12).

Kim, C., & Langari, R. (2010b). (in press). Application of brain limbic system to adaptive cruise control. *International Journal of Vehicle Autonomous Systems*.

Kim, C., & Langari, R. (2011). A mobile robot target tracking via brain limbic system based control. *International Journal of Robotics and Automation*, 26.

Kim, Y., Kim, C., & Langari, R. (2010). Novel bio-inspired smart control for hazard mitigation of civil structures. *Smart Materials and Structures*, *19*(11). doi:10.1088/0964-1726/19/11/115009

Kim, Y., Langari, R., & Hurlebaus, S. (2009). Semiactive nonlinear control of a building structure equipped with a magnetorheological damper system. *Mechanical Systems and Signal Processing*, *23*, 300–315. doi:10.1016/j.ymssp.2008.06.006

Kobori, T., Koshika, N., Yamada, N., & Ikeda, Y. (1991). Seismic response controlled structure with active mass driver system. Part 1: Design. *Earthquake Engineering & Structural Dynamics*, *20*, 133–139. doi:10.1002/eqe.4290200204

Lin, P. Y., Roschke, P. N., & Loh, C. H. (2007). Hybrid base-isolation with magnetorheological damper and fuzzy control. *Structural Control and Health Monitoring*, *14*, 384–405. doi:10.1002/stc.163

Lucas, C., Shahmirzadi, D., & Sheikholeslami, N. (2004). Introducing BELBIC-Brain emotional learning based intelligent controller. *International Journal of Intelligent Automation and Soft Computing*, *10*, 11–22.

Lynch, J. P., Wang, Y., Swartz, R. A., Lu, K. C., & Loh, C. H. (2008). Implementation of a closed-loop structural control system using wireless sensor networks. *Structural Control and Health Monitoring*, *15*, 518–539. doi:10.1002/stc.214

Martinez-Miranda, J., & Aldea, A. (2005). Emotions in human and artificial intelligence. *Computers in Human Behavior*, *21*, 323–341. doi:10.1016/j.chb.2004.02.010

Mehrabian, A. R., & Lucas, C. (2006). Emotional learning based intelligent robust adaptive controller for stable uncertain nonlinear systems. *International Journal of Computational Intelligence*, *2*, 246–253.

Mehrabian, A. R., Lucas, C., & Roshanian, J. (2006). Aerospace launch vehicle control: An intelligent adaptive approach. *Aerospace Science and Technology*, *10*, 149–155. doi:10.1016/j.ast.2005.11.002

Meystel, A. M., & Albus, J. S. (2002). *Intelligent systems: Architecture, design and control*. New York, NY: Wiley Interscience.

Moren, J. (2002). *Emotion and learning-a computational model of the amygdale.* Ph.D. Dissertation Department of Cognitive Science. Lund, Sweden: Lund University.

Moren, J., & Balkenius, C. (2000) A computational model of emotional learning in the amygdale. *Proceedings of the 6th International Conference on the Simulation of Adaptive Behavior*, (pp. 383-391). Cambridge, MA: MIT Press.

Nagarajaiah, S., & Narasimhan, S. (2006). Smart base-isolated benchmark building Part II: Phase I sample controllers for linear isolation systems. *Structural Control and Health Monitoring*, *13*, 589–604. doi:10.1002/stc.100

Nagarajaiah, S., Narasimhan, S., Agrawal, A., & Ping, T. (2009). Benchmark structural control problem for a seismically excited highway bridge. Part III: Phase II sample controller for the fully base-isolated case. *Structural Control and Health Monitoring*, *16*, 549–563. doi:10.1002/stc.293

Nagarajaiah, S., & Spencer, B. F. Jr. (2003). State of the art of structural control. *Journal of Structural Engineering*, *129*, 845–856. doi:10.1061/(ASCE)0733-9445(2003)129:7(845)

Picard, R. (1997). *Affective computing*. Cambridge, MA: MIT Press.

Ping, T., & Agrawal, A. K. (2009). Benchmark structural control problem for a seismically excited highway bridge-Part II: Phase I sample control designs. *Structural Control and Health Monitoring*, *16*, 530–548. doi:10.1002/stc.300

Rolls, E. T. (2000). The orbitofrontal cortex and reward. *Cerebral Cortex*, *10*, 284–294. doi:10.1093/cercor/10.3.284

Rouhani, H., Jalili, M., Araabi, B. N., Eppler, W., & Lucas, C. (2006). Brain emotional learning based intelligent controller applied to neurofuzzy model of micro-heat exchanger. *Expert Systems with Applications*, *32*, 911–918. doi:10.1016/j.eswa.2006.01.047

Rouhani, H., Sadeghzadeh, A., Lucas, C., & Araabi, B. N. (2007). Emotional learning based intelligent speed and position control applied to neurofuzzy model of switched reluctance motor. *Control and Cybernetics*, *36*, 75–95.

Shahmirzadi, D., Langari, R., Ricalde, L. J., & Sanchez, E. N. (2006). Intelligent vs. sliding mode control in rollover prevention of tractor-semitrailers. *Intelligent Journal of Vehicle Autonomous Systems*, *4*, 68–87.

Sheikholeslami, N., Shahmirzadi, D., Semsar, E., Lucas, C., & Yazdanpanah, M. J. (2006). Applying brain emotional learning algorithm for multivariable control of HVAC systems. *Journal of Intelligent & Fuzzy Systems*, *17*, 35–46.

Shook, D. A., Roschke, P. N., & Ozbulut, O. E. (2008). Superelastic semi-active damping of a base-isolated structure. *Structural Control and Health Monitoring*, *15*, 746–768. doi:10.1002/stc.276

Soong, T. T. (1990). *Active structural control: Theory and practice*. Essex, UK: Longman Scientific.

Soong, T. T., & Reinhorn, A. M. (1993). An overview of active and hybrid structural control research in the U.S. *Structural Design of Tall Buildings*, *2*, 192–209. doi:10.1002/tal.4320020303

Spencer, B. F., Dyke, S. J., Sain, M. K., & Carlson, J. D. (1997). Phenomenological model for magnetorheological dampers. *Journal of Engineering Mechanics*, *123*, 230–238. doi:10.1061/(ASCE)0733-9399(1997)123:3(230)

Wang, Y., & Dyke, S. (2008). Smart system design for a 3D base-isolated benchmark building. *Structural Control and Health Monitoring*, *15*, 939–957. doi:10.1002/stc.228

Yao, J. T. P. (1972). Concept of structural control. *Journal of the Structural Division*, *98*(ST7), 1567–1574.

Yoshida, O., & Dyke, S. J. (2004). Seismic control of a nonlinear benchmark building using smart dampers. *Journal of Engineering Mechanics*, *130*, 386–392. doi:10.1061/(ASCE)0733-9399(2004)130:4(386)

Chapter 10
Effective Configurations of Active Controlled Devices for Improving Structural Seismic Response

Yuri Ribakov
Ariel University Center of Samaria, Israel

Grigoriy Agranovich
Ariel University Center of Samaria, Israel

ABSTRACT

Improving structural seismic response using dampers became a widely used method in the recent decades. Various devices were developed for seismic protection of structures and appropriate methods were proposed for effective design of control systems. An actual problem is how many dampers should be used as is their optimal location for yielding the desired structural response with minimum cost. A method for finding effective dampers' placement and using amplifiers for dampers connection was recently proposed in the literature. The current study presents analyses of the amplification and placement of active controlled devices on the efficiency of a control system. A model of a twenty-story structure with active control systems including different dampers configurations is simulated. The response of the structure to natural earthquake excitations is also reported. The results of this study show a method of selecting proper configuration of active devices allowing cost effective control.

DOI: 10.4018/978-1-4666-2029-2.ch010

INTRODUCTION

Reduction of structural responses to earthquakes is a subject that is widely investigated during the last decades. Structural control is known as one of the effective ways for enhancing structural seismic response. Various structural control strategies are developed and implemented in practice. Structural control applications are effectively used in new buildings and also to retrofit existing structures all over the world.

For example, steel moment frames with fluid viscous dampers located at the ground floor are used for seismic retrofitting of a 4-story reinforced concrete building of the Woodland Hotel located in Woodland, California. Seismic rehabilitation of the ten-story MUCTC building in Montreal was achieved by Pall friction dampers in steel bracing. Navy Building in San Diego is equipped with viscoelastic dampers. A tuned mass damper is used in City Corporation Building in NY City. An active mass damper is installed in the Nanjing television tower in China.

For implementation of structural control algorithms passive, semi-active and active devices are used. Passive devices use the energy of structural motion to dissipate energy. This group of devices includes viscous dampers, viscoelastic dampers, friction dampers, tuned mass dampers, base isolation devices, etc. (Soong, 1997). They require no external energy, but the properties of these devices are constant and the forces across these devices are not changed according to any optimal control law.

Modern approaches are developed to improve the efficiency of passive dampers. Seismic design of friction dampers based on the desired structural performance yields effective passive energy dissipation (Tabeshpour, 2010). A gradient-based evolutionary optimization methodology is presented for finding the optimal design of viscoelastic dampers and their supporting members (Fujita, 2010). Finding optimal location and characteristics of triangular adding damping and stiffness dampers in moment resisting steel structures is an additional topic that is investigated (Yousefzadeh, 2011).

Active devices are able to change the control force, applied to the structure according to the optimal control requirements. They allow more effective control, but external energy source is required for activation of these devices. In other words, active controlled devices externally activated and apply control forces to the structure in order to improve its performance. Active devices include active tendons, active tuned mass dampers and actuators.

To reduce the energy, required for activation of the devices, semi-active dampers are used. In these devices a relatively small energy amount is enough to change the dampers properties so that the energy of structural motion would yield damping forces that are close to the optimal control force values. Semi-active devices include active variable stiffness systems, electro-rheological dampers, magneto-rheological dampers, semi-active variable friction dampers, shape memory alloys and piezoelectric materials etc. In order to ensure the structural safety, reliability and durability, pole assignment method, optimal control method and independent model-space control method are usually used. Modern control strategies are also developed for active and semi-active systems (Gu, 2008).

Hybrid applications of active and passive devices are also known. For example, magneto-rheological dampers are successfully used as a part of base isolation systems (Ribakov, 2002). Selective control is an effective algorithm for such systems (Ribakov, 2003). A hybrid isolation system, comprised of a bidirectional roller–pendulum system and augmented by controllable magnetorheological dampers is proposed to reduce the potential for damage to structures and sensitive equipment (Shook, 2007). Comparison of neural network control, LQR/clipped optimal control with variable gains and fuzzy logic control shows that the second is superior to the other in 50% of the investigated cases, while the third performs well for earthquakes with large accelerations. The first is effective in minimizing the acceleration of the superstructure that is subject to moderate excitation. Nonlinear model based control algorithms are developed recently to monitor the magnetorheological damper voltage (Ali, 2009). These techniques are effective under a set of seismic excitations, compared to the performances obtained with a fuzzy based intelligent control algorithm and a widely used clipped optimal strategy.

Many state of the art publications on control applications are published. These publications provide a review of base isolation systems (Kelly, 1986), active control (Soong, 1988, 1990, 1994, Datta, 2003), structural control concepts and strategies (Housner, 1997, Spencer, 2003), etc. In most cases active control systems are designed based on the linear quadratic regulator (LQR) theory or H_∞ control theory, and the state feedback control laws are converted into output feedback ones (Ikeda, 2004).

Structural control should be based on economic principles. With this aim inexpensive control devices should be developed and number of such devices, required for obtaining optimal control, should be minimized. In most structural applications passive or active devices in are connected to diagonal or Chevron braces. When a damper is connected to Chevrone braces the interstory drift and drift velocity are transferred to the damper. If a damper is connected to diagonal braces, the displacement and velocity, transferred to the damper are lower, compared to the interstory drift and drift velocity, respectively.

Several efforts are undertaken to improve the damper efficiency. Various amplification devices are proposed to magnify the displacements and velocities, transferred to dampers, in order to increase energy dissipation in each damper and decrease the number of dampers. Different amplifying devices are developed and proposed to be used for increasing energy dissipation (Hanson, 2001). Such amplifiers include toggle braces (Taylor, 2000, Constantinou, 2001) lever arms (Ribakov, 2000, 2003), scissor jack (Gluck, 1999, Sigaher, 2003, Ribakov, 2006), displacement amplification device based on a gear-type mechanism (Berton, 2005), cables and other configurations (Choi, 2010).

Effective placement of active and passive devices has also high importance. Many techniques were developed to find optimal locations of passive dampers. Parameters of linear viscous dampers that should be connected in each floor of a structure can be obtained using an optimal method based on LQG control (Gluck, 1996). The single mode approach is a special case of this method and it is suitable for structures with one dominant vibration mode. A method for finding the optimal damper locations, minimizing the dynamic compliance of a planar building frame, was developed (Takewaki, 2000). It allows finding an optimal damper positioning sequentially for gradually increasing total damper capacity levels.

Certain locations are advantageous also for placement of actuators in the structure for effective reduction of its dynamic response. Optimal location of actuators in an actively controlled structure was studied in the frame of zero-one optimization problem with a constraint on the number of actuators (Rao, 1991). An optimization scheme, based on genetic algorithm was developed. The maximization of energy dissipated by an active controller was used as the objective function. Locations of the electro-rheological dampers in structures can be also obtained by placing virtual dampers at the locations of interest and computing the power dissipation in the dampers (Chen, 2003).

A general method for optimal application of dampers and actuators in seismic-resistant structures is developed by Cheng (2002). The study includes development of a statistical criterion, formulation of a general optimization problem and establishment of a solution procedure. An empirical procedure to find the optimal locations of actuators by maximizing an optimal locations index is proposed (Pantelides, 1990). The modal responses and earthquake spectra are taken into consideration. Four distinct design criteria, influencing the active control design, are considered to study the optimal actuator placement problem (Rao, 2008). The sensitivities of the four criteria with respect to different earthquake records were also explored.

An algorithm for finding optimal active controlled devices locations is recently proposed (Agranovich, 2010). It is based on LQG design that is carried out using an artificial white noise ground motion. According to this algorithm, it is assumed that active controlled dampers are placed at each floor. The most effective dampers' locations are selected according to maximum contribution to the total energy dissipation. It was demonstrated numerically that the method yields effective improvement of structural seismic response by a limited set of active controlled devices.

For optimal distribution of active controlled devices it is sometimes required to connect more than one device per floor, because the peak force that can be developed in one device is limited. Connecting active dampers to amplifiers can significantly reduce the number of devices. Using less damping units per floor leaves more open bays that is also a very important issue.

This study is focused on analysis of a 20-story active controlled structure described in numerical example. Active devices are located at the floors, where their positive effect is maximal. In cases, when the maximum control force value, required at a certain floor, is higher than the peak force that may be produced in a single device, lever arms are used for connection of active dampers. It allows reduction of dampers and increases the efficiency of control.

FINDING EFFECTIVE DAMPER LOCATIONS

Optimal dampers' location in structures is a problem that is studied for many years (Wu, 1979, Chang, 1980, Hahn, 1992) A wide literature review in this field is given (Liu, 2003). An effective design method is developed recently (Agranovich, 2010). The method is based on simple and logical principles, requiring no changes in the control law. Moreover, it is fast, compared to generic algorithms that are often used for finding optimal dampers' placement. The method does not require defining additional transfer functions or using mode shapes of undamped structure.

According to this method, an artificial earthquake record is modeled and a response of an undamped structure to this earthquake is obtained. After that dampers are connected to the structure at all floors and the structural response to the artificial ground motion is calculated. The control forces correspond to the optimal control law requirements and the number of active controlled devices at each floor is obtained according to a maximum force that can be developed by a single device. Energy at each floor is calculated and its portion in the total energy over the entire structure is obtained. It is further considered that dampers' cost and energy, required to activate them, are limited. Hence, dampers are placed at the most effective positions and their number is increased until desired reduction in seismic response is achieved.

An artificial white noise ground acceleration signal that is used as an earthquake record for finding optimal dampers' locations is generated using an algorithm, implemented in MATLAB routines (Ribakov, 2007). The input parameters for this algorithm are the desired peak ground acceleration (PGA), the desired spectrum bandwidth (BW) and the earthquake duration (t_f). The algorithm and its program realization allow changing the parameters according to the design conditions. To design the active control system the following input parameters have been selected: PGA = 0.3g, BW = 30 Hz, t_f = 50 sec.

After the artificial earthquake is generated, the structure is calibrated based on the modified LQG method (Agranovich, 2010) described below. Control energy distribution between the floors where active control devices are attached is obtained from the calibration of the building with simulated ground motion. At the next stage, based on this energy distribution, the quasi-optimal dampers' location at the stories of the structure is found. The basic assumption for the dampers location stage is that it is more efficient to place dampers at stories with maximum control energy contribution.

The algorithm includes a set of successive improving steps (Agranovich, 2010). At each of these steps a new floor becomes "active" according to the above described assumption, and the dampers' distribution at the "active" floors is updated. After updating the number of "active" floors structural response to the artificial ground motion is simulated. Then, based on the peak control forces at every story, the number of dampers per each of the "active" floors is obtained.

MODIFIED LQG METHOD

The modified LQG method is based on the state model of a structure

$$\dot{d}(t) = Ad(t) + Bu(t) + E\ddot{x}_g(t) \tag{1}$$

and the performance index

$$J = \lim_{T\to\infty} \frac{1}{T} E\left[\int_0^T d^T(t)Qd(t) + u^T(t)Ru(t)dt\right] \tag{2}$$

According to the LQG approach, a system, described by Equation (1) and the optimal control forces $u(t)$ should minimize the performance index (2). An additional assumption is that the optimal feedback is a function of the measurement vector, containing the noised floor accelerations

$$y_m(t) = H_m d(t) + D_m u(t) + F_m \ddot{x}_g(t) + v(t) \tag{3}$$

Matrices H_m, D_m and F_m describe the parameters of the measurement subsystem. Detailed description of these parameters is given in (Spencer, 1999). The ground acceleration $\ddot{x}_g(t)$ and the measurement noise *v(t)* are assumed to be stationary white noises with known intensities. Hence the optimal control force *u(t)* is a function of the measurement vector, containing the noised floors accelerations. The optimal control force is calculated as

$$u(t) = -K \cdot \hat{d}(t) \tag{4}$$

where K is the optimal feedback gains matrix, depending on dampers distribution and performance index J given in Equation (2), $\hat{d}(t)$ is the optimal estimation of structure's state vector *d(t)*, generated by Kalman filter algorithm using the floors' accelerations $y_m(t)$.

The performance index, defined in Equation (2), contains weighting parameters matrices Q_{nxn} and R_{mxm}. In this investigation matrices Q and R are assumed to be diagonal with positive diagonal elements. The dimension m equals to the number of floors with LQG active devices. It is obvious, that the performance index (2) is a function of the weighting parameters Q and R. The optimal choice of their values, according to modified LQG optimization method (Agranovich et al. 2004), is performed by minimizing the global performance index

$$J_G = \sum_{i=1}^{n} \max_{0 \le t \le t_f} \left| d_i(t) \right| \tag{5}$$

considering the following control forces restrictions

$$\max_{0 \le t \le t_f} \left| u_i(t) \right| \le U_{i,\max} \tag{6}$$

For solution of the modified LQG optimization problem (2) and (5) the following algorithm is proposed:

- **Step 1:** $k = 1$. Specifying initial values of $Q_k=Q_0$, $R_k=R_0$.
- **Step 2:** Calculation of $u(t)$, $d(t)$, which minimize the performance index $J = J(Q_k, R_k)$. For the obtained optimal solution find the value of the global performance index J_{Gk} (5) and verify the constraints (6)
- **Step 3:** $k = k+1$. Updating the values of Q_k, R_k, that decrease the global performance index J_{Gk} under the control constraints (6).
- **Step 4:** Repeat steps 1 - 3 until condition $\left| J_{G,k+1} - J_{G,k} \right| < \varepsilon$ is satisfied.

Following the above described algorithm, peak optimal control forces and inter-story drifts should be calculated at Step 2. For this reason response of the optimal controlled structure to the artificial white noise ground motion is simulated.

For carrying out Step 3, any parametrical optimization numerical method can be used. The optimization procedure (Agranovich, 2004) is realized using MATLAB functions "dlqry", "Kalman" (Control System Toolbox) and "fmincon" (Optimization Toolbox).

CRITERIA OF DAMPERS CONFIGURATION EFFICIENCY

For evaluating the efficiency of control systems with limited set of dampers, connected to Chevron braces, the following criteria were proposed (Ribakov, in press):

$$J_1 = \frac{\sum_{i=1}^{NDOF} d_{i,0} - \sum_{i=1}^{NDOF} d_{i,m}}{\sum_{i=1}^{NDOF} d_{i,0} - \sum_{i=1}^{NDOF} d_{i,NDOF}} \cdot 100\,\% \tag{7}$$

where $d_{i,0}$ is the peak inter-story drift at floor i in a structure without dampers, $d_{i,m}$ is the peak inter-story drift at floor i in a structure with optimally distributed dampers located at m active floors and $d_{i,NDOF}$ is the peak inter-story drift at floor i in a structure with optimally distributed dampers located at all floors.

$$J_2 = \frac{\sum_{i=1}^{NDOF} a_{i,0} - \sum_{i=1}^{NDOF} a_{i,m}}{\sum_{i=1}^{NDOF} a_{i,0} - \sum_{i=1}^{NDOF} a_{i,NDOF}} \cdot 100\,\% \tag{8}$$

where $a_{i,0}$ is the peak acceleration at floor i in a structure without dampers, $a_{i,m}$ is the peak acceleration at floor i in a structure with optimally distributed dampers located at m active floors and $a_{i,NDOF}$ is the peak acceleration at floor i in a structure with optimally distributed dampers located at all floors.

$$J_3 = \frac{BS_0 - BS_m}{BS_0 - BS_{NDOF}} \cdot 100\,\% \tag{9}$$

where BS_i is the peak base shear force in a structure without dampers, BS_m is the peak base shear force in a structure with optimally distributed dampers located at m active floors and BS_{NDOF} is the base shear force in a structure with optimally distributed dampers located at all floors.

Similar criteria are proposed to examine the effectiveness of a control system with a limited number of active devices connected to amplifiers:

$$J_4 = \frac{\sum_{i=1}^{NDOF} d_{i,0} - \sum_{i=1}^{NDOF} d_{i,m,AM}}{\sum_{i=1}^{NDOF} d_{i,0} - \sum_{i=1}^{NDOF} d_{i,NDOF}} \cdot 100\% \qquad (10)$$

where $d_{i,m,AM}$ is the peak inter-story drift at floor i in a structure with optimally distributed dampers connected to amplifiers at m active floors.

$$J_5 = \frac{\sum_{i=1}^{NDOF} a_{i,0} - \sum_{i=1}^{NDOF} a_{i,m,AM}}{\sum_{i=1}^{NDOF} a_{i,0} - \sum_{i=1}^{NDOF} a_{i,NDOF}} \cdot 100\% \qquad (11)$$

where $a_{i,m,AM}$ is the peak acceleration at floor i in a structure with optimally distributed dampers, connected to amplifiers at m active floors.

$$J_6 = \frac{BS_0 - BS_{m,AM}}{BS_0 - BS_{NDOF}} \cdot 100\% \qquad (12)$$

where $BS_{m,AM}$ is the peak base shear force in a structure with optimally distributed dampers, connected to amplifiers at m active floors.

AMPLIFYING DEVICES

It is well known that during earthquakes rigid structures have small inter-story drifts and drift velocities. Hence the effect of energy dissipation in damping devices connected to Chevron braces (Figure 1a) is not always high as desired. Using amplifying devices increases the deformations and velocities transferred to dampers and consequently enhances their efficiency. It was demonstrated experimentally and analytically that the toggle brace configuration (Figure 1b) increases energy dissipation (Taylor, 2000, Constantinou, 2001).

A more effective amplifier called a "scissor-jack" (Figure 1d) has demonstrated high magnifying effect (Constantinou, 2000). It was reported that using this configuration reduces the required

Figure 1. Dampers configurations: (a) Chevron brace, (b) toggle brace, (c) lever arm, (d) scissor jack

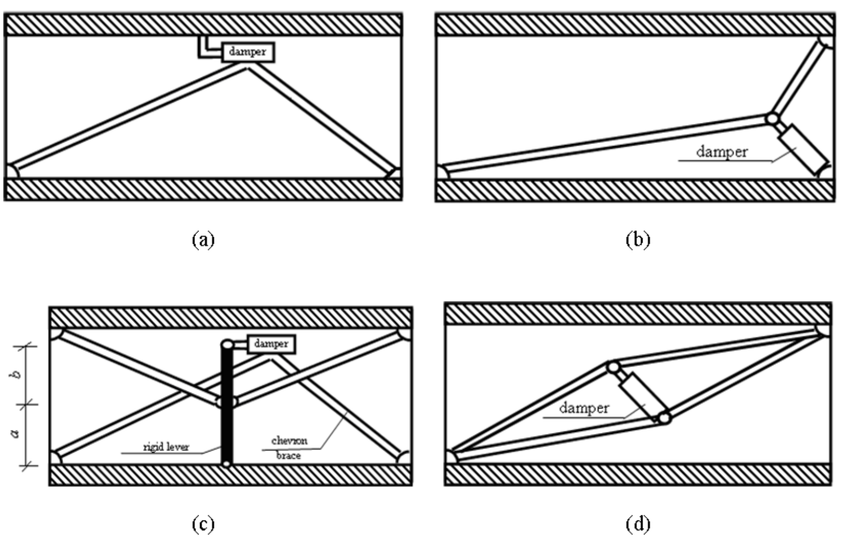

damper force and yields the desired damping effect. Using "scissor-jacks" results in a relatively lower number of damping units required to obtain optimal distribution of devices, compared to toggle braces.

Lever arms (Figure 1c) are proposed to increase the efficiency of damping devices by magnifying the inter-story drifts and drift velocities, transferred from the structure to dampers (Gluck, 1996). This idea was further developed for design of structures with optimal viscous dampers (Ribakov, 2000). The "equivalent" lever arm approach is used to change the effect of off the shelf linear viscous devices yielding an optimal passive control system.

Other effective mechanical amplifying systems are also used for connecting semi-active and active dampers in order to reduce the control forces and the energy required for activation of control devices (Gluck, 2000, Ribakov, 2000). In this study efficiency of lever arm amplifiers for connection of active controlled devices is studied. First optimal locations of control devices are obtained. The amplifiers are used for further decreasing the number of control devices at each floor.

The efficiency of amplifiers can be substantially reduced due to the deformations of connecting elements. A design procedure for lever arm amplifiers, compensating for the bending of structural levers was proposed by Ribakov (2003). It was demonstrated that the proposed design technique is efficient in viscous damped structures. It was shown that the effectiveness of the lever arm amplifier increases for larger amplifying ratios, which depends on the geometry of the system and on the stiffness of the lever arm itself.

If a viscous device is connected to a lever arm, the lever arm deflection decreases the amplification effect. For active controlled actuators the control force usually does not depend on velocity, but the lever arm deflection increases the energy, required for activation of actuators. Following Ribakov (2003), when the desired amplification is determined from other considerations, the height of the Chevron brace l_2 (Figure 2) can be obtained as:

$$l_2 = \frac{H_{st} AL}{1 + AL} \tag{13}$$

where H_{st} is the story height and AL is the amplifying lever ratio for the case of a rigid lever arm:

$$AL = l_2 / l_1 \tag{14}$$

The deflection of the lever arm at each time increment can be expressed as:

$$\Delta = \frac{F_c l_2^2}{3\,EI_{LA}}\left(l_1 + l_2\right) = \frac{F_c l_2^2}{3\,EI_{LA}} H_{st} \tag{15}$$

where F_c and I_{LA} are the force in the actuator and the inertia moment of the lever arm, respectively.

Figure 2. Lever arm calculation scheme

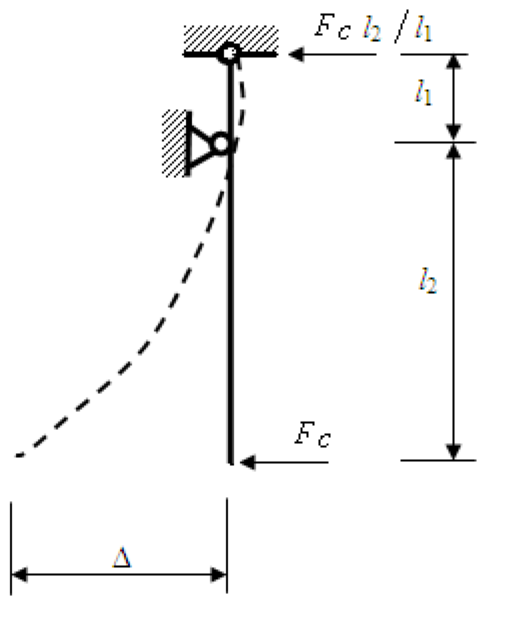

Following Ribakov (2003), the lever arm deflection Δ should be limited by a permitted value, Δ_{perm}, say a proportion of the whole drift d:

$$\Delta \leq \Delta_{perm} = k \cdot d \tag{16}$$

where k is a factor smaller than 1

The effective amplifying ratio of the lever arm system, considering the losses due to bending, AR is

$$AR = \frac{AL \cdot d - \Delta}{d} \tag{17}$$

As it was mentioned above, the losses due to lever arm bending do not require any increase of the optimal control force. They yield additional control energy because the real displacement of the actuator is

$$d_{act} = d \cdot AL + \Delta \tag{18}$$

Knowing the required peak control forces, obtained according to the LQG algorithm, and the maximum forces that may be developed by commercially available actuators, geometry of lever arm amplifiers can be obtained. The section of each lever arm can be selected using the basic design provisions for steel bending elements.

NUMERICAL EXAMPLE

To demonstrate the effectiveness of the proposed method structural seismic response was simulated using originally developed MATLAB routines. The structure selected for this study is a twenty story steel frame shown in Figure 3. It is similar to that used by Spencer *et al.* (1999). The natural damping ratio was assumed to be 2%.

Optimal distribution of dampers for different number of "active" floors was obtained using the

Figure 3. Twenty story steel frame structure

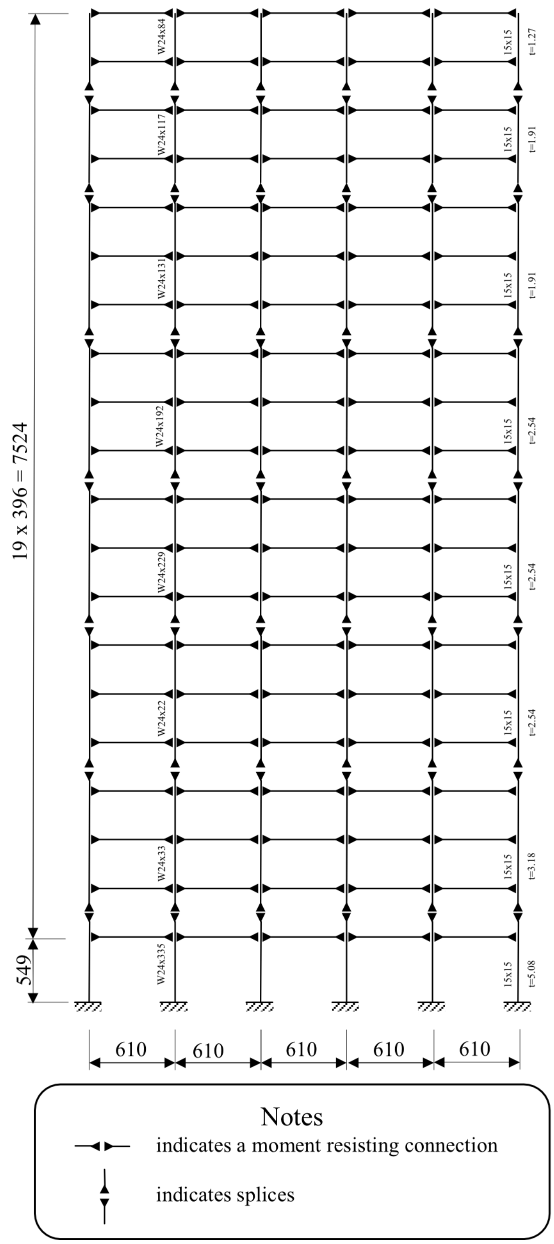

above described procedure. An artificial white noise ground motion with PGA = 0.3g, BW = 30 Hz, t_f = 50 s. was used for this reason. The maximum control force at each damper during this stage was limited to 10% of the story weight and the maximum control force at each floor was limited to 20% of the floor weight. The maximum amplifying lever ratio used in this study was assumed to be 4. Distribution of active controlled devices in the structure for various "active" floors number is shown in Table 1. Following this table, when the number of "active" floors is low, connecting the devices to lever arms decreases the number of dampers by three times and more. The benefit decreases to about 2 times as the number of active floors increases.

At the next stage the earlier defined efficiency criteria (Equations 2, 3, 4, 5, 6, and 7) were calculated. Figure 4 demonstrates efficiency of control systems with various numbers of "active" floors in reduction of structural responses to the white noise ground motion compared to that obtained in the case when all floors are active. As it follows from the figure and from Table 1, when control devices are connected to Chevron braces, if half of the floors in the structure are active (23 devices are used), it is possible to achieve an affect of 70 – 85%, compared with that obtained by a control system with optimally distributed dampers located at all floors (37 devices). When the control devices are connected to lever arms, the same effect may be achieved using just 11 devices.

A similar effect was observed when the structure was subjected to natural ground motions. The following natural earthquake records, scaled to PGA = 0·3 g, were used: El Centro (1940), Kobe (1995) and Hachinohe (1968).

Structural response to these earthquakes was obtained for the following four cases:

- **Case 1:** Structure without dampers;
- **Case 2:** Structure with a control system including optimally distributed dampers, located at all floors and connected to Chevron braces;
- **Case 3:** Structure with a control system including a limited set of optimally distributed dampers, located at *m* active floors and connected to Chevron braces;
- **Case 4:** Structure with a control system including a limited set of optimally distributed dampers, located at *m* active floors and connected to lever arms.

It was assumed that in the frame of this study the number of active floors, *m* is equal to 8. This number of active floors allows an economical solution yielding according to the selected efficiency criteria about 70 - 85% of the effect that may be achieved by an optimal set of active controlled devices located at all floors (see Figure 4). Following Table 1, the optimal solution requires 21 devices connected to Chevron braces or 9 devices connected to lever arms.

Peak floor displacements in the structure under the artificial and natural earthquake records for the four study cases specified above are shown in Figure 5. As it follows from this figure, reduction in peak values of floor displacements under the natural earthquakes were very significant. Using amplifiers allowed reduction of control devices number to 9 and resulted in an effect that was equivalent to that obtained by 21 devices connected to Chevron braces.

Peak values of roof accelerations in the structure are presented in Table 2. Following this table, adding active control devices at all floors (case 2) significantly decreases the peak roof accelerations, compared to the uncontrolled structure (case 1). For the limited set of active control devices (case 3) the decrease in peak roof accelerations was less effective than for case 2.

Roof acceleration time histories are shown in Figure 6. As it follows from this figure, using an optimal set of active controlled devices yields a significant reduction in peak roof accelerations of the structure under all ground motions that were used in the study. Like in the case of peak displacements, also roof accelerations for cases 3 and 4 were equivalent. It proves that using lever arms as amplifiers for connection of active controlled devices (Case 4) yields the same reduction in structural response like an optimal limited set

Table 1. Distribution of active controlled devices in the 20-story structure

Floor	Number of Active Floors																			
	1	**2**	**3**	**4**	**5**	**6**	**7**	**8**	**9**	**10**	**11**	**12**	**13**	**14**	**15**	**16**	**17**	**18**	**19**	**20**
1	$\frac{7}{2}$	$\frac{7}{2}$	$\frac{6}{2}$	$\frac{6}{2}$	$\frac{6}{2}$	$\frac{5}{2}$	$\frac{5}{2}$	$\frac{5}{2}$	$\frac{5}{2}$	$\frac{5}{2}$	$\frac{4}{1}$	$\frac{4}{1}$	$\frac{4}{1}$	$\frac{4}{1}$	$\frac{4}{1}$	$\frac{4}{1}$	$\frac{4}{1}$	$\frac{4}{1}$	$\frac{4}{1}$	$\frac{4}{1}$
2															$\frac{2}{1}$	$\frac{2}{1}$	$\frac{2}{1}$	$\frac{2}{1}$	$\frac{2}{1}$	$\frac{2}{1}$
3																$\frac{2}{1}$	$\frac{2}{1}$	$\frac{2}{1}$	$\frac{2}{1}$	$\frac{2}{1}$
4																	$\frac{2}{1}$	$\frac{2}{1}$	$\frac{1}{1}$	$\frac{1}{1}$
5								$\frac{2}{1}$	$\frac{2}{1}$	$\frac{2}{1}$	$\frac{2}{1}$	$\frac{2}{1}$	$\frac{2}{1}$	$\frac{2}{1}$	$\frac{2}{1}$	$\frac{2}{1}$	$\frac{2}{1}$	$\frac{2}{1}$	$\frac{2}{1}$	$\frac{2}{1}$
6		$\frac{4}{1}$	$\frac{3}{1}$	$\frac{3}{1}$	$\frac{3}{1}$	$\frac{3}{1}$	$\frac{2}{1}$	$\frac{2}{1}$	$\frac{2}{1}$	$\frac{2}{1}$	$\frac{2}{1}$	$\frac{2}{1}$	$\frac{2}{1}$	$\frac{2}{1}$	$\frac{2}{1}$	$\frac{2}{1}$	$\frac{2}{1}$	$\frac{2}{1}$	$\frac{2}{1}$	$\frac{2}{1}$
7				$\frac{3}{1}$	$\frac{3}{1}$	$\frac{2}{1}$	$\frac{2}{1}$	$\frac{2}{1}$	$\frac{2}{1}$	$\frac{2}{1}$	$\frac{2}{1}$	$\frac{2}{1}$	$\frac{2}{1}$	$\frac{2}{1}$	$\frac{2}{1}$	$\frac{2}{1}$	$\frac{2}{1}$	$\frac{2}{1}$	$\frac{2}{1}$	$\frac{2}{1}$
8						$\frac{2}{1}$	$\frac{2}{1}$	$\frac{2}{1}$	$\frac{2}{1}$	$\frac{2}{1}$	$\frac{2}{1}$	$\frac{2}{1}$	$\frac{2}{1}$	$\frac{2}{1}$	$\frac{2}{1}$	$\frac{2}{1}$	$\frac{2}{1}$	$\frac{2}{1}$	$\frac{2}{1}$	$\frac{2}{1}$
9										$\frac{2}{1}$	$\frac{2}{1}$	$\frac{2}{1}$	$\frac{2}{1}$	$\frac{2}{1}$	$\frac{2}{1}$	$\frac{2}{1}$	$\frac{2}{1}$	$\frac{2}{1}$	$\frac{2}{1}$	$\frac{2}{1}$
10														$\frac{2}{1}$	$\frac{2}{1}$	$\frac{2}{1}$	$\frac{2}{1}$	$\frac{2}{1}$	$\frac{2}{1}$	$\frac{2}{1}$
11											$\frac{2}{1}$	$\frac{2}{1}$	$\frac{2}{1}$	$\frac{2}{1}$	$\frac{2}{1}$	$\frac{2}{1}$	$\frac{2}{1}$	$\frac{2}{1}$	$\frac{2}{1}$	$\frac{2}{1}$
12									$\frac{2}{1}$	$\frac{2}{1}$	$\frac{2}{1}$	$\frac{2}{1}$	$\frac{2}{1}$	$\frac{2}{1}$	$\frac{2}{1}$	$\frac{2}{1}$	$\frac{2}{1}$	$\frac{2}{1}$	$\frac{2}{1}$	$\frac{2}{1}$
13													$\frac{2}{1}$	$\frac{2}{1}$	$\frac{2}{1}$	$\frac{2}{1}$	$\frac{2}{1}$	$\frac{2}{1}$	$\frac{2}{1}$	$\frac{2}{1}$
14					$\frac{3}{1}$	$\frac{2}{1}$	$\frac{2}{1}$	$\frac{2}{1}$	$\frac{2}{1}$	$\frac{2}{1}$	$\frac{2}{1}$	$\frac{2}{1}$	$\frac{2}{1}$	$\frac{2}{1}$	$\frac{2}{1}$	$\frac{2}{1}$	$\frac{2}{1}$	$\frac{2}{1}$	$\frac{2}{1}$	$\frac{2}{1}$
15			$\frac{3}{1}$	$\frac{3}{1}$	$\frac{3}{1}$	$\frac{3}{1}$	$\frac{3}{1}$	$\frac{3}{1}$	$\frac{2}{1}$	$\frac{2}{1}$	$\frac{2}{1}$	$\frac{2}{1}$	$\frac{2}{1}$	$\frac{2}{1}$	$\frac{2}{1}$	$\frac{2}{1}$	$\frac{2}{1}$	$\frac{2}{1}$	$\frac{2}{1}$	$\frac{2}{1}$
16							$\frac{2}{1}$	$\frac{2}{1}$	$\frac{2}{1}$	$\frac{2}{1}$	$\frac{2}{1}$	$\frac{2}{1}$	$\frac{2}{1}$	$\frac{2}{1}$	$\frac{2}{1}$	$\frac{2}{1}$	$\frac{2}{1}$	$\frac{2}{1}$	$\frac{2}{1}$	$\frac{2}{1}$
17																	$\frac{2}{1}$	$\frac{2}{1}$	$\frac{2}{1}$	$\frac{1}{1}$
18																		$\frac{2}{1}$	$\frac{1}{1}$	$\frac{1}{1}$
19																			$\frac{1}{1}$	$\frac{1}{1}$
20																				$\frac{1}{1}$
Total	$\frac{7}{2}$	$\frac{11}{3}$	$\frac{12}{4}$	$\frac{15}{5}$	$\frac{18}{6}$	$\frac{18}{7}$	$\frac{19}{8}$	$\frac{21}{9}$	$\frac{21}{10}$	$\frac{23}{11}$	$\frac{24}{12}$	$\frac{26}{13}$	$\frac{28}{14}$	$\frac{30}{15}$	$\frac{32}{16}$	$\frac{34}{17}$	$\frac{36}{18}$	$\frac{38}{18}$	$\frac{37}{19}$	$\frac{37}{20}$

*Note: number of dampers, connected to Chevron braces (numerator) or to amplifiers (denominator)

Figure 4. Efficiency of control system with limited number of active floors under artificial and real earthquakes

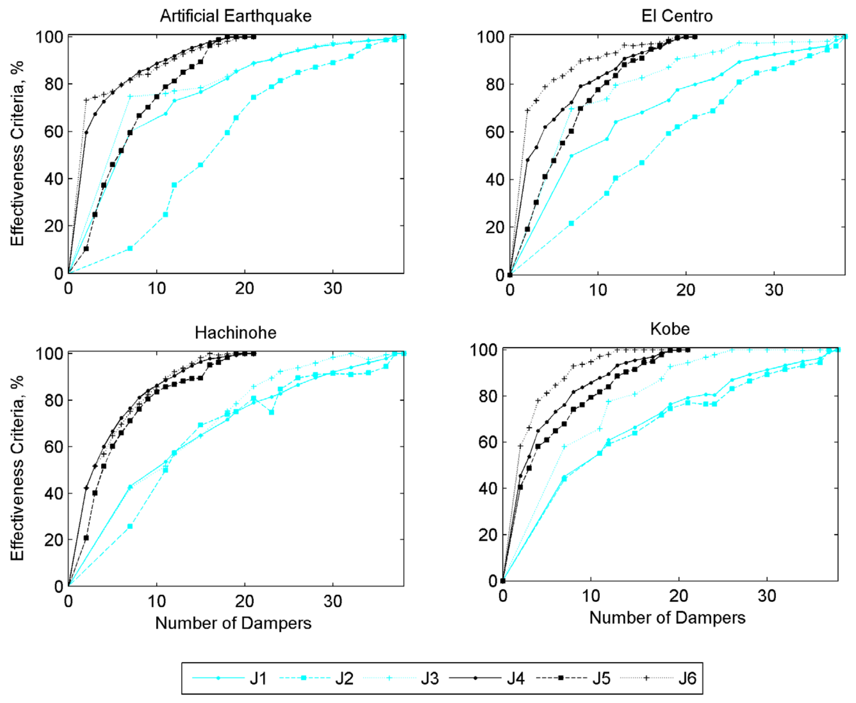

Figure 5. Peak floor displacements under artificial and real earthquakes

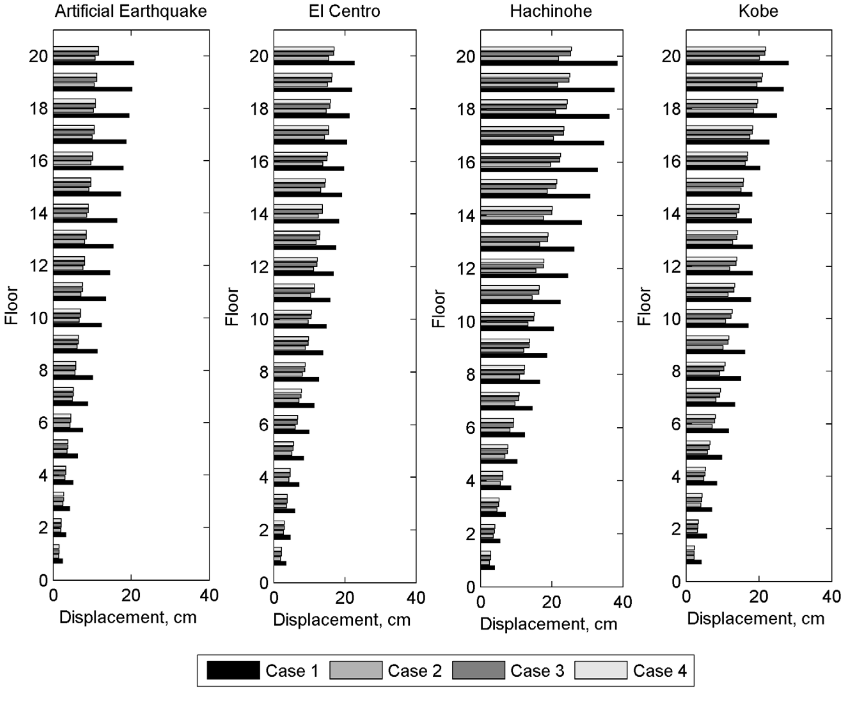

Figure 6. Roof acceleration time histories

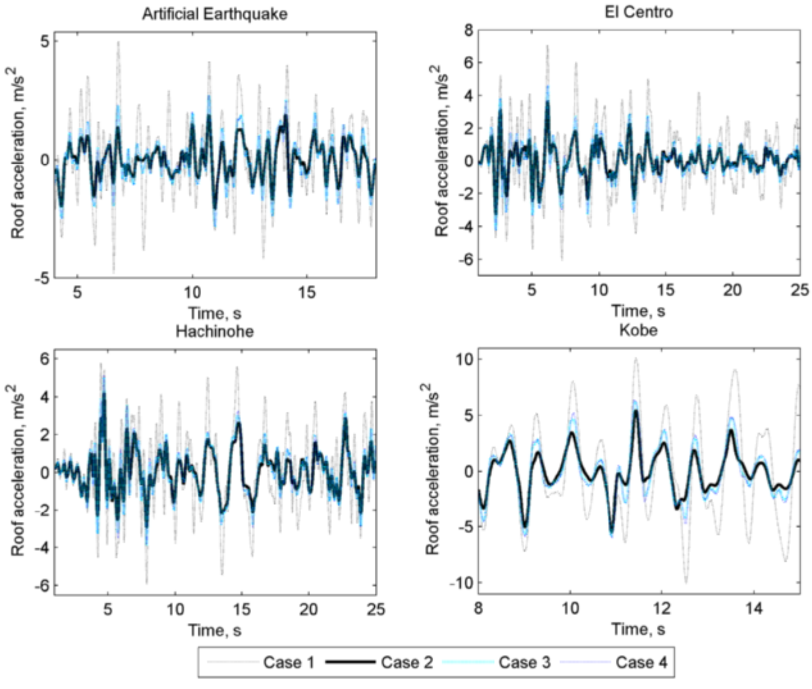

of these devices connected to Chevron braces (Case 3).

CONCLUSION

The effect of a limited set of active controlled devices on structural seismic response was studied. A method for finding the optimal location of control devices yielding the desired structural response by minimum cost was used. The devices were connected to lever arm amplifiers to increase control efficiency.

Analysis of the amplification and active controlled devices placement on efficiency of a control system was performed. A twenty-story framed structure with active control systems including different dampers configurations was simulated. The response of the structure to an artificial white noise ground motion was simulated in order to find the optimal locations of control devices. Behavior of the structure was further investigated under natural earthquake excitations.

It was demonstrated that using an optimal limited set of active controlled devices yields almost the same reduction in structural displacements and accelerations like an optimal set of devices located at all floors. It was further shown that connecting the control devices to lever arms allows getting the same improvement in structural behavior like by connecting them to Chevron braces, but the first configuration requires less devices and enables

Table 2. Peak roof accelerations (m/s²)

Ground motion	Case			
	1	2	3	4
Artificial (white noise)	5.0	2.1	2.8	2.8
El Centro	7.1	3.6	4.6	4.6
Kobe	10.1	5.5	6.2	6.4
Hachinohe	5.9	4.2	5.0	5.2

to obtain more open bays without obstructions, compared to the second.

The results of this study show an attractive way for selection of proper dampers location and configuration, allowing the lowest and most effective control. In the authors' opinion, efficiency of lever arm configuration in active controlled structures, designed using non-linear control algorithms, should be further investigated.

REFERENCES

Agranovich, G., & Ribakov, Y. (2010). A method for efficient placement of semi-active dampers in seismically excited structures. *Structural Control and Health Monitoring*, *17*(5), 513–531.

Agranovich, G., Ribakov, Y., & Blostotsky, B. (2004). A numerical method for choice of weighting matrices in active controlled structures. *Structural Design of Tall and Special Buildings*, *13*, 55–72. doi:10.1002/tal.233

Ali, S. F., & Ramaswamy, A. (2009). Hybrid structural control using magnetorheological dampers for base isolated structures. *Smart Materials and Structures*, *18*(5), 055011. doi:10.1088/0964-1726/18/5/055011

Berton, S., & Bolander, E. B. (2005). Amplification system for supplemental damping devices in seismic applications. *Journal of Structural Engineering*, *131*(6), 979–983. doi:10.1061/(ASCE)0733-9445(2005)131:6(979)

Chang, M. I. J., & Soong, T. T. (1980). Optimal controller placement in modal control of complex systems. *Journal of Mathematical Analysis and Applications*, *75*, 340–358. doi:10.1016/0022-247X(80)90084-0

Chen, S. H., & Yang, G. (2003). A method for determining locations of electro-rheological dampers in structures. *Smart Materials and Structures*, *12*, 164. doi:10.1088/0964-1726/12/2/302

Cheng, F. Y., Jiang, H., & Zhang, X. (2002). Optimal placement of dampers and actuators based on stochastic approach. *Earthquake Engineering and Engineering Vibration*, *1*(2), 237–249. doi:10.1007/s11803-002-0069-y

Choi, H., & Kim, J. (2010). New installation scheme for viscoelastic dampers using cables. *Canadian Journal of Civil Engineering*, *37*, 1201–1211. doi:10.1139/L10-068

Constantinou, M. C., Tsopelas, P., Hammel, W., & Sigaher, A. N. (2000). New configurations of fluid viscous dampers for improved performance. *Passive Control Symposium Proceedings,* Tokyo Institute of Technology, Yokohama, Japan.

Constantinou, M. C., Tsopelas, P., Hammel, W., & Sigaher, A. N. (2001). Toggle-brace-damper seismic energy dissipation systems. *Journal of Structural Engineering*, *127*(2), 105–112. doi:10.1061/(ASCE)0733-9445(2001)127:2(105)

Datta, T. K. (2003). A state-of-the-art review on active control of structures. *ISET Journal of Earthquake Technology*, *40*(1), 1–17.

Fujita, K., Moustafa, A., & Takewaki, I. (2010). Optimal placement of viscoelastic dampers and supporting members under variable critical excitations. *Earthquakes and Structures*, *1*(1), 43–67.

Gluck, J., & Ribakov, Y. (1999). *Practical design of MDOF structures with supplemental viscous dampers using amplifying devices*. International Conference on Earthquake Hazard and Risk in the Mediterranean Region, North Cyprus, October 18-22.

Gluck, J., & Ribakov, Y. (2000). Semi-active friction system with amplifying braces for control of MDOF structures. *Structural Design of Tall Buildings*, *10*(2), 107–120. doi:10.1002/tal.168

Gluck, N., Reinhorn, A. M., Gluck, J., & Levy, R. (1996). Design of supplemental dampers for control of structures. *Journal of Structural Engineering*, *122*(12), 1394–1399. doi:10.1061/(ASCE)0733-9445(1996)122:12(1394)

Gu, Z. Q., & Oyadiji, S. O. (2008). Application of MR damper in structural control using ANFIS method. *Computers & Structures*, *86*(3-5), 427–436. doi:10.1016/j.compstruc.2007.02.024

Hahn, G. D., & Sathiavageeswarm, K. R. (1992). Effects of added-damper distribution on the seismic response of buildings. *Computers & Structures*, *43*(5), 941–950. doi:10.1016/0045-7949(92)90308-M

Hanson, R. D., & Soong, T. T. (2001). Seismic design with supplemental energy dissipation devices. *EERI Monograph Series*, *8*, 47–53.

Housner, G. W., Bergman, L. A., Caughey, T. K., Chassiakos, A. G., Claus, R. O., & Masri, S. F. (1997). Structural control: Past, present and future. *Journal of Engineering Mechanics*, *123*(9), 897–971. doi:10.1061/(ASCE)0733-9399(1997)123:9(897)

Ikeda, Y. (2004). Active and semi-active control of buildings in Japan. *Journal of Japan Association for Earthquake Engineering*, *4*(3), 278–282.

Kelly, J. M. (1986). A seismic base isolation: A review and bibliography. *Soil Dynamics and Earthquake Engineering*, 202–216. doi:10.1016/0267-7261(86)90006-0

Liu, W. (2003). *Optimization strategy for damper configurations of buildings based on performance indices*. Ph. D. Thesis, State University of New York at Buffalo.

Pantelides, C. P., & Cheng, F. Y. (1990). Optimal placement of controllers for seismic structures. *Engineering Structures*, *12*(4), 254–262. doi:10.1016/0141-0296(90)90024-M

Rama Mohan Rao, A., & Sivasubramanian, K. (2008). Optimal placement of actuators for active vibration control of seismic excited tall buildings using a multiple start guided neighbourhood search algorithm. *Journal of Sound and Vibration*, *311*(1-2), 133–159. doi:10.1016/j.jsv.2007.08.031

Rao, S. S., Pan, T. S., & Venkayya, V. B. (1991). Optimal placement of actuators in actively controlled structures using genetic algorithms. *AIAA Journal*, *29*(6), 942–943. doi:10.2514/3.10683

Ribakov, Y. (2003). Selective controlled base isolated multi-story structures with combined damping systems and amplifying braces. *European Earthquake Engineering*, *17*(1), 39–49.

Ribakov, Y., & Agranovich, G. (2007). A roof isolation system with variable friction dampers for seismic protection of multistory buildings. *European Earthquake Engineering*, *21*(1), 10–15.

Ribakov, Y., & Agranovich, G. (in press). Control of structural seismic response by a limited set of active dampers. *Structural Design of Tall and Special Buildings*.

Ribakov, Y., & Dancygier, A. N. (2006). High efficiency amplifiers for viscous damped structures subjected to strong earthquakes. *Structural Design of Tall and Special Buildings*, *15*(2), 221–232. doi:10.1002/tal.292

Ribakov, Y., & Gluck, J. (2002). Selective controlled base isolation system with magnetorheological dampers. *Earthquake Engineering & Structural Dynamics*, *31*(6), 1301–1324. doi:10.1002/eqe.164

Ribakov, Y., Gluck, J., & Gluck, N. (2000). *Practical design of MDOF structures with supplemental viscous dampers using mechanical levers*. ASCE Specialty Conference on Probabilistic Mechanics and Structural Reliability, Notre Dame, U. S. A., 24-26 July, 2000, Paper No 2000-005.

Ribakov, Y., & Reinhorn, A. M. (2003). Design of amplified structural damping using optimal considerations. *Journal of Structural Engineering*, *129*(10), 1422–1427. doi:10.1061/(ASCE)0733-9445(2003)129:10(1422)

Shook, D., Lin, P. Y., Lin, T. K., & Roschke, P. N. (2007). A comparative study in the semiactive control of isolated structures. *Smart Materials and Structures*, *16*, 1433–1446. doi:10.1088/0964-1726/16/4/058

Sigaher, A. N., & Constantinou, M. C. (2003). Scissor-jack-damper energy dissipation system. *Earthquake Spectra*, *19*(1), 133–158. doi:10.1193/1.1540999

Soong, T. T. (1988). State-of-the-art review: Active structure control in civil engineering. *Engineering Structures*, *10*(2), 73–84.

Soong, T. T. (1990). *Active structural control: Theory and practice*. Harlow, UK: Wiley.

Soong, T. T., & Dargush, G. F. (1997). *Passive energy dissipation systems in structural engineering*. London, UK: Wiley.

Soong, T. T., Reinhorn, A. M., Aizawa, S., & Higashino, M. (1994). Recent structural applications of active control technology. *Journal of Structural Control*, *1*(2), 5–21. doi:10.1002/stc.4300010101

Spencer, B. F., Jr., Christenson, R. E., & Dyke, S. J. (1999). Next generation benchmark control problem for seismically excited buildings. *Proceedings of the Second World Conference on Structural Control*, Vol. 2, (pp. 1351–1360). John Wiley & Sons.

Spencer, B. F. Jr, & Nagarajaiah, S. (2003). State of the art of structural control. *Journal of Structural Engineering*, *129*(7), 845–856. doi:10.1061/(ASCE)0733-9445(2003)129:7(845)

Tabeshpour, M. R., & Ebrahimian, H. (2010). Seismic retrofit of existing structures using friction dampers. *Asian Journal of Civil Engineering*, *11*(4), 509–520.

Takewaki, I. (2000). Optimal damper placement for planar building frames using transfer functions. *Structural and Multidisciplinary Optimization*, *20*(4), 280–287. doi:10.1007/s001580050158

Taylor, D. P. (2000). Toggle brace dampers: A new concept for structural control. Advanced technology in structural engineering, *Proceedings of ASCE Structures Congress and Exposition*, Reston.

Wu, Y. W., Rice, R. B., & Juang, J. N. (1979). Sensor and actuator placement for large flexible space structures. *Proceedings of the Joint Automatic Control Conference,* Denver, USA.

Yousefzadeh, A., Sebt, M. H., & Tehranizadeh, M. (2011). The optimal TADAS damper placement in moment resisting steel structures based on a cost-benefit analysis. *International Journal of Civil Engineering*, *9*(1), 23–32.

Chapter 11
Evolutionary Optimization of Passive Compensators to Improve Earthquake Resistance

Rolf Steinbuch
Reutlingen University, Germany

ABSTRACT

Compensators are widely used to influence the dynamic response of excited structures. The coupling of additional masses with defined stiffness and damping to the vibrating elements reduces or avoids unwanted oscillations. In earthquake engineering, compensators often consist of one or a small number of such additional mass-spring combinations. To come up with a good design of the compensators, a multidimensional optimization problem has to be solved. As there might be many local optima, evolutionary approaches are the appropriate choice of the optimization strategy. They start with some basic designs. Then a sequence of generations of design variants is studied. The members of each generation are derived from the parent generation by crossing and mutation. The best kids are the parents of the next generation. Optimization results show that the use of compensating systems may essentially reduce the impact of an earthquake.

INTRODUCTION

Earthquakes are one of the most dangerous and most fatal natural disasters people face. Shock waves impose displacements on the bases of buildings which are excited to dynamic response (Chopra 2000, pp. 197 - 221). The following vibration of the building may cause severe damage leading up to the total collapse of the structure. For tall buildings, the dynamic impact is increased by the deformability of the height. In many designs, the classical approach to improve the load-carrying capacity by increasing the static strength produces no satisfactory results. Consequently dynamic ap-

DOI: 10.4018/978-1-4666-2029-2.ch011

proaches like isolation or compensation have to be used. Isolation is realised by the introduction of efficient intermediate layers at the base of the edifice. Compensation is done by the installation of elastically coupled masses along the building's height.

Compensation is done by introducing fitting sets of masses, springs and dampers which are designed to absorb parts of the earthquake energy. As the impact of an earthquake in terms of amplitude and frequency is not uniquely defined, the compensating system has to respond to a certain variety of excitations. On the other hand, the total mass and space of the compensating system has to be limited since it reduces the usable space of the building.

Compensation systems may be active - using fast control to stimulate accelerations of compensator masses that counteract the external earthquake excitation - or passive - absorbing the energy passed into the structure by an adequate dynamic response. Semi-active dampers, where e.g. the viscosity of the damping fluid changes due to magnetic excitation play an interesting role between the two designs (Han-Rok Ji, H. et al. 2005).

Designing an efficient passive compensating system includes a proposal of position, number and dimension of compensators. For very high buildings, this may include up to 10 or more compensators each defined by mass, stiffness and damping in two horizontal directions resulting in a total of up to 60 or more degrees of freedom to be taken into account for the compensation system. Finding an optimal set of parameters may be a difficult task, as the response surface of the building's loading vs. the parameters of the compensation system may have a large number of local optima. Gradient search strategies tend to converge to the next local optimum, so they are not very efficient. Evolutionary strategies (Rechenberg 1994, pp. 15-44, Gen 2000, pp. 17-34) may be able to cover larger regions of the parameter space, avoiding getting stuck to local maxima.

The application of dynamic loads to simplified models of high buildings allows us to study the response of given compensator designs and to perform an optimization study. It may contribute to a significant reduction of the destructive impact the structure has to withstand during the earthquake.

A short review of the theory and some examples demonstrate the potential of the method proposed. As it is relatively easy to implement and to apply, many variants may be checked, yielding proposals for more detailed studies.

IMPROVE THE STRUCTURAL ABILITY TO WITHSTAND EARTHQUAKE IMPACT

The earthquake loading of a building is understood as a base excitation of the building (Towhata 2008, pp. 67-71, Bozorgnia and Bertero 2004, pp. 2-9 - 2-15). Due to the large mass of the surrounding ground compared to the building's mass, the excitation may be considered as displacement controlled. The interface between the surroundings and the building has to follow these displacements. Any approach to limit or reduce the impact on the building has to take into account this displacement history.

The improvement of the static strength by enforcing the load-carrying elements is not always feasible in an economic and aesthetic way. Consequently we need dynamic approaches. One of the often-used ideas to isolate the building's base from the excited ground shows very promising results (Naeim 1999, pp. 93-119, Ordonez 2002). Isolation implies the uncoupling of the buildings' base from the ground by some less stiff but damping components. Unfortunately, it is not easy and sometimes very expensive to design such an isolating base system for very large and high structures.

Some earthquake resistance improvement may be achieved by local dampers or relatively soft parts in an overall stiff structure (Bozorgnia and

Bertero 2004, pp.10-11 - 10-19). Dampers may absorb some of the impact and help to limit the damage of the building. On the other hand, the deflection required to make the dampers consume energy corresponds to large relative displacements for example between floors, so the local damage could be essential, limiting the further use of the edifice.

The same holds for locally weak designs. They restrict the region of severe destruction to some predefined parts which are capable of withstanding the large deformation. But it might be difficult to repair the deformed sections to re-establish the performance of the original structure. Nevertheless, both ideas help to cut the losses during at least one earthquake. This can be an essential advantage compared to the risk of large destruction without any prevention.

Another approach deals with compensator systems (Chopra 2000, pp. 470-471, Den Hartog 1956, pp. 87-121), which are also called tuned mass dampers or absorbers. It is well known that the Eigen frequencies, the Eigen forms and the amplitudes at a given excitation of a dynamic system change if additional masses and springs are added to the initial system. A qualified selection of springs and masses may reduce the earthquake impact on the building. Some compensating systems work with fluids, being driven through U-shaped piping systems instead of masses and springs. Their function and performance is comparable to the mass-spring systems.

Two main approaches are dealt with in practice. Active systems control the displacements of the compensator masses if sensors indicate ground motion (Chen and Wu 2001, Reiterer and Ziegler 2005, Teuffel 2004). This can be very efficient but requires fast control systems, including actuators which are capable of accelerating large masses in a very short amount of time. Compensators using active control have the advantage to respond in a specific way to the external event.

Passive systems do not need sensors, actors and energy supply but they require large masses and a lot of space for their oscillations. Basically they aim to influence the natural modes of the structure. So a dimensioning may be done by compensation the modal contributions as outlined by Den Hartog (1956, pp. 87-121). Both approaches are used for high buildings and for other dynamically excited structures as well.

Passive systems are installed in some of the most popular high buildings. Examples are the Taipeh101 tower (Eddy 2005), where a 660 metric ton mass is hanging close to the roof at a height of 450m or the Burj al Arab in Dubai (Nawrotzki and Dalmer 2005), a hotel where 11 compensators with a mass of 5 metric tons are installed along the 321m height of the skyscraper.

Especially for bridges there are many ideas known that reduce the vibrations caused by wind or by the traffic on the bridge. One of the most popular examples is the stabilisation of the London millennium bridge (Nawrotzki and Dalmer 2005), which had strongly vibrated but is now stable after a passive compensation system has been installed. But for even more simple structures, compensators are used to improve performance and to avoid damage. Bachmann writes about a diving tower which showed material damage due to large oscillations caused by children swinging it (Bachmann. et al. 1994). A compensator reduced the maximum accelerations from about 3 m/sec^2 to less than 0.5 m/sec^2, so the diving tower could be used again; no further damage was observed.

There is no reason to prefer a special proposal to improve the capability of buildings to withstand earthquakes or other dynamic loading. The decision, which method to use should be based on an open discussion of historical, technical, economical and political aspects.

EVOLUTIONARY OPTIMIZATION OF PASSIVE COMPENSATOR SYSTEMS

The main advantage of passive compensation systems is not to require an active control system to reduce the load or the damage caused by the earthquake. This makes them a favourite in cases where the electric energy supply may fail and destruction of even small parts of the edifice would be equivalent to a total economic loss.

To introduce the way of designing passive compensation systems, we have first sketched the optimization strategy to be applied. A discussion of the basics of compensators follows. Then a simplified model of high and slender structures helps to optimize compensators at high towers. Finally some of the most important results are listed.

Evolutionary Optimization Methods

Optimization is one of the most often used and least understood terms in many parts of our lives, not only in engineering. To avoid any confusion about its use, we have introduced a commonly accepted definition (Steinbuch 2004, pp.188-207) which states that:

Optimization is the process of finding the maximum (or minimum) of a given function

$$z = z(p_1, p_2, p_3, \ldots\ldots p_n) \tag{1}$$

by varying the free parameters $p_1, p_2 \ldots, p_n$ without violation of given boundary conditions

$$p_{i,\min} \leq p_i \leq p_{i,\max} \qquad 1 \leq i \leq n \tag{2}$$

and constraints

$$f_c(p_{c1} \cdot p_{c2}, \cdots p_{cm}) \leq r_c \qquad 0 \leq c \tag{3}$$

related to the problem.

The function z should be defined uniquely and accepted by all participants of the optimization process. The list of free parameters has to be checked for its completeness and the ranges the parameters may assume. Constraints may be given by relations between parameters or physical data of the problem like maximum stress, no penetration of neighbouring parts or other incompatibilities.

Evolutionary Optimization, Terms, and Definitions

Following the theories Darwin proposed 150 years ago, biological species develop as new members of the population are produced by crossing their parents' properties with an additional mutation, a small change of these crossed properties. The new members or individuals who better fit into the requirements of their environment will have a better chance to reproduce. Therefore their properties will become dominant, while those of individuals not fitting well will die out or play a minor role.

To come up with a better understanding of the basic ideas of evolutionary optimization, some definitions may be helpful. It should be noted that not all different schools applying evolutionary optimization strategies use identical terms; sometimes they are even contradictory (Rechenberg 1994, pp. 15-44, Michalewicz 1996, pp. 21-32, Gen and Cheng R. 2000, pp. 17-34). Nevertheless the proposals made here are generally accepted and helpful in many applications.

The central terms in evolutionary optimization used frequently in literature are the following:

- **Objective, Goal, Fitness:** Function measuring the quality of an individual of the population. It is defined by its parameter values. The terms are used interchangeably by different authors.

- **Parameters (Free Parameters):** The free parameters are the data that may be modified to find better values of the objective.
- **Parameter Range:** The parameter range limits the values of the free parameters.
- **Individual:** Individuals are the elements of the sets of parents and kids.
- **Generation:** A generation is one step in the evolutionary process given by a set of parents. The production of a new set of kids defines the genesis of a new generation.
- **Number of Parents per Generation:** This number should be sufficiently large to cover some or many possible parameter combinations.
- **Number of Children per Generation:** This number covers the parameter space. So again a large number is preferred.
- **Pairing:** Pairing is the selection of two individuals of the parent generation to produce one common child. Tests provide efficient strategies of pairing.
- **Kill Parents:** Should old parents survive to be parents in the next generation as well?
- **Crossing:** How are the kids' parameters derived from their parents' values? Figure 1a sketches some of the many ways of defining the child's parameter values from the parents' ones (Steinbuch 2010).
- **Mutation:** Mutation is the modification of the parameter values of an individual. There are infinite possibilities to do mutations, so the different types of mutation have to be checked carefully until some experience is collected. Figure 1b proposes some of the possibilities of mutation in a 2-dimensional parameter space.
- **Mutation Radius:** The mutation radius is the maximum amount that a parameter may be changed in one mutation step (Figure 1b).
- **Selection:** Selection is the process of defining the next parent generation out of the set of kids (including their parents or not) of the current generation. Often selection is done by only taking the best *nparent* kids as new parents.
- **Anisotropy:** Anisotropy is the interdependence between the mutations of parameters (Figure 1b).

There are many other terms used in conjunction with evolutionary or bionic optimization. As there is no generally accepted vocabulary, users reading papers from different authors are advised to carefully check the definitions used.

Gradient and Evolutionary Optimization

Optimization of structures takes place in some steps. First the function of a part or system has to be defined. Next some ideas about the physical realisation are set up and evaluated. A decision about the basic design and the space available yields a first proposal (Steinbuch 2004, p.195).

The following steps deal with the variation of the parameters set during the optimization process. This optimization is often done by gradient or evolutionary strategies. In both cases the free parameters used for the optimization are selected from the total of parameters describing the initial solution. For all of these free parameters, ranges of acceptable values are set. Furthermore necessary relations or constraints between the parameters are identified to exclude impossible or infeasible geometries, penetration of neighbouring components, etc. Care should be taken if there are any restrictions to be checked, e.g. the violation of maximum stress or deflection during a mass reduction study. After this initiation the two strategies split up.

The gradient approach needs one or a small number of good initial designs. For these initial designs the values of the objective are determined. Furthermore the gradient of the objective is found by differentiating the objective with the free parameters:

$$\frac{\partial z}{\partial p_i} \approx \frac{z(p_1, p_2 ..., p_{i-1}, p_i + \Delta p, p_{i+1} .. p_n)}{2\Delta p_i} - \frac{z(p_1, p_2 ..., p_{i-1}, p_i - \Delta p, p_{i+1} .. p_n)}{2\Delta p_i} \tag{4}$$

So the gradient is given by:

$$\nabla z^T = \left(\frac{\partial z}{\partial p_1}, \frac{\partial z}{\partial p_2}, \frac{\partial z}{\partial p_3}, .. \quad . \quad . \quad ., \frac{\partial z}{\partial p_n} \right) \tag{5}$$

We step in the direction of the gradient as long as improvements in the objective are to be observed. Very small or zero gradients indicate the vicinity of a local or global maximum. There the process stops. From the inside of the process there is no chance to decide whether a local or global maximum has been found. Consequently different initial designs should be analysed. If they represent a significant part of the solution space, there may be realistically a chance to find the best or global maximum or at least a very good local maximum.

The evolutionary process starts by defining an initial parent generation (cf. Figure 1c). This may be done by taking some qualified initial designs, mutations of a good initial design or by a random process placing the parents' parameters into the space of allowable ranges.

These parents are paired off. Each pair produces only one child by crossing the parameters in a predefined scheme as shown in Figure 1a (Brieger 2008). The kid's parameters are mutated within the range given by the mutation radius and without violating the allowed parameter ranges (Steinbuch 2010). This step of pairing, crossing and mutation is repeated until the number of required kids has been produced. Care should be taken that a kid does not violate some of the restrictions. In this case, the kid is removed from the population and new kids are produced until the desired number of acceptable members of the new generation is defined. The fitness of the kids is evaluated. From the total of new kids (possibly including some of the parents) the new parent generation is selected, and the cycle restarts.

Figure 1d presents some landscapes of 2D optimization problems. There is no doubt that gradient approaches will be superior in the case of isolated hills; however when applied to multi-hill problems they fail to find the global optimum. Evolutionary strategies are able to detect the absolute maximum at the prize of a large mutation radius and many trials during many generations.

This short outline of evolutionary optimization gives some proposals on how to perform the process. There are many possible variants, so a unique way to do evolutionary optimization does not exist. Users should start with simple but typical problems, testing the influence of the different proposals and learning which specific choice of input performs well for the problem to be handled. Those users should keep in mind that, like in nature, large populations and many generations have to be studied before significant improvements may be observed.

Earthquakes as Mechanical Impact on High Buildings

If we want to perform numerical studies of the impact of earthquake on edifices, we have to reduce the complex event of a real earthquake to a reduced model using a small number of parameters. This reduced model has to be able to represent the most important seismic effects acting on a specific edifice during the event in a realistic and not too conservative way.

Interpretation of Earthquake Pulses

From the mechanical point of view, an earthquake is a displacement controlled transient loading on the ground around the building we are looking at (Chopra 2000, pp. 197-206, Meskouris and Hinzen

Figure 1. Evolutionary optimization

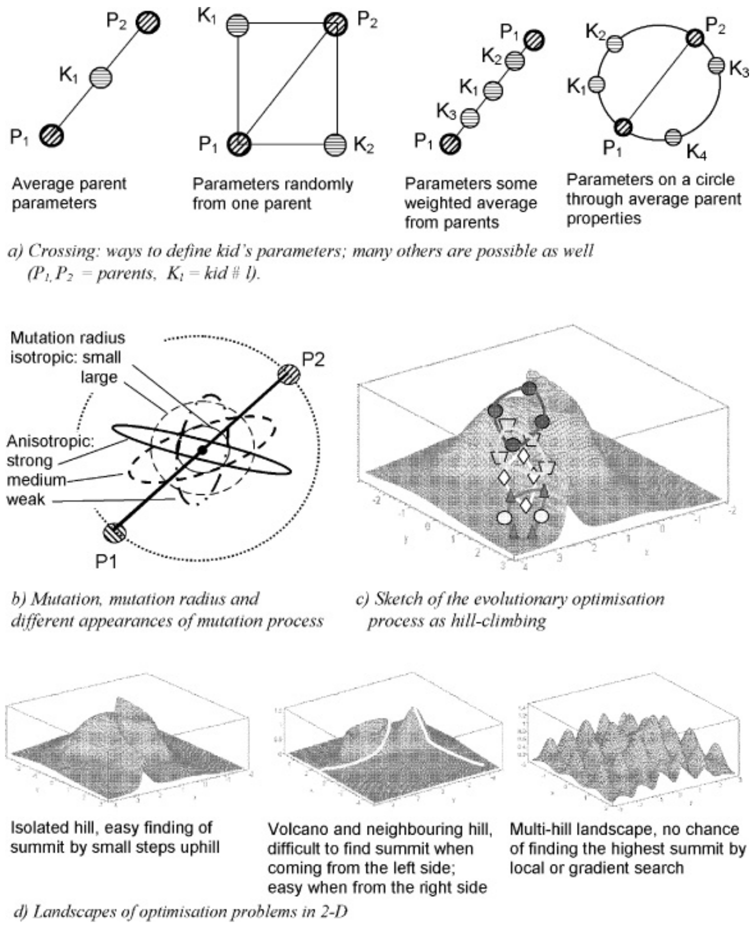

2003, pp. 125-142). Figure 2a shows acceleration records of the Kobe-Earthquake (Berkeley 1995). The total excitation is composed of three dimensional contributions with dominant frequencies in the size of 1 Hz and lasting for some seconds (Figure 2b). Accelerations measured go up to the size of $g = 10\text{m/sec}^2$ or more. In many cases, some preceding and following smaller pulses are registered as well (Meskouris and Hinzen 2003, pp. 80-87).

Interpretation of Earthquake Impact

As there are no specific earthquakes related to different places on earth, earthquake protection in highly endangered zones has to withstand all types of excitation in magnitude and duration to be expected in the specific zone (Towhata 2008, pp. 60-83, Bozorgnia and Bertero 2004, pp. 5-5 - 5-14). Therefore a numerical strategy which is able to deal with all probable types of earthquakes has to be applied. As transient studies deal with only one specific loading system per run, the number of jobs to be done would be very large if we intend to cover a reasonable range of the possible excitations. Therefore a harmonic approach (Chopra 2000, pp. 217-233) seems to be more promising.

To take into account all or much of the possible earthquake displacement time histories, we

Figure 2. Earthquake: acceleration measurement and spectrum

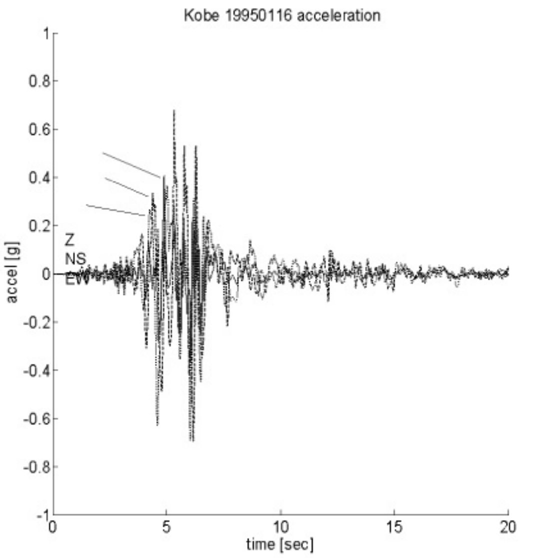

a) measured accelerations at Kobe earthquake

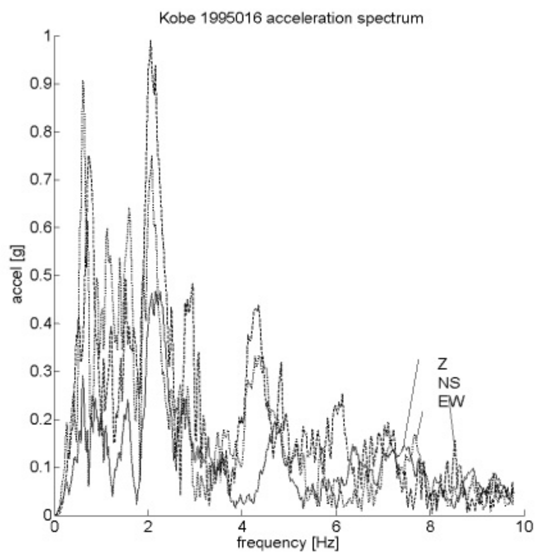

b) spectrum of accelerations of Kobe earthquake

must combine some of the most typical ones by for example, taking the mean of their frequency components. The spectrum of this average earthquake is representative in intensity and frequency as it covers the base terms of the earthquakes to be assumed to act on the building.

Building Response

The ground's seismic time-dependent displacement causes the dynamic response of the structure. We decompose the impact (here interpreted as exciting force) into its frequency components (Figure2b)

$$F = \sum_k F_k e^{i\omega_k t} \qquad \omega_k = k\omega_0 \tag{6}$$

ω_0 being a reasonable base frequency, and check the impact of each frequency on the dynamic system. As one result, we have the response and the elastic energy of the volume of the structure

$$W_{el}(\omega_k) = \frac{1}{2}\int_{Vol} \boldsymbol{\mu}^T_{\max}(\omega_k)\tilde{\mathbf{A}}_{\max}(\omega_k)dVol \tag{7}$$

where $\boldsymbol{\varepsilon}(\omega_k)$ denotes the vector of the strain components and $\boldsymbol{\sigma}(\omega_k)$ the vector of the stress components at the frequency ω_k. The summed response

$$W_{el,tot} = \sum_{k=0}^{k\max} W_{el}(\omega_k) \tag{8}$$

represents the energy input over the frequency range if $\omega_{kmax} = k_{max}\ \omega_0$ stands for a frequency larger than the maximum Eigen frequency to be considered. An optimization of the building's capability to withstand earthquake excitation may be done by minimizing this response or any other appropriate measure.

About Compensators

Compensators are often used to reduce the dynamic response of oscillating systems. Most of the basic formulations are derived by the famous book written by Den Hartog (1956, pp. 87-121). Resonances that would cause inacceptable vibrations are removed by the elastic coupling of additional masses which shift the Eigen frequencies and the amplitudes to regions and values that do not affect the usability of the system. The improvement of the dynamics of bridges and chimneys by compensators is well-known (Nawrotzki 2005). For high buildings passive compensators play an important role as well (Eddy 2005).

One Mass Oscillator and Compensator

From the classical approach of dynamics, it is a good idea to start with a single mass oscillator. It is defined by **the** mass m_1, **the** stiffness k_1 and **the** damping c_1 (Figure 3a). Stiffness and damping are attached to some base which may be fixed in time ($u_g = 0$) or has defined displacements ($u_g = u_g(t)$). The system is excited by either the ground motion $u_g(t)$ or a force $F_1(t)$ acting on the mass m_1. The resulting displacement history $u_l(t)$ may be found by integrating the ODE

$$m\ddot{u}_1 + c\dot{u}_1 + ku_1 = F_1(t) \tag{9}$$

where $F_1(t)$ is either the external force or caused by the displacement $u_g(t)$

$$F_1(t) = k_1\left(u_g(t) - u_1(t)\right) \tag{10}$$

We shall use the complete form of Equation (9) in contradiction to other authors who prefer to divide Equation (9) by the mass and find a dimensionless damping often labelled ζ. The proposal of a viscous damping proportional to the velocity is convenient even if we often do not know exactly which values to use for c.

For the following examples we use a simple dynamic system where

$$\begin{cases} m_1 & = 1 \\ k_1 & = 1 \\ c_1 & = \quad 0.002....0.05 \\ u_{g,\max} & = 1 \\ F_{1,\max} & = 1 \end{cases} \tag{11}$$

so all the other values may be considered as relative values related to this basic data. One result of the ODE (9) is the Eigen frequency of the not damped oscillator

$$\omega_0 = \sqrt{\frac{k_1}{m_1}} \tag{12}$$

1. We usually discuss 3 aspects of the ODE (9):
   Assuming that no external excitation is acting ($F_1(t) = 0$ and $u_g(t) = 0$) yields the Eigen problem

$$m\ddot{u}_1 + c\dot{u}_1 + ku_1 = 0 \tag{13}$$

and the Eigen frequency following Equation (12) for the not damped and

$$\omega_d = \sqrt{\frac{k_1}{m_1} - \frac{c_1^2}{4m_1^2}} = \sqrt{\omega_0^2 - \gamma_1{}^2} \tag{14}$$

where

$$2\gamma_1 = \frac{c_1}{m_1} \tag{15}$$

for the damped system. The resulting displacement-time history is of the type

$$u(t) = u_0 e^{i\omega_d t} e^{-\gamma_1 t} \tag{16}$$

Figure 3. Single-mass oscillator without and with compensator

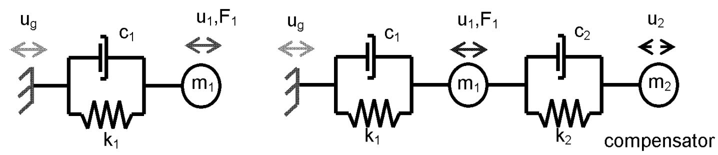

a) Single mass oscillator without and with the compensator: The compensator's mass m_2 is linked to mass m_1 by spring k_2 and damper c_2.

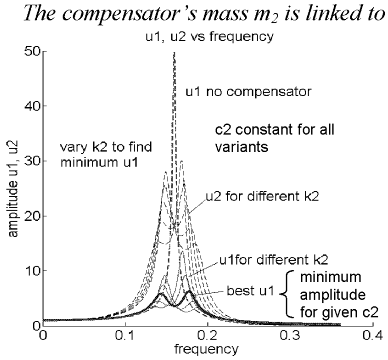

b) Deflection of the masses at a harmonic study: Without the compensator, high resonances occur; a well tuned compensator reduces the maximum amplitude down but has 2 maxima.

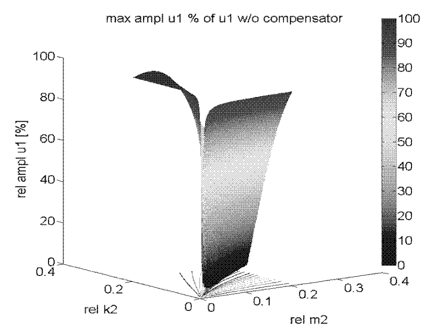

c) Select mass and stiffness for the optimal compensator: Vary mass m_2 and stiffness k_2. Obviously the maximum amplitude of m_1 may be reduced essentially by a good combination of the compensators mass and stiffness.

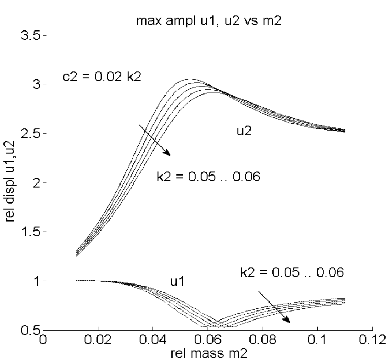

d) Amplitudes vs. compensator mass m_2: Compensators need to be well-tuned to be efficient.

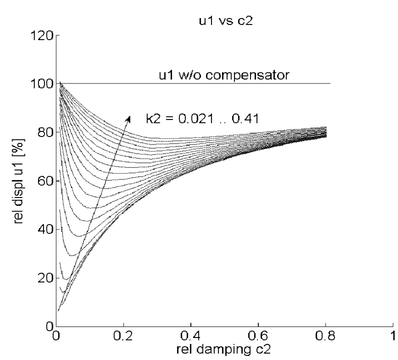

e) Efficiency of the compensator as function of damping c_2. Mass m_2 = .05: Damping that is too large damping reduces the efficiency of the compensator.

The initial deflection u_0 depends on the initial excitation which caused the mass to oscillate.

2. If the force F_1 may be regarded as periodic with a frequency ω_{ex} Equation (9) takes the form

$$m_1\ddot{u}_1 + c_1\dot{u}_1 + k_1u_1 = F_1e^{i\omega_{ex}t} \tag{17}$$

Dividing Equation (17) by m_1 and using

$$f_1 = \frac{F_1}{m_1} \tag{18}$$

$$f_1(t) = f_1e^{i\omega_{ex}t} \tag{19}$$

we find a solution of the type

$$u_1(t) = u_0 e^{-i(\omega_{ex}t-\psi)} \tag{20}$$

for the time after the initial response has been damped away. Substituting (20) in (17) yields solutions for the amplitude

$$\left|u_0(\omega)\right| = \left|\frac{F_1 / m_1}{\omega_0^2 - \omega^2 + 2i\gamma_1\omega}\right| \tag{21}$$

and phase

$$\psi_0(\omega) = \arctan(\frac{2\gamma_1\omega}{\omega_0^2 - \omega^2}) \tag{22}$$

which are the well known relations for harmonic excitation. The amplitude, which is our main concern in the following studies, corresponds to the static solution (ω = 0)

$$\left|u_0(0)\right| = \left|\frac{F_1}{k_1}\right| \tag{23}$$

then increases up to the value:

$$u_{0,\max} = u_0(\omega_0) = \frac{F_1}{\omega_0 c_1} \tag{24}$$

at the Eigen frequency of the non-damped system given by Equation (12). For higher values of ω_{ex} the amplitude and velocity decays with growing ω (cf. Equation (21)), while the acceleration remains in its original range:

$$\begin{cases} u(\omega) \approx \dfrac{const}{\omega^2} \\ \dot{u}(\omega) \approx \dfrac{const}{\omega} \\ \ddot{u}(\omega) \approx const \end{cases} \tag{25}$$

3. For the sake of completeness we add that in the case of a non-periodic force F_1, the ODE (9) may be integrated in time using an appropriate integration scheme such as Newmark's, central differences or any other strategy the user likes to apply.

Our main concern is about the periodic force $F_1(t)$ or displacement $u_g(t)$. From Figure 3b we realise that the amplitudes u_1 will assume large values in the region of the Eigen frequency if the damping is small. If the Eigen frequency is close to the exciting frequency at service conditions, severe damage may be the consequence. To avoid these large amplitudes near the Eigen frequency different proposals are used (cf. Equation (21)):

1. Modify the Eigen frequency by some additional stiffness to shift the Eigen frequency away from the frequency of the dynamic service load.
2. Increase the damping to reduce the maximum amplitudes.
3. Reduce the mass to increase the Eigen frequency and to decrease the amplitude at the critical frequency.
4. Modify the loading to avoid the excitation near the resonance by installing other pumps or engines.

These proposals are often used to qualify dynamic systems. They are very efficient and easy to dimension. Unfortunately, they require changing the main parameters of the dynamic system, which is not always feasible, at least not in a satisfactory and economic way. Many applications of such dynamic improvements may be found in the literature; see for example Chopra (2000, pp. 767-777) or Bozorgnia and Bertero 2004, pp. 10-11 - 10-28). Other approaches deal with changes to the dynamic system by introducing new components. They may be defined by

1. Uncoupling the mass from the ground motion $u_g(t)$ by introducing a base isolation by an elastic and damping layer between surrounding ground and the base of the edifice (Chopra 2000, pp. 741-766).
2. Introducing an additional mass-stiffness-damping element at the mass m_1 to modify the Eigen frequencies (Figure 3a). There may be passive masses or active or semi-active systems using e.g. control to accelerate the mass m_2 to minimise the deflection of the mass m_1. Such mass-stiffness-damping systems are called compensators, absorbers or tuned mass dampers.

For base isolation and controlled compensator systems, more detailed information about the advantages and problems are given by Bozorgnia and Bertero (2004, pp. 11-1 - 11-17) and Xu et al. (2004).

The influence of a compensator on the dynamic response of the initial mass may be learned from Figure 3b. The amplitudes "u_1 for different k_2" are significantly smaller at the Eigen frequency, but have 2 maxima of a significant fraction of the initial maximum amplitude. The maximum amplitude of the "best u_1" proposal one in Figure 3b depends strongly on the damping in the system (Figure 3e). There may be problems since we need to provide space for the corresponding deflections of mass m_2. Figure 3c depicts the dependence of the relative amplitude u_1 compared to the one without compensator on the compensator's mass and stiffness. Even relatively small values of damping mass and stiffness cause strong decreases in the amplitude u_1.

Figure 3d compares the amplitudes u_1 and u_2 for some given stiffness k_2. We realise that the amplitude u_2 increases, but u_1 decreases as m_2 increases down to a minimum of u_1. Further augmentation of m_2 reduces the effect of the compensator, u_1 increases again, but u_2 essentially does not decrease. Figure 3e demonstrates that the use of passive compensators measured as the value u_1 with compensator compared to u_1 without compensator is only efficient if the damping c_2 is relatively small. As soon as the damping is too large, the damper c_2 acts more like a stiff link, increasing the mass m_1 by m_2 but not allowing significant relative displacement. So an independent oscillation of m_2 is suppressed, and the compensator is not efficient.

Multi-Mass Compensator Systems

The idea of a passive compensating device is easily expanded to problems with many degrees of freedom. For the sake of simplicity, we are restraining ourselves here to one-dimensional chains of masses, stiffness and dampers excited at one end of the chain as indicated in Figure 4a. For the following examples we again use data like that proposed in Equation (11).

The corresponding system is given by

$$\mathbf{M}\ddot{\mathbf{u}} + \mathbf{C}\dot{\mathbf{u}} + \mathbf{K}\mathbf{u} = \mathbf{F}(t) \tag{26}$$

where

$$\mathbf{M} = \begin{pmatrix} m_1 & 0 & .. & 0 \\ 0 & m_2 & .. & 0 \\ : & : & :: & : \\ 0 & 0. & .. & m_n \end{pmatrix} \tag{27}$$

denotes the mass matrix which may or may not be diagonal.

Figure 4. Multimass oscillators

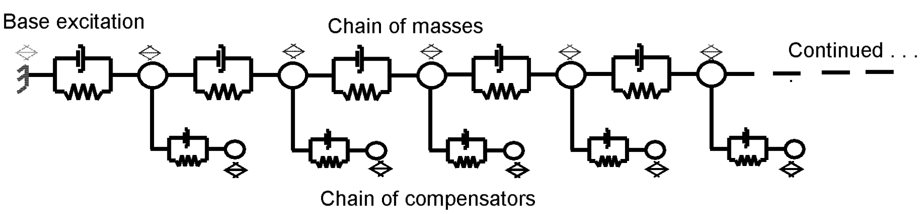

a) Chain of masses and compensators.

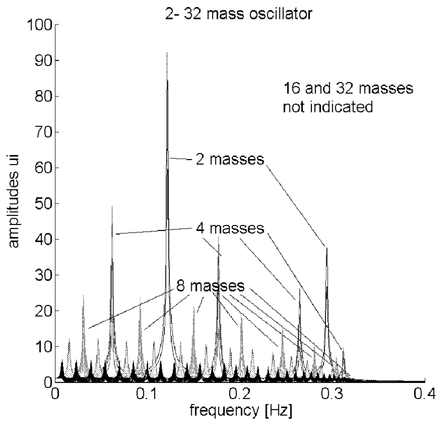

b) Maximum amplitudes as response of multi-mass oscillators: Amplitudes decrease for more masses but energy content remains constant.

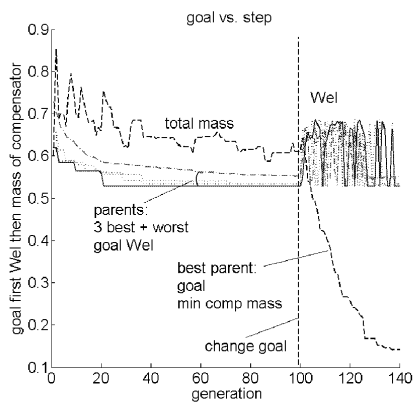

c) Optimisation history of 16 mass oscillator with compensators: After 100 generations the optimisation of the elastic energy (eq. (32)) shows promising results. The next 40 generations are used to reduce the mass of the compensators.

$$\mathbf{C} = \begin{pmatrix} c_1 & 0 & .. & 0 \\ 0 & c_2 & .. & 0 \\ : & : & :: & : \\ 0 & 0 & .. & c_n \end{pmatrix} \tag{28}$$

is the damping matrix if the damping is due to friction related to a fixed environment.

$$\mathbf{C} = \begin{pmatrix} c_{12}+c_g & c_{12} & 0 & . & 0 \\ c_{12} & c_{12}+c_{23} & -c_{23} & . & 0 \\ . & -c_{23} & c_{23}+c_{34} & . & . \\ . & . & . & :: & -c_{n-1,n} \\ 0 & 0 & . & c_{n-1,n} & c_{n-1,n} \end{pmatrix} \tag{29}$$

stands for the damping caused by the relative velocity of two neighbouring masses including c_g, the damping connecting m_1 to the vibrating ground.

$$\mathbf{K} = \begin{pmatrix} k_{12}+k_g & k_{12} & 0 & .. & 0 \\ k_{12} & k_{12}+k_{23} & -k_{23} & .. & 0 \\ 0 & -k_{23} & k_{23}+k_{34} & .. & : \\ : & : & : & :: & -k_{n-1,n} \\ 0 & 0 & . & k_{n-1,n} & k_{n-1,n} \end{pmatrix} \tag{30}$$

is the stiffness matrix including k_g, the stiffness connecting m_1 to the vibrating ground.

Just as with the single mass oscillator, we are primarily interested in the harmonic response. The amplitude of one single-mass point or of some selected mass-points is not representative of the system's energy intake. Instead we take the elastic energy stored in the system as indication of the potential damage:

$$W_{el}(\omega_k) = \frac{1}{2}\mathbf{u}^T(\omega_k)\mathbf{K}\mathbf{u}(\omega_k) \tag{31}$$

(cf. Equation (7) and Equation (8)) either at a given frequency ω or summed over the range of frequencies we are interested in:

$$W_{el,tot} = \sum_{k=0}^{k\max} W_{el}(\omega_k) \tag{32}$$

In Equation (31) **u** stands for the complex displacement derived from Equation (17). The frequency range [0, ω_{max}] should again cover all relevant Eigen frequencies of the problem. Figure 4b compares the amplitudes for dynamic systems (2 − 32 mass oscillators). We see the peaks at the Eigen frequencies and the decreasing amplitudes vs. the increasing number of masses. If we sum the energy (Equation (32)) over the frequency range, we learn that the total elastic energy stored in the chain is nearly constant for the different oscillating systems. This is not a very surprising fact as the external energy is delivered from the same source, the oscillating force or the corresponding ground motion.

To reduce the dynamic response, we may add some compensators here as indicated in Figure 4a. We assume that each mass point has its own compensator. Again we use the summed elastic energy stored in the system (Equation (32)) without the compensators as indication of the internally acting destructive load.

The optimization problem to minimize the energy in the chain is multidimensional now. We use evolutionary approaches to find efficient designs for the compensators' mass and stiffness. We assume the damping to be a small fraction of the stiffness. After some searching of the space of possible values for the m_i, c_i and k_i, we find that the total energy stored in the system may be reduced to about 55% as indicated in Figure 4c for a 16-mass system with additional 16 compensators. The plot shows the fitness function, the elastic energy of the 3 best parents and the worst parent vs. the generation of the optimization process. We used 20 parents, 60 kids and a large mutation radius for 100 generations. In Figure 4c we observe an additional process. Having found an energy level that is close to the minimum of the search, we want to minimise the summed mass of the compensators. Figure 4c indicates that there might be some designs with the same compensation efficiency but essentially smaller masses. We have found compensating systems which are nearly as efficient as the best found up to now but have a significantly smaller mass - about 20% of the mass found before (cf. Figure 4c). So we are able to propose efficient and relatively lightweight designs for compensators of the 16 masses problem. There should be no doubt that this approach may be transferred to other dynamic models with an arbitrary number of masses.

The two step optimisation mentioned above could be easily reduced to a single step process by introducing a combined fitness function by the weighted sum of energy intake (step 1) and mass (step 2). The procedure following Equation (33) is outlined in section 3.5.2. Here we demonstrate the stepped approach to give an idea how to proceed if necessary.

To use the method of modal contributions mentioned above would be a rather tricky task in the case of many compensators applied at many mass points. The interaction of original masses and dampers has to be taken into account, so a multidimensional optimisation problem has to be solved simultaneously. Here evolutionary approaches are superior to conventional gradient methods.

A Simplified Approach to Study Compensators in High Buildings

Dealing with real earthquakes and their impact on buildings requires the use of qualified models of the building including many details. Such models will have large numbers of degrees of freedom (dof). Each floor including its reinforcement and each wall including cut-outs such as doors or windows has to be taken into account.

Problem sizes in the range of at least some 10 000 – 100 000 nodes and elements per floor are not uncommon. At a high building with 100 floors, more than a million nodes define the problem. Consequently every study of such models requires much computing power in terms of storage and computing time. This is generally not a problem using today's computers. Nevertheless the total computing time won't be acceptable if we are going to study many variants to find a satisfactory dynamic response at earthquake excitation.

To come up with faster models, essential reductions are inevitable. A very efficient and common reduction is to handle one or several floors as one beam element taking into account some averaged stiffness, damping and mass distribution (Figure 5a without compensators). A small number of beam elements define the simplified model of a building. This model may be used for a modal, harmonic or transient study analysing large numbers of variants in short times.

Such models help to learn about the Eigen frequencies and the harmonic or transient response at a given excitation. If there is a chance to improve the building by increasing the static strength, changes in the stiffness of the elements may be used to indicate which additional modifications are necessary to reduce the earthquakes' impact on the edifice. More detailed studies using more complex models will then help to decide on the reinforcements to be introduced into the original design.

Beam elements may easily be expanded for the study of compensator systems (Li 2010). To all nodes we add 2 dof to the 6 dof of the beam node (Figure 5b). These 2 dof represent the displacement of the compensator's mass in the 2 plane directions of the floor. They are attached to the corresponding translational dof of the beam via the compensators' stiffness and damping. The mass, stiffness and damping of the compensators are the free parameters for the optimization of a compensation system. At floors without compensators, small values of the compensators' properties produce only negligible effects, so there is no need to use different element types for floors with and without compensator systems (Figure 5a). It is evident that such models allow for fast studies of the dynamic response of structures.

Evolutionary Optimization of Compensators' Positions and Parameters

Having prepared an evolutionary optimization strategy, the application to earthquake resistance follows without many problems. We model the building by the 8 dof/node elements, define a goal or fitness function - a function of the building's response to the earthquake excitation - and try to minimise the goal wrt. the compensators' parameters.

The fitness function is selected according to the phenomena that cause the failure of the building type. It may be any criterion that measures the potential damage of the structure considered. Typical values used are the maximum shear force or the maximum acceleration. Here we prefer the elastic energy of the system without compensators summed over the frequency range of interest (cf. Equation (32)) since it represents some integral value of the earthquake's attack. For more specific and detailed studies, the goal should be adapted according to the available experiences and data.

Figure 5. Simplified building model and optimization results

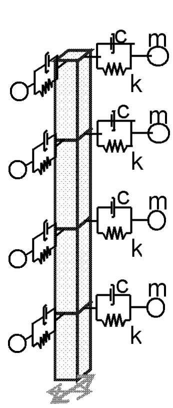

a) Building model including floors and columns vs beam model.

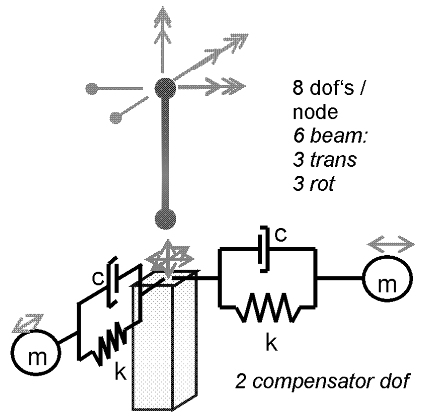

b) Beam element including 2D compensators.

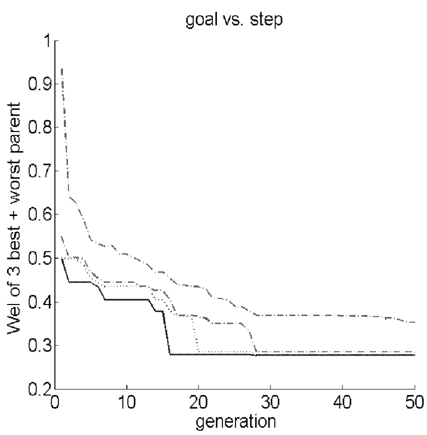

c) Optimisation of a 10 storey building, 3 compensators at floors 5, 8 and 10: Fitness function vs. generation. 3 best and the worst parent of each generation.

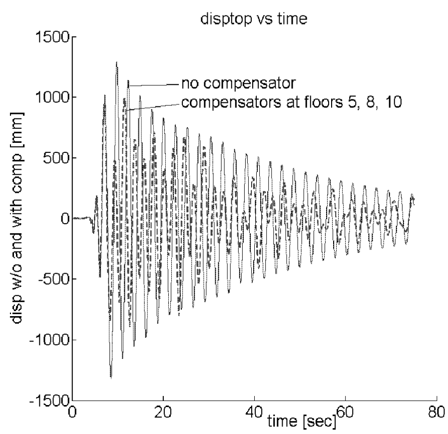

d) Top building deflection w/o and with compensating system vs. time (Kobe NS): After the first impact, the compensating system reduces the amplitude significantly

Parameters of the Optimization Process

The following results are derived from simple examples which may easily be reproduced using conventional results e.g. the modal contributions (Den Hartog 1956 pp. 87-121). Within the numerical tolerances and the scatter of the evolutionary method corresponding results are found.

For the examples outlined, we use a vertical steel structure with a cross section of 5 x 6 m^2 and a height of 100 m. We divide this column in 10 floors where we might apply compensators (cf. Figure 5a). The base excitation is given by the Kobe earthquake NS (Berkeley 1995). The use of any other excitation would yield corresponding results. For real application there should be a comparative analysis with different seismic loadings. The fitness function should then include a summed response of the structure.

We start the optimization of the building by making decisions about some parameters of the optimization job. We define how many compensators are to be installed and on which floors they should be placed. This decision could be the result of an optimization process too. But if we think of a structure with 10 floors, we realise that there are 1024 possible variants of placing compensators, so some reduction of the number of proposals is justified. Table 1 and Figure 6a present the result of such optimizations of the floor number and positioning. The position of the compensators is indicated by a C for the different floors (rows) while the number of compensators increases vertically. It took more than 500h of computing time to find these proposals which we could improve easily by installing the compensators near the maximum amplitudes of the first Eigen frequencies as Figure 6a demonstrates by the curve labelled "engineering proposals." For example placing three compensators at the floors numbered 5 (or even 4), 7 and 9 (or 10) shows a very promising response. This corresponds to the proposals by the conventional modal contribution approach as well.

First we decide about the number and position of compensators. Then we define a range of the dimensions of the compensators' masses, stiffness. Here, once more contradictory effects have to be taken into account. Ranges too small prevent the evolutionary search from finding interesting regions; ranges too large include the danger that the

Table 1. Position of compensators following discrete optimization; Good selection by experienced engineers may yield better results (cf. Figure 6a)

Floor		1	2	3	4	5	6	7	8	9	10
No. of Comp.	1									C	
	2							C		C	
	3				C				C	C	
	4				C	C			C	C	
	5		C			C		C	C	C	
	6	C		C	C			C	C	C	C
	7	C		C		C	C	C		C	C
	8	C	C			C	C	C	C	C	C
	9	C		C	C	C	C	C	C	C	C
	10	C	C	C	C	C	C	C	C	C	C

process converges towards infeasible solutions, as, for example the total weight of the compensators exceeds the building's mass.

Some tests have to be made here like in all evolutionary studies. We remember the example demonstrated in Figure 4c. The fitness function had been switched from the minimal energy to the minimal mass at a reasonable energy level. This is a multi-step approach where different objectives may be helpful. For our 10-storey building

Figure 6. Results of the optimization studies

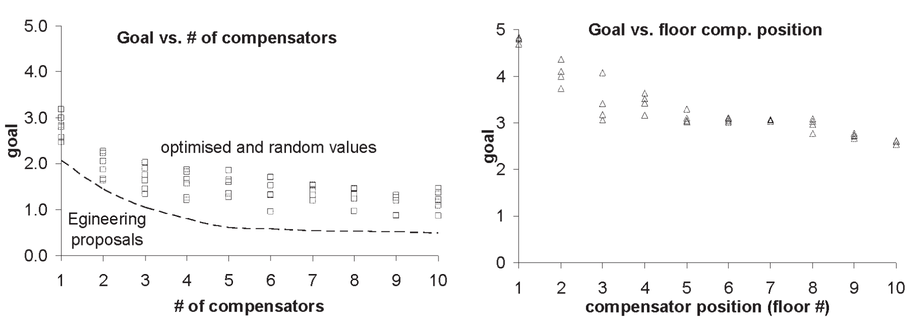

a) Impact W_{el} vs. number of compensators: Optimized and random results compared to proposals based on the maximum amplitude of the first Eigen frequencies. Good engineering guesses prove to be better than jobs optimizing the number and position of the compensators

b) Impact W_{el} vs. position of one compensator: Higher positions are to be preferred, but must not be on the top of the building. Symbols indicate results of different jobs a limitation of the mass to 1%−2% of the mass of a single floor and the stiffness to 10% of the transversal stiffness of the beam elements seems promising as starting values. Figure 3e already proposes using small damping values.

The initial values of the mutation radius should be so large that the parameters of the kids produced by the parents cover an essential part of the total parameter space. On the other hand, a mutation radius which is too large transforms the evolutionary search to a purely random process. A mutation radius which is too small reduces the evolutionary strategy to a local gradient search. Starting with a mutation radius of 25%−50% of the parameter range may help during the initial studies indicating which values to use during the following analysis.

The selection of the number of parents, kids and generations should be done after some preliminary studies of the specific problem. Initial guesses may be the following:

- Let the number of parents be twice the number of free parameters.
- Let the number of kids be twice the number of parents.
- Let the number of generations be in the range of the number of kids.

These starting values together with an appropriate mutation radius will provide ideas on how to proceed. In our compensator optimization study with 10 floors and 3 compensators, the use of 10 parents, 20 kids and 20–40 generations worked well in the initial jobs. Later we increased the data to 20 parents, 50 kids and 100–500 generations.

Many different ways to select the new parents out of a set of kids and perhaps even the old parents exist. It is often a good idea to let some of the best parents survive for at least a limited number of generations. The new parent generation may then be defined by the best of parents and kids of the last generation. It can be useful to expand the region of the parameter space searched by taking some of the not-so-good kids as new parents as well. For studies with relatively small numbers of free parameters as in our problem, parents surviving a long time proved to be accelerating the progress.

Process of Evolutionary Optimization

Evolutionary optimization studies are relatively tolerant and forgive many errors. As long as the mutation radius is not too small, progress will be visible. But like in nature, populations must be sufficiently large and many generations are required before essential progress can be observed. So impatient users or projects where results are required within some hours are not adequate for evolutionary optimization.

To simplify the process of rerunning and evaluation of similar studies, an overlay process creating many jobs and interpreting the most important data could be helpful. If there are qualified ideas on where to locate the best solutions, many parallel studies with slightly different initial data should be performed. Today computing power is available and there is no need to survey the processes. So some nights could be used to run studies on all available computers.

Figure 5c compares the values of the fitness function of the 3 best and the worst parents vs. the generation number. Figure 5d compares the edifice's top deflection vs. time for a structure without and one with a compensation system. Obviously the proposal derived by the analysis outlined is able to reduce the transient impact during the seismic attack.

The example of the changing fitness function (Figure 4c) should be kept in mind once more. If there is a region where the objective assumes acceptable values, why shouldn't we search this region for proposals which optimize other goals? We may transform the damage intensity from the objective to a constraint. Now the search continues for all parameter sets that do not cause a violation of the damage limit to a new objective, for example the minimisation of the compensators mass or the maximum deflection of a compensator. Some cycles help to collect a basic experience. This experience can be used to find satisfactory results.

Combined fitness functions using e.g. the damage impact, the compensators mass and the maximum deflection as contributions work here as well:

$$z(p_1, p_2, \dots p_n) = w_1 z_1(p_1, p_2, \dots p_n) + w_2 z_2(p_1, p_2, \dots p_n) + w_3 z_3(p_1, p_2, \dots p_n) + \dots \quad (33)$$

A well known problem is the definition of the relative weighting factors w_i, which may be avoided when using subsequent optimisation steps, switching old objectives into constraints.

Figure 7a presents a sketch of building with distributed compensators along the height of a building following Fu and Johnson (2009). The main advantage of this approach is not to introduce additional masses into the edifice but to use the fins preventing the sun radiation for the seismic control as well. In contrary to the original active design of Fu and Johnson (2009), we use passive compensators. In our example 20 floors are equipped with such double acting fins. We may use only part of the absorber of each floor as compensator mass. The optimisation now takes place in a combined way as proposed by Equation (33), where the relative weighting for the mass and the energy in the combined objective is $w_2 = w_1$ after scaling both unit mass and unit energy to

Figure 7. Building with distributed compensators

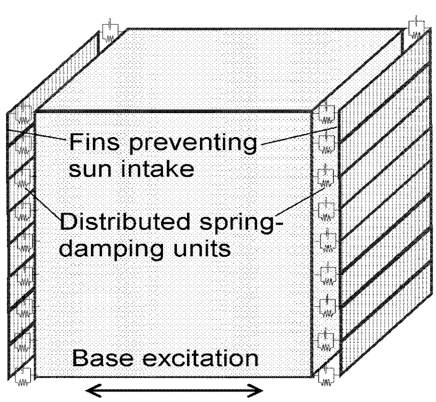

a) Sketch of building with distributed mass damper

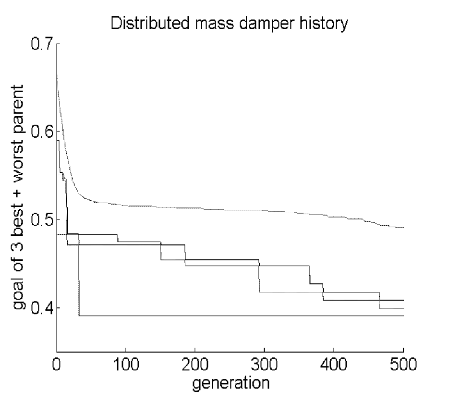

b) Optimization history best and worst parents (normalized values of goal)

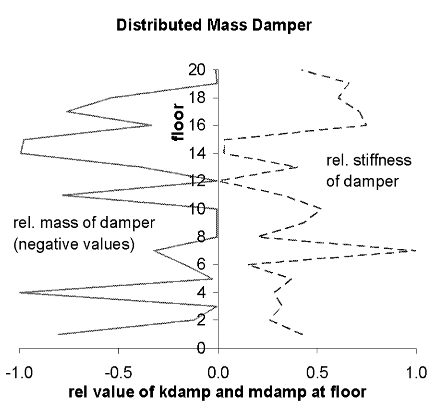

c) Distribution of rel. masses and stiffness along building's height. (rel. masses plotted negative).

Along 20 floors of a building 20 dampers have been installed. The optimisation goal is to minimize the seismic impact and the summed mass of the dampers.
After 500 generations with 50 parents and 100 kids, an essential improvement has been found.
The best design has bee found after 4 generations, the following ones indicate that there are probably no better solutions to occur.
The dampers masses may be applied by using part of the fins of each floor as

the same numerical size. Figure 7b presents the normalized optimisation history. When comparing these results with those of Figure 5c we should remember that now the fitness function is the sum of energy intake and compensator mass. Figure 7c draws the distribution of the stiffness and mass along the buildings height, where we plotted the masses to the left of the vertical axes using the negative value of the mass. Both mass and stiffness are normalized to a predefined value. We realize that there is a large potential of reduction of the impact on the building using a total mass of the compensators of about 2% of the buildings mass. On the other hand it should be mentioned, that this result depends essentially on the definition of the relative weighting factors w_2 and w_1. Switching e.g. to $w_2 = 0.5 * w_1$ yields significantly different results. It is obvious that the design of this absorbing system would be not trivial using conventional methods.

As a general remark it should be mentioned that the evolutionary process including a not-too-small mutation radius is not well-suited for the close approximation of nearby lying local maxima or minima. Therefore it might be a good idea to switch to a local gradient search if one feels that the process is close to an interesting summit (Brieger 2008, Plevris, V. and Papadrakakis, M. 2011).

The method of evolutionary optimization of compensators may be applied to other structures as well. If the mass-, stiffness- and damping-matrices are available, the entries for the additional dof for the compensators may be added and the system solved like outlined. As the time and storage requirements depend on the square of the total number of dof of the dynamic system, the amount of time will grow essentially. Consequently an economical handling of the resources will be needed to come up with reliable results in reasonable time. Grid computing by assembling all the available computing power at night or during lunch breaks proves to be very efficient.

Some Results of the Optimization Studies

The studies performed until now correspond well to the results of other approaches and long-lasting experience in the field. To summarise the most important results, it should be mentioned that

- Essential reduction of the impact of an earthquake up to a factor of 5 and more is possible (Figure 5c).
- Larger numbers of compensators are more efficient (Figure 6a).
- Single compensators at higher floors are more efficient than those at lower floors (Figure 6b).
- At a given number of compensators, an optimal or at least efficient distribution along the building's height may be found (Table 1 and Figure 6a) by the modal contributions.
- Damping should not be too high as it reduces the energy transferred to the compensator mass (Figure 3e).
- Designs for the compensators on different floors are proposed.
- Interaction of the efficiency of compensators may be analysed.

The method proves to be an efficient tool for the design of compensators especially when larger numbers of compensators are to be used.

The large number of jobs to be run keeps seems prohibitive. But if we think of a problem with 40 compensators and 120 dof, the effort of a gradient search is not very much smaller. The numerical derivation (Equation (4)) requires 241 data. If we need 20 steps to find the maximum a total of about 5000 runs have to be performed. As we are not sure, whether our optimisation sticks to the next local maximum, we should repeat the study using different initial values. So numbers of 20 000 or more runs are not uncommon. But then we are in the range of the evolutionary process, so the advantage of the gradient search in the case of a small number of dof has disappeared.

Discussion, Strengths, and Limitations of the Method

Passive compensator systems are used as earthquake prevention installations with satisfactory success. Like any other anti-earthquake strategy, their efficiency is limited by the way they are adapted to the loading history of the expected seismic events. On the other hand, they are useful for many other anti-oscillation applications such as bridges under traffic load or chimneys under wind exposure.

The main advantage of the evolutionary optimisation approach lies in the capability to handle systems with many compensators, especially distributed dampers (Fu and Johnson 2009). In such cases, conventional methods are difficult to apply and tend to find only local maxima of the objective function.

The method outlined shows high potential to improve the design of passive compensator systems to enhance the resistance of buildings. It allows a fast check of many variants and finds even unexpected proposals, as it does not stop at local optima. It is a powerful tool to quantify the effects of the design. Furthermore, due to its drastic simplification of the building, the total system only has a small number of dof. It has to be linear in geometry and stiffness. Such reduced systems always inhibit the danger of ignoring essential properties of the original part. The results should therefore be looked at with sufficient care. It may be helpful as a tool to propose initial designs that may be qualified by more detailed studies. It reduces the numerical effort of the optimization process by a great amount.

Solutions and Recommendations

Optimization is one of the central tasks not only in engineering. Most of our work deals with the improvement of a given design. On the other hand there is no guarantee that we will find the absolute optimum in the case of challenges that are not very trivial. The choice of the optimization strategy therefore has to be made very carefully. Evolutionary procedures are able to cover large regions of parameter spaces even in the case of many local maxima and very irregular landscapes (Figure 1d). But they need very large numbers of trials or individuals. They do not converge very well if a local maximum has to be approached closely, so the option to switch to locally efficient gradient searches should be included.

The use of reduced models always inhibits the loss of information due to reduction. The discrepancy between fast proposals and qualified statements about compensators has to be dealt with. Experience and a critical check of the data produced by the optimization systems are indispensable to interpret the results. Nevertheless, the approach is fast and easy to handle. It may serve as a starting point in compensator design. The idea of introducing extra dof for the compensators may be extended to any other dynamic problem and the evolutionary optimization as well. Motivated engineers will profit from this way of dealing with questions and will surely add new ideas, modifications and extensions as result of their growing experience.

The expansion of the approach to more difficult problems e.g. to non-linear or transient studies may be done without difficulties. But like for all other optimization the large number of variants to be checked is less or more prohibitive as long there is no efficient management of the jobs clusters of computers or any other parallelization.

FUTURE RESEARCH DIRECTIONS

The studies done show that the method proposed may help to accelerate the design of passive compensator systems. The application to real structures and the comparison with more detailed approaches are not yet done. One of the next steps will be the analysis of real buildings equipped with compensators to learn about the possible improvement if one uses this method to dimension the protective equipment. The integration into the design process may be achieved by handling problems like chimneys where passive compensation is used successfully in many applications.

The application to other structures such as bridges will be studied. As many structural analysis codes are designed to deliver the system matrices to the users, the introduction of parameterised compensators causes no problems. An analysis using these matrices and including the compensators produces the fitness values used in the evolutionary optimization process.

The integration of different excitations and the scatter of the structures properties have to be done to provide an estimation of the robustness of the results. This is not a difficult task but has been omitted here for the sake of simplicity.

The optimization of the number and position of compensators takes a very long time if many positions and numbers have to be checked. We did it for some selected applications. The integration of this overlaying optimization is no problem from the theoretical point of view. From the computational aspect, it includes a large increase in the computing power and time used during the total analysis. Therefore, the procedures have to be checked for any potential reduction of the number of individual jobs. There is no doubt that there are related strategies, for example pseudo random searches or swarm strategies (Plevris and Papadrakakis, M. 2011) which often are more efficient than the opulent ones outlined here. But the inherent dangers to destroy the power of the random process by intentional steps should not be underestimated. So in some cases we found that swarm optimisation failed to propose efficient results in the case of out compensation problem, while on the other hand it was much more efficient when applied to other problems.

CONCLUSION

The evolutionary or bionic optimization of passive tuned mass dampers has been studied discussing different aspects. The method outlined has the potential to contribute to more efficient absorbers at reasonable effort. Some of the main findings have to be mentioned to show the advantages of the approach.

The evolutionary optimization of passive compensators applied to simplified models of high buildings has the potential to indicate where and how to use these compensators. The reduction of the earthquakes' impact may be used as an estimate as to whether the compensators are sufficient to prevent severe damage.

Evolutionary optimization helps to find good proposals for multidimensional problems when many local maxima have to be considered. At the prize of large numbers of trials, large sectors of the high dimensional parameter space may be searched. If similar proposals are found when using different initial values and many repetitions, there is some reason to assume that the proposals are very good ones if not even the best. In these cases the method is superior to conventional approaches as it deals with many maxima and may find the best one, where other strategies are likely to converge to suboptimal proposals.

In the case of optimization problems with many degrees of freedom, the disadvantage of the large number of studies becomes less important, as conventional approaches need many calculations as well and are always likely to find only the next local maximum.

Passive compensators are popular not only in earthquake damage control but also for the stabilization of other structures like bridges and chimneys. Their advantage is the independence of active control and the long time availability without much inspection and repair. Their disadvantages are relatively large masses and deflections which have to be integrated into the design. So the idea of distributes dampers using part of the buildings mass like proposed by the Fu and Johnson (2009) should be kept in mind. The efficiency of tuned mass dampers is known, so reliable predictions about the loadings to be withstood without large damage are possible.

Simplified approaches are used throughout the world of engineering. The idea of reducing high buildings to some simple beam elements is not new. Like every simplification, it neglects many details that might be essential in the real structure but are not included in the model. Experienced engineers will use parametric studies to cover the range of possible uncertainties without removing any doubt about the incompleteness of the model.

An evolutionary optimization of the compensating system of high buildings may be done by the approach outlined. It produces many helpful proposals about the number, position and dimension of compensators. Detailed studies of the building taking into account more parameters than the floors' masses and stiffness help to understand the real edifices' response to the earthquake excitation.

REFERENCES

Bachmann, H., & Weber, B. (1995). Tuned vibration absorbers for "lively" structures. *Journal of the International Association for Bridge and Structural Engineering*, *5*(1), 31–36.

Berkeley. (1995). *Kobe earthquake 1995/01/16 20:46, Station Takarazuka*. Retrieved February 1, 2011, from http://peer.berkeley.edu/smcat/data/ath/KOBE/TAZ-UP.AT2

Bozorgnia, Y., & Bertero, V. (2004). *Earthquake engineering*. London, UK: Taylor & Francis, CRC Press. doi:10.1201/9780203486245

Brieger, S., Keller, U., & Steinbuch, R. (2008). *Advanced tools in structural optimization.* Paper presented at Advanced Problems in Mechanics – 2008 Conference, St. Petersburg, Russia.

Chen, G., & Wu, J. (2001). Optimal placement of multiple tuned mass dampers for reducing seismic responses of buildings. *Journal of Structural Engineering*, *127*(9), 1054–1062. doi:10.1061/(ASCE)0733-9445(2001)127:9(1054)

Chopra, A. (2000). *Dynamics of structures: Theory and applications to earthquake engineering*. Upper Saddle River, NJ: Prentice-Hall.

Den Hartog, J. P. (1956). Mechanical vibrations (4th ed.). New York, NY: McGraw-Hill Book Company.

Eddy, N. (2005). *Taipei 101's 730-ton tuned mass damper.* Retrieved February 1, 2011, from http://www.popularmechanics.com/technology/gadgets/news/1612252

Fu, T. S., & Johnson, E. A. (2009). Control strategies for a distributed mass damper system. *Proceedings of the American Control Conference,* St. Louis, MO, USA, June 10-12, 2009 (pp. 3921-3925).

Gen, M., & Cheng, R. (2000). *Genetic algorithms & engineering optimization*. New York, NY: John Wiley & Sons.

Han-Rok Ji, H., et al. (2005). Structural vibration control using semiactive tuned mass damper. *Proceedings of the Eighteenth KKCNN Symposium on Civil Engineering-KAIST6,* December 18-20, 2005, Taiwan.

Li, S. (2010). *Evolutionary optimization of earthquake resistance capacity for high buildings.* Unpublished Master Thesis, University of Reutlingen, Germany.

Meskouris, K., & Hinzen, K. (2003). *Bauwerke und Erdbeben: Grundlagen - Anwendung – Beispiele*. Wiesbaden, Germany: Vieweg +Teubner.

Michalewicz, Z. (1996). *Genetic algorithms + data structures = Evolution programs*. New York, NY: Springer.

Naeim, F., & Kelly, J. M. (1999). *Design of seismic isolated structures: From theory to practice*. New York, NY: John Wiley. doi:10.1002/9780470172742

Nawrotzki, P., & Dalmer, F. (2005). *Der Einfluss von Schwingungstilgern auf die Standsicherheit und Gebrauchstauglichkeit von Bauwerken*. D-A-CH Tagung 2005, Retrieved January 1, 2011 from http://www.gerb.com/de/bibliothek/downloads/dokumente/aKoeln.pdf.

Ordonez, D., Foti, D., & Bozzo, L. (2002). Comparative study of the inelastic response of base isolated buildings. *Earthquake Engineering & Structural Dynamics*, *32*(1), 151–164. doi:10.1002/eqe.224

Plevris, V., & Papadrakakis, M. (2011). A hybrid particle swarm—gradient algorithm for global structural optimization. *Computer-Aided Civil and Infrastructure Engineering*, *26*, 48–68.

Rechenberg, I. (1994). *Evolutionsstrategie '94*. Stuttgart, Germany: Frommann-Holzboog.

Reiterer, M., & Ziegler, F. (2005). Bi-axial seismic activation of civil engineering structures equipped with tuned liquid column dampers. *Journal of Seismology and Earthquake Engineering*, *7*, 45–60.

Steinbuch, R. (2004). *Simulation im konstruktiven Maschinenbau*. Leipzig, Germany: Fachbuchverlag Leipzig.

Steinbuch, R. (2010). Successful application of evolutionary algorithms in engineering design. *Journal of Bionics Engineering*, *7*, 199–210. doi:10.1016/S1672-6529(09)60236-5

Teuffel, P. (2004). *Entwerfen adaptiver Strukturen - Lastpfadmanagement zur Optimierung tragender Leichtbaustrukturen*. Doctoral dissertation, University of Stuttgart, Germany.

Towhata, I. (2008). *Geotechnical earthquake engineering*. Berlin, Germany: Springer Series in Geomechanics and Geoengineering.

Xua, B., Zhishen Wub, Z., Chena, G., & Yokoyamab, K. (2004). Direct identification of structural parameters from dynamic responses with neural networks. *Engineering Applications of Artificial Intelligence*, *17*, 931–943. doi:10.1016/j.engappai.2004.08.010

Chapter 12
Optimum Design of a New Hysteretic Dissipater

Dora Foti
Technical University of Bari, Italy

Riccardo Nobile
University of Salento, Italy

ABSTRACT

In this chapter, a new seismic protection device is proposed. It is designed to dissipate the energy entering a structure subject to seismic action through the activation of hysteresis loops of the material that composes it. These devices are characterized by a high capacity to absorb the seismic energy and the ability to concentrate the damage on it and, consequently, to keep the structure and the structural parts undamaged. Moreover, after a seismic event they can be easily replaced. In particular, this chapter proposes a new shear device that shows the plasticity of some areas of the device at low load levels. In order to maximize the amount of dissipated energy, the design of the device was performed by requiring that the material be stressed in an almost uniform way. In particular, the device is designed to concentrate energy dissipation for plasticity in the aluminum core while the steel parts are responsible to make stiffer the device, limiting out-of-plane instability phenomena. The geometric configuration that maximizes the energy dissipation has been determined using a structural optimization routine of finite element software.

INTRODUCTION

Concept of Structural Control

Traditional techniques for the design of building structures are based on experimentation and on the damage observed during earthquakes. Structural ductility and redundancy are the basis of modern design criteria, giving the possibility of significantly reducing the seismic forces. The result is the design of economic structures that perform satisfactorily during a severe earthquake. However, ductility means damage both in the structural and non-structural elements. Furthermore, the damage may cause the temporal or total arrest of the building. Therefore, in recent years, research

DOI: 10.4018/978-1-4666-2029-2.ch012

is mostly oriented towards finding techniques, which reduce seismic forces, without creating damage in the structure, or concentrating it in certain pre-determined points.

In conventional design practice, energy dissipation is intended to occur in specially detailed critical regions of the structure, usually in the beams near or adjacent to the beam-column joints. Inelastic behaviour in these regions often results in significant damage to the structural members, and although the regions may be well detailed, their hysteretic behaviour will degrade with repeated inelastic cycling. Further, the large interstory drifts required to achieve significant hysteretic energy dissipation in critical regions usually result in substantial damage to non-structural elements such as in-fill walls, partitions, doorways, and ceilings.

A modern tendency in seismic design is to avoid damage in the structure by using specific control techniques.

The control of structures, in fact, was born as a necessity to reduce the effects of vibrations on structures and on structural parts of them. From a broader perspective, control of structures not only refers to civil structures but also to mechanical systems and so on.

Some examples where vibrations are important (not a comprehensive list) are the following:

- Flexible structures (slender) or structures housing sensitive equipment (semiconductor facilities, ultra-precision machinery, measuring instruments)
- Civil engineering: buildings, bridges, offshore structures, slender towers and chimneys, nuclear power plants, telescopes, electric energy transportation lines, perforated elements, cable-ways and high velocity lifts (elevators)
- Aerospace engineering: plane wings, panels, lightweight space structures (free vibrations)
- Automotive engineering: panels, vehicle bodies
- Mechanical engineering: coolers, washing machines, pressing machines, forging machines, flexible robots, pipelines and industrial facilities with dangerous products, shaking tables
- Ships, submarines

The most important problems generated by the vibrations of structures are due to the relative displacements of the structure, which is the displacement between two different points of the structure. As a result, the system is subjected to a fatigue stress with a reduction of its strength and, consequently, a reduction of the structural safety.

In addition, the absolute displacements are cause of problems, as high amplitude could produce uncomfortable noise. The effects of the absolute accelerations must be also considered, as they are especially noticeable on equipment and machines. The human comfort conditions are affected too as high accelerations produce an inertial force on the people preventing them from acting comfortably.

Seismic Control of Structures

In the seismic design, the structures are considered as fixed or jointed to the ground to form a single system with the ground, and the seismic motion causes stresses and deformations. The objective of the resistant design is to make the structure withstand these forces without collapsing. To this end, it is possible to distinguish two levels: for earthquakes with a determinate intensity level (moderate) an absolute absence of damage in the structure and in the non-structural elements is required; for other earthquakes with a higher intensity (and with a less probability of occurrence) it would be acceptable if there were the possibility of localised damage that is not dangerous to the stability of the structure, the possibility of its rehabilitation and the possibility of causing victims.

On the contrary, the mechanisms for control of the seismic response attempt to reduce the seismic forces that act on the structures. These mechanisms are added to the structures to modify their dynamic properties and, in some cases, to increase their energy dissipation capacity.

In the last decades, the number of control devices produced in the world has considerably grown. At the same time, research institutes have devoted much more attention to the analytical and experimental study of structures protected with these devices (Soong and Spencer, 2002).

Control systems can be classified into passive, active, semi-active and hybrid.

Passive Systems

They are the most utilized control systems because many theoretical and experimental studies have been carried out.

They consist of some “inert” mechanical devices (here “inert” does not mean inactive, but that they are not powered and that their behaviour cannot be modified on-line) which are inserted in the structure to dissipate and/or to deflect energy.

In general, passive systems are not able to adapt to the unexpected characteristics of the excitation and in some cases their effect might even be damaging (for instance, as the natural frequencies of the structure are shifted new resonance can occur). However, if the main features of input are known, passive systems are extremely efficient.

Active Systems

These systems behave similarly to passive ones but, instead of inert devices, there are highly powered mechanisms (actuators) that are able to push the structure to counteract the input effect. Hydraulic cylinders driven by servo-valves are examples of actuators. An active control system is composed of a set of sensors to measure on-line the response of the structure (mostly displacements and accelerations), the actuators, a source or reservoir of energy to power the actuators and a controller (typically a computer) that decides the amounts of forces to be exerted by the actuators. These systems operate automatically as a closed loop where the measured response (by the sensors) is used by the controller to calculate (following some strategy -control algorithm-) the forces to be applied (by the actuators) to reduce the vibrations.

An example of an active system is described in Figure 1.The figure shows a mass damper where the connection with the main frame incorporates a powered actuator able to accelerate the auxiliary mass. Horizontal displacements and accelerations in the main structure are measured by sensors (dashed box) and this information goes (dashed arrows) to the actuator, so governing its operation by means of a controller. Such systems are usually known as active mass dampers.

The feasibility and reliability of active systems are controversial because: (i) to accelerate the massive civil engineering constructions large forces are required (consequently, a huge energy source is needed) and (ii) energy supply can be interrupted during a strong input (earthquake, wind, etc.). Therefore, active systems might be more appropriate for reducing the response under minor (or even, frequent) earthquakes. In building structures the feasibility of active control is higher for wind input than for strong seismic excitations because the required control forces are smaller (roughly hundreds of tons compared to thousands).

Figure 1. Example of active (or semi-active) control system (active mass damper)

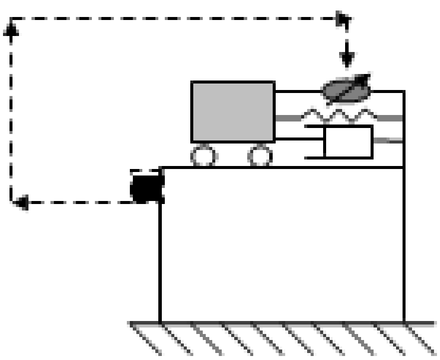

Semi-Active Systems

Their operation is similar to that of active systems but the actuators are only able to restrain the structure instead of having also the capacity of pushing it (in other words, they can take energy from the system but cannot exert energy on it). Consequently, these devices are much smaller (for example hydraulic cylinders with an on/off valve) than those required for active systems, and only a minor amount of energy is required to operate them (typically about 25 W, so some batteries can supply it). Obviously, these systems are more feasible and reliable than the active ones since they do not depend on an external source of energy. It can be said that the performance is better than in the passive case and only slightly worse than in the active one. The same system described in Figure 1 can also represent a semi-active system.

Hybrid Systems

These systems consist of a combination (series of parallel) of active (or semi-active) and passive systems. The efficiency of such co-operation lies in the fact that the passive system can provide the gross reduction of response (by absorbing or deflecting energy) while the active one is used for further lowering (for protection of sensitive equipment, for example) of displacements or accelerations. Figure 2 illustrates an example where an actuator complements passive isolation to reduce high-frequency low-displacement vibrations.

As no big control forces are required, hybrid systems are more feasible and reliable than active ones.

It is remarkable that none of these devices (active, semi-active or passive) is part of the main structure, so they can be temporarily removed for inspection, replacement or repair. Only the case of base isolation is slightly different.

A comparison among the four categories previously described shows that the passive control systems are more feasible and reliable since devices are simpler and do not depend on any source of

Figure 2. Example of hybrid control system

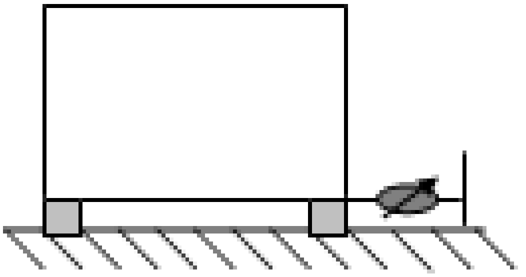

energy. Though they are not as incredibly efficient as the other systems, if properly designed, they can provide excellent results in a wide range of situations. Passive control is clearly more spread than the other systems

Figure 3 shows a classification of the most common systems to control the vibration of structures. The list is not exhaustive because this field is still under research and new mechanisms and devices are being introduced.

Passive control systems, as previously stated, could be defined as «inert» mechanisms added to the structure to improve its behaviour in response to the dynamic forces associated with wind and especially earthquakes. The behaviour of these systems is based on deforming inelastically in response to the excitation.

It is possible to classify the mechanisms of passive control of the seismic response in four classes:

1. **Mechanisms for the Seismic Isolation (Base Isolation) of Vibrations:** Generally, they are put on the base of the structure, with the aim of reducing the seismic forces entering the structure. The structure is partially uncoupled from the foundation by using flexible bearings instead of traditional (rigid) connections. Vibration to be controlled can be transmitted from the ground to the structure or, conversely, from the structure to the ground (vibrating elements isolation).

Figure 3. Earthquake protection systems

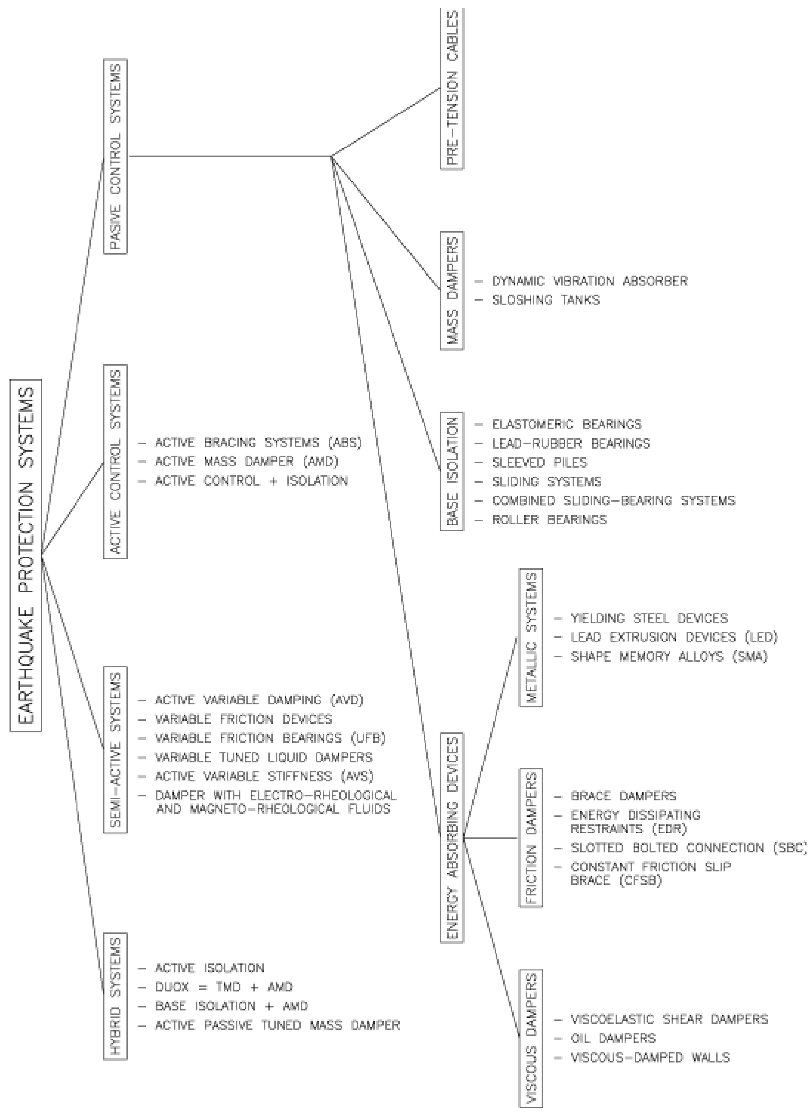

2. **Energy Dissipation Systems:** External devices fixed to the structure dissipate energy. Input: earthquakes, wind, etc. They are installed in the structure with the aim of dissipating most seismic energy entering the same structure (Aiken et al., 1993, Tsai et al., 1993).
3. **Mass Dampers:** They consist in one or more masses added to the structure, generally at the top floor. These masses are made with such dynamic properties that they reduce the response of the structure. Energy is transformed into kinetic energy (translation or rotation) in massive devices (possessing big mass or big moment of inertia). Input: earthquakes, wind, etc.
4. **Pre-Tension Cables:** These cables stiffen the structure and increase the axial load in the columns reducing, in some cases, the rotation of their ends.

The requirements that a mechanism of passive control of the seismic response should guarantee are listed below:

- After the seismic event, the structure must return to its original position (high deformations must not be permitted).
- The daily life of the people living in the structure must not be altered during the checking and restoration phases.
- Utilising mechanisms of this type the initial cost of construction and of the structural reinforcing of the existing building should be reduced.
- The mechanical properties of the devices must not vary substantially with time.
- Maintenance and inspection must not be required except after the occurrence of a severe earthquake; in this case, the operations requested should be simple.

To accomplish all these requirements, a complicated device is not useful, while a simple, economic device with stable behaviour under seismic action is preferable.

The traditional seismic design takes into account that some structural elements enter the inelastic range of behaviour, and the hysteretic energy involved will contribute to reducing the value of the demand of responses during a destructive earthquake. In fact, the conventional design of seismic-resistant structures is based on the concept of ductility and structural redundancy. The forces induced by a severe earthquake are significantly reduced as a function of both concepts, connected with the energy dissipation capacity of the structural elements (Bozzo and Barbat, 1995). A seismic resistant rational design guarantees that for a certain global structural ductility demand the ductility capacity of the elements is not exceeded. Due to uncertainties with non-linear analysis is difficult to estimate precisely the local ductility demands in each section of a structure. Moreover, the traditional building design offers few guarantees of avoiding damage to the non-structural elements during a severe earthquake, so even the restoration of the principal elements could be difficult. Therefore, in the last thirty years several energy dissipation and base isolation systems have been proposed to localise non-linear behaviour in certain pre-defined areas of a structure.

Concept of Energy Dissipation

Energy dissipation systems are able to localise the ductility demand in some “weak” points able to dissipate energy in a stable form and which may be easy to repair. The energy dissipation concept may be understood because of the modern tendency toward seismic-resistant design. In this case, the “weak” points correspond to mechanical elements, which dissipate energy in a stable form. In the event of a severe earthquake, and if the devices are damaged, they may be replaced without disturbing the use of the building.

In antiseismic design the mechanical elements that are able to dissipate energy are called energy dissipative devices (EDDs); this modern approach to seismic resistant design is now spreading and widening, also thanks to the development of devices obtained by using innovative materials or materials traditionally utilized for different use.

EDDs are inserted into a structure so that when it vibrates, they deform and dissipate energy. After the biggest earthquakes, such devices can be easily replaced. In this way, they do not require any major structural flexibility in the system, since the damage (permanent deformation) is concentrated in the device. In this way, the other structural elements remain elastic.

There are many systems with the objective of dissipating the seismic energy and some of them have been utilised in buildings and bridges (Jara et al 1992, Hanson et al. 1992).

In general, the significant reduction of structural response to severe earthquakes utilizing energy dissipaters depends on their number, position in the building, the type of dissipater and its design able to dissipate a great amount of the seismic energy.

In summary, until now, the dissipaters that have been developed are based on the following principles:

- Plastic deformation of metals
- Friction
- Elastomers with high damping capacity
- Viscous fluid damping devices

The design of these devices is greatly influenced by their force-displacement characteristics and those of the building where they are installed.

One of the first buildings equipped with energy dissipaters were the Twin Towers in New York. These buildings incorporated many hundreds of devices in the column-beam joints to increase the structural damping for vibration control of wind gusts.

Energy dissipaters present some advantages respect to other control techniques such as base isolation. They do not require either construction or design techniques that differ from those used in conventional buildings; energy dissipaters are efficient in high and low rise buildings and their unit cost is often low. Figure 4 shows a building equipped with energy dissipaters installed in the middle of the diagonals or at their connection with the beams. These elements dissipate energy through the relative displacements between the floors.

Hysteretic Dissipaters

As part of the passive control techniques, special attention is given to devices that help to dissipate the energy entering a structure during an earthquake, through the activation of hysteresis loops in the material of the device itself (Skinner et al. 1980, Bozzo et al. 1998), thus avoiding plastic action of structural elements. Therefore, it is

Figure 4. Building with energy dissipaters

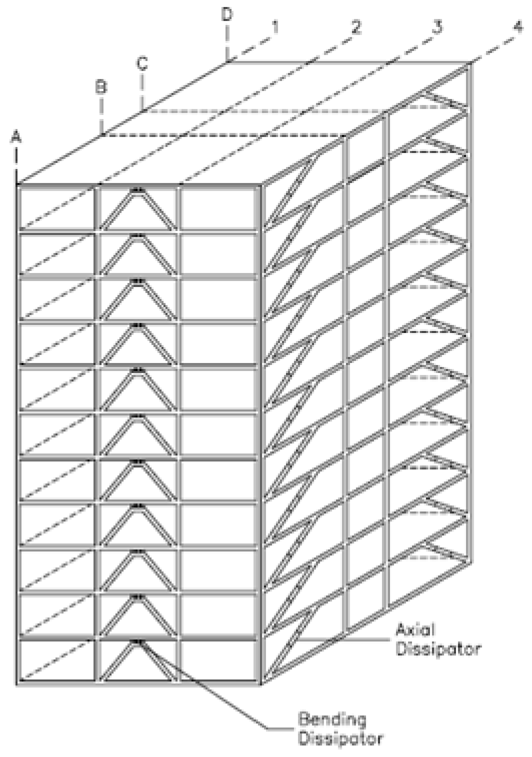

evident that the energy dissipation takes place only for drifts of a magnitude greater than that activates the plastic behavior of the material. In particular, metallic devices show a stable behavior under cyclic loading, producing a large hysteretic cycle that depends on the strength of the material.

Generally, the devices possess a large hysteretic energy dissipation capacity in relation to their size. However, the introduction of these devices in the building increases the stiffness of the structure and reduces the drifts that concentrate the damage on the device. The limitation of these devices is that the energy dissipation capability is only activated after the activation of large excursions into the inelastic range and, as a result, they are not effective for small vibrations of the drift that produces the yield in the material composing the device.

Dissipaters Based on Metal Plasticization

Metallic systems are relatively simple to construct and it is easy to change their dimensions. Conceptually, the seismic design of structures with yielding of steel devices is similar to the conventional design of buildings based on ductility with the additional requirement of a limited number of available devices.

In literature, several metallic systems have been proposed for their wider development and use in buildings and structures: lead extrusion devices, torsion beams, dampers with bending deformation. A wide variety of different types of devices have been developed that utilise bending, shear, or extensional deformation modes into their plastic range. Important desirable features of these systems are stable behaviour, long-term reliability, and generally good resistance to environmental and temperature factors.

Yielding steel systems represent a sub-group of the metallic systems (Chan et al., 2009). They are modelled with different shapes (“X”-shaped, triangle-shaped, and “U”-shaped) so that the yielding is spread uniformly throughout the material. The result is a device that is able to sustain repeated inelastic deformations in a stable manner, avoiding stress concentrations and low cycle fatigue.

A convenient location of these “connections” is in the diagonal-beam joint. In this case, the bracing system must be substantially stiffer than the surrounding structure. The introduction of such a heavy bracing system into a structure may be prohibitive unless the system is efficient. The sizes of these braces and the dissipative capacity of the device must be calibrated to have the highest seismic energy dissipation.

In the following, a new metal dissipater has been proposed. It is designed to yield under a shear force and dissipate energy for hysteresis of the material that composes it. Since the amount of energy dissipation depends not only by device dimension and by geometry but also by stiffness of the hosting structure, it is clear that the choice of dissipater constructive details is critical in determining the real efficacy of the protective system. Therefore, the design process presented here starts from a panel geometry defined through geometrical parameters. These parameters are then chosen using an optimization routine having the aim of maximizing the energy dissipation phenomena in the device. For this purpose, a simple and well-established optimization strategy has been selected among all the possible strategies developed in the technical literature for the structural optimization (Kirsch 1993, Spillers and MacBain 2009).

PROPOSAL FOR A NEW HYSTERETIC DISSIPATOR

Description of the Device

Hysteretic dissipaters for passive seismic protection of buildings are able to dissipate high amounts of input energy during an earthquake thanks to the large plastic behavior of the material utilized in their manufacturing (Nakashima et al 1994, Nakashima 1995, Rai et al. 1998, Yamaguchi et al. 1998, De Matteis et al 2007).

In passive metal devices, the effectiveness of dissipation depends on two main characteristics: first, the low value of displacement at which the hysteresis loops are activated in the material area, which ensures the protection of structures for small vibration, and secondly a large plastic field, which maximizes the energy dissipation. These two requirements are in conflict, since the use of a small device allows reducing the load activation level, but the amount of dissipated energy is also reduced being proportional to the volume of material involved in dissipation processes.

In order to satisfy these demands, a new dissipation mechanism has been proposed. The initial idea was to consider a device where the use of two different coupled materials could accomplish the different requirements. The fundamental idea was to obtain a high reduction of the effects of an earthquake on a building utilizing a material such as aluminum with a low yielding limit that could dissipate a good amount of seismic energy for hysteresys. The first device consists in a shear panel composed of a central aluminum plate and two steel side plates (Foti et al. 1999, Foti et al. 2000). A series of shaking-table tests were performed on this preliminary aluminum-steel device (Bairrao R. et, al., 2000) and a good behavior but also some critical points were observed. In particular, the efficacy of the panel was sensibly reduced by the difficulty in assuring a correct load transmission between plates of steel and aluminum.

Starting from these observations, Fe360 steel and a 1000 series aluminum alloy plate were chosen respectively for the outside plates and for the central device (Diaferio et al. ECSC 2008, Foti et al. 2010). A low yield stress and a large plastic range, increasing the extent of yielding even at low loads (Table 1), characterize the 1000 series alloys.

The proposed configuration provides adequate stiffness to increase the limit of instability in the shear panel. This latter feature is important to reduce the possibility of out-of-plane instability of the device. Steel plates provide the necessary stiffness to the panel, while the aluminum is the element that dissipates energy. The steel plates have rectangular openings (Figure 5), from which the central aluminum plate emerges for a few millimeters. This solution ensures that the panel behaves as desired, particularly assuring that the load is transmitted between the aluminum and steel, avoiding the possibility of slippage. This behavior is achieved in part with the aluminum protrusions into the openings of the steel panels, which provide a barrier to slipping. Moreover, all the three plates are connected through bolts to enhance connectivity between the plates. The design of the device obviously took into account how it has to be connected to the structure to be protected. To facilitate the inclusion of the panel in different structures, a standard configuration shown in Figure 6 has been designed where two diagonal bracings are bolted to the frame and welded to a plate where the device will be installed. Maximum dimension of the area provided for the panel is 470x600 mm. This particular configuration will be assumed in the following for the panel dimensioning and for the experimental test.

Table 1. Mechanical properties of steel and aluminum utilized in the device

Materials properties		Fe360	Series 1000 Al
σ_y	Yielding stress [N/mm^2]	235	30
σ_R	Ultimate tensile stress [N/mm^2]	360	90
A	Rupture elongation [%]	26	40
E	Young modulus [N/mm^2]	206000	70000
H	Plastic modulus [N/mm^2]	20000	5000

Optimum Design of the Device

The considerations reported before allowed to define the standard configuration of device, but were not exhaustive to define the geometrical configuration of the panel, that is the definition of the design parameters showed in Figure 5. This problem represents a classical case in which a structural optimization procedure can help to define the final geometry of the device. To improve the dissipation behavior of the device, the shape design of the dissipater was thought to be obtained from an optimization study with the principal aim to get the maximum amount of energy dissipated by the device during a seismic event.

The optimization procedure consists in assigning a possible form and shape to the initial panel, while some dimensions and characteristics have been maintained in a parametric form. Literature is very rich about optimization procedure starting from simple linear approach to more sophisticated and non linear approach (Kirsch 1993, Spillers and MacBain 2009). In this case, the authors choose to consider an optimization procedure integrated

Figure 5. Geometrical parameters of the aluminum-steel device

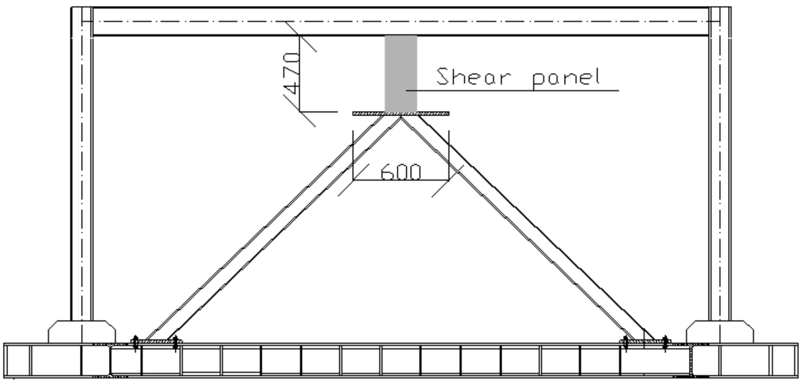

Figure 6. Positioning of the device in the structure

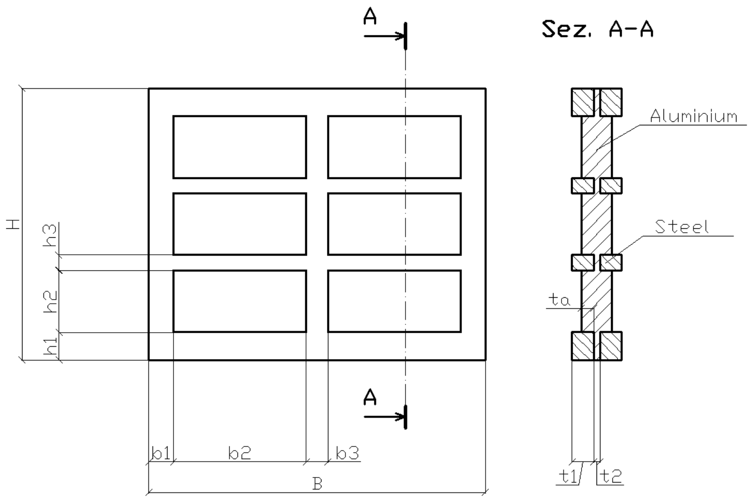

with commercial FEM code, simple to use and with a relatively low computing time. In particular optimization method consists in a random design generation followed by a sub-problem approximation run that were performed using ANSYS program. A solid FEM model of the panel has been built for the optimization analysis using element SOLID90 at 20 nodes, having a parabolic shape function. Maximum dimension of elements in thickness direction was fixed to 0.5 mm, therefore the number of nodes were about 15000, depending from the design values of the plate thickness. The mechanical behavior of steel and aluminum has been described by a bi-linear behavior, whose parameters were defined according to the properties listed in Table 1. In this analysis, the panel was modeled as fixed at the base and with a double pendulum at the top, to reflect the installation of the device in a frame (Figure 6).

The load condition considered for the optimization analysis corresponds to a top displacement of the panel of 4 mm, equal to 0.2% of the interstory height of the frame, the last being between 2.5 and 3.0 m. This top displacement must be maintained due to the working constraint of the shaking-table used for the experimental test.

The optimization routine is carried out in two step: a first random design generation is used to explore all the design space obtaining at least a number of 30 feasible solution; in a second time the best two feasible solutions are used as starting points of sub-problem approximation runs. In this manner, it is possible to reduce the risk of obtaining a local optimum solution with a relatively small increase of computational time.

The described optimization routine took into account some constraints in order to meet the space provided in the frame and to avoid failure.

The analysis proposed considered four different constraints:

1. The stress in the aluminum, whose maximum value was assumed coincident with the ultimate tensile stress, equal to 90 MPa (cf. Table 1);
2. The overall height of the panel, which was allowed to vary in the range 420-470 mm on the basis of the considerations relative to the maximum acceptable size for the test frame, as shown in Figure 6;
3. The width of the panel, which was allowed to vary in the range 100-250 mm, depending on the dimensions of the plates for mounting the dissipaters in the 3D frame.
4. Transversal load, corresponding to the maximum horizontal displacement of 4 mm, which was initially limited to 20 kN, so that the resulting panel is compatible with the test frame where it will be mounted for next shaking table tests (see par. 4).

The fourth constraint was added to obtain several panel configurations with different stiffnesses, so that they can be adapted to a structure with different behavior from one another. The stiffness of the panel to be mounted in a structure, in fact, must be appropriate to the stiffness of the structure to be protected.

At the conclusion of this process, the optimization routine provides the optimal geometric configuration corresponding to that for which the plastic strain energy takes the maximum value over all those examined.

With reference to the choice of the geometrical parameters that allow the description of the configuration of the panel, Table 2 shows the variation of the parameters ranges and the final configuration chosen. The optimized panel obtained for 20 kN transversal load is represented in Figure 7.

Table 2. Variability range of the geometrical parameters and the optimization results

Geometrical Parameters		Variability Range	Optimal Configuration	Final Configuration
n_x	Horizontal window	2-6	3	3
n_y	Vertical window	1-4	4	4
b_1	Width of the lateral steel stiffener [mm]	5-10	9.5	8
b_2	Width of the aluminium window [mm]	30-200	46.4	40
b_3	Width of the internal steel stiffener [mm]	5-10	8.4	8
h_1	Height of the external steel stiffener [mm]	5-10	9.8	10
h_2	Height of the aluminium window[mm]	30-200	110.8	100
h_3	Height of the internal steel stiffener [mm]	5-10	10.9	10
t_1	Thickness of the steel plate [mm]	1-4	1	1
t_2	Thickness of the aluminium plate[mm]	1-4	2.5	3
t_a	Projection of the aluminium plate [mm]	1-4	2.7	3

Figure 7. Details of the construction of the aluminum-steel device corresponding to 20 kN transversal load: the device has 12 openings (n_x=3 in horizontal and n_y=4 in vertical) and b_1=8 mm, b_2=40 mm, b_3=8 mm, h_1=10 mm, h_2=100 mm, h_3=10 mm, t_1=1 mm, t_2=3 mm, t_a=3 mm.

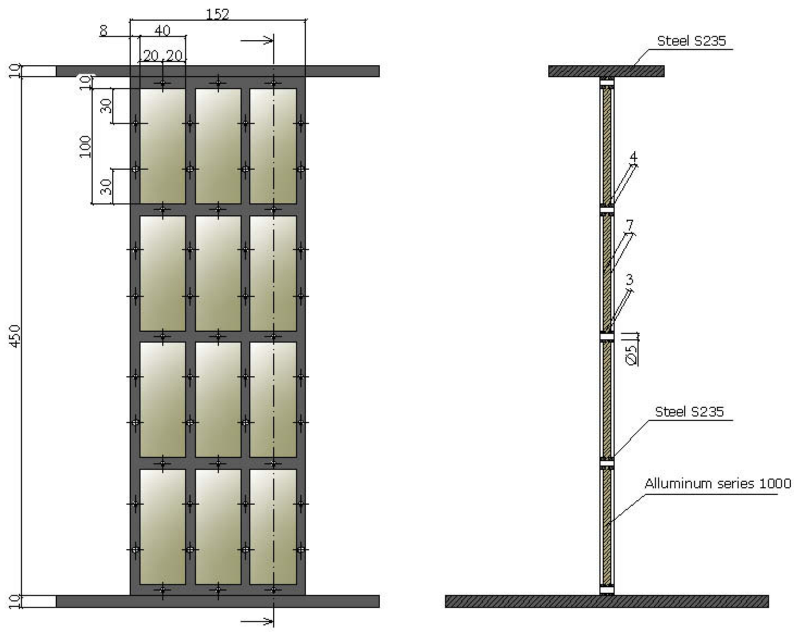

Extension of the Optimum Design to Devices with Different Shear Loads

The same procedure was then extended to different geometrical configurations of the shear panel simply by changing a particular design parameter, the constraint of the maximum transverse load. Since an effective dissipation can be obtained only if panel and structure stiffness are comparable, it is possible to define a series of panels, designed to protect frames that have different structural stiffness. This objective was achieved by changing the maximum shear force and keeping unchanged the other parameters and constraints. In this way, the optimization procedure automatically selects the best solution for each class of the shear load. The farther design cases considered are those related to load values of 40 kN, 80 kN and 100 kN. The results obtained for the optimal configuration are presented in Table 3, while in Figure 8 the details of construction of the 40 kN panel are reported. Each column is identified by a name that represents the best solution obtained using the maximum shear load reported in the column headers. It may be noted that this name identifies an average range of the transverse load that can ensure a proper use of the panel. For a relatively low increase in the shear load, the best solution is achieved mainly by changing the thickness and the dimensions of the window of the aluminum panel. Instead, the solution obtained for a shear load of 100 kN differs significantly, since the aluminum window is almost doubled in width. In other words, the increase of the amount of transversal load initially produces a moderate increase and then a higher increase of the panel width.

Once the optimization procedure has been used to determine more geometrical configurations of the panels, their behavior has been numerically evaluated: it consists essentially of the link between the top displacement and the applied shear load. Again, the models include the nonlinear

Table 3. Optimal values of the geometrical parameters for different service loads

		20 kN	40 kN	80 kN	100 kN
Geometrical Parameters		*[10-20 kN]*	*[20-40 kN]*	*[40-80 kN]*	*[80-150 kN]*
n_x	Horizontal windows	3	3	3	3
n_y	Vertical windows	4	4	4	4
b_1	Width of the lateral steel reinforcing [mm]	8	8	12	15
b_2	Width of the aluminum window[mm]	40	60	70	180
b_3	Width of the internal steel reinforcing [mm]	8	8	12	15
h_1	Height of the external steel reinforcing [mm]	10	10	15	10
h_2	Height of the aluminum window [mm]	100	100	95	100
h_3	Height of the internal steel reinforcing[mm]	10	10	15	10
t_1	Thickness of the steel plate [mm]	1	4	3	4
t_2	Thickness of the aluminum plate[mm]	3	1	3	2
t_a	Projection of the aluminum plate [mm]	3	3	3	2

behavior of the materials in order to determine the behavior of the panel during yielding. The characteristic curves obtained are reported and compared in Figure 9.

Subsequently, a buckling analysis was performed on each panel class in order to determine the conditions corresponding to the possibility of instability. The beginning of instability phenomena leads to a quick panel stiffness reduction and it represents a limiting condition for the real utilization of the device. It would be desirable that the transversal top displacement corresponding to this condition could be higher than 4 mm, which is the maximum acceptable interstory drift of the structure to be protected. Figures 10, 11, 12, and 13 report the map of the plastic deformation and the first mode of instability for each of the panels examined. The first mode of instability is shown in the mentioned figures and it occurs for 3.928 mm, 3.532 mm, 5.328 mm, 3.208 mm, respectively, for panels of 20 kN, 40 kN, 80 kN and 100 kN. These values, especially for 40 kN and 100 kN devices, are lower than the design value of 4 mm, but they can be considered sufficiently close to the limit value in order to assure a correct behavior of the panel.

Summarizing, it is possible to propose a design procedure for this new aluminum-steel dissipater in the range of shear forces 0-150 kN. At design of the structure, the technician must choose the most appropriate panel to be included in the structure. The choice must be made based on the shear force expected for the panel, once it is inserted into the structure. Therefore, the size of the force must be assessed by a numerical model of a structure without dissipaters but equipped with the same braces that will be utilized to install the devices.

The methodology to perform a proper evaluation of this force and, consequently, the correct selection of the panel to install, is as follows:

1. Definition of a simplified model of the structure where the diagonal braces will be modified to connect directly the end to the structure, that is removing the panel itself.
2. Perform a seismic analysis of the simplified model and evaluating the maximum shear force that is generated at the point where the panel will be added to the structure.
3. Select the device for which the previously determined shear force will be within the operational range of the panel.

Figure 8. Constructive details of the aluminum steel devices corresponding to 40 kN ltransversal load: the device has 12 openings (n_x= 3 in horizontal and n_y= 4 in vertical) and b_1= 8 mm, b_2=60 mm, b_3=8 mm, h_1=10 mm, h_2=100 mm, h_3=10 mm, t_1=4 mm, t_2=1 mm, t_a=3 mm.

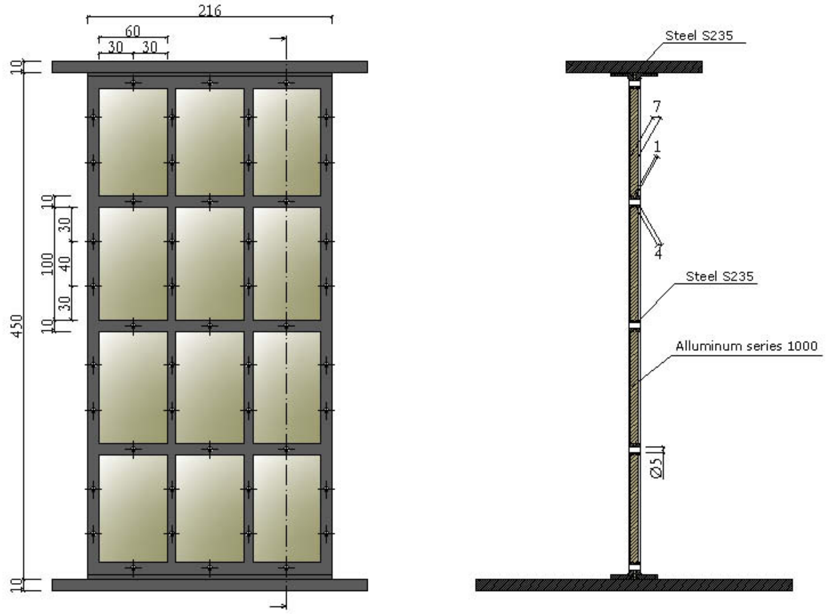

Figure 9. Comparison of the global behavior for different shear panels

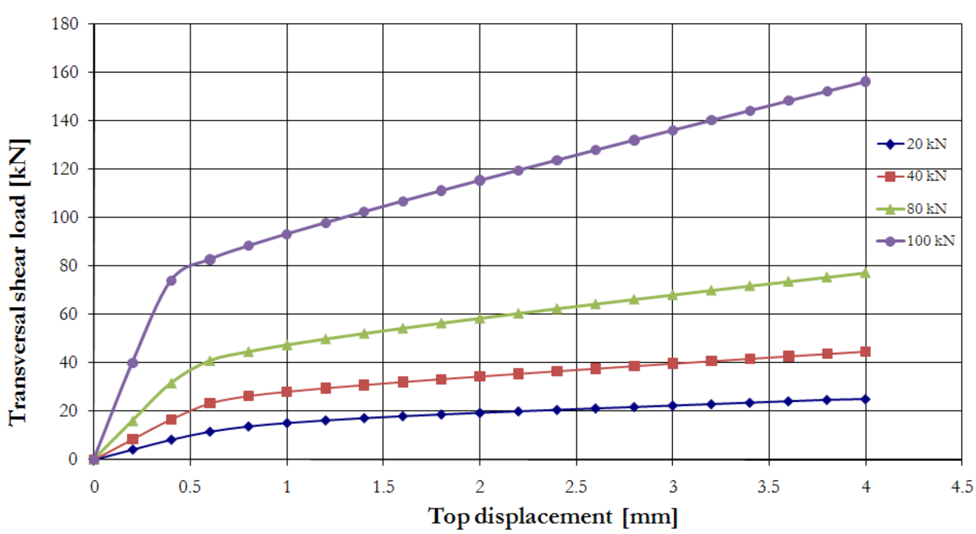

Figure 10. a) Plastic deformation and b) instability mode of the 20 kN aluminum device with 12 openings

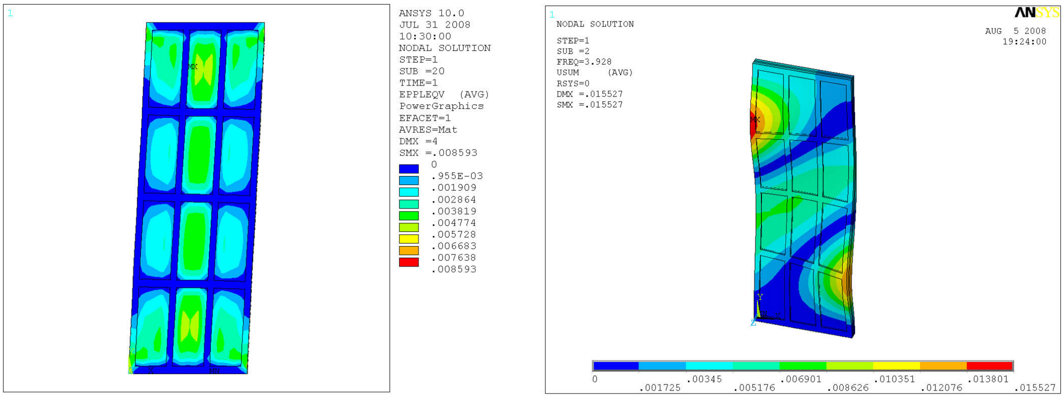

a) b)

Figure 11. a) Plastic deformation and b) instability mode of the 40 kN device with 12 openings

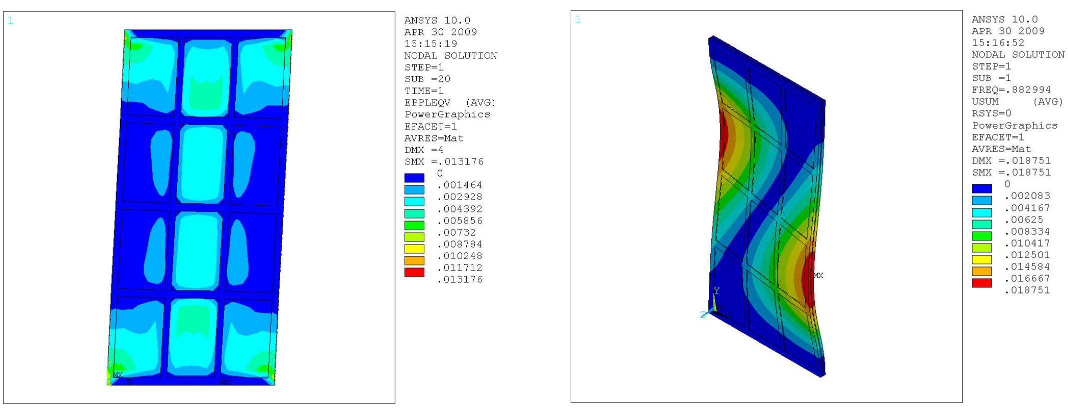

a) b)

Figure 12. a) Plastic deformation and b) instability mode of the 80 kN device with 12 openings

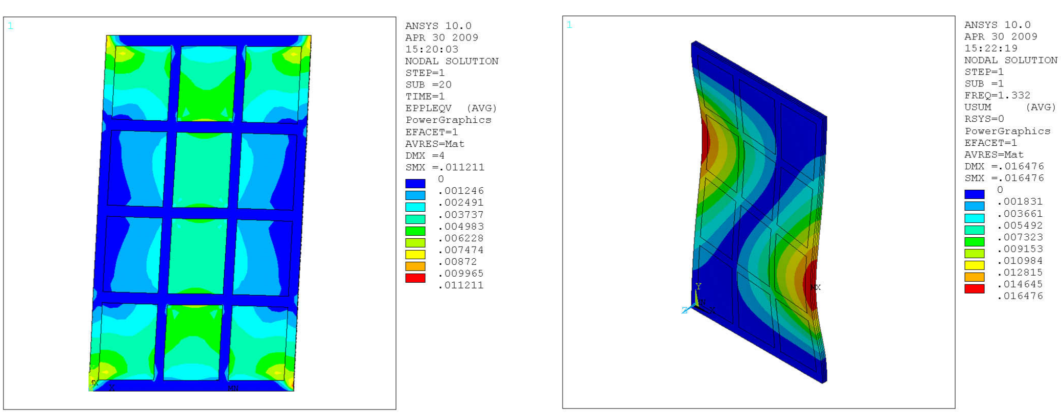

a) b)

Figure 13. a) Plastic deformation and b) instability mode of the 100 kN device with 12 openings

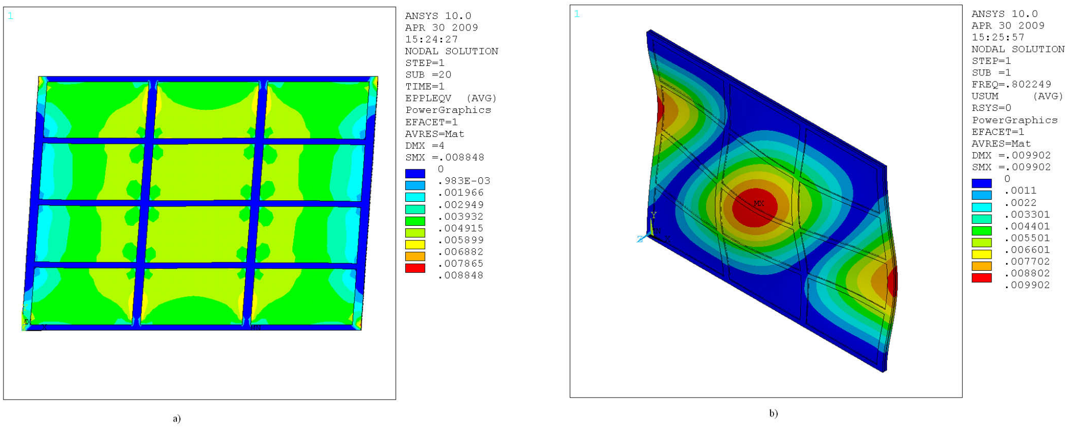

CHARACTERIZATION TESTS

Testing Setup

The test equipment was designed to reproduce the working conditions of the panels in the 3D frame previously described. In particular, a steel frame consisting of a base beam (HEB 120), two vertical elements (HEB120) and a top beam (HEB 120) was built (Diaferio et al. WCEE 2008, Diaferio et al. 2009). At the center of the top beam, a 250-kN actuator Enerpac was connected. In this way, it is possible to apply a load cycle to a pair of panels, installed in the frame as shown in Figure 14. Consequently, the load transmitted from the actuator is divided equally into the two panels, even in the presence of distortions or misalignments. The panels are perfectly fixed in correspondence of the columns, which are bolted in the same manner provided for mounting the 3D frame for the shaking table tests (see par. 4), while at the top, considering the symmetry of the test system, the panels can only be subjected to vertical displacements. By using the software SAP2000, the test frame has been verified in correspondence of the maximum applied load of 80 kN, assuming the frame to be externally isostatic and loaded by two forces of 80 kN, one acting upward in the middle of the top transverse beam and one acting downward at the junction between the two devices for a maximum load of 40 kN.

The test frame was used to perform tests on the following devices:

- Device of 20 kN
- Device of 20 kN, without the central aluminum plate
- Device to 40 kN
- Device to 40 kN, without the central aluminum plate

Tests have been carried out at the Laboratory "M. Salvati" of the Department of Civil and Environmental Engineering of the Technical University of Bari.

Figure 14. Testing frame

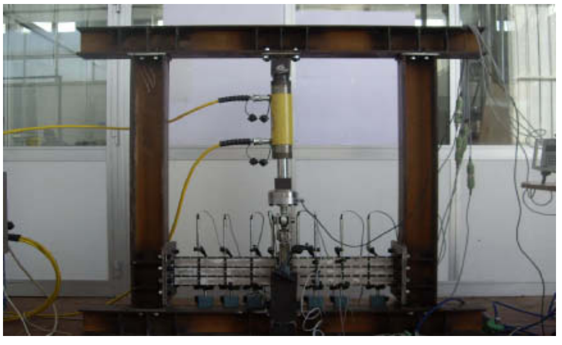

During the tests the actuator displacements and the displacements in correspondence of the horizontal stiffeners of the panels have been measured through 8 LVDTs with a stroke of 10 mm and accuracy <0.10% (Figure 15). A 100 kN load cell measures the load applied at any time. It was thus possible to determine the force-displacement plots described in the following section.

Results of the Characterization Tests

The devices first tested were the 20 kN type. They were subject to subsequent load cycles from zero to a maximum load in both directions. In subsequent cycles, maximum load was increased up to failure. Load cycles having maximum loads greater than 20 kN are performed in one direction only.

These preliminary tests were completed when the welding at the base of the panels began to failure (Figure 16). The crisis of welding has also led to a slip out of the plane of the device, as best it can be seen in Figure 17. For this reason the details have been improved, shifting the welding of the steel plates in points farther from the fixed joints with the base plate, keeping always the dimensions obtained from the optimization procedure.

The structural behavior of the panels is represented by the applied load against displacement, as reported in Figure 18 for 20 kN panel, with the details improved after the first preliminary tests. The same plot obtained for 40 kN panel is reported in Figure 19.

From the various load cycles, it is possible to confirm that the area of hysteresis, corresponding to the energy dissipated by the device, starts from the earliest load cycles, and increases significantly with increasing load level. The origin of this dissipation resides on two dominant factors:

- Friction between the plates of steel and aluminum
- Yielding of materials, presumably aluminum

Figure 20 shows the cyclical characteristics curves considering the peaks of the different hysteresis cycles for 20 kN and 40 kN panels. Each characteristic curve is just the constitutive law of the respective panel: it is the one that should be considered if the panel is subject to repeated strain over time, as in the case of an earthquake. This curve shows what was previously stated about the hysteresis loops, namely that the panel has an overall non-linear behavior due to the dissipative phenomena.

The experimental curve differs from the numerical one not only for the lower slope of the initial part, but also for the lower value of the

Figure 15. Displacement transducers LVDT installed on the panels: a) global view and b) particular in correspondence of load axis

Figure 16. Collapse of the welding of the 20 kN dissipater after the first characterization tests

a) b)

Figure 17. Configuration at the end of the test: a) out-of-plane instability of the dissipater, b) permanent deformation in the dissipaters with lateral reinforcement

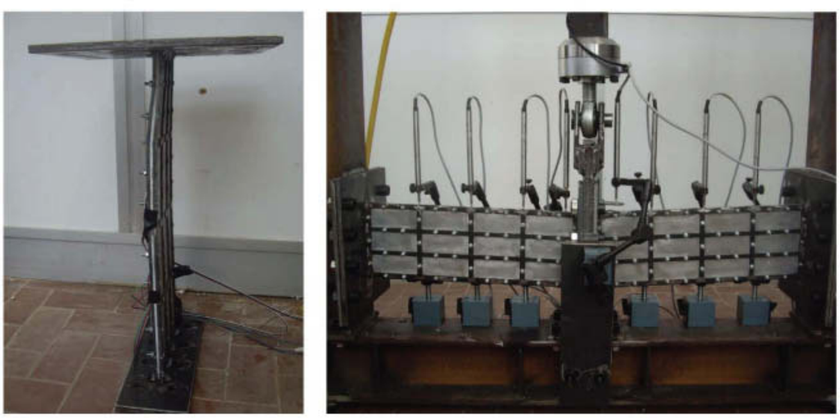

lateral force reached in the non-linear part. It is certainly possible to identify the causes to justify this large discrepancy. The first is intrinsic to the test mode and should be attributed to the recovery of existing clearance throughout the test system, as well as the deformability of the frame used to load the devices. The second, instead, is to be attributed to the simplification introduced in the model and not necessarily realized in the real panel. This simplification consists in considering the existence of a perfect solidarity between the steel and aluminum plates that make up the panel. In reality the load transfer between these plates is ensured by the friction forces and the

Figure 18. Force-displacement plot of the 20 kN dissipater

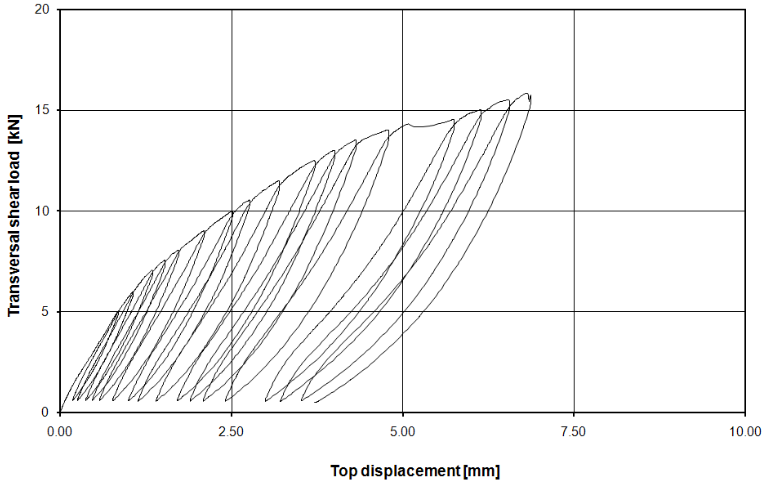

Figure 19. Load-displacement plot of 40 kN dissipater

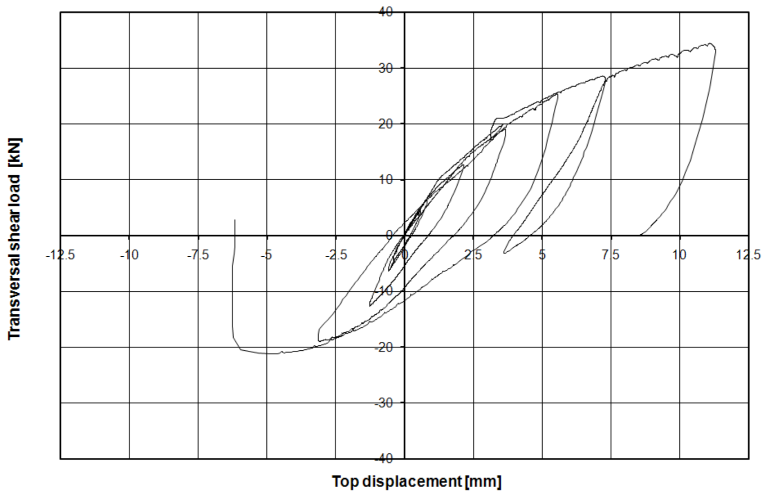

Figure 20. Envelope of the cyclic curves: constitutive law of the dissipation devices

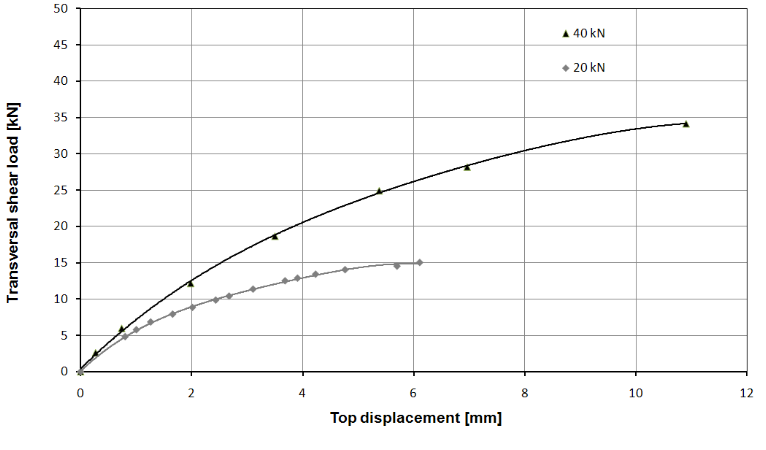

obstacle constituted by the aluminum windows. Despite these strengths, it is not possible to exclude the existence of micro- slips between the plates that give the panel softness greater than that, which is possible to calculate with a numerical model.

This hypothesis is confirmed if the experimental and numerical behaviors of the panel without the internal aluminum plate are compared. In this case, in fact, both for 20 kN and 40 kN panel, the two curves are practically coincident, if we except the non linear region (Figure 21). Therefore, the difference existing in the behavior of the dissipater can be recognized in the slippage between the three different panels that constitute each device.

Finally, the two devices with the aluminum plate have been compared considering the normalized transversal load and top displacement, which are the ratio of these quantities to the maximum values measured for each panel. The result is reported in Figure 22, showing that the two panels have an identical behavior but at different load and displacement levels. This fact demonstrates the reliability of the design process used to establish the optimal values of the geometrical parameters of the device.

SHAKING-TABLE TESTS

Test Setup

The device of 20 kN described in the previous paragraphs was subjected to shaking table tests (Ponzo et al. 2007, Gattulli et al. 2007, Serino et al. 2007), installing four of them in a steel frame in scale 2:3 (Figure 23). The frame had a 3m x 4m plane section and consisted of four HEB140 profile columns positioned at the corners and IPE180 profile beams welded to columns. The two levels were at an equal height of about 2 m, while the columns emerged of 0.50 m from the top floor.

The two floors consisted of A55/P600 section corrugated sheets with a thickness of 0.8 mm and completed by a jet of concrete. At the ground floor, two horizontal diagonals were fitted, made with HEA160 profiles, while in the vertical planes two HEA100 profiles diagonals on each floor were installed (Figure 23c) to allow the mounting of the dissipaters. In particular, the devices had to be bolted to a plate, welded at the top of the diagonals, and to the beam of the upper floor. In this way, all rotations at the ends of the dissipaters had been avoided.

The frame had been subjected to seven signals of natural earthquakes whose spectrum is compatible with the one of Eurocode 8 for type A ground. Tests had been performed scaling the signals from 10% to 100%.

The test frame had been equipped with numerous displacement and acceleration transducers. In particular, the displacements at the base level and at the first and second floors were measured. Moreover, a displacement transducer was positioned in order to measure the transversal displacement of each dissipating device. Finally, acceleration in transversal and longitudinal directions was measured at the first and at the second floors (Diaferio et al. 2010). Due to the geometrical configurations of the panel and of the frame, it was not possible to mount a load cell to measure the transversal shear load acting on each panel.

Results of the Shaking-Table Tests

Since it is fundamental to report in a plot the shear load and the transversal displacement of each panel in order to verify that effectively the device was subjected to dissipating and hysteretic phenomena during shaking-table tests, the shear load had been evaluated by means of the acceleration measured at each floor.

The model used at this purpose considers that the inertia loads at each floor cause the transversal loads acting on the panels. Assuming the floor as a rigid body, its motion could be expressed by the components of the accelerations of the centroid G along the L and T directions (Figure 24a), al_G

Figure 21. Comparison of experimental and numerical behaviors of device without the aluminum plate: a) 20 kN and b) 40 kN panel

a)

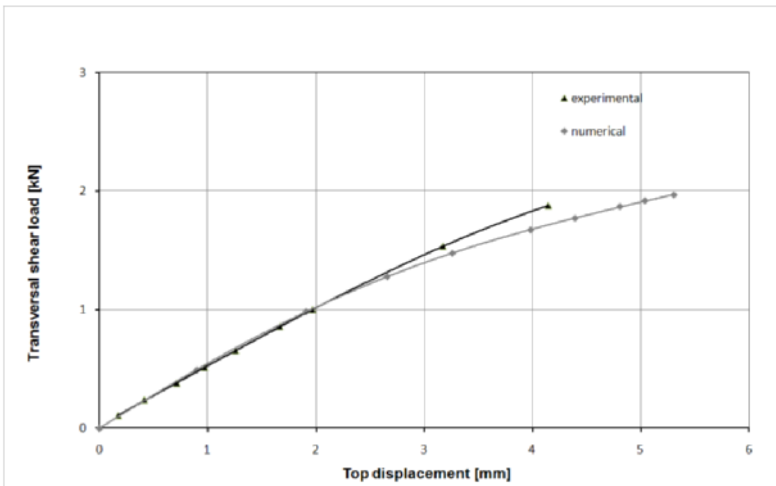

b)

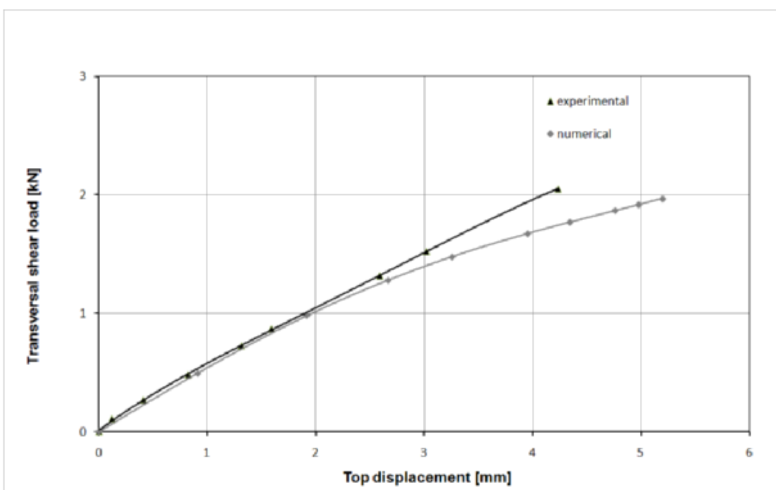

and at_G, respectively, the angular velocity ω and the angular acceleration α. Since transversal and longitudinal accelerations have been measured in points 1 and 2 of each floor (Figure 24a), the aforementioned kinematic parameters had been evaluated and, by means of the constrain equations representing the rigid floor (see the equations in Figure 24b), the longitudinal and transversal accelerations in correspondence of the East and West panels were determined.

Observing that these accelerations are directly proportional to the inertia loads that acts on each panel, it is possible to use longitudinal acceleration al_W and al_E and measured transversal displacements of each panel to describe, at least qualitatively, the hysteresis cycle. These graphs have been plotted for each test condition and for each panel. In particular, Figure 25 shows the hysteresis cycles for the panels mounted on the first floor, where shear loads originated by seismic action is maximum. The plots are referred to a

Figure 22. Comparison of normalized hysteresis cycle of 20 kN and 40 kN panels

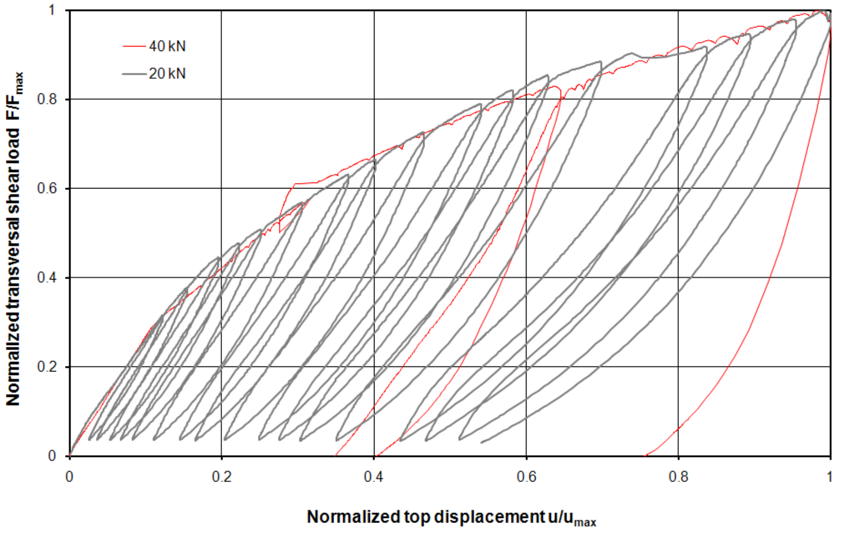

Figure 23. 2:3 scaled steel frame built in the Laboratory of Structural Engineering of the University of Basilicata, Potenza: a) plane view, b) 3D-view, c) vertical view in the XZ plane, d) vertical view in the YZ plane

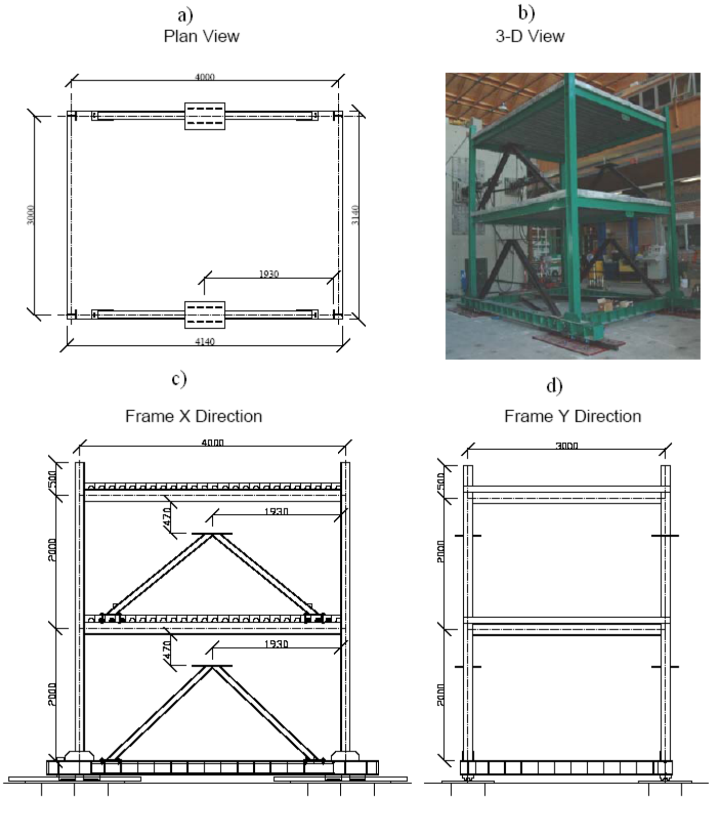

Figure 24. Model of the steel frame floor: a) acceleration measurements; b) kinematic model

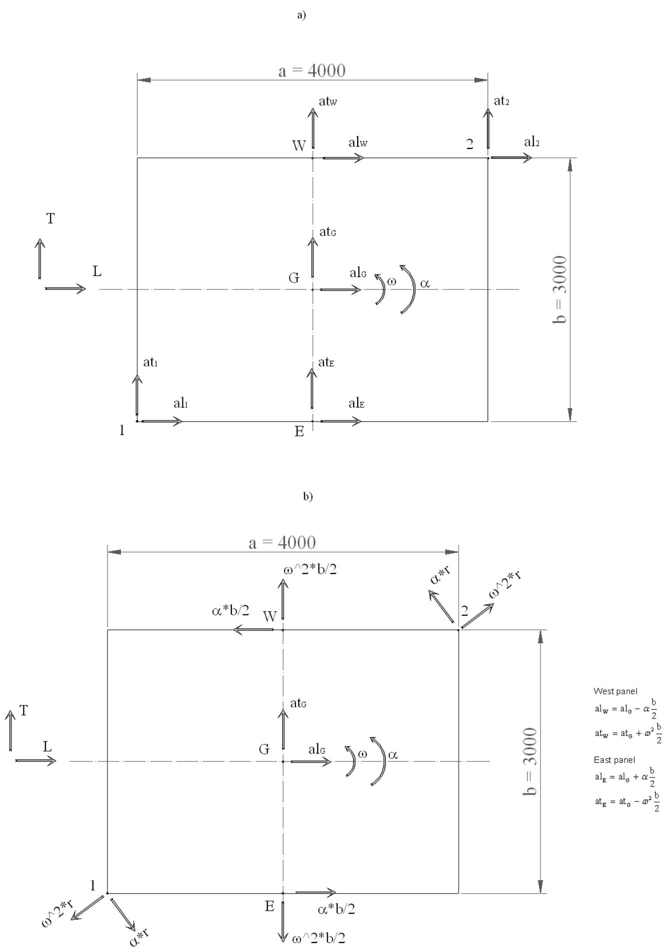

signal input corresponding to S2-000196xa earthquake scaled at 50%.

It can be observed that the two panels have a different behaviour. In particular, the West panel, corresponding to Figure 25a, seems to have been interested by an excessively limited shear load. For this panel the hysteresis cycle is practically absent. The behaviour of the East panel is different. In fact, the acceleration that interested this panel, and subsequently the correspondent shear load, has been relevant and a hysteresis cycle appeared, confirming the possibility of the device to dissipate seismic energy. This aspect regarding the two hysteresis cycles has been confirmed by the data obtained from all the other seismic tests that have been carried out. However, it is noticeable that the differences existing in the two hysteresis cycles, very limited in the initial tests that have been performed at a very low seismic intensity, become more important at higher seismic levels. Moreover, at the end of the test program, it has been observed that the West panel presented a crack failure of the welding that joined the panel to the horizontal base plate, while this failure was absent in other panels. Therefore, it is possible that the results obtained for the West panel of the first floor could be largely influenced by a welding defect that caused its premature failure. Probably this failure appeared since the initial tests at a lower intensity. Therefore, this

Figure 25. Hysteresis cycle of dissipating devices at the first floor: a) West panel; b) East panel

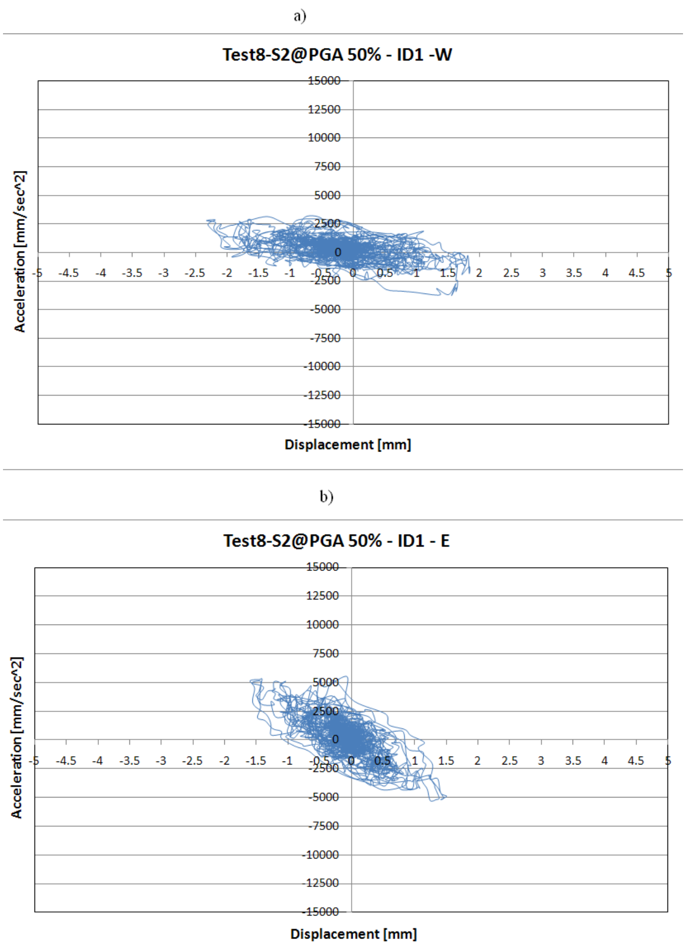

panel was inefficacious in the subsequent tests, as showed by the hysteresis cycles reported in Figure 25a.

CONCLUSION

The purpose of this research was to design a new energy dissipation device to be used for passive seismic protection of structures. The dissipater is made of steel and aluminum and its geometric configuration was determined using a structural optimization routine. The optimization method is simple and has been arranged to adapt its behavior to the demands of the device in dissipating the maximum seismic energy entering the structure. This procedure has been used to determine the geometry of four different panels, differing for the maximum transversal load that they can act when inserted in a structure.

The optimized configurations of the panel have been then modeled using ANSYS FEM software in order to calculate the non-linear structural behavior and the maximum transversal top displacement tolerable before the beginning of elastic instability phenomena.

A simple design method of choosing the most appropriate panel to be inserted into a structure to protect it from a seismic point of view has been proposed.

Static and shacking table characterization tests have been performed to determine the experimental behavior of the device. The tests have been performed on 20 kN and 40 kN devices with and without the central aluminum plate. The results showed the effectiveness of the device in dissipating the seismic energy, following the design prescriptions imposed in the optimization procedure.

ACKNOWLEDGMENT

This study has been funded by Strategic Project PS060 – "Innovative structures and Advanced Material Experimentation" – S.I.S.M.A. – Apulia Region.

TEC s.r.l. is also gratefully acknowledged for providing the devices.

REFERENCES

Aiken, I. D., Nims, D. K., Whittaker, A. S., & Kelly, J. M. (1993). Testing of passive energy dissipation systems. *Earthquake Spectra*, *9*(3), 335–370. doi:10.1193/1.1585720

Bairrao, R., Duque, J., & Foti, D. (2000). *Shaking table tests on shear panels for the seismic protection of buildings*. Report n. 304/00 –C3ES, Laboratorio Nacional de Engenharia Civil (LNEC).

Bozzo, L. M., & Barbat, A. H. (1995). *Tecnicas avanzadas de diseño sismorresistente*. Perù: CAPECO Lima. (in Spanish)

Bozzo, L. M., Chais, X., & Torres, L. (1998). A shear type energy dissipator for the protection of masonry infill walls. *Proceedings of the Sixth U.S. National Conference on Earthquake Engineering*, Seattle.

Chan, R. W. K., Albermani, F., & Williams, M. S. (2009). Evaluation of yielding shear panel device for passive energy dissipation. *Journal of Constructional Steel Research*, *65*, 260–268. doi:10.1016/j.jcsr.2008.03.017

De Matteis, G., Mazzolani, F. M., & Panico, S. (2007). Pure aluminium shear panels as dissipative devices in moment-resisting steel frames. *Earthquake Engineering & Structural Dynamics*, *36*(7), 841–859. doi:10.1002/eqe.656

Diaferio, M., Foti, D., & Nobile, R. (2008a). Design optimization of aluminium-steel devices for passive protection of structures. *4th Conference on Structural Control (ECSC2008)*, St. Petersburg, Russia.

Diaferio, M., Foti, D., & Nobile, R. (2008b). Aluminium-steel energy dissipators for passive protection of structures. *14th World Conference on Earthquake Engineering* – 12-17 October 2008, Beijing, China.

Diaferio, M., Foti, D., & Nobile, R. (2009). Hysteretic dissipators made of aluminium and steel: Optimal design and preliminary characterization tests. *International Journal of Advanced Structural Engineering*, *1*(1), 77–92.

Diaferio, M., Foti, D., & Nobile, R. (2010). *The dynamic experimental behavior of a new aluminium passive protection device in a 3d frame*. 14th European Conference on Earthquake Engineering – 30.08-03.09.2010, Ohrid, Republic of Macedonia.

Foti, D., & Diaferio, M. (1999). *Shear panels for seismic protection of buildings*. 4th European Conference of Structural Dynamics–EURODYN'99, Prague, Czech Republic.

Foti, D., Diaferio, M., & Nobile, R. (2010). Optimal design of a new seismic passive protection device made in aluminium and steel (Technical Note). *Structural Engineering & Mechanics*, *35*(1), 119–122.

Foti, D., & Nobile, R. (2000). *Characterization tests of new aluminium and steel energy dissipating devices*. 5th International Conference on Computational Structures Technology: Identification, Control and Optimisation of Engineering Structures. Leuven, Belgium: Civil-Comp Press.

Gattulli, V., Lepidi, M., & Potenza, F. (2007). *Identification of analytical and finite element model for the Jetpacs three-dimensional frame*. Jetpacs Report No. 2, Research Project No. 7 of 2005-2008 ReLuis Project, Naples, Italy.

Hanson, R. D., Xia, C., & Su, Y. F. (1992). Design of supplemental steel damping devices for buildings. *Proceedings of the 10WCEE*, Madrid, Spain, (pp. 4139-4142).

Jara, J. M., Vargas, E., Galindo, C., Gonzalez, R., & Gòmez, C. (1992). Seismic performance of buildings with energy dissipating systems. *Proceedings of the 10WCEE*, Madrid, Spain, (pp. 2455-2460).

Kirsch, U. (1993). *Structural optimization: Fundamentals and applications*. Springer.

Nakashima, M. (1995). Strain-hardening behavior of shear panels made of low-yield steel. I: Test. *Journal of Structural Engineering*, *121*(12), 1742–1749. doi:10.1061/(ASCE)0733-9445(1995)121:12(1742)

Nakashima, M., Iwai, S., Iwata, M., Takeuchi, T., Konomi, S., Akazawa, T., & Saburi, K. (1994). Energy dissipation behavior of shear panels made of low yield steel. *Earthquake Engineering & Structural Dynamics*, *23*(12), 1299–1313. doi:10.1002/eqe.4290231203

Oh, S.-H., Kim, Y.-J., & Ryu, H.-S. (2009). Seismic performance of steel structures with slit dampers. *Engineering Structures*, *31*, 1997–2008. doi:10.1016/j.engstruct.2009.03.003

Ponzo, F. C., Cardone, D., Di Cesare, A., Moroni, C., Nigro, D., & Vigoriti, G. (2007). *Dynamic tests on Jetpacs steel frame experimental model set up*. Jetpacs Report No. 3, Research Project No. 7 of 2005-2008 ReLuis Project, Naples, Italy.

Rai, D. C., & Wallace, B. J. (1998). Aluminium shear-link for enhanced seismic resistance. *Earthquake Engineering & Structural Dynamics*, *27*(4), 315–342. doi:10.1002/(SICI)1096-9845(199804)27:4<315::AID-EQE703>3.0.CO;2-N

Serino, G., Chandrasekaran, S., Marsico, M. R., & Spizzuoco, M. (2007). *Description and analytical modeling of the Jetpacs steel frame prototype*. Jetpacs Report No. 1, Research Project No. 7 of 2005-2008 ReLuis Project, Naples, Italy.

Skinner, R. I., Tayler, R. G., Heine, A. J., & Robinson, W. J. (1980). Hysteretic dampers for the protection of structures from earthquakes. *Bulletin of the New Zealand National Society for Earthquake Engineering*, *13*(1).

Soong, T. T., & Spencer, B. F. Jr. (2002). Supplemental energy dissipation: State-of-the-art and state-of-the practice. *Engineering Structures*, *24*, 243–259. doi:10.1016/S0141-0296(01)00092-X

Spillers, W. R., & MacBain, K. M. (2009). *Structural optimization*. Springer.

Tsai, K.-C., Chen, H.-W., Hong, C.-P., & Su, Y.-F. (1993). Design of steel triangular plate energy absorber for seismic resistance construction. *Earthquake Spectra*, *9*(3), 505–528. doi:10.1193/1.1585727

Yamaguchi, T., Takeuchi, T., Nagao, T., Suzuki, T., Nakata, Y., Ikebe, T., & Minami, A. (1998). Seismic control devices using low-yield-point steel, (pp. 65-72). Nippon Steel Technical Report No. 77. Chiba, Japan: Nippon Steel Corporation.

Chapter 13
Nonlinear Structural Control Using Magnetorheological Damper

Shaikh Faruque Ali
Swansea University, UK

Ananth Ramaswamy
Indian Institute of Science, India

ABSTRACT

This chapter provides an introduction to semi active control of base isolated buildings using magnetorheological (MR) dampers. Recently developed nonlinear control algorithms are discussed. First a fuzzy logic control (FLC) is designed to decide how much voltage is required to be supplied to the MR damper for a desired structural response. The FLC is optimized using micro genetic algorithm. A novel geometric approach is developed to optimize the FLC rule base. Experiments are undertaken to access the efficacy of the optimal FLC. Secondly the chapter develops two model based control algorithms based on dynamic inversion and integrator backstepping approaches. A three storey base isolated building is used for experimental and numerical studies. A numerical comparison is shown with clipped optimal control.

INTRODUCTION

Civil engineering structures, e.g., tall buildings, long span bridges, deep water offshore platforms, nuclear power plants, etc., have become more costly, complex and serve more critical functions. The consequences of their failure are catastrophic. Devastations in the past and recent earthquakes have shown that the understanding of building physics under seismic motion has increased which has improved the design of building and international building codes too. But we are still

DOI: 10.4018/978-1-4666-2029-2.ch013

at the mercy of the nature as one concern that still remains is that no structure can be built to with stand all possible loads. The uncertainty in future loadings and few fold increase in cost of construction never allow the engineers to design and built a structure that can withstand all possible loading conditions. The best alternative is to supplement structures with added devices such that they can take care of any unforeseen events and loadings. For an example, recent earthquake followed by a tsunami in Japan (11th March 2011) has not only devastated but wiped out cities. Strict building codes and added damping to the structures have saved Japan from wider destructions as noted in various international newspapers worldwide (Glanz and Onishi, 2011; Ross, 2011).

Seismic base isolation is an old, widely accepted and implemented structural mechanism due to its robustness and ease in deployment. Following the Northridge earthquake (1994), and Kobe earthquake (1995), the interest of structural engineers in understanding near-source ground motions has enhanced (Soong and Spencer, 2002). Documents published after these earthquakes emphasized the issue of large base displacements because of the use of none or little isolation damping (of viscous type only) prior to these events. More recent studies have investigated analytically and experimentally, the efficiency of various dissipative mechanisms to protect seismic isolated structures from recorded near source long period, pulse-type, high-velocity ground motions. Consequently, hybrid isolation systems, seismic base isolation supplemented with active/semi-active damping mechanisms, have become the focus of current research trend in structural vibration control.

The recent focus on hybrid mechanism is to augment base isolation devices with semi-active magnetorheological (MR) dampers for efficient structural vibration control. MR dampers provide hysteretic damping and can operate with battery power (Dyke et al., 1996; Ali and Ramaswamy, 2008a).

The use of MR damper as a semi-active device involves two steps:

1. Development of a model to describe the MR damper hysteretic behaviour
2. Development of a proper nonlinear control algorithm to monitor MR damper current / voltage supply

The present chapter deals with the development of nonlinear control strategies to use with MR damper for base isolated buildings. The chapter unfolds in two interlinked areas. First an intelligent fuzzy logic control (FLC) scheme is developed to monitor the MR damper voltage input. The FLC is optimized using micro genetic algorithm. An experimental study is undertaken to access the efficacy of the optimal FLC in real time and to verify the numerical studies. Next the chapter provides insight to two newly developed model based nonlinear control techniques, viz, a dynamic inversion based MR damper monitoring and an integrator backstepping based MR damper monitoring. These two control algorithms are studied through numerical simulations.

The chapter is organized as follows: the next section provides a comprehensive review of literature on nonlinear control schemes to monitor MR damper for structural applications. Next, development of an optimal FLC using micro genetic algorithm is shown in details. A novel geometric scheme is developed to optimize the FLC such that a few optimization variables are required. Experimental study carried out to access the efficiency of the FLC is detailed next. The chapter then introduces the nonlinear control schemes. The mostly used clipped optimal control scheme is discussed. Emphasis is given to recently developed backstepping and dynamic inversion based control schemes. Results of numerical simulations of the nonlinear algorithms are provided and discussed thereafter. Finally the chapter concludes with a future direction of research.

BACKGROUND AND LITERATURE REVIEW

A control system can be classified as passive, active, hybrid, or semi-active based on the level of energy required and the type of control devices employed. Among these systems, the semi-active approach has recently received considerable attention because of its significant adaptability without large power requirements like active systems and is as reliable as passive systems. Rapid-response, fail-safe, low power requirement, simple interfaces between electronic controls and mechanical systems are some characteristics of magnetorheological (MR) devices that have attracted significant research interest for using them as semi-active control devices in applications of vibration mitigation (Soong and Spencer, 2002; Dyke et al., 1996). In particular, it has been found that MR dampers can be designed to be very effective vibration control actuators. In civil engineering, MR damper applications have mainly centered around the structural vibration control under wind and earthquake excitations (Dyke et al., 1996; Ali and Ramaswamy, 2008a). The automotive industry has been interested in developing applications of these materials, for example, for engine mounts, shock absorbers, clutches, and seat dampers (Karnopp et al., 1974).

Magnetorheological dampers are nonlinear devices due to their inherent hysteretic damping characteristics. The nonlinear hysteretic characteristic can be varied (monitored) by changing the input voltage to the damper. The nonlinear hysteretic behaviour and voltage monitoring make the design of suitable control algorithms that can provide a smooth change in voltage, an interesting and challenging task.

Control algorithms available in the literature map control force required to an equivalent voltage and then supply that voltage into the damper. This inverse mapping of force to voltage makes the choice and development of control algorithms more complicated. Semi-active control algorithms mostly use an ‘on–off’ or ‘bang–bang’ strategy for MR applications. The ‘on–off’ nature of these algorithms neither provide a smooth change in MR damper voltage input nor do they consider all possible voltage values within its full range (Jung et al., 2005).

A wide range of theoretical and experimental studies has been performed to assess the efficacy of MR dampers as semi-active devices (Jung et al., 2005; Shook et al., 2007). In one of the first examinations, Karnopp et al. (1974) proposed a ‘skyhook’ damper control algorithm for a vehicle suspension system and demonstrated that this system offers improved performance over a passive system when applied to a single-degree-of-freedom (SDOF) system. Feng and Shinozuka (1990) proposed a bang–bang control approach. Lyapunov function based approaches are studied and reported by Leitmann (1994), Sahasrabudhe and Nagarajaiah (2005). Dyke et al. (1996) proposed a clipped optimal control algorithm based on acceleration feedback for the MR damper. In this approach, a linear optimal controller, combined with a force feedback loop, was designed to adjust the command voltage of the MR damper. The command signal was set at either zero or the maximum value depending on how the damper force compared with the target optimal control force. The target optimal control can be obtained from the H2/LQG (linear quadratic Gaussian) (Dyke et al., 1996) and Lyapunov based methods (Sahasrabudhe and Nagarajaiah, 2005).

The use of MR dampers as supplementary damping device to base isolated structures is promoted and validated by researchers across the world through benchmark studies on buildings (Narasimhan et al., 2006, Nagarajaiah and Narasimha, 2006, Narasimhan et al. 2008) and bridge (Agrawal et al. 2009). Interested readers are directed to special issues by Nagarajaiah et al. (2008) and Agrawal and Nagarajaiah (2009) and articles in these special issues for the details of problem definition and control techniques used on the benchmark structures.

The main disadvantage of the clipped optimal strategy is that it tries to change the voltage of the MR damper directly from 0 to its maximum value (in the present case 5 V), without any intermediate voltage supply. This makes the controller a sub-optimal one. This swift change in voltage leads to a sudden rise in the external control force, which increases the system responses (Ali and Ramaswamy, 2008a, 2009b). Moreover, the clipped optimal strategy needs the measurement of the force the damper provides. The mathematical information regarding the structure is used for the calculation of the numerically obtained control forces to compare with the experimentally obtained damper force. Based on the compared result an on–off strategy is used to keep the damper input voltage to zero or to change it to maximum, and vice versa. Therefore, there is a need for control algorithms which can change the MR damper voltage, slowly and smoothly, such that all voltage values between maximum and zero voltage can be covered based on the feedback from the structure.

In this context various intelligent methods (neural controllers (Xu et al., 2003) and non-adaptive and adaptive fuzzy controllers by Ali and Ramaswamy (2008a)) have been tried in which the damper monitoring voltage is directly set based on system feedback. Ali and Ramaswamy (2008a) reported a comparison of adaptive, non-adaptive, and Lyapunov based clipped optimal strategies for a nonlinear base isolated benchmark building. One main disadvantage of the intelligent controllers is that they are mostly problem oriented, and therefore a more general approach to voltage monitoring still remains unexplored. Furthermore, neither the intelligent controllers nor the model based clipped optimal controllers consider the effect of the input voltage on the commanded voltage dynamics (the voltage that actually goes to the coil to create a magnetic flux). The dynamics matters less when the supplied voltage is a constant and does not vary. When the supplied voltage to the MR damper is varied based on the system responses and desired performance of the system, the difference in the supplied voltage and the commanded voltage plays a crucial role.

This chapters provides details of an optimal fuzzy logic control, a clipped optimal control, a dynamic inversion control and integrator back-stepping based control for MR damper monitoring. Next section provides details of MR damper modeling.

MAGNETORHEOLOGICAL DAMPERS

An MR damper consists of a hydraulic cylinder containing MR fluid that, in the presence of a magnetic field, can reversibly change from a free-flowing, linear viscous fluid to a semi-solid with controllable yield strength in a fraction of a second (Ali and Ramaswamy 2009b; Wang and Liao, 2011). An MR fluid is a suspension of micron-sized magnetically soft particles in a carrier liquid (such as water, mineral or synthetic oil), that exhibits dramatic changes in rheological properties. Under the influence of a magnetic field these particles arrange themselves to form very strong chains of fluxes (Yang et al., 2004; Wereley and Pang, 1998). Once aligned in this manner, the particles are restrained from moving away from their respective flux lines and act as a barrier preventing the flow of the carrier fluid.

A RD-1005-3 MR damper, manufactured by Lord Corporation, which is used for the experimental and numerical studies, is discussed here. The damper is 208mm long in its extended position, and provides a stroke of ± 25 mm. The input voltage can be varied to a maximum of 2.5V (continuous supply) and 5V (intermittent supply). A simple Bouc–Wen model, developed by Spencer et al. (1997) has been explored to characterize the MR damper. The force $f_c(t)$ provided by an MR damper as predicted by the Bouc–Wen model is given by

$$f_c(t) = k_0 x_{mr}(t) + c_0 \dot{x}_{mr}(t) + \alpha z_{mr}(t,x) \tag{1}$$

$$\dot{z} = -\gamma \left|\dot{x}_{mr}\right| z_{mr} \left|z_{mr}\right|^{n-1} - \beta \dot{x}_{mr} \left|z_{mr}\right|^{n} + A \dot{x}_{mr} \tag{2}$$

where x_{mr} is the displacement at the damper location; z_{mr} is the evolutionary variable, and γ, β, n, A are parameters controlling the linearity in the unloading and the smoothness of the transition from the pre-yield to the post-yield region. The functional dependence of the device parameters on the command voltage v_c is expressed as

$$\alpha(v_c) = \alpha_a + \alpha_b v_c; \qquad c_0(v_c) = c_{0a} + c_{0b} v_c$$
$$k_0(v_c) = k_{0a} + k_{0b} v_c \tag{3}$$

The six parameters $\left(c_0,\ k_0,\ \alpha,\ \gamma\ ,\ \beta, A\right)$ are estimated on the basis of minimizing the error between the model-predicted force (u) and the force obtained in the experiment (details are given in Ali & Ramaswamy (2009b)). In addition, the resistance and inductance present in the circuit introduce a dynamics into this system. This dynamics of the electrical part has been accounted for by the first-order filter on the control input given by

$$\dot{v}_c = -\eta(v_c - v_a) \tag{4}$$

where η is the time constant associated with the first-order filter and v_a is the voltage supplied to the current driver. The MR damper parameters used in the study reported in this chapter are given in Table 1.

INTELLIGENT FUZZY LOGIC BASED CONTROL DESIGN

Zadeh (1965) introduced fuzzy set theory to treat imprecision and uncertainty that is often present in implementation of problems in real world. Mamadani (1974), by applying Zadeh's theories of linguistic approach and fuzzy inference, successfully used the if-then rule on the automatic operating control of steam generator. Since then fuzzy control theory has been applied to a number of linear and nonlinear systems.

Fuzzy logic control (FLC) is a simulation of logical reasoning of human brain; it maps an input space to a corresponding output space based on fuzzy rules specified in if-then format known as knowledge base. Fuzzy logic-based control includes a fuzzification interface, an inference engine and a defuzzification interface. For details

Table 1. Parameter values for magnetorheological damper

Parameter	Value	Parameter	Value
α_a	1.95×10^5 Nm^{-1}	α_b	3.94×10^5 Nm^{-1}A^{-1}
c_{0a}	8.67×10^2 Nsm^{-1}	c_{0b}	4.15×10^3 Nsm^{-1}A^{-1}
k_{0a}	7.51×10^2 Nsm^{-1}	k_{0b}	3.46×10^3 Nsm^{-1}A^{-1}
η	190 s^{-1}	n	2
γ	2.85	β	5.42
A	12.26		

about FLC and definitions of important terms related to FLC the readers are directed to Ali and Ramaswamy (2007, 2009a) and the references therein. The inference engine has a dual role in fuzzy control theory. It maps the input fuzzified variables to the output variables based on user-defined rules known as knowledge base. It also provides a decision based on the results obtained from implementation of these rules. Usually, the rule base of the fuzzy controller is formed from operator experience and expert knowledge (Casciati et al., 1995). The more the control rules, the more the efficiency of the control system. Control rules are usually in the form of if-then rules to link input to the output variables. Fuzzy 'if' is called antecedent; 'then' is called consequence. For example rule R_i: if relative velocity is positive large; and acceleration is positive large; then the control current is positive large; where, i = 1,..., n; where n represents the total number of control rules. The initial FLC rule base adopted in this study (which is modified based on evolutionary optimization) is shown in the Table 2. This rule base pattern is based on first mode of vibration of structures (Ahlawat and Ramaswamy, 2004).

Optimal Fuzzy Logic Control

The selection of fuzzy parameters, especially the rule base structure is based on trial and error approach. A number of optimization schemes are studied and reported in the literature to select optimal rule base structure, like, the Michigan technique (Ishibuchi et al., 1997), the iterative rule techniques, the Pittsburgh approach (Driankov et al., 1992; Ishibuchi et al., 1997), etc. In this study, a geometric interpretation to the rule-base structure is given and based on that a relatively simple optimization scheme is adopted, which requires very few optimization variables.

Table 2. Initial inference rules for FLC used in the study

	Acceleration					
Velocity	NL	NL	NE	ZE	PO	PL
	NE	NL	NE	NS	NS	ZE
	ZE	NE	NS	ZE	ZE	ZE
	PO	NS	ZE	ZE	ZE	PS
	PL	ZE	ZE	ZE	PS	PO

The FLC considered in this chapter has two input variables, namely, acceleration and relative velocity, at the damper location and provides MR damper voltage as an output. The input/output variables are normalized over the UOD (universe of discourse) of [−1, 1]. The input variables range their respective UODs using five equally spaced 'gbell' shaped membership functions (MFs) (NL = negative large, NS = negative small, ZE = zero, PS = positive small, PL = positive large). Seven equally spaced 'gbell' shaped MFs have been used to define the output voltage ($v(t) \in [0, 1]$), (PO = positive; NE = negative MFs are extra). The extreme MFs for input variables are kept unbounded in the respective positive (s-shaped) and negative (z-shaped) UOD. This is done to consider the values of input that are outside the range of the UOD. It is to be noted that the output contains negative values, which is done to keep symmetry about zero in UOD.

Optimization of the FLC is attempted with a priori information in relation to the number of rules and the number of MFs that give meaning to those rules as noted earlier. Fuzzy input scaling gains, membership function parameters and the fuzzy rule base are optimized. The method proposed in this study considers only ten variables to obtain an optimal FLC structure. The MF properties altered by optimization are MF shape, MF centre shift, and MF slope at 0.5 membership grade. The adaptive rule base design will be elaborated in this section, for adaptive membership function design and more detail study the readers are requested to follow Ali and Ramaswamy (2009a). The application of adaptive FLC to benchmark nonlinear building is reported in Ali and Ramaswamy (2008).

Adaptive Rule Base Design

A geometric approach has been adopted to optimize the rule base, such that it takes fewer variables for rule base optimization. In this approach we keep the symmetry in the rule base as shown in Table 2 about the premise [0; 0] intact. The following assumptions consistent with structural control design are made while designing the rule base.

- To design an optimal rule base for the structural system we take advantage of the fact that control force input to the structure should increase when the structural responses increases, i.e., the extreme input values (premise) result in an extreme output values (consequent), mid-range input values result in mid-range output values and small/zero input values result in small/zero output. This rule base pattern is true for both the negative and positive portion of universe of discourse (UOD).
- Larger control force is provided by the MR damper with larger input current. Therefore input current to the MR damper is consistent with the structural responses.

To describe the optimization approach we define a 'premise coordinate system' which is as shown in Figure 1, a coordinate system formed by the MFs of the two inputs relative velocity and acceleration. The consequent MFs are to be placed at the nodal locations formed by the connection of two MFs of each input variables.

Encoding the Rule Base for Optimization

In this geometric approach the consequent space is overlaid upon the 'premise coordinate system' and is in effect partitioned into seven small non-overlapping regions, where each region represents a consequent fuzzy set (see Figure 1). To design

Figure 1. Fuzzy optimal rule base design strategy

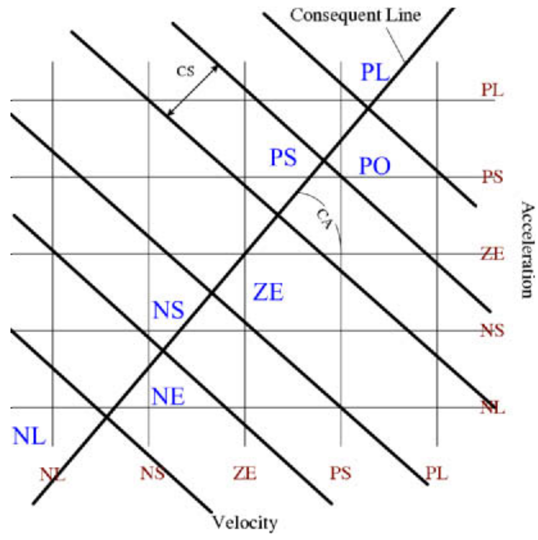

an optimal rule base we define a consequent line as shown in Figure 1. The line is made pivotal on premise zero-zero position (i.e., both inputs being zero) and it is free to rotate over the consequent space and therefore the rule base adapts according to the optimization scheme. Each region represents a consequent fuzzy set. It is to be noted that the rule base remains symmetrical whatever be the position of the consequent line.

The rule base is extracted by determining the consequent region in which each premise combination point lies. The geometric approach is made possible using only two parameters (CA and CS).

1. **Slope of the Consequent Line Angle (CA):** It has been used to create different output space partitions. The angle is encoded to cover angles between $0-180^{\circ}$. As the consequent space is symmetric and the output u(t) ranges between [0, 1], $0–180^{\circ}$ is equivalent to $0-360^{\circ}$.
2. **Consequent-Region Spacing (CS):** As shown in Figure 1, CS represents the space spanned by each of the consequent variables i.e., (NL, NE, NS, ZE, PS, PO, PL) over the consequent region. A CS of value one is used

to define the distance between the premise points along the premise line.

Thus only two variables are required to be encoded for optimization of the rule base. Making consequent line angle to be 45° and consequent region spacing to be 1, we get a rule base as shown in Table 2 analogous to the rule base that can be derived from the first mode vibration of the structure.

A micro genetic algorithm (μ-GA) (Krishnakumar, 1989; Ali and Ramaswamy, 2009a) is used to optimize the fuzzy logic control parameters. Figure 2 demonstrates the computational flow of micro genetic algorithm. For the GA used in this study, each chromosome represents a complete FLC inference system i.e., membership function optimization parameters, fuzzy input-output scaling gains and the rule base optimization parameters. The rule base is modified using a geometric approach keeping the symmetry in the rule base structure as noted earlier. This reduces the computational overhead of the optimization scheme.

For the present study an off-line trained FLC is adopted. The off-line training is carried out by providing an initial base displacement of 0.025m and then allowing the hybrid system to come to rest. The FLC that minimizes the following cost function is adopted for the study.

$$J_{ga} = \left\| \frac{x_b}{x_{b_{unc}}} \right\| + \left\| \frac{\ddot{x}_b}{\ddot{x}_{b_{unc}}} \right\| \tag{5}$$

The above cost function considers minimization (L_2 norm) of the ratio of base displacement (x_b) with controller and base displacement $\left(x_{b_{unc}}\right)$ without the controller, at the same time minimizing the corresponding ratio of acceleration norms. The rule base obtained from this optimization is then used to control the hybrid base isolated building.

Figure 2. Flow diagram of FLC optimization using micro genetic algorithm

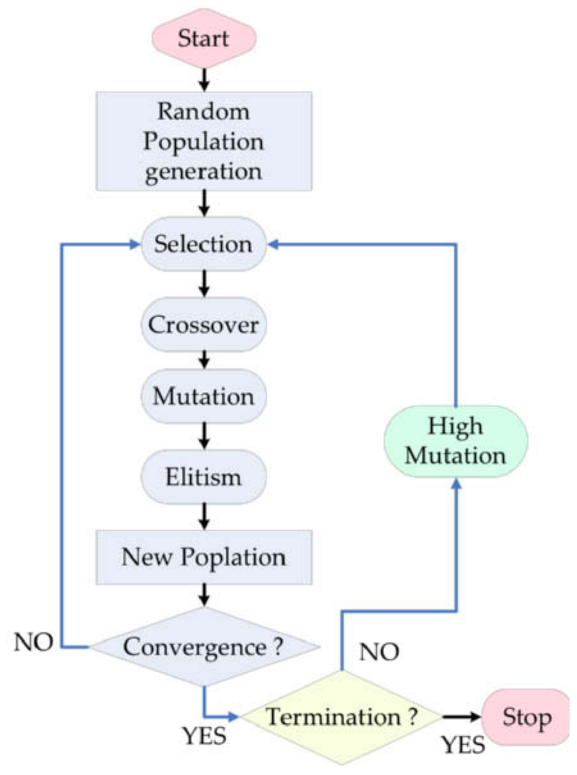

Apart from the inherent advantages of the FLC i.e., robust to uncertainty, noise etc., one important advantage of using FLC in present situation is that the voltage output, *v(t)* from the FLC, unlike the clipped optimal, can take any value in the range [0, 1]. Therefore FLC covers the full voltage range available for the damper. In the process, the voltage switch is gradual and does not jump between zero and maximum. Secondly, μ-GA used for the optimization process is computationally less intensive.

EXPERIMENTAL VERIFICATION OF OPTIMAL FUZZY CONTROL

A three storey base isolated building is considered for the experimental evaluation. The schematic diagram of the experimental test set-up for the control of the hybrid base isolated building using optimal FLC is shown in Figure 3. The hybrid isolation is achieved using four sliding bearing at the four column bases of the building and an MR damper connected at the base. In the experimental set up GA based optimal FLC is used as the controller. The stiffness of the bearing at the base is augmented using four linear springs placed co-axially with the sliding bearings. Figure 4a shows a photograph of the experiment with LVDT positions. Figure 4b shows connections at the base in fixed base condition, base isolated condition and the MR damper connection. Acceleration responses and inter-storey drifts are measured on all floors. In addition, acceleration and relative displacement (*w.r.t.* shake table) at the base isolator and acceleration and absolute displacement of the shake table are measured. Velocity at each floor is hardware integrated from the acceleration data.

Data acquisition is carried out using Dewetron acquisition system at a sampling rate of 1 kHz. For real time control implementation, dSPACE real-time controller, which has an on-board digital signal processor (DSP) is used. Thus the processing speed depended only on the DSP, which is designed specifically for real-time tasks. The optimal FLC is encoded in MATLAB Simulink using real time workshop (RTW) interface and dSPACE hardware and software. The isolator acceleration at the damper location and pseudo velocity are used as feedback to the RTW to obtain the voltage to be supplied to the MR damper. Figure 5 shows the Simulink block diagram of the controller implementation. The embedded fuzzy function contains the off-line simulated optimal fuzzy parameters and the rule base. The fuzzy parameters and the rule base are specifically optimized for this particular experiment.

Base Isolated Building Model and System Identification

For the simulation and experimental study presented in this chapter a three-storey base isolated building is considered. A single MR damper is connected at the base of the building. Base isolated buildings are designed such that the superstructure remains elastic. Hence, the superstructure is modeled as a three-dimensional linear elastic shear

Figure 3. Schematic diagram of the experimental set-up

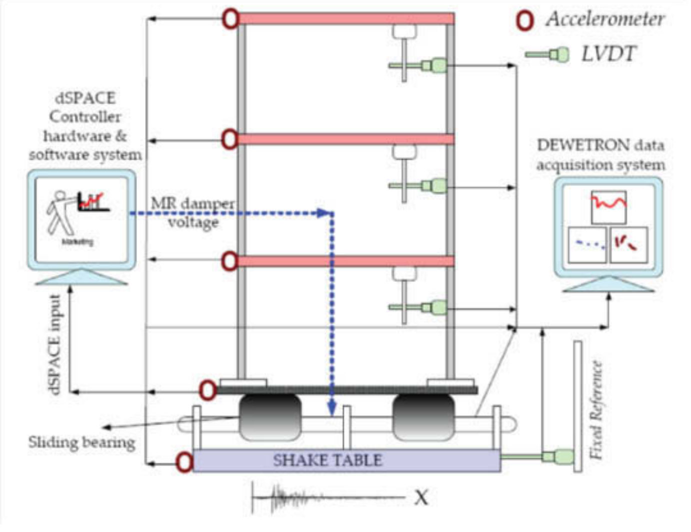

Figure 4. a) Photograph of the experimental set-up; b) Photograph of the experimental set-up showing the base connections

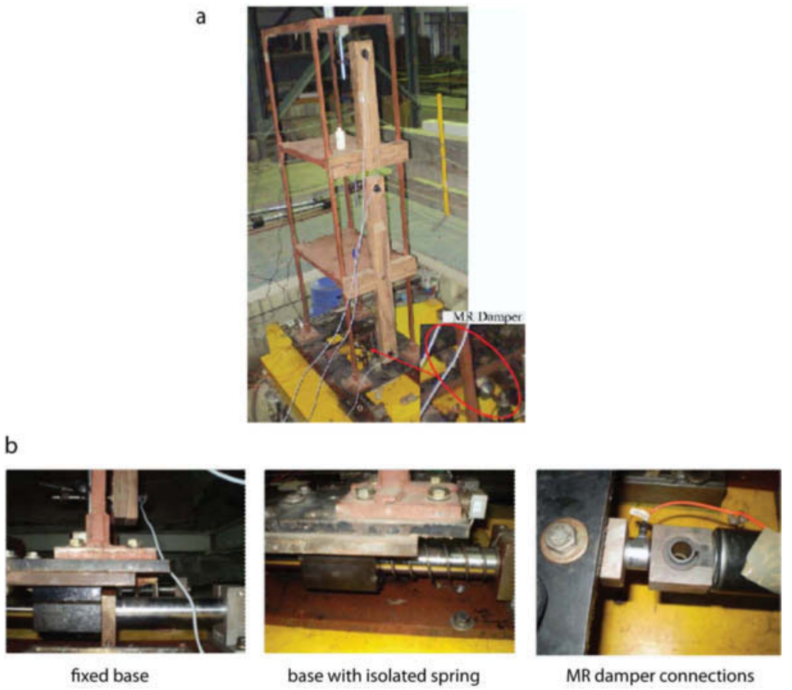

Figure 5. Matlab Simulink diagram for the FLC implementation in the experiments

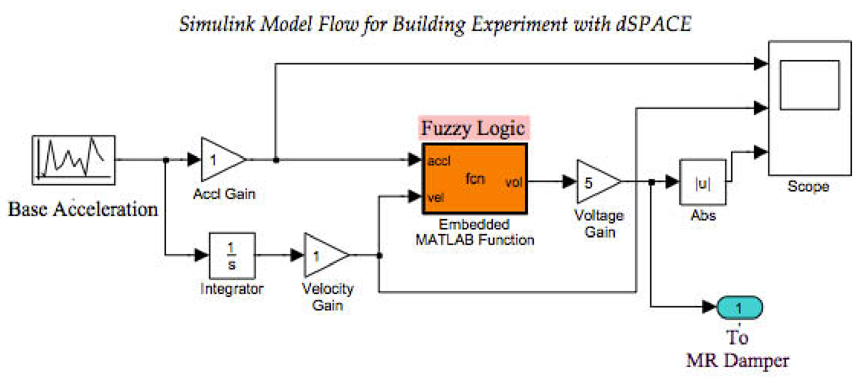

building. The equation of motion for the elastic superstructure is expressed in the following form

$$M_a\ddot{U} + C_a\dot{U} + K_aU = -M_aR\left(\ddot{U}_g + \ddot{U}_b\right) \tag{6}$$

where M_a is the superstructure mass matrix, C_a and K_a are the superstructure damping and stiffness matrices, respectively, in the fixed-base case, and R is the matrix of earthquake influence coefficients. Furthermore, $\ddot{U}$, $\dot{U}$, and U represent the floor acceleration, velocity, and displacement vectors relative to the base, respectively. $\ddot{U}_b$ is the vector of base accelerations (at isolation level) relative to the ground, and $\ddot{U}_g$ is the vector of ground accelerations. The equation of motion for the base is given as follows

$$R^T M_a \left[\ddot{U} + R\left(\ddot{U}_g + \ddot{U}_b\right)\right] + m_b\left(\ddot{U}_g + \ddot{U}_b\right) + c_b \dot{U}_b + k_b U_b + f_c = 0 \tag{7}$$

where f_c is the force across the MR damper. Subscript (b) represents parameters from the base of the building.

Impulse hammer tests (IHT) are conducted to determine the building parameters without isolator attached and sinusoidal base excitation is used to determine the damping characteristics of the sliding bearings. The stiffness at the base provided by the linear springs is determined experimentally using a servo hydraulic closed loop universal test rig. As noted earlier a simple Bouc-Wen model is used to describe the MR damper hysteretic characteristic. Details of experiments on MR damper are discussed in Ali and Ramaswamy (2009b).

For IHT, impulsive force is given at the top floor and the acceleration responses are measured at all the floors along the direction of impulse. The frequency response functions (FRFs) characteristic of the building is obtained in IOtech DaqBoard-2000 device and with DaisyLab Software (Ver. 7.02). From the FRFs, natural frequencies, damping coefficients and the mass normalized mode shapes of the fixed base building are determined using 'MEscope' software. Finally, the building parameters for analytical simulations (mass, damping and stiffness) are updated to match experimentally obtained results using particle swarm optimization (PSO).

Model updating aims at introducing correction to an initial model so that it predicts accurate and reliable dynamic behavior of the structure. The process of updating is performed by adjusting parameters of the initial model in such a way that the difference between analytical results and experimental data is minimized.

For optimization using PSO the building is idealized to be a three storey shear building model. PSO is used to minimize the cost function as given in Equation (8).

$$\psi = W_\omega J_\omega + W_\varsigma J_\varsigma + W_\phi J_\phi \tag{8}$$

where J_ω, J_ς and J_φ are the cost function components related to the natural frequencies, damping coefficients and mode shapes, respectively, and W_ω, W_ς and W_φ are the relative weight factors. The cost functions J_ω and J_ς are given as:

$$J_\omega = \sum_{k=1}^{3}\left(\frac{\omega_k^m - \omega_k^a}{\omega_k^m}\right)^2 \qquad J_\varsigma = \sum_{k=1}^{3}\left(\frac{\zeta_k^m - \zeta_k^a}{\zeta_k^m}\right)^2 \tag{9}$$

whereas the cost function related to mode shapes (J_φ) of the building is given by:

$$J_\phi = \sum_{k=1}^{3}\left\{\left(MSF\phi_k^m - \phi_k^a\right)^T\left(MSF\phi_k^m - \phi_k^a\right)\right\} \tag{10}$$

ω_k, ς_k, and φ_k are the kth natural frequency, coefficient of damping and mode shape vector, respectively. The superscripts (m) and (a) represent measured and analytical data, respectively and (T) is the transpose operator. MSF is the modal scale factor that is used to keep the experimental and analytical mode shapes at equal scale (Ewins, 2000). Equal weight factors for J_ω, J_ς and J_φ, i.e., $W_\omega = 1/3$, $W_\varsigma = 1/3$ and $W_\varphi = 1/3$ are assumed.

The obtained updated mass (M_a), damping (C_a) and stiffness (K_a) matrices are as given in Equation (11).

$$M_a = \begin{bmatrix} 62.76 & 0 & 0 \\ 0 & 64.20 & 0 \\ 0 & 0 & 59.40 \end{bmatrix} kg$$

$$C_a = \begin{bmatrix} 5.23 & -2.23 & 0 \\ -2.23 & 2.33 & -0.1 \\ 0 & -0.1 & 0.1 \end{bmatrix} \times 10^2 \frac{Ns}{m}$$

$$K_a = \begin{bmatrix} 1.04 & -0.74 & 0 \\ -0.74 & 1.49 & -0.76 \\ 0 & -0.76 & 0.76 \end{bmatrix} \times 10^2 \frac{N}{m} \quad (11)$$

Figures 6a and 6b show the comparison of amplitude and phase angles for experimental and analytical models measured at third floor respectively. Both the initial and updated analytical FRFs are presented to show the convergence of updated model using PSO algorithm. Initial model refers to system parameters prior to the PSO runs. There is a small peak at 27.1Hz in the experimental curve, which may be attributed to some transverse motion present in the structure due to the inherent eccentricity in the model introduced in the fabrication process. This is not analyzed further as the analytical predictions of the experiments are quite close to the test results across different displacement and acceleration time-histories. Figure 7 shows the progress in PSO convergence as the number of generations in the optimization increased.

The mass of the base is measured to be 38 kg. The stiffness of the linear springs attached coaxially with the sliding isolator is measured using servo-hydraulic testing machine. The stiffness of each of the springs is found to be 2.162kN/m. A nonlinear frictional damping $\left(f_b = \mu w z_w\right)$ is considered for the isolator, where μ is the coefficient of friction (Sahasrabuddhe and Nagarajaiah, 2005; Madden et al., 2002) and is given by

$$\mu = \mu_{\max} - (\mu_{\max} - \mu_{\min})e^{-\lambda|\dot{x}_b|} \quad (12)$$

where μ ranges from $\mu_{\max}$ at large velocities of sliding to $\mu_{\min}$ at very low velocities. λ is a constant having units of time per unit length and $\dot{x}_b$ is the velocity across the isolator. The value to

Figure 6. FRF measured at third floor showing amplitude and phase angle on the initial guess, updated model and the experimental obtained FRF

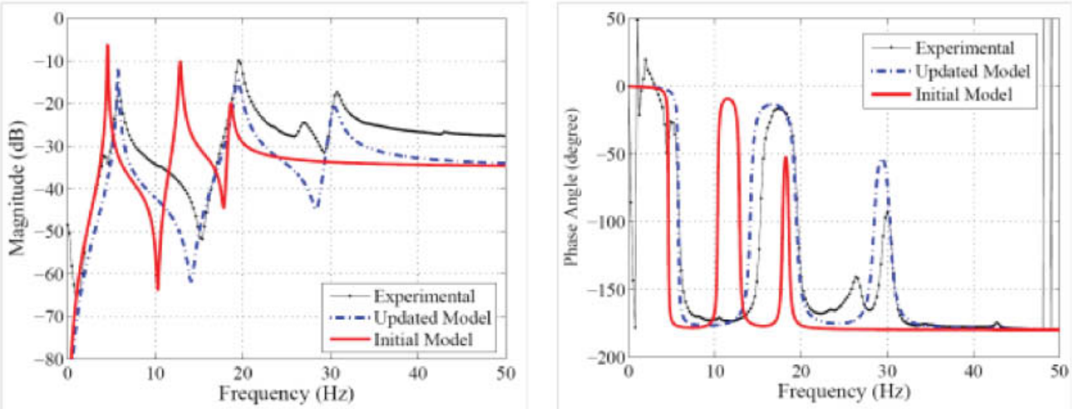

a) Amplitude of FRF

b) Phase angle

Figure 7. PSO convergence for all cost functions showing the decay in total cost function value and the respective vales in the each associated costs

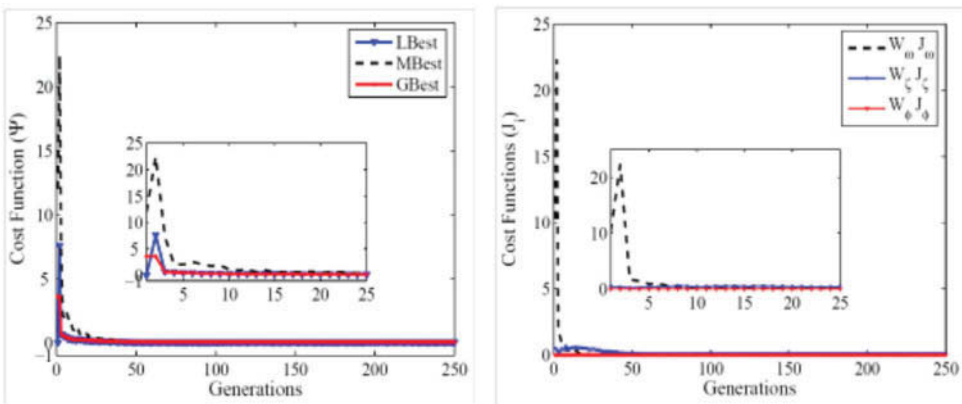

a) PSO convergence: Multi-objective cost function b) PSO convergence: J_ω J_ζ and J_ϕ

$\mu_{\max}$ and $\mu_{\min}$ are determined through experiments tests.

The Wen's hysteretic variable (z_w) is given by (Sahasrabuddhe and Nagarajaiah, 2005),

$$Y\dot{z}_w + \gamma_w \mid \dot{x}_b \mid z_w + \beta_w \dot{x}_b z_w^2 - A_w \dot{x}_b = 0 \tag{13}$$

where the constants Y, A_w, γ_w, and β_w are the shape parameters of the hysteretic loop which are calibrated using the experimental data. Tests with sinusoid input excitations at the base are carried out with varied frequencies ranging from 1Hz to 3Hz and amplitudes ranging from 2mm to 10mm, to determine frictional damping at the sliding isolator. Particle swarm optimization algorithm is used to optimize the variables $\mu_{\min}$, $\mu_{\max}$, Y and λ. The values for A_w, γ_w, and β_w are considered as 1, 0.9 and 0.1, respectively (Sahasrabuddhe and Nagarajaiah, 2005; Madden et al., 2002). The optimal values for the variables are obtained as $\mu_{\min} = 2853$, $\mu_{\max} = 1.1303$, $Y = 0.2526$ and $\lambda = 0.6191$.

Hybrid Semi Active Control of Base Isolated Building

Experimental and numerical studies of the building with GA-FLC monitored MR damper for eight earthquake records are carried out. For brevity, results are reported only for N. Palm Springs earthquake excitation. The time history and the frequency content of the excitation are shown in Figure 8. It should be noted that most of the energy of the excitation is localized below 5Hz of frequency. This shows that the first mode of the base isolated building will be highly effected by the N. Palm Springs earthquake excitation. In the present section we discuss the experimental results obtained on the three storey base isolated building and compare them with that of results obtained from the numerical simulations.

The responses measured in the experimental study are all the floor inter-storey drifts, relative base displacement, absolute displacement at shake table and acceleration at all the floors, base and shake table. Experimental data are acquired using Dewetron acquisition system at a sampling rate of 1kHz. The acquisition system has a low pass filter of 30 Hz. No further data filtering is carried out offline. Control actions are computed using

Figure 8. Seismic input excitation: N. Palm Springs (Frequency content upto 30 Hz)

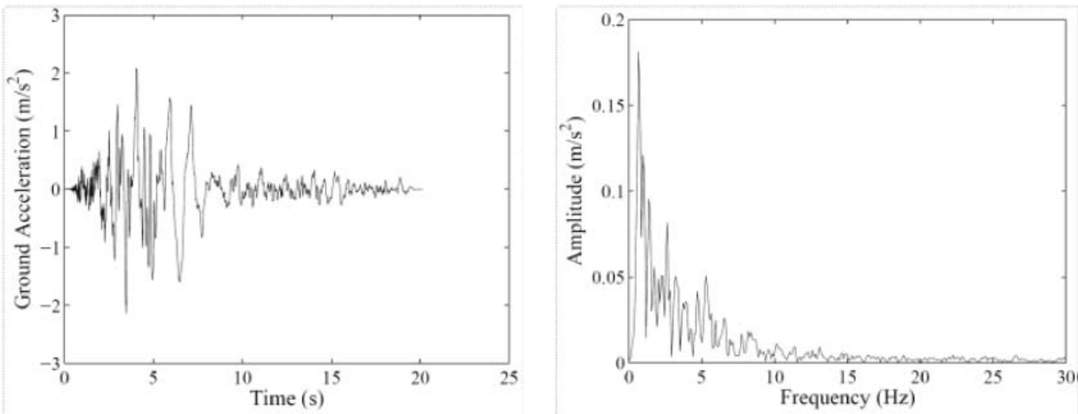

a) N. Palm Spring earthquake excitation

b) Frequency content of N. Palm Spring

a DSP-based, real-time controller manufactured by dSPACE. As noted earlier the FLC is encoded in MATLAB Simulink using real time workshop (RTW) interface and dSPACE hardware and software. The base plate acceleration at the damper location and pseudo velocity (obtained by integrating acceleration data in real time) are used as a feedback to the RTW to decide on the voltage required by the MR damper based on encoded FLC algorithm.

Figure 9 shows the isolator displacement and acceleration for both experimental and numerical results. The peak isolator relative displacement is found to be 0.1615m, where as the analytically obtained maximum isolator drift is 0.1339m. This shows a good match between the analytically and experimentally obtained results. A phase shift is observed between the experimental and the analytical results. This is due to the shake table dynamics that has introduced a phase lag between the original seismic displacement data and the data obtained as an output from the shake table.

Figure 10 shows the floor inter-storey drift and acceleration response of the base isolated

Figure 9. Isolator responses of simple base isolated building (N. Palm Springs)

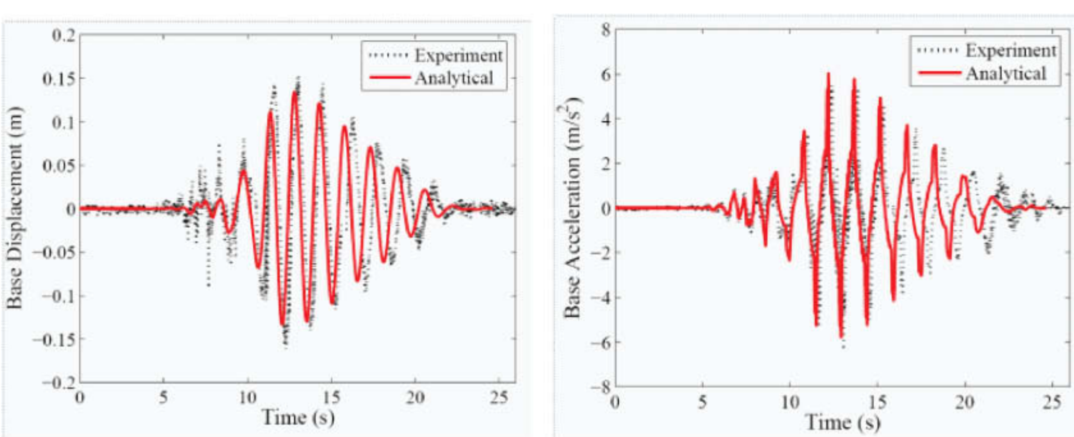

a) Isolator displacement

b) Isolator acceleration

building. From Figures 10, 11, 12, 13, 14, and 15 one can see a good correlation between the experimental and analytical responses. The floor inter-storey response plots in Figures 10, 11, and 12 show a noisy output from the capacitance type LVDT.

The responses of the base isolated building with the MR damper monitored by GAFLC are shown in Figures 16 through 23. A good agreement is seen between experimental and numerical results except in the case of isolator displacement (Figure 16). The experimental peak displacement in the GA-FLC case is found to be 0.0028m which is less than simple base isolated case (without MR damper attached). This reduction in isolator displacement has resulted in the increase in the isolator acceleration (from 6.207m/s^2 in base isolation case to 7.95 m/s^2 in hybrid base isolation case). But the increase is not as much as compared to benefit obtained from reducing the base displacement. Table 3 reports the comparative values obtained in three different cases, fixed base building i.e., building without any control mechanism; building with only base isolation and building with hybrid isolation mechanism.

Seismic isolators reduce the super structure drift and acceleration at the cost of increased displacement at the base. The theory is that most of the earthquake input energy is dissipated at the base level with little to pass to the super structure. But in near field seismic motions the base itself experiences out of limit base displacement. This on the other hand increases safety concern, as with little moment capacity at the base, large base deflection can topple the building or the building may collide with nearby structures. The hybrid

Figure 10. First floor drift of simple base isolated building without control (N. Palm Springs)

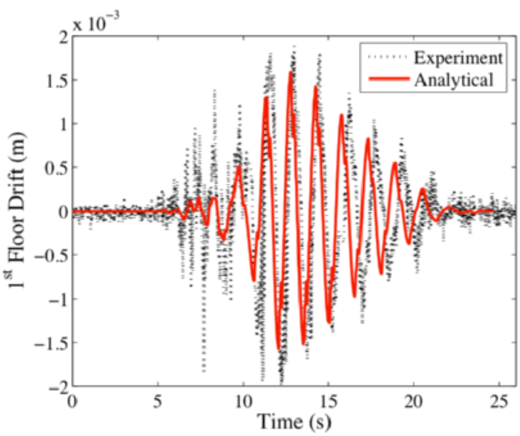

Figure 11. Second floor drift of simple base isolated building without control (N. Palm Springs

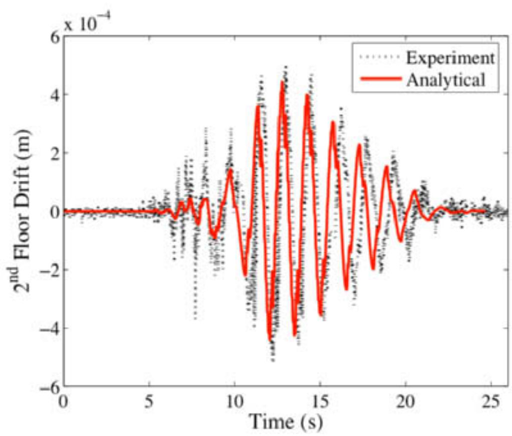

Table 3. Experimental results: peak responses under N. Palm Springs earthquake

Test Case	Relative Displacement (x10^{-2}m)				Floor Acceleration (m/s^2)			
	Base	FF	SF	TF	Base	FF	SF	TF
Fixed Base	0 0	0 2363	0 0656	0 0259	0 00	4 1331	3 1831	4 4149
Base Isolated	16 145	0 1993	0 0520	0 0387	6 2067	3 4458	3 1298	4 0787
Hybrid Isolation	0 2859	0 1026	0 0320	0 0235	7 9447	1 944	1 7624	2 2667

Figure 12. Third floor drift of simple base isolated building without control (N. Palm Springs)

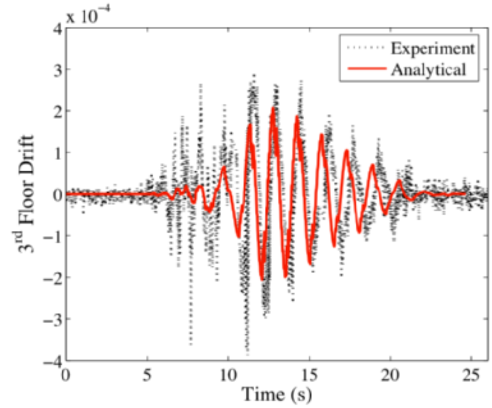

Figure 13. First floor acceleration of simple base isolated building without control (N. Palm Springs)

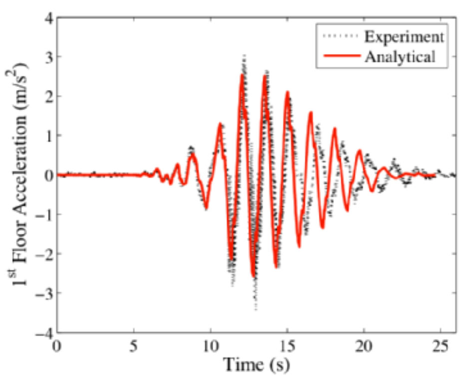

Figure 14. Second floor acceleration of simple base isolated building without control (N. Palm Springs)

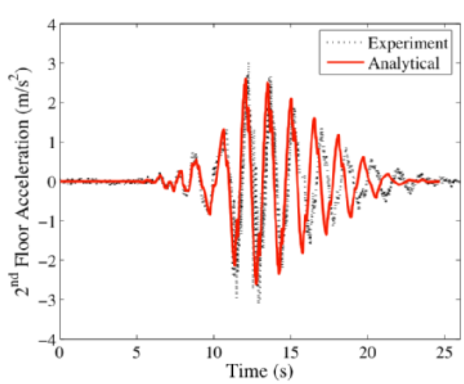

Figure 15. Third floor acceleration of simple base isolated building without control (N. Palm Springs)

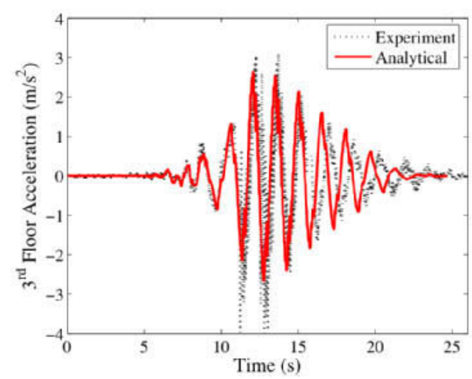

Figure 16. Base displacement of hybrid semi active base isolated building with optimal FLC driven MR damper (N. Palm Springs)

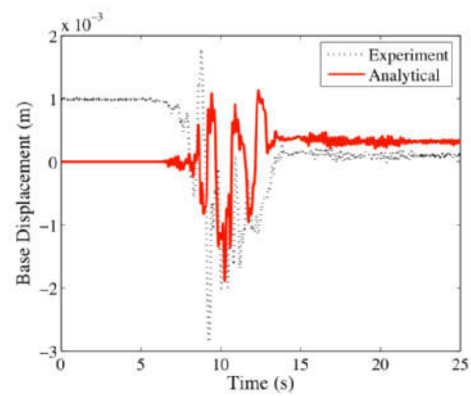

Figure 17. First floor drift of hybrid semi active base isolated building with optimal FLC driven MR damper (N. Palm Springs)

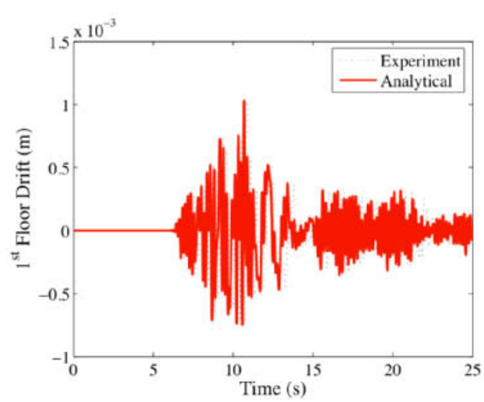

Figure 18. Second floor drift of hybrid semi active base isolated building with optimal FLC driven MR damper (N. Palm Springs)

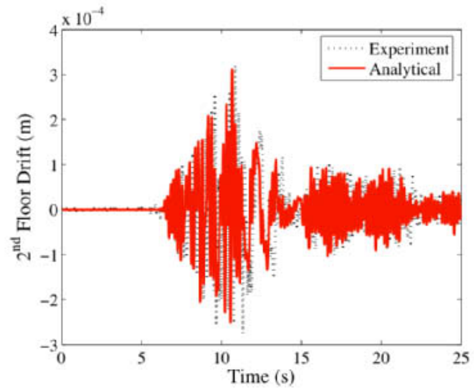

Figure 19. Third floor drift of hybrid semi active base isolated building with optimal FLC driven MR damper (N. Palm Springs)

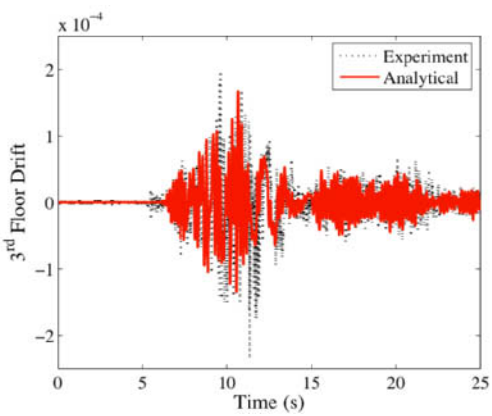

Figure 20. Base acceleration of hybrid semi active base isolated building with optimal FLC driven MR damper (N. Palm Springs)

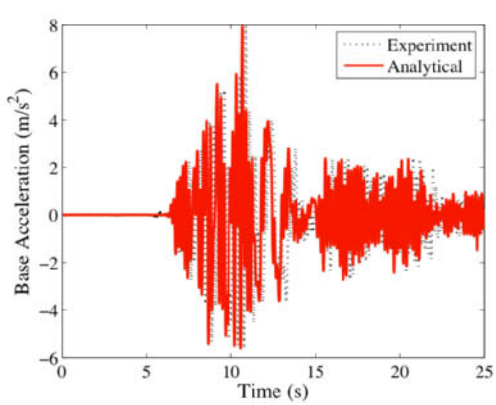

Figure 21. First floor acceleration of hybrid semi active base isolated building with optimal FLC driven MR damper (N. Palm Springs)

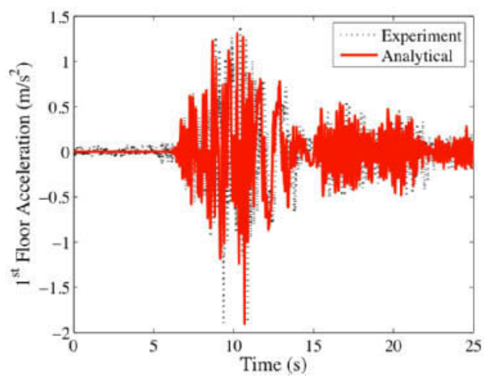

Figure 22. Second floor acceleration of hybrid semi active base isolated building with optimal FLC driven MR damper (N. Palm Springs)

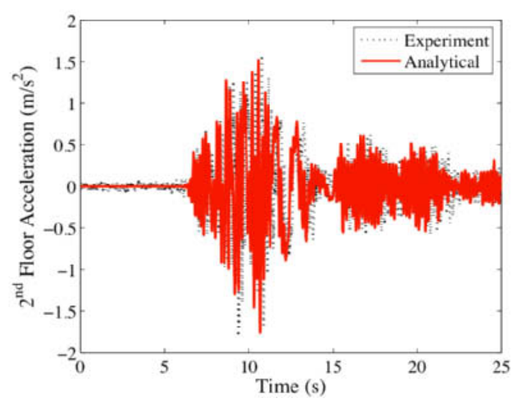

Figure 23. Third floor acceleration of hybrid semi active base isolated building with optimal FLC driven MR damper (N. Palm Springs)

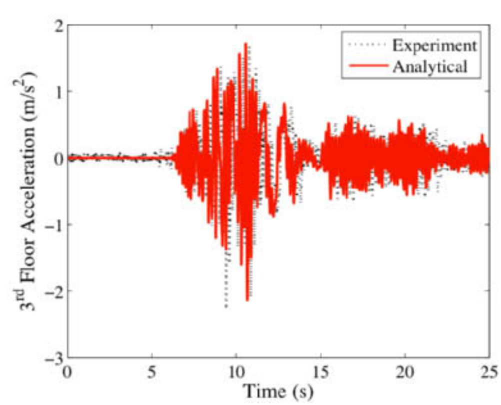

base isolation mechanism minimizes the drift demand on the isolators. Therefore, the isolator displacement is reduced when the MR damper is attached. In this case MR damper absorbs a part of the input seismic energy and dissipate it as heat energy. But reducing isolator displacement increases the super structure drift and acceleration, as well as, the acceleration at the isolation level. Therefore, addition of damping devices increases the acceleration level as they decrease the isolator displacement. This can be observed in Figure 9 through Figure 23. Therefore, too much or high damping i.e., using full capacity of MR damper will not allow the base to act as isolator and too low damping i.e., using MR damper in zero voltage will not reduce the base displacement as required. A trade-off should be considered between zero and maximum voltage supply to the damper. This is achieved using GA optimized FLC (GAFLC).

Another important motivation behind the adoption of FLC based MR damper monitoring is to provide smooth voltage (variable voltage) update across the MR damper. Figure 24 shows the voltage input to the MR damper under N. Palm Springs seismic motion. The variable voltage input to the MR damper is evident from the Figure 24.

Figure 24. Voltage input to the MR damper using optimal FLC (N. Palm Springs)

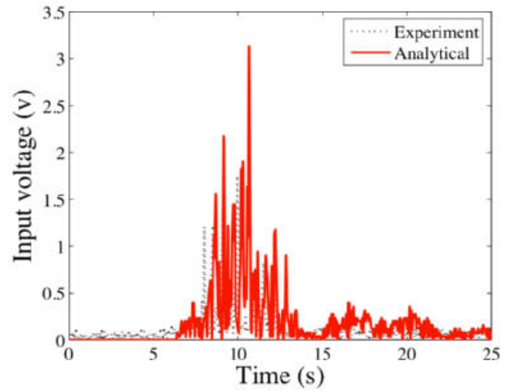

NONLINEAR CONTROL STRATEGIES

As has been discussed earlier, MR damper input voltage monitoring algorithms are developed in the framework of intelligent based control schemes and model based control schemes. Intelligent controllers are efficient in controlling the structural displacements responses with slight increase in the structural acceleration response. This makes the application of intelligent method based control algorithm interesting.

Intelligent controllers need training for its optimal performance and consequently are model specific. Moreover, stability criteria are not well developed in these algorithms. This drawback of intelligent controllers limits their applications in structural vibration control. On the other hand properly designed model based controllers provide better stability but they are vulnerable to parameter uncertainty.

In this section numerical study on two model based stable controllers to monitor MR damper input voltage using feedback from structural responses is reported. Nonlinear control algorithms like dynamic inversion (Isidori, 1995, Ali and Padhi, 2009) and integral backstepping (Krstic et al., 1995; Krstic and Smyshlyaev, 2007) are used to design semi-active control algorithms. The dynamics of supplied and commanded current input to MR damper is considered while designing these nonlinear algorithms.

Clipped Optimal Control

The clipped optimal control algorithm is proposed by Dyke et al, (1996). It is currently the most widely used algorithm for MR damper control. This strategy consists of a bang–bang (on–off) type of controller that causes the damper to generate a desirable control force which is determined by an 'ideal' active controller (in state feedback form). A force feedback loop is used to produce the desired control force, f_d, which is determined by a linear optimal controller, $K_k(s)$, based on the measured structural responses, y and the measured damper force, f_c at the current time.

The damper force is then calculated by

$$f_d = L^{-1}\left\{-K_k(s)L\left(\begin{matrix} y \\ f_c \end{matrix}\right)\right\} \tag{14}$$

where $L(.)$ is the Laplace transform operator. The linear controller is usually obtained using H_2 or LQG strategies. The applied voltage, v_a, to the MR damper can be commanded and not the damper force; hence when the actual force being generated by the MR damper, f_c, equals the desirable force, f_d, the voltage applied remains the same. Again, when the magnitude of the force f_c is smaller than the magnitude of f_d and both forces have the same sign, then the voltage applied is set to its maximum level, to increase the damper force. Otherwise, the voltage is set to zero.

This algorithm for selecting the voltage signal is described by

$$v_a = v_{\max} H(f_d - f_c)f_c \tag{15}$$

where $v_{\max}$ is the voltage level associated with the saturation of the magnetic field in the MR damper, and $H(.)$ is the Heaviside step function operator.

The performance of the clipped optimal control algorithm has been evaluated through numerical simulations (Dyke et al., 1996) and demonstrated for multiple MR dampers in Jansen and Dyke (2000). Jansen and Dyke (2000) also presented a comparison with other algorithms. In all cases the clipped optimal controller is found to satisfactorily reduce the structural responses and outperform passive control strategies.

The main disadvantage of the clipped optimal strategy is that it tries to change the voltage of the MR damper from zero to its maximum value, which makes the control force suboptimal. Moreover, sometimes this swift change in voltage and therefore sudden rise in external control force increases the system responses, which may lead to an inelastic response of the structure. Therefore there is, indeed, a need for better control algorithms that can change the MR damper voltage slowly and smoothly, such that all voltages between maximum and zero voltage can be covered based on the feedback from the structure. In addition, the algorithm needs to consider the dynamics between the applied voltage and the commanded voltage (given by Equation (4)). Intelligent control algorithms are used to solve the first of the above-mentioned constraints but the inclusion of supplied to commanded voltage dynamics is not addressed.

Dynamic Inversion Control

Dynamic inversion (DI) control methodology is a member of feedback linearization control techniques and is applied to different types of aircraft applications (Reiner et al., 1995). In this technique the existing deficient or undesirable dynamics in the system are nullified and replaced by designer specified desirable dynamics (Reiner et al., 1995; Ali and Padhi, 2009). This tuning of system dynamics is accomplished by a careful algebraic selection of a feedback function. It is for this reason that the DI methodology is also called the feedback linearization technique. Details of feedback linearization and DI can be found in Marquez (2003).

Like all other model based systems, a fundamental assumption in this approach is that the plant dynamics are perfectly modeled, and therefore can be cancelled exactly by the feedback functions. Here also we assume that no uncertainty is involved in the plant dynamics and parameters. Here, DI is used as a two-stage controller formulation. The first stage contains a primary controller, which provides the force required to obtain a desired closed loop response of the system. Then, DI maps the required force to required voltage to be supplied to the MR damper. Therefore the overall control scheme forms a new two-stage stabilizing state feedback control design approach.

To formulate the proposed two-stage controller let us consider a system in state space form as given by

$$\dot{X} = AX + Bu + E\ddot{x}_g \tag{16}$$

where $X \in R^n$ is the state of the system, u ∈ R1 is the damper force, and $\ddot{x}_g$ is the input excitation to the system. $A \in R^{n\times n}$, $B \in R^{n\times 1}$, and $E \in R^{n\times 1}$ are the system state matrix, controller location vector, and influence vector for support excitation, respectively.

$$f_c = c_0\dot{x}_{mr} + k_0 x_{mr} + \alpha z_{mr} \tag{17}$$

where f_c is the MR damper force. For simplification, we assume a perfectly observable and controllable system, and the all states are measurable.

Primary Controller Design

An LQR (linear quadratic regulator) is considered as the first-stage or primary controller. LQR is designed to obtain the optimal force required to minimize the cost function defined as

$$J_1 = \lim_{\tau\to\infty} \frac{1}{\tau}\left[\int_0^\tau \left\{X^T Q X + u^T R u\right\} dt\right] \tag{18}$$

where Q and R are weighting matrices used to appropriately weight the states and calculate the controller force required. Minimization of the performance index in Equation (27) with the system dynamics Equation (25) as a constraint gives a state feedback form of the control force required (Ali and Ramaswamy 2009c).

$$f(t) = -K_g X \tag{19}$$

where K_g is the feedback gain matrix and X the states. The feedback gain (K_g) can be calculated or can be obtained using the '*lqr*' function available with the Control Toolbox in MATLAB. Once the state feedback form of the optimal control force has been obtained, it is necessary to compute the voltage to be supplied to the MR damper such that the MR damper provides similar control force. Dynamic inversion is used to obtain a closed form solution of the input voltage to be supplied to the MR damper in order to obtain the desired optimal force.

Secondary Controller Design

The secondary controller is designed with a goal to minimize the error between the primary controller and the control force supplied by the MR damper in L_2 norm sense. Let us define an error term as follows

$$e = \frac{1}{2}\left(u - f\right)^2 \tag{20}$$

The idea is to minimize the error, e in an exponential decay fashion. Therefore a first order dynamics is considered for the error variable.

$$\begin{gathered}\dot{e} + k_e e = 0 \\ \left(\dot{u} - \dot{f}\right)\left(u - f\right) + \frac{k_e}{2}\left(u - f\right)^2 = 0\end{gathered} \tag{21}$$

In Equation (21), $k_e > 0$ serves as a gain. One may choose it as $k_e = \dfrac{1}{\tau_c}$, where $\tau_c > 0$ serves as a 'time constant' for the error e to decay. Choice of k_e determines the stability of the controller and its tracking efficiency. It should be noted that Equation (21) contain the dynamics of the primary control force, $\dot{f}$ and the force provided by the MR damper, $\dot{u}$. Equation (19) provides f and Equation (1) provides $u = f_c$, which are given in Equations (22) and (23), respectively

$$\dot{f}(t) = -K_g \dot{X} \tag{22}$$

$$\begin{aligned} \dot{u} = &\left(c_{0a}\ddot{x}_{mr} + K_{0a}\dot{x}_{mr} + \alpha_a \dot{z}_{mr}\right) \\ &-\left(c_{0b}\dot{x}_{mr} + K_{0b}x_{mr} + \alpha_b z_{mr}\right)\eta\hat{v}_c \\ &+\left(c_{0a}\ddot{x}_{mr} + K_{0a}\dot{x}_{mr} + \alpha_a \dot{z}_{mr}\right)\hat{v}_c \\ &+\left(c_{0b}\dot{x}_{mr} + K_{0b}x_{mr} + \alpha_b z_{mr}\right)v_a \end{aligned} \tag{23}$$

The voltage supplied to the MR damper is represented by v_a whereas the voltage driving the magnetic flux, i.e., at the damper magnetic coils (also known as commanded voltage), is represented by v_c. $\hat{v}_c$ represents the measured value of the commanded voltage obtained from on-line integration using Simulink. Substituting $\dot{u}$ from Equation (23) into Equation (21), the following simplified form of the supply voltage is obtained:

$$v_a = \left\{\begin{matrix} \dot{f} + \dfrac{k_e}{2}\left(u - f\right) - \left(c_{0a}\ddot{x}_{mr} + K_{0a}\dot{x}_{mr} + \alpha_a \dot{z}_{mr}\right) \\ -\left(c_{0b}\dot{x}_{mr} + K_{0b}x_{mr} + \alpha_b z_{mr}\right)\eta\hat{v}_c \\ +\left(c_{0a}\ddot{x}_{mr} + K_{0a}\dot{x}_{mr} + \alpha_a \dot{z}_{mr}\right)\hat{v}_c \end{matrix}\right\} \times\left(c_{0b}\dot{x}_{mr} + K_{0b}x_{mr} + \alpha_b z_{mr}\right) \tag{24}$$

It is to be noted that when the system dynamics at the damper location goes to zero (particularly at steady state) or in any situation where the states simultaneously go to zero, an unstable situation may arise in the computed applied voltage. However, this is unlikely as in that case the prescribed force by the primary controller should be zero and the algorithm ends up in a $\frac{0}{0}$ position. To avoid such a numerically unstable situation, the supply voltage near the zero state condition is redefined as

$$v_{a\,\text{redefined}} = \left\{\begin{matrix} 0 & x_{mr} < tol_1 \text{and } \dot{x}_{mr} < tol_2 \\ v_a & \text{otherwise} \end{matrix}\right\} \tag{25}$$

Backstepping Control Design

The DI technique designed in the previous section considers the input voltage dynamics of the MR damper in its algorithm development. Nevertheless it has a drawback in that one needs to design an intermediate controller like H2/LQG and then employ dynamic inversion to determine the voltage required to be supplied to the MR damper such that the control force prescribed by the intermediate controller is supplied. The main scope of this section is to design a stable semi-active controller maintaining the good features of the DI algorithms but eliminating the intermediate primary controller, and for this the integral backstepping controller proposed by Krstic et al., (1995) is adopted in this study.

In recent adaptive and robust control literature, the backstepping design provides a systematic framework for the design of tracking and regulation strategies, suitable for a large class of state feedback linearizable nonlinear systems. Integrator backstepping is used to systematically design controllers for systems with known nonlinearities. The approach can be extended to handle systems with unknown parameters, via adaptive backstepping. However, adaptive backstepping design for nonlinear control may dramatically increase the complexity of the controller. In this chapter, integrator backstepping is applied to deduce the voltage required by the MR damper to minimize the structural responses.

This is also a two-stage control design. In the first stage a Lyapunov control is designed to stabilize the dynamics of the structural system. Next, considering the MR damper input voltage dynamics, a second Lyapunov based control is developed to stabilize the full system, considering both the structural system and the MR damper. It is assumed that the three storey building behaves as a SDOF system due to the presence of base isolation (Chopra, 2005). The integral backstepping based semi-active MR damper voltage monitoring is developed for a SDOF system.

System Model

An SDOF model is considered with an MR damper connected to it. The linear dynamics of SDOF systems with an MR damper is given by

$$m\ddot{x} + c\dot{x} + kx + u(t) = -m\ddot{x}_g \tag{26}$$

where m, c, and k are the mass, damping, and stiffness of the SDOF system and $(\cdot)$ denotes the derivative *w.r.t.* time, t. $u(t) = f_c$ is the MR damper control force and $\ddot{x}_g$ is the external excitation force. $u(t)$ is added as the system restoring force as the MR damper acts as a passive device in the absence of driver voltage. Substitute $u(t) = f_c(t)$ from Equation (1) to Equation (26). Rewriting the closed loop system dynamics and considering the MR damper dynamics (and neglecting the external excitation) in state space form, one gets

$$\begin{aligned} \dot{X} &= F_1(t,X) + G_1(t,X)v_c \\ \dot{v}_c &= F_2(t,X,i_c) + G_2(t,X,i_c)v_a \end{aligned} \tag{27}$$

where X, F1, G1, F2 and G2 are given in Equation (28).

$$\begin{aligned} &X = \left[x_1, x_2, x_3\right]^T; \\ &x_1 = x = x_{mr};\ x_2 = \dot{x} = \dot{x}_{mr};\ x_3 = z_{mr} \\ &F_1 = \begin{bmatrix} x_2 - \frac{1}{m}\left\{\left(k + k_{0a}\right)x_1 + \left(c + c_{0a}\right)x_2 + \alpha_a x_3\right\} - \\ \gamma\left|x_2\right|x_3\left|x_3\right|^{n-1} - \beta x_2\left|x_3\right|^n + Ax_2 \end{bmatrix} \\ &G_1 = \begin{bmatrix} 0 & -\frac{1}{m}\left\{k_{0b}x_1 + c_{0b}x_2 + \alpha_b x_3\right\} & 0 \end{bmatrix}^T \\ &F_2 = -\eta i_c;\ G_2 = \eta; \end{aligned} \tag{28}$$

The variable $x_3 = z_{mr}$ is responsible for the hysteretic behaviour of the MR damper and it evolves with time. Therefore it is a hidden variable and is considered as an additional state variable.

Backstepping Controller Design

Equation (27) is in a second-order strict feedback form. Let us define a dummy variable v_{dum} such that it satisfies the following relation:

$$v_a = \frac{1}{G_2(t,X,v_c)}\left(v_{dum} - F_2(t,X,v_c)\right) \tag{29}$$

The dummy variable v_{dum} is defined to convert the second-order strict feedback system to a simplified form amenable for integrator backstepping application. Combining Equations (27) and (29), we reduce the strict feedback system to an integrator backstepping form:

$$\begin{aligned} \dot{X} &= F_1(t,X) + G_1(t,X)v_c \\ \dot{v}_c &= v_{dum} \end{aligned} \tag{30}$$

The design objective is the state variable $X \to 0$ as the time $t \to \infty$. The control law can be synthesized in two steps. We regard the commanded voltage, v_c, to the damper as the real voltage driver, first. By choosing the Lyapunov candidate function of the system as

$$V_1 = \frac{1}{2}(kx_1^2 + mx_2^2 + qx_3^2) \tag{31}$$

$$\dot{V}_1 = \begin{bmatrix} -\left\{\left(c + c_{0a}\right)x_2^2 + \gamma q\left|x_2 x_3\right| x_3^2\right\} \\ -\begin{Bmatrix} k_{0a}x_1 x_2 + \left(\alpha_a - Aq\right)x_2 x_3 + q\beta x_2 x_3^3 \\ +\left(k_{0b}x_1 x_2 + c_{0b}x_2^2 + \alpha_b x_2 x_3\right)v_c \end{Bmatrix} \end{bmatrix} \tag{32}$$

To design a stable closed loop system the Lyapunov time-derivative $\dot{V}_1$ should be made negative-definite. The first term in $\dot{V}_1$, i.e., $\left\{\left(c + c_{0a}\right)x_2^2 + \gamma q\left|x_2 x_3\right| x_3^2\right\}$, is free of the voltage variable v_c and is negative-definite $\forall\left(x_1, x_2, x_3\right)$ q is a positive constant given by $\frac{\alpha_a}{A}$. Out of many solutions, we select the designed commanded voltage $v_{c_{dzs}}$ to be

$$v_{c_{des}} = \frac{k_d x_1^2 - K_{0a}x_1 x_2 - q\beta x_2 x_3^3}{k_{0b}x_1 x_2 + c_{0b}x_2^2 + \alpha_b x_2 x_3} \tag{33}$$

where $k_d \geq 0$ is a positive constant to be decided by the designer. This simple form makes $\dot{V}_1 = -\left\{\left(c + c_{0a}\right)x_2^2 + \gamma q\left|x_2 x_3\right| x_3^2 + k_d x_1^2\right\} \leq 0, \forall X \neq 0$

In the present analysis, $k_d = 1$ is considered. There can be a numerical stability problem, when all $x_1 \to 0$, $x_2 \to 0$ and $x_3 \to 0$ simultaneously. Therefore, a tolerance is set for all the state variables, below which the damper input voltage is kept at zero.

Nevertheless, v_c is a state variable, and perfect tracking to $v_{c_{des}}$ is desired and hardly achieved in reality. Therefore, an error variable e (given in Equation (34)) is defined as the error between the target and the designed.

$$e = v_c - v_{c_{des}} \tag{34}$$

The error dynamics is given by

$$\begin{aligned} \dot{e} &= \dot{v}_c - v_{c_{des}} \\ &= v_{dum} - v_{c_{des,X}}\dot{X} \end{aligned} \tag{35}$$

where $v_{c_{des,X}}$ is the derivative of $v_{c_{des}}$ *w.r.t.* state X. Choosing a second Lyapunov function as $V_2 = V_1 + \frac{1}{2}e^2$ and the voltage variable v_{dum} as given in Equation (36), it can be shown that the system defined in Equation (30) becomes asymptotically stable (see Marquez, (2003); Krstic et al., (1995)).

$$\begin{aligned} v_{dum} = v_{c_{des},X}&\left[F_1(t,X) + G_1(t,X)v_c\right] \\ &- V_{1,X}.G_1(t,X) - K(v_c - v_{c_{des}}) \end{aligned} \tag{36}$$

with F_1 and G_1 defined in Equation (28); $K > 0$ is any constant to be decided by the designer. For our analysis K=1 is considered. The voltage applied to the MR damper can be obtained by substituting Equation (36) into equation (29).

NUMERICAL SIMULATION OF NONLINEAR CONTROL STRATEGIES

Numerical simulations are carried out with eight earthquake records. For the sake of brevity results are reported for Big Bear earthquake excitation with recorded magnitude 6.4 M on 28th June 1992 at San Bernardino Hospitality, California. Figure 25 shows the time history of the input excitation and frequency spectrum. It is to be noted that the frequency spectrum shows high peaks at low frequency, which excites low frequency structures like base isolated buildings. Mathematical model of the three storey base isolated building shown in Figure 4 is used for the study. A classical damping at the base is considered for the numerical analysis at 2% of the critical. The MR damper parameters taken for the present analysis are given in Table 1. The maximum input voltage allowed for the damper is 5V. The damper can provide a maximum force of ±2250 N.

Numerical simulations are carried out for micro-GA optimized FLC, clipped optimal control, dynamic inversion based MR damper monitoring and with integrator backstepping control of MR damper voltage input.

Results for GAFLC are shown in Figures 14 and 15. Figure 26 shows the displacement and acceleration time histories at the base and at the third storey of the building. Both the uncontrolled and controlled time histories are shown in same plot for better comparison of the responses. The peak displacement response of the isolator in simple isolation condition is found to be 0.1229m, which is reduced to 0.0015m and the third floor drift is decreased from 0.0020m in uncontrolled condition to 0.0015m in MR damper controlled case. Since the MR damper decreases the isolator displacement, the isolator acceleration goes up. The base acceleration of 2.3214m/s^2 in uncontrolled case is increased to 7.7440m/s^2 in the MR controlled case but the third floor acceleration is decreased from 2.3631 m/s^2 in uncontrolled case to 2.0381m/s^2. Figure 27 shows the voltage time history and the corresponding control force supplied by the MR damper.

A LQR based clipped optimal control strategy is considered for the comparison purposes. The LQR is designed with the weights same as considered for the dynamic inversion based control case. The matrix $Q = 5 \times 10^3 \times I_{8\times8}$ and $R = 1 \times 10^{-4}$ are considered for the study. $I_{8\times8}$ is an identity matrix of dimension (8×8).

Figure 28 shows the time histories of the uncontrolled and controlled system responses (displacement and acceleration) of base isolator and at the third floor. The peak displacement response of the isolator in simple isolation condition has been found to be 0.1229m, which is reduced to 0.0010m. The third floor time histories also show decrease displacement responses from 0.0020m in uncontrolled condition to 0.0016m in MR damper controlled case, which is a slight decrease in displacement response when compared with other control techniques.

Since the MR damper decreases the isolator displacement, the isolator acceleration increases. The base acceleration of 2.3214m/s^2 in uncontrolled case is increased to 8.2796m/s^2 in the MR controlled case. The third floor acceleration is

Figure 25. Seismic input excitation: Big Bear earthquake (Frequency content up to 30 Hz)

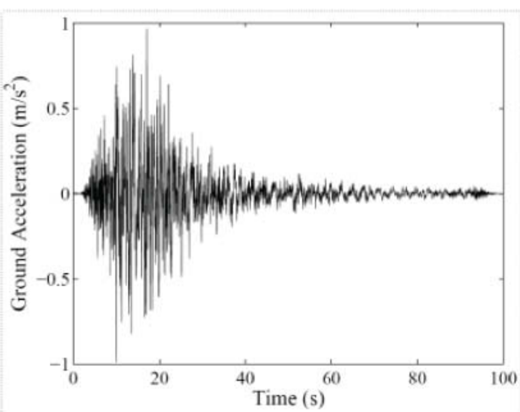

a) Big Bear earthquake excitation

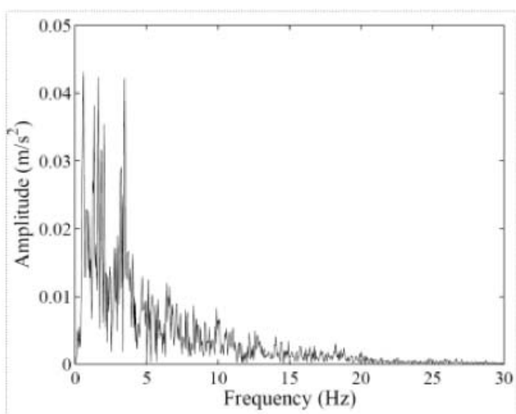

b) Frequency content of Big Bear

Figure 26. Base isolator and third-floor displacement and acceleration responses under Big Bear earthquake for GA-FLC based MR damper monitoring

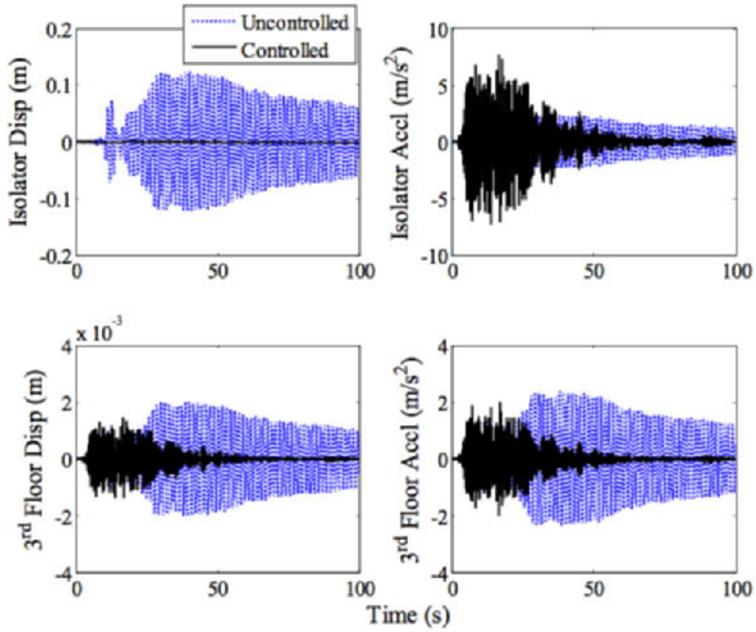

also increased from 2.3631 m/s^2 in uncontrolled case to 2.5526m/s^2 in clipped optimal case.

Figure 29 shows the input voltage to the MR damper and the corresponding control force at the damper location. The voltage plot is shown from 20s to 40s of the voltage time history. As is seen from Figure 29 there are frequent jumps in the voltage plot from zero to maximum 5V. This is same all through. It is to be noted that the maximum allowed input voltage is not supplied for all the time, which is observed in the clipped optimal case.

Figure 27. Voltage input and control force under Big Bear earthquake for GA-FLC based MR damper monitoring

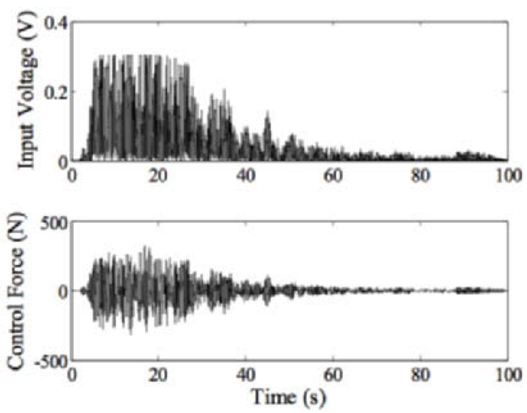

For dynamic inversion based control law the primary control force is obtained using LQR algorithm ('lqr' function available with Control Toolbox. The matrix $Q = 5 \times 10^3 \times I_{8\times8}$ and $R = 1 \times 10^{-4}$ are considered for the study. $I_{8\times8}$ is an identity matrix of dimension (8×8). The gain k_e is taken as 10. The tolerance values in Equation (25) are taken as $tol_1 = 1 \times 10^{-5}$ m and $tol_2 = 1 \times 10^{-5}$ m/s.

Figure 30 shows the time histories of the uncontrolled and controlled system responses (displacement and acceleration) of base isolator and at the third floor under Big-bear ground motion. The uncontrolled (simple base isolation) and controlled (hybrid isolation) displacement and ac-

Figure 28. Base isolator and third-floor displacement and acceleration responses under Big Bear earthquake for clipped optimal based MR damper monitoring

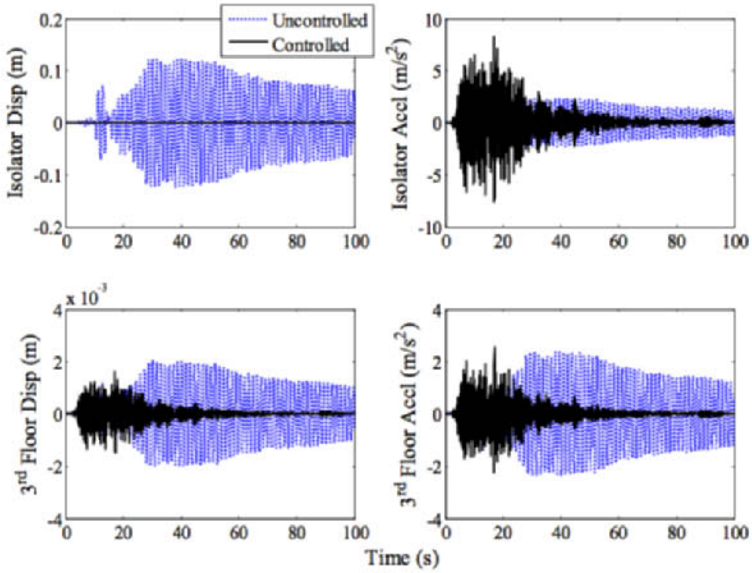

celeration responses are shown together for better comparison. The peak displacement response of the isolator in simple isolation condition has been found to be 0.1229m, which is reduced to 0.0070m by the DI monitored MR damper. The third floor time histories also show a decrease displacement response from 0.0020m in uncontrolled condition to 0.0011m in MR damper controlled case.

Figure 29. Voltage input and control force under Big Bear earthquake for clipped optimal based MR damper monitoring

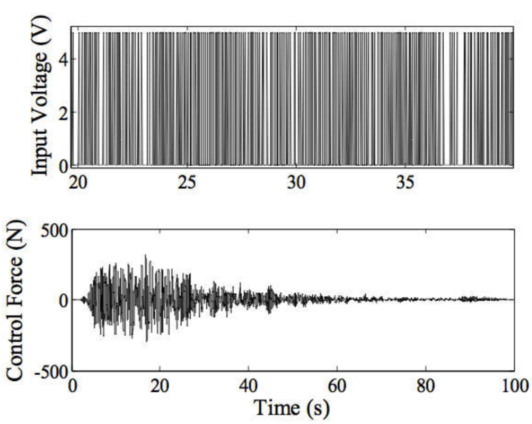

The acceleration response at the isolator level is increased whereas at the superstructure it is reduced due to the implementation of MR damper. Since the MR damper decreases the isolator displacement, the isolator acceleration increases. The base acceleration of 2.3214m/s^2 in uncontrolled case is increased to 6.5054m/s^2 in the MR controlled case. This rise is due to some sudden peaks in the acceleration response. Figure 30 reveals that this is not always the case all along the time history of the input excitation. For the third floor the acceleration is reduced from 2.3631 m/s^2 to 1.6068m/s^2.

Figure 31 shows the input voltage to the MR damper and the corresponding control force at the damper location. It is to be noted that the maximum allowed input voltage is not supplied for all the time, which is observed in the clipped optimal case.

Base isolated structures behave as a rigid mass over the base under seismic ground motion (Cho-

Figure 30. Base isolator and third-floor displacement and acceleration responses under Big Bear earthquake for dynamic inversion based MR damper monitoring

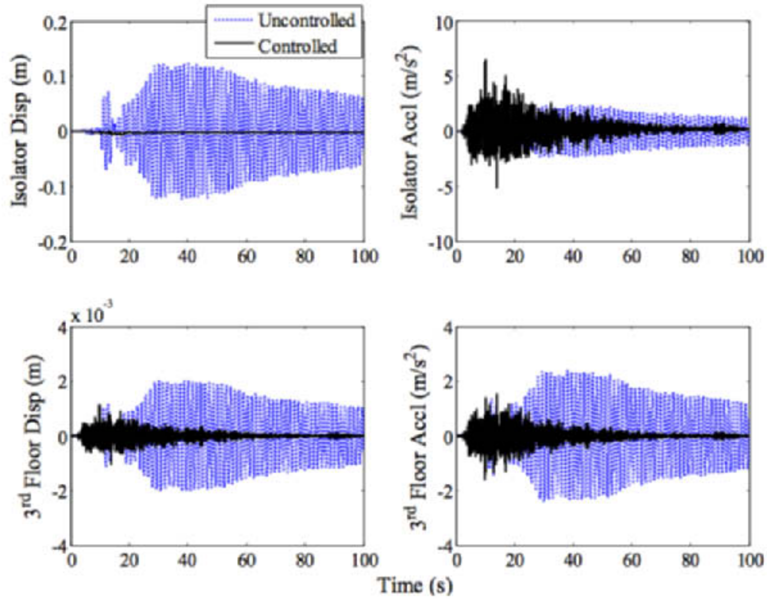

pra, 2005). Therefore SDOF models provide good approximation to these systems for quick calculation under ground motion. The integrator backstepping based algorithm is developed assuming a SDOF system with mass equal to the total mass of the three storey base isolated building and stiffness equal to that of the base stiffness. The tolerances for the simulation studies with backstepping are set to $tol_1 = 1 \times 10^{-5}$ m for isolator displacement and $tol_2 = 1 \times 10^{-5}$ for isolator velocity.

Figure 32 shows the time histories of the uncontrolled (simple isolation) and controlled system (hybrid isolation) responses of base isolator and at the third floor. The peak displacement response of the isolator is reduced from 0.1229m to 0.0061m by the integral backstepping monitored MR damper. The isolator acceleration has been observed to increase from 2.3214m/s^2 to 3.326m/s^2 with backstepping control, which is a smaller increase in comparison to that obtained through DI control.

The third floor displacement has also been minimized from 0.0020m in uncontrolled (simple isolation) condition to 0.0007m in MR damper controlled (hybrid isolation) case and at the same time it has managed to keep the acceleration response reduced (2.2361 m/s^2 in uncontrolled case

Figure 31. Voltage input and control force under Big Bear earthquake for dynamic inversion based MR damper monitoring

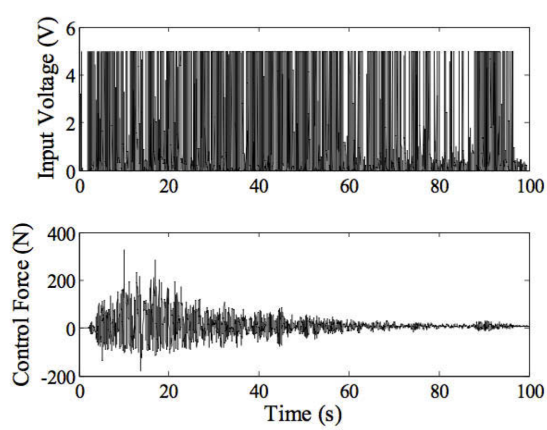

Figure 32. Base isolator and third-floor displacement and acceleration responses under Big Bear earthquake for integrator backstepping based MR damper monitoring

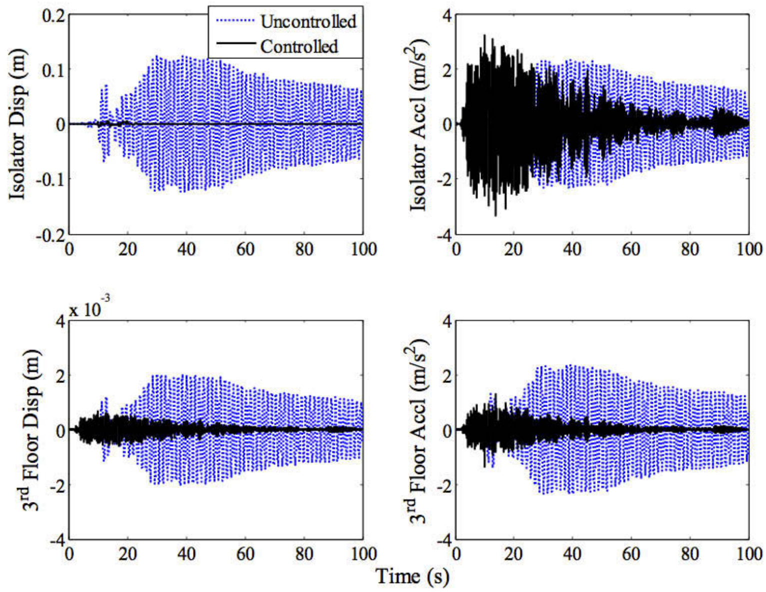

to 1.3729 m/s² in controlled case). The control force provided by the MR damper and the corresponding input voltages to the MR damper are shown in Figure 33. It is clear from the input voltage time history shown in Figure 33 that only a small amount current input is needed to mitigate the vibration. Therefore, switching the input current from zero to maximum based on system responses decreases the system performance under seismic motions.

It is observed from above discussions that worst control cases are seen in clipped optimal and in GA based optimal FLC. The reason for clipped optimal case is that it tries to provide a full voltage supply or zero to the damper. Therefore either it tries to over dampen the structure or it provides less than required damping. When the damper gets full voltage supply it tries to reduce the displacement and that on the other hand increases the acceleration at the base level.

This scenario is not seen in the cases of dynamic inversion control and in integrator backstepping control as they provide the required voltage to the MR damper.

Figure 33. Voltage input and control force under Big Bear earthquake for integrator backstepping based MR damper monitoring

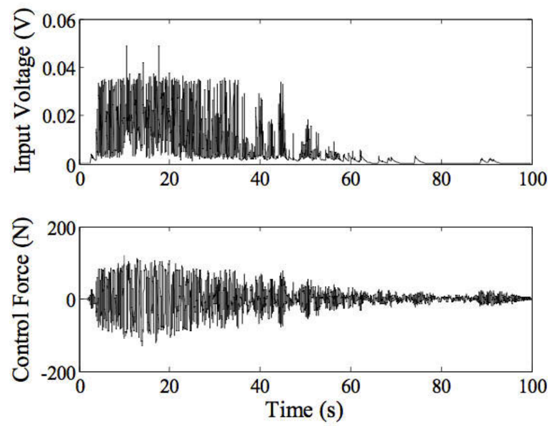

CONCLUSION

The nonlinear force-input voltage relation of MR damper introduces challenges in modeling the damper characteristic as well as in developing proper control strategy to effectively use the damper capacity. Existing model based algorithms switch the MR damper input voltage between zero and maximum, based on force feedback from the damper and the desired control force. Another drawback of the existing algorithms is that none of them consider the dynamics of the input voltage in to the algorithm. These two drawbacks in existing control schemes formed two objectives of the present chapter. In this chapter, development of various nonlinear control schemes are shown along with the most widely used linear control method. First a fuzzy logic based intelligent control a technique is studied. Various parameters, the membership function and the fuzzy rule base are optimized using micro-genetic algorithm. A novel geometric way of designing the fuzzy rule base is shown. The FLC system is optimized for a three storey base isolated building, which is then used to control the building in real time experiments. The experimental details and results are also reported. The results show a good match between the experimental and numerical analysis. The optimal FLC is seen to control the system responses as desired.

In a separate section two model-based semi-active control algorithms are developed using modern nonlinear control techniques. The developed algorithms not only update the voltage supply to the damper smoothly, but also take care of the MR damper supplied to commanded voltage dynamics in the algorithms. Furthermore, unlike other model based control algorithms, the proposed algorithms do not switch between zero and maximum voltage values, and as a consequence they provide all voltages within zero and the maximum allowed as an input to the damper. Numerical studies are conducted in the same three storey base isolated building. A comparison with the widely used clipped optimal and optimal FLCs is shown. From the results reported, it can be concluded that the performance of the proposed nonlinear controllers are better than those from the widely used clipped optimal and optimal FLCs. Both clipped optimal and optimal FLCs decrease the isolator displacement but at the cost of an increase in base and superstructure acceleration. The dynamic inversion and the integrator backstepping controllers provide a tradeoff between the isolator displacement and superstructure acceleration responses, offering the engineer a suite of options for selecting a design.

FUTURE RESEARCH DIRECTIONS

There are still many issues that need to be addressed and further explored in the area of response control of structures, such as the development of highly efficient and reliable control systems, large scale testing of various control devices, applications of control in the design and retrofit of structures, code adoption of seismic protective systems in future design guidelines, etc. In terms of the application of seismic protective systems in earthquake engineering, ground motion characteristics need to be better addressed in the future design and application of various control systems.

Based on the present study following recommendation for future studies can be suggested

- Due to hardware constraints and the computational efforts required in real time optimization using genetic algorithm, the experimental study is performed using offline optimization. The experimental study can be conducted using various hardware that are specifically made for GA optimization. Further investigation can be carried out with 3D building considering bi-directional seismic excitation supplied simultaneously and considering the torsional response of building in the analysis.

- Model based semi-active control algorithms are very sensitive to the accuracy of the mathematical model of the structure. The proposed model based algorithms should be supported with procedures to identify structural parameters. This remains to be further investigated using adaptive backstepping, fuzzy backstepping, etc. Robust backstepping technique may be further explored to minimize the sensitivity of the model based algorithms to noise.
- Along with the mathematical models for the structures, neuro based training algorithms should be supplemented to consider the uncertainty in modeling arising out of the flexibility at connections, effect of nonlinearity (material and geometric), etc. Thereafter the controller should be designed on these hybrid models.
- Powering active/semi-active devices is concern to engineers. Although semi active devices operate at battery power, maintenance and mounting of sensors and control devices at remote locations provides challenge and are not cost effective. Therefore, coming up with self powered, less energy consuming devices and sensors remains an effective choice in future. In this context one can design self powered MR dampers, which will be cost effective and environmental friendly.

REFERENCES

Agrawal, A. K., & Nagarajaiah, S. (2009). Benchmark structural control problem for a seismically excited highway bridge—Part I and II. *Structural Control and Health Monitoring, Special Issue*, *16*(5), 503–528. doi:10.1002/stc.336

Agrawal, A. K., Tan, P., Nagarajaiah, S., & Zhang, J. (2009). Benchmark structural control problem for a seismically excited highway bridge—Part I: Phase I problem definition. *Structural Control and Health Monitoring, Special Issue*, *16*(5), 509–529. doi:10.1002/stc.301

Ahlawat, A. S., & Ramaswamy, A. (2004). Multiobjective optimal fuzzy logic controller driven active and hybrid control systems for seismically excited nonlinear buildings. *Journal of Engineering Mechanics*, *130*(4), 416–423. doi:10.1061/(ASCE)0733-9399(2004)130:4(416)

Ali, S. F., & Padhi, R. (2009). Active vibration suppression of nonlinear beams using optimal dynamic inversion. *Journal of Systems and Control Engineering*, *223*(5), 657–672.

Ali, S. F., & Ramaswamy, A. (2007). Developments in structural optimization and applications to intelligent structural vibration control. In Lagaros, N., & Tsompanakis, Y. (Eds.), *Intelligent computational paradigms in earthquake engineering* (pp. 125–247). Hershey, PA: Idea Group Publishing. doi:10.4018/978-1-59904-099-8.ch006

Ali, S. F., & Ramaswamy, A. (2008). GA optimized FLC driven semi-active control for phase II smart nonlinear base isolated benchmark building. *Structural Control and Health Monitoring*, *15*, 797–820. doi:10.1002/stc.272

Ali, S. F., & Ramaswamy, A. (2009a). Optimal fuzzy logic control for MDOF structural systems using evolutionary algorithms. *Engineering Applications of Artificial Intelligence*, *22*(3), 407–419. doi:10.1016/j.engappai.2008.09.004

Ali, S. F., & Ramaswamy, A. (2009b). Testing and modeling of MR damper and its application to SDOF systems using integral backstepping technique. *Journal of Dynamic Systems, Measurement, and Control*, *131*, 021009. doi:10.1115/1.3072154

Ali, S. F., & Ramaswamy, A. (2009c). Optimal dynamic inversion based semi-active control of benchmark bridge using MR dampers. *Structural Control and Health Monitoring*, *16*(5), 564–585. doi:10.1002/stc.325

Casciati, F., Faravelli, L., & Yao, T. (1995). The tuning of fuzzy controllers for active structural control. *Applications of Statistics and Probability*, *2*, 741–746.

Chopra, A. K. (2005). *Dynamics of structures: Theory and application to earthquake engineering*. New Delhi, India: Pearson Education.

Driankov, D., Hellendoorn, H., & Reinfrank, M. (1992). *An introduction to fuzzy control*. Kolkata, India: Narosa Publishing House.

Dyke, S. J., Spencer, B. F. Jr, Sain, M. K., & Carlson, J. D. (1996). Modeling and control of magnetorheological dampers for seismic response reduction. *Smart Materials and Structures*, *5*, 565–575. doi:10.1088/0964-1726/5/5/006

Ewins, D. J. (2000). *Modal testing: Theory, practice and application* (2nd ed.). Hertfordshire, UK: Research Studies Press Ltd.

Feng, Q., & Shinozuka, M. (1990) Use of a variable damper for hybrid control of bridge response under earthquake. In G. Housner & S. Masri (Eds.), *Proceedings of the US National Workshop on Structural Control Research*, University of Southern California, Los Angeles, (pp. 107–112).

Glanz, J., & Onishi, N. (2011, March 12). Japans strict building codes saved lives. *The New York Times*. Retrieved March 14, 2011, from http://www.nytimes.com/2011/03/12/world/asia/12codes.html?_r=2

Ishibuchi, H., Nakashima, T., & Murata, T. (1997). Comparison of the Michigan and Pittsburgh approaches to the design of fuzzy classification systems. *Electronics and Communications in Japan*, *80*(12), 10–19. doi:10.1002/(SICI)1520-6440(199712)80:12<10::AID-ECJC2>3.0.CO;2-W

Jansen, L. M., & Dyke, S. J. (2000). Semi-active control strategies for MR dampers: Comparative study. *Journal of Engineering Mechanics*, *126*, 795–803. doi:10.1061/(ASCE)0733-9399(2000)126:8(795)

Jung, H. J., Choi, K. M., Spencer, B. F. Jr, & Lee, I. W. (2005). Application of some semi-active control algorithms to a smart base isolated building employing MR dampers. *Structural Control and Health Monitoring*, *13*(2-3), 693–704. doi:10.1002/stc.106

Karnopp, D. C., Crosby, M. J., & Harwood, R. A. (1974). Vibration control using semi-active force generators. *Journal of Engineering for Industries*, *96*(2), 619–626. doi:10.1115/1.3438373

Krishnakumar, K. (1989). Microgenetic algorithms for stationary and non-stationary function optimization. In G. Rodriguez (Ed.), *Proceedings of SPIE Intelligent Control and Adaptive Systems,* Vol. 1196, (pp. 289–296).

Krstic, M., Kanellakopoulos, I., & Kokotovic, P. V. (1995). *Nonlinear and adaptive control design*. New York, NY: Wiley.

Krstic, M., & Smyshlyaev, A. (2007). Backstepping boundary control—A tutorial. *Proceedings of the American Control Conference*, New York City, NY, July, (pp. 870–875).

Leitmann, G. (1994). Semi-active control for vibration attenuation. *Journal of Intelligent Material Systems and Structures*, *5*, 841–846. doi:10.1177/1045389X9400500616

Madden, G. J., Symans, M. D., & Wongprasert, N. (2002). Experimental verification of seismic response of building frame with adaptive sliding base-isolation system. *Journal of Structural Engineering*, *128*(4), 1037–1045. doi:10.1061/(ASCE)0733-9445(2002)128:8(1037)

Mamadani, E. H. (1974). Application of fuzzy logic algorithms for control of simple dynamic plant. *Proceedings of the Institution of Electrical Engineers*, *29*, 1585–1588. doi:10.1049/piee.1974.0328

Marquez, H. J. (2003). *Nonlinear control systems: Analysis and design*. New York, NY: Wiley Interscience.

Nagarajaiah, S., & Narasimhan, S. (2006). Smart base isolated benchmark building part II: phase I sample controllers for linear isolation systems. *Journal of Structural Control and Health Monitoring*, *13*(2-3), 589–604. doi:10.1002/stc.100

Nagarajaiah, S., Narasimhan, S., & Johnson, E. A. (2008). Structural control benchmark problem: Phase II—Nonlinear smart base-isolated building subjected to near-fault earthquakes. *Journal of Structural Control and Health Monitoring*, *15*(5), 653–656. doi:10.1002/stc.280

Narasimhan, S., Nagarajaiah, S., & Johnson, E. A. (2008). Smart base isolated benchmark building part IV: phase II. Sample controller for nonlinear isolation systems. *Journal of Structural Control and Health Monitoring*, *15*(2-3), 657–672. doi:10.1002/stc.267

Narasimhan, S., Nagarajaiah, S., Johnson, E. A., & Gavin, H. P. (2006). Smart base isolated benchmark building part I: Problem definition. *Journal of Structural Control and Health Monitoring*, *13*(2-3), 573–588. doi:10.1002/stc.99

Reiner, J., Balas, G. J., & Garrard, W. L. (1995). Robust dynamic inversion for control of highly maneuverable aircraft. *Journal of Guidance, Control, and Dynamics*, *18*, 18–24. doi:10.2514/3.56651

Ross, M. (2011, March 14). Building codes spared Tokyo from wider destruction. *ABC News.* Retrieved March 14, 2011, from http://www.abc.net.au/news/stories/2011/03/14/3163447.htm?section=justin

Sahasrabudhe, S., & Nagarajaiah, S. (2005). Experimental study of sliding base-isolated building with magnetorheological dampers in near fault earthquakes. *Journal of Structural Engineering*, *131*, 1025–1034. doi:10.1061/(ASCE)0733-9445(2005)131:7(1025)

Shook, D., Lin, P. Y., Lin, T. K., & Roschke, P. N. (2007). A comparative study in the semi-active control of isolated structures. *Smart Materials and Structures*, *16*, 1433–1446. doi:10.1088/0964-1726/16/4/058

Soong, T. T., & Spencer, B. F. (2002). Supplemental energy dissipation: State of the art and state of the practice. *Engineering Structures*, *24*, 243–259. doi:10.1016/S0141-0296(01)00092-X

Spencer, B. F. Jr, Dyke, S. J., Sain, M. K., & Carlson, J. D. (1997). Phenomenological model for magnetorheological dampers. *Journal of Engineering Mechanics*, *123*, 230–238. doi:10.1061/(ASCE)0733-9399(1997)123:3(230)

Wang, D. H., & Liao, W. H. (2011). Magnetorheological fluid dampers: A review of parametric modelling. *Smart Materials and Structures*, *20*, 023001. doi:10.1088/0964-1726/20/2/023001

Wereley, N. M., & Pang, L. (1998). Nondimensional analysis of semi-active electrorheological and magnetorheological dampers using approximate parallel plate models. *Smart Materials and Structures*, *7*(5), 732–743. doi:10.1088/0964-1726/7/5/015

Xu, Z. D., Shen, Y. P., & Guo, Y. Q. (2003). Semi-active control of structures incorporated with magnetorheological dampers using neural-networks. *Smart Materials and Structures*, *12*(1), 80–87. doi:10.1088/0964-1726/12/1/309

Yang, G., Spencer, B. F., Jung, H. H., & Carlson, J. D. Jr. (2004). Dynamic modeling of large-scale magnetorheological damper systems for civil engineering applications. *Journal of Engineering Mechanics*, *130*, 1107–1114. doi:10.1061/(ASCE)0733-9399(2004)130:9(1107)

Zadeh, L. A. (1965). Fuzzy sets. *Information and Control*, *8*, 338–353. doi:10.1016/S0019-9958(65)90241-X

Chapter 14
Comparative Study on Multi-Objective Genetic Algorithms for Seismic Response Controls of Structures

Young-Jin Cha
The City College of New York, USA

Yeesock Kim
Worcester Polytechnic Institute, USA

ABSTRACT

This chapter introduces three new multi-objective genetic algorithms (MOGAs) for minimum distributions of both actuators and sensors within seismically excited large-scale civil structures such that the structural responses are also minimized. The first MOGA is developed through the integration of Implicit Redundant Representation (IRR), Genetic Algorithm (GA), and Non-dominated sorting GA 2 (NSGA2): NS2-IRR GA. The second one is proposed by combining the best features of both IRR GA and Strength Pareto Evolutionary Algorithm (SPEA2): SP2-IRR GA. Lastly, Gene Manipulation GA (GMGA) is developed based on novel recombination and mutation mechanism. To demonstrate the effectiveness of the proposed three algorithms, two full-scale twenty-story buildings under seismic excitations are investigated. The performances of the three new algorithms are compared with the ones of the ASCE benchmark control system while the uncontrolled structural responses are used as a baseline. It is shown that the performances of the proposed algorithms are slightly better than those of the benchmark control system. In addition, GMGA outperforms the other genetic algorithms.

DOI: 10.4018/978-1-4666-2029-2.ch014

INTRODUCTION

In recent years, structural control technology has attracted a great attention from the society of civil engineering because the properties of structural systems can be modified in real time without adding too much mass to mitigate severe damage and protect structural poverty and human lives from attacking strong natural hazards such as winds, waves, and earthquakes (Kobori et al. 1991; Soong and Reinhorn 1993; Housner et al. 1994; Adeli and Saleh 1999; Kim et al. 2009; 2010a; 2010b; Cha and Agrawal 2011). As a result of this, a lot of control strategies have been proposed. In general, structural control systems can be classified into three different categories: passive, active, and semi-active control systems (Spencer and Nagarajaiah 2003). It is generally said that the passive control system is the most stable and reliable control method because it does not require external power supply, but utilizes material yielding forces or viscosity of fluids or friction forces. Representatives of the passive control devices include viscous fluid damper, viscoelastic damper, friction damper, tuned mass damper, tuned liquid damper, tuned liquid column damper, base isolation systems, etc. Although it is relatively easy and cheap to install into civil structures, the parameters of the passive systems cannot be adjusted during earthquake events. On the other hand, active control systems can adjust control forces according to the maginitude and spectrum of external loads and structural responses. Thus, active control systems are more effective in mitigating natural hazards of large-scale civil structures than the passive systems. However, the active control system requires large external power supply to offer desired control forces that derive actuators. Although semi-active control systems have been proposed to compenstate the drawbacks of the active and passive systems, it is beyond the scope of this book chapter. This study focuses on the application of structural active control systems to large-scale civil structures. Another important thing along with the developed control algorithms and control devices is the mechanism of optimal placement of control devices and sensors within structures. However, the optimal placement of control devices/sensors has not been much investigated even though it can significantly contribute to the improvement of control performance. With this in mind, we propose three new different multi-objective optimization algorithms of not only finding minimum distributions of both actuators and sensors, but also minimizing the seismic responses of structures.

To date, the impact of optimal placement of control devices in large-scale civil structures has been investigated. Arbel (1981) found optimal locations of actuators in an oscillatory dynamic system using controllability measures. DeLorenzo (1990) optimized the placement of actuators and sensors in a solar optical telescope system using successive approximation-based weight-selection technique. Chen et al (1991) used simulated annealing (SA) for finding optimal placement of active/passive members of truss structures. GA was applied to an active truss structure for finding optimal locations of actuators (Rao et al. 1991). Onoda and Hanawa (1992) applied GA to an actuator placement optimization for correcting statistical static distortion of truss structures. Furuya and Haftka (1995) applied GA to optimization problems of finding optimal actuator locations within large space structures. Dhingra and Lee (1995) applied a hybrid gradient based GA to an across-four space structure for finding actuator locations and minimum weights of structures. Liu et al. (1997) used SA to solve an integrated structural topology and actuator placement problem of structures. Agrawal and Yang (1999) studied a variety of heuristic search algorithms for optimal placement of energy dissipative devices within buildings, including Sequential, Worst-Out-Best-In, and Exhaustive Single Point Substitution methods. Linear quadratic Gaussian-based Pareto optimal trade-off curves have been proposed by Brown et al. (1999) for various placements of actuators and sensors in structures. Li et al. (2000; 2004) developed a multi-level GA to optimize both actuator locations and state feedback control gains for structural control system design. GA is also applied to a forty-story high-rise building to find the optimal locations of the pre-defined number of actuators (Abdullah et al. 2001). Cheng et al. (2002) applied a sequential iterative procedure for optimal placement of dampers and actuators to a seismically excited three-story building. A step-by-step procedure for optimal placement of piezoelectric friction dampers in a seismically excited building is proposed by Chen and Chen (2002; 2004). Liu et al. (2003) adopted GA for optimal actuator distribution within a seismically excited sixteen-story tall building. Wongprasert and Symans (2004) proposed an optimal location of passive control devices within the ASCE nonlinear benchmark building. Yang et al. (2005) applied SA to an optimization problem of finding best locations of active bars in smart structures. Amini and Tavassoli (2005) applied artificial neural networks to the optimal actuator placement problems for seismic response control of a twelve-story building structure. Tan et al. (2005) applied GA to optimization problems of finding optimal actuator locations and control gains for hazard mitigation of a forty-story shear building and a nine-story irregular structure. Moita et al. (2006) applied an SA to laminated reinforced composite structures to maximize the effectiveness of piezoelectric actuators. Rao and Sivasubramanian (2008) proposed a novel multiple start guided neighborhood search (MSGNS) algorithm by integration of the best features of SA and Tabu search algorithms for optimal placement of actuators within seismically excited tall buildings.

However, there is minimal study of GA-based multi-objective optimal formulations for minimum distributions of both actuators and sensors as well as minimum structural responses of large-scale infrastructures under seismic excitations. Several previous studies used a simple GA to solve this optimal distribution of the actuators and sensors. However, it might not be easy to solve highly complex optimization problems, e.g., multi-objective formulations of large-scale complex structure-control systems. Even though it can handle the complex problem, it may require high computational cost (Raich and Ghaboussi 1998). With this in mind, this book chapter introduces three novel multi-objective genetic algorithms (MOGA) with the capacity of robust and efficient problem solving for optimal placement of control devices and sensors in large civil structures such that the performance on the interstory drifts of structures is also satisfied: 1) the proposed first MOGA is developed through the integration of an implicit redundant representation genetic algorithm (IRR GA) (Raich 1999) and a strength Pareto evolutionary algorithm 2 (SPEA2), namely, SP2-IRR GA (Cha et al. 2011a) ; 2) the second one is an integrated model of a non-dominated sorting genetic algorithm 2 (NSGA-II) (Deb et al. 2000) and IRR GA, namely, NS2-IRR GA (Cha et al. 2011b); 3) gene manipulation genetic algorithm (GMGA) (Cha et al. 2011a) by applying engineering judgment concept as a genetic operator. To investigate the effectiveness of the newly proposed algorithms, full-scale twenty-story buildings are investigated. To implement active structural control systems into the large frame structures, the linear quadratic Gaussian (LQG) algorithm, hydraulic actuators, and accelerometers are used. In this book chapter, multi-objective optimization problems are formulated using two tradeoff objective functions of the number of actuators and sensors, and the interstory drifts of the frame structures.

MULTI-OBJECTIVE GENETIC ALGORITHMS

The basic idea of a simple GA (SGA), which is developed by Goldberg (1989), coming from natural selection in Darwin's theory is composed of four steps: 1) evaluation of each individual's fitness in the problem environment, 2) selection of a new individual to fill new population based on the fitness values, 3) interchanging gene information between strings (i.e. individuals) by using genetic operators such as crossover and mutation. The cycle of these four steps, which is called genetic loop, is repeated until the population converges or pre-defined criteria are satisfied. Although the SGA has significant problem solving performance for the single objective problem domain, it shows limitation for solving multi-objective problems by formulating a composite, weighted single fitness function. The objectives conflict each other in most cases, i.e., if performance of an objective is improved, the performance of other objectives may be degraded. The optimization of control device and sensor layout with best efficiency and minimum control cost as defined in this research effort is a typical conflicting objective problem: minimum distributions of both control devices and sensors installed and minimum interstory drift of controlled structure, which is the set of equally optimal solutions, called Pareto-optimal solutions.

To investigate more robust Pareto-optimal set for the two conflict objectives, this research studies three multi-objective genetic algorithms (MOGA): The first MOGA is developed through the integration of Implicit redundant representation (IRR) genetic algorithm (GA) and Non-dominated sorting GA 2 (NSGA2): NS2-IRR GA. The second one is proposed by combining the best features of both IRR GA and Strength Pareto Evolutionary Algorithm (SPEA2): SP2-IRR GA. Lastly, Gene Manipulation GA (GMGA) is developed based on novel recombination and mutation mechanism. The main difference among these MOGA lies in the ranking mechanism at the selection step in the genetic loop. Diverse ranking processes have been developed to assign reasonable relative fitness values among individuals. Another difference lies in sharing or strength measures used to promote diversity across the Pareto-optimal front. The other difference lies in storing non-dominated individuals found during the genetic loop. However the other steps are very similar in information exchange step. In order to find and keep Pareto fronts which are evenly and equally considering conflicting objectives, two advanced MOGA are used in this research effort: NSGA-II and SPEA2. These methods are explained in greater detail in the following section.

NS2-IRR GA

Implict Redundant Representation (IRR) Genetic Algorithm (GA)

The SGA which uses binary or real-coded encoding policies is fairly good to represent single objective problem. To solve multi-objective problems, new appropriate encoding policy is required to consider highly complex optimization problems, in particular, requiring high-cost computation. To consider high nonlinear solution domain, a novel encoding policy, which is implicit redundant representation genetic algorithm (IRR GA), is proposed by Raich and Ghaboussi (1998). The IRR GA is composed of gene locator (GL) which indicates starting points of the gene instance which has design variables and redundant segments which do not use for design variables at current generation but it may be used at other generations by becoming gene instances by genetic operators as shown in Figure 1. This redundant segment can keep useful design information and can dynamically trip during the binary strings. This implicit coding policy can solve complex multi-objective problems. The IRR GA is integrated with non-dominated sorting genetic algorithms and strength Pareto evolutionary algorithms.

Non-Dominated Sorting GA

In most cases, the optimal solution for each objective for the design problem in numerous engineering areas may usually be different to each other (Hans 1988). For example, if drivers want to drive fast, the vehicle consumes more

Figure 1. IRR GA representation (Cha et al. 2011a)

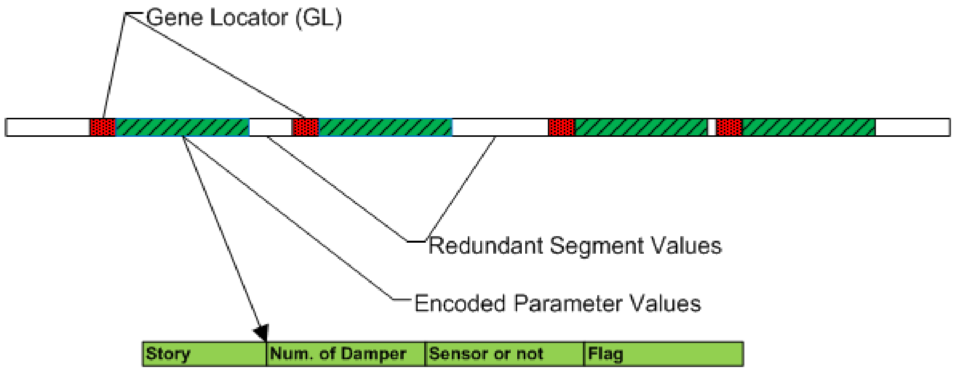

fuel, i.e., when the vehicle driver tries to operate the vehicle with high speed, the consumption of gas generally would increase. Therefore, there can be a lot of solutions satisfying each objective. Each solution would not be covered by the other solutions; this kind of solution set is called Pareto tradeoff optimal curve as shown in Figure 2.

Non-Dominated Pareto Ranking

To investigate multi-objective optimization problems, Goldberg (1989) applied a non-dominated Pareto ranking and its selection method to achieve a set of optimal solutions. To find the non-dominated Pareto curve, the estimated value of each individual objective function is compared with all of the population individuals and then, the first non-dominated front is determined. Without the first non-dominated front set, the same selection procedure is repeated until all the individuals in the population are assigned in a front with a rank. These individuals with the assigned ranks can be used to select individuals as mating pools for the next population. The first non-dominated set has a higher probability to be chosen by the selection operator. However, from the non-dominated Pareto ranking mechanism, the optimal solution can be easily converged to local optima; thus, the sharing function (Goldberg 1989) is adopted to evenly scatter the individuals to feasible regions.

The concepts of sharing functions and crowding operators to scatter the individuals to feasible areas are discussed next.

Crowding Operator and Sharing Function

In general, evolutionary algorithms converge to a single solution when limited population sets are used even though the final goal is to find multiple optima. This local convergence phenomenon is called genetic drift (De Jong 1975). Thus, Holland (1975) proposed the use of an environmental niche

Figure 2. Non-dominated Pareto curve (Cha 2008)

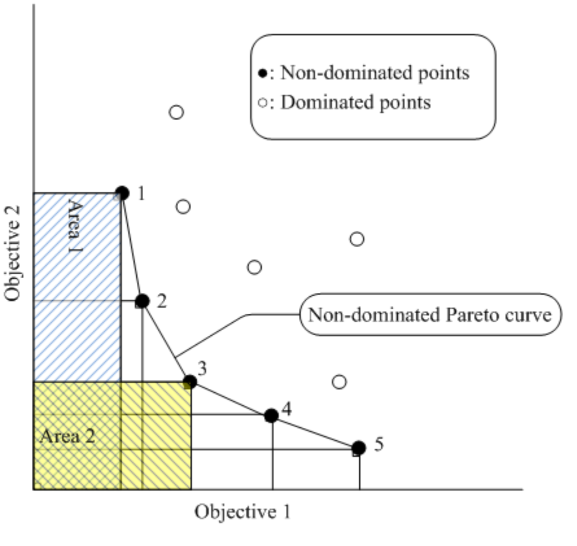

and crowding operators to keep genetic drift from the genetic algorithm application. The role of the crowding operators is to identify how many individuals dominate the environmental niche. Then, the competition for the next generation in selection step increases rapidly. The individuals have the lower possibilities to survive in next generation. The percentage of the population that is allowed to reproduce is called generation gap. The number of individuals that are initially selected as candidates to be replaced by a particular offspring is called the crowding factors (Shrinivas and Deb 1994; Coello et al. 2001).

A sharing function that is achieved by performing the selection is suggested by Goldberg and Richardson (1987). The sharing function defines the degraded fitness values obtained by dividing the original fitness function value of an individual by a quantity proportional to the number of individuals around it (Shrinivas and Deb 1994). Goldberg and Richardson (1987) defined a sharing function $sh(d_{ij})$, and the sharing function can be expressed as different functions by using the power factor α which is generally 1, but it will be dependent on the optimization problem characteristics. The general format of the sharing function is (Goldberg and Richardson 1987)

$$sh(d_{ij}) = \left\{ \begin{matrix} 1 - \left(\dfrac{d_{ij}}{\sigma_{share}} \right)^{\alpha}, & \text{if } d_{ij} < \sigma_{share} \\ 0, & \text{otherwise} \end{matrix} \right\}, \tag{1}$$

where d_{ij} is the metric distance between the individual string i, j, and σ_{share} is the sharing parameter or radius to control the range of the sharing. From the sharing function, the modified fitness is defined as (Goldberg and Richardson 1987)

$$f_{s_i} = \frac{f_i}{\sum_{j=1}^{M} sh(d_{ij})}, \tag{2}$$

where M is the number of individuals located in vicinity of the i^{th} individual and d_{ij} is the p-dimensional Euclidean distance (Coello et al. 2001)

$$d_{ij} = \sqrt{\sum_{k=1}^{p} (x_{k,i} - x_{k,j})^2}, \tag{3}$$

where p refers to the number of variables encoded in the evolutionary algorithms. As σ_{share} value is generally selected between 1 to 2, Deb et al (1989) suggested an equation to determine the value of the sharing parameters (Coello et al. 2001)

$$\sigma_{share} = \frac{r}{\sqrt[p]{q}} = \frac{\sqrt{\sum_{k=1}^{p} (x_{k,\max} - x_{k,\min})^2}}{\sqrt[p]{2q}}, \tag{4}$$

where r is the volume of a p-dimensional hypersphere of the radius of σ_{share} and q is the number of Pareto-solutions that GAs need to find. These non-dominated Pareto ranking and sharing functions will be the backbone of the proposed multi-objective genetic algorithms (MOGAs).

Multi-Objective Genetic Algorithms (MOGA)

Fonseca and Fleming (1993) proposed a modification of the simple genetic algorithm (SGA) at the selection level. The basic concepts of the proposed MOGA are the ranking based on the Pareto dominance and sharing function. The Pareto dominance-based rank is the same as one plus the number that certain individual dominates as shown in Figure 3. Thus, the rank of a non-dominated individual should be 1 and the other dominated individuals are penalized by the degree of the population density. The main selection mechanism is that all the current individuals are sorted according to the rank and assigned as fitness to individuals by interpolating from the best to the worst ones. The best will have the largest value while the other individuals will be also assigned fitness values. The average fitness values of same rank individuals are then calculated. The average fitness value is assigned to the same rank individuals. Therefore, all the individuals in same rank have the same probability to be selected for the next generation.

The main drawback of MOGA is that the block type of the fitness assignment for individuals of the same rank is exposed to large selection pressure, resulting in premature convergence of the population. It implies two different vectors with the same objective function values and then performs the sharing function. However, it cannot exist simultaneously in the population under this scheme. The performance of MOGA is dependent on the value of the sharing factors (Srinivas and Deb 1994; Coello et al. 2001). In other words, it might be difficult for the traditional MOGA to guarantee the unbiased and even Pareto sets. To overcome this disadvantage, a non-dominated sorting genetic algorithm (NSGA) is proposed.

Figure 3. Multi-objective ranking based on the Pareto dominance

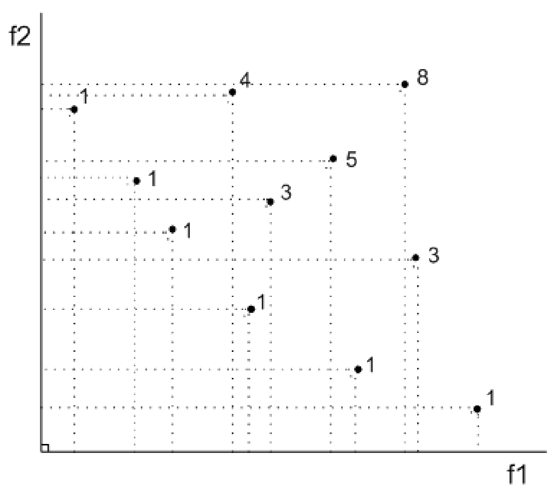

Non-Dominate Sorting Genetic Algorithm (NSGA)

Srinivas and Deb (1994) developed the non-dominated sorting genetic algorithm (NSGA). The NSGA offers an unbiased Pareto optimal set. The NSGA only differs from the SGA in the selection operators. The population is ranked on the basis of its non-domination characteristics. To keep specific individuals from the premature convergence and in order to maintain diversity and multiple optimal points, the procedure is (1) The non-dominated individuals are found and then each is given an equal reproductive potential value (2) Then the sharing method is applied by assigning a degraded fitness value that is obtained by dividing the equal reproductive potential value by a quantity proportional to the number of individuals around it using Equation (1) (Goldberg and Richardson 1987). These classifying and sharing processes are performed on the entire population. Naturally, the second new dummy set fitness value should be kept smaller than the minimum shared dummy fitness set. However, this NSGA requires complex optimization procedures, resulting in high computational cost. Thus, Deb et al. (2000) proposed a modification of the original NSGA, namely, NSGA II.

Non-Dominated Sorting Genetic Algorithm 2 (NSGA-II)

Deb at al. (2000) proposed an enhanced version of the NSGA to remove the disadvantages of the NSGA and improve its performance. The drawbacks of the NSGA are (Deb at al. 2000)

- High computational complexity of the non-dominated sorting: in case of large population size, the population needs to be sorted every generation

- Lack of elitism
- Requirements of specifying the sharing parameter σ_{share}

With the non-dominated sorted current population P, the non-dominated fronts will be added to the parent population composed of non-dominated individuals E until the size exceeds beyond the specified population size in order to fill the population for the next generation E. The individuals in E are assigned via the crowding distance. To estimate the density of individuals surrounding a particular point in the phenotype non-dominated Pareto front graph, the average distance of the two points on either side of this point along with each of the objectives is used as crowding distance. This crowding distance is used for estimating the size of the largest Cuboid enclosing the point i without including any other point in the population. The crowding distance,

$I\left[i\right]_{\text{distance}}$ is (Deb et al. 2000)

$$I\left[i\right]_{\text{distance}} = I\left[i\right]_{\text{distance}} + (I\left[i+1\right]m - I\left[i-1\right]m) \tag{5}$$

where m is the number of objectives and $I[i]_{\text{distance}}$ is the m^{th} objective function value of the i^{th} individual in the set I. The non-dominated individual E is also sorted according to the crowded comparison operator. The crowded comparison operator $\geq_n$ is (Deb et al. 2000)

$$i \geq_n j \text{ if } (i_{rank} < j_{rank}) \text{ or } ((i_{rank} = j_{rank}) \text{ and } (i_{\text{distance}} > j_{\text{distance}})) \tag{6}$$

where n is the n^{th} crowding selection; $\geq_n$ is the crowded comparison operator; i_{rank} is non-dominated rank; and i_{distance} is local crowding distance. From Equation (6), it can be inferred that an individual with the lower rank is selected while if two points are in the same front, the individual with the larger local crowding distance is selected.

Hybrid NS2-IRR GA

The NS2-IRR GA (Cha 2008; Cha et al 2011b) is developed through the integration of an advanced selection method (i.e., NSGA-II) for multi-objective problems and a dynamic search encoding policy (i.e., IRR GA) to consider high complex control device layout optimization problem. The proposed MOGA algorithm flowchart is shown in Figure 4 in detail. This algorithm is composed of mainly 4 steps:

1. Initialization of population (P_0) by randomly generated binary numbers (i.e., 0 and 1)
2. Evaluation of each binary of population (P_0)
3. Non-dominated sorting based on NSGA-II algorithm using fitness values of current population and previous non-dominated population set (Q_t)
4. Genetic operation to generate child population for the next generation

For the second step, to calculate the fitness values of the current population, the H_2 / LQG control system is investigated by considering controllability and stability of the closed loop control system using control devices and sensors layout information offered from each individual binary of current population. For the third step the non-dominated sorting is performed to calculate rank (F_i) of each non-dominated curve. If it is the first generation, non-dominated sorted fronts of the current population are assigned same fitness values for each front. However from the second generation, these non-dominated curves are filled to P_{t+1} population without overflow of the pre-defined size (N) of P_{t+1} population. To fill the

Figure 4. Flow chart of NS2-IRR GA (Cha 2008)

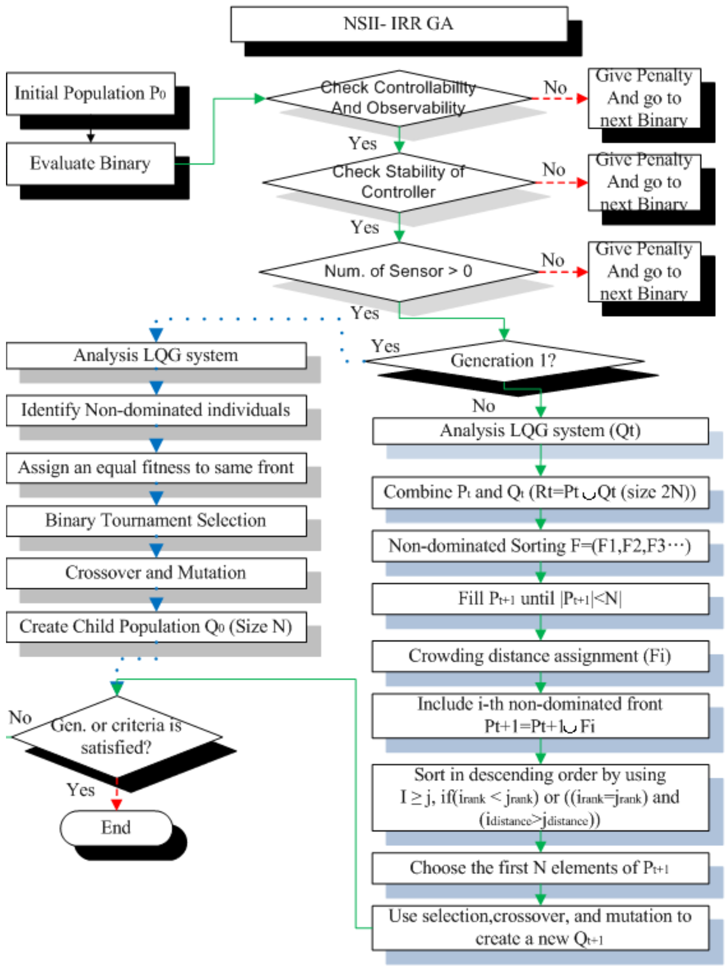

P_{t+1} the crowding distances are assigned to the best remedy rank F_i using Equation (5). By adding F_i to P_{t+1} and sorting in descending order by using Equation (6), the first N number of individuals is selected. For the fourth step, Q_{t+1} is generated by crossover and mutation operator. This iteration will continue until satisfying the GA criteria or reaching the predefined maximum generation. Although the performance of the NS2-IRR GA is good, it is often difficult to guarantee diverse optimal solution sets. However, a solution can be found in the modified strength Pareto evolutionary algorithm.

SP2-IRR GA

Strength Pareto Evolutionary Algorithm (SPEA)

Zitzler and Thiele (1999) proposed the strength Pareto evolutionary algorithm (SPEA) with combination of several features of multi-objective evolutionary algorithms in a unique manner. The SPEA has some similarities in its process to other evolutionary algorithms (Zitzler and Thiele 1999) in that it

- Stores the non-dominated solutions found so far in an external population.
- Uses the concept of the Pareto dominance in order to assign scalar fitness values to individuals.
- Performs clustering to reduce the number of non-dominated solutions stored without destroying the characteristics of the tradeoff front.

The originalities of the SPEA method are as follows:

- It combines the above three techniques as a single algorithm.
- Irrespective of the dominancy of members of the population, the individual fitness is calculated only from the solutions of external sets.
- The individuals of the external set will participate in the selection process.
- The Pareto-based new niching method which does not rely on any sharing or niche radius is developed to sustain diversity in the population (Zitzler and Thiele 1999).

The non-dominated sorting and assigning fitness are a little bit different with the previously reviewed GAs. The individuals in the archive set are ranked and then the individuals in current population are evaluated. The fitness of the archive set is defined as (Zitzler and Thiele 1999)

$$s_i = \frac{n}{N+1} \tag{7}$$

where n is the number of individuals in P that are covered by i, and N is the size of P. The fitness of the current population is calculated by summing the strengths of all the external non-dominated solutions i that cover j. The equation is expressed as (Zitzler and Thiele 1999)

$$f_i = 1 + \sum_{i, i \succeq j} s_i \tag{8}$$

where $f_j \in [1, N]$. When the size of the archive set is more than the defined size, the clustering analysis is carried out and then prunes the inferior individuals. The average linkage method (Morse 1980) is suggested as the clustering analysis. The first step is initialing cluster set C, and the next step is calculating the distance d of two cluster c_1 and c_2. The equation of d is expressed (Zitzler and Thiele 1999) as

$$d = \frac{1}{\left|c_1\right| \cdot \left|c_2\right|} \cdot \sum_{i_1 \in c_1, i_2 \in c_2} \left\| i_1 - i_2 \right\| \tag{9}$$

where the metric $\|\cdot\|$ is the distance between two individuals i_1 and i_2. Two clusters c_1 and c_2 are determined with a minimal distance d; and then, the chosen clusters are added to the larger cluster; finally, the reduced non-dominated set is computed by selecting a representative individual per each cluster (Zitzler and Thiele 1999).

Strength Pareto Evolutionary Algorithm 2 (SPEA2)

A modified version of the SPEA (i.e., SPEA2) is suggested by Zitzler et al. (2001, 2002). The main improvements are (Zitzler et al. 2001, 2002):

- A fine-grained fitness assignment strategy
- Density estimation technique
- Enhanced archive truncation method

In the fitness assignment of this algorithm, both non-dominated individuals and dominated individuals are considered simultaneously to avoid the situation that individuals are dominated by the same archived members as shown in Figure 5. As

Figure 5. Fitness and strength calculation method of SPEA2 (Cha2008)

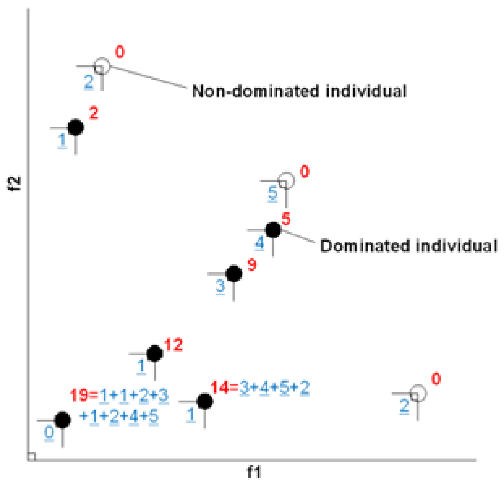

a first step to calculate the row fitness, the strength values of the current population and archive set are calculated. The strength value of an individual is the number of individuals that is dominated in the current and archived population. With these defined strength values, the row fitness value is determined by adding the strength values of its dominators in the archive and current population (Zitzler et al 2001).

One difference in the SPEA2 mechanism is a truncation operator. The truncation operator is performed to sustain the archive set size. In case the archive size is smaller than the defined size, the number of shortage individual is coped from the current population to archive. In case the archive size is bigger than the defined size, the individual that has the minimum distance to another individual is chosen for removal, but if there are several individuals with the same minimum distance, the tie is broken by considering the second smallest distances.

Hybrid SP2-IRR GA

The SP2-IRR GA (Cha 2008; Cha et al. 2011a) is proposed through the integration of an advanced selection method (i.e., SPEA2) and dynamic search encoding policy (i.e., IRR GA). The developed algorithm is shown in Figure 6. This algorithm is also characterized as mainly 4 steps:

1. Initialization of population (P_0) and archive (E_0) by randomly generated binary numbers (i.e., 0 and 1)
2. Evaluation of each binary of the population P_0 for the first generation or P_t for the t-th generation)
3. Non-dominated sorting based on SPEA2 algorithm using fitness values of current population and previous archive set (E_t)
4. Genetic operation to generate child population for the next generation.

For the third step the strength values are calculated by $S(i) = \left|\left\{ j \middle| j \in P_t + E_t \wedge i \succ j \right\}\right|$ and $R(i) = \sum_{j \in P_t + E_t \wedge j \succ i} S(j)$. And density estimation is carried to get final fitness by summing $R(i)$ and $D(i)$ for each individual. All non-dominated individuals in P_t and E_t to E_{t+1}. If the size of the E_{t+1} is bigger than predefined size of archive, truncation operation is carried out to cut out and sustain the size of archive, and if it is smaller than the predefined size of archive, the archive is filled with best dominated individuals of P_t and E_t. By tournament selection, the new P_{t+1} is filled. For the fourth step the general genetic operator is carried out to create new parent population $\left(P_{t+1}\right)$.

Gene Manipulation Genetic Algorithm

Using a flexible implicit redundant representation encoding method, the number of control devices on a specific floor and the sensor locations are specified. To enhance the search performance and reduce the simulation time, new genetic algorithm is proposed. Gene manipulation genetic algorithm (GMGA) (Cha 2008) uses engineering judgment to create encoding variables to search non-dominated individuals based on novel recombination/mutation mechanism. The novel mechanism uses average, maximum, minimum, and random perturbation values of the variables of each two adjacent non-dominated individuals of current Pareto-optimal front. To define the percentage of individuals in current population that undergo gene manipulation process, GMGA uses a gene manipulation ratio (GMR) which ranges from 0.1 to 0.3 in research investigated (Cha 2008). The other remaining population is filled with individuals that undergo traditional genetic operating process such as crossover and mutation. The gene manipulation procedures of the GMGA are (Cha et al. 2009; Cha et al. 2011a):

1. Non-dominated sorting in the current population using any MOGA selection method such as NSGA series or SPEA series
2. Define GMR to determine the number of individuals that undergo gene manipulation process and determine exact number of each number that is created between individuals in Pareto front (see Equation 10)
3. Select representative individuals in each identified section of the Prato front to be used for new individuals created
4. Generate new gene instances using one of four gene manipulation mechanisms.
5. Insert created gene instances in the representative individuals
6. Integrate individuals created based on gene manipulation and created based on traditional genetic procedure to make child population for next generation.

The number of new individuals to create in each section of the Pareto-optimal front can be calculated (Cha 2009):

$$\text{Number of new string (i)} = \text{round}\left(\frac{\text{Each distance (i)}}{\text{Total distance}} \times \text{Pop. Size} \times \text{GMR}\right) \quad (10)$$

An example that identifies how the gene manipulation process is working to create new individuals in sections between non-dominated individuals is shown in Figure 7. The GMR is 0.1 and population size is 100 and then 10 new individuals will be generated using GMGA. The two adjacent individuals are selected from the current Pareto-optimal front. Based on Euclidean distance between the individuals in Pareto-optimal front, the numbers of new individuals for each section are determined using Equation (10). Several new gene instances are created using one of four gene manipulation mechanisms to generate a new individual in a specific section as shown in Figure 7. New gene instance variable are generated using four operations (Cha 2008) as stated in Equations (11)-(14) (Cha et al. 2011a):

for s=1:t {

if k <= number of new individuals created in each section, s (i.e. create the first new individual)

for v=1:n{

$$P_n(s,k,v) = \frac{1}{j}\left(\sum_{i=1}^{j} P_c(v,i)\right) \quad (11)$$

Figure 6. Flow chart of SP2-IRR GA (Cha 2008)

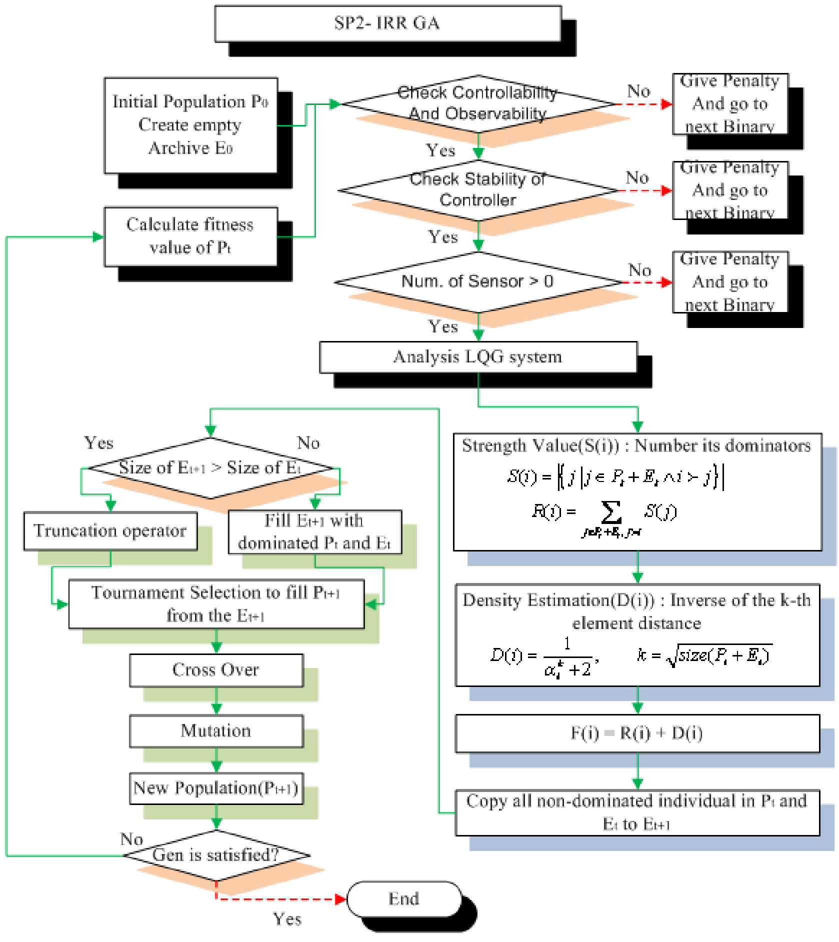

k=*k*+1

if *k* <= number of new individuals created in each section, *s* (i.e. create the second new individual)

for *v*=1:*n*{

$$P_n(s,k,v) = \max_{i=1}^{j}(P_c(v,i)) \tag{12}$$

k=*k*+1

if *k* <= number of new individuals created in each section, *s* (i.e. create the third new individual)

for *v*=1:*n*{

$$P_n(s,k,v) = \min_{i=1}^{j}(P_c(v,i)) \tag{13}$$

k=*k*+1

while *k* <= number of new individuals created in each section, *s*(i.e. create the remaining new individuals)

for *v*=1:*n*{

$$P_n(s,k,v) = \operatorname*{rand\ between}_{i=1}^{j}(P_c(v,i)) \tag{14}$$

Figure 7. Determining the number of individuals to create between selected Pareto-optimal individuals (Cha et al. 2011a)

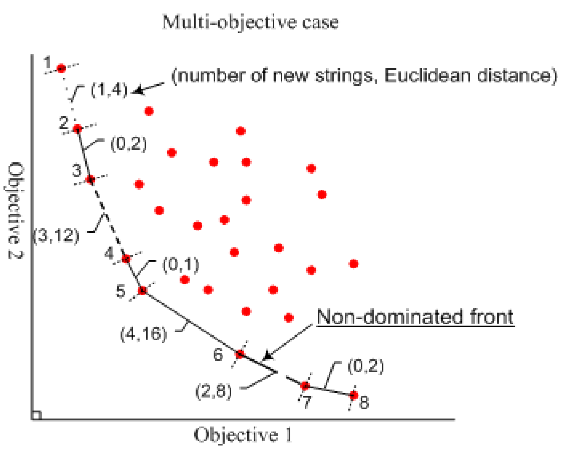

k=k+1

where v is number of design variable parameters encoded in a IRR individual, t is the number of Pareto-optimal front sections determined between every two individuals lying on the front (Figure 7 identifies 7 sections along the Pareto-optimal front), j is number of individuals bounding the Pareto-optimal front sections ($j = 2$ for problems with two objectives and $j = 3$ for problems with three-objectives), and k is the number of new individuals to be created in each section, s, determined using Eq. 10, $P_n(s,k,v)$ is the new parameter value for the v-th parameter in the k-th new individual in the s-th section of the Pareto-optimal front, and $P_c(v,i)$ is the v-th current parameter value, which may be determined by the gene instance with the highest flag value if there are duplicate story gene instances in the current individual.

The gene instances of the first new individual are generated using average value of the variables. The second one is created by maximum values of the variables, the third using the minimum values, and the fourth and later individuals, only if the number of new individuals in specific section is bigger than 4, are generated using random values bounded between the decoded variables. The created values are encoded based on binary and this new gene instance is inserted at specific location of the representative individuals as shown in Figure 8. The flag values are used and the larger flag valued gene instances is selected for to insert the new gene instance when there are more than one gene instances that express the same story information.

As a final step, the newly created individuals are added to individuals which are created by standard genetic operation to create new child population for the next generation. The benefit of using the proposed GMGA to obtain a set of near-optimal control device and sensor layout designs for larger, more complex problems is investigated in this research effort.

EXAMPLE

Optimal Formulation

In this chapter, a multi-objective optimization problem is formulated in terms of the distribution of both device and sensor and interstory drift responses of structures. The maximum drift is a normalized measure (Barroso 1999, Barroso et al. 2002)

$$J_1 = \max\left\{\max_{t,i}\frac{\left|d_i^c(t)\right|}{h_i}\right\}, \tag{15}$$

$$J_2 = \text{Summation of the number of control devices and sensors,}$$

Figure 8. Insertion of new gene instances into selected Pareto-optimal front IRR GA encoded individuals (Cha et al. 2008)

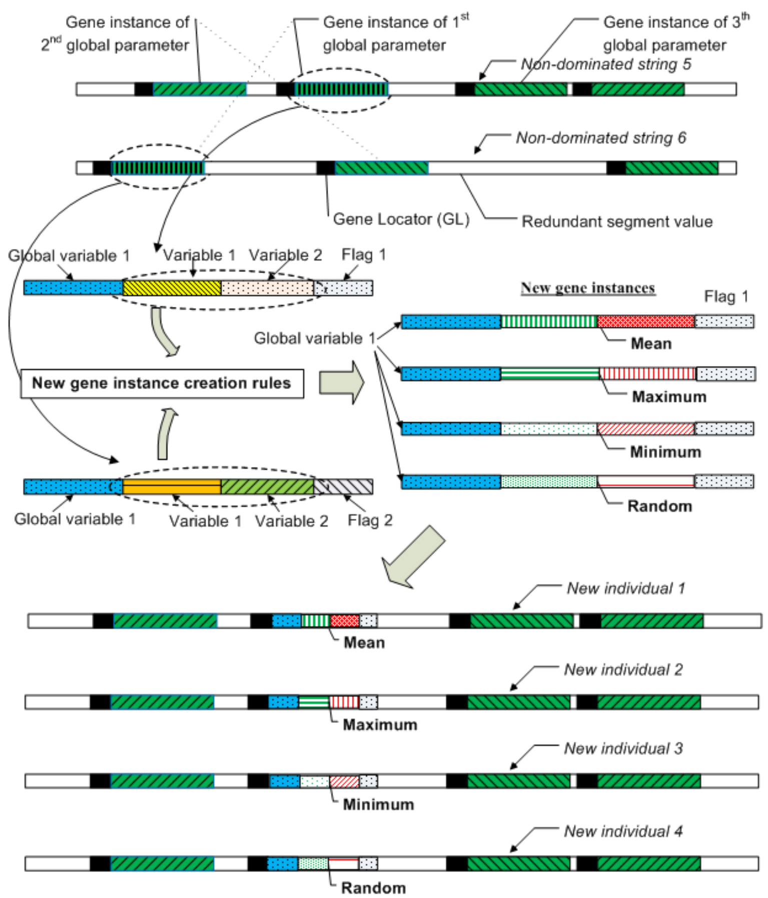

where h_i, $d_i^c(t)$, and $d_i^u(t)$ are the height of each story i, controlled and uncontrolled interstory drifts of the above ground floors.

Case Study Model: Three-Dimensional (3D) Twenty-Story Building

To date, although a number of articles on structural control for hazard mitigation of civil structures have been investigated, most of the studies have been focused on 2D structural models. In particular, almost all articles that study optimal placement of actuators and sensors within large civil structures have been mainly dealt with 2D structures. However, since the 2D analysis model often leads to underestimation of structural behavior, 3D analysis of large civil structures may be necessary (Kim and Adeli 2005).

This book chapter presents a 3D structural model to investigate the effectiveness of optimal placement of actuators and sensors within practical large civil buildings. In this research, the 2D twenty-story control benchmark building proposed by (Spencer et al. (1999); Ohtori et al. (2004) is extended into a 3D frame structure. The 3D twenty-story building is composed of moment resisting frames with five bays in NS-direction and six bays in EW-direction. Mass, stiffness, and damping matrix in stiff and weak direction are developed using finite element models with lumped seismic mass, Ritz method and static condensation approach. The damping matrix is defined by 2% proportional Rayleigh damping. A 3D twenty-story frame structure with the reduced 60 DOFs is developed using the pre-determined stiff and weak direction as shown in Figure 9. The lateral and transversal stiffness are calculated to eradicate zero mess degree-of-freedom (DOF). The mass matrix $\mathbf{M}_{\mathbf{3D20s}}$ is defined for the 3D system as

$$\mathbf{M}_{\mathbf{3D20s}} = \begin{bmatrix} 2\mathbf{M}_x & \mathbf{0} & \mathbf{0} \\ \mathbf{0} & 2\mathbf{M}_y & \mathbf{0} \\ \mathbf{0} & \mathbf{0} & \mathbf{M}_r \end{bmatrix} \tag{16}$$

where $\mathbf{M}_x = \mathbf{M}_y$ is the 20x20 seismic mass matrix in weaker and stiffer direction of 3D structures and $\mathbf{M}_r = \mathbf{M}_x(b^2 + d^2)/12$ where b and d are longitudinal and transverse length of structures, respectively. The stiffness matrix $\mathbf{k}_{\text{story}}$ of each story is defined as (Chopra 2000)

$$\mathbf{k}_{\text{story}} = \begin{bmatrix} k_{xB} + k_{xC} & 0 & (d/2)(k_{xC} - k_{xB}) \\ 0 & k_y & ek_y \\ (d/2)(k_{xC} - k_{xB}) & ek_y & e^2 k_y + (d^2/4)(k_{xB} + k_{xC}) \end{bmatrix} \tag{17}$$

where k_{xB}, k_y and k_{xC} are the lateral stiffness of the frame B, A, and C, respectively; d and e are the distances from the center of axis to each frame as shown in Figure 10; and the stiffness matrix $\mathbf{k}_{\text{story}}$ is extended into a global stiffness matrix $\mathbf{K}_{\mathbf{3D20s}}$. The moment of inertia of the diaphragm about the vertical axis passing through O in Figure 10 is determined by (Chopra 2000)

$$\mathbf{I}_{\mathbf{o}} = \mathbf{M}(b^2 + d^2)/12 \tag{18}$$

Figure 9. Three-dimensional twenty-story building model

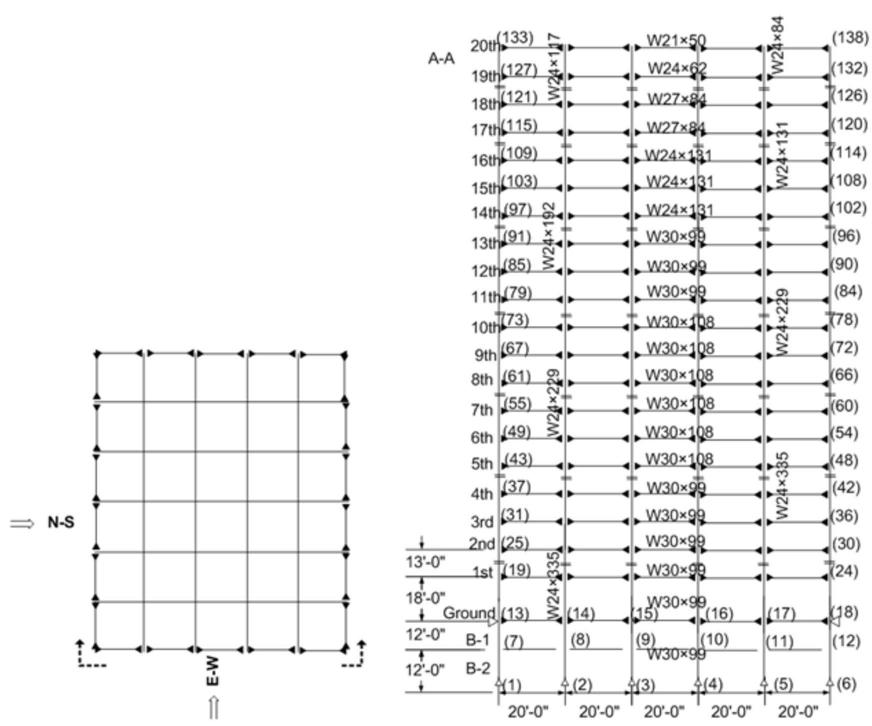

Figure 10. Stiffness of two-way asymmetric system (Chopra 2000)

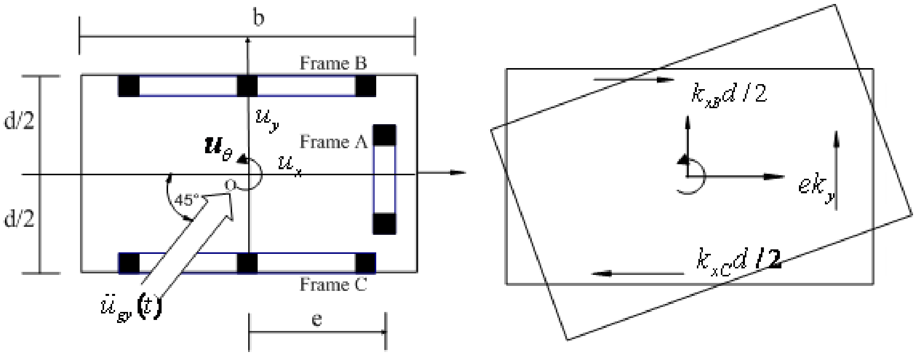

where $\mathbf{M}$ is the seismic mass matrix of the 20-story building and b and d are the distances of structural plan of the NS- and EW-directions, respectively. Finally, the governing equation of motion is

$$\begin{aligned}\mathbf{M}_{\mathbf{3D20s}}\ddot{\mathbf{x}} + \mathbf{C}_{\mathbf{3D20s}}\dot{\mathbf{x}} + \mathbf{K}_{\mathbf{3D20s}}\mathbf{x} = \\ -\mathbf{M}_{\mathbf{3D20s}}\mathbf{G}_{\mathbf{3D20s}}\ddot{x}_g + \mathbf{P}_{\mathbf{3D20s}}\mathbf{f}_{\mathbf{3D20s}}\end{aligned} \tag{19}$$

where $\mathbf{K}_{\mathbf{3D20s}}$ (60x60) is the global stiffness matrix, $\mathbf{M}_{\mathbf{3D20s}}$ (60x60) is the global mass matrix, $\mathbf{C}_{\mathbf{3D20s}}$ (60x60) is the global damping matrix that is defined by 2% proportional Rayleigh damping, $\mathbf{G}_{\mathbf{3D20s}}$ is ground motion matrix, $\mathbf{P}_{\mathbf{3D20s}}$ is a location vector of the control device forces, and $\mathbf{f}_{\mathbf{3D20s}}$ is the control force input. The 2nd order differential equations can be transformed into the 1st order state space equations

$$\dot{\mathbf{x}} = \mathrm{A}\mathrm{x} + \mathrm{B}\mathrm{f} + \mathrm{E}\ddot{x}_g \tag{20}$$

$$\mathrm{y}_{\mathrm{m}} = \mathrm{C}_{\mathrm{m}}\mathrm{x} + \mathrm{D}_{\mathrm{m}}\mathrm{f} + \mathrm{F}_{\mathrm{m}}\ddot{x}_g + \mathrm{v} \tag{21}$$

$$\mathbf{y}_{\mathbf{r}} = \ddot{\mathbf{x}} + \mathbf{C}_{\mathbf{r}}\mathbf{x} + \mathbf{D}_{\mathbf{r}}\mathbf{f} + \mathbf{F}_{\mathbf{r}}\ddot{x}_g \tag{22}$$

where $\mathbf{x}$ is the state vector, $\mathbf{f}$ is control force input, $\mathbf{y}_{\mathbf{m}}$ is the vector corresponding to the measured output, $\mathbf{y}_{\mathbf{r}}$ is the vector of regulated responses, $\mathbf{v}$ is a measurement noise vector, and $\mathbf{C}_{\mathbf{r}}$, $\mathbf{D}_{\mathbf{r}}$, and $\mathbf{F}_{\mathbf{r}}$ depend on the sensor locations and the number of actuators and locations, and

$$\mathbf{A} = \begin{bmatrix} \mathbf{0}_{ndof\times ndof} & \mathbf{I}_{ndof\times ndof} \\ -\mathbf{M}_{\mathbf{3D20s}}{}^{-1}\mathbf{K}_{\mathbf{3D20s}\ ndof\times ndof} & -\mathbf{M}_{\mathbf{3D20s}}{}^{-1}\mathbf{C}_{\mathbf{3D20s}\ ndof\times ndof} \end{bmatrix}, \tag{23}$$

$$\mathbf{B} = \begin{bmatrix} \mathbf{0}_{ndof\times ndof} \\ \mathbf{M}_{\mathbf{3D20s}}{}^{-1}\mathbf{f}_{a}{}''_{\ ndof\times ndof} \end{bmatrix}, \tag{24}$$

$$\mathbf{C}_{\mathrm{m}} = \begin{bmatrix} \mathbf{I}_{ndof\times ndof} & \mathbf{0}_{ndof\times ndof} \\ \mathbf{0}_{3\times 3} & \mathbf{I}_{ndof\times ndof} \\ -\mathbf{M}_{\mathbf{3D20s}}{}^{-1}\mathbf{K}_{\mathbf{3D20s}\ ndof\times ndof} & -\mathbf{M}_{\mathbf{3D20s}}{}^{-1}\mathbf{C}_{\mathbf{3D20s}\ ndof\times ndof} \end{bmatrix}, \tag{25}$$

$$\mathbf{D}_{\mathbf{m}} = \begin{bmatrix} \mathbf{0}_{ndof\times ndof} \\ \mathbf{0}_{ndof\times ndof} \\ \mathbf{f}_{\mathbf{a}}(\mathbf{M}_{\mathbf{3D20s}}{}^{-1}{}''_{\ ndof\times ndof}) \end{bmatrix}, \tag{26}$$

$$\mathbf{E} = \begin{bmatrix} \mathbf{0}_{ndof\times 1} \\ -\mathbf{G}_{\mathbf{3D20s}\ ndof\times 1} \end{bmatrix}, \tag{27}$$

$$\mathbf{F_m} = \begin{bmatrix} \mathbf{0}_{ndof\times 1} \\ \mathbf{0}_{ndof\times 1} \\ -\mathbf{ones}_{ndof\times 1} \end{bmatrix}. \qquad (28)$$

where *ndof* is 20 for the 20-story 2D model and 60 for the 20 story 3D structural model, $\mathbf{G}$ is a vector defining the loading of ground acceleration onto the evaluation model, and $\mathbf{f}_a$ is the control device force of 1000 kN.

Simulation

Figures 11 and 12 for the 2D twenty-story building compare the maximum displacements and drift responses respectively, under a variety of earthquake excitations: El-Centro, Hachinohe, Northridge, Kobe earthquakes. As shown in the figures, all the proposed algorithms (IRR-NS2 GA, IRR-SP2 GA, and GMGA) improve the performance of the benchmark control system. Figure 13 shows the time histories of displacement responses of the proposed GMGA and benchmark controllers while the uncontrolled responses are used as a baseline. As seen in Figure 13, the performance of the proposed GMGA is slightly better than the one of the benchmark control system. Figure 14 compares the dynamic responses of the 3D building structure. It is demonstrated that the newly proposed algorithm is very effective in reducing the dynamic responses of seismically excited large-scale building structures. Note that it can be found that the performance of the GMGA is nearly the same with NS2-, and SP2-IRR GAs from Figure 11 and Figure 12, however the CPU running time is highly reduced by using GMGA as shown in Figure 15.

FUTURE RESEARCH DIRECTIONS

The near-optimal locations and numbers of the sensors are critical to the active control performance to reduce structural responses and damage

Figure 11. Maximum displacement responses (El-Centro, Hachinohe, Northridge, and Kobe earthquakes)

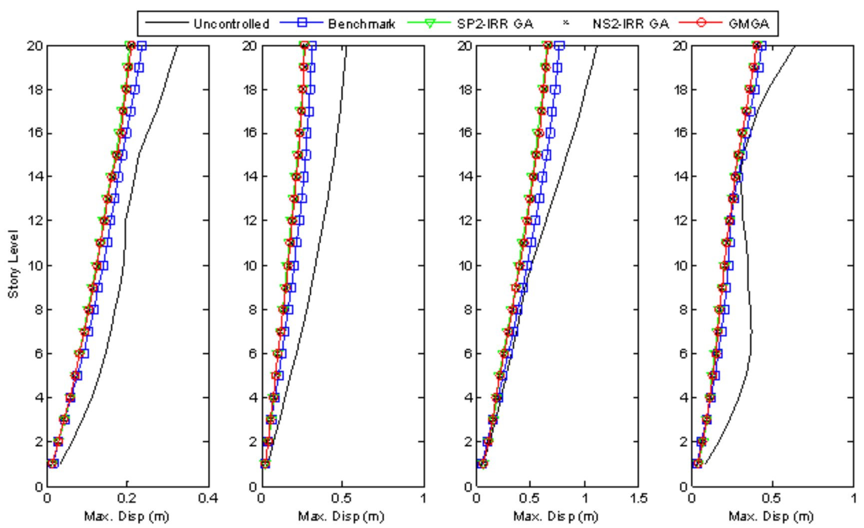

Figure 12. Maximum drift ratio responses (El-Centro, Hachinohe, Northridge, and Kobe earthquakes)

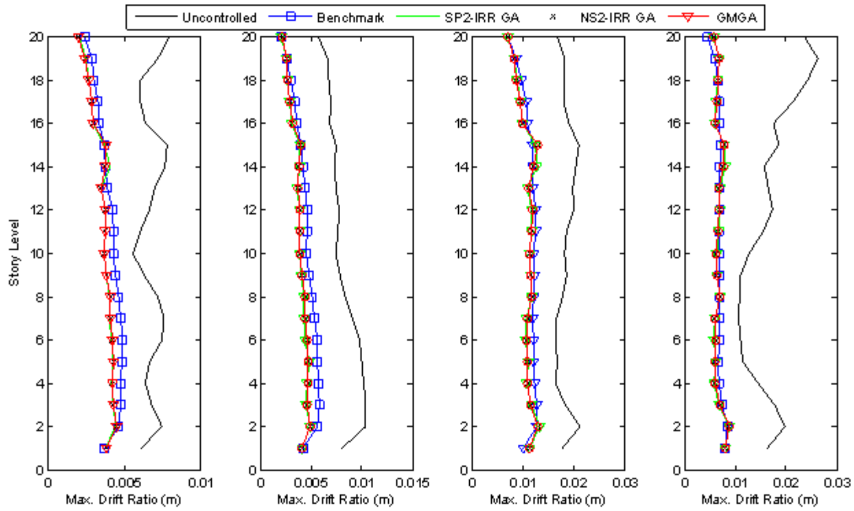

of high-rise buildings. In near future, sensitivity analyses of the sensor fault (Sharifi et al. 2010) and structural damage to the performance of the optimal control devices layouts in high-rise buildings will be investigated.

CONCLUSION

To date, most encoding policies of genetic algorithms (GAs) are based on binary or real-coded encoding. However, these encoding policies may not be appropriate for solving highly complex and computationally intensive optimization problems, e.g., large-scale infrastructure design and analysis problems. To address the issue, this book chapter presents three novel frameworks of multi-objective genetic algorithms (MOGAs) for integrated optimal design of actively controlled large-scale infrastructures under seismic excitation, by combining the best features of several GAs. The first MOGA is developed through the integration of an implicit redundant representation (IRR) genetic algorithm (GA) and a non-dominated sorting II (NS2) GA. The second is proposed by combining the IRR-GA and a strength Pareto evolutionary algorithm 2 (SPEA 2). The last one is Gene Manipulation GA (GMGA) that is developed based on novel recombination and mutation mechanism. The MOGAs are formulated as optimization problems of finding optimal locations and number of actuators and sensors within seismically excited large-scale civil structures such that dynamic responses of structures are also minimized. To implement active control systems into seismically excited structures, linear quadratic regulator (LQR)-based controllers, Kalman estimators, hydraulic actuators, and accelerometers are used. To demonstrate the effectiveness of the proposed three MOGAs, twenty-story two dimensional (2D) and three dimensional (3D) building models are developed using the finite element method. To excite those large-scale building models, a variety of earthquakes are used as external loads. Further, the performances of the three MOGAs are compared in terms of convergence rate, Pareto fronts, the time history responses, and maximum interstory responses. It is shown from the simulations that the proposed MOGAs are very effective in finding not only optimal locations and numbers of actua-

Figure 13. Displacement time history responses (El-Centro, Hachinohe, Northridge, and Kobe earthquakes)

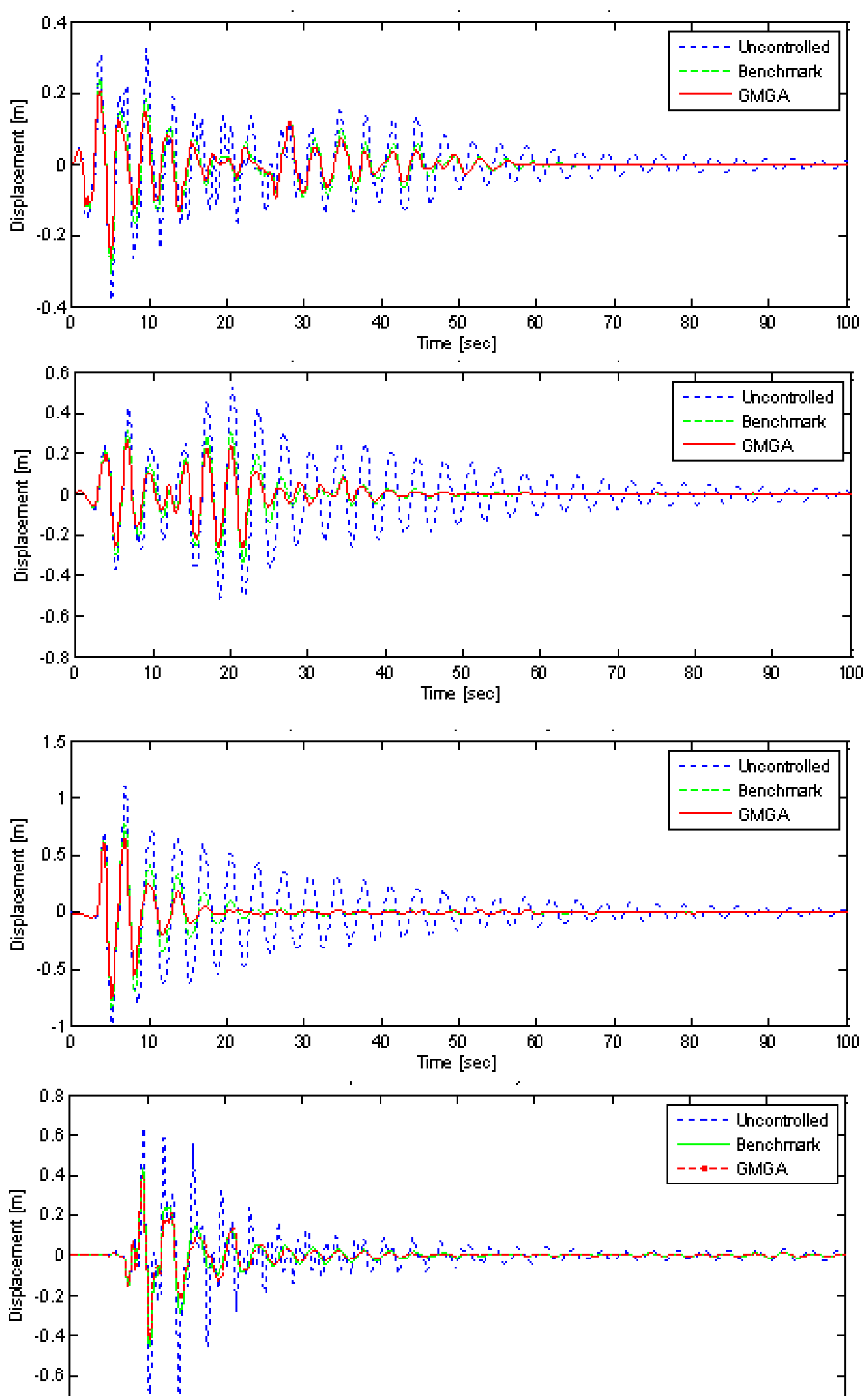

Figure 14. Dynamic responses of the 3D building under a variety of earthquake excitations

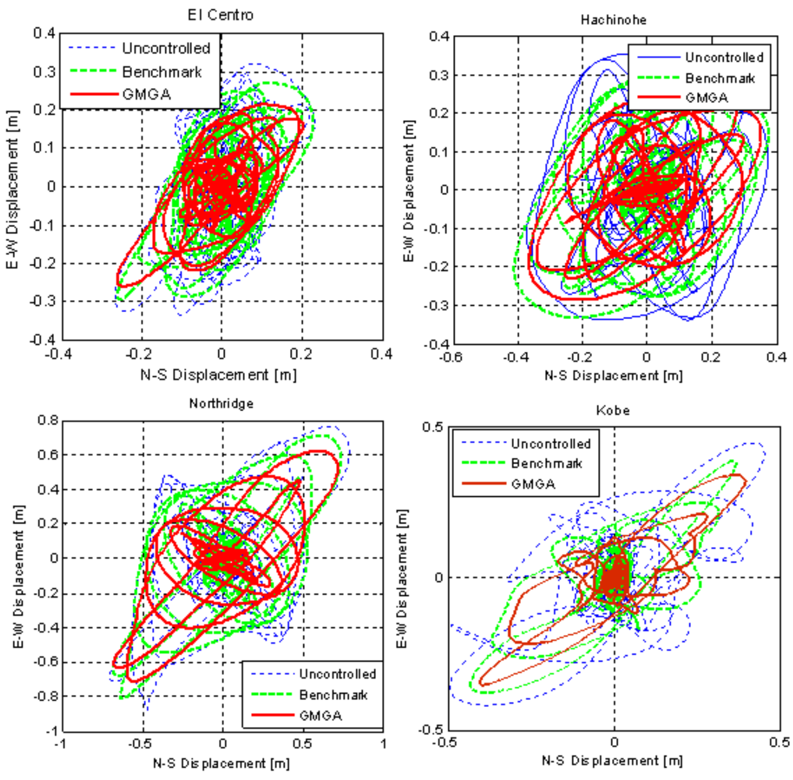

Figure 15. Performance comparisons of the number of generations and CPU running time

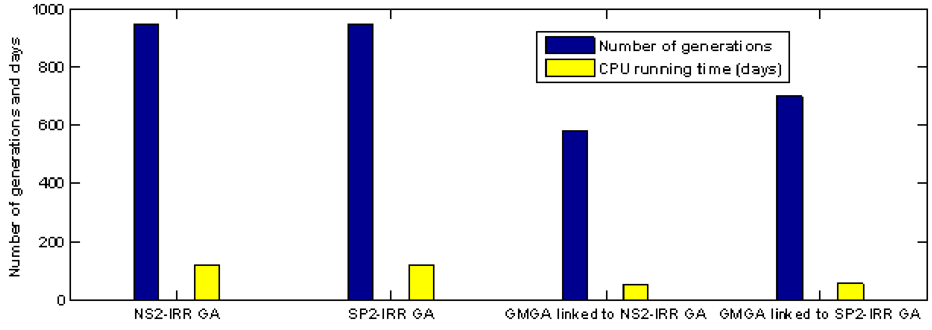

tors and sensors, but also minimum responses of the buildings under earthquake excitation. The simulation also shows that the proposed MOGAs are effectively capable of finding a set of optimal solutions. In particular, GMGA outperforms over NS2-IRR GA and SP2-IRR GA in terms of computational time.

REFERENCES

Adeli, H. and Saleh, A. (1999). *Control, optimization, and smart structures: High performance bridges*.

Agrawal, A. K., & Yang, J. N. (1999). Optimal placement of passive dampers on seismic and wind-excited buildings using combinatorial optimization. *Journal of Intelligent Material Systems and Structures*, *10*, 997–1014.

Amini, F., & Tavassoli, M. R. (2005). Optimal structural active control force, number and placement of controllers. *Engineering Structures*, *27*(9), 1306–1316. doi:10.1016/j.engstruct.2005.01.006

Arbel, A. (1981). Controllability measures and actuator placement in oscillatory systems. *International Journal of Control*, *33*(3), 565–574. doi:10.1080/00207178108922941

Barroso, L. R. (1999). *Performance evaluation of vibration controlled steel structures under seismic loading*. PhD Thesis, Department of Civil and Environmental Engineering, Stanford University, Stanford, CA.

Barroso, L. R., Breneman, S. E., & Smith, H. A. (2002). Performance evaluation of controlled steel frames under multi-level seismic loads. *Journal of Structural Engineering*, *128*(11), 1368–1378. doi:10.1061/(ASCE)0733-9445(2002)128:11(1368)

Brown, A. S., Ankireddi, S., & Yang, H. T. Y. (1999). Actuator and sensor placement for multi-objective control of structures. *Journal of Structural Engineering*, *125*, 757–765. doi:10.1061/(ASCE)0733-9445(1999)125:7(757)

Cha, Y.-J. (2008). *Structural control architecture optimization for 3-D systems using advanced multi-objective genetic algorithms*. Ph.D. dissertation, Zachry Department of Civil Engineering, Texas A&M University, College Station, TX.

Cha, Y.-J., & Agrawal, A. K. (2011). (in press). Decentralized output feedback polynomial control of seismically excited structures using genetic algorithm. *Journal of Structural Control & Health Monitoring*. doi:10.1002/stc.486

Cha, Y.-J., Kim, Y., Raich, A. M., & Agrawal, A. K. (2011b). (in press). Multi-objective formulation for actuator and sensor layouts of actively controlled 3D buildings. *Journal of Vibration and Control*.

Cha, Y.-J., Raich, A. M., & Barroso, L. R. (2009). *Near-optimal structural control architectures of active devices and sensors using gene manipulation genetic algorithms.* 8th World Congress on Structural and Multidisciplinary Optimization, Lisbon, Portugal, June 1-5.

Cha, Y.-J., Raich, A. M., Barroso, L. R., & Agrawal, A. K. (2011a). Optimal placements of active control devices and sensors in frame structures using multi-objective genetic algorithms. *Journal of Structural Control & Health Monitoring*. DOI: 10.1002/stc.468

Chen, C. C., & Chen, G. D. (2002). Nonlinear control of a 20-story steel building with active piezoelectric friction dampers. *International Journal of Structural Engineering and Mechanics*, *4*(1), 21–38.

Chen, G., & Chen, C. (2004). Semiactive control of the 20-story Benchmark building with piezoelectric friction dampers. *Journal of Engineering Mechanics*, *130*(4), 393–400. doi:10.1061/(ASCE)0733-9399(2004)130:4(393)

Chen, G. S., Rruno, R. J., & Salama, M. (1991). Optimal placement of active/passive members in truss structures using simulated annealing. *AIAA Journal*, *29*(8), 1327–1334. doi:10.2514/3.10739

Cheng, F. Y., Jiang, H., & Zhang, X. (2002). Optimal placement of dampers and actuators based on stochastic approach. *Earthquake Engineering and Engineering Vibration*, *1*(2), 237–249. doi:10.1007/s11803-002-0069-y

Chopra, A. K. (2000). *Dynamics of structures theory and applications to earthquake engineering*. New Jersey: Prentice Hall.

Coello, C. A., Veldhuizen, D. A., & Lamont, G. B. (2001). *Evolutionary algorithms for solving multi-objective problem*. New York, NY: Kluwer Academic Publisher.

Deb, K., Agrawal, S., Pratab, A., & Meyarivan, T. (2000). *A fast elitist non-dominated sorting genetic algorithm for multi-obejective optimization: NSGA-II. KanGAL Report 200001*. Kanpur, India: Indian Institute of Technology.

Deb, K., Goldberg, D. E., & Chaffer, J. D. S. (1989). An investigation of niche and species formation in genetic function optimization. *Proceedings of the Third International Conference on Genetic Algorithms*, (pp. 42-50). Morgan Kauffman

DeJong, A. K. (1975). *An analysis of the behavior of a class of genetic adaptive systems.* PhD Dissertation, University of Michigan.

DeLorenzo, M. L. (1990). Sensor and actuator selection for large space structure control. *Journal of Guidance, Control, and Dynamics*, *13*(2), 249–257. doi:10.2514/3.20544

Dhingra, A. K., & Lee, B. H. (1995). Multiobjective design of actively controlled structures using a hybrid optimization method. *International Journal for Numerical Methods in Engineering*, *38*(20), 3383–3401. doi:10.1002/nme.1620382003

Fonseca, C. M., & Fleming, P. J. (1995). An overview of evolutionary algorithms in multiobjective optimization. *Evolutionary Computation*, *3*(1), 1–16. doi:10.1162/evco.1995.3.1.1

Furuya, H., & Haftka, R. T. (1995). Placing actuators on space structures by genetic algorithms and effectiveness indices. *Structural Optimization*, *9*(2), 69–75. doi:10.1007/BF01758822

Goldberg, D. E. (1989). *Genetic algorithms in search, optimization, and machine learning*. New York, NY: Addison-Wesley.

Goldberg, D. E., & Richardson, J. (1987). Genetic algorithm with sharing for multimodal function optimization. In J. J. Grefenstette (Ed.), *Genetic Algorithms and their Applications: Proceedings of the Second International Conference on Genetic Algorithms*, (pp. 41-49). Hillsdale, NJ: Lawrence Erlbaum.

Hans, A. E. (1988). Multicriteria optimization for highly accurate systems. In W. Stadler (Ed.), *Multicriteria optimization in engineering and sciences, Mathematical concepts and methods in science and engineering, 19*, 309-352. New York, NY: Plenum Press.

Holland, J. (1975). *Adaptation in natural and artificial systems*. Ann Arbor, MI: The University of Michigan Press.

Horn, J., & Nafpliotis, N. (1993). *Multiobjective optimization using the niched Pareto genetic algorithm*. IlliGAL Report 93005, Illinois Genetic Algorithms Lab., Univ. Illinois, Urbana-Champaign.

Housner, G. W., Masri, S. F., & Chassiakos, A. G. (1994). *Proceeding of the 1st World Conference on Structural Control.*

Kim, H., & Adeli, H. (2005). Hybrid control of irregular steel highrise building structures under seismic excitations. *International Journal for Numerical Methods in Engineering*, *63*, 1757–1774. doi:10.1002/nme.1336

Kim, Y., Langari, R., & Hurlebaus, R. (2009). Semiactive nonlinear control of a building structure equipped with a magnetorheological damper system. *Mechanical Systems and Signal Processing*, *20*, 300–315. doi:10.1016/j.ymssp.2008.06.006

Kim, Y., Langari, R., & Hurlebaus, R. (2010a). Control of a seismically excited benchmark building using linear matrix inequality-based semiactive nonlinear fuzzy control. *Journal of Structural Engineering*, *136*(8), 1023–1026. doi:10.1061/(ASCE)ST.1943-541X.0000192

Kim, Y., Langari, R., & Hurlebaus, R. (2010b). Novel bio-inspired smart control for hazard mitigation of civil structures. *Smart Materials and Structures*, *19*. doi:10.1088/0964-1726/19/11/115009

Kobori, T., Koshika, N., Yamada, N., & Ikeda, Y. (1991). Seismic response controlled structure with active mass driver system. Part 1: Design. *Earthquake Engineering & Structural Dynamics*, *20*, 133–139. doi:10.1002/eqe.4290200204

Li, Q. S., Liu, D. K., Fang, J. Q., & Tam, C. M. (2000). Multi-level optimal design of buildings with active control under winds using genetic algorithms. *Journal of Wind Engineering and Industrial Aerodynamics*, *86*(1), 65–86. doi:10.1016/S0167-6105(00)00004-0

Li, Q. S., Liu, D. K., Tang, J., Zhang. N., & Tam. C. M. (2004). Combinatorial optimal design of number and positions of actuators in actively controlled structures using genetic algorithms. Journal of Sound and Vibration, *270*(4-50), 611-624.

Liu, D. K., Yang, Y. L., & Li, Q. S. (2003). Optimum positioning of actuators in tall buildings using genetic algorithm. *Computers & Structures*, *81*(32), 2823–2827. doi:10.1016/j.compstruc.2003.07.002

Liu, X., Begg, D. W., & Matravers, D. R. (1997). Optimal topology/actuator placement design of structures using SA. *Journal of Aerospace Engineering*, *10*, 119–125. doi:10.1061/(ASCE)0893-1321(1997)10:3(119)

Moita, J. M., Correia, V. M., Martins, P. G., Soares, C. M., & Soares, C. A. (2006). Optimal design in vibration control of adaptive structures using a simulated annealing algorithm. *Thirteenth International Conference on Composite Structures - ICCS, 75*(1-4), 79-87.

Ohtori, Y., Christenson, R. E., Spencer, B. F. Jr, & Dyke, S. J. (2004). Benchmark control problems for seismically excited nonlinear buildings. *Journal of Engineering Mechanics*, *130*(4), 366–385. doi:10.1061/(ASCE)0733-9399(2004)130:4(366)

Onoda, J., & Hanawa, Y. (1992). Actuator placement optimization by genetic and improved simulated annealing algorithms. *AIAA Journal*, *31*(6), 1167–1169. doi:10.2514/3.49057

Raich, A. M. (1999). *An evolutionary based methodology for representing and evolving structural design solutions*. Ph.D. dissertation, Department of Civil and Environmental Engineering, University of Illinois, Urbana-Champaign, IL.

Raich, A. M., & Ghaboussi, J. (1998). Evolving structural design solution using an implicit redundant genetic algorithm. *Structural Multidisciplinary Optimization*, *20*, 222–231. doi:10.1007/s001580050150

Rao, R., Mohan, A., & Sivasubramanian, K. (2008). Optimal placement of actuators for active vibration control of seismic excited tall buildings using a multiple start guided neighborhood search (MSGNS) algorithm. *Journal of Sound and Vibration*, *311*(1-2), 133–159. doi:10.1016/j.jsv.2007.08.031

Rao, S. S., Pan, T., & Venkayya, V. B. (1991). Optimal placement of actuators in actively controlled structures using genetic algorithms. *AIAA Journal*, *29*(6), 942–943. doi:10.2514/3.10683

Reigles, D. G., & Symans, M. (2006). Supervisory fuzzy control of a base-isolated benchmark building utilizing a neuro-fuzzy model of controllable fluid viscous dampers. *Structural Control and Health Monitoring*, *13*, 724–747. doi:10.1002/stc.108

Richardson, A., & Abdullah, M. M. (2002). Sensor/actuators placement on civil structures using a real coded genetic algorithm. *Proceedings of the SPIE-The International Society for Optimal Engineering*, *4696*, 244–255.

Schaffer, J. D. (1985). Multiple objective optimization with vector evaluated genetic algorithms. *Proceedings of the First International Conference on Genetic Algorithms*, (pp. 93-100). Hillsdale, NJ: Lawrence Erlbaum Associates.

Sharifi, R., Kim, Y., & Langari, R. (2010). Sensor fault isolation and detection of smart structures. *Smart Materials and Structures*, *12*(10). doi:doi:10.1088/0964-1726/19/10/105001

Soong, T. T., & Reinhorn, A. M. (1993). An overview of active and hybrid structural control research in the U.S. *Structural Design of Tall Buildings*, *2*, 192–209. doi:10.1002/tal.4320020303

Spencer, B. F., Jr., Christenson, R. E., & Dyke, S. J. (1999). Next generation benchmark control problem for seismically excited buildings. In T. Kobori, et al., (Eds.), *Proceeding of the 2nd World Conference on Structural Control*, Vol. 2, (pp. 1135-1360). New York, NY: Wiley.

Spencer, B. F. Jr, & Nagarajaiah, S. (2003). State of the art of structural control. *Journal of Structural Engineering*, *129*(7), 845–856. doi:10.1061/(ASCE)0733-9445(2003)129:7(845)

Srinivas, N., & Deb, K. (1994). Multiobjective optimization using nondominated sorting in genetic algorithms. *Journal of Evolutionary Computation*, *2*(3), 221–248. doi:10.1162/evco.1994.2.3.221

Suresh, S., Narasimhan, S., & Sundararajan, N. (2008). Adaptive control of nonlinear smart base-isolated building using Gaussian kernel functions. *Structural Control and Health Monitoring*, *15*, 585–603. doi:10.1002/stc.217

Tan, P., Dyke, S. J., Richardson, A., & Abdullah, M. (2005). Integrated device placement and control design in civil structures using genetic algorithms. *Journal of Structural Engineering*, *131*(10), 1489–1496. doi:10.1061/(ASCE)0733-9445(2005)131:10(1489)

Tewari, A. (2002). *Modern control design with Matlab and Simulink*. New York, NY: John Wiley & Sons, Ltd.

The Mathworks. (2007). *MATLAB/Simulink*. Natick, MA: Author.

Wongprasert, N., & Symans, M. D. (2004). Application of a genetic algorithm for optimal damper distribution within the nonlinear seismic benchmark building. *Journal of Engineering Mechanics*, *130*(4), 401–406. doi:10.1061/(ASCE)0733-9399(2004)130:4(401)

Yang, F., Sedaghati, R., Younesian, D., & Esmailzadeh, E. (2005). Optimal placement of active bars in smart structures. *Proceedings of the IEEE International Conference on Mechatronics & Automation*, Niagara Falls Canada, (pp. 1-6).

Yao, J. T. P. (1972). Concept of structural control. *ASCE Journal of Strucutral Division*, *98*(ST7), 1567–1574.

Zitzler, E., Deb, K., & Thiele, L. (1999). Comparison of multiobjective evolutionary algorithms: Empirical results. *Evolutionary Computation*, *8*(2), 173–195. doi:10.1162/106365600568202

Zitzler, E., Laumanns, M., & Thiele, L. (2002a). *SPEA2: Improving the Strength Pareto Evolutionary Algorithm for Multiobjecitve Optimization.* Technical Report 103, Computer Engineering and Networks Laboratory (TIK), Swiss Federal Institute of Technology (ETH) Zurich, Switzerland.

Zitzler, E., Laumanns, M., & Thiele, L. (2002b). SPEA2: Improving the strength pareto evolutionary algorithm for multiobjecitve optimization. In Giannakoglou, K., Tsahalis, D., Periaux, J., Papailiou, K., & Fogarty, T. (Eds.), *Evolutionary methods for design, optimization and control*. Barcelona, Spain.

Zitzler, E., Laumanns, M., & Thiele, L. (2001). *SPEA2: Improving the Strength Pareto Evolutionary Algorithm. Technical Report 103*. Computer Engineering and Networks Laboratory (TIK), Swiss Federal Institute of Technology (ETH) Zurich, Gloriastrasse 35, CH-8092 Zurich, Switzerland. 2001.

About the Contributors

Nikos D. Lagaros is a Lecturer at the Institute of Structural Analysis and Seismic Research of the School of Civil Engineering, National Technical University of Athens and at the School of Corps of Engineers of the Hellenic Army since 2007. He is serving as Treasurer of the Greek Association for Computational Mechanics, while he acts as NSF panellist at the Directorate for Engineering Civil, Mechanical and Manufacturing Innovation, since 2010. Dr. Lagaros provides consulting, peer-review and expert-witness services to private companies and federal government agencies in Greece. A focus of his consulting work is the assessment of buildings after earthquake events and the development of technical software. The results of his research activity encompass a wide range of topics with an interdisciplinary character in the field of computational mechanics. His published research work contains: 70 peer-reviewed journal papers, 1 book, 6 contributed books, 2 international conference proceedings, 15 chapters in international books, and 135 papers in international conferences.

Vagelis Plevris is an Assistant Professor at the Department of Civil and Structural Engineering Educators, School of Pedagogical & Technological Education (ASPETE) in Athens, Greece and a Research Associate at the School of Civil Engineering, National Technical University of Athens (NTUA). He holds a Bachelor's in Civil Engineering, an MSc in Earthquake Engineering, a PhD in Computational Mechanics from NTUA and also a Master's in Business Administration from the Athens University of Economics and Business. His research work focuses mainly on computational earthquake engineering, design optimization, reliability analysis of structures and neural networks applications in structural engineering. His published research work includes more than 10 peer-reviewed journal papers, 4 contributed books as editor, 4 chapters in international scientific books, and 22 papers in international conferences.

Chara Ch. Mitropoulou is a Post-Doctoral Researcher at the Institute of Structural Analysis and Seismic Research of the School of Civil Engineering, National Technical University of Athens. She holds BSc, MSc, and Ph.D. degrees in Civil Engineering from the National Technical University of Athens. She has participated in a number of research projects and consultancies in the areas of structural analysis and structural dynamics, shape, sizing and topology optimum design of structures, mathematical programming, performance based design of RC and steel structures, as well as life cycle cost and fragility assessment of structures. Her publications include 4 book chapters, 2 papers in non-referred international scientific journals, 7 publications in referred international scientific journals, and 13 papers in conference proceedings.

* * *

Shaikh Faruque Ali is a Newton International Fellow in the Swansea University, Swansea, UK from January 2010. Before this he was a Post-Doctoral Research Fellow in Automatic Control Laboratory, IUT-Longwy, CRAN-CNRS, Nancy University, France. Dr. Ali obtained his doctorate in the Department of Civil Engineering at Indian Institute of Science, Bangalore in 2008. Dr. Ali's current research area is energy harvesting and structural control. He is particularly interested in semi-active vibration control using magneto-rheological devices. His works include both development of suitable control algorithms for civil structures and its experimental verification. His interest surrounds techniques from intelligent methods, like fuzzy logic, artificial neural network, genetic algorithms, et cetera. He is also interested in backstepping design and optimal dynamic inversion techniques. He has published more than 11 research articles in various international journals, 1 book and 1 book chapter, and more than 20 peer reviewed international conference papers. He has served as a reviewer for various international journals.

Grigoriy Agranovich received a Diploma with first class honors in Electrical Engineering in Sevastopol (Ukraine) in 1971 and defended his PhD dissertation at the Leningrad Aerospace University (Russia) in 1978. He joined the Department of Technical Cybernetics at the Technical University of Sevastopol in Ukraine and worked there till 1998. Since 1999 he is a faculty member at the Department of Electrical Engineering and Electronics at the Ariel University Center of Samaria (Israel). Prof. Agranovich is supervising students specializing in control. His research interests include control systems, structural control, optimization, vibration, et cetera. He has published about 50 chapters in edited books and papers in refereed journals, presented many lectures at international and national conferences, and prepared 12 research reports.

Athol Carr received his PhD from the University of California, Berkeley in 1967. He joined the Department of Civil Engineering at the University of Canterbury in 1968 and teaching Structural Mechanics, Dynamics, and Finite Element Methods. After 43 years he retired in April 2010 and was awarded the status of Professor Emeritus at the University of Canterbury. His major research interests are non-linear dynamic analyses and earthquake engineering. Over the past 30 years he has developed the non-linear time-history program Ruaumoko. Professor Carr is a Member of ASCE, a Fellow of IPENZ and has been made a Life-member of the NZ Society for Earthquake Engineering. Professor Carr is a member of the faculty of the Rose School (The European School of Advanced Studies in Reduction of Seismic Risk) in Pavia, Italy. He is an Adjunct Professor at the Earthquake Engineering Research Centre, University of Iceland. He has had a major interest the modelling of damping in structures for over 30 years and has led a number of research projects in applying viscous and non-viscous damping systems to structures to reduce their earthquake response.

Young-Jin Cha is serving as Postdoctoral Researcher at City College of City University of New York. He received his M.S. degree in Civil Engineering from Yonsei University, Seoul Korea in 2002 and his Ph.D. degree in Structural Engineering from Texas A&M University, College Station, Texas in 2008. He is the author of 3 book/book chapters, including 18 technical papers in various fields of multi-objective optimizations, passive, active and semi-active control systems, and smart sensing. His main scientific interests are structural control, system identification, structural health monitoring, multi-objective optimization, heuristic search methods and neural networks. He is currently serving as reviewer for the *Journal of Bridge Engineering and Structural Control* and *Health Monitoring*.

Gian Paolo Cimellaro is currently Chair of the ASCE Disaster Resilience of Structures, Infrastructures and Communities Subcommittee and Assistant Professor in the Politecnico di Torino. He received his Ph.D. degree in Civil Engineering, University at Buffalo (SUNY), NY, USA in 2008, M.S. Earthquake Engineering, University at Buffalo (SUNY), NY 2005; BS Civil Engineering, University of Rome "La Sapienza" 2001. He recently received the Fib Achievement Award for Young Engineers 2011 to recognize outstanding contribution to structural concrete, sponsored by *fib*. Dr. Cimellaro primary field of investigation is earthquake engineering with emphasis on defining quantification of resilience of physical infrastructural systems. He is currently P.I. of the Project ICRED- Integrated Community Resilience of European Disasters. He has authored 23 journal papers and 50 international conference proceedings, and 3 book chapters. For details please refer to URL: http://www.cimellaro.com.

Rajesh Dhakal received his PhD from the University of Tokyo in 2000 and is currently working as an Associate Professor of Structural and Earthquake Engineering at University of Canterbury. His research interests are in the areas of performance based earthquake engineering, seismic risk assessment, and advancement of seismic design technologies. He has published more than 150 technical papers in different aspects of structural and earthquake engineering. Dr Dhakal has received numerous awards, including the prestigious EQC-NZSEE Ivan Skinner award for advancement of earthquake engineering research in New Zealand. Dr. Dhakal is also a Chartered Professional Engineer in New Zealand, and currently serving as an Editorial Board member of five international Civil/Structural engineering journals; including the Associate Editorship of the prestigious ASCE *Journal of Structural Engineering*.

Anthony Blakeborough is a Professor in the Department of Engineering Science at the University of Oxford. He holds MA and PhD degress from the University of Cambridge, and was part of the team that set up the UK's leading shaking table facility at Bristol University before moving to Oxford. He recently held a visiting research fellowship at the University of California, Berkeley. His has broad research interests in structural engineering, including earthquake engineering, vibration of grandstands and footbridges, and the modelling of crowds.

Dora Foti is Associate Professor of Structural Engineering at the Polytechnic of Bari. She has taught courses of Design of bridges, Construction Engineering and Elements of Earthquake Engineering at the Faculty of Civil Engineering. She has lectured at numerous seminars and training courses as well as at Italian and foreigner universities and research institutes. She is author of about 100 scientific publications in the field of Structural Engineering, where she developed mainly issues related to the seismic behavior of structures and the study of the effects of dynamic loads on bridges. She is member of the scientific board the PhD course in "Sciences of Civil and Environmental Engineering" at the Polytechnic of Bari.

Markus Hochrainer, born 03/08 1973, received the Ph.D. degree in 2001 from the Vienna University of Technology, Austria, the M.S. degree in 1997 from Loughborough University, UK, and a M.S degree in 1996 from the Johannes Kepler University Linz, Austria. His main research interests include active and passive control of vibrations, system simulation and identification, theoretical and experimental modal analysis, hardware in the loop simulations, acoustics, and sound emission. He is the author or co-author of more than 30 papers. From 2001 to 2006 he was project engineer at Geoconsult, a civil engineering office where he focused on sound and vibration emissions from railway and underground projects. In 2006 he joined the University of Applied Sciences in Wiener Neustadt where he is currently head of the dynamics laboratory.

Theodore Karavasilis holds a Diploma, MSc, and PhD degrees in Civil Engineering from the University of Patras, Greece. He served as Post-Doctoral Researcher (2007-2009) in the ATLSS Center of Lehigh University (USA) and as Departmental Lecturer in Civil Engineering (2010-2011) at the University of Oxford. He was appointed Assistant Professor in Structural Engineering in the School of Engineering of the University of Warwick in 2011. He is a Visiting Academic Fellow of the Department of Engineering Science of the University of Oxford. He conducts research on the development of resilient minimal-damage structural systems under extreme loads (earthquakes, wind, blast). His expertise includes steel structures design, earthquake engineering, self-centering systems, smart materials and devices; nonlinear finite element implementation; and real-time hybrid testing.

Yeesock Kim currently holds the position as the Assistant Professor of Structural Engineering at the Department of Civil and Environment Engineering at Worcester Polytechnic Institute (WPI), Massachusetts, USA. He was a postdoctoral researcher of Control Engineering at the Department of Mechanical Engineering at Texas A&M University, College Station, USA, in 2007-2010. He is the author of 6 book/book chapters, including 42 technical papers in various fields of smart structures, vibration control, system identification, and control theory. At WPI, he teaches Smart Structures, Smart Infrastructure Analysis and Design, Structural Dynamics, and Structural Analysis and Design. He is also currently serving on the IEEE Control Systems Society Editorial Board.

Chang Won Kim received his BS and MS Degree from the School of Mechanical Engineering, Pusan National University in February 2003 and August 2005, respectively. During his Master's course, February 2004–2005, he was granted Abroad Cooperative Research funding by the Korean Science and Engineering Foundation, and worked in the Delft University of Technology, the Netherlands. He received his Doctor of Philosophy Degree in Mechanical Engineering at Texas A&M University in 2010. As a Post Doctoral Research Associate his research interests include bio-inspired control and control function management focusing on vehicle autonomy and advanced safety of autonomous vehicle systems.

Reza Langari received his B.Sc., M.Sc. and Ph.D. from the University of California at Berkeley in 1981, 1983, and 1991, respectively. He has worked for Measurex Corporation, Integrated Systems, Inc, and Insight Development Corporation and has held research positions at NASA Ames Research Center, Rockwell International Science Center (RISC) and United Technologies Research Center (UTRC.) Dr. Langari's expertise is in the area of computational intelligence with application to mechatronic systems. He is the co-author of the textbook, *Fuzzy Logic: Intelligence, Control and Information*, Prentice Hall, 1999 and co-editor of *Fuzzy Control: Synthesis and Analysis*, Wiley, 2000 as well Industrial Applications of Fuzzy Systems (IEEE Press, 1995.) He has served as Associate Editor of *IEEE Transactions on Fuzzy Systems, IEEE Transactions on Vehicular Technologies,* as well as the *ASME Journal of Dynamic Systems, Measurement and Control.*

Roman Lewandowski received his M.S., Ph.D. degree and Habilitation in Civil Engineering from Poznan University of Technology in 1973, 1982, and 1994, respectively. Currently he is a Professor at the Poznan University of Technology, Faculty of Civil and Environmental Engineering, Poznan, Poland. He is an author or co-author of one book and numerous pre-reviewed publications, mainly in the area of dynamics of structures and in the passive and active control of vibrations of structures. He is a member of the Polish Society for Theoretical and Applied Mechanics and the Polish Association for Computational Mechanics. His main research interests are non-linear vibration of structures and reduction of vibrations by means of passive, active, and semi-active methods.

Aiqun Li, male, born in Anhui province of China in July of 1962, is a Professor and Ph.D supervisor in the School of Civil Engineering at Southeast University now and is engaged in the health monitoring and vibration control of civil engineering. He obtained Doctor's Degree of Structure Engineering from Southeast University in 1992. He is the winner of National Outstanding Youth Fund and the national candidate of new century talents project, and got the governmental special allowance of the state council. He is also the editor of the *Journal of Asian Building and Engineering* and the member of the fifth discipline evaluation expert group of the state council degree committee. In recent years, he had taken charge of more than ten national key projects and owned seventeen patents, as well as published more than one hundred papers in domestic and international journals.

Chi-Chang Lin received his Ph.D. degree of Civil Engineering at the State University of New York at Buffalo in USA in 1989. He joined the Department of Civil Engineering at National Chung Hsing University (NCHU) in Taiwan in 1989 and was promoted to a full Professor in 1996. He has been a Distinguished Professor of Civil Engineering at NCHU since 2007. Dr. Lin was the department chair of Civil Engineering, Dean of College of Engineering, Director of Center for Environmental Restoration and Disaster Reduction (CERDR) and the Vice President of NCHU. He was also a Visiting Scholar at the University of California at Berkeley in 2002 and the University of Delaware in 2010. His research interests include structural health monitoring, passive and active control of structures, earthquake engineering, train-induced vibration, and soil-structure interaction. He has authored and co-authored more than 100 technical papers in international scientific journals and conferences. Dr. Lin has received numeral awards and honors including Distinguished Research Award from Taiwan National Science Council, Excellence Teacher Award of Taichung City, and Outstanding Engineering Professor Award from Taiwan Chinese Institute of Engineers. He is active in community service and serves as a board member in various national technical organizations in Taiwan. He is currently a Fellow of the Chinese Institute of Civil and Hydraulic Engineering.

Riccardo Nobile is Assistant Professor of Machine Design and Experimental Mechanics at the University of Salento in Italy. Main research interests are fatigue of base and welded materials, experimental techniques for the evaluation and monitoring of fatigue damage process, experimental and numerical evaluation of residual stress, and mechanical characterization of innovative materials and structures.

Zdzislaw Pawlak received the Ph.D. in Civil Engineering from the Poznan University of Technology in 2001. Currently he is an Assistant Professor at the Faculty of Civil and Environmental Engineering, Poznan University of Technology, Poland. He is the author or co-author of several pre-reviewed publications in the area of mechanics of structures. He is a member of the Polish Society for Theoretical and Applied Mechanics. He has been active in the design and construction of engineering structures for the past fifteen years. His main research interests are in passive methods of reduction of structure vibration.

Saeid Pourzeynali has received his Master's of Structural Engineering in 1989 from the Tehran University, Iran. He joined University of Guilan, Rasht, Iran as a Lecturer in the Dept. of Civil Engineering in June, 1991. Dr. Pourzeynali went on to accomplish his Ph. D. in Structural Engineering from IIT Delhi, India, in 1998, and came back in 2001 to the University of Guilan. His interests span a wide range of specialized fields like structural dynamics, earthquake engineering, random vibrations, reliability analysis, structural control and optimization, and dynamics of cable supported bridges. Dr. Pourzeynali has a record of 20 M. Sc. guidance, more than 20 years of teaching experiences, publication of more than 80 international journal and conference papers. Dr. Pourzeynali has received various awards among which the notable one is the "2004 best research study on cable supported bridges" from the Vice-Chancellor for Research of the University of Guilan.

Arun Puthanpurayil received his MSc. in Earthquake and Civil Engineering Dynamics from the University of Sheffield in 2007 and is currently a PhD. Student in the Department of Civil Engineering at University of Canterbury. Before joining the department as a PhD. Candidate, Arun was working as a Design Engineer for a multi-national company called Gifford for 3 years. He has been responsible for structural design of buildings of varying complexities and functionalities with a specific emphasis on their dynamic performances during extreme events like blast and earthquake. To till date he has published 10 technical papers in journals and various international conferences mostly focusing on earthquake engineering.

Ananth Ramaswamy is a Professor in the Department of Civil Engineering, Indian Institute of Science, Bangalore, India. He has done his B. Tech from Indian Institute of Technology, Madras (IITM) in 1985. He has completed his MS from University of California at Davis in 1986 and obtained his Doctorate from Louisiana State University in 1992. Research interest of Prof. Ananth Ramaswamy involves various interdisciplinary subjects and broadly encircles: analysis and design of reinforced concrete structures, pre-stressed and fiber reinforced concrete, bridge engineering, structural and shape optimization, FRP composites, smart materials, and vibration control. He has published more than 30 research papers in various international journals, 2 book chapters and more than 45 national and international conference papers. He has served as a reviewer for various prestigious national and international journals.

Yuri Ribakov studied Structural Engineering in Ukraine and received a Diploma with first class honors in 1991. In 2000 he joined the Department of Civil Engineering at the Ariel University Center of Samaria (Israel) and in 2001 got a PhD degree from the Technion – Israel Institute of Technology In 2001 he was a visiting researcher at the Structural Engineering and Earthquake Simulation Laboratory in the State University of New York at Buffalo and since 2002 till 2003 a Humboldt Research Fellow at the University of Leipzig (Germany). Presently Prof. Y. Ribakov is a head of civil engineering department at Ariel University Center of Samaria. His research interests include structural control, dampers, base isolation, reinforced concrete, engineering education, et cetera. He published more than 70 chapters in edited books and papers in refereed journals, presented about 50 lectures at international conferences. He is an active editorial board member of international journals and conferences.

Shide Salimi has received her B. Sc. degree in Civil Engineering in 2007 from the IKIU Qazvin, Iran. She has also received her M. Sc. degree in Structural Engineering form MAU, Ardabil, Iran in 2011. Her fields of interests are dynamics, earthquake engineering, robust design, structural control and optimization, and intelligent control. In addition, she has published some conference and journal papers about tuned mass damper design, fuzzy semi-active tuned mass damper design, and active tuned mass damper design.

Rolf Steinbuch studied Mathematics and Physics at the University of Ulm. After 5 years with Siemens/KWU (now AREVA), where he was doing research in the field of fracture mechanics, he moved to Daimler, where he was responsible for nonlinear studies in the field of safety and reliability analysis. Since 1993 he works at Reutlingen University. He teaches mechanics, numerics, and simulation. His research fields cover optimization, acoustics, and nonlinear problems. As consultant he supports the introduction of CAE-tools to the industry. He has been publishing some books and many papers on simulation, acoustics, and optimisation. As visiting Professor he spent time at different universities in Europe and Africa.

Teng Tong, male, born in Jiangsu province of China in October of 1988, is the postgraduate in the School of Civil Engineering at Southeast University now and is engaged in the dynamic analysis of bridge engineering. He had won scholarships for many times and published several papers in domestic and international journals. At present he is taking part in the segmental prefabricated assembly method of approach span part of the 4th Yangtze River Bridge in Nanjing.

Jer-Fu Wang received his Ph.D. degree from the Department of Civil Engineering, National Chung Hsing University (NCHU) in Taiwan in 2001. He continued his research as a post-doctor at NCHU after graduation. He was a visiting scholar at University of California at Berkeley in 2002, at University of California at San Diego in 2005-2006, and at the Hong Kong Polytechnic University in 2008 for the health monitoring of the Canton Tower in China. He joined 921 Earthquake Museum of Taiwan, National Museum of Natural Science as an Assistant Research Fellow in 2009. Dr. Wang's research interests include structural health monitoring, seismic resistance evaluation, and structural control. He is also a professional planner on science and disaster prevention exhibits and activities. The earthquake museum he works for is one of the few earthquake museums in the world, which preserves unique fault ruptures and collapsed school buildings caused by the Taiwan Chi-Chi Earthquake (M7.3) in September 21, 1999.

Hao Wang, male, born in Jiangxi province of China in September of 1980, is an Associate Researcher in the School of Civil Engineering at Southeast University. His major research interests are the structural health monitoring, the anti-earthquake analysis and wind induced vibration of long span bridges. He obtained Master's Degree of the Bridge & Tunnel Engineering from Central South University in 2004 and Doctor's Degree of Disaster Prevention and Mitigation Engineering & Sheltering Engineering from Southeast University in 2007, and studied at University of Illinois at Urbana-Champaign (UIUC) from 2009 to 2010 as visiting scholar. He is member of ASCE and the secretary general of China branch of International Association for Bridge Maintenance and Safety, and has published more than fifty journal papers. In recent years, he has presided or taken part in many national key projects including the researches on the Runyang Suspension Bridge and Sutong Cable-stayed Bridge.

Jessica K. Whittle holds a BSc with honours (2006) and an MSc in Civil Engineering (2007) from the University of Oklahoma (USA) in addition to a PhD in Engineering Science from the University of Oxford (2011). Dr. Whittle received an NSF Graduate Research Fellowship (USA) and an award at the Institution for Structural Engineers (UK) Young Researchers Conference in 2009. She also joined the UK Earthquake Engineering Field Investigation Team on a field mission to Padang, Indonesia after the September 30, 2009 earthquake. Her research interests are in earthquake engineering and structural design, optimal dissipative device distribution, disaster mitigation training, and low-cost seismic design for developing areas.

Martin Williams is a Professor in the Department of Engineering Science at the University of Oxford, where he has been based since 1989. He holds BSc and PhD degress in Civil Engineering from the University of Bristol. He has held visiting appointments at the University of British Columbia, UNAM Mexico City and the University of Queensland, and is a Fellow of both the Institution of Civil Engineers and the Institution of Structural Engineers. His research interests cover a wide range of structural dynamics problems, including earthquake engineering, development of novel hybrid test methods, dynamic human-structure interaction, and dynamics of historic masonry structures.

Rui Zhou, male, born in Jiangxi province of China in March of 1988, is the postgraduate in the School of Civil Engineering at Southeast University now and is engaged in the dynamic analysis of bridge engineering. He had attended the 19th national bridge academic conference in Shanghai, 2009 and the 1st nation disaster prevention and mitigation engineering academic conference in Nanjing, 2011. In addition, he has won scholarships for many times and had published three papers in domestic and international journals. At present he is taking part in the earthquake simulation multiple shaking table experiment of a three towers cable-stayed bridge.

Franz Ziegler, born 12/12 1937, held a chaired Professorship in Civil Engineering at the Vienna University of Technology, Austria from 1972 until his retirement in 2006. He received a Mechanical Engineering Diploma in 1961 and Doctor techn. from the same University in 1964. He was awarded Dr.H.C. of the St. Petersburg State Polytechnic University in 1996. Main research interests are vibrations and control, waves, and fluid-structure interaction. He is the author or co-author of more than 200 papers, several handbook-articles and two books. Since 1982 he is the Editor of the international journal *Acta Mechanica*. He held visiting professorships at Cornell, Northwestern, Stanford, and Stuttgart University. He is an Honorary Fellow of IIAV and a Fellow of ASME, Fellow of the Austrian Academy of Sciences and Academician of both, the Russian Academy of Sciences and the Russian Academy of Natural Sciences. In 2002 he was awarded as Honorary Professor of the Perm State Technical University, Russia. He served his terms as IUTAM Secretary-General, as GAMM-President and Vice-President and as President of IIAV (2006-2008). From 1982 to 2011 he served as the chairman of the Austrian Association of Earthquake Engineering and Structural Dynamics (OGE) and was elected as a Honorary Member 2011. In 1997 he received the *Peter-Kapitza-Medal* of the Russian Academy of Natural Sciences and the *Golden-Ikarus-Medal* of the University of Crete, Greece. In 2003 he was the first recipient of the EUROMECH-Solid-Mechanics-Prize.

Zhouhong Zong, male, born in Jiangsu province of China in October of 1966, is a Professor and Ph.D supervisor in the School of Civil Engineering at Southeast University, as well as the laboratory Director of Civil Engineering now. He is engaged in the health monitoring and safety assessment of bridge engineering. He obtained Doctor's Degree of Bridge & Tunnel Engineering from Southwest Jiaotong University in 1998 and was selected as the new century excellent talent in institutions of higher education of Fujian province in 2006. He is member of China civil engineering society and the civil engineering instrument equipment tendering evaluation experts of the Ministry of Education. In recent years, he had taken charge of many important engineering projects, for example, the national natural science foundation projects, the scientific and technological key projects of Fujian province, and the economical traffic development projects of Fujian province.

Compilation of References

Abdel-Ghaffar, A. M. (2000). Vibration studies and tests of a suspension bridge. *Computers & Structures*, *76*(6), 787–797.

Abdel-Ghaffar, A. M., & Rubin, L. I. (1982). Suspension bridge response to multiple-support excitations. *Journal of Engineering Mechanics*, *108*(2), 419–435.

Abdel-Ghaffar, A. M., & Rubin, L. I. (1983a). Vertical seismic behavior of suspension bridges. *Earthquake Engineering & Structural Dynamics*, *11*(1), 1–19. doi:10.1002/eqe.4290110103

Abdel-Ghaffar, A. M., & Rubin, L. I. (1983b). Lateral earthquake response of suspension bridges. *Journal of Engineering Mechanics*, *109*(3), 664–675.

Abe, M., & Fujino, Y. (1994). Dynamic characterization of multiple tuned mass dampers and some design formulas. *Earthquake Engineering & Structural Dynamics*, *23*, 813–835. doi:10.1002/eqe.4290230802

Abe, M., & Fujino, Y. (1998). Optimal design of passive energy dissipation devices for seismic protection of bridges. [in Japanese]. *J Struct Mech Earthquake Eng*, *605*(45), 41–52.

Abe, M., & Igusa, T. (1995). Tuned mass dampers for structures with closely spaced natural frequencies. *Earthquake Engineering & Structural Dynamics*, *24*, 247–261. doi:10.1002/eqe.4290240209

Abe, M., & Igusa, T. (1996). Semiactive dynamic vibration absorbers for controlling transient response. *Journal of Sound and Vibration*, *198*, 547–569. doi:10.1006/jsvi.1996.0588

Adeli, H. and Saleh, A. (1999). *Control, optimization, and smart structures: High performance bridges*.

Adeli, H., & Saleh, A. (1999). *Control, optimization, and smart structures: High-performance bridges and buildings of the future*. New York, NY: John Wiley & Sons, Inc.

Adhikari, S. (2000). *Damping models for structural vibration.* PhD Dissertation, University of Cambridge.

Adhikari, S., & Woodhouse, J. (2003). Quantification of non-viscous damping in discrete linear systems. *Journal of Sound and Vibration*, *260*, 499–518. doi:10.1016/S0022-460X(02)00952-5

Agranovich, G., & Ribakov, Y. (2010). A method for efficient placement of semi-active dampers in seismically excited structures. *Structural Control and Health Monitoring*, *17*(5), 513–531.

Agranovich, G., Ribakov, Y., & Blostotsky, B. (2004). A numerical method for choice of weighting matrices in active controlled structures. *Structural Design of Tall and Special Buildings*, *13*, 55–72. doi:10.1002/tal.233

Agrawal, A. K., & Yang, J. N. (2000). Semiactive control strategies for building subject to near-field earthquakes. *Proceedings of SPIE 3988, Vol. 359. Smart Structures and Materials 2000: Smart Systems for Bridges, Structures, and Highways* (pp. 359-370). Newport Beach, CA, USA.

Agrawal, A. K., & Nagarajaiah, S. (2009). Benchmark structural control problem for a seismically excited highway bridge—Part I and II. *Structural Control and Health Monitoring, Special Issue*, *16*(5), 503–528. doi:10.1002/stc.336

Agrawal, A. K., Tan, P., Nagarajaiah, S., & Zhang, J. (2009). Benchmark structural control problem for a seismically excited highway bridge—Part I: Phase I problem definition. *Structural Control and Health Monitoring, Special Issue*, *16*(5), 509–529. doi:10.1002/stc.301

Agrawal, A. K., & Yang, J. N. (1999). Optimal placement of passive dampers on seismic and wind-excited buildings using combinatorial optimization. *Journal of Intelligent Material Systems and Structures*, *10*, 997–1014.

Agrawal, A. K., & Yang, J. N. (2000). Design passive energy dissipation systems based on LQR methods. *Journal of Intelligent Material Systems and Structures*, *10*, 933–944. doi:10.1106/FB58-N1DG-ECJT-B8H4

Agrawal, A. K., Yang, J. N., & Wu, J. C. (1998). Application of optimal polynomial controller to a benchmark problem. *Earthquake Engineering & Structural Dynamics*, *27*, 1291–1302. doi:10.1002/(SICI)1096-9845(1998110)27:11<1291::AID-EQE784>3.0.CO;2-M

Ahlawat, A. S., & Ramaswamy, A. (2004). Multi-objective optimal fuzzy logic controller driven active and hybrid control systems for seismically excited nonlinear buildings. *Journal of Engineering Mechanics*, *130*(4), 416–423. doi:10.1061/(ASCE)0733-9399(2004)130:4(416)

Ahmadi, G. (1979). On the application of the critical excitation method to aseismic design. *Journal of Structural Mechanics*, *7*, 55–63. doi:10.1080/03601217908905312

Aiken, I. D., Nims, D. K., Whittaker, A. S., & Kelly, J. M. (1993). Testing of passive energy dissipation systems. *Earthquake Spectra*, *9*(3), 335–370. doi:10.1193/1.1585720

Ajeet, S. K., & Shirkhande, M. (2007). Optimal placement of supplemental dampers in seismic design of structures. *Japanese Society of Engineering Education*, *9*(3), 125–135.

Ali, S. F., & Padhi, R. (2009). Active vibration suppression of nonlinear beams using optimal dynamic inversion. *Journal of Systems and Control Engineering*, *223*(5), 657–672.

Ali, S. F., & Ramaswamy, A. (2007). Developments in structural optimization and applications to intelligent structural vibration control. In Lagaros, N., & Tsompanakis, Y. (Eds.), *Intelligent computational paradigms in earthquake engineering* (pp. 125–247). Hershey, PA: Idea Group Publishing. doi:10.4018/978-1-59904-099-8.ch006

Ali, S. F., & Ramaswamy, A. (2008). GA optimized FLC driven semi-active control for phase II smart nonlinear base isolated benchmark building. *Structural Control and Health Monitoring*, *15*, 797–820. doi:10.1002/stc.272

Ali, S. F., & Ramaswamy, A. (2009). Hybrid structural control using magnetorheological dampers for base isolated structures. *Smart Materials and Structures*, *18*(5), 055011. doi:10.1088/0964-1726/18/5/055011

Ali, S. F., & Ramaswamy, A. (2009a). Optimal fuzzy logic control for MDOF structural systems using evolutionary algorithms. *Engineering Applications of Artificial Intelligence*, *22*(3), 407–419. doi:10.1016/j.engappai.2008.09.004

Ali, S. F., & Ramaswamy, A. (2009b). Testing and modeling of MR damper and its application to SDOF systems using integral backstepping technique. *Journal of Dynamic Systems, Measurement, and Control*, *131*, 021009. doi:10.1115/1.3072154

Ali, S. F., & Ramaswamy, A. (2009c). Optimal dynamic inversion based semi-active control of benchmark bridge using MR dampers. *Structural Control and Health Monitoring*, *16*(5), 564–585. doi:10.1002/stc.325

Alkhatib, R., Jazar, G. N., & Golnaraghi, M. F. (2004). Optimal design of passive linear suspension using genetic algorithm. *Journal of Sound and Vibration*, *275*, 665–691. doi:10.1016/j.jsv.2003.07.007

Amini, F., & Tavassoli, M. R. (2005). Optimal structural active control force, number and placement of controllers. *Engineering Structures*, *27*(9), 1306–1316. doi:10.1016/j.engstruct.2005.01.006

Andrzej, S., Przemyslaw, K., & Jan, H. S. (2008). Damage identification in skeletal structures using the virtual distortion method in frequency domain. *Mechanical Systems and Signal Processing*, *22*(8), 1826–1839. doi:10.1016/j.ymssp.2008.03.009

Arbel, A. (1981). Controllability measures and actuator placement in oscillatory systems. *International Journal of Control*, *33*(3), 565–574. doi:10.1080/00207178108922941

Ashour, S. A., & Hanson, R. D. (1987). *Elastic seismic response of buildings with supplemental damping. Report No. UMCE- 87-1*. Department of Civil Engineering, University of Michigan.

Atashkari, K., Nariman-zadeh, N., Jamali, A., & Pilechi, A. (2005). Thermodynamic Pareto optimization of turbojet using multi-objective genetic algorithm. *International Journal of Thermal Sciences*, *44*(11), 1061–1071. doi:10.1016/j.ijthermalsci.2005.03.016

Autodesk, Inc. (2010). *Autodesk® Robot™ structural analysis*. San Rafael, CA: Author.

Aydin, E., Boduroglub, M. H., & Guney, D. (2007). Optimal dampers placements for seismic rehabilitation of planar building structures. *Engineering Structures*, *29*, 176–185. doi:10.1016/j.engstruct.2006.04.016

Baburaj, V., & Matsukai, Y. (1994). A study on the material damping of thin angle-ply laminated plates. *Journal of Sound and Vibration*, *172*(3), 415–419. doi:10.1006/jsvi.1994.1184

Bachmann, H. (2010). Seismic upgrading of a fire-brigade building by base isolation in Basel, Switzerland. *Structural Engineering International*, *20*(7), 268–274. doi:10.2749/101686610792016880

Bachmann, H., & Weber, B. (1995). Tuned vibration absorbers for “lively” structures. *Journal of the International Association for Bridge and Structural Engineering*, *5*(1), 31–36.

Bagley, R. L., & Torvik, P. J. (1989). Fractional calculus – A different approach to the analysis of viscoelastically damped structures. *AIAA Journal*, *27*, 1412–1417. doi:10.2514/3.10279

Bairrao, R., Duque, J., & Foti, D. (2000). *Shaking table tests on shear panels for the seismic protection of buildings*. Report n. 304/00 –C3ES, Laboratorio Nacional de Engenharia Civil (LNEC).

Balkenius, C., & Moren, J. (2001). Emotional learning: A computational model of the amygdala *Cybernetics and Systems*. *International Journal (Toronto, Ont.)*, *32*, 611–636.

Bandstra, J. P. (1983). Comparison of equivalent viscous damping in discrete and continuous vibrating system. *Transaction of ASME, Journal of Vibration, Acoustics*. *Stress and Reliabilityin Design*, *105*, 382–392. doi:10.1115/1.3269117

Banks, H. T., & Inman, D. J. (1991). On damping mechanisms in beams. *Transactions of ASME*. *Journal of Applied Mechanics*, *58*, 716–723. doi:10.1115/1.2897253

Bao, Y. D., Wu, Y. P., He, Y., et al. (2004). An improved AHP method in performance assessment. *WCICA 2004-Fifth World Congress on Intelligent Control and Automation, Conference Proceedings,* Vol. 1, (pp. 177-180).

Barroso, L. R. (1999). *Performance evaluation of vibration controlled steel structures under seismic loading*. PhD Thesis, Department of Civil and Environmental Engineering, Stanford University, Stanford, CA.

Barroso, L. R., Breneman, S. E., & Smith, H. A. (2002). Performance evaluation of controlled steel frames under multi-level seismic loads. *Journal of Structural Engineering*, *128*(11), 1368–1378. doi:10.1061/(ASCE)0733-9445(2002)128:11(1368)

Bechara, A., Damasio, H., & Damasio, A. R. (2000). Emotion, decision making and the orbitofrontal cortex. *Cerebral Cortex*, *10*, 295–307. doi:10.1093/cercor/10.3.295

Berkeley. (1995). *Kobe earthquake 1995/01/16 20:46, Station Takarazuka*. Retrieved February 1, 2011, from http://peer.berkeley.edu/smcat/data/ath/KOBE/TAZ-UP.AT2

Bernal, D. (1994). Viscous Damping in inelastic structural response. *Journal of Structural Engineering*, *120*(4), 1240–1254. doi:10.1061/(ASCE)0733-9445(1994)120:4(1240)

Berton, S., & Bolander, E. B. (2005). Amplification system for supplemental damping devices in seismic applications. *Journal of Structural Engineering*, *131*(6), 979–983. doi:10.1061/(ASCE)0733-9445(2005)131:6(979)

Bishop, R. E. D., & Webourn, D. B. (1952). The problem of the dynamic vibration absorber. *Engineering*, *174*, 769.

Blasco, X., Herrero, J. M., Sanchis, J., & Martinez, M. (2008). A new graphical visualization of n-dimensional Pareto front for decision-making in multiobjective optimization. *Information Sciences*, *178*(20). doi:10.1016/j.ins.2008.06.010

Bozorgnia, Y., & Bertero, V. (2004). *Earthquake engineering*. London, UK: Taylor & Francis, CRC Press. doi:10.1201/9780203486245

Bozzo, L. M., Chais, X., & Torres, L. (1998). A shear type energy dissipator for the protection of masonry infill walls. *Proceedings of the Sixth U.S. National Conference on Earthquake Engineering*, Seattle.

Bozzo, L. M., & Barbat, A. H. (1995). *Tecnicas avanzadas de diseño sismorresistente*. Perù: CAPECO Lima. (in Spanish)

Branke, J. (1998). Creating robust solutions by means of an evolutionary algorithm. *Proceedings of the International Conference on Parallel Problem Solving from Nature*, (pp. 119–128).

Brieger, S., Keller, U., & Steinbuch, R. (2008). *Advanced tools in structural optimization.* Paper presented at Advanced Problems in Mechanics – 2008 Conference, St. Petersburg, Russia.

Brown, A. S., Ankireddi, S., & Yang, H. T. Y. (1999). Actuator and sensor placement for multiobjective control of structures. *Journal of Structural Engineering*, *125*, 757–765. doi:10.1061/(ASCE)0733-9445(1999)125:7(757)

Cao, H., & Li, Q. S. (2004). New control strategies for active tuned mass damper systems. *Computers & Structures*, *82*, 2341–2350. doi:10.1016/j.compstruc.2004.05.010

Cao, H., Reinborn, A. M., & Soong, T. T. (1998). Design of an active mass damper for a tall TV tower in Nanjing, China. *Engineering Structures*, *20*(3), 134–143. doi:10.1016/S0141-0296(97)00072-2

Carr, A. J. (1997). Damping models for inelastic structures. *Proceedings of Asia Pacific Vibration Conference '97*, Kyongju, Korea, Nov. 9–13, Vol. 1 (pp. 287–293).

Carr, A. J. (2005). Damping models for time-history structural analyses. *Proceedings of Asia Pacific Vibration Conference '05*, Langkawi, Malaysia, Nov 27 (pp. 42–48).

Carr, A. J. (2007). *Ruaumoko manual - Theory* (pp. 3–14). University of Canterbury Press.

Casciati, F., Faravelli, L., & Yao, T. (1995). The tuning of fuzzy controllers for active structural control. *Applications of Statistics and Probability*, *2*, 741–746.

Cha, Y.-J. (2008). *Structural control architecture optimization for 3-D systems using advanced multi-objective genetic algorithms*. Ph.D. dissertation, Zachry Department of Civil Engineering, Texas A&M University, College Station, TX.

Cha, Y.-J., Raich, A. M., & Barroso, L. R. (2009). *Near-optimal structural control architectures of active devices and sensors using gene manipulation genetic algorithms.* 8th World Congress on Structural and Multidisciplinary Optimization, Lisbon, Portugal, June 1-5.

Cha, Y.-J., Raich, A. M., Barroso, L. R., & Agrawal, A. K. (2011a). Optimal placements of active control devices and sensors in frame structures using multi-objective genetic algorithms. *Journal of Structural Control & Health Monitoring.* DOI: 10.1002/stc.468

Chandra, M., & Langari, R. (2006). Analytical study of a control algorithm based on emotional processing. *Proceedings of the the American Control Conference,* (pp. 3433-3438). Minneapolis, MN: IEEE.

Chang, C. M., Park, K. S., Mullenix, A., & Spencer, B. F. Jr. (2008). Semiactive control strategy for a phase II smart base isolated benchmark building. *Structural Control and Health Monitoring*, *15*, 673–696. doi:10.1002/stc.269

Chang, M. I. J., & Soong, T. T. (1980). Optimal controller placement in modal control of complex systems. *Journal of Mathematical Analysis and Applications*, *75*, 340–358. doi:10.1016/0022-247X(80)90084-0

Chang, M. L., Lin, C. C., Ueng, J. M., Hsieh, K. H., & Wang, J. F. (2010). Experimental study on adjustable tuned mass damper to reduce floor vibration due to machinery. *Structural Control and Health Monitoring*, *17*(5), 532–548.

Chang, T. S., & Singh, M. P. (2009). Mechanical model parameters for viscoelastic dampers. *Journal of Engineering Mechanics*, *135*, 581–584. doi:10.1061/(ASCE)0733-9399(2009)135:6(581)

Chang, T., & Singh, M. P. (2002). Seismic analysis of structures with a fractional derivative model of viscoelastic dampers. *Earthquake Engineering and Engineering Vibration*, *1*, 251–260. doi:10.1007/s11803-002-0070-5

Chan, R. W. K., Albermani, F., & Williams, M. S. (2009). Evaluation of yielding shear panel device for passive energy dissipation. *Journal of Constructional Steel Research*, *65*, 260–268. doi:10.1016/j.jcsr.2008.03.017

Charney, F. A. (2008). Unintended consequences of modelling damping in structures. *Journal of Structural Engineering*, *134*(4), 581–592. doi:10.1061/(ASCE)0733-9445(2008)134:4(581)

Cha, Y.-J., & Agrawal, A. K. (2011). (in press). Decentralized output feedback polynomial control of seismically excited structures using genetic algorithm. *Journal of Structural Control & Health Monitoring*. doi:10.1002/stc.486

Cha, Y.-J., Kim, Y., Raich, A. M., & Agrawal, A. K. (2011b). (in press). Multi-objective formulation for actuator and sensor layouts of actively controlled 3D buildings. *Journal of Vibration and Control*.

Chen, C. C., & Chen, G. D. (2002). Nonlinear control of a 20-story steel building with active piezoelectric friction dampers. *International Journal of Structural Engineering and Mechanics*, *4*(1), 21–38.

Cheng, F. Y., & Pantelides, C. P. (1988). *Optimal placement of actuators for structural control*. Technical Report NCEER-88-0037, National Centre for Earthquake Engineering Research, State University of New York, Buffalo, N.Y.

Chen, G. S., Rruno, R. J., & Salama, M. (1991). Optimal placement of active/passive members in truss structures using simulated annealing. *AIAA Journal*, *29*(8), 1327–1334. doi:10.2514/3.10739

Chen, G., & Chen, C. (2004). Semiactive control of the 20-story Benchmark building with piezoelectric friction dampers. *Journal of Engineering Mechanics*, *130*(4), 393–400. doi:10.1061/(ASCE)0733-9399(2004)130:4(393)

Chen, G., & Wu, J. (2001). Optimal placement of multiple tuned mass dampers for reducing seismic responses of buildings. *Journal of Structural Engineering*, *127*(9), 1054–1062. doi:10.1061/(ASCE)0733-9445(2001)127:9(1054)

Cheng, F. Y., Jiang, H., & Zhang, X. (2002). Optimal placement of dampers and actuators based on stochastic approach. *Earthquake Engineering and Engineering Vibration*, *1*(2), 237–249. doi:10.1007/s11803-002-0069-y

Chen, S. H., & Yang, G. (2003). A method for determining locations of electro-rheological dampers in structures. *Smart Materials and Structures*, *12*, 164. doi:10.1088/0964-1726/12/2/302

Chey, M. H., Chase, J. G., Mander, J. B., & Carr, A. J. (2009). *Energy-dissipative semi-active tuned mass damper building systems for structural damage reduction*. Paper presented at the International Symposium.

Choi, H., & Kim, J. (2010). New installation scheme for viscoelastic dampers using cables. *Canadian Journal of Civil Engineering*, *37*, 1201–1211. doi:10.1139/L10-068

Chopra, A. (2000). *Dynamics of structures: Theory and applications to earthquake engineering*. Upper Saddle River, NJ: Prentice-Hall.

Chopra, A. K. (2000). *Dynamics of structures, Theory and applications to earthquake engineering*. Upper Saddle River, NJ: Prentice Hall.

Chopra, A. K. (2005). *Dynamics of structures: Theory and application to earthquake engineering*. New Delhi, India: Pearson Education.

Christopoulos, C., & Filiatrault, A. (2006). *Principles of passive supplemental damping and seismic isolation*. Pavia, Italy: IUSS Press.

Cimellaro, G. P. (2007). Simultaneous stiffness-damping optimization of structures with respect to acceleration, displacement and base shear. *Engineering Structures*, *29*, 2853–2870. doi:10.1016/j.engstruct.2007.01.001

Cimellaro, G. P., Lavan, O., & Reinhorn, A. M. (2009). Design of passive systems for control of inelastic structures. *Earthquake Engineering & Structural Dynamics*, *38*, 783–804. doi:10.1002/eqe.867

Cimellaro, G. P., & Retamales, R. (2007). Optimal softening and damping design for buildings. *Structural Control and Health Monitoring*, *14*(6), 831–857. doi:10.1002/stc.181

Cimellaro, G. P., Soong, T. T., & Reinhorn, A. M. (2009). Integrated design of controlled linear structural systems. *Journal of Structural Engineering*, *135*(7), 853–862. doi:10.1061/(ASCE)ST.1943-541X.0000032

Clerc, M. (2006). *Particle swarm optimization*. Wiley-ISTE. doi:10.1002/9780470612163

Coello, C. A., Veldhuizen, D. A., & Lamont, G. B. (2001). *Evolutionary algorithms for solving multi-objective problem*. New York, NY: Kluwer Academic Publisher.

Connor, J. J., & Klink, B. S. A. (1996). *Introduction to motion-based design*. WIT Press.

Connor, J. J., Wada, A., Iwata, M., & Huang, Y. H. (1997). Damage-controlled structures, I: Preliminary design methodology for seismically active regions. *Journal of Structural Engineering*, *123*(4), 423–431. doi:10.1061/(ASCE)0733-9445(1997)123:4(423)

Constantinou, M. C., Tsopelas, P., Hammel, W., & Sigaher, A. N. (2000). New configurations of fluid viscous dampers for improved performance. *Passive Control Symposium Proceedings,* Tokyo Institute of Technology, Yokohama, Japan.

Constantinou, M. C., Soong, T. T., & Dargush, G. F. (1998). *Passive energy dissipation systems for structural design and retrofit. Monograph No.1*. Buffalo, NY: Multidisciplinary Center for Earthquake Engineering Research.

Constantinou, M. C., & Tadjabakhsh, I. G. (1983). Optimum design of a first story damping system. *Computers & Structures*, *17*(2), 305–310. doi:10.1016/0045-7949(83)90019-6

Constantinou, M. C., Tsopelas, P., Hammel, W., & Sigaher, A. N. (2001). Toggle-brace-damper seismic energy dissipation systems. *Journal of Structural Engineering*, *127*(2), 105–112. doi:10.1061/(ASCE)0733-9445(2001)127:2(105)

CSI. (2009). *SAP2000, version 11*. Berkeley, CA: Computers and Structures, Inc.

Datta, T. K. (1996). *Control of dynamic response of structures*. Indo-US Symposium on Emerging Trends in Vibration and Noise Engineering, 18-20 March.

Datta, T. K. (2003). A state-of-the-art review on active control of structures. *ISET Journal of Earthquake Technology*, *40*(1), 1–17.

De Matteis, G., Mazzolani, F. M., & Panico, S. (2007). Pure aluminium shear panels as dissipative devices in moment-resisting steel frames. *Earthquake Engineering & Structural Dynamics*, *36*(7), 841–859. doi:10.1002/eqe.656

De Silva, C. W. (1981). An algorithm for the optimal design of vibration controllers for flexible systems. *Journal of Sound and Vibration*, *75*(4), 495–502. doi:10.1016/0022-460X(81)90437-5

De Silva, C. W. (2007). *Vibration damping, control, and design*. Boca Raton, FL: CRC Press/Taylor & Francis Group.

Deb, K., & Gupta, H. (2004). *Introducing robustness in multi-objective optimization*. Technical Report (KanGAL Report No. 2004016), Department of Mechanical Engineering, Indian Institute of Technology, Kanpur, India.

Deb, K., Goldberg, D. E., & Chaffer, J. D. S. (1989). An investigation of niche and species formation in genetic function optimization. *Proceedings of the Third International Conference on Genetic Algorithms*, (pp. 42-50). Morgan Kauffman

Deb, K., Agrawal, S., Pratab, A., & Meyarivan, T. (2000). *A fast elitist non-dominated sorting genetic algorithm for multi-obejective optimization: NSGA-II. KanGAL Report 200001*. Kanpur, India: Indian Institute of Technology.

Deb, K., Agrawal, S., Pratap, A., & Meyarivan, T. (2002). A fast and elitist multi-objective genetic algorithm: NSGA-II. *IEEE Transactions on Evolutionary Computation*, *6*(2), 182–197. doi:10.1109/4235.996017

DeJong, A. K. (1975). *An analysis of the behavior of a class of genetic adaptive systems.* PhD Dissertation, University of Michigan.

DeLorenzo, M. L. (1990). Sensor and actuator selection for large space structure control. *Journal of Guidance, Control, and Dynamics*, *13*(2), 249–257. doi:10.2514/3.20544

Den Hartog, J. P. (1956). Mechanical vibrations (4th ed.). New York, NY: McGraw-Hill Book Company.

Derham, C. J., Kelly, J. M., & Thomas, A. G. (1985). Nonlinear natural rubber bearings for seismic isolation. *Nuclear Engineering and Design*, *84*(3), 417–428. doi:10.1016/0029-5493(85)90258-4

Dhingra, A. K., & Lee, B. H. (1995). Multiobjective design of actively controlled structures using a hybrid optimization method. *International Journal for Numerical Methods in Engineering*, *38*(20), 3383–3401. doi:10.1002/nme.1620382003

Diaferio, M., Foti, D., & Nobile, R. (2008a). Design optimization of aluminium-steel devices for passive protection of structures. *4th Conference on Structural Control (ECSC2008)*, St. Petersburg, Russia.

Diaferio, M., Foti, D., & Nobile, R. (2008b). Aluminium-steel energy dissipators for passive protection of structures. *14th World Conference on Earthquake Engineering* – 12-17 October 2008, Beijing, China.

Diaferio, M., Foti, D., & Nobile, R. (2010). *The dynamic experimental behavior of a new aluminium passive protection device in a 3d frame*. 14th European Conference on Earthquake Engineering – 30.08-03.09.2010, Ohrid, Republic of Macedonia.

Diaferio, M., Foti, D., & Nobile, R. (2009). Hysteretic dissipators made of aluminium and steel: Optimal design and preliminary characterization tests. *International Journal of Advanced Structural Engineering*, *1*(1), 77–92.

Drenick, R. F. (1970). Model-free design of aseismic structures. *Journal of the Engineering Mechanics Division*, *96*(4), 483–493.

Drenick, R. F. (1973). Aseismic design by way of critical excitation. *Journal of the Engineering Mechanics Division*, *99*(4), 649–667.

Drenick, R. F. (1977a). On a class of non-robust problems in stochastic dynamics. In Clarkson, B. L. (Ed.), *Stochastic problems in dynamics* (pp. 237–255). London, UK: Pitman.

Drenick, R. F. (1977b). The critical excitation of nonlinear systems. *Journal of the Engineering Mechanics Division*, *44*(2), 333–336.

Drenick, R. F., & Park, C. B. (1975). Comments on worst inputs and a bound on the highest peak statistics of a class of non-linear systems. *Journal of Sound and Vibration*, *41*, 129–131. doi:10.1016/S0022-460X(75)80203-3

Driankov, D., Hellendoorn, H., & Reinfrank, M. (1992). *An introduction to fuzzy control*. Kolkata, India: Narosa Publishing House.

Dühring, M. B., Jensen, J. S., & Sigmund, O. (2008). Acoustic design by topology optimization. *Sound and Vibration*, *317*(3), 557–575. doi:10.1016/j.jsv.2008.03.042

Dyke, S. J., Spencer, B. F. Jr, Sain, M. K., & Carlson, J. D. (1996). Modeling and control of magnetorheological dampers for seismic response reduction. *Smart Materials and Structures*, *5*, 565–575. doi:10.1088/0964-1726/5/5/006

Eddy, N. (2005). *Taipei 101's 730-ton tuned mass damper.* Retrieved February 1, 2011, from http://www.popularmechanics.com/technology/gadgets/news/1612252

Engelen, K., Ramon, H., Saeys, A., Franssens, W., & Anthonis, J. (2007). Positioning and tuning of viscous damper on flexible structure. *Journal of Sound and Vibration*, *304*, 845–862. doi:10.1016/j.jsv.2007.03.020

Erkus, B., Abe, M., & Fujino, Y. (2002). Investigation of semi-active control for seismic protection of elevated highway bridges. *Structure Engineering*, *24*(3), 281–293. doi:10.1016/S0141-0296(01)00095-5

Ernst, J. H. (1965). Der E-Modul von Seilen unter Berucksichtigung des Durchhanges. *Der Bauingenieur*, *40*(2), 52–55.

Ewins, D. J. (2000). *Modal testing: Theory, practice and application* (2nd ed.). Hertfordshire, UK: Research Studies Press Ltd.

Falcon, K. C., Stone, B. J., Simcock, W. D., & Andrew, C. (1967). Optimization of vibration absorbers: A graphical method for use on idealized systems with restricted damping. *Journal of Mechanical Engineering Science*, *9*, 374–381. doi:10.1243/JMES_JOUR_1967_009_058_02

Fan, L. C. (1997). *Seismic analysis of bridge*. Shanghai, China: Tongji University Press.

FEMA. (2000). *FEMA 356: Prestandard and commentary for the seismic rehabilitation of buildings*. Washington, DC: Federal Emergency Management Agency.

Feng, Q., & Shinozuka, M. (1990) Use of a variable damper for hybrid control of bridge response under earthquake. In G. Housner & S. Masri (Eds.), *Proceedings of the US National Workshop on Structural Control Research*, University of Southern California, Los Angeles, (pp. 107–112).

Fonseca, C. M., & Fleming, P. J. (1993). Genetic algorithms for multi-objective optimization: formulation, discussion and generalization. In S. Forrest (Ed.), *Proceedings of the Fifth International Conference on Genetic Algorithms*, Morgan Kaufmann, San Mateo, CA, (pp. 416–423).

Fonseca, C. M., & Fleming, P. J. (1995). An overview of evolutionary algorithms in multiobjective optimization. *Evolutionary Computation*, *3*(1), 1–16. doi:10.1162/evco.1995.3.1.1

Foti, D., & Diaferio, M. (1999). *Shear panels for seismic protection of buildings.* 4th European Conference of Structural Dynamics–EURODYN'99, Prague, Czech Republic.

Foti, D., & Nobile, R. (2000). *Characterization tests of new aluminium and steel energy dissipating devices*. 5th International Conference on Computational Structures Technology: Identification, Control and Optimisation of Engineering Structures. Leuven, Belgium: Civil-Comp Press.

Foti, D., Diaferio, M., & Nobile, R. (2010). Optimal design of a new seismic passive protection device made in aluminium and steel (Technical Note). *Structural Engineering & Mechanics*, *35*(1), 119–122.

Frahm, H. (1911). *Devices for damping vibrations of bodies*. U.S. Patent, 989, 958.

Fu, C. (2008). *Effective damping of vibrations of plan-asymmetric buildings.* Doctoral dissertation, Vienna University of Technology, Austria. Retrieved from http://www.ub.tuwien.ac.at/diss/AC05037516.pdf

Fu, T. S., & Johnson, E. A. (2009). Control strategies for a distributed mass damper system. *Proceedings of the American Control Conference,* St. Louis, MO, USA, June 10-12, 2009 (pp. 3921-3925).

Fu, C., & Ziegler, F. (2010). Vibration prone multi-purpose buildings and towers effectively damped by tuned liquid column-gas dampers. *Asian Journal of Civil Engineering*, *10*(1), 21–56.

Fujita, K., Moustafa, A., & Takewaki, I. (2010). Optimal placement of viscoelastic dampers and supporting members under variable critical excitations. *Earthquakes and Structures*, *1*(1), 43–67.

Fujita, K., Moustafa, A., & Takewaki, I. (2010a). Optimal placement of viscoelastic dampers and supporting members under variable critical excitations. *Earthquakes and Structures*, *1*, 43–67.

Fujita, K., Yamamoto, K., & Takewaki, I. (2010b). An evolutionary algorithm for optimal damper placement to minimize interstorey-drift transfer function in shear building. *Earthquakes and Structures*, *1*, 289–306.

Furuya, O., Hamazaki, H., & Fujita, S. (1998). Study on proper distribution of storey-installation type damper for vibration control of slender structures using genetic algorithm. *Joint Pressure Vessels and Piping Conference, 364*, 297-304.

Furuya, H., & Haftka, R. T. (1995). Placing actuators on space structures by genetic algorithms and effectiveness indices. *Structural Optimization*, *9*(2), 69–75. doi:10.1007/BF01758822

Garcia, D. L. (2001). A simple method for the design of optimal damper configuration in MDOF structures. *Earthquake Spectra*, *17*(3), 38–398. doi:10.1193/1.1586180

Garcia, D. L., & Soong, T. T. (2002). Efficiency of a simple approach to damper allocation in MDOF structures. *Journal of Structural Control*, *9*(1), 19–30. doi:10.1002/stc.3

Gattulli, V., Lepidi, M., & Potenza, F. (2007). *Identification of analytical and finite element model for the Jetpacs three-dimensional frame*. Jetpacs Report No. 2, Research Project No. 7 of 2005-2008 ReLuis Project, Naples, Italy.

Gazi, V., & Passino, K. M. (2011). *Swarm stability and optimization*. Springer Verlag. doi:10.1007/978-3-642-18041-5

Gen, M., & Cheng, R. (1997). *Genetic algorithms and engineering design*. John Wiley & Sons Inc.

Gen, M., & Cheng, R. (2000). *Genetic algorithms & engineering optimization*. New York, NY: John Wiley & Sons.

Glanz, J., & Onishi, N. (2011, March 12). Japans strict building codes saved lives. *The New York Times*. Retrieved March 14, 2011, from http://www.nytimes.com/2011/03/12/world/asia/12codes.html?_r=2

Gluck, J., & Ribakov, Y. (1999). *Practical design of MDOF structures with supplemental viscous dampers using amplifying devices*. International Conference on Earthquake Hazard and Risk in the Mediterranean Region, North Cyprus, October 18-22.

Gluck, J., & Ribakov, Y. (2000). Semi-active friction system with amplifying braces for control of MDOF structures. *Structural Design of Tall Buildings*, *10*(2), 107–120. doi:10.1002/tal.168

Gluck, N., Reinhorn, A. M., Gluck, J., & Levy, R. (1996). Design of supplemental dampers for control of structures. *Journal of Structural Engineering*, *122*(12), 1394–1399. doi:10.1061/(ASCE)0733-9445(1996)122:12(1394)

Gluck, N., Reinhorn, A., & Levy, R. (1996). Design of supplemental dampers for control of structures. *Journal of Structural Engineering*, *122*(12), 1394–1399. doi:10.1061/(ASCE)0733-9445(1996)122:12(1394)

Goldberg, D. E., & Richardson, J. (1987). Genetic algorithm with sharing for multimodal function optimization. In J. J. Grefenstette (Ed.), *Genetic Algorithms and their Applications: Proceedings of the Second International Conference on Genetic Algorithms*, (pp. 41-49). Hillsdale, NJ: Lawrence Erlbaum.

Goldberg, D. E. (1989). *Genetic algorithms in search, optimization, and machine learning*. New York, NY: Addison-Wesley.

Grover, G. K. (1996). *Mechanical vibrations* (6th ed.). Roorkee, India: University of Roorkee.

Gurgoze, M., & Muller, P. C. (1992). Optimal positioning of dampers in multi-body systems. *Journal of Sound and Vibration*, *158*(3), 517–530. doi:10.1016/0022-460X(92)90422-T

Gu, Z. Q., & Oyadiji, S. O. (2008). Application of MR damper in structural control using ANFIS method. *Computers & Structures*, *86*(3-5), 427–436. doi:10.1016/j.compstruc.2007.02.024

Hahn, G. D., & Sathiavageeswaran, K. R. (1992). Effects of added-damper distribution on the seismic response of buildings. *Computers & Structures*, *43*(5), 941–950. doi:10.1016/0045-7949(92)90308-M

Hall, J. F. (2006). Problems encountered from the use (or misuse) of Rayleigh damping. *Earthquake and Structural Dynamics*, *35*, 522–545.

Han-Rok Ji, H., et al. (2005). Structural vibration control using semiactive tuned mass damper. *Proceedings of the Eighteenth KKCNN Symposium on Civil Engineering-KAIST6,* December 18-20, 2005, Taiwan.

Hans, A. E. (1988). Multicriteria optimization for highly accurate systems. In W. Stadler (Ed.), *Multicriteria optimization in engineering and sciences, Mathematical concepts and methods in science and engineering, 19*, 309-352. New York, NY: Plenum Press.

Hanson, R. D., Xia, C., & Su, Y. F. (1992). Design of supplemental steel damping devices for buildings. *Proceedings of the 10WCEE*, Madrid, Spain, (pp. 4139-4142).

Hanson, R. D., & Soong, T. T. (2001). *Seismic design with supplemental energy dissipation devices. EERI Monograph No. 8*. Oakland, CA: Earthquake Engineering Research Institute.

Heo, G., Wang, M. L., & Satpathi, D. (1997). Optimal transducer placement for health monitoring of long span bridge. *Structure Engineering*, *16*(7-8), 495–502.

He, W. L., Agrawal, A. K., & Mahmoud, K. (2001). Control of seismically excited cable-stayed bridge using resetting semiactive stiffness dampers. *Bridge Engineering*, *6*(6), 376–384. doi:10.1061/(ASCE)1084-0702(2001)6:6(376)

Hidaka, S., Ahn, Y. K., & Morishita, S. (1999). Adaptive vibration control by a variable-damping dynamic absorber using ER fluid. *Journal of Vibration and Acoustics*, *121*, 373–378. doi:10.1115/1.2893990

Hoang, N., & Warnitchai, P. (2005). Design of multiple tuned mass dampers by using a numerical optimizer. *Earthquake Engineering & Structural Dynamics*, *34*, 125–144. doi:10.1002/eqe.413

Hochrainer, M. J. (2001). *Control of vibrations of civil engineering structures with special emphasis on tall buildings*. Doctoral dissertation, Vienna University of Technology, Austria. Retrieved from http://www.ub.tuwien.ac.at/diss/AC03322409.pdf

Hochrainer, M. J. (2005). Tuned liquid column damper for structural control. *Acta Mechanica*, *175*(1-4), 57–76. doi:10.1007/s00707-004-0193-z

Hochrainer, M. J., & Ziegler, F. (2006). Control of tall building vibrations by sealed tuned liquid column dampers. *Structural Control and Health Monitoring*, *13*(6), 980–1002. doi:10.1002/stc.90

Holland, J. (1975). *Adaptation in natural and artificial systems*. Ann Arbor, MI: The University of Michigan Press.

Horn, J., & Nafpliotis, N. (1993). *Multiobjective optimization using the niched Pareto genetic algorithm*. IlliGAL Report 93005, Illinois Genetic Algorithms Lab., Univ. Illinois, Urbana-Champaign.

Housner, G. W., Masri, S. F., & Chassiakos, A. G. (1994). *Proceeding of the 1st World Conference on Structural Control.*

Housner, G. W., Bergman, L. A., Caughey, T. K., Chassiakos, A. G., Claus, R. O., & Masri, S. F. (1997). Structural control: Past, present and future. *Journal of Engineering Mechanics*, *123*(9), 897–971. doi:10.1061/(ASCE)0733-9399(1997)123:9(897)

Hrovat, D., Barak, P., & Rabins, M. (1983). Semi-active versus passive or active tuned mass damper for structural control. *Journal of the Engineering Mechanics Division*, *109*, 691–705. doi:10.1061/(ASCE)0733-9399(1983)109:3(691)

Huffmann, G., Freeman, R. A., & Brown, C. W. (1987). Dao Khanong cable stayed bridge: Tuned mass dampers in deck and pylon. *Proceedings of International Conference on Cable Stayed Bridges*, Bangkok, (pp. 1485-93).

Huo, L. S., Li, H. N., & Sun, L. (2001). Parameter study of TLCD control system excited by multidimensional ground motions. *Earthquake Engineering and Engineering Vibration*, *4*(21), 147–153.

Hurlebaus, S., & Gaul, L. (2006). Smart structure dynamics. *Mechanical Systems and Signal Processing*, *20*, 255–281. doi:10.1016/j.ymssp.2005.08.025

Ikeda, Y. (2004). Active and semi-active control of buildings in Japan. *Journal of Japan Association for Earthquake Engineering*, *4*(3), 278–282.

Ioi, T., & Ikeda, K. (1978). On the dynamic vibration damped absorber of the vibration system. *Bulletin of Japanese Society of Mechanical Engineering*, *21*(151), 64–71. doi:10.1299/jsme1958.21.64

Ishibuchi, H., Nakashima, T., & Murata, T. (1997). Comparison of the Michigan and Pittsburgh approaches to the design of fuzzy classification systems. *Electronics and Communications in Japan*, *80*(12), 10–19. doi:10.1002/(SICI)1520-6440(199712)80:12<10::AID-ECJC2>3.0.CO;2-W

Iyengar, R. N. (1970). *Matched inputs.* Report No. 47, Series J, Center for Applied Stochastics, Purdue University, W. Lafayette, IN.

Iyengar, R. N. (1989). Critical seismic excitation for structures. *Proceedings of the 5th ICOSSAR*, San Francisco. New York, NY: ASCE Publications.

Iyengar, R. N., & Manohar, C. S. (1985). System dependent critical stochastic seismic excitations. *M15/6, Proceedings of the 8th International Conference on SMiRT*, Brussels, Belgium.

Iyengar, R. N. (1972). Worst inputs and a bound on the highest peak statistics of a class of non-linear systems. *Journal of Sound and Vibration*, *25*, 29–37. doi:10.1016/0022-460X(72)90593-7

Iyengar, R. N., & Manohar, C. S. (1987). Nonstationary random critical seismic excitations. *Journal of Engineering Mechanics*, *113*(4), 529–541. doi:10.1061/(ASCE)0733-9399(1987)113:4(529)

Jaishi, B., & Ren, W. X. (2005). Structural finite element model updating using ambient vibration test results. *Structure Engineering*, *131*(4), 617–628. doi:10.1061/(ASCE)0733-9445(2005)131:4(617)

Jamali, M. R., Dehyadegari, M., Arami, A., Lucas, C., & Navabi, Z. (2009). Real-time embedded emotional controller. *Neural Computing & Applications*, *19*(1). doi:doi:10.1007/s00521-008-0227-x

Jangid, R. S. (1995). Dynamic characteristics of structures with multiple tuned mass dampers. *Structural Engineering & Mechanics*, *3*, 497–509.

Jansen, L. M., & Dyke, S. J. (2000). Semi-active control strategies for the MR damper: A comparative study ASCE. *Journal of Engineering Mechanics*, *126*, 795–803. doi:10.1061/(ASCE)0733-9399(2000)126:8(795)

Jara, J. M., Vargas, E., Galindo, C., Gonzalez, R., & Gòmez, C. (1992). Seismic performance of buildings with energy dissipating systems. *Proceedings of the 10WCEE*, Madrid, Spain, (pp. 2455-2460).

Jennige, R. L., & Frohrib, D. A. (1977). Alternative tuned absorbers for steady state vibration control of tall structures. *Journal of Mechanical Design*, *77*(84), 1–7.

Jones, D. I. G. (2001). *Handbook of viscoelastic vibration damping*. Chichester, UK: Wiley.

Juang, J. N. (1997). System realization using information matrix. *Journal of Guidance, Control, and Dynamics*, *21*(3), 492–500. doi:10.2514/2.4068

Jung, H. J., Choi, K. M., Spencer, B. F. Jr, & Lee, I. W. (2005). Application of some semi-active control algorithms to a smart base isolated building employing MR dampers. *Structural Control and Health Monitoring*, *13*(2-3), 693–704. doi:10.1002/stc.106

Karamodin, A., & Kazemi, H. (2010). Semi-active control of structures using neuro-predictive algorithm for MR dampers. *Structural Control and Health Monitoring*, *17*, 237–253.

Kareem, A., & Kline, S. (1995). Performance of multiple mass dampers under random loading. *Journal of Structural Engineering*, *121*, 348–361. doi:10.1061/(ASCE)0733-9445(1995)121:2(348)

Karnopp, D. C., Crosby, M. J., & Harwood, R. A. (1974). Vibration control using semi-active force generators. *Journal of Engineering for Industries*, *96*(2), 619–626. doi:10.1115/1.3438373

Kaveh, A., & Talatahari, S. (2009). Particle swarm optimizer, ant colony strategy and harmony search scheme hybridized for optimization of truss structures. *Computers & Structures*, *87*, 267–283. doi:10.1016/j.compstruc.2009.01.003

Kawashima, K., & Unjoh, S. (1994). Seismic response control of bridges by variable dampers. *Journal of Structural Engineering*, *120*(9), 2583–2601. doi:10.1061/(ASCE)0733-9445(1994)120:9(2583)

Kelly, J. M., & Hasegawa, K. (1992). *Application of a mass damping system to bridge structures*. Report No. UCB/EERC 92/12. Berkeley, CA: Earthquake Engineering Research Center.

Kelly, J. M., & Tsztoo, D. F. (1977). Energy absorbing devices in structures under earthquake loading. *6th World Conference on Earthquake Engineering*, New Delhi, Vol. 2, (pp. 139-1374).

Kelly, J. M. (1986). A seismic base isolation: A review and bibliography. *Soil Dynamics and Earthquake Engineering*, 202–216. doi:10.1016/0267-7261(86)90006-0

Kelly, J. M. (1996). *Earthquake-resistant design with rubber* (2nd ed.). London, UK: Springer-Verlag.

Kelly, J. M., Skinner, R. I., & Heine, A. J. (1972). Mechanisms of energy absorption in special devices for use in earthquake resistant structures. *Bulletin of the New Zealand National Society for Earthquake Engineering*, *5*, 78–89.

Kelly, T. E. (2001). *Base isolation of structures: Design guidelines*. Holmes Consulting Group Ltd.

Kennedy, J., & Eberhart, R. (2001). *Swarm intelligence*. San Francisco, CA: Morgan Kaufmann Publishers.

Khalid, B. (2010). *Control of seismically forced vibrations of asymmetric buildings by means of a novel base isolation system.* Doctorial dissertation, Vienna University of Technology, Austria. Retrieved from http://www.ub.tuwien.ac.at/diss/AC07809200.pdf

Khalid, B., & Ziegler, F. (2009). Experimental verification of control of asymmetric building vibrations by tuned liquid column gas dampers. *Proceedings of the 3rd International Conf. Experiments / Process / System Modeling / Simulation and Optimisation*, Athens, 8-11 July, 2009. Retrieved from http://epsmso.gr/2009/default.htm, CD-ROM paper: epsmso09_142.pdf

Khalid, B., & Ziegler, F. (2010). A novel base isolation system for asymmetric buildings effectively damped by tuned liquid column-gas dampers. *Proceedings of the 14th European Conference on Earthquake Engineering* (14. ECEE), Ohrid, 30. 08.- 03. 09. 2010. Abstract ID 1048. Retrieved from http://www.14ecee mk/

Kim, C., & Langari, R. (2009). Target tracking control of a mobile robot using a brain limbic system based control strategy. *Proceedings IEEE International Conference on Intelligent Robots and Systems,* (pp. 5095-5064). St. Louis, MO: IEEE.

Kim, C., & Langari, R. (2010a). Brain limbic system based intelligent controller application to lane change maneuver. *Vehicle System Dynamics*, *49*(12).

Kim, C., & Langari, R. (2010b). (in press). Application of brain limbic system to adaptive cruise control. *International Journal of Vehicle Autonomous Systems*.

Kim, C., & Langari, R. (2011). A mobile robot target tracking via brain limbic system based control. *International Journal of Robotics and Automation*, 26.

Kim, H., & Adeli, H. (2005). Hybrid control of irregular steel highrise building structures under seismic excitations. *International Journal for Numerical Methods in Engineering*, *63*, 1757–1774. doi:10.1002/nme.1336

Kim, Y., Kim, C., & Langari, R. (2010). Novel bio-inspired smart control for hazard mitigation of civil structures. *Smart Materials and Structures*, *19*(11). doi:10.1088/0964-1726/19/11/115009

Kim, Y., Langari, R., & Hurlebaus, R. (2009). Semiactive nonlinear control of a building structure equipped with a magnetorheological damper system. *Mechanical Systems and Signal Processing*, *20*, 300–315. doi:10.1016/j.ymssp.2008.06.006

Kim, Y., Langari, R., & Hurlebaus, R. (2010a). Control of a seismically excited benchmark building using linear matrix inequality-based semiactive nonlinear fuzzy control. *Journal of Structural Engineering*, *136*(8), 1023–1026. doi:10.1061/(ASCE)ST.1943-541X.0000192

Kim, Y., Langari, R., & Hurlebaus, R. (2010b). Novel bio-inspired smart control for hazard mitigation of civil structures. *Smart Materials and Structures*, *19*. doi:10.1088/0964-1726/19/11/115009

Kirsch, U. (1993). *Structural optimization: Fundamentals and applications*. Springer.

Klocke, F., Weck, M., & Schell, H. (1997). Evaluating alternative production cycles using the extended fuzzy AHP method. *European Journal of Operational Research*, *100*(2), 351–366. doi:10.1016/S0377-2217(96)00295-0

Knowles, J., & Corne, D. (1999). The Pareto archived evolution strategy: A new baseline algorithm for multi-objective optimization. *Proceedings of the 1999 Congress on Evolutionary Computation, IEEE Service Center,* Piscataway, NJ, (pp. 98–105).

Kobori, T., Koshika, N., Yamada, N., & Ikeda, Y. (1991). Seismic response controlled structure with active mass driver system. Part 1: Design. *Earthquake Engineering & Structural Dynamics*, *20*, 133–139. doi:10.1002/eqe.4290200204

Krishnakumar, K. (1989). Microgenetic algorithms for stationary and non-stationary function optimization. In G. Rodriguez (Ed.), *Proceedings of SPIE Intelligent Control and Adaptive Systems,* Vol. 1196, (pp. 289–296).

Krstic, M., & Smyshlyaev, A. (2007). Backstepping boundary control—A tutorial. *Proceedings of the American Control Conference*, New York City, NY, July, (pp. 870–875).

Krstic, M., Kanellakopoulos, I., & Kokotovic, P. V. (1995). *Nonlinear and adaptive control design*. New York, NY: Wiley.

Lavan, O., & Levy, R. (2004). Optimal design of supplemental viscous dampers for linear framed structures. *Proceedings of 13th World Conference on Earthquake Engineering,* Paper no: 42.

Lavan, O., Cimellaro, G. P., & Reinhorn, A. M. (2008). Noniterative optimization procedure for seismic weakening and damping of inelastic structures. *Journal of Structural Engineering*, *134*(10), 1638–1648. doi:10.1061/(ASCE)0733-9445(2008)134:10(1638)

Lavan, O., & Dargush, G. F. (2009). Multi-objective Evolutionary seismic design with passive energy dissipation systems. *Journal of Earthquake Engineering*, *13*, 758–790. doi:10.1080/13632460802598545

Lavan, O., & Levy, R. (2005). Optimal design of supplemental viscous dampers for irregular shear frames in the presence of the yielding. *Earthquake Engineering & Structural Dynamics*, *34*, 889–907. doi:10.1002/eqe.458

Lavan, O., & Levy, R. (2006). Optimal peripheral drift control of 3D irregular framed structures using supplemental viscous dampers. *Journal of Earthquake Engineering*, *10*(6), 903–923. doi:10.1080/13632460609350623

Lavan, O., & Levy, R. (2006a). Optimal design of supplemental viscous dampers for linear framed structures. *Earthquake Engineering & Structural Dynamics*, *35*(3), 337–356. doi:10.1002/eqe.524

Lavan, O., & Levy, R. (2006b). Optimal peripheral drift control of 3D irregular framed structures using supplemental viscous dampers. *Journal of Earthquake Engineering*, *10*(6), 903–923. doi:10.1080/13632460609350623

Lavan, O., & Levy, R. (2009). Simple iterative use of Lyapunov's solution for the linear optimal seismic design of passive devices in framed buildings. *Journal of Earthquake Engineering*, *13*, 650–666. doi:10.1080/13632460902837736

Leger, P., & Dussault, S. (1992). Seismic energy dissipation in MDOF structures. *Journal of Structural Engineering*, *118*(5), 1251–1269. doi:10.1061/(ASCE)0733-9445(1992)118:5(1251)

Leitmann, G. (1994). Semi-active control for vibration attenuation. *Journal of Intelligent Material Systems and Structures*, *5*, 841–846. doi:10.1177/1045389X9400500616

Levy, R., & Lavan, O. (2006). Fully stressed design of passive controllers in framed structures for seismic loadings. *Structural and Multidisciplinary Optimisation*, *32*(6), 485–498. doi:10.1007/s00158-005-0558-5

Levy, R., & Lavan, O. (2009). Quantitative comparison of optimization approaches for the design of supplemental damping in earthquake engineering practice. *Journal of Structural Engineering*, *135*(3), 321–325. doi:10.1061/(ASCE)0733-9445(2009)135:3(321)

Lewandowski, R. (2008). Optimization of the location and damping constants of viscous dampers. In B. H. V. Topping & M. Papadrakakis (Eds.), *Proceedings of the Ninth International Conference on Computational Structures Technology, Civil-Comp Press, Stirlingshire, Scotland*, Athens, Greece, 2-5 September, 2008, Paper 193, (pp. 1-16).

Lewandowski, R., & Pawlak, Z. (2010). Dynamic analysis of frames with viscoelastic dampers modelled by rheological models with fractional derivatives. *Journal of Sound and Vibration*, *330*, 923–936. doi:10.1016/j.jsv.2010.09.017

Li, Q. S., Liu, D. K., Tang, J., Zhang. N., & Tam. C. M. (2004). Combinatorial optimal design of number and positions of actuators in actively controlled structures using genetic algorithms. Journal of Sound and Vibration, *270*(4-50), 611-624.

Li, S. (2010). *Evolutionary optimization of earthquake resistance capacity for high buildings.* Unpublished Master Thesis, University of Reutlingen, Germany.

Li, C. (2000). Performance of multiple tuned mass dampers for attenuating undesirable oscillations of structures under the ground acceleration. *Earthquake Engineering & Structural Dynamics*, *29*, 1405–1421. doi:10.1002/1096-9845(200009)29:9<1405::AID-EQE976>3.0.CO;2-4

Li, C. (2002). Optimum multiple tuned mass dampers for structures under the ground acceleration based on DDMF and ADMF. *Earthquake Engineering & Structural Dynamics*, *31*, 897–919. doi:10.1002/eqe.128

Li, C., & Liu, Y. (2003). Optimum multiple tuned mass dampers for structures under the ground acceleration based on the uniform distribution of system parameters. *Earthquake Engineering & Structural Dynamics*, *32*, 671–690. doi:10.1002/eqe.239

Li, H., & Ni, X. (2007). Optimization of non-uniformly distributed multiple tuned mass damper. *Journal of Sound and Vibration*, *308*, 80–97. doi:10.1016/j.jsv.2007.07.014

Lin, C. C., Hu, C. M., Wang, J. F., & Hu, R. Y. (1994). Vibration control effectiveness of passive tuned mass dampers. *Journal of the Chinese Institute of Engineers*, *17*, 367–376. doi:10.1080/02533839.1994.9677600

Lin, C. C., Ueng, J. M., & Huang, T. C. (1999). Seismic response reduction of irregular buildings using passive tuned mass dampers. *Engineering Structures*, *22*(5), 513–524. doi:10.1016/S0141-0296(98)00054-6

Lin, C. C., Wang, C. E., Wu, H. W., & Wang, J. F. (2005). On-line building damage assessment based on earthquake records. *Smart Materials and Structures*, *14*, S137–S153. doi:10.1088/0964-1726/14/3/017

Lin, C. C., Wang, J. F., & Chen, B. L. (2005). Train-induced vibration control of high-speed railway bridges equipped with multiple tuned mass dampers. *Journal of Bridge Engineering*, *10*(4), 398–414. doi:10.1061/(ASCE)1084-0702(2005)10:4(398)

Lin, C. C., Wang, J. F., Lien, C. H., Chiang, H. W., & Lin, C. S. (2010). Optimum design and experimental study of multiple tuned mass dampers with limited stroke. *Earthquake Engineering & Structural Dynamics*, *39*, 1631–1651. doi:10.1002/eqe.1008

Lin, C. C., Wang, J. F., & Ueng, J. M. (2001). Vibration control identification of seismically excited m.d.o.f structure-PTMD systems. *Journal of Sound and Vibration*, *240*(1), 87–115. doi:10.1006/jsvi.2000.3188

Lin, P. Y., Chung, L. L., & Loh, C. H. (2005). Semiactive control of building structures with semiactive tuned mass damper. *Computer-Aided Civil and Infrastructure Engineering*, *20*, 35–51. doi:10.1111/j.1467-8667.2005.00375.x

Lin, P. Y., Roschke, P. N., & Loh, C. H. (2007). Hybrid base-isolation with magnetorheological damper and fuzzy control. *Structural Control and Health Monitoring*, *14*, 384–405. doi:10.1002/stc.163

Li, Q. S., Liu, D. K., Fang, J. Q., & Tam, C. M. (2000). Multi-level optimal design of buildings with active control under winds using genetic algorithms. *Journal of Wind Engineering and Industrial Aerodynamics*, *86*(1), 65–86. doi:10.1016/S0167-6105(00)00004-0

Liu, W. (2003).*Optimization strategy for damper configurations of buildings based on performance indices*. Ph. D. Thesis, State University of New York at Buffalo.

Liu, D. K., Yang, Y. L., & Li, Q. S. (2003). Optimum positioning of actuators in tall buildings using genetic algorithm. *Computers & Structures*, *81*(32), 2823–2827. doi:10.1016/j.compstruc.2003.07.002

Liu, W., Tong, M., & Lee, G. (2005). Optimization methodology for damper configuration based on building performance indices. *Journal of Structural Engineering*, *131*(11), 1746–1756. doi:10.1061/(ASCE)0733-9445(2005)131:11(1746)

Liu, X., Begg, D. W., & Matravers, D. R. (1997). Optimal topology/actuator placement design of structures using SA. *Journal of Aerospace Engineering*, *10*, 119–125. doi:10.1061/(ASCE)0893-1321(1997)10:3(119)

Loh, C. H., Lin, P. Y., & Chung, N. H. (2000). Design of dampers for structures based on optimal control theory. *Earthquake Engineering & Structural Dynamics*, *29*, 1307–1323. doi:10.1002/1096-9845(200009)29:9<1307::AID-EQE972>3.0.CO;2-D

Lopez-Garcia, D. (2001). A simple method for the design of optimal damper configurations in MDOF structures. *Earthquake Spectra*, *17*(3), 387–398. doi:10.1193/1.1586180

Lopez-Garcia, D., & Soong, T. T. (2002). Efficiency of a simple approach to damper allocation in MDOF structures. *Journal of Structural Control*, *9*, 19–30. doi:10.1002/stc.3

Lucas, C., Shahmirzadi, D., & Sheikholeslami, N. (2004). Introducing BELBIC-Brain emotional learning based intelligent controller. *International Journal of Intelligent Automation and Soft Computing*, *10*, 11–22.

Lynch, J. P., Wang, Y., Swartz, R. A., Lu, K. C., & Loh, C. H. (2008). Implementation of a closed-loop structural control system using wireless sensor networks. *Structural Control and Health Monitoring*, *15*, 518–539. doi:10.1002/stc.214

Madden, G. J., Symans, M. D., & Wongprasert, N. (2002). Experimental verification of seismic response of building frame with adaptive sliding base-isolation system. *Journal of Structural Engineering*, *128*(4), 1037–1045. doi:10.1061/(ASCE)0733-9445(2002)128:8(1037)

Main, J. A., & Krenk, S. (2005). Efficiency and tuning of viscous dampers on discrete systems. *Journal of Sound and Vibration*, *286*, 97–112. doi:10.1016/j.jsv.2004.09.022

Mamadani, E. H. (1974). Application of fuzzy logic algorithms for control of simple dynamic plant. *Proceedings of the Institution of Electrical Engineers*, *29*, 1585–1588. doi:10.1049/piee.1974.0328

Maplesoft Inc. (n.d.). *Maple 13.02*. Waterloo, Canada: Author.

Marquez, H. J. (2003). *Nonlinear control systems: Analysis and design*. New York, NY: Wiley Interscience.

Martinez-Miranda, J., & Aldea, A. (2005). Emotions in human and artificial intelligence. *Computers in Human Behavior*, *21*, 323–341. doi:10.1016/j.chb.2004.02.010

Martinez-Rodrigo, M., & Romero, M. L. (2003). An optimum retrofit strategy for moment resisting frames with nonlinear viscous dampers for seismic applications. *Engineering Structures*, *25*(2), 913–925. doi:10.1016/S0141-0296(03)00025-7

Matsagar, V. A., & Jangid, R. S. (2003). Seismic response of base-isolated structures during impact with adjacent structures. *Engineering Structures*, *25*, 1311–1323. doi:10.1016/S0141-0296(03)00081-6

Matsagar, V. A., & Jangid, R. S. (2004). Influence of isolator characteristics on the response of base-isolated structures. *Engineering Structures*, *26*, 1735–1749. doi:10.1016/j.engstruct.2004.06.011

McCormick, J., Aburano, H., Ikenaga, M., & Nakashima, M. (2008). Permissible residual deformation levels for building structures considering both safety and human elements. *Proceedings of the 14th World Conference on Earthquake Engineering*, Beijing, China, Paper No. 05-06-0071.

Mead, D. J. (1999). *Passive vibration control*. Chichester, UK: Wiley.

Mehrabian, A. R., & Lucas, C. (2006). Emotional learning based intelligent robust adaptive controller for stable uncertain nonlinear systems. *International Journal of Computational Intelligence*, *2*, 246–253.

Mehrabian, A. R., Lucas, C., & Roshanian, J. (2006). Aerospace launch vehicle control: An intelligent adaptive approach. *Aerospace Science and Technology*, *10*, 149–155. doi:10.1016/j.ast.2005.11.002

Meo, M., & Zumpano, G. (2005). On the optimal sensor placement techniques for a bridge structure. *Structure Engineering*, *27*(10), 1488–1497. doi:10.1016/j.engstruct.2005.03.015

Meskouris, K., & Hinzen, K. (2003). *Bauwerke und Erdbeben: Grundlagen - Anwendung – Beispiele*. Wiesbaden, Germany: Vieweg +Teubner.

Meystel, A. M., & Albus, J. S. (2002). *Intelligent systems: Architecture, design and control*. New York, NY: Wiley Interscience.

Michalewicz, Z. (1996). *Genetic algorithms + data structures = Evolution programs*. New York, NY: Springer.

Mikhailov, L. (2004). Group prioritization in the AHP by fuzzy preference programming method. *Computers & Operations Research*, *31*(2), 293–301. doi:10.1016/S0305-0548(03)00012-1

Milman, M. H., & Chu, C.-C. (1994). Optimization methods for passive damper placement and tuning. *Journal of Guidance, Control, and Dynamics*, *17*(4), 848–856. doi:10.2514/3.21275

Ming, T. Z., Hu, G. W., & Huang, W. (2007). Multiple-objective optimum design of pavement system for long-span steel bridges. *China Civil Engineering*, *40*(2), 70–73.

Moita, J. M., Correia, V. M., Martins, P. G., Soares, C. M., & Soares, C. A. (2006). Optimal design in vibration control of adaptive structures using a simulated annealing algorithm. *Thirteenth International Conference on Composite Structures - ICCS, 75*(1-4), 79-87.

Moren, J. (2002). *Emotion and learning-a computational model of the amygdale.* Ph.D. Dissertation Department of Cognitive Science. Lund, Sweden: Lund University.

Moren, J., & Balkenius, C. (2000) A computational model of emotional learning in the amygdale. *Proceedings of the 6th International Conference on the Simulation of Adaptive Behavior*, (pp. 383-391). Cambridge, MA: MIT Press.

Moreschi, L. M. (2000). *Seismic design of energy dissipation systems for optimal performance.* PhD. Dissertation, Virginia Polytechnic Institute and State University.

Morgenstern, J. (199, May 295). City perils: The fifty-nine-story crisis. *The New Yorker*, 45-53. Retrieved from http://www.duke.edu/~hpgavin/ce131/citicorp1 htm

Movaffaghi, H., & Friberg, O. (2006). Optimal placement of dampers in structure using genetic algorithm. *Engineering Computations*, *23*(6), 597–606. doi:10.1108/02644400610680324

Müller, P. C., & Schiehlen, W. O. (1976). *Lineare Schwingungen*. Wiesbaden, Germany: Akademische Verlagsgesellschaft.

Mulligan, K. (2007). *Experimental and analytical studies of semi-active and passive structural control of buildings*. PhD Thesis, University of Canterbury, Christchurch, New Zealand.

Mulligan, K., Chase, J. G., Mander, J. B., Fougere, M., Deam, B. L., Danton, G., & Elliot, R. B. (2006). Hybrid experimental analysis of semi-active rocking wall systems. *Proceedings of the New Zealand Society of Earthquake Engineering Conference (NZSEE)*, Napier, New Zealand.

Mulligan, K., Miguelgorry, M., Novello, V., Chase, J. G., Mander, J. B., & Rodgers, G. … Horn, B. (2007). *Semi-active tuned mass damper systems.* 19th Australasian Conference on Mechanics of Structures and Materials (ACMSM), Christchurch, New Zealand.

Muravski, G. B. (2004). On frequency independent damping. *Journal of Sound and Vibration*, *274*, 653–668. doi:10.1016/j.jsv.2003.05.012

Murphy, T. P., & Collins, K. R. (2004). Retrofitting suspension bridges using distributed dampers. *Structure Engineering*, *130*(10), 1466–1474. doi:10.1061/(ASCE)0733-9445(2004)130:10(1466)

Naeim, F., & Kelly, J. M. (1999). *Design of seismic isolated structures, Earthquake resistant design.* Nabuto, J., Fujino, Y., & Ito, M. (1988). A study of the effectiveness of TMD to suppress a coupled flutter of bridge deck. *Journal of JSCE, October*, 413-16.

Naeim, F., & Kelly, J. M. (1999). *Design of seismic isolated structures: From theory to practice*. New York, NY: John Wiley. doi:10.1002/9780470172742

Nagarajaiah, S., & Narasimhan, S. (2006). Smart base-isolated benchmark building Part II: Phase I sample controllers for linear isolation systems. *Structural Control and Health Monitoring*, *13*, 589–604. doi:10.1002/stc.100

Nagarajaiah, S., Narasimhan, S., Agrawal, A., & Ping, T. (2009). Benchmark structural control problem for a seismically excited highway bridge. Part III: Phase II sample controller for the fully base-isolated case. *Structural Control and Health Monitoring*, *16*, 549–563. doi:10.1002/stc.293

Nagarajaiah, S., Narasimhan, S., & Johnson, E. A. (2008). Structural control benchmark problem: Phase II—Nonlinear smart base-isolated building subjected to near-fault earthquakes. *Journal of Structural Control and Health Monitoring*, *15*(5), 653–656. doi:10.1002/stc.280

Nagarajaiah, S., & Spencer, B. F. Jr. (2003). State of the art of structural control. *Journal of Structural Engineering*, *129*, 845–856. doi:10.1061/(ASCE)0733-9445(2003)129:7(845)

Nakamura, T., & Tsuji, M. (1996). Inverse damping perturbation for stiffness design of shear buildings. *Journal of Structural Engineering*, *122*(6), 617–625. doi:10.1061/(ASCE)0733-9445(1996)122:6(617)

Nakashima, M., & Mitani, T. (1996b). Distribution of energy input and dissipation along stories in steel building structures with hysteretic dampers. *Proceedings of the 11th World Conference on Earthquake Engineering 1996*, Paper No. 260.

Nakashima, M. (1995). Strain-hardening behavior of shear panels made of low-yield steel. I: Test. *Journal of Structural Engineering*, *121*(12), 1742–1749. doi:10.1061/(ASCE)0733-9445(1995)121:12(1742)

Nakashima, M., Iwai, S., Iwata, M., Takeuchi, T., Konomi, S., Akazawa, T., & Saburi, K. (1994). Energy dissipation behavior of shear panels made of low yield steel. *Earthquake Engineering & Structural Dynamics*, *23*(12), 1299–1313. doi:10.1002/eqe.4290231203

Nakashima, M., Saburi, K., & Tsuji, B. (1996a). Energy input and dissipation behaviour of structures with hysteretic dampers. *Earthquake Engineering & Structural Dynamics*, *25*, 483–496. doi:10.1002/(SICI)1096-9845(199605)25:5<483::AID-EQE564>3.0.CO;2-K

Narasimhan, S., Nagarajaiah, S., & Johnson, E. A. (2008). Smart base isolated benchmark building part IV: phase II. Sample controller for nonlinear isolation systems. *Journal of Structural Control and Health Monitoring*, *15*(2-3), 657–672. doi:10.1002/stc.267

Narasimhan, S., Nagarajaiah, S., Johnson, E. A., & Gavin, H. P. (2006). Smart base isolated benchmark building part I: Problem definition. *Journal of Structural Control and Health Monitoring*, *13*(2-3), 573–588. doi:10.1002/stc.99

Nawrotzki, P., & Dalmer, F. (2005). *Der Einfluss von Schwingungstilgern auf die Standsicherheit und Gebrauchstauglichkeit von Bauwerken*. D-A-CH Tagung 2005, Retrieved January 1, 2011 from http://www.gerb.com/de/bibliothek/downloads/dokumente/aKoeln.pdf.

Oh, S.-H., Kim, Y.-J., & Ryu, H.-S. (2009). Seismic performance of steel structures with slit dampers. *Engineering Structures*, *31*, 1997–2008. doi:10.1016/j.engstruct.2009.03.003

Ohtori, Y., Christenson, R. E., Spencer, B. F., & Dyke, S. J. (2004). Nonlinear benchmark control problem for seismically excited buildings. *Journal of Engineering Mechanics*, *130*(4), 366–385. doi:10.1061/(ASCE)0733-9399(2004)130:4(366)

Ohtori, Y., Christenson, R. E., Spencer, B. F. Jr, & Dyke, S. J. (2004). Benchmark control problems for seismically excited nonlinear buildings. *Journal of Engineering Mechanics*, *130*(4), 366–385. doi:10.1061/(ASCE)0733-9399(2004)130:4(366)

Onoda, J., & Hanawa, Y. (1992). Actuator placement optimization by genetic and improved simulated annealing algorithms. *AIAA Journal*, *31*(6), 1167–1169. doi:10.2514/3.49057

Ordonez, D., Foti, D., & Bozzo, L. (2002). Comparative study of the inelastic response of base isolated buildings. *Earthquake Engineering & Structural Dynamics*, *32*(1), 151–164. doi:10.1002/eqe.224

Ormondroyd, J., & Den Hartog, J. P. (1928). The theory of the dynamic vibration absorber. *Transactions of the American Society of Mechanical Engineers*, *50*, 9–22.

Palazzo, B., Petti, L., & De Iuliis, M. (2004). A modal approach to optimally place dampers in framed structures. *Proceedings of 13th World Conference on Earthquake Engineering,* Paper no: 769.

Pantelides, C. P., & Cheng, F. Y. (1990). Optimal placement of controllers for seismic structures. *Engineering Structures*, *12*(4), 254–262. doi:10.1016/0141-0296(90)90024-M

Paola, M. D., & Navarra, G. (2009). Stochastic seismic analysis of MDOF structures with nonlinear viscous dampers. *Structural Control and Health Monitoring*, *16*(3), 303–318. doi:10.1002/stc.254

Pareto, V. (1927). *Manuel d'e'conomie politique*. Paris, France: Giard.

Park, Y. J., Cho, H. S., & Cha, D. H. (1995). Genetic algorithm-based optimization of fuzzy logic controller using characteristic parameters. *Proceedings of the IEEE International Conference on Evolutionary Computation* (pp. 831-836).

Park, K. S., Koh, H. M., Ok, S. Y., & Seo, C. W. (2005). Supervisory control of earthquake-excited cable-stayed bridges. *Engineering Structures*, *27*, 1086–1100. doi:10.1016/j.engstruct.2005.02.007

Park, S. W. (2001). Analytical modelling of viscoelastic dampers for structural and vibration control. *International Journal of Solids and Structures*, *38*, 8065–8092. doi:10.1016/S0020-7683(01)00026-9

Pawlak, Z., & Lewandowski, R. (2010). Optimization of viscoelastic dampers as described by the fractional rheological model. In B. H. V. Topping et al., (Eds.), *Proceedings of The Tenth International Conference on Computational Structural Technology*, (pp. 1-15). Stirlingshire, UK: Civil-Comp Press.

PEER. (2005). *Next generation attenuation relationships – Strong motion database*. Pacific Earthquake Engineering Research Center. Retrieved from http://peer.berkeley.edu/nga.

Picard, R. (1997). *Affective computing*. Cambridge, MA: MIT Press.

Ping, T., & Agrawal, A. K. (2009). Benchmark structural control problem for a seismically excited highway bridge-Part II: Phase I sample control designs. *Structural Control and Health Monitoring*, *16*, 530–548. doi:10.1002/stc.300

Pinkaew, T., & Fujino, Y. (2001). Effectiveness of semi-active tuned mass dampers under harmonic excitation. *Engineering Structures*, *23*(7), 850–856. doi:10.1016/S0141-0296(00)00091-2

Pintér, J. (2008). *Global optimization*. Retrieved from http://mathworld.wolfram.com/GlobalOptimization html

Plevris, V., & Papadrakakis, M. (2011). A hybrid particle swarm—gradient algorithm for global structural optimization. *Computer-Aided Civil and Infrastructure Engineering*, *26*, 48–68.

Podlubny, I. (1999). *Fractional differential equations*. Academic Press.

Ponzo, F. C., Cardone, D., Di Cesare, A., Moroni, C., Nigro, D., & Vigoriti, G. (2007). *Dynamic tests on Jetpacs steel frame experimental model set up*. Jetpacs Report No. 3, Research Project No. 7 of 2005-2008 ReLuis Project, Naples, Italy.

Pourzeynali, S., & Datta, T. K. (2002). Control of flutter of suspension bridge deck using TMD. *International Journal of Wind and Structure*, *5*(5), 407–422.

Pourzeynali, S., & Datta, T. K. (2005). Semi active fuzzy control of suspension bridge flutter. *Journal of Structural Engineering*, *131*(6), 900–912. doi:10.1061/(ASCE)0733-9445(2005)131:6(900)

Pourzeynali, S., & Esteki, S. (2009). Optimization of the TMD parameters to suppress the vertical vibrations of suspension bridges subjected to earthquake excitations. *Iranian International Journal of Engineering*. *IJE Transaction B (Application)*, *22*(1), 23–34.

Pourzeynali, S., Lavasani, H. H., & Modarayi, A. H. (2007). Active control of high rise building structures using fuzzy logic and genetic algorithms. *Engineering Structures*, *29*, 346–357. doi:10.1016/j.engstruct.2006.04.015

Pourzeynali, S., & Mousanejad, T. (2010). Optimization of semi-active control of seismically excited buildings using genetic algorithms. *Scientia Iranica, Transaction A*. *Civil Engineering (New York, N.Y.)*, *17*(1), 26–38.

Pourzeynali, S., & Zarif, M. (2008). Multi-objective optimization of seismically isolated high-rise building structures using genetic algorithms. *Journal of Sound and Vibration*, *311*, 1141–1160. doi:10.1016/j.jsv.2007.10.008

Puthanpurayil, A. M., Dhakal, R. J., & Carr, A. J. (2011). Modelling of in-structure damping damping: A review of the state of the art. *Proceedings of 9th Pacific Conference on Earthquake Engineering,* Paper no: 091.

Raich, A. M. (1999). *An evolutionary based methodology for representing and evolving structural design solutions*. Ph.D. dissertation, Department of Civil and Environmental Engineering, University of Illinois, Urbana-Champaign, IL.

Raich, A. M., & Ghaboussi, J. (1998). Evolving structural design solution using an implicit redundant genetic algorithm. *Structural Multidisciplinary Optimization*, *20*, 222–231. doi:10.1007/s001580050150

Rai, D. C., & Wallace, B. J. (1998). Aluminium shear-link for enhanced seismic resistance. *Earthquake Engineering & Structural Dynamics*, *27*(4), 315–342. doi:10.1002/(SICI)1096-9845(199804)27:4<315::AID-EQE703>3.0.CO;2-N

Rama Mohan Rao, A., & Sivasubramanian, K. (2008). Optimal placement of actuators for active vibration control of seismic excited tall buildings using a multiple start guided neighbourhood search algorithm. *Journal of Sound and Vibration*, *311*(1-2), 133–159. doi:10.1016/j.jsv.2007.08.031

Rana, R., & Soong, T. T. (1998). Parametric study and simplified design of tuned mass dampers. *Engineering Structures*, *202*(3), 193–204. doi:10.1016/S0141-0296(97)00078-3

Rao, R., Mohan, A., & Sivasubramanian, K. (2008). Optimal placement of actuators for active vibration control of seismic excited tall buildings using a multiple start guided neighborhood search (MSGNS) algorithm. *Journal of Sound and Vibration*, *311*(1-2), 133–159. doi:10.1016/j.jsv.2007.08.031

Rao, S. S., Pan, T. S., & Venkayya, V. B. (1991). Optimal placement of actuators in actively controlled structures using genetic algorithms. *AIAA Journal*, *29*(6), 942–943. doi:10.2514/3.10683

Rechenberg, I. (1994). *Evolutionsstrategie '94*. Stuttgart, Germany: Frommann-Holzboog.

Reid, T. J. (1956). Free vibration and hysteretic damping. *Journal of Royal Aeronautical Society*, *60*, 283.

Reigles, D. G., & Symans, M. (2006). Supervisory fuzzy control of a base-isolated benchmark building utilizing a neuro-fuzzy model of controllable fluid viscous dampers. *Structural Control and Health Monitoring*, *13*, 724–747. doi:10.1002/stc.108

Reiner, J., Balas, G. J., & Garrard, W. L. (1995). Robust dynamic inversion for control of highly maneuverable aircraft. *Journal of Guidance, Control, and Dynamics*, *18*, 18–24. doi:10.2514/3.56651

Reiterer, M. (2004). *Damping of vibrational civil engineering structures with emphasis on bridges*. Doctoral dissertation, Vienna University of Technology, Austria. Retrieved from http://www.ub.tuwien.ac.at/diss/AC04250350.pdf

Reiterer, M., & Ziegler, F. (2004). Bi-axial seismic activation of civil engineering structures equipped with tuned liquid column dampers. *Journal of Seismology and Earthquake Engineering*, *6*(3), 45–60.

Reiterer, M., & Ziegler, F. (2005). Bi-axial seismic activation of civil engineering structures equipped with tuned liquid column dampers. *Journal of Seismology and Earthquake Engineering*, *7*, 45–60.

Reiterer, M., & Ziegler, F. (2006). Control of pedestrian-induced vibrations of long-span bridges. *Structural Control and Health Monitoring*, *13*, 1003–1027. doi:10.1002/stc.91

Ribakov, Y., Gluck, J., & Gluck, N. (2000). *Practical design of MDOF structures with supplemental viscous dampers using mechanical levers*. ASCE Specialty Conference on Probabilistic Mechanics and Structural Reliability, Notre Dame, U. S. A., 24-26 July, 2000, Paper No 2000-005.

Ribakov, Y. (2003). Selective controlled base isolated multi-story structures with combined damping systems and amplifying braces. *European Earthquake Engineering*, *17*(1), 39–49.

Ribakov, Y., & Agranovich, G. (2007). A roof isolation system with variable friction dampers for seismic protection of multistory buildings. *European Earthquake Engineering*, *21*(1), 10–15.

Ribakov, Y., & Agranovich, G. (in press). Control of structural seismic response by a limited set of active dampers. *Structural Design of Tall and Special Buildings*.

Ribakov, Y., & Dancygier, A. N. (2006). High efficiency amplifiers for viscous damped structures subjected to strong earthquakes. *Structural Design of Tall and Special Buildings*, *15*(2), 221–232. doi:10.1002/tal.292

Ribakov, Y., & Gluck, J. (2002). Selective controlled base isolation system with magnetorheological dampers. *Earthquake Engineering & Structural Dynamics*, *31*(6), 1301–1324. doi:10.1002/eqe.164

Ribakov, Y., & Reinhorn, A. M. (2003). Design of amplified structural damping using optimal considerations. *Journal of Structural Engineering*, *129*(10), 1422–1427. doi:10.1061/(ASCE)0733-9445(2003)129:10(1422)

Richardson, A., & Abdullah, M. M. (2002). Sensor/actuators placement on civil structures using a real coded genetic algorithm. *Proceedings of the SPIE-The International Society for Optimal Engineering*, *4696*, 244–255.

Robinson, W. H. (1982). Lead rubber hysteretic bearing suitable for protecting structures during earthquakes. *Earthquake Engineering & Structural Dynamics*, *10*, 593–604. doi:10.1002/eqe.4290100408

Rodellar, J., & Manosa, V. (2003). A robust tendon control scheme for a class of cable-stayed structures. *Proceedings of the 3rd Conference on Structural Control,* Vol. 3. (pp. 184-190). Como, Italy.

Rolls, E. T. (2000). The orbitofrontal cortex and reward. *Cerebral Cortex*, *10*, 284–294. doi:10.1093/cercor/10.3.284

Ross, M. (2011, March 14). Building codes spared Tokyo from wider destruction. *ABC News.* Retrieved March 14, 2011, from http://www.abc.net.au/news/stories/2011/03/14/3163447.htm?section=justin

Rossikhin, Y. A., & Shitikova, M. V. (2001). A new method for solving dynamic problems of fractional derivative viscoelasticity. *International Journal of Engineering Science*, *39*(2), 149–176. doi:10.1016/S0020-7225(00)00025-2

Rouhani, H., Jalili, M., Araabi, B. N., Eppler, W., & Lucas, C. (2006). Brain emotional learning based intelligent controller applied to neurofuzzy model of micro-heat exchanger. *Expert Systems with Applications*, *32*, 911–918. doi:10.1016/j.eswa.2006.01.047

Rouhani, H., Sadeghzadeh, A., Lucas, C., & Araabi, B. N. (2007). Emotional learning based intelligent speed and position control applied to neurofuzzy model of switched reluctance motor. *Control and Cybernetics*, *36*, 75–95.

RWDI Consultant Engineers, (2011). *Projects from RWDI.* Retrieved March 28, 2011, from http://www.rwdi.com/project/one_wall_centre

Saaty, T. L. (1980). *The analytic hierarchy process*. New York, NY: McGraw-Hill.

Sadek, F., Mohraz, B., Taylor, A. W., & Chung, R. M. (1997). A method of estimating the parameters of tuned mass dampers for seismic applications. *Earthquake Engineering & Structural Dynamics*, *26*, 617–635. doi:10.1002/(SICI)1096-9845(199706)26:6<617::AID-EQE664>3.0.CO;2-Z

Sahasrabudhe, S., & Nagarajaiah, S. (2005). Experimental study of sliding base-isolated building with magneto-rheological dampers in near fault earthquakes. *Journal of Structural Engineering*, *131*, 1025–1034. doi:10.1061/(ASCE)0733-9445(2005)131:7(1025)

Schaffer, J. D. (1985). Multiple objective optimization with vector evaluated genetic algorithms. In J. J. Grefenstette (Ed.), *Proceedings of the First International Conference on Genetic Algorithms and their Applications,* (pp. 93–100). London, UK: Lawrence Erlbaum.

Serino, G., Chandrasekaran, S., Marsico, M. R., & Spizzuoco, M. (2007). *Description and analytical modeling of the Jetpacs steel frame prototype*. Jetpacs Report No. 1, Research Project No. 7 of 2005-2008 ReLuis Project, Naples, Italy.

Shahmirzadi, D., Langari, R., Ricalde, L. J., & Sanchez, E. N. (2006). Intelligent vs. sliding mode control in rollover prevention of tractor-semitrailers. *Intelligent Journal of Vehicle Autonomous Systems*, *4*, 68–87.

Sharifi, R., Kim, Y., & Langari, R. (2010). Sensor fault isolation and detection of smart structures. *Smart Materials and Structures*, *12*(10). doi:doi:10.1088/0964-1726/19/10/105001

Sheikholeslami, N., Shahmirzadi, D., Semsar, E., Lucas, C., & Yazdanpanah, M. J. (2006). Applying brain emotional learning algorithm for multivariable control of HVAC systems. *Journal of Intelligent & Fuzzy Systems*, *17*, 35–46.

Shin, Y. C., & Xu, C. (2009). *Intelligent systems modeling, optimization, and control*. New York, NY: Taylor & Francis Group.

Shook, D. A., Roschke, P. N., & Ozbulut, O. E. (2008). Superelastic semi-active damping of a base-isolated structure. *Structural Control and Health Monitoring*, *15*, 746–768. doi:10.1002/stc.276

Shook, D., Lin, P. Y., Lin, T. K., & Roschke, P. N. (2007). A comparative study in the semiactive control of isolated structures. *Smart Materials and Structures*, *16*, 1433–1446. doi:10.1088/0964-1726/16/4/058

Shukla, A. K., & Datta, T. K. (1999). Optimal use of viscoelastic dampers in building frames for seismic force. *Journal of Structural Engineering*, *125*(4), 401–409. doi:10.1061/(ASCE)0733-9445(1999)125:4(401)

Sigaher, A. N., & Constantinou, M. C. (2003). Scissor-jack-damper energy dissipation system. *Earthquake Spectra*, *19*(1), 133–158. doi:10.1193/1.1540999

Sikaroudi, H., & Chandler, A. M. (1992). Structure-foundation interaction in the earthquake response of torsionally asymmetric buildings. *Soil Dynamics and Earthquake Engineering*, *11*(1), 1–16. doi:10.1016/0267-7261(92)90022-6

Singh, M. P., & Chang, T. S. (2009). Seismic analysis of structures with viscoelastic dampers. *Journal of Engineering Mechanics*, *135*, 571–580. doi:10.1061/(ASCE)0733-9399(2009)135:6(571)

Singh, M. P., & Moreschi, L. M. (2001). Optimal seismic response control with dampers. *Earthquake and Structural Dynamics*, *30*(4), 553–572. doi:10.1002/eqe.23

Singh, M. P., & Moreschi, L. M. (2002). Optimal placement of dampers for passive response control. *Earthquake and Structural Dynamics*, *31*(4), 955–976. doi:10.1002/eqe.132

Skibniewski, M. J. (1988). Framework for decision-making on implementing robotics in construction. *Journal of Computing in Civil Engineering*, *2*(2), 188–200. doi:10.1061/(ASCE)0887-3801(1988)2:2(188)

Skibniewski, M., & Chao, L. C. (1992). Evaluation of advanced construction technology with AHP method. *Journal of Construction Engineering and Management*, *118*(3), 577–593. doi:10.1061/(ASCE)0733-9364(1992)118:3(577)

Skinner, R. I., Kelly, J. M., & Heine, A. J. (1975). Hysteretic damper for earthquake resistant structures. *Earthquake Engineering & Structural Dynamics*, *3*(3), 287–296. doi:10.1002/eqe.4290030307

Skinner, R. I., Tayler, R. G., Heine, A. J., & Robinson, W. J. (1980). Hysteretic dampers for the protection of structures from earthquakes. *Bulletin of the New Zealand National Society for Earthquake Engineering*, *13*(1).

Smyrou, E., Priestley, M. J., & Carr, A. J. (2011). Modelling of elastic damping in nonlinear time-history analyses of cantilever RC walls. *Bulletin of Earthquake Engineering*, *9*(5). doi:10.1007/s10518-011-9286-y

Somerville, P., Smith, N., Punyamurthula, S., & Sun, J. (1997). *Development of ground motion histories for phase 2 of the FEMA/SAC steel project*. Report No. SAC/BD-97/04.

Soong, T. T. (1988). State-of-the-art review: Active structure control in civil engineering. *Engineering Structures*, *10*(2), 73–84.

Soong, T. T. (1990). *Active structural control: Theory and practice*. Harlow, UK: Wiley.

Soong, T. T., & Constantinou, M. C. (1994). *Passive and active structural vibration control in civil engineering*. New York, NY: Springer.

Soong, T. T., & Dargush, G. (1997). *Passive energy dissipation systems in structural engineering*. Chichester, UK: John Wiley & Sons.

Soong, T. T., & Reinhorn, A. M. (1993). An overview of active and hybrid structural control research in the U.S. *Structural Design of Tall Buildings*, *2*, 192–209. doi:10.1002/tal.4320020303

Soong, T. T., Reinhorn, A. M., Aizawa, S., & Higashino, M. (1994). Recent structural applications of active control technology. *Journal of Structural Control*, *1*(2), 5–21. doi:10.1002/stc.4300010101

Soong, T. T., & Spencer, B. F. (2002). Supplemental energy dissipation: State of the art and state of the practice. *Engineering Structures*, *24*, 243–259. doi:10.1016/S0141-0296(01)00092-X

Spencer, B. F., Jr., Christenson, R. E., & Dyke, S. J. (1999). Next generation benchmark control problem for seismically excited buildings. In T. Kobori, et al., (Eds.), *Proceeding of the 2nd World Conference on Structural Control*, Vol. 2, (pp. 1135-1360). New York, NY: Wiley.

Spencer, B. F., Dyke, S. J., Sain, M. K., & Carlson, J. D. (1997). Phenomenological model for magnetorheological dampers. *Journal of Engineering Mechanics*, *123*, 230–238. doi:10.1061/(ASCE)0733-9399(1997)123:3(230)

Spencer, B. F. Jr, & Nagarajaiah, S. (2003). State of the art of structural control. *Journal of Structural Engineering*, *129*(7), 845–856. doi:10.1061/(ASCE)0733-9445(2003)129:7(845)

Spillers, W. R., & MacBain, K. M. (2009). *Structural optimization*. Springer.

Srinivas, N., & Deb, K. (1994). Multi-objective optimization using non-dominated sorting in genetic algorithm. *Evolutionary Computation*, *2*(3), 221–248. doi:10.1162/evco.1994.2.3.221

Steinbuch, R. (2004). *Simulation im konstruktiven Maschinenbau*. Leipzig, Germany: Fachbuchverlag Leipzig.

Steinbuch, R. (2010). Successful application of evolutionary algorithms in engineering design. *Journal of Bionics Engineering*, *7*, 199–210. doi:10.1016/S1672-6529(09)60236-5

Suresh, S., Narasimhan, S., & Sundararajan, N. (2008). Adaptive control of nonlinear smart base-isolated building using Gaussian kernel functions. *Structural Control and Health Monitoring*, *15*, 585–603. doi:10.1002/stc.217

Symans, M. D., & Constantinou, M. C. (1999). Semi-active control systems for seismic protection of structures: A state-of-the-art review. *Engineering Structures*, *21*, 469–487. doi:10.1016/S0141-0296(97)00225-3

Symans, M. D., & Kelly, S. W. (1999). Fuzzy logic control of bridge structures using intelligent semi-active seismic isolation systems. *Earthquake Engineering & Structural Dynamics*, *28*(1), 37–60. doi:10.1002/(SICI)1096-9845(199901)28:1<37::AID-EQE803>3.0.CO;2-Z

Tabeshpour, M. R., & Ebrahimian, H. (2010). Seismic retrofit of existing structures using friction dampers. *Asian Journal of Civil Engineering*, *11*(4), 509–520.

Takewaki, I. (1997). Optimal damper placement for minimum transfer function. *Earthquake Engineering & Structural Dynamics*, *26*(11), 1113–1124. doi:10.1002/(SICI)1096-9845(199711)26:11<1113::AID-EQE696>3.0.CO;2-X

Takewaki, I. (1997a). Optimal damper placements for minimum transfer functions. *Earthquake Engineering & Structural Dynamics*, *26*(11), 1113–1124. doi:10.1002/(SICI)1096-9845(199711)26:11<1113::AID-EQE696>3.0.CO;2-X

Takewaki, I. (1997b). Efficient redesign of damped structural systems for target transfer functions. *Computer Methods in Applied Mechanics and Engineering*, *147*(3-4), 275–286. doi:10.1016/S0045-7825(97)00022-4

Takewaki, I. (1998). Optimal damper positioning in beams for minimum dynamic compliance. *Computer Methods in Applied Mechanics and Engineering*, *156*(1-4), 363–373. doi:10.1016/S0045-7825(97)00221-1

Takewaki, I. (1999). Displacement-acceleration control via stiffness-damping collaboration. *Earthquake Engineering & Structural Dynamics*, *28*, 1567–1585. doi:10.1002/(SICI)1096-9845(199912)28:12<1567::AID-EQE882>3.0.CO;2-1

Takewaki, I. (2000). Optimal damper placement for planar building frames using transfer functions. *Structural and Multidisciplinary Optimization*, *20*(4), 280–287. doi:10.1007/s001580050158

Takewaki, I. (2000a). Optimal damper placement for critical excitation. *Probabilistic Engineering Mechanics*, *15*(4), 317–325. doi:10.1016/S0266-8920(99)00033-8

Takewaki, I. (2000b). *Effective damper placement for critical excitation* (pp. 558–561). Confronting Urban Earthquakes, Report of Fundamental Research on the Mitigation of Urban Disasters Caused by Near-Field Earthquakes.

Takewaki, I. (2000c). A new probabilistic critical excitation method. *Journal of Structural and Construction Engineering*, *533*, 69–74.

Takewaki, I. (2000d). A nonstationary random critical excitation method for MDOF linear structural models. *Journal of Structural and Construction Engineering*, *536*, 71–77.

Takewaki, I. (2001a). Anewmethod for nonstationary random critical excitation. *Earthquake Engineering & Structural Dynamics*, *30*(4), 519–535. doi:10.1002/eqe.21

Takewaki, I. (2001b). Nonstationary random critical excitation for nonproportionally damped structural systems. *Computer Methods in Applied Mechanics and Engineering*, *190*(31), 3927–3943. doi:10.1016/S0045-7825(00)00354-6

Takewaki, I. (2001c). Nonstationary random critical excitation for acceleration response. *Journal of Engineering Mechanics*, *127*(6), 544–556. doi:10.1061/(ASCE)0733-9399(2001)127:6(544)

Takewaki, I. (2001d). Critical excitation for elastic–plastic structures via statistical equivalent linearization. *Probabilistic Engineering Mechanics*, *17*(1), 73–84. doi:10.1016/S0266-8920(01)00030-3

Takewaki, I. (2001e). Critical excitation for MDOF elastic–plastic structures via statistical equivalent linearization. *Journal of Structural Engineering*, *47B*, 187–194.

Takewaki, I. (2001f). Probabilistic critical excitation for MDOF elastic–plastic structures on compliant ground. *Earthquake Engineering & Structural Dynamics*, *30*(9), 1345–1360. doi:10.1002/eqe.66

Takewaki, I. (2001g). Maximum global performance design for variable critical excitations. *Journal of Structural and Construction Engineering*, *539*, 63–69.

Takewaki, I. (2004a). Critical envelope functions for non-stationary random earthquake input. *Computers & Structures*, *82*(20–21), 1671–1683. doi:10.1016/j.compstruc.2004.04.004

Takewaki, I. (2004b). Bound of earthquake input energy. *Journal of Structural Engineering*, *130*(9), 1289–1297. doi:10.1061/(ASCE)0733-9445(2004)130:9(1289)

Takewaki, I. (2005). Bound of earthquake input energy to soil–structure interaction systems. *Soil Dynamics and Earthquake Engineering*, *25*(7–10), 741–752. doi:10.1016/j.soildyn.2004.11.017

Takewaki, I. (2007). *Critical excitation methods in earthquake engineering*. Netherlands: Elsevier.

Takewaki, I. (2009). *Building control with passive dampers: Optimal performance based design for earthquakes*. London, UK: John Wiley & Sons. doi:10.1002/9780470824931

Takewaki, I., Fujita, K., Yamamoto, K., & Takabatake, H. (2010). Smart passive damper control for greater building earthquake resilience in sustainable cities. *Sustainable Cities and Society*, *1*(1). doi:doi:10.1016/j.scs.2010.08.002

Takewaki, I., & Nakamura, T. (1995). Hybrid inverse mode problems for FEM-shear models. *Journal of Engineering Mechanics*, *121*(8), 873–880. doi:10.1061/(ASCE)0733-9399(1995)121:8(873)

Takewaki, I., & Nakamura, T. (1997). Hybrid inverse mode problems for a structure-foundation system. *Journal of Engineering Mechanics*, *123*(4), 312–321. doi:10.1061/(ASCE)0733-9399(1997)123:4(312)

Takewaki, I., & Uetani, K. (1999). *Optimal damper placement in shear-flexural building models. Proceedings of second world conference on structural control* (*Vol. 2*, pp. 1273–1282). Chichester, UK: John Wiley & Sons Ltd.

Takewaki, I., & Yoshitomi, S. (1998). Effects of support stiffnesses on optimal damper placement for a planar building frame. *Journal of the Structural Design of Tall Buildings*, *7*(4), 323–336. doi:10.1002/(SICI)1099-1794(199812)7:4<323::AID-TAL115>3.0.CO;2-L

Takewaki, L. (2009). *Building control with passive dampers. Optimal performance-based design for earthquakes*. Singapore: Wiley. doi:10.1002/9780470824931

Tan, P., Dyke, S. J., Richardson, A., & Abdullah, M. (2005). Integrated device placement and control design in civil structures using genetic algorithms. *Journal of Structural Engineering*, *131*(10), 1489–1496. doi:10.1061/(ASCE)0733-9445(2005)131:10(1489)

Tarics, A. G. (1984). *The implementation of base isolation for the Foothill Communities Law and Justice Center*. Report to NSF and County of San Bernardino, San Francisco.

Taylor, D. P. (2000). Toggle brace dampers: A new concept for structural control. Advanced technology in structural engineering, *Proceedings of ASCE Structures Congress and Exposition*, Reston.

Taylor, D. P. (1999). *Buildings: Design for damping*. New York, NY: Taylor Devices Inc.

Teramura, A., & Yoshida, O. (1996). Development of vibration control system using u-shaped water tank. In *Proceedings of the 11th World Conference on Earthquake Engineering* (Sociedad Mexicana de Ingenieria Sismica, A.C.), paper no. 1343, Elsevier Science Ltd.

Teuffel, P. (2004). *Entwerfen adaptiver Strukturen - Lastpfadmanagement zur Optimierung tragender Leichtbaustrukturen*. Doctoral dissertation, University of Stuttgart, Germany.

Tewari, A. (2002). *Modern control design with Matlab and Simulink*. New York, NY: John Wiley & Sons, Ltd.

The Mathworks. (2007). *MATLAB/Simulink*. Natick, MA: Author.

Towhata, I. (2008). *Geotechnical earthquake engineering*. Berlin, Germany: Springer Series in Geomechanics and Geoengineering.

Trombetti, T., & Silvestri, S. (2004). Added viscous dampers in shear type structures: The effectiveness of mass proportional damping. *Journal of Earthquake Engineering*, *8*(2), 275–313. doi:10.1080/13632460409350490

Trombetti, T., & Silvestri, S. (2006). On the modal damping ratios of shear-type structures equipped with Rayleigh damping systems. *Journal of Sound and Vibration*, *292*(1-2), 21–58. doi:10.1016/j.jsv.2005.07.023

Trombetti, T., & Silvestri, S. (2007). Novel schemes for inserting seismic dampers in shear type systems based upon the mass proportional component of Rayleigh damping matrix. *Journal of Sound and Vibration*, *302*(3), 486–526. doi:10.1016/j.jsv.2006.11.030

Trombetti, T., Silvestri, S., & Ceccoli, C. (2003). *On the first modal damping ratio of MPD and SPD systems. Technical Report, Department DISTART*. Italy: University of Bologna.

Tsai, K.-C., Chen, H.-W., Hong, C.-P., & Su, Y.-F. (1993). Design of steel triangular plate energy absorber for seismic resistance construction. *Earthquake Spectra*, *9*(3), 505–528. doi:10.1193/1.1585727

Tsuji, M., & Nakamura, T. (1996). Optimum viscous dampers for stiffness design of shear buildings. *Journal of the Structural Design of Tall Buildings*, *5*, 217–234. doi:10.1002/(SICI)1099-1794(199609)5:3<217::AID-TAL70>3.0.CO;2-R

Ueng, J. M., Lin, C. C., & Wang, J. F. (2008). Practical design issues of tuned mass dampers for torsionally-coupled buildings under earthquake loadings. *Structural Design of Tall and Special Buildings*, *17*(3), 133–165. doi:10.1002/tal.336

Val, V. D., & Segal, F. (2005). Effect of damping model on pre-yielding earthquake response of structures. *Engineering Structures*, *27*, 1968–1980. doi:10.1016/j.engstruct.2005.06.018

Viana, F. A. C., Kotinda, G. I., Rade, D. A., & Steffen, V. (2008). Tuning dynamic vibration absorbers by using ant colony optimization. *Computers & Structures*, *86*, 1539–1549. doi:10.1016/j.compstruc.2007.05.009

Viola, E., & Guidi, F. (2009). Influence of the supporting braces on the dynamic control of buildings with added viscous dampers. *Structural Control and Health Monitoring*, *16*(3), 267–286. doi:10.1002/stc.234

Wada, A., Huang, Y., & Bertero, V. V. (2004). Innovative strategies in earthquake engineering. In Bozorgnia, Y., & Bertero, V. V. (Eds.), *Earthquake engineering: From engineering seismology to performance-based engineering* (pp. 10-1–10-33). London, UK: CRC Press.

Wang, H., Li, A. Q., & Miao, C. Q. (2005). FE model and model updating of Runyang Suspension Bridge. *The 2nd International Conference on Structural Health Monitoring of Intelligent Infrastructure,* (pp. 1235-1241).

Wang, D. H., & Liao, W. H. (2011). Magnetorheological fluid dampers: A review of parametric modelling. *Smart Materials and Structures*, *20*, 023001. doi:10.1088/0964-1726/20/2/023001

Wang, H., Li, A. Q., & Guo, T. (2006). Compositive optimal control of the seismic response for super-long-span suspension bridges. *Hunan University*, *33*(3), 6–10.

Wang, H., Li, A. Q., & Miao, C. Q. (2005). FE model updating and validating of Runyang Suspension Bridge based on SHMS. *Southeast University*, *21*(4), 474–479.

Wang, J. F., & Lin, C. C. (2005). Seismic performance of multiple tuned mass dampers for soil-irregular building interaction systems. *International Journal of Solids and Structures*, *42*(20), 5536–5554. doi:10.1016/j.ijsolstr.2005.02.042

Wang, J. F., Lin, C. C., & Chen, B. L. (2003). Vibration suppression for high speed railway bridges using tuned mass dampers. *International Journal of Solids and Structures*, *40*(2), 465–491. doi:10.1016/S0020-7683(02)00589-9

Wang, J. F., Lin, C. C., & Lian, C. H. (2009). Two-stage optimum design of tuned mass dampers with consideration of stroke. *Structural Control and Health Monitoring*, *16*, 55–72. doi:10.1002/stc.312

Wang, Y., & Dyke, S. (2008). Smart system design for a 3D base-isolated benchmark building. *Structural Control and Health Monitoring*, *15*, 939–957. doi:10.1002/stc.228

Warburton, G. B. (1982). Optimum absorber parameters for various combinations of response and excitation parameters. *Earthquake Engineering & Structural Dynamics*, *10*, 381–401. doi:10.1002/eqe.4290100304

Wereley, N. M., & Pang, L. (1998). Nondimensional analysis of semi-active electrorheological and magnetorheological dampers using approximate parallel plate models. *Smart Materials and Structures*, *7*(5), 732–743. doi:10.1088/0964-1726/7/5/015

Whittle, J. K., Williams, M. S., Karavasilis, T. L., & Blakeborough, A. (2011). A comparison of viscous damper placement methods for improving seismic building design. *Journal of Earthquake Engineering*, 15.

Wirsching, P. H., & Campbell, G. W. (1974). Minimal structural response under random excitation using the vibration absorbers. *Earthquake Engineering & Structural Dynamics*, *2*, 303–312. doi:10.1002/eqe.4290020402

Wongprasert, N., & Symans, M. D. (2004). Application of a genetic algorithm for optimal damper distribution within the nonlinear seismic benchmark building. *Journal of Engineering Mechanics*, *130*(4), 401–406. doi:10.1061/(ASCE)0733-9399(2004)130:4(401)

Woodhouse, J. (1998). Linear damping models for structural vibration. *Journal of Sound and Vibration*, *215*(3), 547–569. doi:10.1006/jsvi.1998.1709

Wu, Y. W., Rice, R. B., & Juang, J. N. (1979). Sensor and actuator placement for large flexible space structures. *Proceedings of the Joint Automatic Control Conference,* Denver, USA.

Wu, B., Ou, J. P., & Soong, T. T. (1997). Optimal placement of energy dissipation devices for three-dimensional structures. *Engineering Structures*, *19*(2), 113–125. doi:10.1016/S0141-0296(96)00034-X

Wu, W.-H., Wang, J. F., & Lin, C. C. (2001). Systematic assessment of irregular building-soil interaction using efficient modal analysis. *Earthquake Engineering & Structural Dynamics*, *30*, 573–594. doi:10.1002/eqe.25

Xi, L. (1999). *Analysis and design of building structures with supplemental lead dampers under earthquake and wind loads.* PhD. Dissertation, University of Canterbury, Christchurch.

Xua, B., Zhishen Wub, Z., Chena, G., & Yokoyamab, K. (2004). Direct identification of structural parameters from dynamic responses with neural networks. *Engineering Applications of Artificial Intelligence*, *17*, 931–943. doi:10.1016/j.engappai.2004.08.010

Xu, K., & Igusa, T. (1992). Dynamic characteristics of multiple substructures with closely spaced frequencies. *Earthquake Engineering & Structural Dynamics*, *21*(12), 1059–1070. doi:10.1002/eqe.4290211203

Xu, Z. D., Shen, Y. P., & Guo, Y. Q. (2003). Semi-active control of structures incorporated with magnetorheological dampers using neural-networks. *Smart Materials and Structures*, *12*(1), 80–87. doi:10.1088/0964-1726/12/1/309

Xu, Z. D., Shen, Y. P., & Zhao, H. T. (2003). A synthetic optimization analysis method on structures with viscoelastic dampers. *Soil Dynamics and Earthquake Engineering*, *23*, 683–689. doi:10.1016/j.soildyn.2003.07.003

Xu, Z. D., Zhao, H. T., & Li, A. Q. (2004). Optimal analysis and experimental study on structures with viscoelastic dampers. *Journal of Sound and Vibration*, *273*(3), 607–618. doi:10.1016/S0022-460X(03)00522-4

Yamaguchi, T., Takeuchi, T., Nagao, T., Suzuki, T., Nakata, Y., Ikebe, T., & Minami, A. (1998). Seismic control devices using low-yield-point steel, (pp. 65-72). Nippon Steel Technical Report No. 77. Chiba, Japan: Nippon Steel Corporation.

Yamaguchi, H., & Harnpornchai, N. (1993). Fundamental characteristics of multiple tuned mass dampers for suppressing harmonically forced oscillations. *Earthquake Engineering & Structural Dynamics*, *22*, 51–62. doi:10.1002/eqe.4290220105

Yang, F., Sedaghati, R., Younesian, D., & Esmailzadeh, E. (2005). Optimal placement of active bars in smart structures. *Proceedings of the IEEE International Conference on Mechatronics & Automation*, Niagara Falls Canada, (pp. 1-6).

Yang, G., Spencer, B. F., Jung, H. H., & Carlson, J. D. Jr. (2004). Dynamic modeling of large-scale magnetorheological damper systems for civil engineering applications. *Journal of Engineering Mechanics*, *130*, 1107–1114. doi:10.1061/(ASCE)0733-9399(2004)130:9(1107)

Yang, J. N., & Agrawal, A. K. (2002). Semi-active hybrid control systems for nonlinear buildings against near-field earthquakes. *Engineering Structures*, *24*, 271–280. doi:10.1016/S0141-0296(01)00094-3

Yang, J. N., Kim, J. H., & Agrawal, A. K. (2002). Optimal design of passive energy dissipation systems based on $H\infty$ and H_2 performances. *Earthquake Engineering & Structural Dynamics*, *31*, 921–936. doi:10.1002/eqe.130

Yao, J. T. P. (1972). Concept of structural control. *ASCE Journal of Strucutral Division*, *98*(ST7), 1567–1574.

Ye, A. J., Hu, S. D., & Fan, L. C. (2004). Seismic displacement control for super-long-span cable-stayed bridges. *China Civil Engineering Journal*, *37*(12), 38–43.

Yoshida, O., & Dyke, S. J. (2004). Seismic control of a nonlinear benchmark building using smart dampers. *Journal of Engineering Mechanics*, *130*, 386–392. doi:10.1061/(ASCE)0733-9399(2004)130:4(386)

Yousefzadeh, A., Sebt, M. H., & Tehranizadeh, M. (2011). The optimal TADAS damper placement in moment resisting steel structures based on a cost-benefit analysis. *International Journal of Civil Engineering*, *9*(1), 23–32.

Zadeh, L. A. (1965). Fuzzy sets. *Information and Control*, *8*, 338–353. doi:10.1016/S0019-9958(65)90241-X

Zareian, F., & Medina, R. A. (2010). A practical methof for proper modelling of structural damping in inelastic plane structural systems. *Computers & Structures*, *88*, 45–53. doi:10.1016/j.compstruc.2009.08.001

Zhang, J. M., & Xiao, R. C. (2005). Study on the pre-arranged angle of girders in construction state for a thousand-meter scale cable-stayed bridge. *Computational Mechanics*, *22*(5), 618–622.

Zhang, Q., Zhu, S. T., & Zhou, Z. W. (2005). Study of advanced evaluation system based on a fuzzy AHP method for nuclear reactors. *Nuclear Power Engineering*, *26*(1), 91–95.

Zhang, R. H., & Soong, T. T. (1992). Seismic design of viscoelastic dampers for structural applications. *Journal of Structural Engineering*, *118*(5), 1375–1392. doi:10.1061/(ASCE)0733-9445(1992)118:5(1375)

Zhu, H. P., Ge, D. D., & Huang, X. (2010). Optimum connecting dampers to reduce the seismic responses of parallel structures. *Journal of Sound and Vibration*, *330*. doi:doi:10.1016/j.jsv.2010.11.016

Ziegler, F. (1998). Mechanics of solids and fluids, 2nd ed. New York, NY: Springer.

Ziegler, F. (2008). Special design of tuned liquid column-gas dampers for the control of spatial structural vibrations. *Acta Mechanica*, *201*, 249–267. doi:10.1007/s00707-008-0062-2

Ziegler, F., & Khalid, B. (2011). A novel base isolation system for asymmetric buildings in seismic active zones: damping supplied by tuned liquid column-gas dampers. In Belyaev, A. K., Irschik, H., & Krommer, M. (Eds.), *Advanced dynamics and model based control of structures and machines* (pp. 225–234). Wien, Austria: Springer-Verlag. doi:10.1007/978-3-7091-0797-3_26

Zitzler, E., & Thiele, L. (1998). *An evolutionary algorithm for multi-objective optimization: The strength Pareto approach.* Technical Report 43, Computer Engineering and Federal Institute of Technology, Zurich.

Zitzler, E., Laumanns, M., & Thiele, L. (2001). *SPEA2: Improving the Strength Pareto Evolutionary Algorithm. Technical Report 103*. Computer Engineering and Networks Laboratory (TIK), Swiss Federal Institute of Technology (ETH) Zurich, Gloriastrasse 35, CH-8092 Zurich, Switzerland. 2001.

Zitzler, E., Laumanns, M., & Thiele, L. (2002a). *SPEA2: Improving the Strength Pareto Evolutionary Algorithm for Multiobjecitve Optimization.* Technical Report 103, Computer Engineering and Networks Laboratory (TIK), Swiss Federal Institute of Technology (ETH) Zurich, Switzerland.

Zitzler, E., Deb, K., & Thiele, L. (1999). Comparison of multiobjective evolutionary algorithms: Empirical results. *Evolutionary Computation*, *8*(2), 173–195. doi:10.1162/106365600568202

Zitzler, E., Laumanns, M., & Thiele, L. (2002b). SPEA2: Improving the strength pareto evolutionary algorithm for multiobjecitve optimization. In Giannakoglou, K., Tsahalis, D., Periaux, J., Papailiou, K., & Fogarty, T. (Eds.), *Evolutionary methods for design, optimization and control*. Barcelona, Spain.

Zuo, L., & Nayfeh, S. (2003). The multi-degree-of-freedom tuned-mass damper for suppression of single-mode vibration under random and harmonic excitation. *ASME. Proceedings on Mechanical Vibration & Noise*, *5*, 2051–2061.

Zuo, L., & Nayfeh, S. A. (2005). Optimization of the individual stiffness and damping parameters in multiple-tuned-mass-damper system. *Journal of Vibration and Acoustics*, *127*(1), 77–83. doi:10.1115/1.1855929

INDEX

IndexTerms	**Links**		

Q

R

S

IndexTerms	**Links**